KIT SCIENTIFIC REPORTS 7764

Proceedings of the 15th International Workshop on Beryllium Technology (BeWS-15)

September, 14-15, 2022, Karlsruhe, Germany

Pavel Vladimirov, Christopher Dorn, Ramil Gaisin (eds.)

KIT Scientific Publishing

Pavel Vladimirov, Christopher Dorn, Ramil Gaisin (eds.)

Proceedings of the 15th International Workshop on Beryllium Technology (BeWS-15)

September, 14-15, 2022, Karlsruhe, Germany

Karlsruhe Institute of Technology

KIT SCIENTIFIC REPORTS 7764

Proceedings of the 15th International Workshop on Beryllium Technology (BeWS-15)

September, 14-15, 2022, Karlsruhe, Germany

by
Pavel Vladimirov, Christopher Dorn, Ramil Gaisin (eds.)

Scientific
Publishing

Report-Nr. KIT-SR 7764

Impressum

KIT Scientific Publishing

Karlsruher Institut für Technologie (KIT)
KIT Scientific Publishing
Straße am Forum 2
D-76131 Karlsruhe

KIT Scientific Publishing is a registered trademark
of Karlsruhe Institute of Technology.
Reprint using the book cover is not allowed.

www.ksp.kit.edu

Print on Demand 2023 – Gedruckt auf FSC-zertifiziertem Papier

ISSN 1869-9669
ISBN 978-3-7315-1284-4
DOI 10.5445/KSP/1000156312

Table of contents

Executive Summary

The 15th International Workshop on Beryllium Technology (BeWS-15) was initially planned to be held as a satellite meeting of the SOFT-32 in Dubrovnik, Croatia in 2021. Due to the global COVID pandemic the SOFT-32 conference was held as a virtual event only and the International Organizing Committee (IOC) of the BeWS-15 decided to postpone the workshop until in person participation will be possible.

Finally, the Workshop was held as a joint event combining both the BeWS-15 and an industrial forum BeYOND-IX during 14-15 September 2022 in Karlsruhe, Germany with a great success. The workshop was organized by the Karlsruhe Institute of Technology. A company Karlsruhe Beryllium Handling Facility (KBHF) headed by A. Goraieb and Dr. M. Lemmens was responsible for the industrial forum and helped us with the organization of joint social events as well as. Due to still difficult pandemic situation in Asia, it was decided to organize the workshop as a hybrid event, i.e., provide a possibility for the participants having difficulties with travel with online access.

Participants came mainly from Germany, the US, the UK, Kazakhstan, Latvia, Czech Republic, Japan, Sweden, France and China, totaling 55 persons, which was not expected immediately after the global pandemic.

The BeWS-15 program agenda comprised two keynote presentations, which were followed by five technical sessions.

The first session was devoted to the memory of our colleague and friend Prof. Dr. Glen Longhurst who passed away on May 12, 2021. The session was started with the presentation given by Dr. Milan Zmitko from F4E, who reported on the status of Be neutron multiplier materials for the ITER Test Blanket Module (TBM) program and overviewed developments and opened issues. The final keynote was presented by Dr. Jae-Hwan Kim, QST, Japan, who gave an overview on R&D on Neutron Multipliers in Japan.

The five technical sessions featured presentations on

- “News from Industry” with contributions from Materion, USA, and Ulba Metallurgical Plant, Kazakhstan;
- Reports from big facilities “DEMO, ITER & JET” with contributions on the current advanced EU DEMO HCPB breeding blanket design, regulatory situation of Beryllium in EU and France, as well as investigation of JET beryllium tiles;
- The session on “Beryllides” summarized activities in this area performed worldwide by various institutions in Kazakhstan, KIT, Germany and QST, Japan;
- In the session on “Modeling and experimental validation” both high-quality experimental and simulation results on beryllium and beryllides were presented;
- The session “Mechanical properties and irradiation damage” contained contributions on mechanical and microstructural changes of beryllium and beryllides after helium implantation, creep of beryllium pebbles after irradiation as well as thermos-mechanical properties of beryllide pebbles.

The last day of the joint event was devoted to the industrial forum BeYOND-IX where contributions from Fusion-Start-Ups and Health & Safety aspects of beryllium fabrication and study were interchanged. This day has started from a Lab Tour visit to the Karlsruhe Beryllium Handling Facility situated in KIT Campus North.

The Prof. Mario Dalle Donne Memorial Award (MDDMA) was presented for the first time at the BeWS-11 in Barcelona to recognize researchers with outstanding achievements in beryllium-related research. This year, the IOC of BeWS awarded this prize to Mr. Aniceto Goraieb, the KBHF leader, based on his numerous technological achievements in beryllium-related research over the past decades. For him it was a special pleasure to receive this award as he was a student of Prof. M. Dalle Donne.

The IOC of BeYOND industrial forum decided to establish a Glen Longhurst Award for people working on the edge between industry and technological applications of beryllium materials. The Prof. Glen Longhurst Award was presented for the first time to Mr. Christopher Dorn for his long-term support for R&D on beryllium materials for their application for fusion technology working as one of the chief managers at Materion Inc. in USA, keeping beryllium safety standards and services at ITER in France and at JET in UK, and running his own consulting company on beryllium business.

SESSION 1

In memory of Glen Longhurst

In memory of Glen Longhurst (1943-2022)

Pavel V. Vladimirov[1], Christopher K. Dorn[2]

[1]Karlsruhe Institute of Technology, Institute for Applied Materials - Applied Materials Physics, 76344 Eggenstein-Leopoldshafen, Germany
[2]Be4FUSION LLC, Upland, California, U.S.A.

This presentation is devoted to the memory of our colleague and dear friend, Prof. Dr. Glen Longhurst, who passed away on May 12, 2021.

Together with Mario Dalle Donne, Hiroshi Kawamura and Vladimir Shestakov, Glen was one of the co-founders of the Beryllium Workshop in 1991. After that, he was a member of the International Organizing Committee (IOC) for many years, and he actively worked on further development of the Workshop Series. In 2005, Glen hosted the BeWS-7 in Santa Barbara, California, USA as a satellite meeting of the ICFRM-12 conference, and the workshop was a great success. In 2012 during the BeWS-10 in Karlsruhe, he suggested the establishment of the Mario Dalle Donne Memorial award to honor outstanding contributions by scientists working in beryllium area.

In the field of beryllium technology, Glen was well known for his investigations of beryllium behavior under irradiation, its handling, recycling, application for fusion and, especially, for his studies on the retention of accumulated tritium within beryllium. Glen developed the Tritium Migration Analysis Program (TMAP) for simulation of tritium transport and release, which has survived through seven major releases and is still regarded as the gold standard in the field today.

A special award for lifetime achievement, in particular, for the establishment and development of the BeWS series, was presented to Prof. Emeritus G. Longhurst during the previous BeWS-14 held in Long Beach, California, USA in 2019. The following slides share some memories from this event.

To honor Glen's achievements, the IOC of the BeYOND Industrial Forum has decided to establish a Glen Longhurst Memorial Award for exceptional persons working on the edge between industry and technological applications of beryllium materials.

Glen will be forever enshrined in our hearts as an outstanding scientist, a great personality, and a wonderful friend to us all.

Corresponding Author:

Dr. Pavel Vladimirov
pavel.vladimirov@kit.edu
Karlsruhe Institute of Technology
P.O. Box 3640
76021 Karlsruhe
Germany

Karlsruhe Institute of Technology

In Memory of Glen Longhurst

Pavel Vladimirov and Christopher Dorn

KIT – The Research University in the Helmholtz Association

www.kit.edu

Karlsruhe Institute of Technology

Glen Longhurst: 1943-2021

Dr. Glen Longhurst was one of the co-founders of the Beryllium Workshop in 1991. He also served on the IOC for many years and worked to develop the BeWS series.

Glen was well known for his investigations of beryllium behavior under irradiation and, especially, for his studies on the retention of accumulated tritium within beryllium. Glen developed the Tritium Migration Analysis Program (TMAP) for simulation of tritium release and transport, which has survived through seven major releases and is still regarded as the gold standard in the field today.

A special award for lifetime achievement, in particular, for the establishment and development of the BeWS series, was presented to Prof. Longhurst during the BeWS-14 held in Long Beach, California, USA in October 2019.

In memory of Glen Longhurst

Department of Metallic Alloys, Institute for Applied Materials - Applied Materials Physics

IAM Institute for Applied Materials

Karlsruhe Institute of Technology

Lifetime achievement awards were presented to Drs. Longhurst and Kawamura, two of the original co-founders of the Beryllium Workshop series. The ceremony took place at the BeWS-14 workshop dinner aboard the Hotel Queen Mary, a former British passenger ship, in Long Beach, California, USA in October 2019.

3 14.09.2022 In memory of Glen Longhurst

Department of Metallic Alloys, Institute for Applied Materials - Applied Materials Physics

IAM Institute for Applied Materials

Karlsruhe Institute of Technology

Glen Longhurst, pictured here with Aniceto Goraieb, Managing Director of KBHF, the Karlsruhe Beryllium Handling Facility, after the awards ceremony at the BeWS-14 workshop dinner aboard the Hotel Queen Mary.

4 14.09.2022 In memory of Glen Longhurst

Department of Metallic Alloys, Institute for Applied Materials - Applied Materials Physics

IAM Institute for Applied Materials

From left to right: Aniceto Goraieb of the KBHF in Germany, Glen Longhurst, and his wife Jean, shown here at the BeWS-14 workshop dinner aboard the Hotel Queen Mary.

5 14.09.2022 In memory of Glen Longhurst

Department of Metallic Alloys, Institute for Applied Materials - Applied Materials Physics

The Last Slide from Glen's Last Presentation

G. Longhurst, "Evolution of the Beryllium Workshop Series", presented at the BeWS-14, Long Beach, California, USA, 24-25 October 2019.

6 14.09.2022 In memory of Glen Longhurst

Department of Metallic Alloys, Institute for Applied Materials - Applied Materials Physics

The HCPB Test Blanket Module: Current Status in Development and Qualification of Beryllium Materials and an Overview of Open Issues

Milan Zmitko[1], P. Vladimirov[2], V. Chakin[2], A. Spagnuolo[3]

[1]*Fusion for Energy (F4E), TBMs and Materials Development, Barcelona, Spain*
[2]*Institut fuer Materialforschung I, KIT, Karlsruhe, Germany*
[3]*EUROfusion - Programme Management Unit, Boltzmannstrasse 2, Garching, Germany*

One of the reference tritium Breeder Blanket concepts developed in the Europe that will be tested in ITER machine under the form of Test Blanket Module (TBM) is the Helium-Cooled Pebble-Bed (HCPB) TBM concept in which lithiated ceramic pebbles are used as a tritium breeder and beryllium/beryllides pebbles as a neutron multiplier material. This concept uses the EUROFER97 reduced activation ferritic-martensitic (RAFM) steel as a structural material and pressurized helium for heat extraction (8 MPa, 300-500ºC).

The paper gives a brief general description of the HCPB TBM design and the main design requirements including the requirements to beryllium multiplier material. The ITER HCPB TBM development and qualification plan with identification of the main milestones will be presented, taking into account recently signed EU-KO TBM Partnership agreement between Fusion for Energy and ITER Korea.

The main part of the paper will be devoted to the presentation of beryllium materials development strategy, qualification plan and overview of the current status of research, development and characterization.

The achieved results on fabrication technologies development, materials characterization and performance under TBM/DEMO relevant conditions, including the performance under neutron irradiation and thermo-mechanical performance will be briefly overviewed and a new neutron irradiation experiment, foreseen for the functional materials (i.e. beryllium materials and ceramic breeder pebbles), will be introduced.

A special attention will be focused on technical issues related to the HCPB TBM design and manufacturing, like for instance, Be/ceramic breeder pebbles filling procedure and realization of post-weld heat treatment operations during the course of TBM box manufacturing, and an assessment of their possible implications.

Corresponding Author:

Dr. Milan Zmitko
milan.zmitko@f4e.europa.eu
Fusion for Energy (F4E)
c/ Josep Pla 2 – Torres Diagonal Litoral B3
08019 Barcelona, Spain

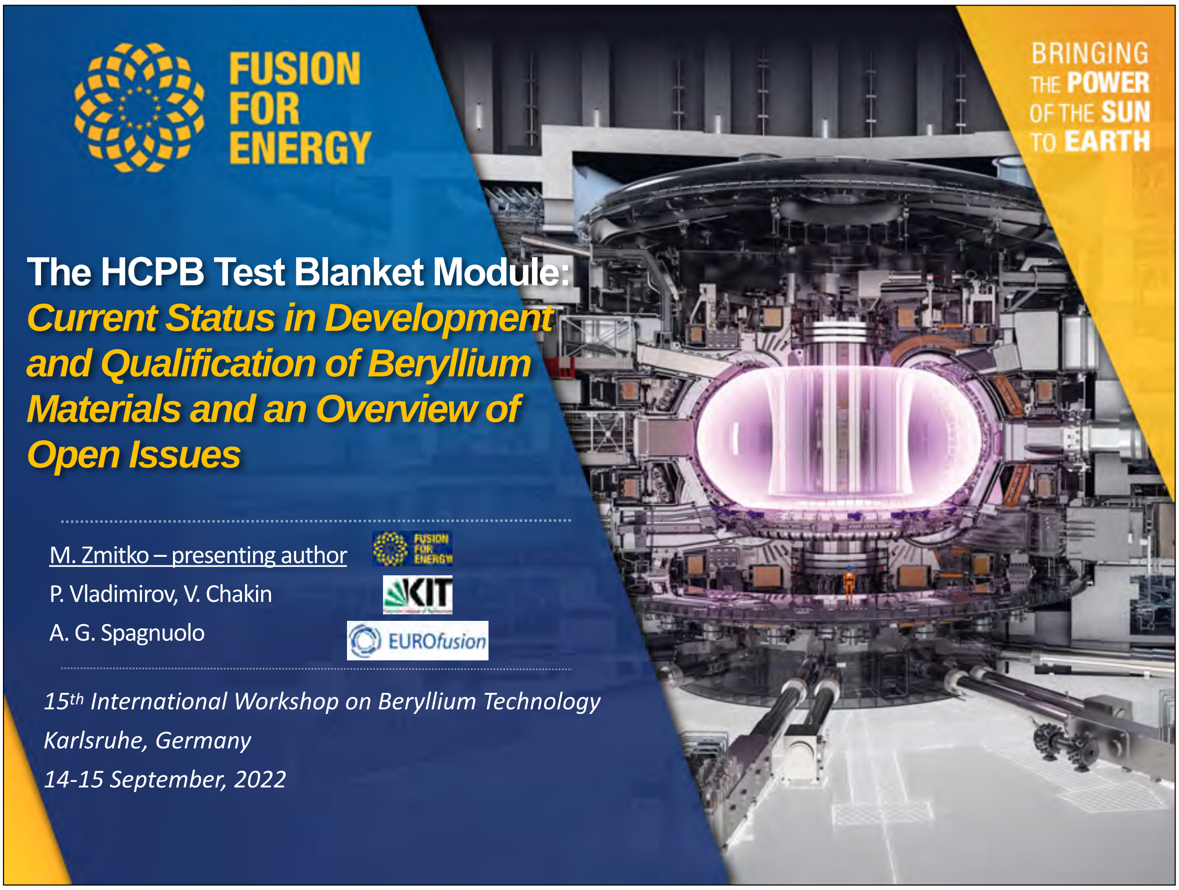
FUSION FOR ENERGY
BRINGING THE POWER OF THE SUN TO EARTH
The HCPB Test Blanket Module:
Current Status in Development and Qualification of Beryllium Materials and an Overview of Open Issues
M. Zmitko – presenting author
P. Vladimirov, V. Chakin
A. G. Spagnuolo
KIT
EUROfusion
15th International Workshop on Beryllium Technology
Karlsruhe, Germany
14-15 September, 2022

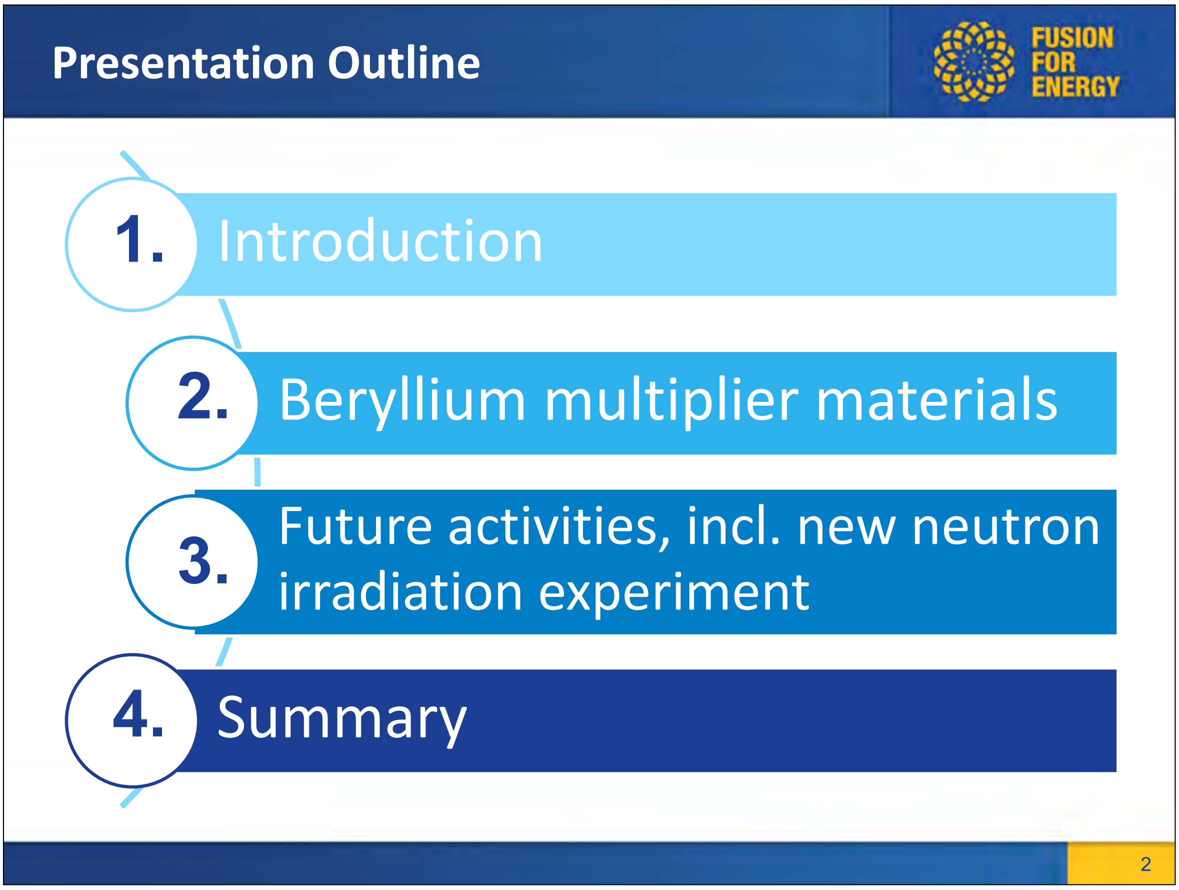
Presentation Outline
FUSION FOR ENERGY
1. Introduction
2. Beryllium multiplier materials
3. Future activities, incl. new neutron irradiation experiment
4. Summary
2

FUSION FOR ENERGY

1. Introduction

3

Test Blanket Systems testing at ITER

FUSION FOR ENERGY

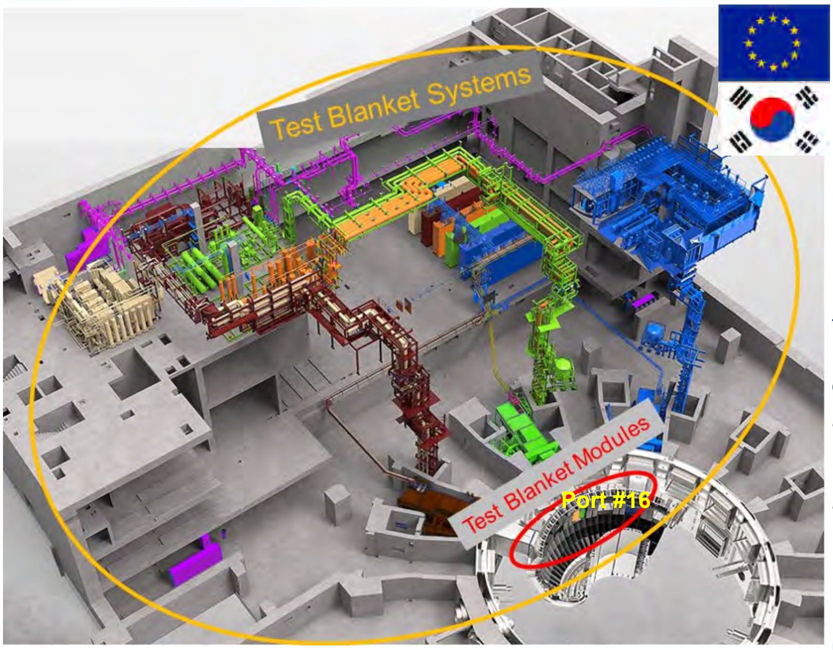

"The TBM project provides test blankets to test and validate design concepts of tritium breeding blankets relevant to a power-producing reactor."
(from ITER Project Requirements)

Europe proposes **two Test Blanket Systems,** aiming to test **two types of tritium breeding materials and two coolants:**

- Liquid metal: Pb-16Li & pressurized water coolant → **WCLL TBM**
- Pebbles bed: Li ceramic & high-pressure helium coolant → **HCPB TBM (Collaboration Agreement with KODA – HCCP TBM)**

EUROFER97 structural material (RAFM steel)

4

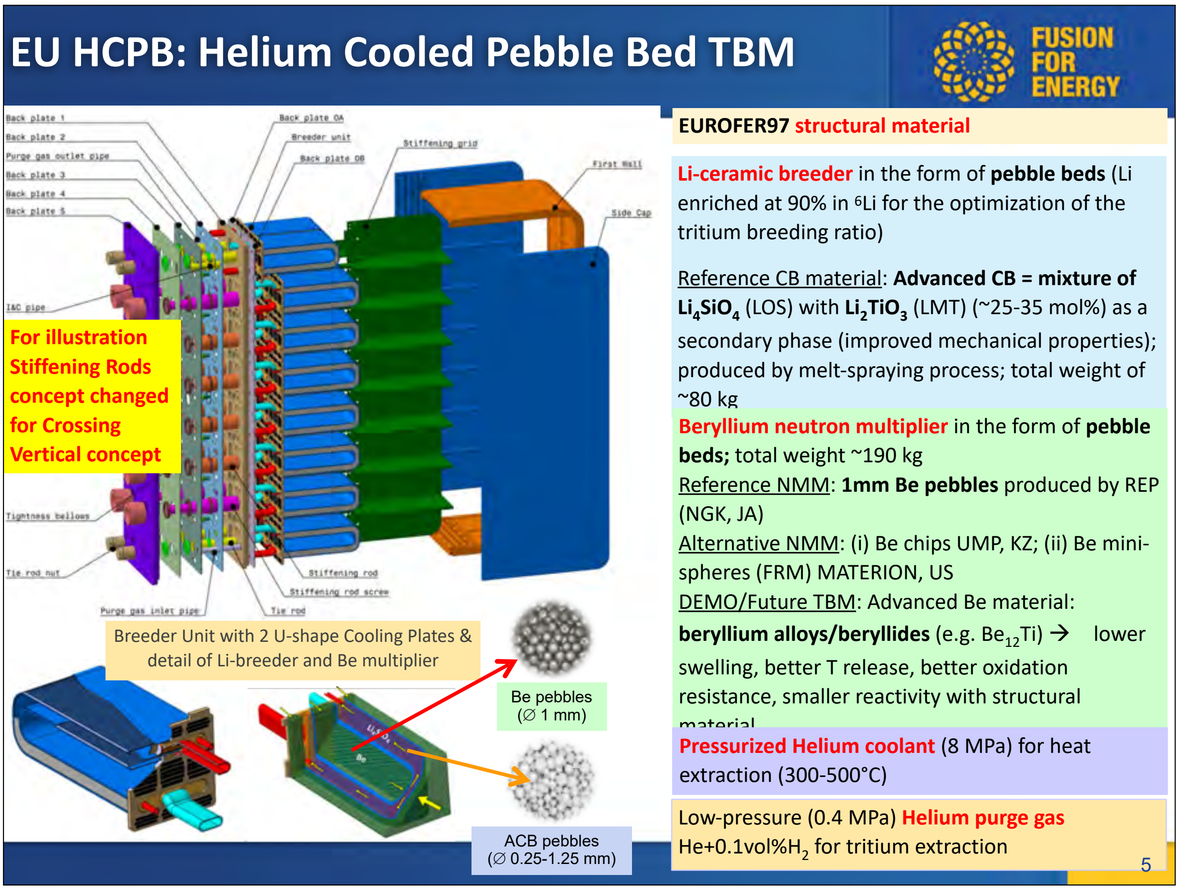
EU HCPB: Helium Cooled Pebble Bed TBM
FUSION FOR ENERGY
Back plate 1
Back plate 2
Purge gas outlet pipe
Back plate 3
Back plate 4
Back plate 5
Back plate 0A
Breeder unit
Back plate 0B
Stiffening grid
First Wall
Side Cap
I&C pipe
Tightness bellows
Tie rod nut
Purge gas inlet pipe
Tie rod
Stiffening rod
Stiffening rod screw
For illustration Stiffening Rods concept changed for Crossing Vertical concept
Breeder Unit with 2 U-shape Cooling Plates & detail of Li-breeder and Be multiplier
Be pebbles (∅ 1 mm)
ACB pebbles (∅ 0.25-1.25 mm)
EUROFER97 structural material
Li-ceramic breeder in the form of pebble beds (Li enriched at 90% in 6Li for the optimization of the tritium breeding ratio)
Reference CB material: Advanced CB = mixture of Li4SiO4 (LOS) with Li2TiO3 (LMT) (~25-35 mol%) as a secondary phase (improved mechanical properties); produced by melt-spraying process; total weight of ~80 kg
Beryllium neutron multiplier in the form of pebble beds; total weight ~190 kg
Reference NMM: 1mm Be pebbles produced by REP (NGK, JA)
Alternative NMM: (i) Be chips UMP, KZ; (ii) Be mini-spheres (FRM) MATERION, US
DEMO/Future TBM: Advanced Be material: beryllium alloys/beryllides (e.g. Be12Ti) → lower swelling, better T release, better oxidation resistance, smaller reactivity with structural material
Pressurized Helium coolant (8 MPa) for heat extraction (300-500°C)
Low-pressure (0.4 MPa) Helium purge gas He+0.1vol%H2 for tritium extraction
5

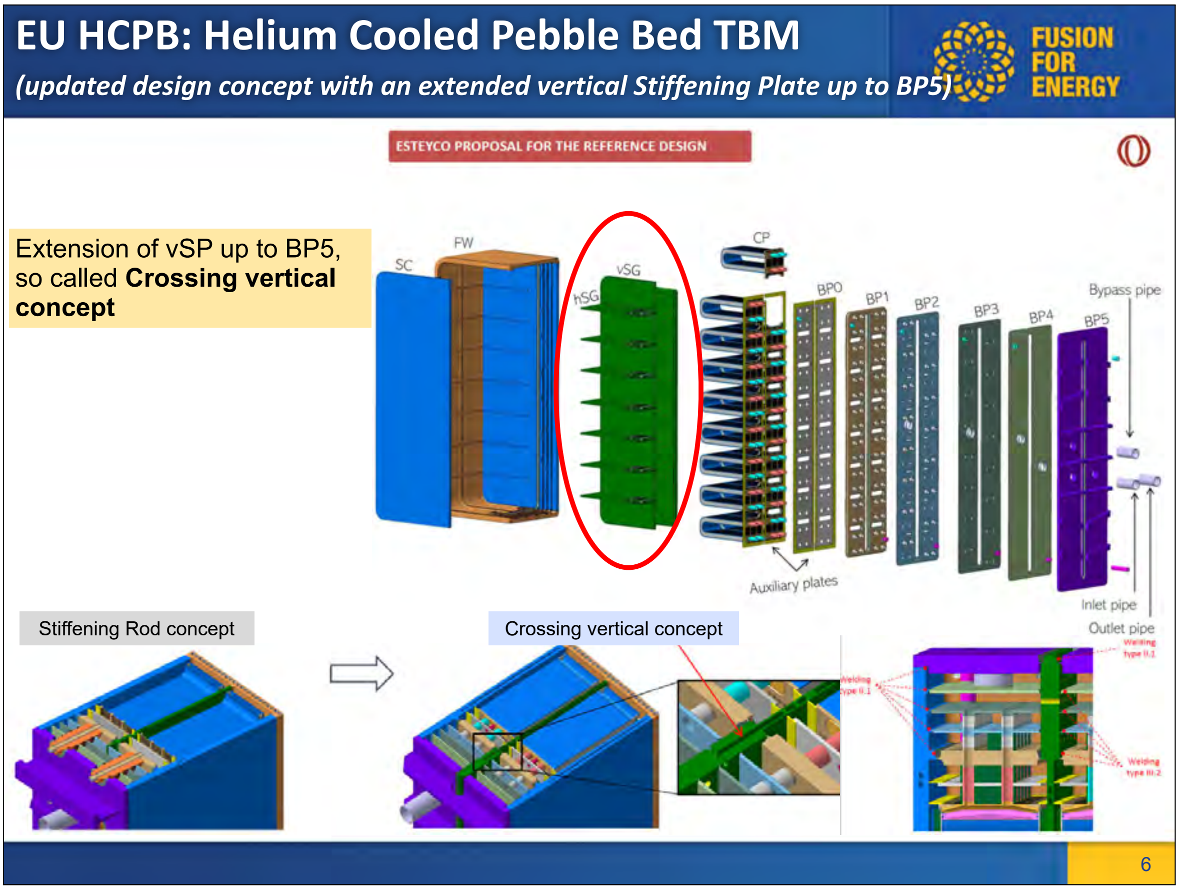
EU HCPB: Helium Cooled Pebble Bed TBM
(updated design concept with an extended vertical Stiffening Plate up to BP5)
FUSION FOR ENERGY
ESTEYCO PROPOSAL FOR THE REFERENCE DESIGN
Extension of vSP up to BP5, so called Crossing vertical concept
SC
FW
hSG
vSG
CP
BP0
BP1
BP2
BP3
BP4
BP5
Bypass pipe
Auxiliary plates
Inlet pipe
Outlet pipe
Stiffening Rod concept
Crossing vertical concept
6

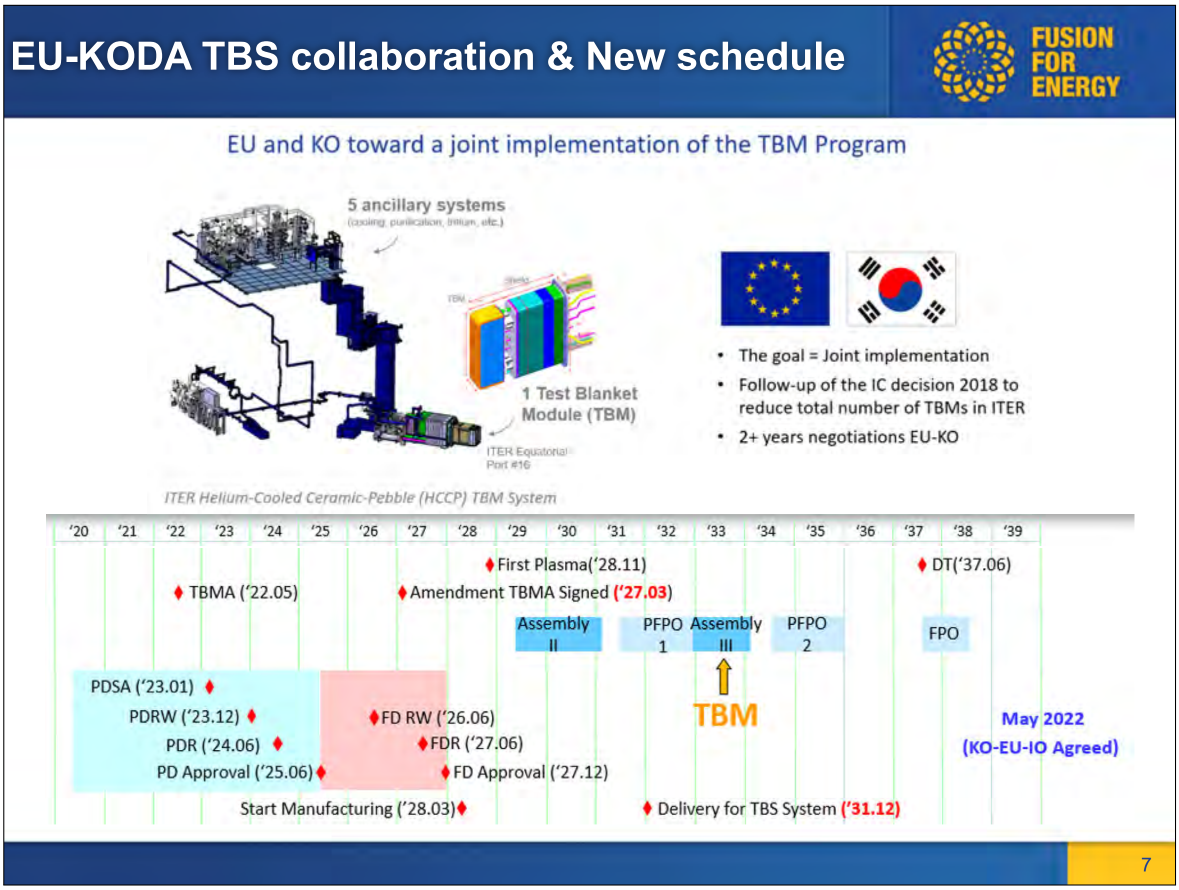
EU-KODA TBS collaboration & New schedule
FUSION FOR ENERGY
EU and KO toward a joint implementation of the TBM Program
5 ancillary systems
1 Test Blanket Module (TBM)
ITER Helium-Cooled Ceramic-Pebble (HCCP) TBM System
The goal = Joint implementation
Follow-up of the IC decision 2018 to reduce total number of TBMs in ITER
2+ years negotiations EU-KO
'20 '21 '22 '23 '24 '25 '26 '27 '28 '29 '30 '31 '32 '33 '34 '35 '36 '37 '38 '39
First Plasma('28.11)
DT('37.06)
TBMA ('22.05)
Amendment TBMA Signed ('27.03)
Assembly II
PFPO 1
Assembly III
PFPO 2
FPO
PDSA ('23.01)
PDRW ('23.12)
PDR ('24.06)
PD Approval ('25.06)
FD RW ('26.06)
FDR ('27.06)
FD Approval ('27.12)
TBM
May 2022
(KO-EU-IO Agreed)
Start Manufacturing ('28.03)
Delivery for TBS System ('31.12)
7

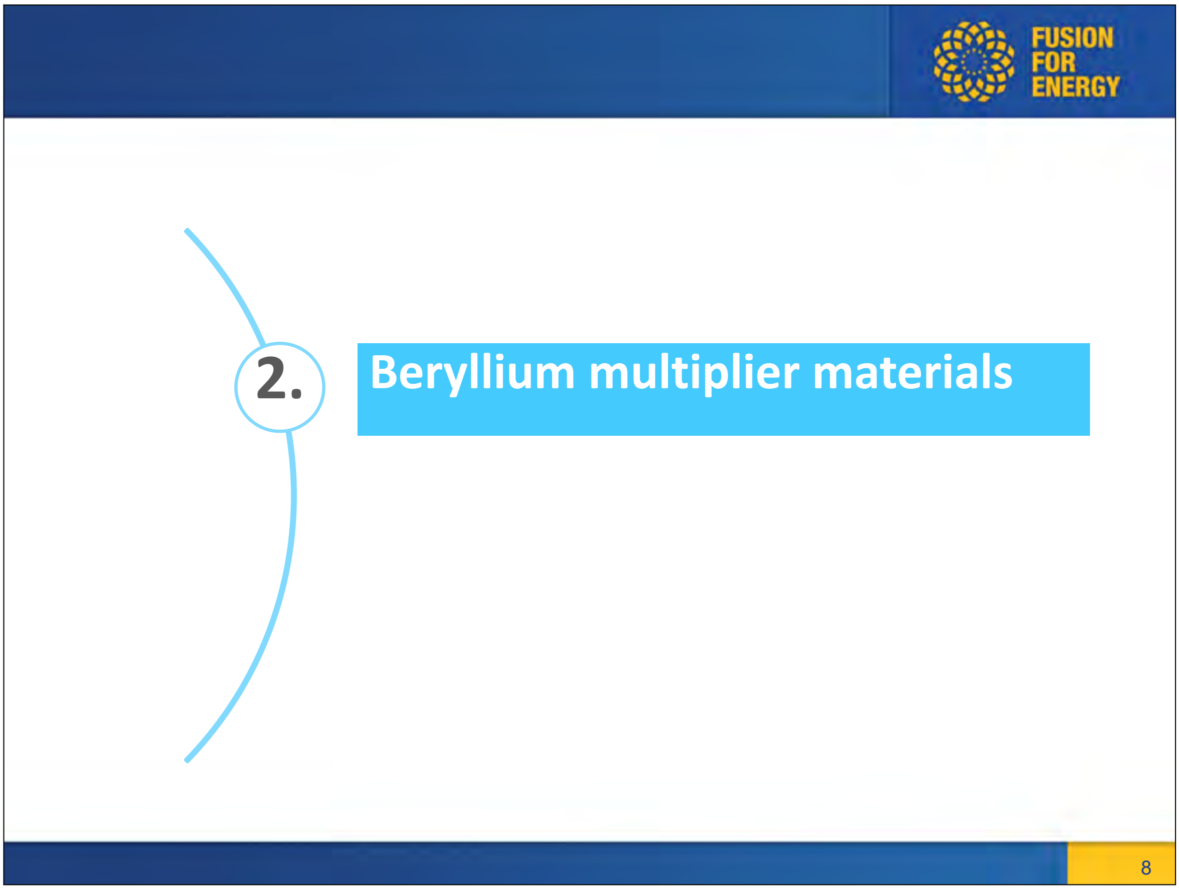
FUSION FOR ENERGY
2.
Beryllium multiplier materials
8

Functional Requirements for Functional Materials

FUSION FOR ENERGY

General requirements come from DEMO objectives with a short-term objective to characterize & qualify Functional Materials (Li-ceramics breeder and Be materials) for a use in the ITER TBM

- Neutronic performances for T self-sufficiency (TBR ≥ 1.1)
- Temperature control of the pebble beds during operation in the temperature window of ~400-920ºC for the CB and ~300-650ºC for Be (PBTM issues/aspects)
- Sufficient long lifetime → (i) neutron irradiation resistance without significant changes of thermo-physical and mechanical properties; (ii) withstanding stresses induced under DEMO-relevant operating conditions without excessive fragmentation and flow resistance of the purge gas (CB and Be pebble beds do not have a structural function)
- Material compatibility between the FMs and EUROFER (up to max. T~ 550ºC), in the reference purge gas He+0.1vol%H_2)
- Low tritium residence time/tritium retention in the Li-ceramics pebbles; efficient tritium extraction → purge gas chemistry optimization
- Low tritium retention in the Be pebbles to minimize tritium inventory → safety aspect
- As low as possible activation under neutron irradiation (impurities level control; e.g. U, Co, Ni, Al, Fe,…) → for recycling / reprocessing (in the view of DEMO/future FPR) and waste management
- Limit/predict hydrogen and passive heat release during accidental conditions below safety limits (Be/steam/water interaction)

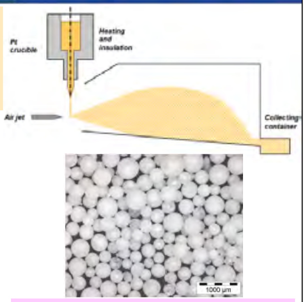

Schematic representation of melt-spray process for LOS pebbles

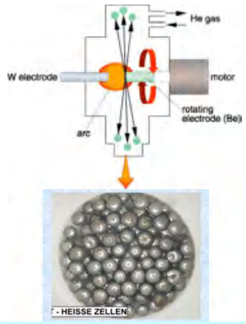

1 mm Be pebbles NGK (JA) Rotation Electrode Process (REP)

9

Beryllium materials R&D activities: Material Assessment and Database Reports

FUSION FOR ENERGY

Material Assessment Report (MAR) and **Material Database Report** (MDBR) → collection of **available out-of-pile & in-pile data/characterization results**; input for **TBM and DEMO design activities**

KIT	KIT Document Ref. No.	Version	Date	Page
	MAT-GEW-1238031-RD-016D01-01	1.0	29-May-15	2 of 113

Part 01: Intermediate Be MAR Update

Material Assessment Report
on
Be Pebble Beds for EU HCPB Test Blanket Module

Table of Content

Table of Content - continuation

10

HIDOBE irradiation campaign & PIE

FUSION FOR ENERGY

High Dose Beryllium fission reactor irradiation program (**HIDOBE**)

- blanket relevant temperatures (425-750°C)
- pebbles of 0.5, 1 and 2 mm produced by REP (NGK, Japan); Be and $Be_{12}Ti$ (Be-5at%Ti and Be-7at%Ti) pellets
- Constrained & unconstrained Be pebbles

Objectives :

(i) Beryllium behaviour under DEMO relevant He/dpa ratios and temperatures
(ii) Tritium inventory as affected by microstructure, swelling, creep
(iii) Pebble beds thermo-mechanical behaviour under neutron irradiation

HIDOBE-01 irradiation rig:
3000 appm He (DEMO: ~18,000 appm); 18 dpa in Be
Irradiation completed - 665 FPD
PIE completed in 2012

HIDOBE-02 irradiation rig:
6000 appm He; 36 dpa in Be
Irradiation completed - 1274 FPD
PIE completed in 2017

HIDOBE Irradiation rig

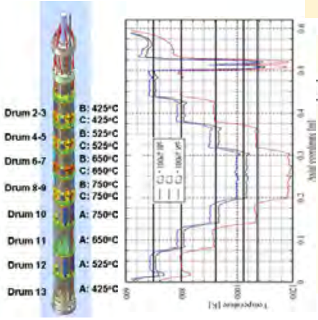

HIDOBE Irradiation program vs. DEMO

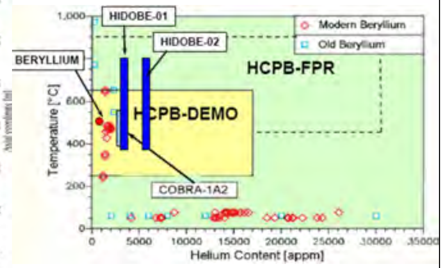

NRG

Post Irradiation Examination (2012-2017):

- Dimensional stability, size distribution, porosity [**performed by NRG**]
- Microstructure and morphology (OM, SEM, TEM, XRD) [**KIT & NRG**]
- Tritium and He release (TPD) [**NRG & KIT**]
- Mechanical properties – Vickers hardness, creep [**KIT**]
- Thermal properties (LFA) [**NRG**]

11

HIDOBE Post-Irradiation Examination Microstructure of Be pebbles

FUSION FOR ENERGY

Effect of irradiation temperature on surface oxidation layer

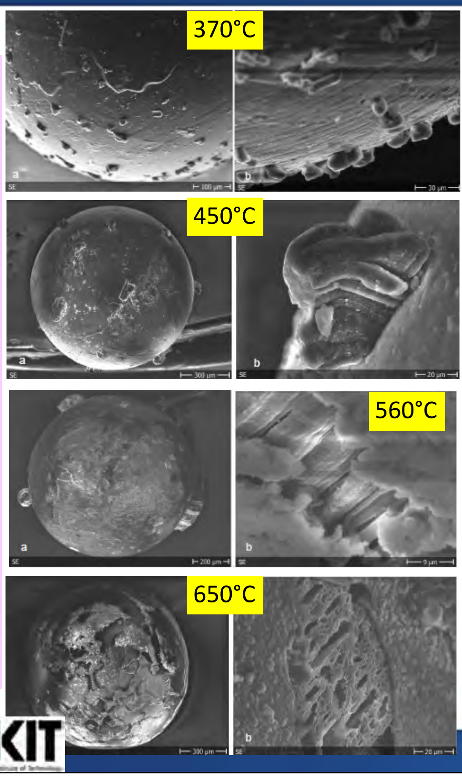

KIT

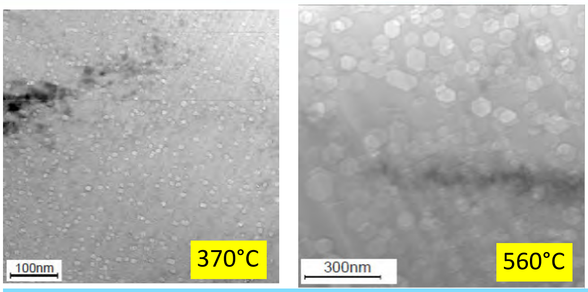

TEM images of He bubbles in 1 mm Be pebbles (hexagonal shape)

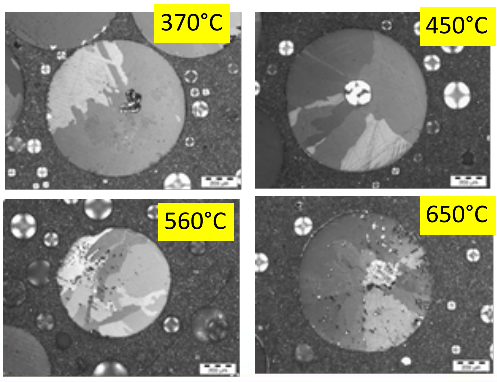

Cross sections (OM) of irradiated unconstrained Be pebbles of 1 mm → formation of bubbles and pores

12

HIDOBE Post-Irradiation Examination
Tritium release characteristics

FUSION FOR ENERGY

Temperature Programmed Desorption (TPD)

Tritium and He release from 0.5 mm unconstrained pebble, irrad. at 560°C

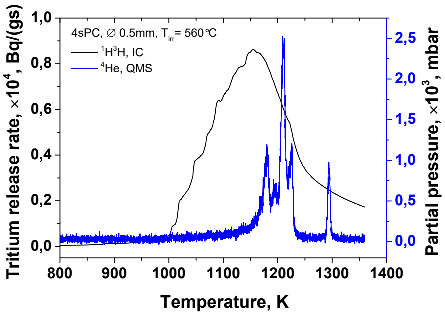

Tritium and He release from 1 mm constrained pebble, irrad. at 480°C

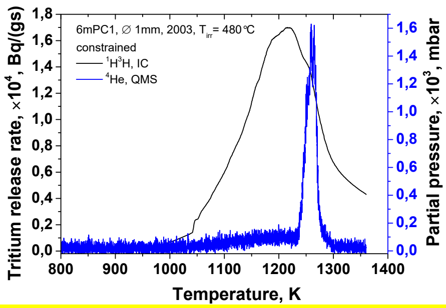

- Tritium released predominantly as HT
- One broad peak for T (830-1070°C) independently of irrad. temperature
- Slow T release starts always at 670-730°C

- He released sometimes in several peaks
- He release starts at 830-930°

Residual Tritium retention of 1 mm Be pebbles as a function of irrad. temperature (related to with theoretically calculated values of T production)

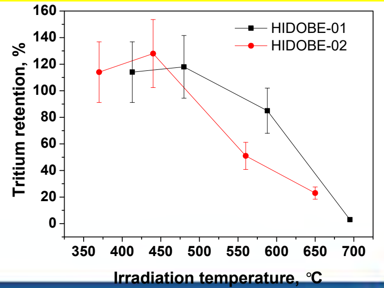

13

HIDOBE Post-Irradiation Examination
Microstructure of Be pebbles

FUSION FOR ENERGY

Swelling of 1 mm **unconstrained Be pebbles** as a function of the irradiation temperature

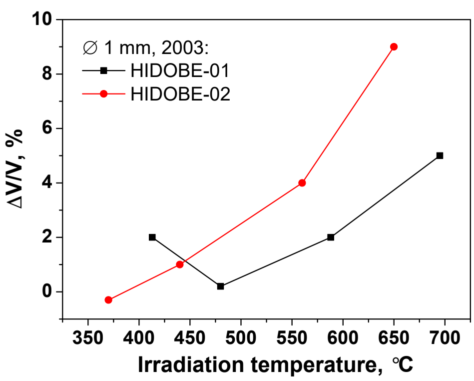

Swelling of **Be-7Ti pellets** as a function of irradiation temperature

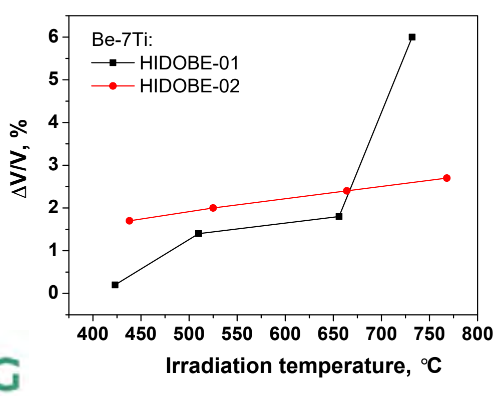

- Swelling depends significantly on irradiation temperature
- Swelling of Be pebbles remains under ~10%
- Swelling of beryllide pellets remains under ~5%

14

Beryllium materials R&D activities: HIDOBE-01/02 PIE results

FUSION FOR ENERGY

Summary of the main PIE results:

Microstructure:

- Strongly depends on irradiation temperatures independently for irradiated constrained/ unconstrained Be pebbles. No significant pore or bubble formations occur at 425 and 525ºC. Irradiations at 650 and 750ºC lead to intensive pore formation resulting swelling up to the highest value of 7 %.
- No compact oxidation layer is observed on the surface regions at 425 and 525 ºC. However, strong oxidation occurs after irradiation at 650 and 750ºC where the thickness of BeO layers on the pebble surfaces can reach 10-25 µm.

Tritium release:

- One peak is observed (at TPD) in the temperature range ~900-1100ºC independently to the irradiation temperature or the pebbles bed state (constrained/unconstrained).
- Tritium is released mainly in the form of HT.
- Irradiation temperature influences the amount of Tritium released/retained throughout irradiation: it increases significantly above 650ºC; at 750ºC, the residual Tritium measured in irradiated samples is 6 to 8 times lower than in samples irradiated at lower temperature.

15

Characterization of reference Be pebbles

FUSION FOR ENERGY

Characterization of as-received Be pebbles supplied by NGK Insulators Ltd., Japan

KIT

- 1 mm Be pebbles produced by Rotation Electrode Process (REP)
- Over 90% of pebbles in the size range of 890-1220 µm

Microstructure of Be pebbles

Chemical analyses obtained by Ion Beam (in ppm)

Element	Content	Element	Content
Mg	56±12	Cr	123±35
Al	780±87	Mn	81±28
Si	529±95	Fe	1082±242
P	31±24	Co	<4
S	13±4	Ni	188±22
Cl	7±1	Cu	75±23
Ca	67±63	W	27
Sc	18±9	U	<7
Ti	204±39		

Be oxidation in steam

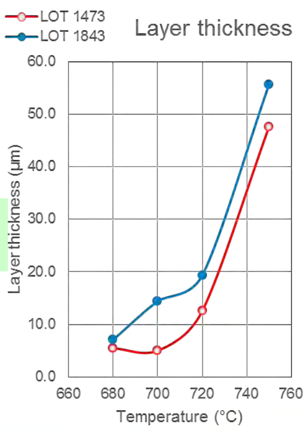

Interaction of Be pebbles with air and steam → reaction kinetic

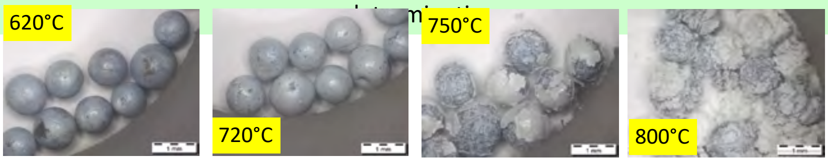

Be specimens after reaction with steam at different temperatures

16

Complementary Be pebbles oxidation studies (REM / NGK & FRM / MATERION pebbles)

FUSION FOR ENERGY

Be pebbles oxidation studies at air (600-1000°C)

Air

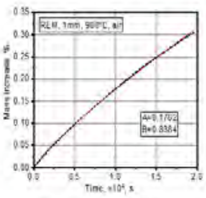

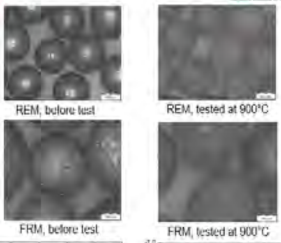

The curves were fitted using equation $\Delta m = At^B$

The oxidation surface layer is protective if b>1 because the reaction rate decreases with t, non-protective if b<1. B connects with b by the relation $b = 1/B$

The temperature dependence of A is described by the Arrhenius equation $A = C\exp(-E_a/kT)$

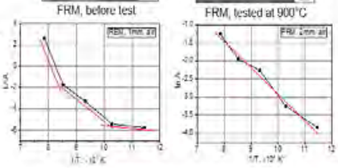

Lot	Activation energy of oxidation E_a in air, eV		
REM, Ø 1 mm, Lot 1805-20	0.24 for 600-700°C	1.81 for 700-900°C	5.61 for 900-1000°C
FRM, Ø 2 mm	0.61 for 600-1000°C		

Be pebbles oxidation studies at steam (500-750°C)

Steam

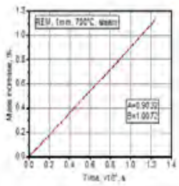

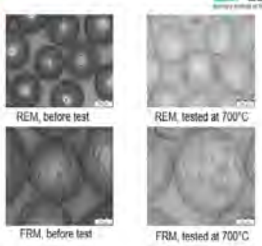

The curves were fitted using equation $\Delta m = At^B$

The oxidation surface layer is protective if b>1 because the reaction rate decreases with t, non-protective if b<1. B connects with b by the relation $b = 1/B$

The temperature dependence of A is described by the Arrhenius equation $A = C\cdot\exp(-E_a/kT)$

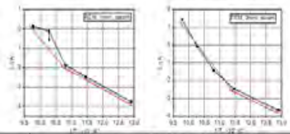

Lot	Activation energy of oxidation E_a in steam, eV	
REM, Ø 1 mm, Lot 1805-20	0.78 for 500-650°C	1.69 for 650-750°C
FRM, Ø 2 mm	0.74 for 500-600°C	2.00 for 600-750°C

1. The 2 mm Be pebbles fabricated by the FRM show **similar corrosion behavior** to the 1 mm REM Be pebbles.
2. An intensive **oxidation in air starts since 700-800°C**.
3. In steam, both kinds of Be pebbles have a **protective oxide surface layer up to 650-700°C**. **Since 700-750°C, the oxide layer is already not protective**. The temperatures of **700-750°C are critical for the use of Be pebbles** in contact with water steam **even during a short time exposure**.
4. The intensive reaction with water steam should be **avoided in fusion reactors** because it results in the **hydrogen production** bearing **a risk of hydrogen gas explosion**.

17

Tritium release characteristics (REM & FRM pebbles)

FUSION FOR ENERGY

Tritium release rate from Ø 1 mm beryllium pebbles produced by REM and FRM

Total tritium accumulation from Ø 1 mm beryllium pebbles produced by REM and FRM

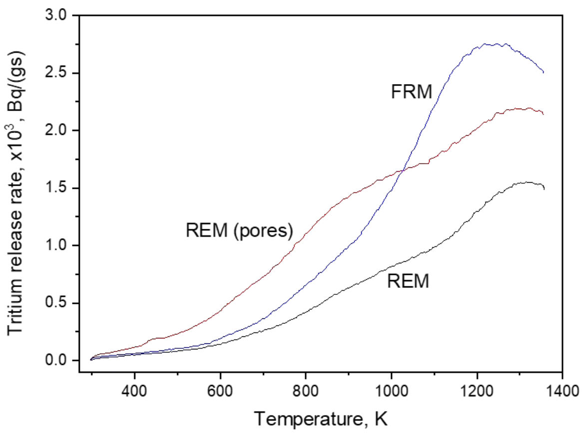

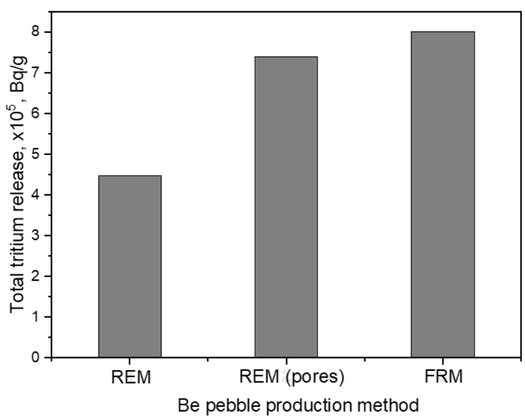

Temperature Programmed Desorption (TPD)

18

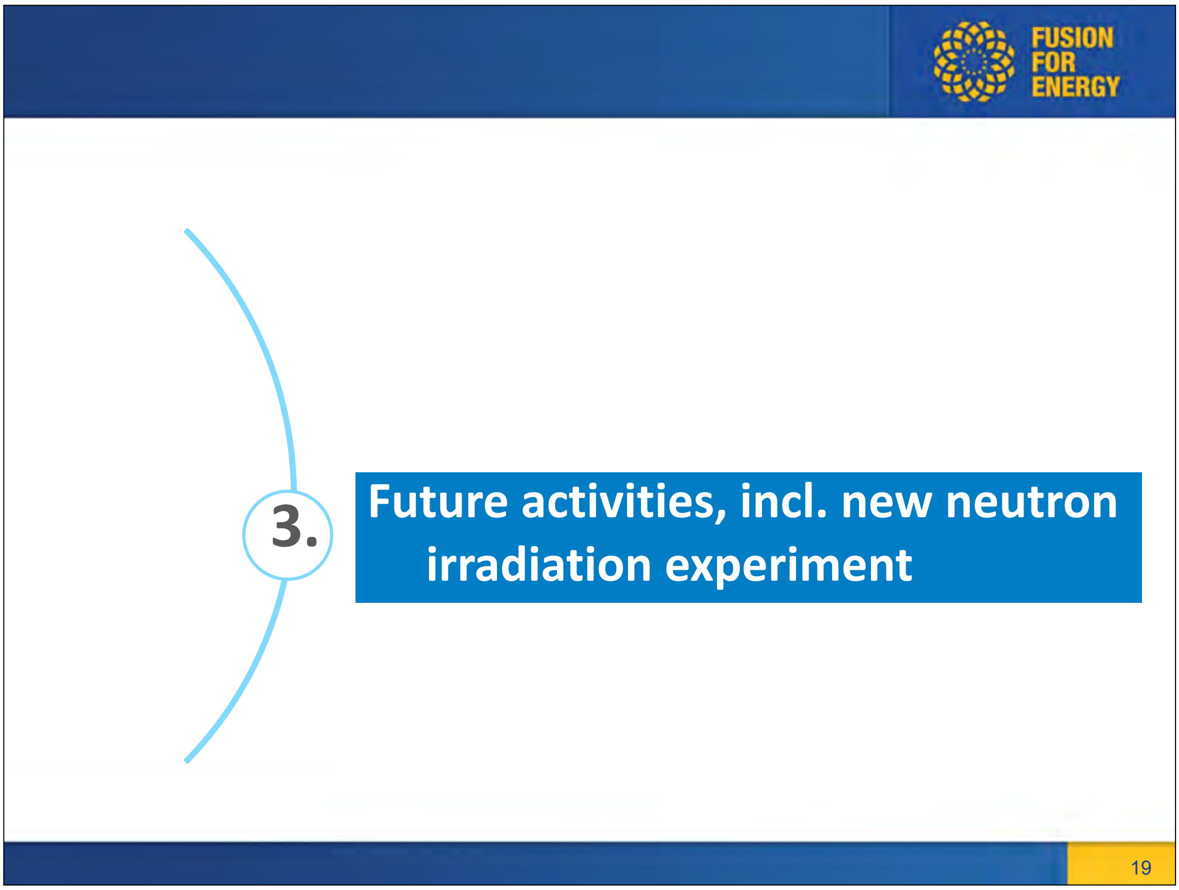
FUSION
FOR
ENERGY
3.
Future activities, incl. new neutron irradiation experiment
19

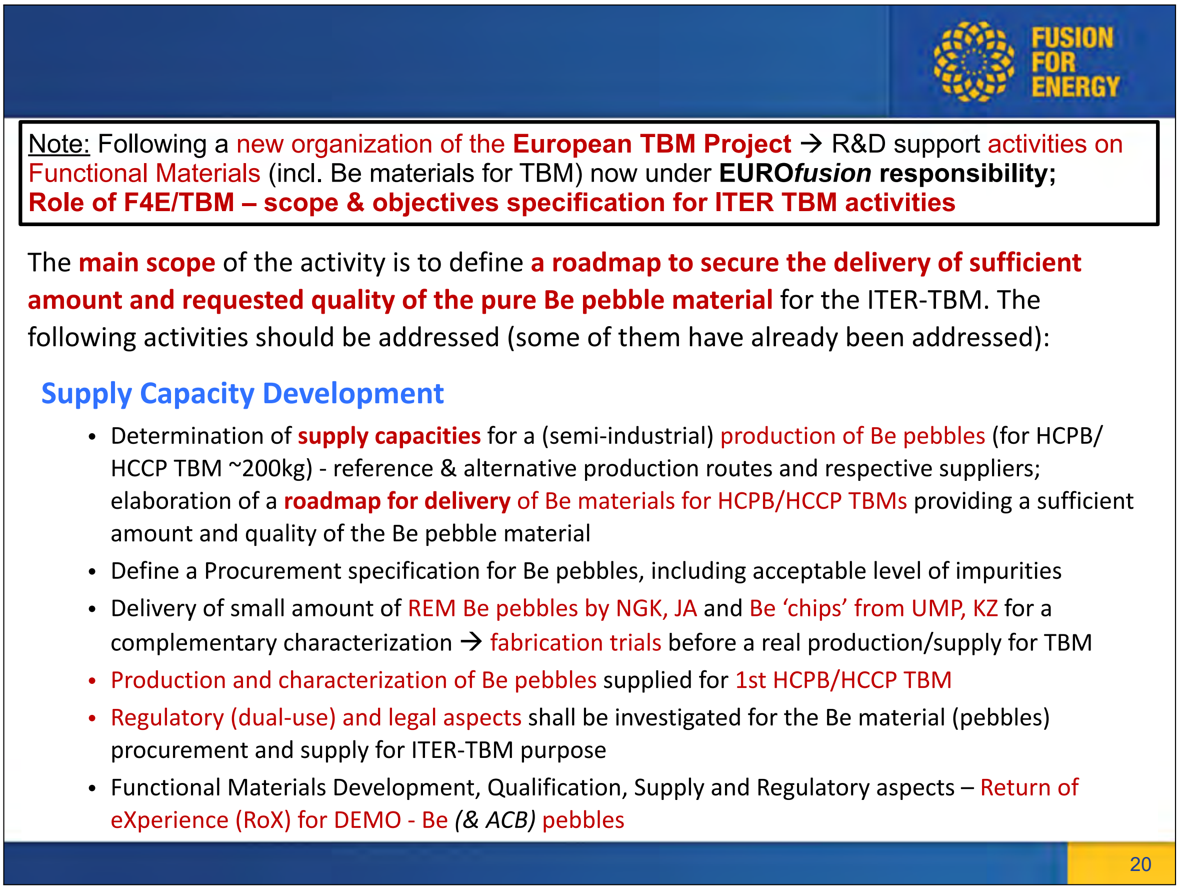
FUSION
FOR
ENERGY
Note: Following a new organization of the European TBM Project → R&D support activities on Functional Materials (incl. Be materials for TBM) now under EUROfusion responsibility;
Role of F4E/TBM – scope & objectives specification for ITER TBM activities
The main scope of the activity is to define a roadmap to secure the delivery of sufficient amount and requested quality of the pure Be pebble material for the ITER-TBM. The following activities should be addressed (some of them have already been addressed):
Supply Capacity Development
• Determination of supply capacities for a (semi-industrial) production of Be pebbles (for HCPB/ HCCP TBM ~200kg) - reference & alternative production routes and respective suppliers; elaboration of a roadmap for delivery of Be materials for HCPB/HCCP TBMs providing a sufficient amount and quality of the Be pebble material
• Define a Procurement specification for Be pebbles, including acceptable level of impurities
• Delivery of small amount of REM Be pebbles by NGK, JA and Be 'chips' from UMP, KZ for a complementary characterization → fabrication trials before a real production/supply for TBM
• Production and characterization of Be pebbles supplied for 1st HCPB/HCCP TBM
• Regulatory (dual-use) and legal aspects shall be investigated for the Be material (pebbles) procurement and supply for ITER-TBM purpose
• Functional Materials Development, Qualification, Supply and Regulatory aspects – Return of eXperience (RoX) for DEMO - Be (& ACB) pebbles
20

Development & Qualification

- Characterization of Be pebbles **produced with an alternative production route** based on fluoride reduction method (FRM, Materion, US) and Ulba Be 'chips' (UMP, KZ) → i.e. chemical composition, impurities, microstructure, porosity, thermo-mechanical properties, oxidation characteristics, tritium release characteristics,…)
  - Characterization of FRM Be pebbles supplied by MATERION, US → high level of impurities detected *(activity already performed)*
- Complementary **oxidation studies** of reference NGK Be pebbles in air and water vapor; experiments at temperatures not covered by the previous activity *(activity already performed)*
- **Update** of the existing Functional Materials properties database (Version for HCPB/HCCP PDR in 2023)
- Definition and realization of **a new neutron irradiation campaign for ACB and Be materials** → very important step in the **Functional Materials qualification** for their use in the ITER-TBM
- Production & characterization of **NMM samples** (Be pebbles & beryllides) **for a new irradiation experiment**
- Experimental study on development of a **filling procedure** for CB and Be pebbles into the HCPB/HCCP Breeder Units, taking into account the TBM assembly sequence and post-weld heat treatments (PWHT)
- **Update** of the existing Functional Materials properties database (Version for HCPB/HCCP FDR in 2027)
- *Important activity for ACB (for info): Modelling of dust formation/re-suspension mechanisms in the Breeder Unit and V&V with experiments → a safety-related aspect*

21

Functional Materials Neutron Irradiation

- **New neutron irradiation campaign** of the Advanced Ceramic Breeder (ACB) and Neutron Multiplier Material (NMM) → irradiation facility(ies) under discussion/assessment *(WWR-K, Almaty - Kazachstan; BR2, SCK-CEN Mol – Belgium)*
- Definition of the **scope of the experiment**, **experimental matrix, experimental conditions** and **PIE** for both ACB and NMM *(on-going)*
- Design of irradiation rig for Functional Materials new irradiation test (conceptual & detailed design) and the rig manufacturing
- Characterization of Be pebbles for new irradiation test (Be pebbles produced by both reference REM and alternative FRM & Ulba Be chips)
- New irradiation experiment realization *(irradiation parameters and exp. conditions still TBD)*
  - irradiation temperatures of the irradiated materials (irradiation temperatures for the ACB in the range of 500-900°C, of 350-650°C for pure Be pebble materials and of up 1000°C for beryllides)
  - irradiation dose / neutron fluence (target irradiation dose for the ACB is ~2-3 dpa *in steel*, for Be pebbles ~2 dpa)
  - type of the experiment (i.e. materials irradiation for subsequent PIE, in-situ on-line tritium release measurement for the ACB, compatibility test with structural material)
- Post-irradiation activities (dismantling, retrieval of irradiation drums, transport, waste management and permanent storage)
- Post-irradiation examination of Be materials
  - Be pebbles microstructure and morphology with OM, SEM, TEM
  - Dimensional stability (swelling), pebbles' size distribution, close and open porosity
  - Mechanical properties (e.g. Vicker's hardness, creep behavior)
  - Tritium and Helium release characteristics (with Temperature Programmed Desorption (TPD) process)
  - Be pebbles compatibility with EUROFER97 structural material

22

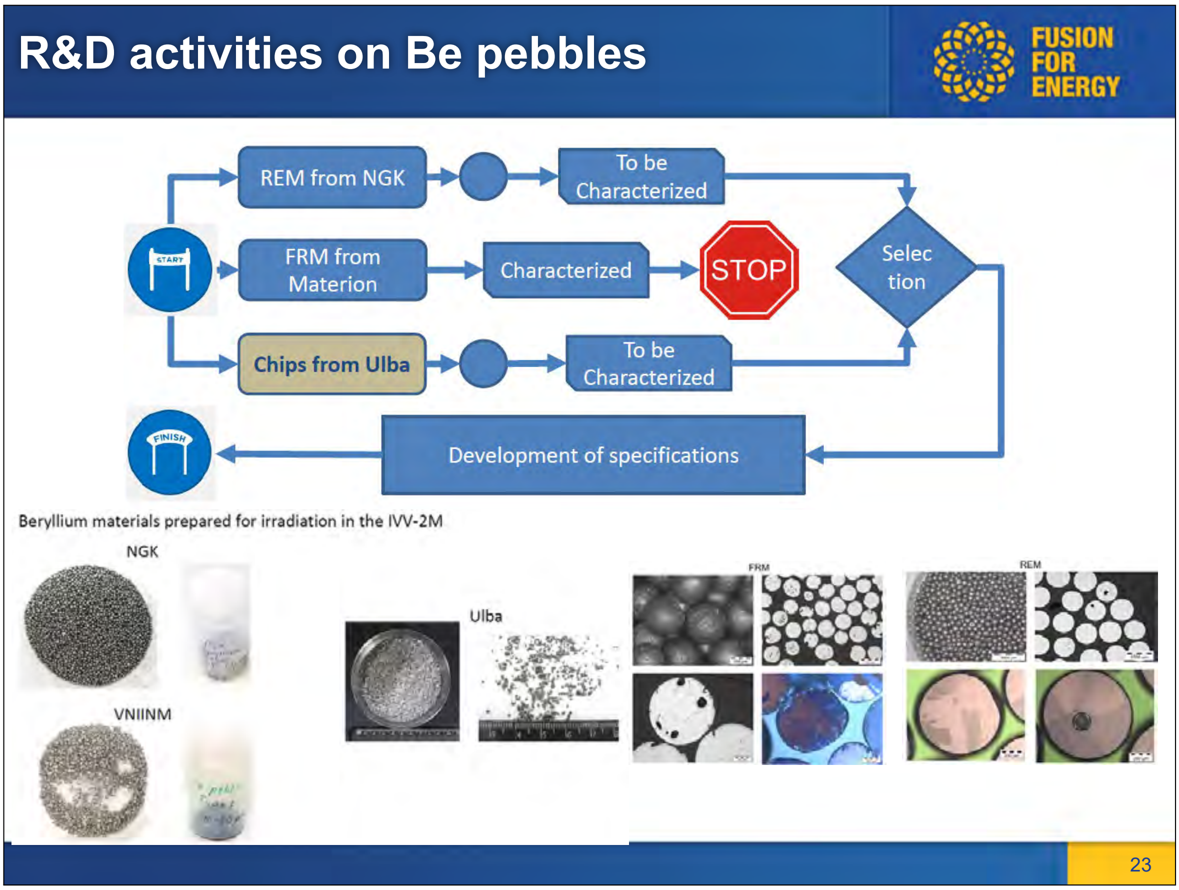
R&D activities on Be pebbles
FUSION FOR ENERGY
REM from NGK
To be Characterized
START
FRM from Materion
Characterized
STOP
Selec tion
Chips from Ulba
To be Characterized
FINISH
Development of specifications
Beryllium materials prepared for irradiation in the IVV-2M
NGK
VNIINM
Ulba
FRM
REM
23

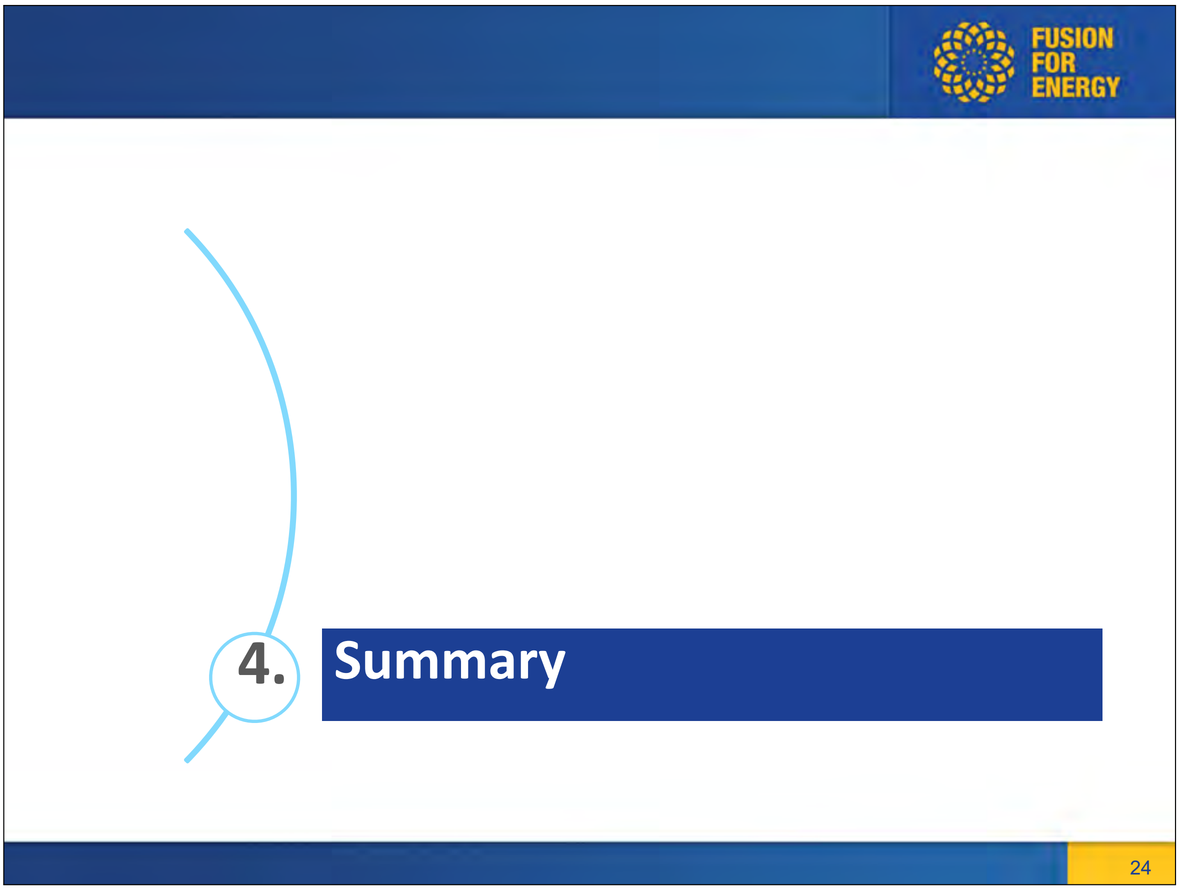
FUSION FOR ENERGY
4.
Summary
24

Summary

FUSION FOR ENERGY

Beryllium Multiplier Materials:

- The 1 mm Be pebbles produced by REP are at present the reference multiplier material for the first HCPB/HCCP TBM breeder blanket concept
- The reference Be pebbles/pebble beds are widely characterized, both out-of-pile & in-pile → available data collected in the MAR and MDBR
- At later stages of ITER operation, beryllides pebbles (e.g. $Be_{12}Ti$) could be tested when production technology and product characterization is mature enough
- The HIDOBE PIE results provided very important information crucial for qualification and licensing of Be pebbles material for its use in the HCPB TBM at ITER
  - Irradiation temperature most significantly affects the development of the material properties → microstructure, tritium retention and release (mainly in HT form)
- Identification of an alternative production route for Be pebbles, including necessary characterization and qualification for ITER TBM use
- Identification of supply capacities and elaboration of a delivery roadmap for both reference and alternative Be pebbles to be used in ITER TBMs
- New neutron irradiation experimental campaign under definition & planning; testing of alternative Be pebbles and beryllides *(together with advanced ceramic breeder pebbles)*

25

FUSION FOR ENERGY

Thank you for your attention

Follow us on:

www.f4e.europa.eu

www.twitter.com/fusionforenergy

www.youtube.com/fusionforenergy

www.linkedin.com/company/fusion-for-energy

www.flickr.com/photos/fusionforenergy

Overview of R&D activities on Neutron Multipliers in QST

Jae-Hwan Kim, Taehyun Hwang, Yutaka Sugimoto, Suguru Nakano, Yoshiaki Akatsu,
Masaru Nakamichi

National Institutes for Quantum Science and Technology, Aomori, Japan

DEMO reactors require advanced neutron multipliers that have higher stability at high temperature. Beryllium intermetallic compounds (beryllides) are the most promising advanced neutron multipliers. Development of the advanced neutron multipliers has been started between Japan and the EU in the DEMO R&D of the International Fusion Energy Research Centre (IFERC) project as a part of the Broader Approach activities. In Japan, beryllides fabrication R&D has been carried out in the DEMO R&D building at IFERC, Rokkasho.

Since beryllides are too brittle to produce the pebbles, establishing fabrication techniques for beryllides is a key issue for development of the advanced neutron multipliers. Conventional syntheses of the beryllides involve a powder metallurgy process involving a hot isostatic pressing method, a casting method, and an arc-melting method. However, beryllides synthesized conventionally are so brittle that it was not easy to fabricate the block or rod type by these methods.

On the other hand, a plasma sintering method has been proposed as a new technique for beryllides synthesis and joining because this method results in powder surface activation that enhances powder particle sinterability and reduces high temperature exposure. From the results of beryllide synthesis experiments, it was clarified that the not only disk type but rod type of beryllide has been successfully fabricated by the plasma sintering method.

To fabricate the beryllide pebbles using the plasma-sintered beryllide rod, a rotating electrode method (REM) was selected because the experience base for its use is broad for not only Be pebbles but also metallic pebbles in general industry. The result of beryllide granulation revealed that the prototypic beryllide pebbles with 0.5 mm to 2.5 mm in average diameter were successfully fabricated. In this study, the recent progress on R&Ds of beryllides as the advanced neutron multipliers in Japan will be presented.

Corresponding Author:

Dr. Jae-Hwan Kim
kim.jaehwan@qst.go.jp
2-166 Omotedate, Obuchi, Rokkasho, Aomori 039-3212, JAPAN

The 15th International Workshop on Beryllium Technology,
Karlsruhe Institute of Technology, Germany, 14-15 Sept, 2022

Overview of R&D activities on Neutron Multipliers in QST

Outline

1. Necessity of advanced neutron multipliers
2. Synthesis of single-phased beryllides
3. Granulation of beryllide pebbles
4. Characterization of beryllide pebbles
5. A joining process to F82H by plasma sintering
6. Summary

IFERC

Jae-Hwan KIM, Taehyun Hwang, Yutaka Sugimoto, Suguru Nakano, Yoshiaki Akatsu, Masaru Nakamichi

QST

National Institutes for Quantum Science and Technology, QST

Jae-Hwan Kim | BeWS-15, KIT| 14th 15th Sept. 2022 | page (1/24)

1. Necessity of advanced neutron multipliers
2. Synthesis of single-phased beryllides
3. Granulation of beryllide pebbles
4. Characterization of beryllide pebbles
5. A joining process to F82H by plasma sintering
6. Summary

Jae-Hwan Kim | BeWS-15, KIT| 14th 15th Sept. 2022 | page (2/24)

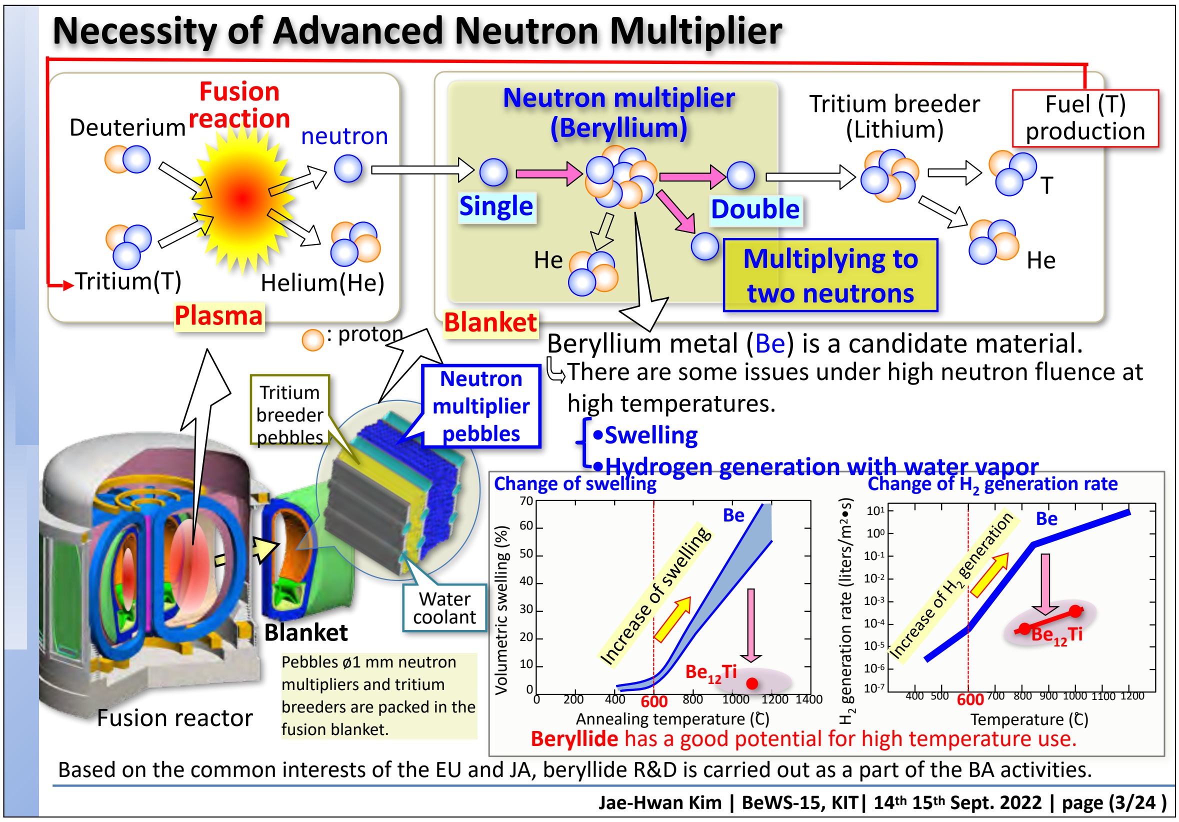

1. Necessity of advanced neutron multipliers

2. Synthesis of single-phased beryllides

3. Granulation of beryllide pebbles

4. Characterization of beryllide pebbles

5. A joining process to F82H by plasma sintering

6. Summary

Jae-Hwan Kim | BeWS-15, KIT| 14th 15th Sept. 2022 | page (4/24)

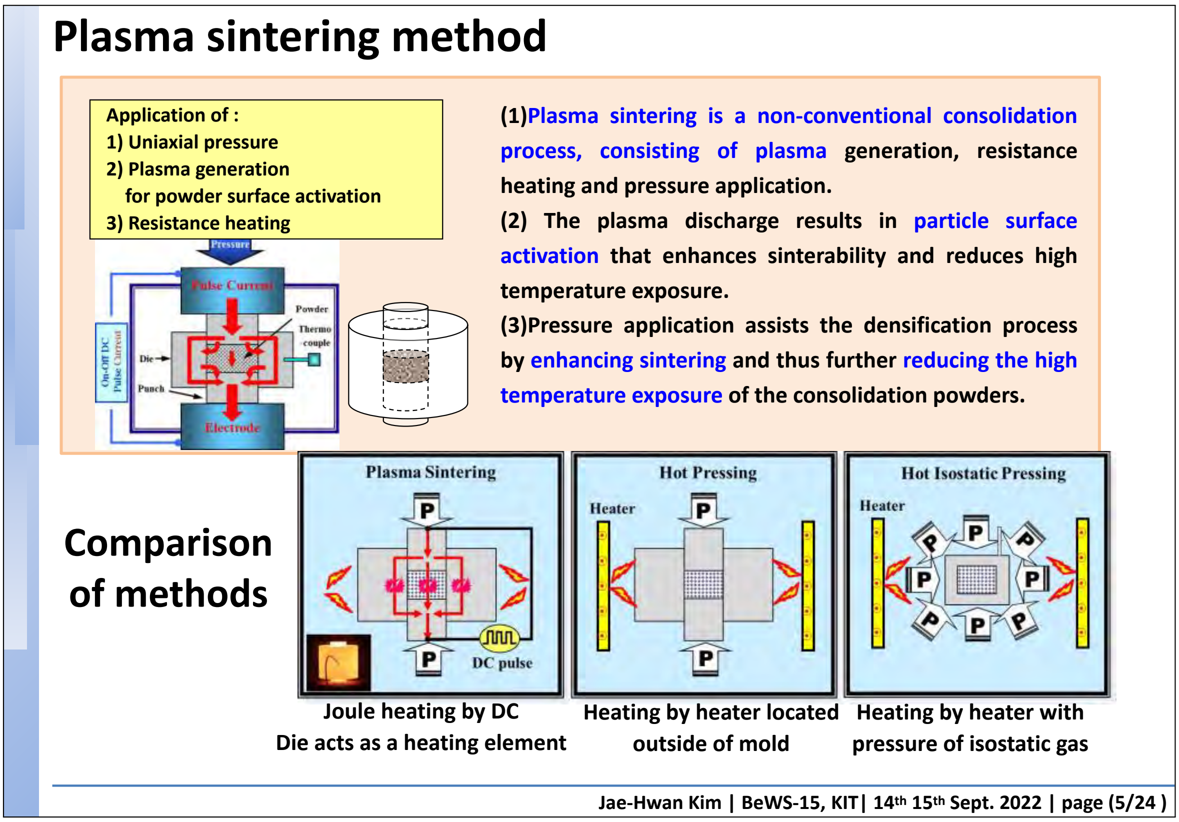
Plasma sintering method
Application of :
1) Uniaxial pressure
2) Plasma generation
for powder surface activation
3) Resistance heating
Pressure
Pulse Current
Powder
Thermo couple
Die
Punch
On-Off DC Pulse Current
Electrode
(1)Plasma sintering is a non-conventional consolidation process, consisting of plasma generation, resistance heating and pressure application.
(2) The plasma discharge results in particle surface activation that enhances sinterability and reduces high temperature exposure.
(3)Pressure application assists the densification process by enhancing sintering and thus further reducing the high temperature exposure of the consolidation powders.
Comparison of methods
Plasma Sintering
DC pulse
Hot Pressing
Heater
Hot Isostatic Pressing
Heater
Joule heating by DC
Die acts as a heating element
Heating by heater located outside of mold
Heating by heater with pressure of isostatic gas
Jae-Hwan Kim | BeWS-15, KIT| 14th 15th Sept. 2022 | page (5/24)

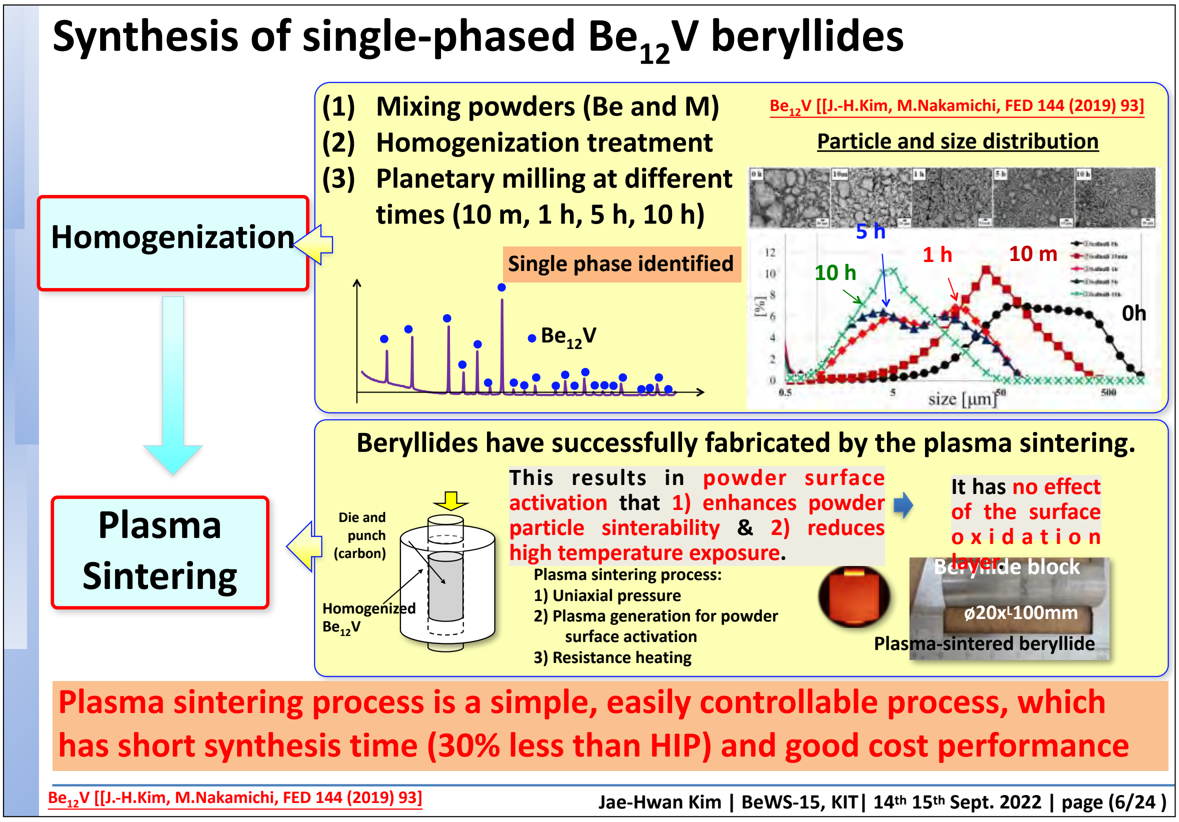
Synthesis of single-phased $Be_{12}V$ beryllides
(1) Mixing powders (Be and M)
(2) Homogenization treatment
(3) Planetary milling at different times (10 m, 1 h, 5 h, 10 h)
$Be_{12}V$ [[J.-H.Kim, M.Nakamichi, FED 144 (2019) 93]
Particle and size distribution
Homogenization
Single phase identified
$Be_{12}V$
5 h
10 h
1 h
10 m
0h
size [µm]
Beryllides have successfully fabricated by the plasma sintering.
Die and punch (carbon)
Homogenized $Be_{12}V$
This results in powder surface activation that 1) enhances powder particle sinterability & 2) reduces high temperature exposure.
It has no effect of the surface oxidation layer.
Plasma sintering process:
1) Uniaxial pressure
2) Plasma generation for powder surface activation
3) Resistance heating
Beryllide block
ø20xL100mm
Plasma-sintered beryllide
Plasma Sintering
Plasma sintering process is a simple, easily controllable process, which has short synthesis time (30% less than HIP) and good cost performance
$Be_{12}V$ [[J.-H.Kim, M.Nakamichi, FED 144 (2019) 93]
Jae-Hwan Kim | BeWS-15, KIT| 14th 15th Sept. 2022 | page (6/24)

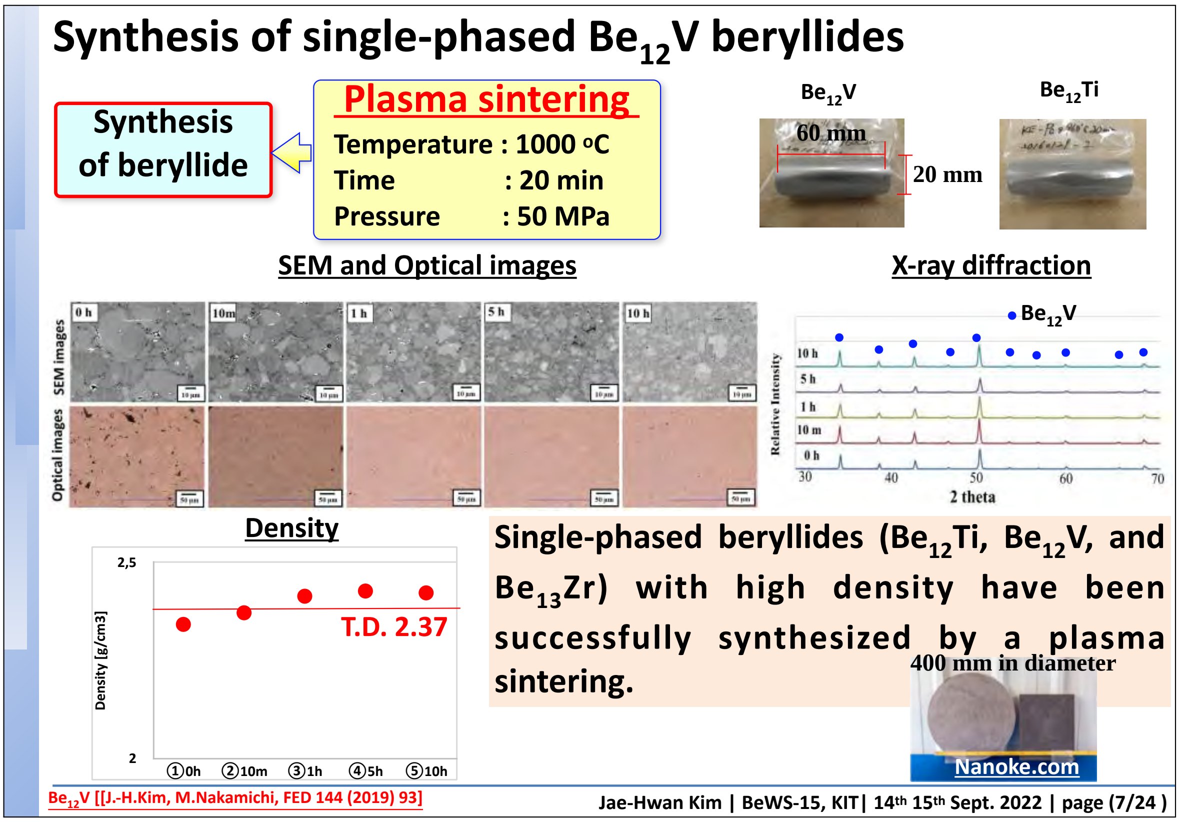
Synthesis of single-phased Be12V beryllides
Synthesis of beryllide
Plasma sintering
Temperature : 1000 ºC
Time : 20 min
Pressure : 50 MPa
Be12V
Be12Ti
60 mm
20 mm
SEM and Optical images
X-ray diffraction
SEM images
Optical images
Relative Intensity
2 theta
Density
T.D. 2.37
Density [g/cm3]
Single-phased beryllides (Be12Ti, Be12V, and Be13Zr) with high density have been successfully synthesized by a plasma sintering.
400 mm in diameter
Nanoke.com
Be12V [[J.-H.Kim, M.Nakamichi, FED 144 (2019) 93]
Jae-Hwan Kim | BeWS-15, KIT| 14th 15th Sept. 2022 | page (7/24)


1. Necessity of advanced neutron multipliers
2. Synthesis of single-phased beryllides
3. Granulation of beryllide pebbles
4. Characterization of beryllide pebbles
5. A joining process to F82H by plasma sintering
6. Summary
Jae-Hwan Kim | BeWS-15, KIT| 14th 15th Sept. 2022 | page (8/24)

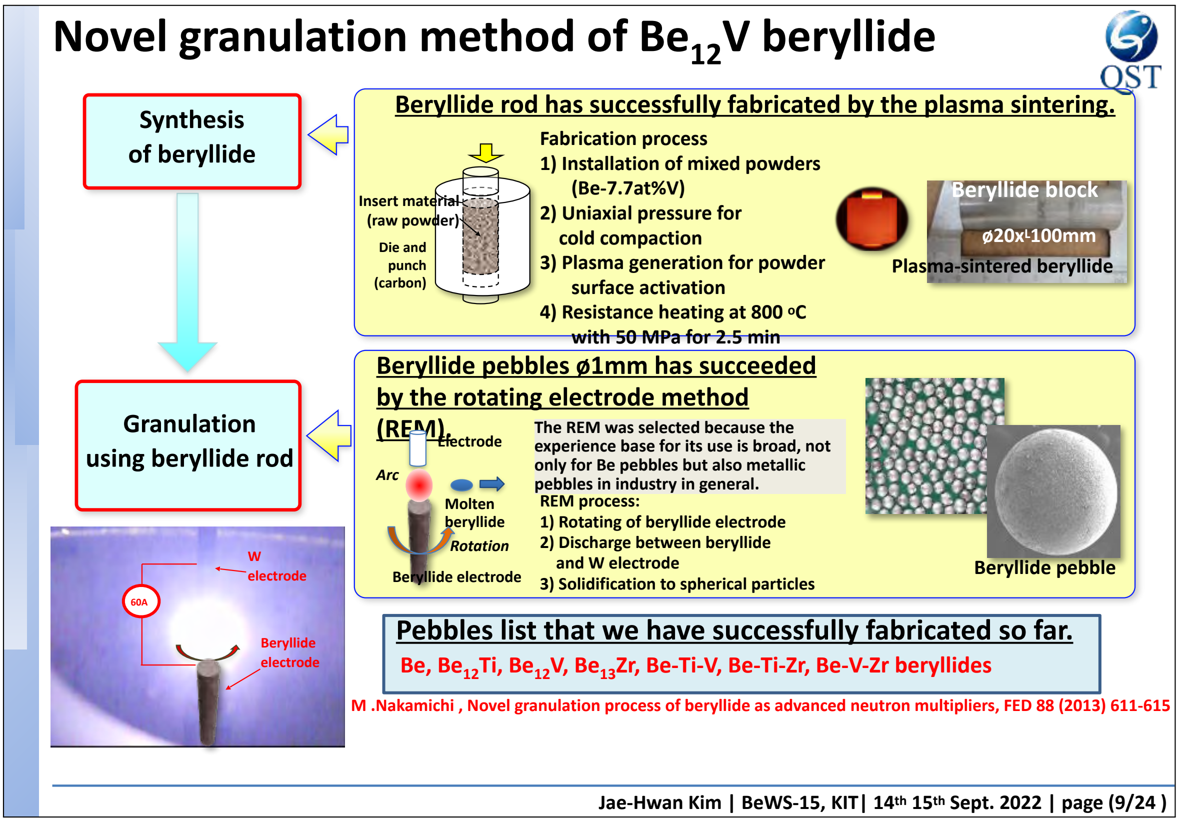

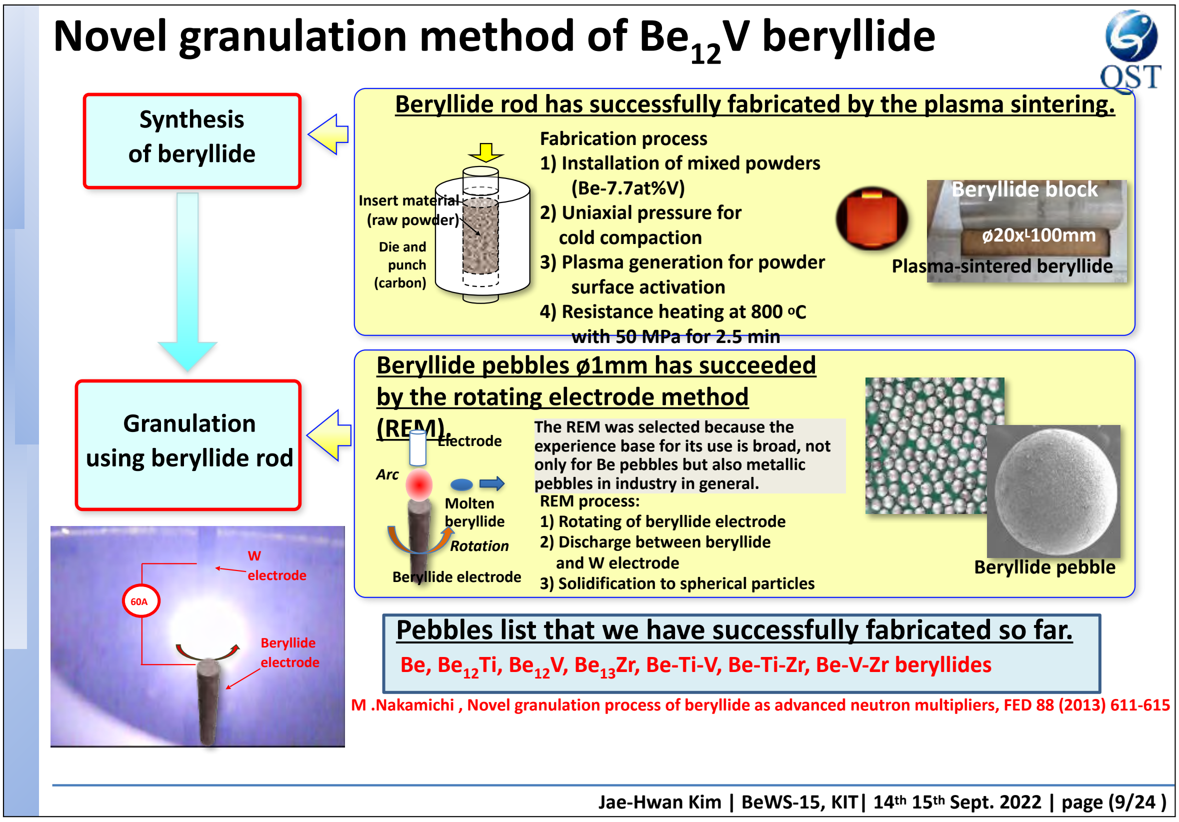
Novel granulation method of Be12V beryllide
QST
Synthesis of beryllide
Granulation using beryllide rod
Beryllide rod has successfully fabricated by the plasma sintering.
Insert material (raw powder)
Die and punch (carbon)
Fabrication process
1) Installation of mixed powders (Be-7.7at%V)
2) Uniaxial pressure for cold compaction
3) Plasma generation for powder surface activation
4) Resistance heating at 800 °C with 50 MPa for 2.5 min
Beryllide block
ø20xL100mm
Plasma-sintered beryllide
Beryllide pebbles ø1mm has succeeded by the rotating electrode method (REM).
Electrode
Arc
Molten beryllide
Rotation
Beryllide electrode
The REM was selected because the experience base for its use is broad, not only for Be pebbles but also metallic pebbles in industry in general.
REM process:
1) Rotating of beryllide electrode
2) Discharge between beryllide and W electrode
3) Solidification to spherical particles
Beryllide pebble
W electrode
60A
Beryllide electrode
Pebbles list that we have successfully fabricated so far.
Be, Be12Ti, Be12V, Be13Zr, Be-Ti-V, Be-Ti-Zr, Be-V-Zr beryllides
M .Nakamichi , Novel granulation process of beryllide as advanced neutron multipliers, FED 88 (2013) 611-615
Jae-Hwan Kim | BeWS-15, KIT| 14th 15th Sept. 2022 | page (9/24)

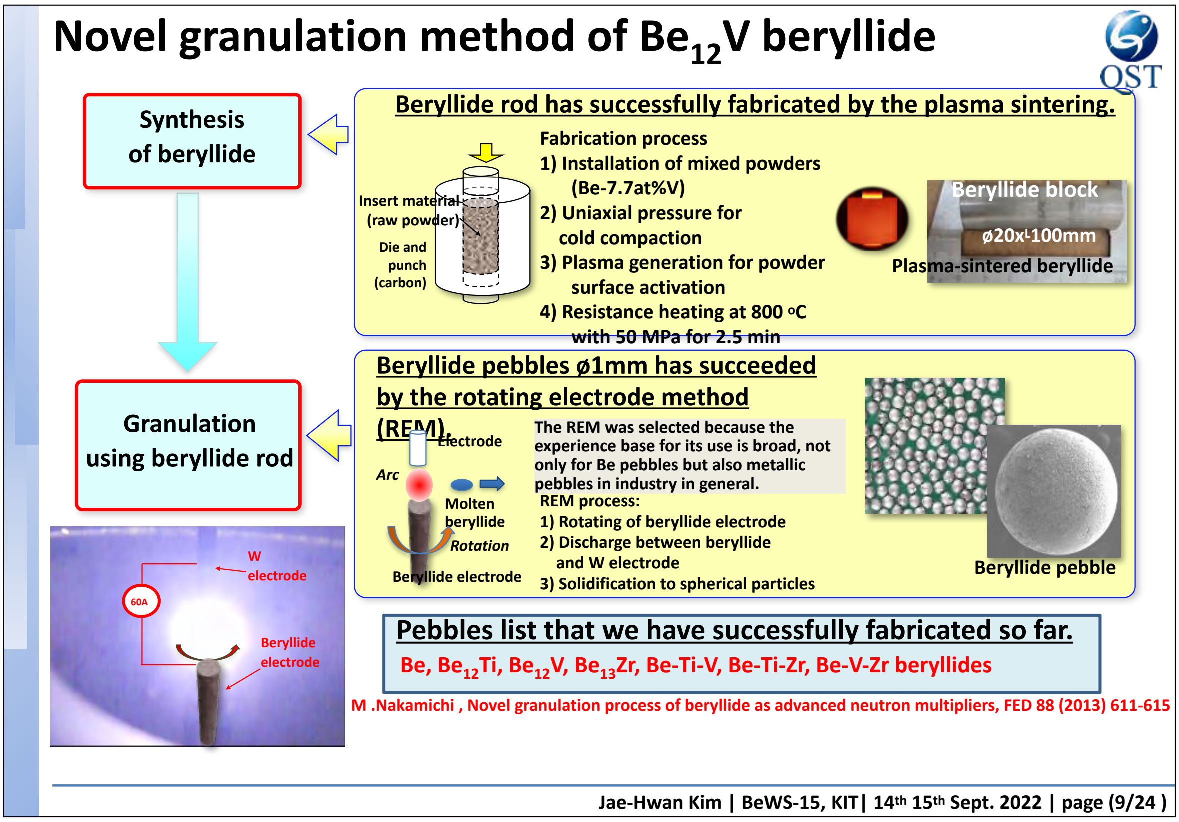

Novel granulation method of Be12V beryllide
QST
Synthesis of beryllide
Beryllide rod has successfully fabricated by the plasma sintering.
Fabrication process
1) Installation of mixed powders (Be-7.7at%V)
2) Uniaxial pressure for cold compaction
3) Plasma generation for powder surface activation
4) Resistance heating at 800 °C with 50 MPa for 2.5 min
Insert material (raw powder)
Die and punch (carbon)
Beryllide block
ø20xL100mm
Plasma-sintered beryllide
Granulation using beryllide rod
Beryllide pebbles ø1mm has succeeded by the rotating electrode method (REM).
Electrode
Arc
Molten beryllide
Rotation
Beryllide electrode
The REM was selected because the experience base for its use is broad, not only for Be pebbles but also metallic pebbles in industry in general.
REM process:
1) Rotating of beryllide electrode
2) Discharge between beryllide and W electrode
3) Solidification to spherical particles
Beryllide pebble
W electrode
60A
Beryllide electrode
Pebbles list that we have successfully fabricated so far.
Be, Be12Ti, Be12V, Be13Zr, Be-Ti-V, Be-Ti-Zr, Be-V-Zr beryllides
M .Nakamichi , Novel granulation process of beryllide as advanced neutron multipliers, FED 88 (2013) 611-615
Jae-Hwan Kim | BeWS-15, KIT| 14th 15th Sept. 2022 | page (9/24)

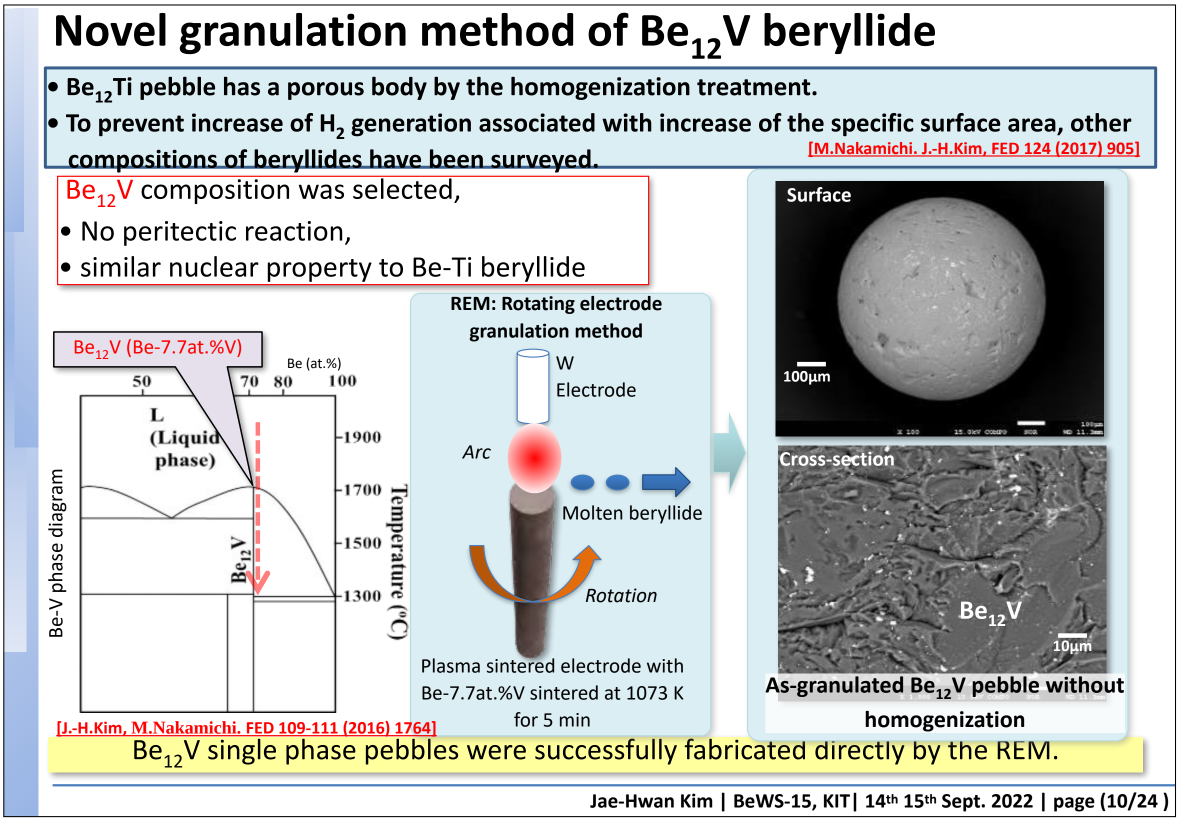

Novel granulation method of Be12V beryllide
• Be12Ti pebble has a porous body by the homogenization treatment.
• To prevent increase of H2 generation associated with increase of the specific surface area, other compositions of beryllides have been surveyed.
[M.Nakamichi. J.-H.Kim, FED 124 (2017) 905]
Be12V composition was selected,
• No peritectic reaction,
• similar nuclear property to Be-Ti beryllide
Be12V (Be-7.7at.%V)
Be (at.%)
50 70 80 100
L (Liquid phase)
1900
1700
1500
1300
Be12V
Temperature (°C)
Be-V phase diagram
[J.-H.Kim, M.Nakamichi. FED 109-111 (2016) 1764]
REM: Rotating electrode granulation method
W Electrode
Arc
Molten beryllide
Rotation
Plasma sintered electrode with Be-7.7at.%V sintered at 1073 K for 5 min
Surface
100μm
Cross-section
Be12V
10μm
As-granulated Be12V pebble without homogenization
Be12V single phase pebbles were successfully fabricated directly by the REM.
Jae-Hwan Kim | BeWS-15, KIT| 14th 15th Sept. 2022 | page (10/24)

Optimization of granulation process

Pebble size is under control by a rotating speed

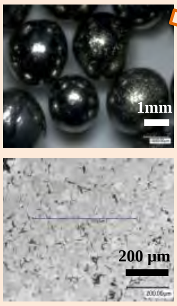

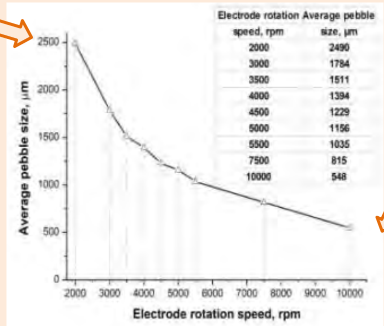

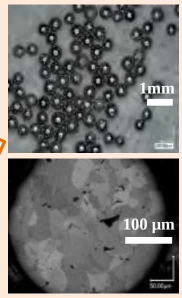

Pebble packing factor (targeting to 80%)

Single packing

Binary packing

	Pebble size	Container dia., mm	Packing factor%
Single packing	0.3-0.5	10	64.9
	0.425-0.6	10	64.8
	2.36-2.8	30	63.5
Binary packing	2.38-2.8 /0.3-0.5	30	81.0

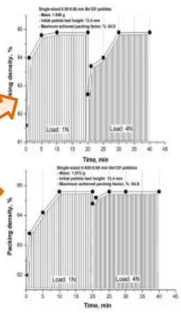

[P. Kurinskiy, J.-H.Kim, M. Nakamichi, FED 146 (2019) 656]

Jae-Hwan Kim | BeWS-15, KIT| 14th 15th Sept. 2022 | page (11/24)

1. Necessity of advanced neutron multipliers
2. Synthesis of single-phased beryllides
3. Granulation of beryllide pebbles
4. **Characterization of beryllide pebbles**
5. A joining process to F82H by plasma sintering
6. Summary

Jae-Hwan Kim | BeWS-15, KIT| 14th 15th Sept. 2022 | page (12/24)

Thermal conductivity of Be and $Be_{12}V$ pebble beds

Packing fraction variation by vibration

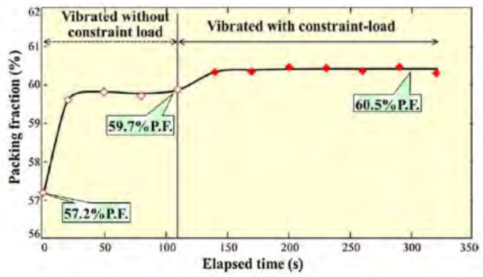

Packing fraction vs surface roughness

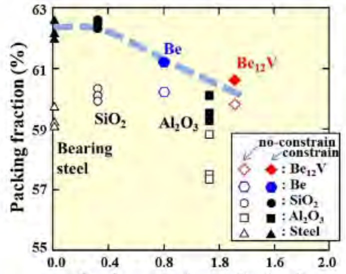

Schematic of hot wire method

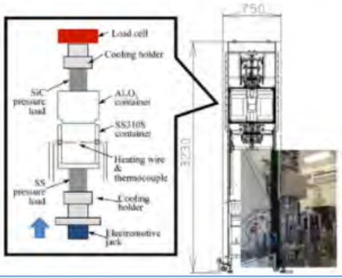

Effective thermal conductivity

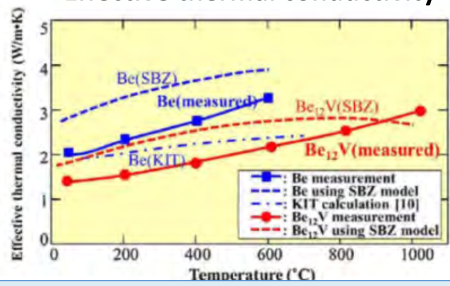

It was clear that the effective thermal conductivity of the $Be_{12}V$ pebble bed was lower by 33 % than that of Be pebble bed at 873 K.

[M. Nakamichi, J.-H.Kim, P. Kurinskiy, FED 136 (2018) 125-127]

Jae-Hwan Kim | BeWS-15, KIT| 14th 15th Sept. 2022 | page (13/24)

Critical issues on H_2 generation reaction in LOCA

Japan has adopted water coolant solid breeder blanket concept for ITER and DEMO. Assuming Loss Of Coolant Accident in the blanket, H_2 generation behavior of neutron multiplier (beryllium and beryllides) should be clarified.

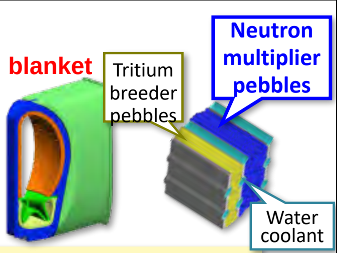

H_2 generation reaction of beryllides pebbles under Ar with the addition of H_2O (1~15%) were examined using a Thermo-Gravimetry/Differential Scanning Calorimetry apparatus connected with a gas chromatography.

Schematic flow diagram of test apparatus

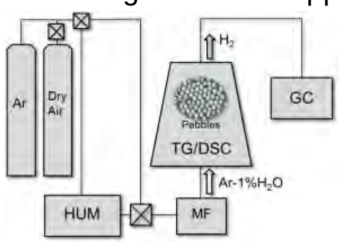

DSC : Differential Scanning Calorimetry apparatus
GC : Gas Chromatographic apparatus
HUM: Water vapor generation apparatus
MF : Mass flow controller

Conditions

- Apparatus :
  - DSC : STA-499, Netzsch, Japan.
  - GC : CP-490, Agilent, USA.
  - HUM : HC-9800, Netzsch, Japan.
- Heating rate : 10 K/min
- Atmosphere : Ar with 1~15% H_2O
- Temperature: ~1473 K
  (Ar gas flow during temperature ramping)

Jae-Hwan Kim | BeWS-15, KIT| 14th 15th Sept. 2022 | page (14/24)

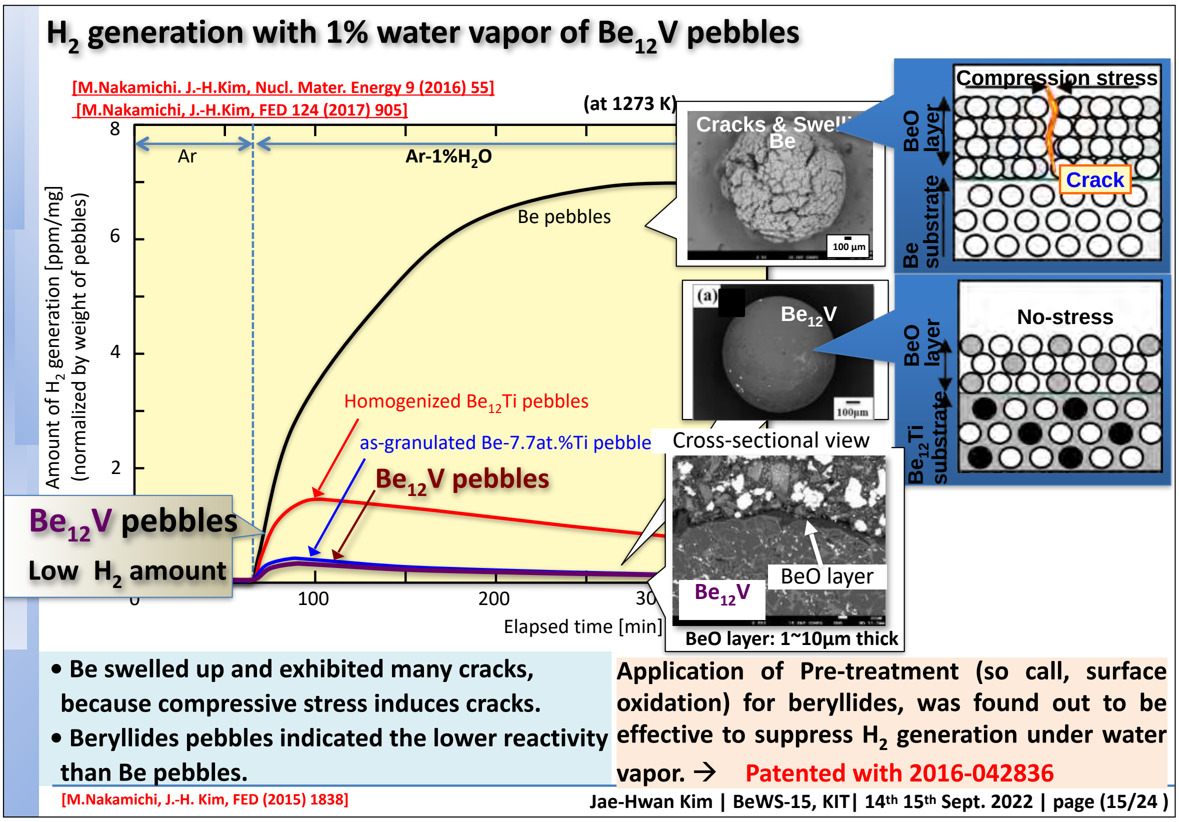
H2 generation with 1% water vapor of Be12V pebbles
[M.Nakamichi. J.-H.Kim, Nucl. Mater. Energy 9 (2016) 55]
[M.Nakamichi, J.-H.Kim, FED 124 (2017) 905]
(at 1273 K)
Ar
Ar-1%H2O
Be pebbles
Homogenized Be12Ti pebbles
as-granulated Be-7.7at.%Ti pebble
Be12V pebbles
Amount of H2 generation [ppm/mg] (normalized by weight of pebbles)
Elapsed time [min]
Be12V pebbles
Low H2 amount
Cracks & Swell
Be
Be12V
Cross-sectional view
BeO layer
Be12V
BeO layer: 1~10μm thick
Compression stress
Crack
BeO layer
Be substrate
No-stress
BeO layer
Be12Ti substrate
• Be swelled up and exhibited many cracks, because compressive stress induces cracks.
• Beryllides pebbles indicated the lower reactivity than Be pebbles.
Application of Pre-treatment (so call, surface oxidation) for beryllides, was found out to be effective to suppress H2 generation under water vapor. → Patented with 2016-042836
[M.Nakamichi, J.-H. Kim, FED (2015) 1838]
Jae-Hwan Kim | BeWS-15, KIT| 14th 15th Sept. 2022 | page (15/24)

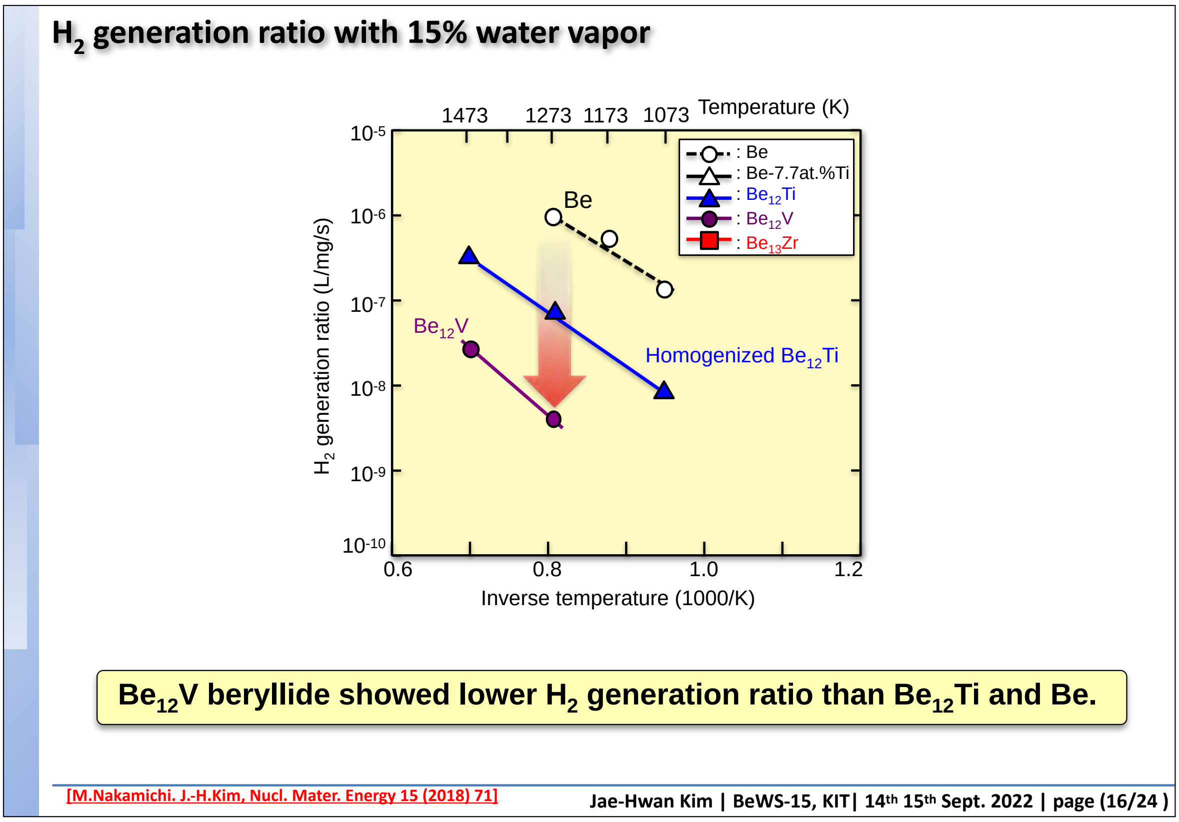
H2 generation ratio with 15% water vapor
Temperature (K)
1473
1273
1173
1073
H2 generation ratio (L/mg/s)
Inverse temperature (1000/K)
: Be
: Be-7.7at.%Ti
: Be12Ti
: Be12V
: Be13Zr
Be
Be12V
Homogenized Be12Ti
Be12V beryllide showed lower H2 generation ratio than Be12Ti and Be.
[M.Nakamichi. J.-H.Kim, Nucl. Mater. Energy 15 (2018) 71]
Jae-Hwan Kim | BeWS-15, KIT| 14th 15th Sept. 2022 | page (16/24)

17

Deuterium Desorption and retention properties

- 3keV-D_2^+, 1x10^{22} D/m², R.T. and TDS with 1 K/s (ramping speed)

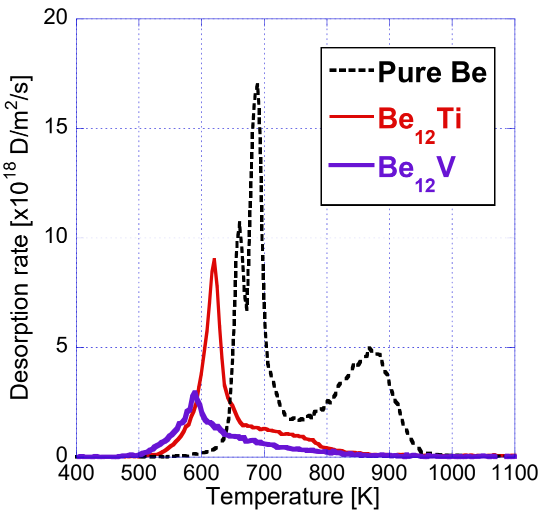

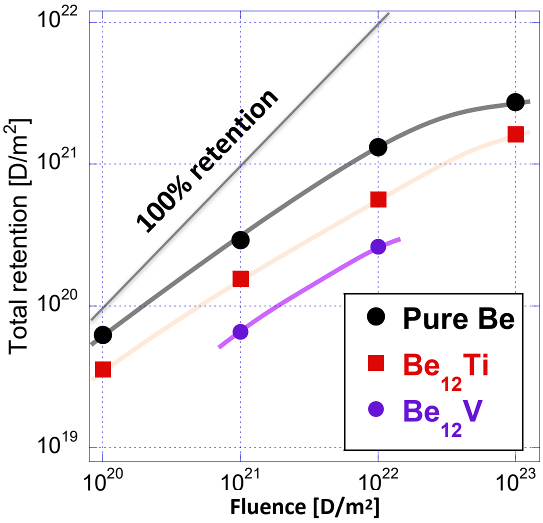

Due to the small desorption from beryllides, the total retentions of deuterium in beryllides were evaluated to be ~50% in $Be_{12}Ti$ and ~20% in $Be_{12}V$ of that in pure Be.

[M.Nakamichi. J.-H.Kim, Nucl. Mater. Energy 9 (2016) 55]

Jae-Hwan Kim | BeWS-15, KIT| 14th 15th Sept. 2022 | page (17/24)

1. Necessity of advanced neutron multipliers
2. Synthesis of single-phased beryllides
3. Granulation of beryllide pebbles
4. Characterization of beryllide pebbles
5. **A joining process to F82H by plasma sintering**
6. Summary

Jae-Hwan Kim | BeWS-15, KIT| 14th 15th Sept. 2022 | page (18/24)

Application of joining process

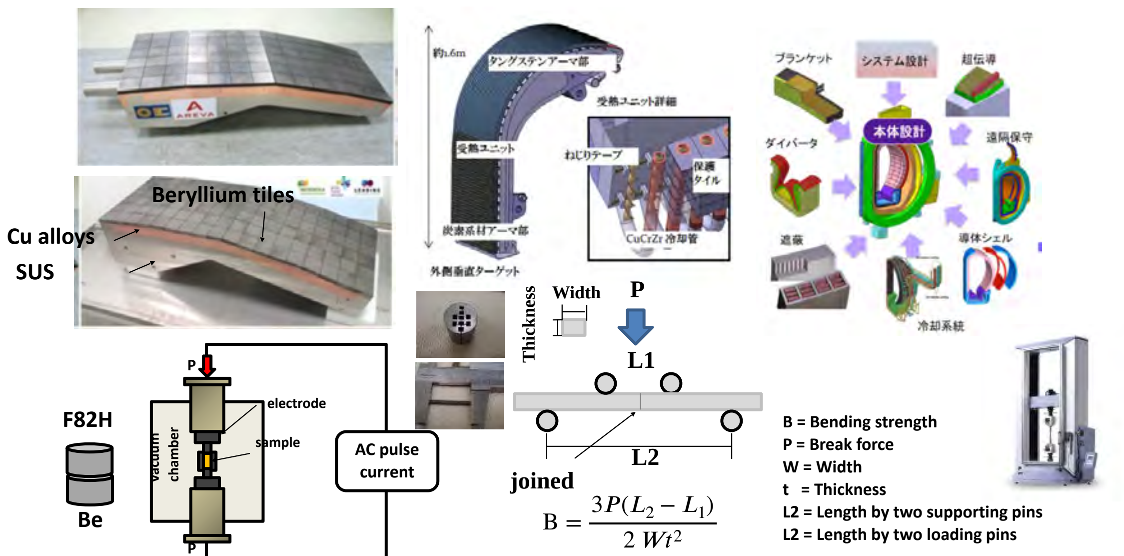

- Sintering temp. : 923、1023、1123 K
- Sintering time : 30m、60m、90m
- Sintering pressure : 15 kN

Dimension : 3㎜ x 3㎜ x 35㎜
Sample number : N= 3
Bonding strength was measured

[Jae-Hwan Kim, et al, Materials 13 (2021) 6348]

Jae-Hwan Kim | BeWS-15, KIT| 14th 15th Sept. 2022 | page (19/24)

Results (1) : Mapping and activation energy for growth

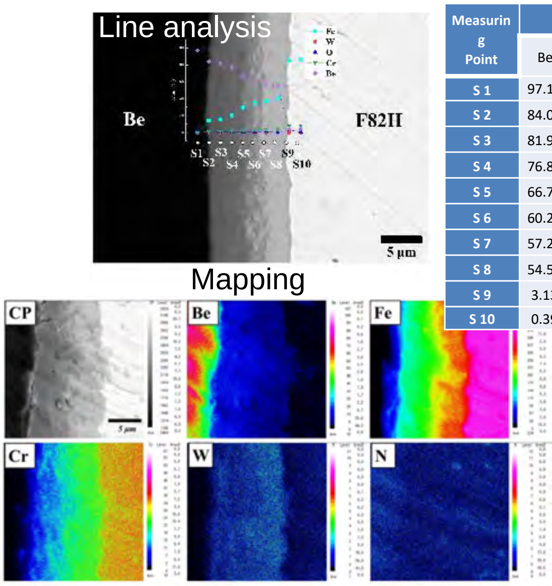

Measuring Point	Composition (at.%)					Estimated Compounds
	Be	Fe	Cr	W	O	
S 1	97.16	0.44	0.02	0.00	2.38	Be
S 2	84.03	14.02	1.23	0.10	0.62	$Be_{12}Fe$
S 3	81.91	15.80	1.50	0.12	0.68	$Be_{12}Fe$
S 4	76.88	20.25	1.89	0.17	0.80	$Be_{12}Fe$, Be_5Fe
S 5	66.78	29.53	2.64	0.23	0.83	Be_5Fe, Be_2Fe
S 6	60.21	35.25	3.40	0.32	0.82	Be_5Fe, Be_2Fe
S 7	57.29	37.34	3.65	0.35	1.37	Be_2Fe
S 8	54.53	41.03	4.01	0.34	0.08	Be_2Fe
S 9	3.13	86.14	7.89	1.88	0.95	Be_2Fe, F82H
S 10	0.39	89.16	8.19	1.68	0.57	F82H

Arrhenius Plot

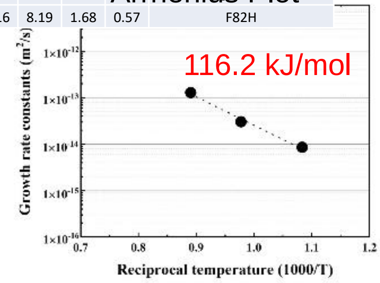

In the reaction layer, it was found out that Be-Fe compounds, $Be_{12}Fe$, Be_5Fe, Be_2Fe were formed.

By the thicknesses of joined samples at 923, 1023 and 1123 K for 90 min, the growth rate was evaluated, indicating the activation energy is 116.2 kJ/mol.

[Jae-Hwan Kim, et al, Materials 13 (2021) 6348]

Jae-Hwan Kim | BeWS-15, KIT| 14th 15th Sept. 2022 | page (20/24)

Results (2) : Bonding strength and thickness

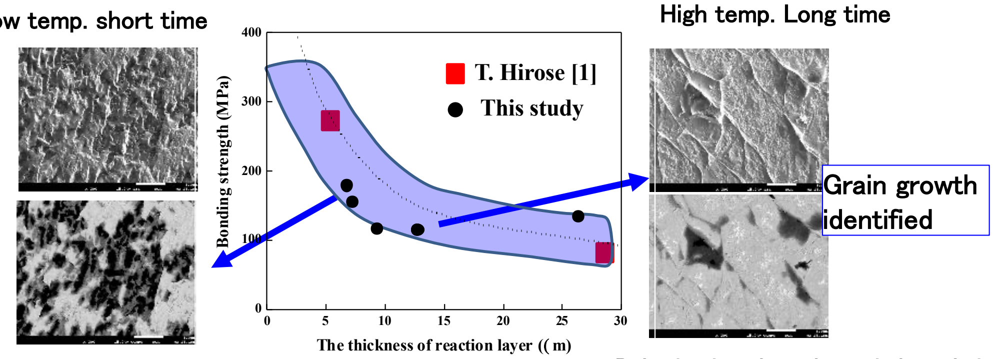

[1] T. Hirose et. al., Fusion Eng Des., 85 (2010) 809-812

❑ The bonding strength of the joined materials was inversely proportional to the thickness of the reaction layer.

❑The difference in the fracture behaviour induced by either the delamination of grains or delamination along grain boundaries is attributed to the difference in the bonding strength.

[Jae-Hwan Kim, et al, Materials 13 (2021) 6348]

Jae-Hwan Kim | BeWS-15, KIT| 14th 15th Sept. 2022 | page (21/24)

Summary

- Single phased $Be_{12}V$ beryllide blocks and pebbles were successfully fabricated directly either by a plasma sintering and by the rotating electrode granulation method (REM) using the plasma-sintered beryllides electrodes, respectively.
- Optimization of granulation for $Be_{12}V$ pebbles led to being able to fabricate not only small (0.5mm) but also big (2.5mm) pebbles and binary packing fraction reached into over 80 %.
- Beryllides ($Be_{12}V$) had much lower H_2 generation ratio under H_2O than Be and lower D retention than Be.
- A new neutron irradiation campaign will be performed for newly developed beryllides (for instance, single phase $Be_{12}V$, ternary beryllides etc.) to verify superiority of swelling and tritium retention over Be.

Jae-Hwan Kim | BeWS-15, KIT| 14th 15th Sept. 2022 | page (22/24)

- A joining process between Be and F82H by plasma sintering was tried. It was clear that the bonding strength of the joined materials was inversely proportional to the thickness of the reaction layer.

Jae-Hwan Kim | BeWS-15, KIT| 14th 15th Sept. 2022 | page (23/24)

Thank you for your kind attention

Jae-Hwan Kim | BeWS-15, KIT| 14th 15th Sept. 2022 | page (24/24)

SESSION 2

News from Industry

Overview of the United States Beryllium Industry - 2022 Update

Keith Smith[1]

[1] *Materion – Brush Inc, Elmore, Ohio USA*

Beryllium is a critical material of construction for the ITER First Wall Panels. The supply and fabrication of beryllium is key to the success of the ITER project. This presentation will provide an updated overview of the US beryllium industry including mining, manufacturing, and fabrication capabilities. Beryllium raw material availability, ITER relevant First Wall beryllium grades, engineering, and program management services provided in support to those products will be discussed. Additionally, activities related to process improvements within Materion's beryllium manufacturing plants including activities related to the manufacturing and purification of beryllium containing molten salt (FLIBE) be addressed.

Corresponding Author:

Keith J. Smith
Keith.smith@materion.com
Materion Brush Inc.
14710 West Portage River South Rd
Elmore, OH 43416
USA

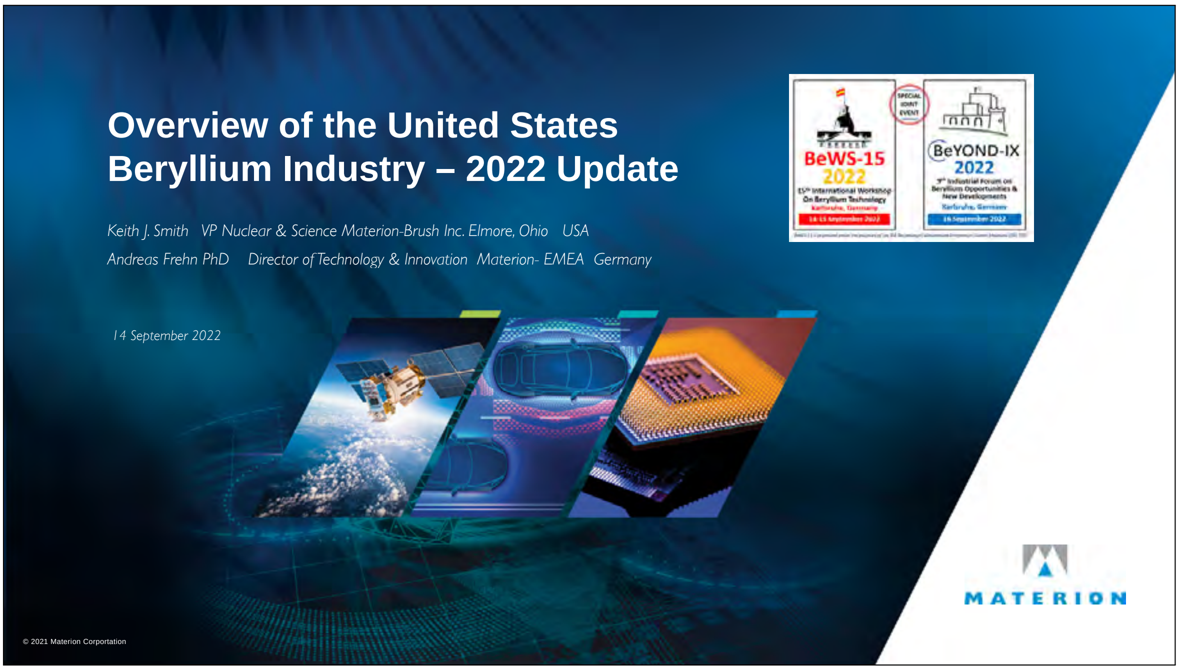

Overview of the United States Beryllium Industry – 2022 Update
Keith J. Smith VP Nuclear & Science Materion-Brush Inc. Elmore, Ohio USA
Andreas Frehn PhD Director of Technology & Innovation Materion- EMEA Germany
14 September 2022
BeWS-15 2022
BeYOND-IX 2022
MATERION
© 2021 Materion Corporation

Materion at a Glance…
A global high-tech solutions provider of performance alloys, precision optics and advanced materials
100+ years of materials knowledge
Publicaly traded since 1972 - NYSE (MTRN)
In excess of $1 billion in sales
32 WORLDWIDE LOCATIONS
3,400 EMPLOYEES
62 COUNTRIES SERVED
MATERION
2
© 2022 Materion Corporation


M IN DS OVER M ATERIALS™
Our People Make the Difference
Materials scientists
Chemists & physicists
Applications & sales engineers
Manufacturing & process engineers
Customer-focused teams
Technical support staff
Supply chain, logistics, & materials management experts
Innovative. Motivated. Dedicated.
MATERION

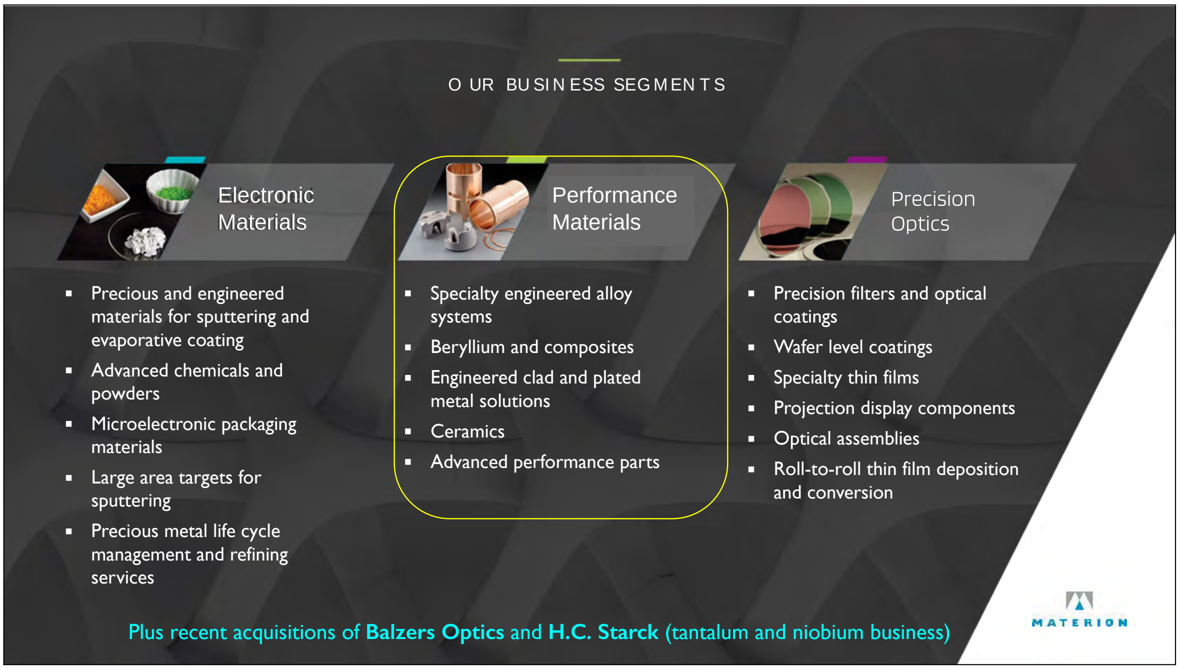
O UR BUSIN ESS SEGMEN T S
Electronic Materials
Precious and engineered materials for sputtering and evaporative coating
Advanced chemicals and powders
Microelectronic packaging materials
Large area targets for sputtering
Precious metal life cycle management and refining services
Performance Materials
Specialty engineered alloy systems
Beryllium and composites
Engineered clad and plated metal solutions
Ceramics
Advanced performance parts
Precision Optics
Precision filters and optical coatings
Wafer level coatings
Specialty thin films
Projection display components
Optical assemblies
Roll-to-roll thin film deposition and conversion
Plus recent acquisitions of Balzers Optics and H.C. Starck (tantalum and niobium business)
MATERION


OUR GLOBAL MARKETS
51% Performance Materials
34% Electronic Materials
15% Precision Optics
25% Semiconductor
20% Industrial
12% Aerospace and Defense
10% Automotive
8% Consumer Electronics
6% Energy
5% Telecom and Data Center
14% Other
MATERION


Beryllium Supply Chain
MATERION

Materion – Beryllium Processing

- Materion is the largest producer of beryllium containing materials in the world. **Be mining – Be extraction – Be production – Be machining**
  - We **operate and invest** in the most modern beryllium production facilities.
  - Over $100,000,000 (US) has been invested over the past 15 years.
  - **New investments:** New Machining facility, Upgrade of the Primary Beryllium … type Manufacturing Facility, Mining …



Mining

•Materion operates a beryllium mine in the **Topaz-Spor Mountain** area of western Utah.

•The mineral is identified as **bertrandite**, a hydrous beryllium silicate ($Be_4Si_2O_7(OH)_2$)

•Materion holds estimated ore reserves for 70 years of production.

•USGS estimates 21,000tons of Be reserves @ Utah.



8

Materion Resources, Delta, Utah

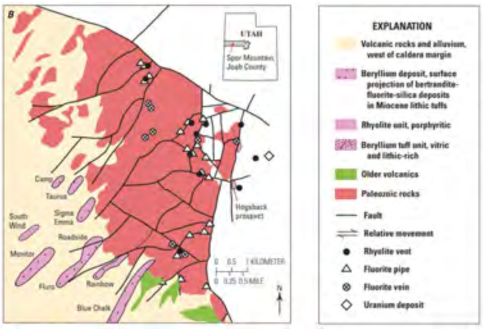

9

MATERION

Materion Resources, Delta, Utah

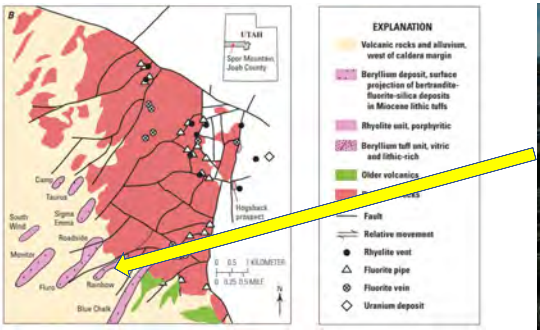

9 © 2021 Materion Corportation

MATERION

Beryllium Mine Production

World Mine Production and Reserves:

	Mine production[8, 9] 2020	Mine production[8, 9] 2021[e]	Reserves[10]
United States	165	170	The United States has very little beryl that can be economically hand sorted from pegmatite deposits. The Spor Mountain area in Utah, an epithermal deposit, contains a large bertrandite resource, which is being mined. Proven and probable bertrandite reserves in Utah total about 20,000 tons of contained beryllium. World beryllium reserves are not available.
Brazil	[e]3	3	
China	70	70	
Madagascar	[e]1	1	
Mozambique	[e]3	3	
Nigeria	[e]1	1	
Rwanda	[e]1	1	
Uganda	7	7	
World total (rounded)	250	260	

World Resources:[10] The world's identified resources of beryllium have been estimated to be more than 100,000 tons. About 60% of these resources are in the United States; by tonnage, the Spor Mountain area in Utah, the McCullough Butte area in Nevada, the Black Hills area in South Dakota, the Sierra Blanca area in Texas, the Seward Peninsula in Alaska, and the Gold Hill area in Utah account for most of the total.

U.S. Geological Survey, Mineral Commodity Summaries, January 2022

MATERION

10

Performance Materials

- The only fully integrated manufacturer of Beryllium and Beryllium containing materials in the world.
  - Mining
  - Extraction
  - Conventional Metal Processing - CuBe/ CuNiSn/NiBe
  - Ceramic processing (BeO, Al_2O_3, others)
  - Powder metallurgy (Be, Al-Be, others)
  - Metal Matrix Composites (Al-B4C, Al-SiC, others)
  - Clad and Plated Metal Strip
  - Machining - Fabrication

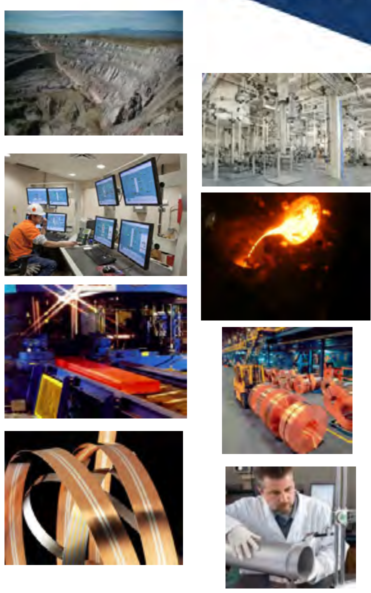

MATERION

11

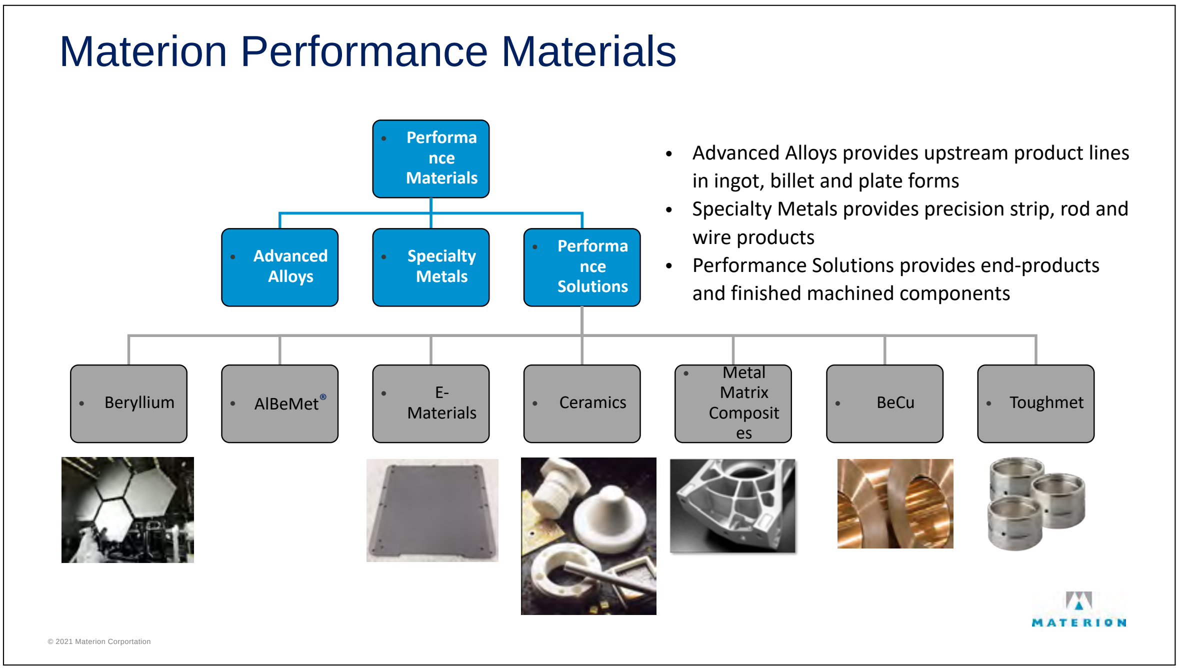
Materion Performance Materials
Performance Materials
Advanced Alloys
Specialty Metals
Performance Solutions
Advanced Alloys provides upstream product lines in ingot, billet and plate forms
Specialty Metals provides precision strip, rod and wire products
Performance Solutions provides end-products and finished machined components
Beryllium
AlBeMet®
E-Materials
Ceramics
Metal Matrix Composites
BeCu
Toughmet
MATERION
© 2021 Materion Corportation


Beryllium Products
MATERION
Beryllium:
Seven commercial grades of Beryllium metal:
S-200-F, S-200-F-H, S-200-F-C, I-70, S-65, I-220, I-220-H
Block, Parts, Sheet, Extrusions
Beryllium Foil – multiple grades (Materion Electrofusion)
Ultra High-purity Beryllium
Beryllium hydroxide
Beryllium fluoride
AlBeMet – Be-38Al
AlBeCast – Investment cast Al-Be
Be/BeO Composites (E-Material)
BeO ceramic components
Cu-Be Alloys
13
13

S-65 Vacuum Hot Pressed Beryllium

- A Materion standard product produced for over 40 years.
- Fully qualified for ITER.
- Baseline FW beryllium for ITER.

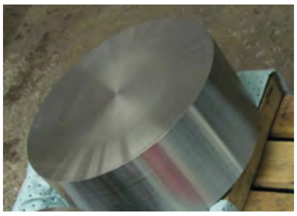

SPEC SHEET

S-65
BERYLLIUM GRADE

1. SCOPE

This specification defines the requirements for a structural grade of hot pressed beryllium block which is designated S-65. This material is recommended for applications requiring higher purity.

2. CHEMICAL COMPOSITION

2.1. The chemical composition shall conform to the following:

Beryllium Assay, % minimum (1)	99.2
Beryllium Oxide, % maximum (2)	0.9
Al, % maximum (3)	0.05
C, % maximum (4)	0.09
Fe, % maximum (3)	0.08
Mg, Cr, each % maximum (3)	0.01
Ni, Cu, Ti, Zr, each, % maximum (3)	0.025
Zn, Mn, Ag, Co, Pb, Ca, Mo, each, % maximum (3)	0.005
Silicon, % maximum (3)	0.045
U, % maximum (5)	0.015
Other Metallic Impurities, each, % maximum (3)	0.04

Note:
(1) Difference (i.e. 100%-other elements)
(2) Leco Inert Gas Fusion
(3) Spectrochemical Methods
(4) Leco Combustion
(5) Glow Discharge Mass Spectrometry, Neutron Activation Analysis or Fluorescence

MATERION

14

Beryllium Fabrication

- **Materion – Fabrication and Program Management**
  - Fabricated Solutions Group – Elmore, Ohio
  - Application engineering
  - Program management.

- **US Domestic Fabrication Capabilities**
  - All fabricators maintain various levels of program management and applications engineering support to customers.

MATERION

15

US Beryllium Fabrication Sources

- **Materion** – Elmore, OH
- **General Dynamics** – Cullman, AL
- **LA Gauge** – Sun valley, CA
- **Peregrine Falcon** – Pleasanton, CA
- **Hardric Laboratories, Inc.** Waltham, MA
- **WessDel** – San Jose, CA
- **Rev Manufacturing** – Plamdale, CA
- **Coherent, Inc.** – Richmond, CA
- **Skinner Machining** – Cleveland, OH

16


Continuing to Accelerate Our Transformation Strategy
WHERE WE WERE
(Before 2017)
Origins as a mining and metals-focused producer in 1931
Strong heritage of beryllium expertise
Several acquisitions broaden portfolio, creating the foundation for Electronic Materials and Precision Optics segments
WHERE WE ARE
(2017 – 2021)
Becoming a global leader in advanced materials solutions through organic initiatives and strategic acquisitions
Implemented One Materion strategy focused on driving profitable growth
Increased investment in R&D fueling innovation; significantly expanding growth pipeline through customer collaborations
Transformed financial profile, doubling margins and returns
WHERE WE ARE GOING
(2022+)
Accelerating global leadership in advanced materials solutions for evolving growth megatrends
Delivering step-change organic and inorganic growth initiatives, driving transformative profitable growth
Investing to deliver next generation solutions to support customer roadmaps
Building on our leading positions in all major geographies
Driving above-market top line growth and mid teens margins with strong ROIC
MATERION

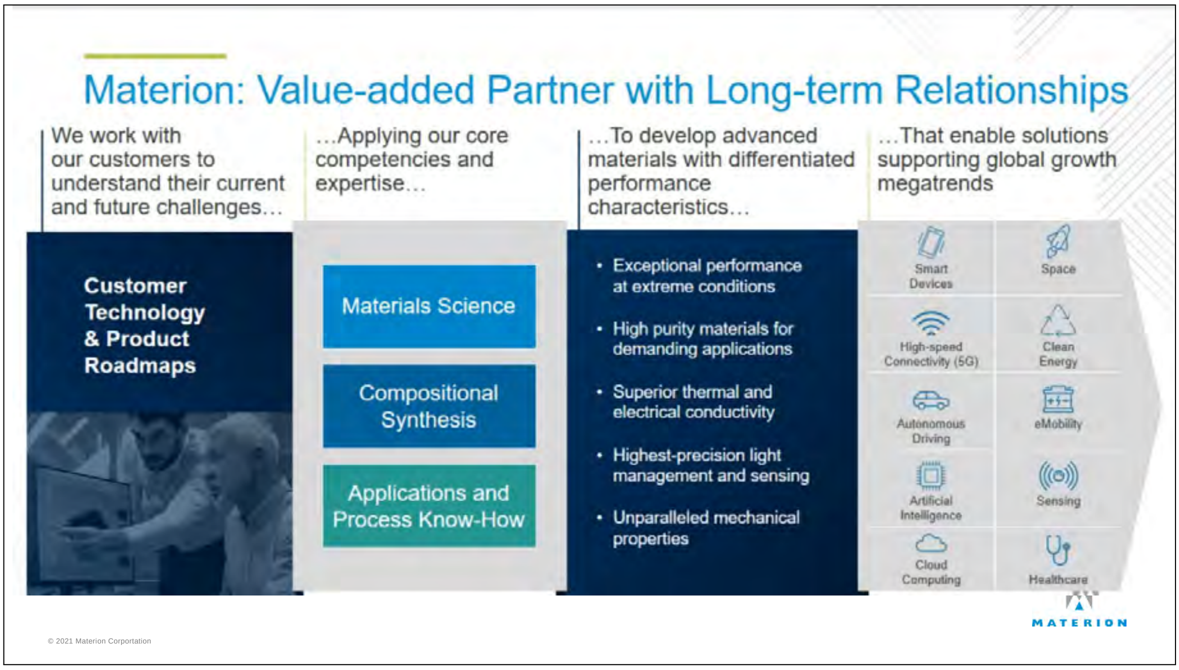
Materion: Value-added Partner with Long-term Relationships
We work with our customers to understand their current and future challenges…
…Applying our core competencies and expertise…
…To develop advanced materials with differentiated performance characteristics…
…That enable solutions supporting global growth megatrends
Customer Technology & Product Roadmaps
Materials Science
Compositional Synthesis
Applications and Process Know-How
Exceptional performance at extreme conditions
High purity materials for demanding applications
Superior thermal and electrical conductivity
Highest-precision light management and sensing
Unparalleled mechanical properties
Smart Devices
Space
High-speed Connectivity (5G)
Clean Energy
Autonomous Driving
eMobility
Artificial Intelligence
Sensing
Cloud Computing
Healthcare
MATERION
© 2021 Materion Corporation

FLiBe Molten Salt Production

Kairos Power

- **Materion** and **Kairos Power** are collaborating to produce FLIBE, a molten fluoride salt, as a coolant for the **K**airos **P**ower **F**luoride salt-cooled **H**igh temperature **R**eactor (KP-FHR).
- The facility has been constructed at Materion's Elmore, Ohio plant.
- Materion will operate the facility and provide both BeF_2 and LiF.

wnn world nuclear news — Celebrating 15 years —

Energy & Environment | New Nuclear | Regulation & Safety | Nuclear Policies | Corporate | Uranium & Fuel |

Materion to supply coolant for Kairos molten salt reactor

27 May 2020

Share

Kairos Power of the USA has entered into a strategic collaboration with advanced materials supplier Materion Corporation to develop a reliable and cost-effective supply of coolant for its fluoride salt-cooled, high-temperature reactor (KP-FHR). Materion will supply beryllium fluoride, technical consultation, key interfaces and support services.

MATERION

Molten Salt Purification Plant

Kairos Power

- ➢ **FLiBe Purification Facility**
  - ➢ **Kairos Power / Materion Joint agreement to produce FLiBe (BeF_2 + LiF)**

MATERION

Molten Salt Purification Plant

KAIROS POWER AND MATERION CORPORATION COMMISSION MOLTEN SALT PURIFICATION PLANT TO PRODUCE COOLANT FOR HIGH-TEMPERATURE MOLTEN SALT REACTORS

ELMORE, Ohio – July 19, 2022 – As part of a Cooperative Development Agreement with Materion Corporation, Kairos Power has commissioned a Molten Salt Purification Plant (MSPP) at the Materion campus in Elmore, Ohio. The plant, designed by Kairos Power, will produce large quantities of high-purity fluoride salt coolant to be used in high-temperature molten salt reactors, a clean, affordable and safe nuclear energy solution with the potential to transform the global energy landscape.

Kairos Power's fluoride salt-cooled high-temperature reactor (KP-FHR) technology is cooled by a mixture of lithium fluoride and beryllium fluoride salts known as "Flibe" which is chemically stable and operates at low pressure. This molten salt coolant will be used in Kairos Power's Engineering Test Unit (ETU), and the Hermes demonstration reactor, as well as future commercial KP-FHR reactors.

As an industry leader in the production and manufacturing of beryllium-based materials, Materion supplies beryllium fluoride for MSPP and contributes requisite expertise staffing and operating the plant. The decision to locate MSPP at Materion's Elmore facility reinforces a long-term, strategic commitment by both companies to demonstrate leadership in molten salt production.

MATERION

22

Additive Manufacturing

- Materion has initiated a comprehensive Additive manufacturing program.
- State of the art AM development center has been built at the Materion Technology and Innovation Center in Ohio.
- More detail will be discussed in a separate presentation this week.

MATERION

23


Newton Acquisition Overview
OUR TEAM:
140 Employees
OUR EXPERIENCE:
70+ Years
OUR SITE:
Located in Massachusetts, USA
ISO 9001 certified
20,300 m2
OUR METALS:
Tantalum
Niobium
OUR MARKETS:
Electronics
Chemicals & Superconductors
Aerospace & Defense
MATERION
24
© 2021 Materion Corporation

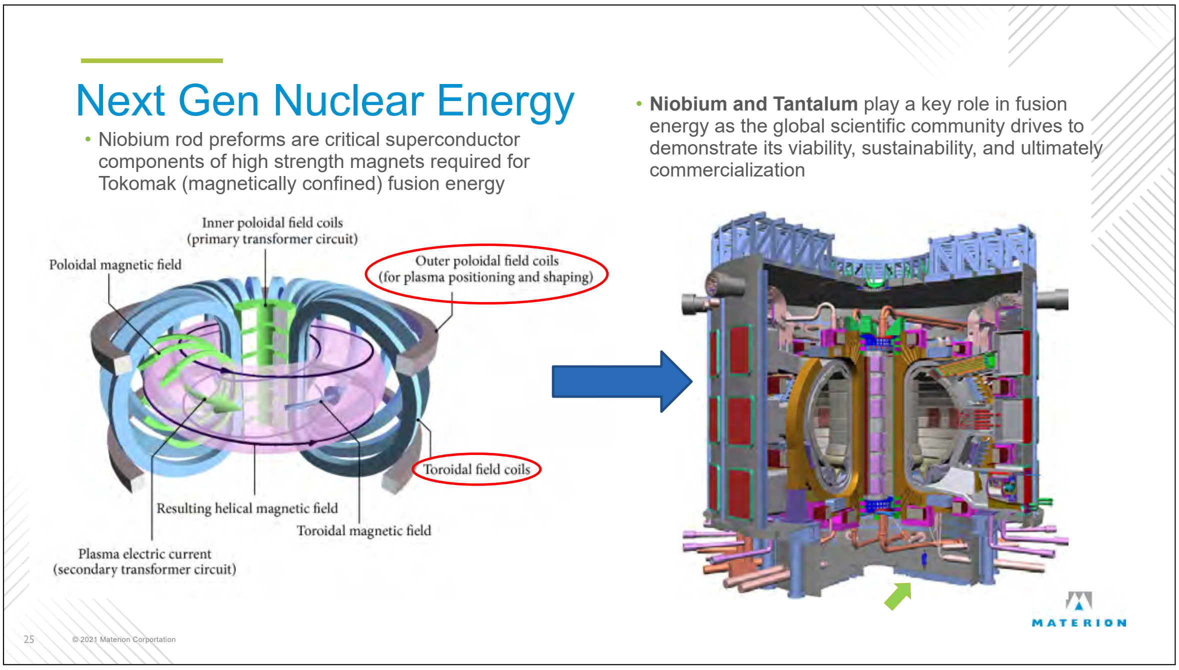
Next Gen Nuclear Energy
• Niobium rod preforms are critical superconductor components of high strength magnets required for Tokomak (magnetically confined) fusion energy
• Niobium and Tantalum play a key role in fusion energy as the global scientific community drives to demonstrate its viability, sustainability, and ultimately commercialization
Inner poloidal field coils
(primary transformer circuit)
Poloidal magnetic field
Outer poloidal field coils
(for plasma positioning and shaping)
Toroidal field coils
Resulting helical magnetic field
Toroidal magnetic field
Plasma electric current
(secondary transformer circuit)
MATERION
25
© 2021 Materion Corporation

Superconductor Industry

Applications

- MRI and NMR
- Mass spectroscopy
- **Nuclear fusion energy**
- Magnetic levitation
- Particle accelerators

Superconducting Filaments – Nb rod preforms

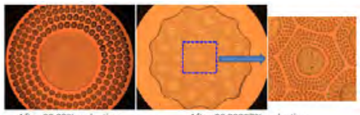

Niobium and Tantalum Products

- Sheet
- Rod
- Wire

MATERION

26

JWST – First Images

The **James Webb Space Telescope** is an **all-Beryllium telescope.**

The mirrors and structures are beryllium. The company also supplied additional beryllium components, electronic packages, and optical filters and coatings.

MATERION

27

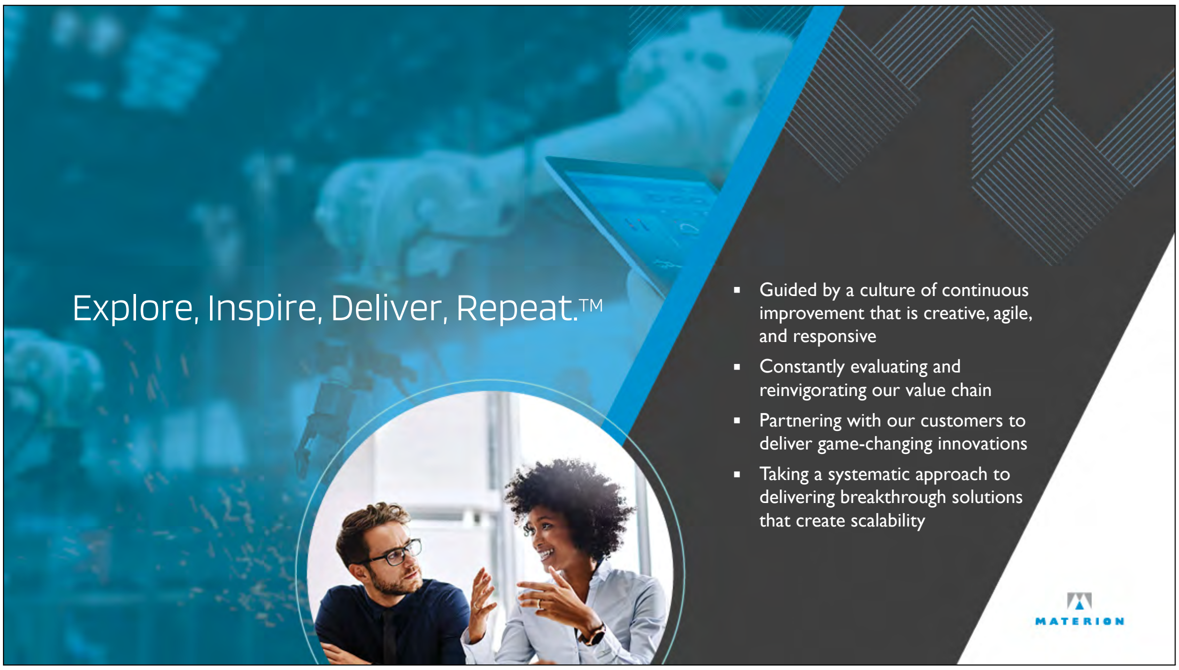

Explore, Inspire, Deliver, Repeat.™
Guided by a culture of continuous improvement that is creative, agile, and responsive
Constantly evaluating and reinvigorating our value chain
Partnering with our customers to deliver game-changing innovations
Taking a systematic approach to delivering breakthrough solutions that create scalability
MATERION

Beryllides - experience of UMP JSC in development and testing

Ye. Frants, M. Kolmakov, B. Zorin, M. Kylyshkanov, M Podoinikov, S. Udartsev, A. Vechkutov

"Ulba Metallurgical Plant" JSC,
Ust-Kamenogorsk, Republic of Kazakhstan.

Intermetallic compounds of beryllium (beryllides) have outstanding characteristics in terms of heat resistance, hardness, and resistance to oxidation. For this reason, beryllides have potential applications in nuclear and thermonuclear energy, aerospace, instrumentation and other industries.

To date, the process of producing billets and products from beryllides has not passed into the stage of stable industrial production.

In recent years, UMP JSC has been making efforts to develop and implement technologies for producing billets and products from various beryllides, as well as testing and studying the properties of beryllides.

This article presents information on the results of producing billets and products from tantalum, titanium and chromium beryllides, as well as resource thermocyclic tests under conditions simulating the thermal modes of operation of helium-cooled blanket modules of the DEMO/may be ITER reactor.

Corresponding Author:

Ye. Frants
FrantsEV@ulba.kz

102, Abay Avenue, Ust-Kamenogorsk,
070005, Republic of Kazakhstan

Beryllides - experience of UMP JSC in development and testing

Ye. Frants, M. Kolmakov, B. Zorin, M. Kylyshkanov, M. Podoinikov, S. Udartsev, A. Vechkutov

Ulba Metallurgical Plant JSC, Ust-Kamenogorsk, Kazakhstan

P. Vladimirov, V. Chakin, R. Gaisin

Karlsruhe Institute of Technology, Germany

Ulba Metallurgical Plant, Kazakhstan

Uranium
Beryllium
Tantalum & Niobium
HF acid

Big press

Beryllium smelting furnace

2 Sergey Udartsev Ulba Metallurgical Plant

History of Be production in Ulba

1951 $Be(OH)_2$ and BeO

1955 Metallic Be

1958 BeO ceramics

1963 Be billets and parts

1971 Be powders

1973 Hot working of Be

2001 Beryllium-copper alloys (beryllium bronze)

2015 Beryllides

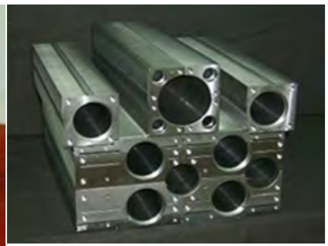

3 Sergey Udartsev Ulba Metallurgical Plant

Advantages of beryllides

- High melting point
- Heat resistance
- High specific strength
- Hardness
- Resistance to oxidation at high temperature
- High (n,2n) reaction rate for MBe_{12} type of beryllides

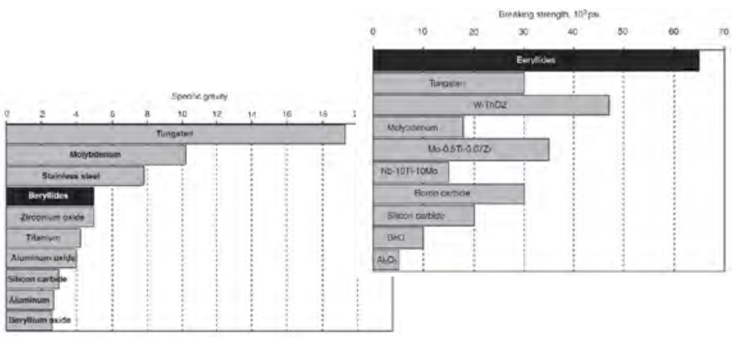

4 Sergey Udartsev Ulba Metallurgical Plant


Tantalum beryllide Ta2Be17
ULBA
Ta2Be17
5.05 g/cm3
Tmp=1980°C
Dmax = 45 mm
Hmax = 50 mm
Thmax = 4 mm
5
Sergey Udartsev
Ulba Metallurgical Plant

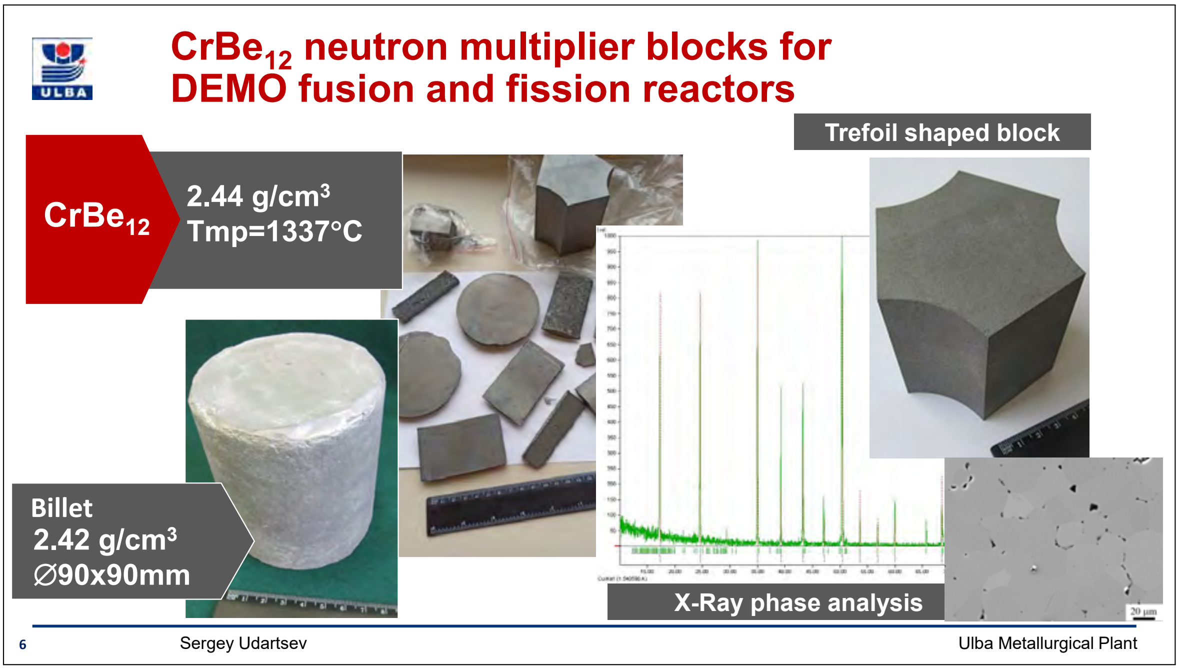
CrBe12 neutron multiplier blocks for
DEMO fusion and fission reactors
ULBA
CrBe12
2.44 g/cm3
Tmp=1337°C
Trefoil shaped block
Billet
2.42 g/cm3
∅90x90mm
X-Ray phase analysis
6
Sergey Udartsev
Ulba Metallurgical Plant

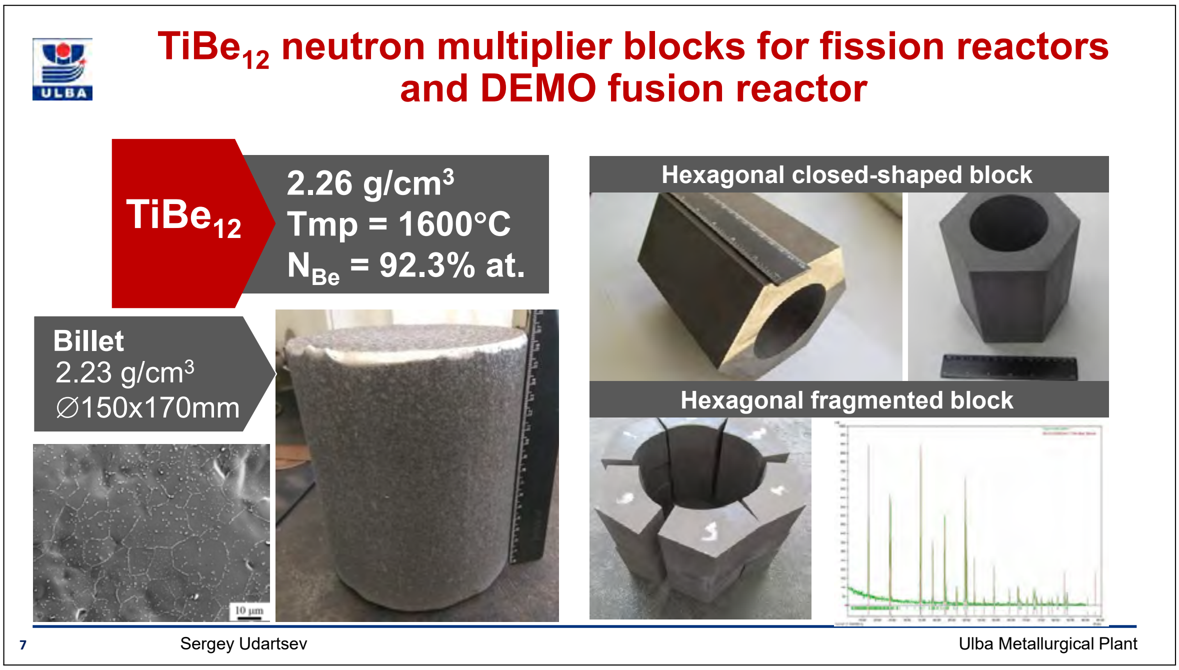
ULBA
TiBe12 neutron multiplier blocks for fission reactors and DEMO fusion reactor
TiBe12
2.26 g/cm3
Tmp = 1600°C
NBe = 92.3% at.
Billet
2.23 g/cm3
∅150x170mm
10 µm
Hexagonal closed-shaped block
Hexagonal fragmented block
7
Sergey Udartsev
Ulba Metallurgical Plant

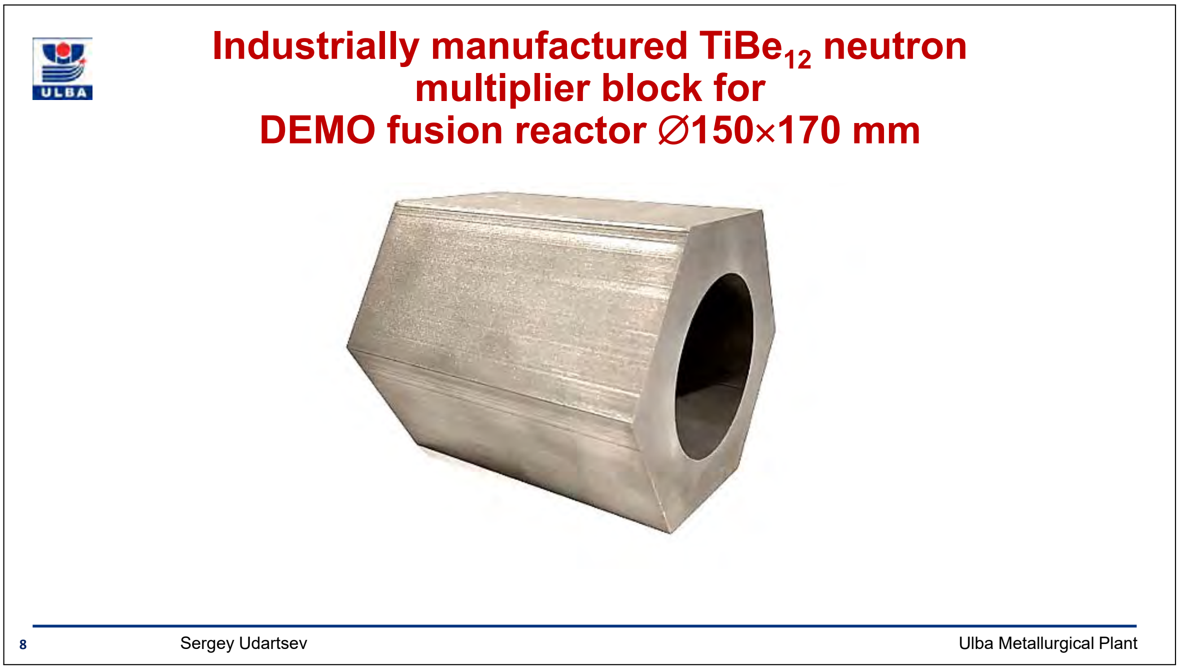
ULBA
Industrially manufactured TiBe12 neutron multiplier block for DEMO fusion reactor ∅150×170 mm
8
Sergey Udartsev
Ulba Metallurgical Plant

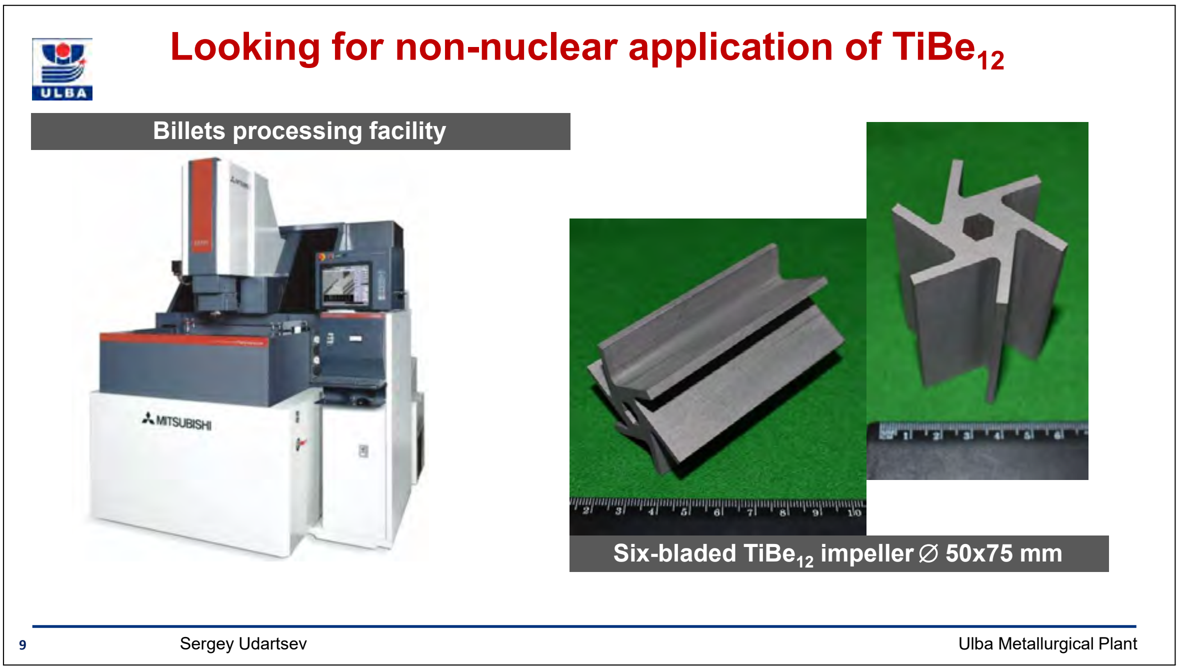
Looking for non-nuclear application of TiBe12
ULBA
Billets processing facility
MITSUBISHI
Six-bladed TiBe12 impeller ∅ 50x75 mm
9
Sergey Udartsev
Ulba Metallurgical Plant

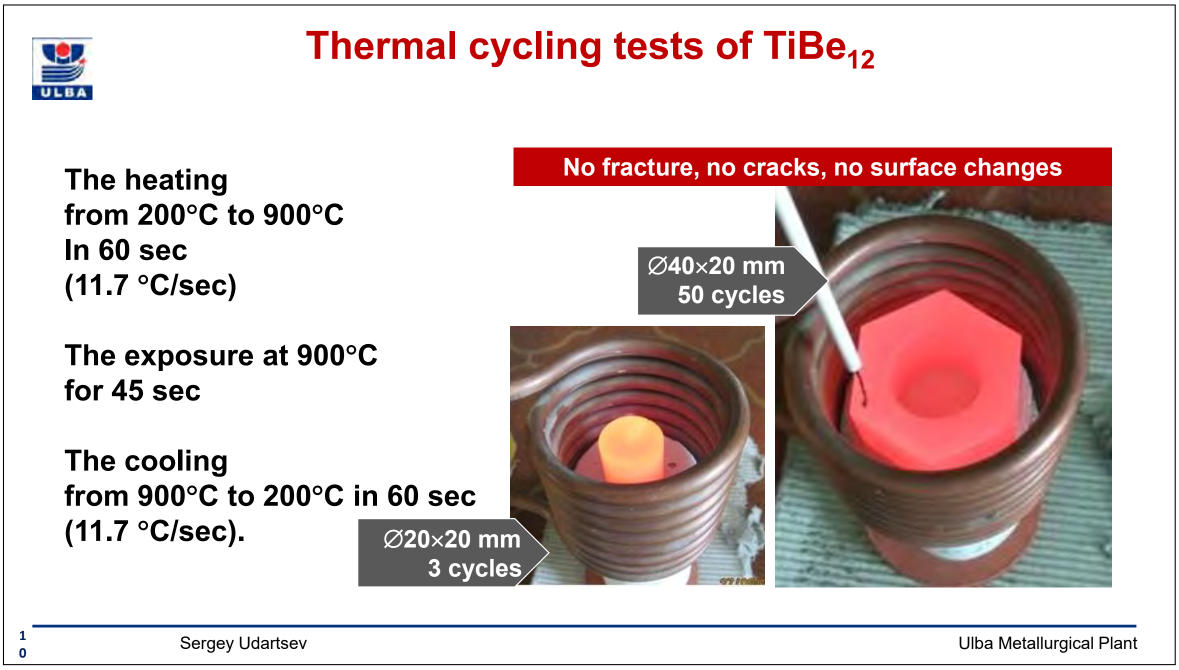
Thermal cycling tests of TiBe12
ULBA
The heating
from 200°C to 900°C
In 60 sec
(11.7 °C/sec)
The exposure at 900°C
for 45 sec
The cooling
from 900°C to 200°C in 60 sec
(11.7 °C/sec).
No fracture, no cracks, no surface changes
∅40×20 mm
50 cycles
∅20×20 mm
3 cycles
10
Sergey Udartsev
Ulba Metallurgical Plant

Thermal cycling tests of $TiBe_{12}$

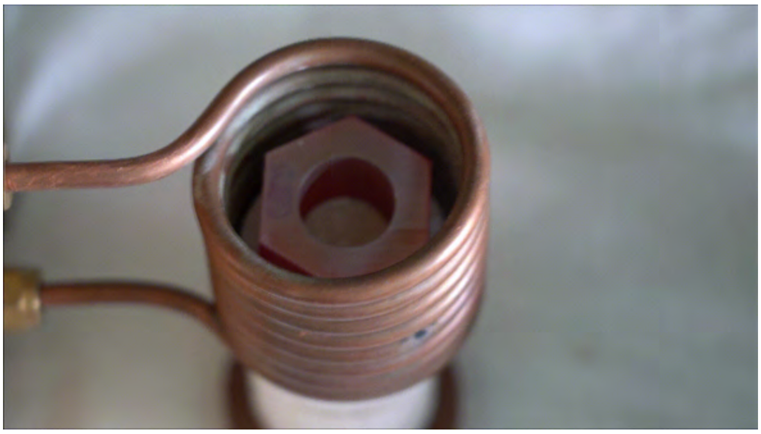

11 Sergey Udartsev Ulba Metallurgical Plant

Thermal cycling of large $TiBe_{12}$ samples

150×30×40 mm

Tmin 350°C
Tmax 850 °C
The heating rate
1.4, 0.3, 0.6 °C/sec
The cooling rate 0.6 °C/sec
in air atmosphere

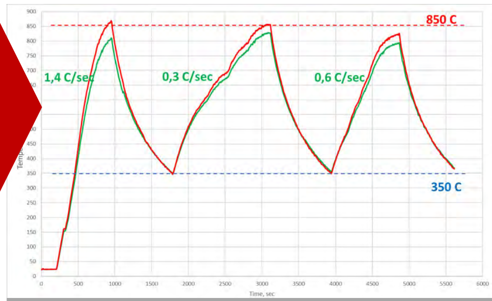

No fracture,
no cracks,
no surface changes

12 Sergey Udartsev Ulba Metallurgical Plant

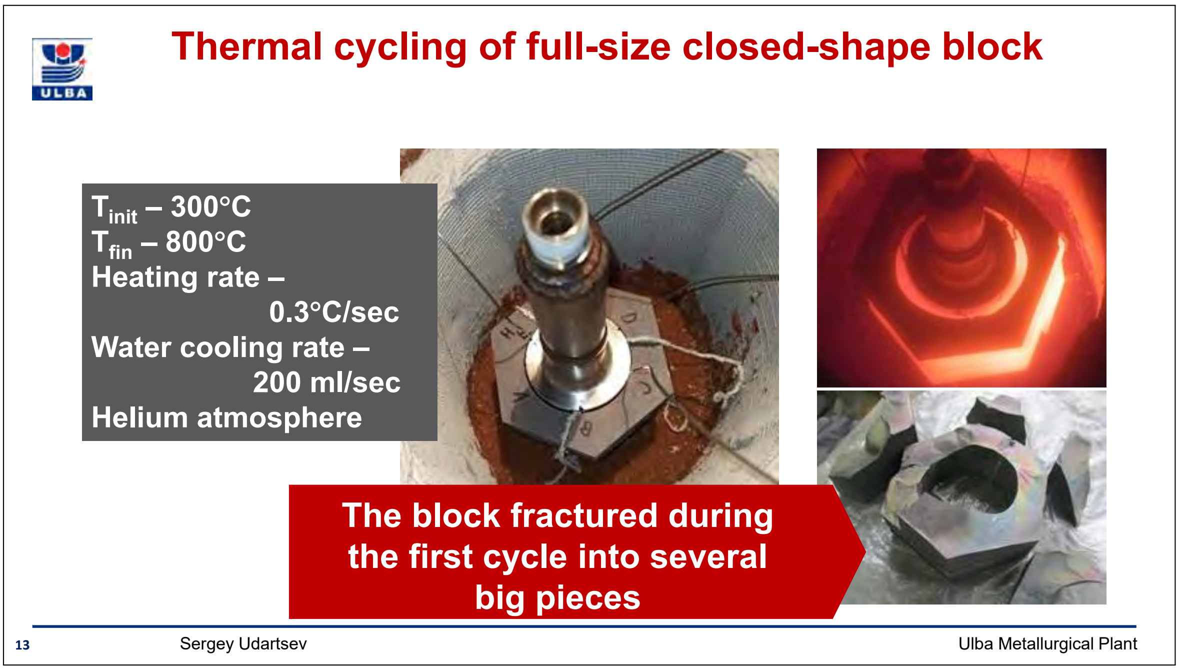
ULBA
Thermal cycling of full-size closed-shape block
T init – 300°C
T fin – 800°C
Heating rate – 0.3°C/sec
Water cooling rate – 200 ml/sec
Helium atmosphere
The block fractured during the first cycle into several big pieces
13
Sergey Udartsev
Ulba Metallurgical Plant

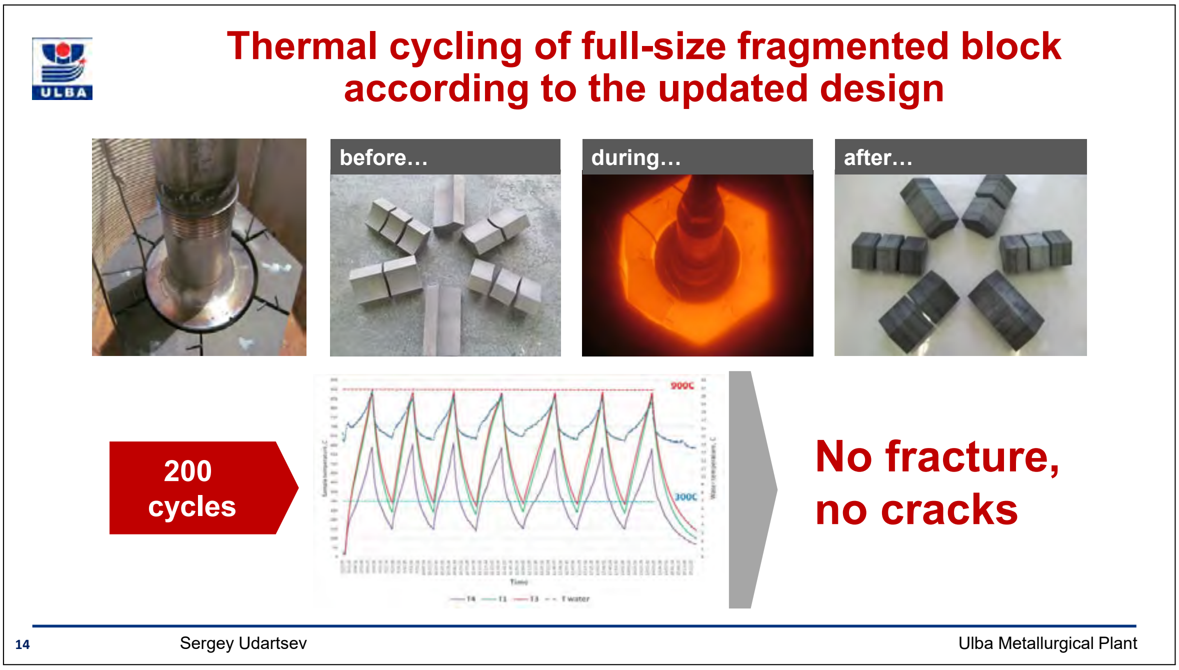
ULBA
Thermal cycling of full-size fragmented block according to the updated design
before…
during…
after…
200 cycles
900C
300C
No fracture, no cracks
14
Sergey Udartsev
Ulba Metallurgical Plant

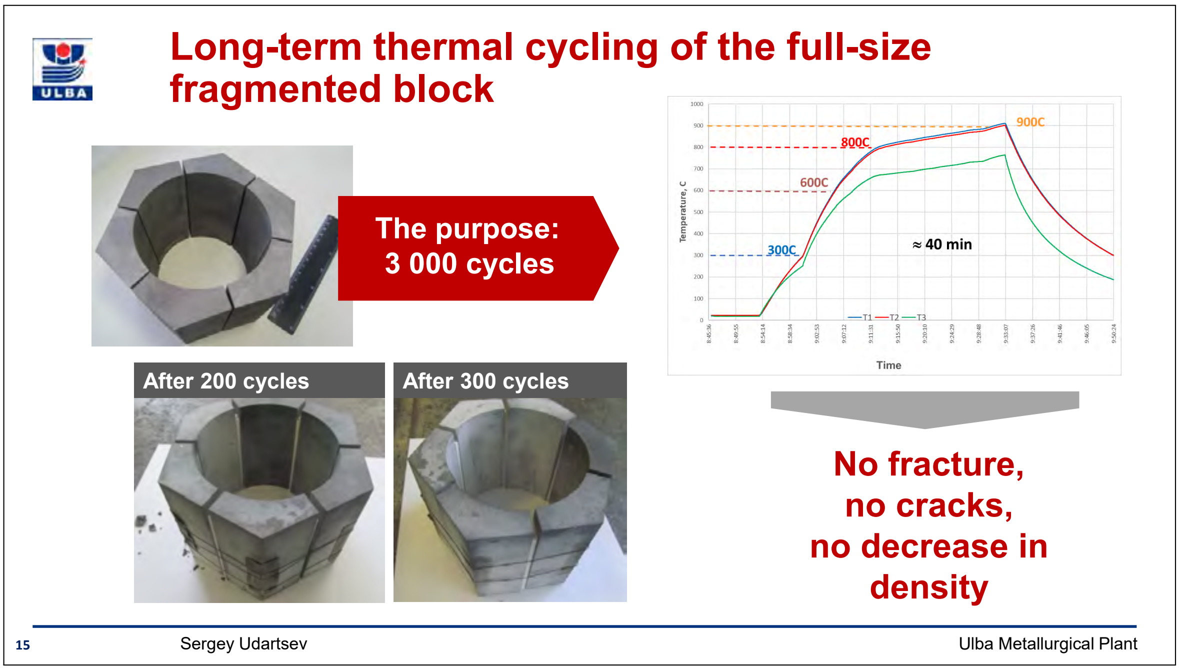
ULBA
Long-term thermal cycling of the full-size fragmented block
The purpose:
3 000 cycles
900C
800C
600C
300C
≈ 40 min
Temperature, C
Time
T1
T2
T3
After 200 cycles
After 300 cycles
No fracture,
no cracks,
no decrease in
density
15
Sergey Udartsev
Ulba Metallurgical Plant


ULBA
Accelerated time-laps video of one thermal cycle
16
Sergey Udartsev
Ulba Metallurgical Plant

Conclusions

Test prototypes for the high temperature application were manufactured from Ta_2Be_{17}.

Sufficiently dense homogeneous products from chromium beryllide $CrBe_{12}$ with a size of ∅ 90×90 mm were successfully fabricated. Production can be scaled up to much larger workpieces.

Sufficiently dense homogenous titanium beryllide $TiBe_{12}$ billets ∅150×170 mm and various products for nuclear and non-nuclear applications can be manufactured by UMP on industrial facilities

17 Sergey Udartsev Ulba Metallurgical Plant

Thank you for your attention!

We invite you to cooperation!

18 Sergey Udartsev Ulba Metallurgical Plant

Beryllium Additive Manufacturing

FritzCarl Grensing[1,2], Andreas Frehn[3], Carole Trybus[2], Andrew Ruzek[2], Rhea Christopherson[2], Jacob Huxol[2]

[2] Materion – Performance Materials, Elmore, Ohio USA
[3]Materion,- Performance Materials, Stuttgart, Germany

Beryllium components have historically been produced via powder metallurgy processes followed by subtractive machining operations. In the last 25 years, rapid advances in additive manufacturing have occurred in aluminum, titanium and many other materials while little to no work was done on beryllium. In 2021 Materion installed the first dedicated beryllium additive manufacturing laboratory with the goal of both developing additive technology for beryllium materials and understanding and mitigating the Environmental, Health and Safety issues associated with additively processing beryllium. Metallurgical results obtained will be described as well and the EHS data.

[1]Corresponding Author:

Dr. FritzCarl Grensing
Fritz.Grensing@materion.com
Materion Brush Inc.
14710 West Portage River South Rd
Elmore, OH 43416
USA


Beryllium Additive Manufacturing
Dr Fritz-Carl Grensing VP Technology & Innovation Materion-Brush, Inc. Elmore, Ohio USA
Keith J. Smith VP Nuclear & Science Materion-Brush Inc. Elmore, Ohio USA
Dr. Andreas Frehn Director of Technology Materion- EMEA, Germany
BeWS-15
2022
BeYOND-IX
2022
MATERION
© 2021 Materion Corportation

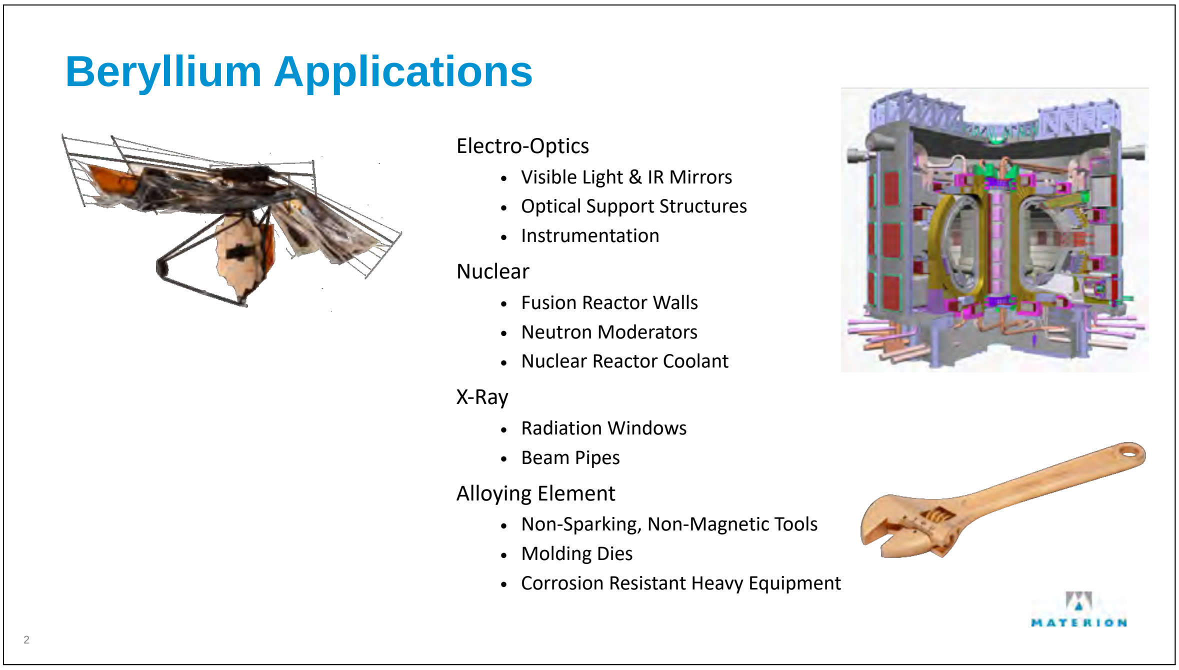
Beryllium Applications
Electro-Optics
• Visible Light & IR Mirrors
• Optical Support Structures
• Instrumentation
Nuclear
• Fusion Reactor Walls
• Neutron Moderators
• Nuclear Reactor Coolant
X-Ray
• Radiation Windows
• Beam Pipes
Alloying Element
• Non-Sparking, Non-Magnetic Tools
• Molding Dies
• Corrosion Resistant Heavy Equipment
MATERION
2

Potential Materials for AM

Beryllium (Be)
- Current technology has very high buy to fly ratios, long lead times, and limited flexibility
- Best AM value proposition

Aluminum-Beryllium (AlBe)
- Alternative to Be in lightweight and stiff applications
- Lower material and machining costs than Be
- More damage tolerant than Be
- Used in sensors, electronics, and housings

Beryllides (Beryllium-transition metal alloys)
- Lightweight with very high melting points
- Significant research on binary systems

Beryllium Oxide (BeO)
- Thermally conductive but electrically insulating ceramic
- Thermal spreaders and power applications

MATERION

3

History of Be-Based AM

2004-2008: Materion led E-Beam Powder Bed Fusion Efforts on AlBe
- Very early ARCAM machine with minimal control systems
- Lack of sufficient thermal control resulted in defects
- Materion concluded that AM system controls needed further maturation

2008-2018: Materion continued to keenly follow and assess the technical developments in additive manufacturing

2019: Materion concluded sufficient advancement in AM has been achieved to deliver the required quality and flexibility to produce parts on a commercial scale
- Performed in-depth review of the AM industry, evaluated 92 equipment vendors on a ranked matrix and determined the best available technology for Be-based AM

2020: Commissioned our Safe Be Materials AM Lab

2021: Work on Be materials began

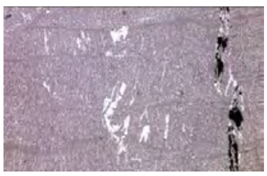

MATERION

4


Materion Additive Manufacturing Laboratory
Formative
Subtractive
Additive
Materion has built a laboratory to investigate and develop multiple additive manufacturing processes for Beryllium containing and other advanced materials.
Due to health and safety considerations for Be, the laboratory has strict access, ventilation, and environmental controls.
In addition to developing the technology, the laboratory will validate the appropriate health and safety procedures for Additively Manufacturing Beryllium and other advanced materials.
MATERION
5

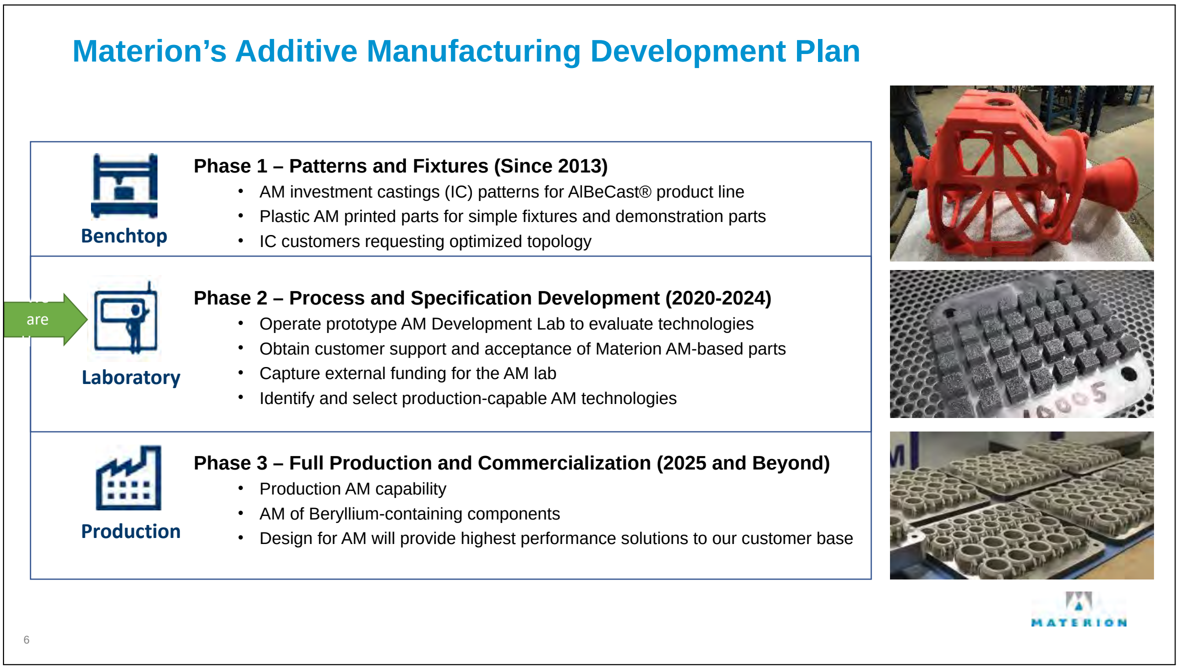
Materion's Additive Manufacturing Development Plan
Benchtop
Phase 1 – Patterns and Fixtures (Since 2013)
• AM investment castings (IC) patterns for AlBeCast® product line
• Plastic AM printed parts for simple fixtures and demonstration parts
• IC customers requesting optimized topology
are
Laboratory
Phase 2 – Process and Specification Development (2020-2024)
• Operate prototype AM Development Lab to evaluate technologies
• Obtain customer support and acceptance of Materion AM-based parts
• Capture external funding for the AM lab
• Identify and select production-capable AM technologies
Production
Phase 3 – Full Production and Commercialization (2025 and Beyond)
• Production AM capability
• AM of Beryllium-containing components
• Design for AM will provide highest performance solutions to our customer base
MATERION
6

Laser Powder Bed Fusion (LPBF) Of Beryllium

Beryllium LPBF had never been attempted before, so fundamental development necessary.

- Melt Pool Size
- Layer Thickness
- Energy Density
- Scan Velocity
- Stress Relief

These parameters require optimization based on the characterization of the resultant material.

- Volumetric Density
- Microstructural Analysis

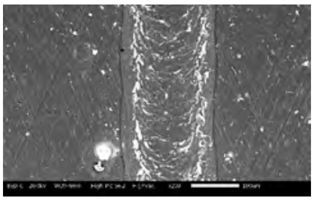

MATERION

7

Materion Proprietary and Confidential

Laser Powder Bed Fusion (LPBF) Of Beryllium

Current best recipe has minimal porosity and an intertwined columnar grain structure.

- Result after hundreds of samples
- Still significant room for improvement
- Initial mechanical property testing is underway

Surface roughness, support structures and other build requirements need to be developed.

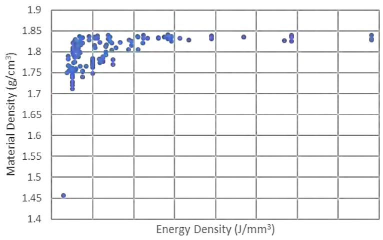

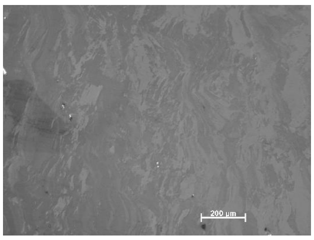

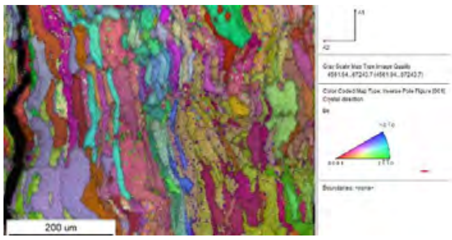

8

Binder Jet Printing of Beryllium

Parallel efforts to development binder jetting printing of beryllium.

- Green components can demonstrate through features (Walls and Gaps).

Densification upon sintering remains a challenge.

- Density is not expected to match that of laser powder bed fusion, however, further densification is desired.
- Trials to improve densification are ongoing.

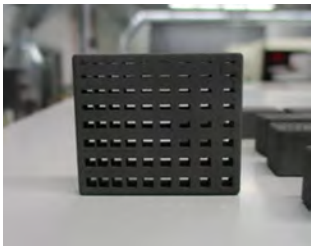

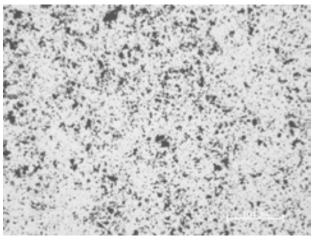

MATERION

9

Supporting Capabilities and Heritage Systems

Gas Atomization, Powder Processing and Characterization
Hot Isostatic Pressing, Post Processing and Machining
Chemical, Mechanical and Microscopic Analysis
Metrology, NDT and Radiography
Beryllium Metallurgical Expertise
Labs and Testing Capabilities

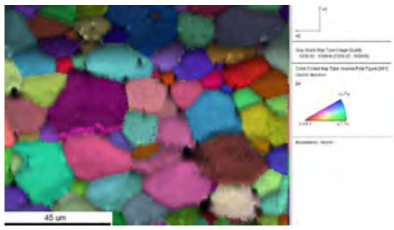

MATERION

10

Conclusions

- Materion is developing additive manufacturing for beryllium and other specialty engineered materials.
- Current efforts are in the laboratory phase and not yet commercialized.
- As additive manufacturing of beryllium approaches maturity, industrial partners and future customers will be needed for trade studies, pathfinder parts and specification evaluation.
- The goal is to bring a robust beryllium additive manufacturing solution to market and change the paradigm of beryllium utilization.

MATERION

11

SESSION 3

DEMO, ITER & JET

Current design of the EU DEMO Helium Cooled Pebble Bed breeding blanket

Guangming Zhou[1], Francisco A. Hernández[1]

[1]*Karlsruhe Institute of Technology*

In the Work Package Breeding Blanket (WPBB) of the European DEMO program, the Helium Cooled Pebble Bed (HCPB) breeding blanket is one of the two driver-blanket candidates for the European DEMO and to be tested as test blanket module (TBM) in ITER. In the Pre-Concept Design (PCD) phase (2014-2020), within the framework of the EUROfusion consortium in Europe, the design of the HCPB breeding blanket has been changed to address various challenges facing the HCPB blanket concept. One of the big challenges was the use of Beryllium pebbles as the neutron multiplier in the previous design. Irradiation campaign showed that the tritium retention in the Be pebbles could impose severe safety issues and exceed the tritium limit of EU DEMO. Beryllides, on the other hand, have better properties in terms of volumetric swelling, tritium retention, irradiation and melting temperature.

This talk will focus on the current design status of the European DEMO HCPB breeding blanket and conclude with future activities in the Concept Design phase (2021-2027).

Corresponding Author:
Dr. Guangming Zhou
guangming.zhou@kit.edu

Institute for Neutron Physics and Reactor Technology (INR),
Karlsruhe Institute of Technology (KIT),
Hermann-von-Helmholtz-Platz 1,
76344 Eggenstein-Leopoldshafen, Germany

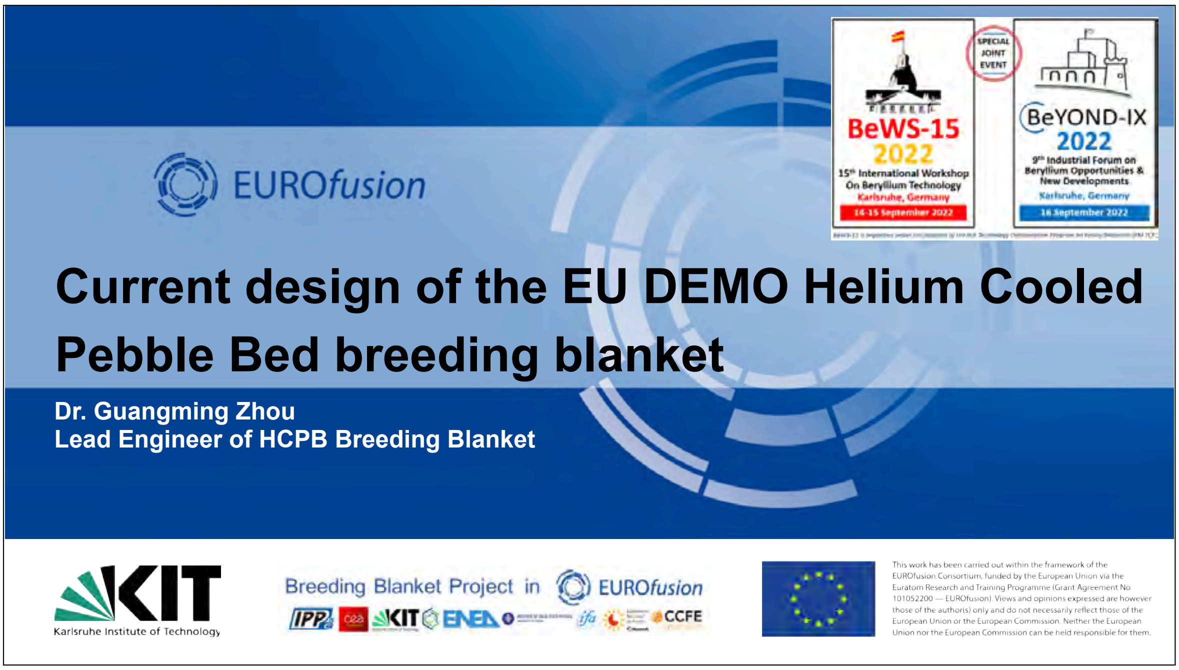
EUROfusion
BeWS-15 2022
15th International Workshop On Beryllium Technology
Karlsruhe, Germany
14-15 September 2022
SPECIAL JOINT EVENT
BeYOND-IX 2022
9th Industrial Forum on Beryllium Opportunities & New Developments
Karlsruhe, Germany
16 September 2022
Current design of the EU DEMO Helium Cooled Pebble Bed breeding blanket
Dr. Guangming Zhou
Lead Engineer of HCPB Breeding Blanket
KIT
Karlsruhe Institute of Technology
Breeding Blanket Project in EUROfusion
IPP
cea
KIT
ENEA
CCFE

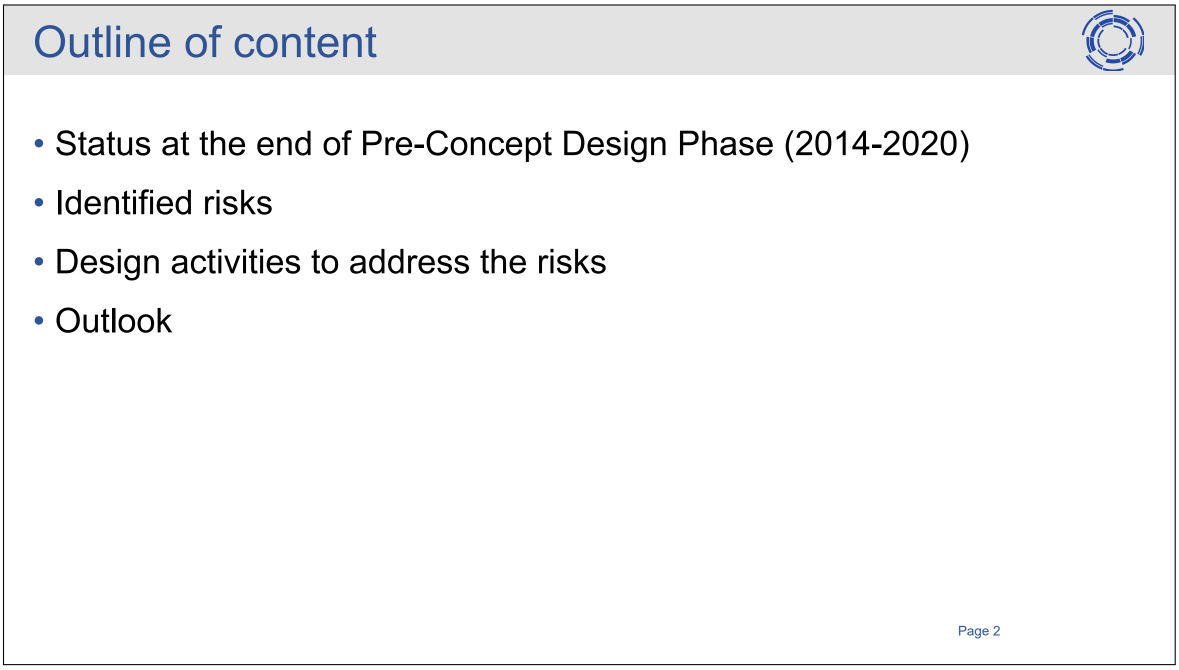
Outline of content
• Status at the end of Pre-Concept Design Phase (2014-2020)
• Identified risks
• Design activities to address the risks
• Outlook
Page 2

Status at the end of Pre-Concept Design Phase (2014-2020)

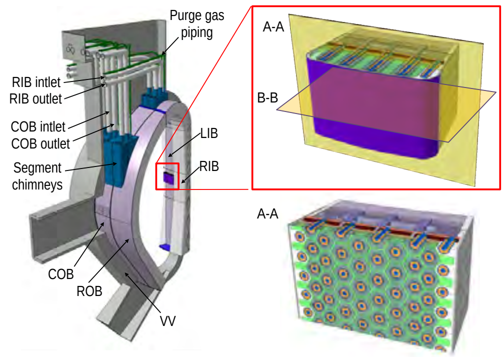

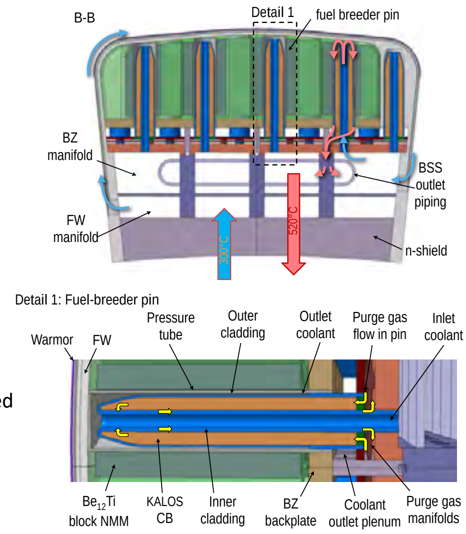

- Coolant: He @80 bar, 300-520°C
- Fuel-breeder pins containing advanced ceramic breeder (ACB) pebble bed
- Pins inserted into blocks of Be12Ti neutron multiplier
- Structural steel: Eurofer97
- Purge gas: He + 0.1vol% H_2 @2 bar
- Easier manufacturing, easier filling of pebbles
- NA, TH & TM; TBR = 1.20; Ppump per blower < 6 MW; satisfying shielding

Page 3

Identified risks related to HCPB BB

1. Low reliability of BB system under DEMO conditions [due to welds failure]
2. Loss of structural integrity of beryllide blocks
3. High pressure drops in coolant loop contributing to total high pumping power
4. Large tritium permeation rates at the interface of breeder-coolant loop
5. Low BB shielding capability
6. Degradation of Eurofer at contact with pebbles in purge gas environment
7. Reduction of structural integrity of blanket during shutdown due to Eurofer irradiation embrittlement
8. Low TRL of Codes & Standards for design of DEMO components

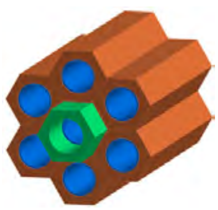

$Be_{12}Ti$ block NMM

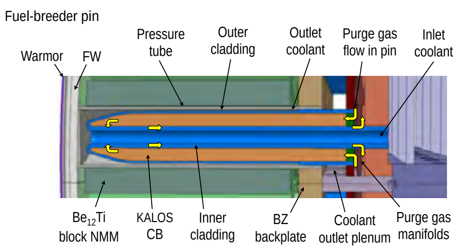

4

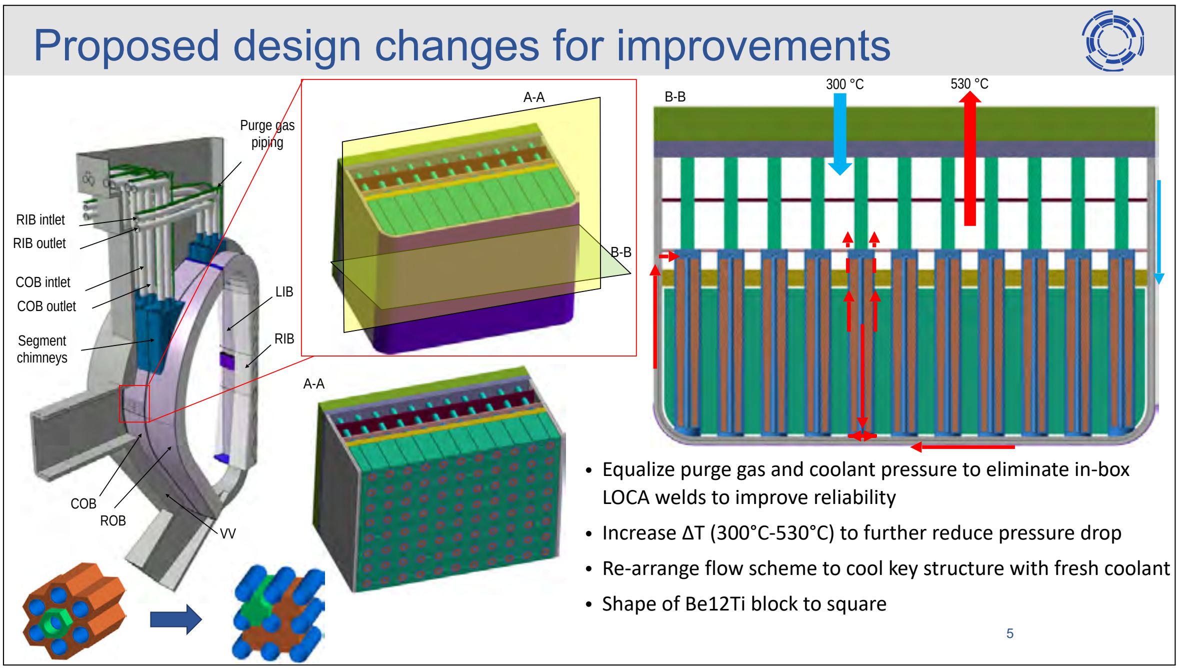

Proposed design changes for improvements
Purge gas piping
RIB intlet
RIB outlet
COB intlet
COB outlet
Segment chimneys
LIB
RIB
COB
ROB
VV
A-A
B-B
300 °C
530 °C
• Equalize purge gas and coolant pressure to eliminate in-box LOCA welds to improve reliability
• Increase ΔT (300°C-530°C) to further reduce pressure drop
• Re-arrange flow scheme to cool key structure with fresh coolant
• Shape of Be12Ti block to square
5

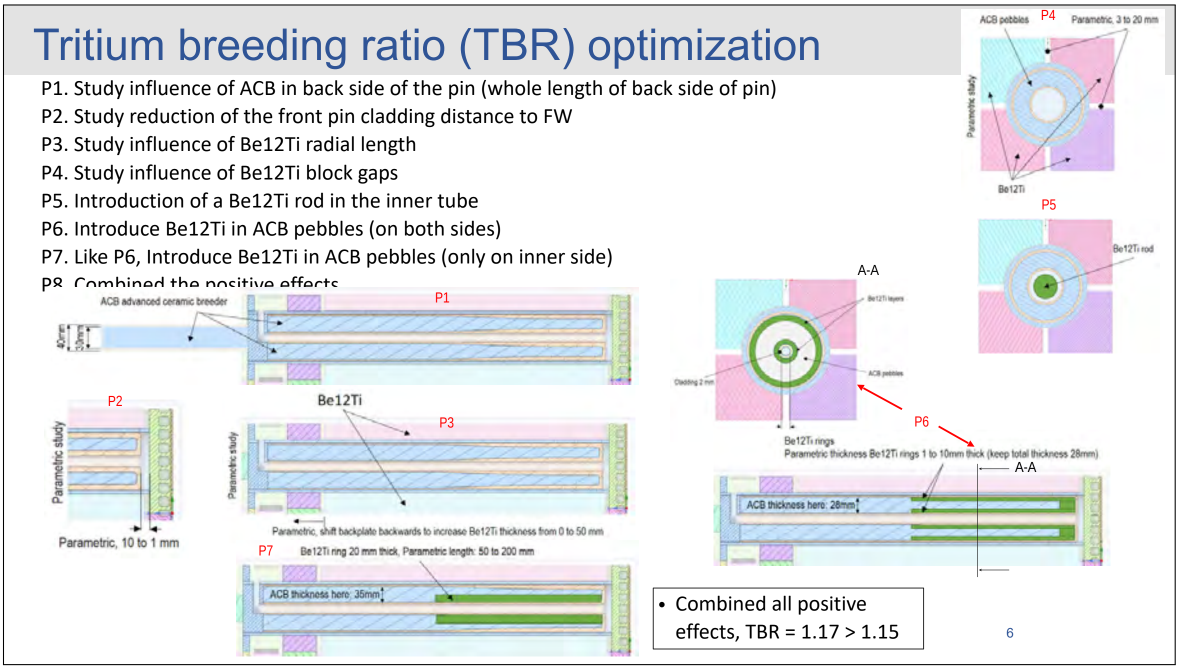

Tritium breeding ratio (TBR) optimization
P1. Study influence of ACB in back side of the pin (whole length of back side of pin)
P2. Study reduction of the front pin cladding distance to FW
P3. Study influence of Be12Ti radial length
P4. Study influence of Be12Ti block gaps
P5. Introduction of a Be12Ti rod in the inner tube
P6. Introduce Be12Ti in ACB pebbles (on both sides)
P7. Like P6, Introduce Be12Ti in ACB pebbles (only on inner side)
P8. Combined the positive effects
ACB advanced ceramic breeder
P1
P2
Parametric, 10 to 1 mm
Be12Ti
P3
Parametric, shift backplate backwards to increase Be12Ti thickness from 0 to 50 mm
P7
Be12Ti ring 20 mm thick, Parametric length: 50 to 200 mm
ACB thickness here: 35mm
P4
ACB pebbles
Parametric, 3 to 20 mm
Be12Ti
P5
Be12Ti rod
A-A
P6
Be12Ti rings
Parametric thickness Be12Ti rings 1 to 10mm thick (keep total thickness 28mm)
ACB thickness here: 28mm
• Combined all positive effects, TBR = 1.17 > 1.15
6

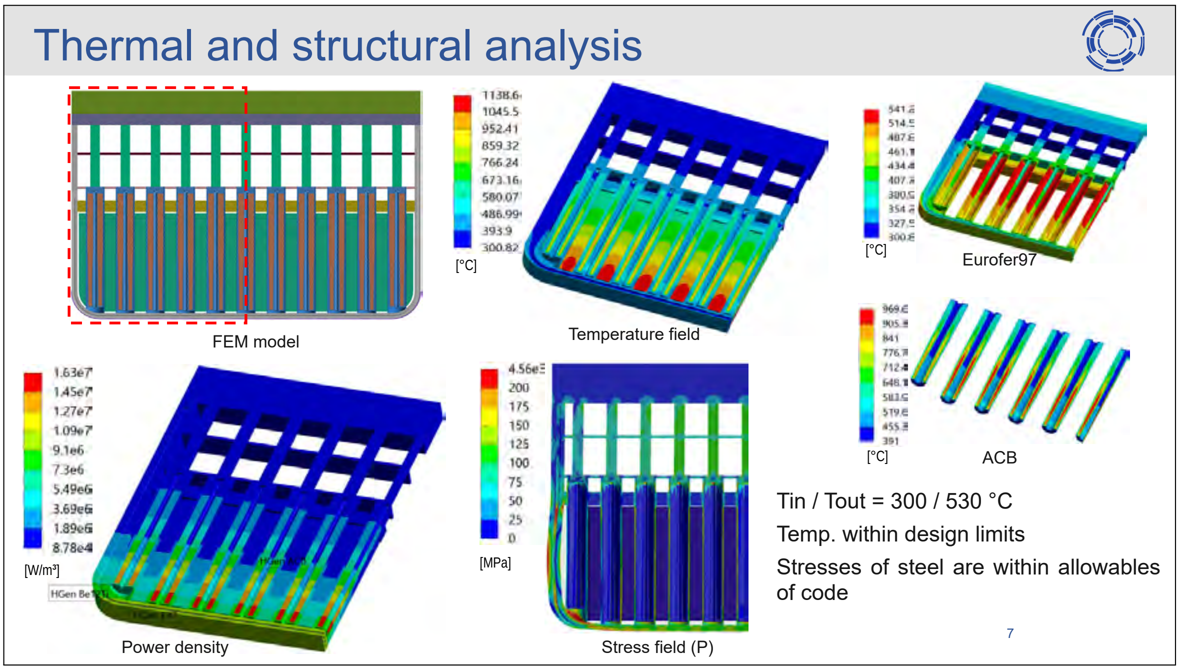
Thermal and structural analysis
FEM model
[°C]
Temperature field
[°C]
Eurofer97
[°C]
ACB
[W/m³]
Power density
[MPa]
Stress field (P)
Tin / Tout = 300 / 530 °C
Temp. within design limits
Stresses of steel are within allowables of code
7

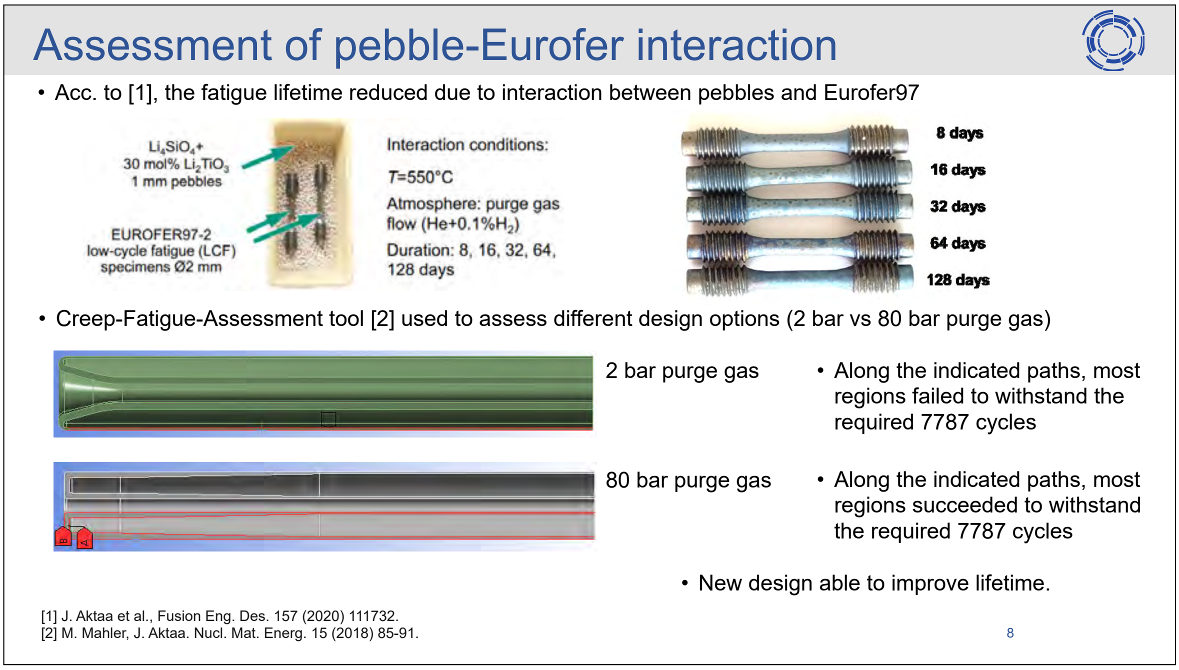
Assessment of pebble-Eurofer interaction
• Acc. to [1], the fatigue lifetime reduced due to interaction between pebbles and Eurofer97
Li4SiO4+ 30 mol% Li2TiO3 1 mm pebbles
EUROFER97-2 low-cycle fatigue (LCF) specimens Ø2 mm
Interaction conditions:
T=550°C
Atmosphere: purge gas flow (He+0.1%H2)
Duration: 8, 16, 32, 64, 128 days
8 days
16 days
32 days
64 days
128 days
• Creep-Fatigue-Assessment tool [2] used to assess different design options (2 bar vs 80 bar purge gas)
2 bar purge gas
• Along the indicated paths, most regions failed to withstand the required 7787 cycles
80 bar purge gas
• Along the indicated paths, most regions succeeded to withstand the required 7787 cycles
• New design able to improve lifetime.
[1] J. Aktaa et al., Fusion Eng. Des. 157 (2020) 111732.
[2] M. Mahler, J. Aktaa. Nucl. Mat. Energ. 15 (2018) 85-91.
8

Shielding design (1/2)

- Parametric neutronics analysis [3]
  3D MCNP model by SuperMC
  - *Baseline*: 15 cm Eurofer
  - *v1*: 1 cm B_4C, 14 cm Eurofer
  - *v2*: 2 cm B_4C, 13 cm Eurofer
  - …
  - *v5*: 5 cm B_4C, 10 cm Eurofer
  - …
  - *v10*: 10 cm B_4C, 5 cm Eurofer
- Tritium and helium production in B4C

Part of MCNP6 model

Cases	Nuclear heating at 1st cm of TFC (limit: 5e-5)	Neutron flux at 1st cm of TFC (limit: 1e9)	dpa/fpy at 1st cm of TFC (limit: 1.6e-5)	dpa/fpy at 1st cm of VV (limit: 4.5e-1)	He production at 1st cm of VV (limit: 0.16)
	W/cm³	n/cm²/s			appm/fpy
Baseline	8.69e-5	2.21e9	1.81e-5	1.53e-1	0.56
v1	7.36e-5	2.07e9	1.69e-5	1.28e-1	0.42
v2	6.83e-5	2.29e9	1.24e-5	9.27e-2	0.35
v3	5.37e-5	1.82e9	1.42e-5	9.43e-2	0.29
v4	5.16e-5	1.74e9	1.50e-5	8.58e-2	0.27
v5	4.72e-5	1.66e9	1.40e-5	7.70e-2	0.24
v6	4.16e-5	1.57e9	1.41e-5	6.94e-2	0.22
v7	3.69e-5	1.47e9	1.41e-5	6.29e-2	0.18
v8	3.32e-5	1.43e9	1.24e-5	5.76e-2	0.17
v9	3.30e-5	1.41e9	1.27e-5	5.52e-2	0.16
v10	3.24e-5	1.40e9	1.24e-5	5.27e-2	0.15
v5_inverted	4.06e-5	1.65e9	1.28e-5	7.46e-2	0.19
v10_inverted	2.81e-5	1.33e9	1.16e-5	5.07e-2	0.14

Negligible, 120 kg T/fpy in EU-DEMO → 1e-28 [Pa·m³/(s·m²)] << Outgassing limit 1e-11

Maximum T and He production is in v10, 1.84 mole (5.52 g) T per FPY, 500 mole (2 kg) He per FPY in EU-DEMO

At least 9 cm B4C is needed for meeting all the requirements.
Due to fragmentation of B4C, container of B4C is needed.
Nuclear heating in B4C and Eurofer used as input for structural design of the shield.

[3] I. Palermo et al., ICRS 14/RPSD 2022. September 25-29, 2022. Seattle, WA.

9

Shielding design (2/2)

- Structural design

To confine the fragmentation, B4C is designed to be contained.

Concept 1: Radiation, shield fixed to cover plate

Concept 2: Contact, shield fixed to BSS backplate

Concept 3: Contact, shield fixed to BSS backplate with external clamping

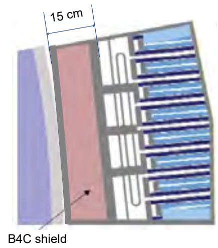

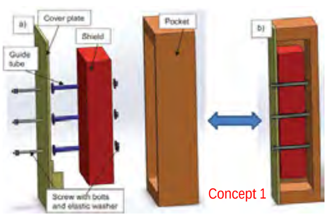

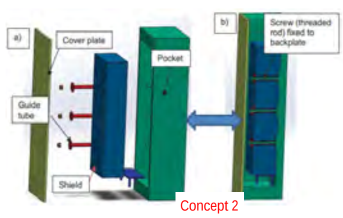

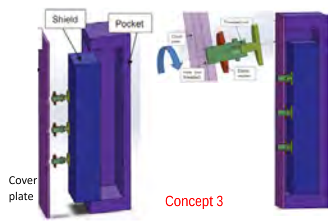

10

Global segment hydraulics

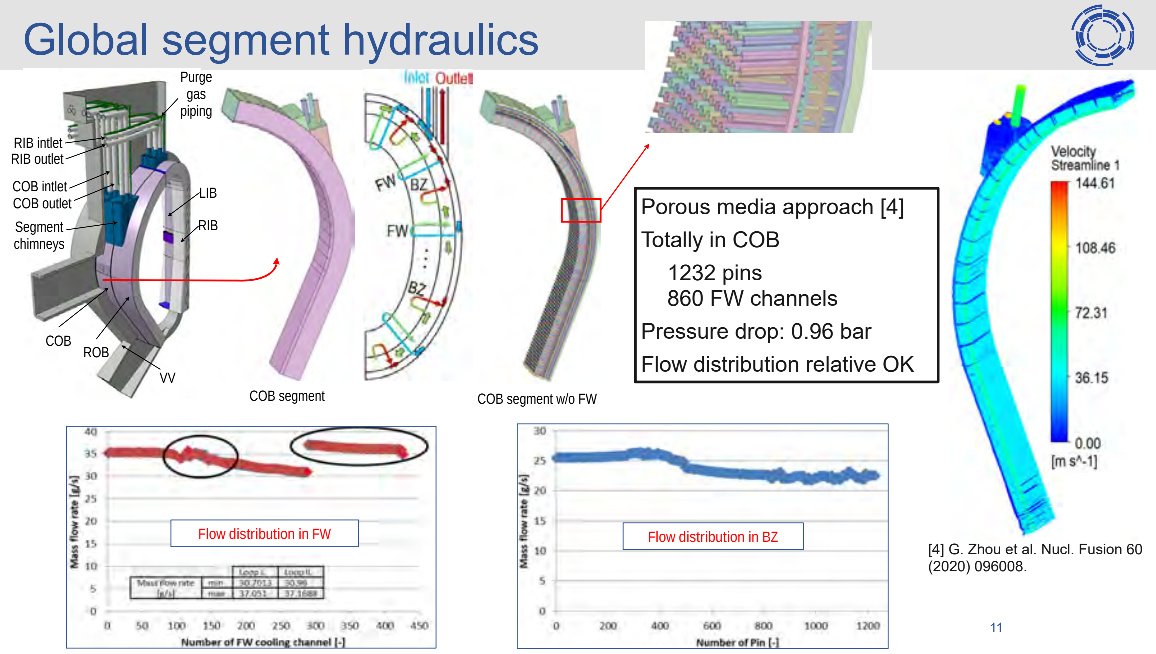

[4] G. Zhou et al. Nucl. Fusion 60 (2020) 096008.

11

Tritium Extraction and Removal (TER) system

- Reference design
  - ➢ Two stages in series
    First the adsorption of Q2O on the Reactive Molecular Sieve Bed (RMSB), thereafter the adsorption of Q2 on the Cryogenic Molecular Sieve Bed (CMSB) at 77 K. Q = H, D, T
  - ➢ Tritium recovered via isotope exchange on RMSB and by heating-up of the CMSB.
  - ➢ Extrapolated to DEMO scale is realized with industry.
- Outlook
  - ➢ 80 bar purge gas, introduced to improve reliability of BB, results show that TER operating at 80 bar not a issue.
  - ➢ CMSB requires large amount of liquid N2, getter bed is explored as alternative.
  - ➢ Wetted purge gas to have a higher isotopic exchange rate compared to H2 and oxidized Q2, reducing permeation.

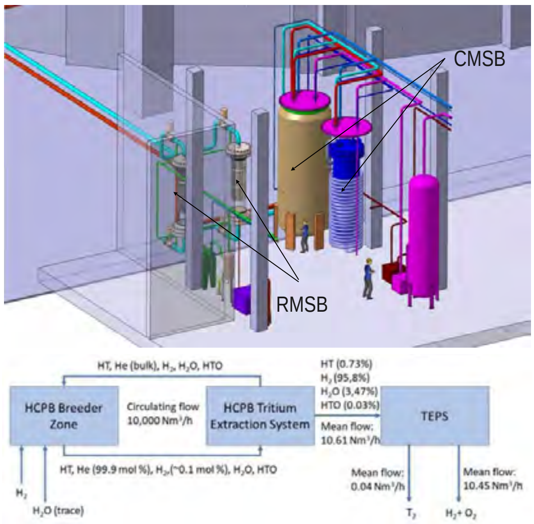

[5] I. Cristescu et al., Fusion Eng. Des. 158 (2020) 111558.

12

Tritium permeation analysis

- 3D component level solver [6]
  - ➢ Developed based on the OpenFOAM and benchmarked with TMAP 7
  - ➢ T release model
    - Grain surface release model based on irradiation T release experiment [7]

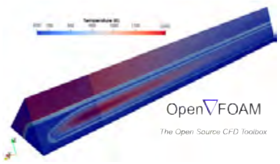

Temp. field of 1/6 fuel-breeder pin

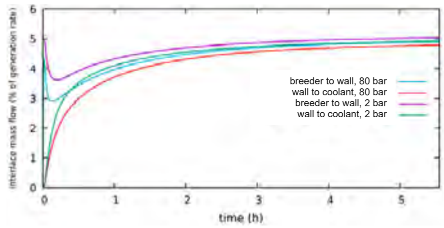

Permeation under equal volumetric flow

- T permeation analysis
  - ➢ T permeation analysis under 2 bar pressure purge gas vs 80 bar pressure purge gas, with same H2 partial pressure
  - ➢ Wetted purge gas vs dry purge gas

Purge gas	Permeation to coolant	Wall T inventory
200Pa H2, no H2O	0.077% of T generation 290 mg/d	65 ng
200Pa H2 + 200Pa H2O	0.022% of T generation 83 mg/d	19.2 ng

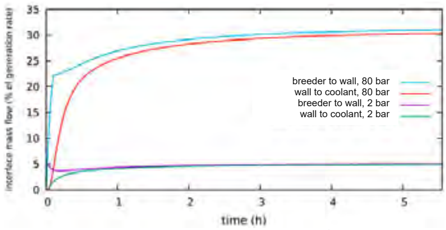

Permeation under equal mass flow

[6] V. Pasler et al., Applied Sciences 11 (2021) 3481.
[7] T. Kinjyo et al. Fusion Engineering and Design 81 (2006) 573-577.

13

Outlook

- At end of 2022, the milestone of preliminary conceptual design of the HCPB blanket shall be reached.
- At second half of 2024, the milestone of reference conceptual design for the HCPB blanket shall be reached, together with R&D programme.
- At the end of 2024, the driver blanket for EU-DEMO will be selected from the HCPB and WCLL concepts.
- From 2025 to 2027, the selected blanket will be further consolidated and qualified via design and R&D activities.

14

Contributors & Acknowledgements

Guangming Zhou[1*], Francisco A. Hernández[1, 2], Jarir Aktaa[1], David Alonso[3], Frederik Arbeiter[1], Lorenzo V. Boccaccini[1], Ion Cristescu[1], Antonio Froio[4], Christophe Garnier[5], Mathias Jetter[1], Xue Zhou Jin[1], Marc Kamlah[1], Béla Kiss[6], Christine Klein[1], Christina Koehly[1], Ivan Maione[1], Luis Maqueda[3], Carlos Moreno[7], Ivo Moscato[2,8], Iole Palermo[7], Jin Hun Park[1], Volker Pasler[1], Dario Passafiume[1], Pavel Pereslavtsev[1], Anoop Retheesh[1], Álvaro Yáñez[3]

*Guangming.Zhou@kit.edu

[1]*Karlsruhe Institute of Technology (KIT), Eggenstein-Leopoldshafen, Germany*

[2]*EUROfusion Programme Management Unit, Garching, Germany*

[3]*ESTEYCO, Madrid, Spain*

[4]*Dipartimento Energia, Politecnico di Torino, Turin, Italy*

[5]*French Alternative Energies and Atomic Energy Commission (CEA), Cadarache, France*

[6]*Budapest University of Technology and Economics (BME), Budapest, Hungary*

[7]*CIEMAT, Fusion Technology Division, Madrid, Spain*

[8]*University of Palermo, Palermo, Italy*

This work has been carried out within the framework of the EUROfusion Consortium, funded by the European Union via the Euratom Research and Training Programme (Grant Agreement No 101052200 — EUROfusion). Views and opinions expressed are however those of the author(s) only and do not necessarily reflect those of the European Union or the European Commission. Neither the European Union nor the European Commission can be held responsible for them.

Regulatory situation of Beryllium in EU and France – Update
Beryllium Good Practices at the Workplace - Be Responsible Program - Update

Angélique RENIER[1,2]

[1] *NGK BERYLCO FRANCE*
[2]*Beryllium Science and Technology (BeST) association*

Since the last Beyond event that I attended in Karlsruhe, Germany, in 2018, the regulatory situation of beryllium in EU has evolved.

At EU level, a harmonized Occupational Exposure Limit (OEL) for beryllium has been adopted in July 2019. Member States had 2 years to implement it in their national law. Furthermore, Beryllium has been assessed for an eventual restriction in the Electrical and Electronic Equipment (EEE) under the RoHS Directive (Restriction of Hazardous Substances in EEE). The assessment started in February 2018 and the conclusion has been published in March 2021 by the European Commission: it is not recommended to restrict beryllium. Another important point is that it was decided to keep beryllium in the list of Critical Raw Materials (CRM) for the EU (last list published in September 2020). Lastly, this presentation could be the opportunity to introduce new concepts currently discussed in the frame of the green deal and the Chemicals Strategy for Sustainability, including the ongoing revision of the main EU chemicals regulations (REACH and other sectorial directives). Essential Use Concept, Safe Use Concept or General Risk Approach are emerging new concepts which could have impacts on beryllium.

At French level, ITER being based in France, it is important to mention the implementation of the EU OEL in France since the 1st March 2022 (Decree No. 2021-1849 of December 28, 2021).

In a second part of the presentation, I suggest to introduce the Be Responsible Program (www.berylliumsafety.eu) developed by the Beryllium Association (BeST) in which NGK is involved and our actions to promote these good practices to the users of our beryllium-containing products. I was honored to present our beryllium good practices in the frame of trainings for ITER beryllium workers organized by INSTN (Institut des Sciences et Techniques du Nucléaire), several sessions in French and English. As French SME processing articles in copper-beryllium alloys, we also were very honored to share our experience during the conference on occupational cancers organized as part of the French Presidency of the European Union on March 07 and 08, 2022 in Paris.

Corresponding Author:
Mrs. Angélique RENIER
Chemicals Engineer (CPE Lyon, France, 1993)
Communication and Environment Manager at NGK BERYLCO France
& Secretary General of the Beryllium Association BeST
renier@ngkbf.com
NGK BERYLCO FRANCE, 103 Quai Jean-Pierre Fougerat CS 20017 44220 COUËRON, FRANCE

NGK BERYLCO
www.ngk-alloys.com

BeYOND-IX 2022
Angélique RENIER, NGK BERYLCO France
and BeST (Beryllium Science and Technology Association)

Updated regulatory situation of beryllium
& Good Practices Program at the workplace « Be Responsible »

BeST
Beryllium Science & Technology Association

Be Responsible
Beryllium Product Stewardship

1. **Regulatory situation of beryllium: last update**
   - ☑ Context reminder (main uses, risk & CLP classification)
   - ☑ Be Occupational Exposure Limit: CMD Directive (2019) & French transposition (2022)
   - ☑ RoHS Directive (Restriction of Hazardous Substances in EEE): Be evaluation (2020)
   - ☑ EU CRM (Critical Raw Materials) list: Be still CRM in 2020, next list 2023
   - ☑ Chemicals Strategy for Sustainability CSS (Green Deal): ongoing REACH revision and new concepts

2. **Good Practices Program Be Responsible: last update**
   - ☑ Be Responsible Program developed by BeST www.berylliumsafety.eu
   - ☑ Webinars
   - ☑ Trainings for ITER workers
   - ☑ NGK Beryllium testimony at the French Presidency of the EU

1

NGK BERYLCO
www.ngk-alloys.com

1. Regulatory situation of beryllium in EU: update

☑ **Context Reminders:**

- ➢ NGK BERYLCO activity: manufacturing and sales of articles in copper-beryllium alloys CuBe2 (strips, rolls, plates, rods, bars, wires etc..)
- ➢ Subsidary of the NGK Insulators LTD Group including 3 divisions :
  - Digital Society (Electronic components and devices, New Metals)
  - Energy & Industry (Insulators, Energy storage, Industrial processes)
  - Environment (Ceramic filters, Sensors)
- ➢ Beryllium: natural element (4th of the periodic table). Mainly extracted in US (80%) and mainly used as alloying element in copper at 2% to date (80% out of the 400 M tons produced /year)
- ➢ 2% of beryllium in copper substantially increases the mechanical performances of copper without impairing its conductivity. Best possible combination mechanical resistance/conductivity
- ➢ Main uses of CuBe2 alloys : connectors and contactors, electrical and electronic equipment. Main applications: Automobile, Aeronautic, Aerospace, Telecommunication, Computers, Home Appliances, Photovoltaic, Defense

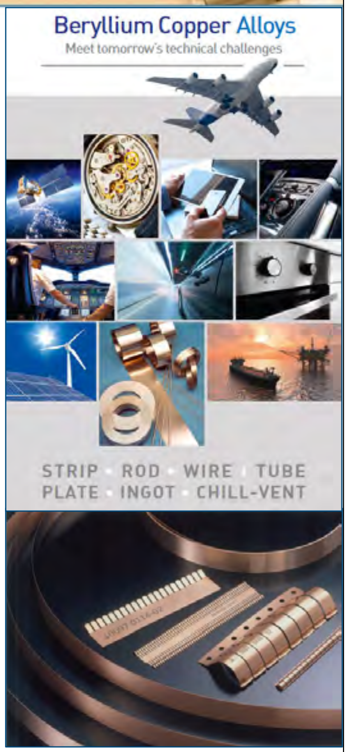

2

NGK BERYLCO
NGK www.ngk-alloys.com

☑ **Risk and classification:**

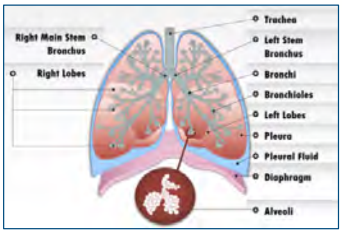

- Risk by inhalation of fine airborne particles (< 10 microns). Risk limited to the workplace. Individuals who are sensitized (allergic) to beryllium and exposed can develop a chronic lung disease : Chronic Beryllium Disease (CBD) also called berylliosis. This is the consequence of a reaction of the immune system at the level of pulmonari alveoli (formation of granulomas). CBD can be treated but is not curable. It can be fatal.
- EU CLP Regulation (Classification): Beryllium is classified Carcinogen 1B (H350i : can cause cancer by inhalation) for all forms insoluble (metal) and soluble (compounds).

004-001-00-7	beryllium	231-150-7	7440-41-7	Carc. 1B Acute Tox. 2 (*) Acute Tox. 3 (*) STOT RE 1 Eye Irrit. 2 STOT SE 3 Skin Irrit. 2 Skin Sens. 1	H350i H330 H301 H372 (**) H319 H335 H315 H317	GHS06 GHS08 Dgr	H350i H330 H301 H372 (**) H319 H335 H315 H317			

- Recent epidemiologic studies (Dr. Paolo Boffetta) found no excess cancer risk in workers at plant sites that only used insoluble forms of beryllium. The Beryllium association BeST aims to reclassify beryllium metal as Carcinogen 2 differently from beryllium compounds. Ongoing revision of the EU CLP is an opportunity.
- REACH evaluation (Risk Management Option Analysis RMOA published by BAuA in 2016):
  Beryllium is **not Substance of Very high concern** SVHC on the candidate list,
  not under authorization, not under professional restriction.

REACH COMPLIANCE

3

NGK BERYLCO
NGK www.ngk-alloys.com

☑ **New EU and French Beryllium Occupational Exposure Limit OEL:**

- **Beryllium has been included in the Carcinogen and Mutagen Directive CMD** on 11 **July 2019 (3rd revision)**:
  Directive (EU) 2019/983 amending 2004/37/EC : **0.6 µg/m³** to be followed by **0.2** in July 2026

DIRECTIVE (EU) 2019/130 OF THE EUROPEAN PARLIAMENT AND OF THE COUNCIL

of 16 January 2019

amending Directive 2004/37/EC on the protection of workers from the risks related to exposure to carcinogens or mutagens at work

ANNEX

In point A of Annex III to Directive 2004/37/EC, the following rows are added:

Name of agent	EC No (1)	CAS No (2)	Limit values						Notation	Transitional measures
			8 hours (3)			Short-term (4)				
			mg/m^3 (5)	ppm (6)	f/ml (7)	mg/m^3 (5)	ppm (6)	f/ml (7)		
'Cadmium and its inorganic compounds	—	—	0,001 (11)	—	—	—	—	—		Limit value 0,004 mg/m^3 (12) until 11 July 2027
Beryllium and inorganic beryllium compounds	—	—	0,0002 (11)	—	—	—	—	—	dermal and respiratory sensitisation (13)	Limit value 0,0006 mg/m^3 until 11 July 2026

20.6.2019 EN

- **National transposition of the EU CMD Directive in France**: French Decree 2021-1849 published on 28 December 2021 and entered into force on **1st March 2022**
  - → **French OEL** previously indicative at 2 µg/m³ now **binding at 0.6 µg/m³**
  - → **0.2 µg/m³ in 2026**
- No over-transposition in EU Member States except (< 200 ng): Germany(140), Belgium(50), Denmark (20)

4

NGK BERYLCO
www.ngk-alloys.com

☑ **Beryllium evaluation under the RoHS Directive:**
(Restriction of Hazardous Substances in Electrical and Electronic Equipment EEE)

- Beryllium is not restricted under RoHS (Annex II of RoHS: 10 substances restricted to date including lead, mercury, cadmium and hexavalent chromium)
- A new evaluation of Beryllium has been launched in February 2018 for a possible restriction under RoHS (Pack 15 featuring 7 substances including beryllium)
- The evaluation report dated November 2020 has been published by the European Commission in February 2021
- Conclusion: **« the inclusion of beryllium and BeO in ANNEX II of RoHS is currently not recommended »**
- Excerpts: « High technological importance of beryllium for the EEE sector » « especially as it comes to medical and safety relevant products » « the health hazards of beryllium and BeO, in particular CBD and even beryllium sensitisation can be regulated through an Occupational Exposure Limit » « progress in implementaing exposure controls in order to meet established OELs of 0.6/0.2 µg/m³ for airborne beryllium at mechanical and thermal plants throughout the EU » « same measures can reduce the release of other pollutants »
- Ongoing RoHS general review expected for 2023

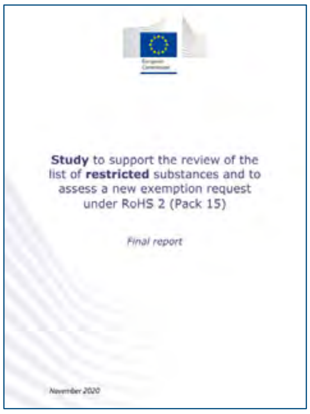

RoHS Ready

5

NGK BERYLCO
www.ngk-alloys.com

☑ **Beryllium Critical Raw Material (CRM) to the EU:**

- Beryllium is in the CRM list since the first list in 2011
- CRM List updated every 3 years:
  2011 (14 CRMs) - 2014 (20) - 2017 (27) – **2020 (30)**
- New list expected in 2023 (BeST involoved in ongoing workshops: SCREEN, MSA)
- 3 criteria:
  - Supply risk
  - Economic importance
  - Non-substitutability
- BeST member of the CRM Alliance: « need of a unique approach in regulation and policymaking when addressing CRMs to avoid overregulation, innovation barriers, loss of EU competitiveness and societal well-being »

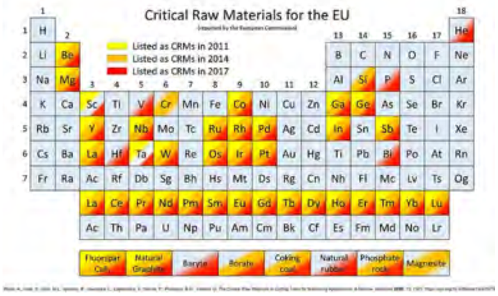

Where the EU sources from?

6

NGK BERYLCO
www.ngk-alloys.com

☑ **Chemical Strategy for Sustainability CSS (EU Green Deal):**

➢ Ongoing review of REACH and CLP regulations + RoHS and ELV Directives

➢ REACH and RoHS revision proposals expected for 2023. BeST proactive in workshops and public consultations

➢ 2 new concepts to be introduced:
- Essential Use Concept EUC
- Generic Risk Managemet Approach GRA

➢ Simplistic hazard-based approachs in which the real risks are not considered (risk = hazard X exposure). Impact on innovation, competitiveness of the EU industry and achievement of Green Deal objectives.

➢ BeST is defending a « safe use approach », i.e. a risk-based approach versus a mere hazard-based approach. Common position of EU industry (ASMOR : Alliance for Sustainable Management of chemical Risk)

➢ More than 80 actions in the CSS are to be implemented by 2024. Other vigilance point: Sustainable Product Initiative & Circular Economy Action Plan (Safe and sustainable by Design SSdB concept, mandatory recycling targets)

➢ BeST message:
"BeST stresses the need for a coherent and balanced approach. The regulatory actions stemming from the CSS should be developed in coordinated manner, coupled with proper impact assessments to determine benefits and drawbacks. To meet the green deal challenges, we will need to use hazardous chemicals. Simplistic and unscientific statements on phasing out hazardous chemicals will be counterproductive. A real risk-based approach is essential: Risk = Hazard x Exposure. "

7

NGK BERYLCO
www.ngk-alloys.com

2. Good Practices – Beryllium Product Stewardship Program – Be Responsible

☑ **Be Responsible Program www.berylliumsafety.eu**

Be Responsible
Beryllium Product Stewardship

➢ Launched by BeST in 2017

➢ Website accessible (free of charge) in English : www.berylliumsafety.eu

➢ Summarized web version **in all European languages** including French : www.berylliumsecurite.fr and German www.berylliumsicherheit.de

➢ **Kit of 12 guides** available in English and French (+ DE, IT, SP) :
✓ 3 generic guides : Health and Safety / Hygiene & Personal Protective Equipment / Exposure assessment
✓ 9 guides for the most frequent operations in industry
Low inhalation concern operations (CNC machining / Sawing / Stamping)
Likely inhalation risk operations (Machining by Electro-erosion EDM / Sandblasting, grinding, rectification, polishing / Fusion / Foundry / Heat Treatment/ Forging / Welding)

Official Campaign Partner
Healthy Workplaces
2018 - 2019

8

NGK BERYLCO
www.ngk-alloys.com

➢ Indentification of **sources of exposure**

SOURCES OF EXPOSURE

All operations performed on beryllium-containing alloys must be performed with appropriate work practices and engineering controls designed to control the release or generation of airborne beryllium-containing dust, mist or fume. The following tables provide a summary of those processes that typically present low inhalation concern (green) and those that present a likely inhalation hazard (yellow).

Low Inhalation Concern Operations			Likely Inhalation Hazard Operations		
Adhesive Bonding	Filing by Hand	Roll Bonding	Abrasive Blasting	Forging	Resistance Welding
Age Hardening (<950°F)	Gun Drilling	Rotary forging	Abrasive Processing	Grinding	Roller Burnishing
Assembly	Hand Solvent Cleaning	Sawing (tooth blade)	Abrasive Sawing	Heat Treating (in air)	Sand Blasting
Bending	Handling	Shearing	Annealing	High Speed Machining (>10,000 rpm)	Sand Casting
Blanking	Heading	Shipping	Brazing	Honing	Sanding
Bonding	Heat Treating (inert atmosphere)	Sizing	Bright Cleaning	Hot Forging	Scrap Management (Clean)
Boring	Inspection	Skiving	Brushing	Hot Rolling	Sectioning
Broaching	Machining	Slitting	Buffing	Investment Casting	Slab Milling
CNC Machining	Metallography	Stamping	Burnishing	Lapping	Soldering
Cold Forging	Milling	Straightening	Casting	Laser Cutting	Solution Management
Cold Heading	Packaging	Stretch Bend Leveling	Centerless Grinding	Laser Machining	Spot Welding
Cold Pilger	Painting	Stretcher Leveling	Chemical Cleaning	Laser Scribing	Sputtering
Cold Rolling	Physical Testing	Tapping	Chemical Etching	Laser Marking	Swaging
Cutting	Piercing	Tensile Testing	Chemical Milling	Laser Welding	Torch cutting (i.e., oxy-acetylene)
Deburring (non-grinding)	Pilger	Thread Rolling	Coolant Management	Laundering	Water-jet Cutting
Deep Hole Drilling	Plating	Trepanning	Deburring (grinding)	Melting	Welding (ARC, TIG, MIG, etc.)
Drawing	Pressing	Tumbling	Destructive Testing	Photo-Etching	Wire Electrical Discharge Machining (WEDM)
Drilling	Radiography/X-ray	Turning	Dross Handling	Pickling	
Dry Tumbling	Reaming	Ultrasonic Cleaning	Electrical Chemical Machining (ECM)	Point and Chamfer	
Electroless Plating	Ring Forging	Ultrasonic Testing	Electrical Discharge Machining (EDM)	Polishing	
Electroplating	Ring Rolling	Upsetting	Electron Beam Welding (EBW)	Process Ventilation Maintenance	
Extrusion					

Be Responsible
Beryllium Product Stewardship

9

NGK BERYLCO
www.ngk-alloys.com

➢ **Beryllium worker protection model** based on 8 principles : limiting the emission and dispersion of fine particles

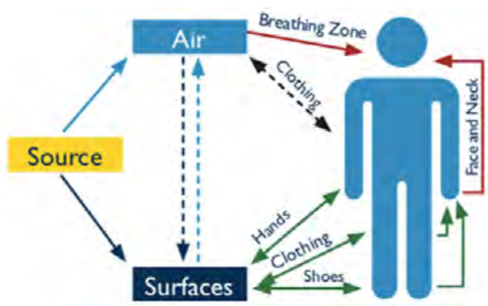

1. Keep Beryllium Out of the Lungs
2. Keep Beryllium Off the Skin
3. Keep Beryllium Off of the Clothes
4. Keep Beryllium at the Source
5. Keep Beryllium in the Work Area
6. Keep Beryllium on the Plant Site
7. Keep Beryllium Work Areas Clean
8. Keep Beryllium Workers Prepared

Be Responsible
Beryllium Product Stewardship

10

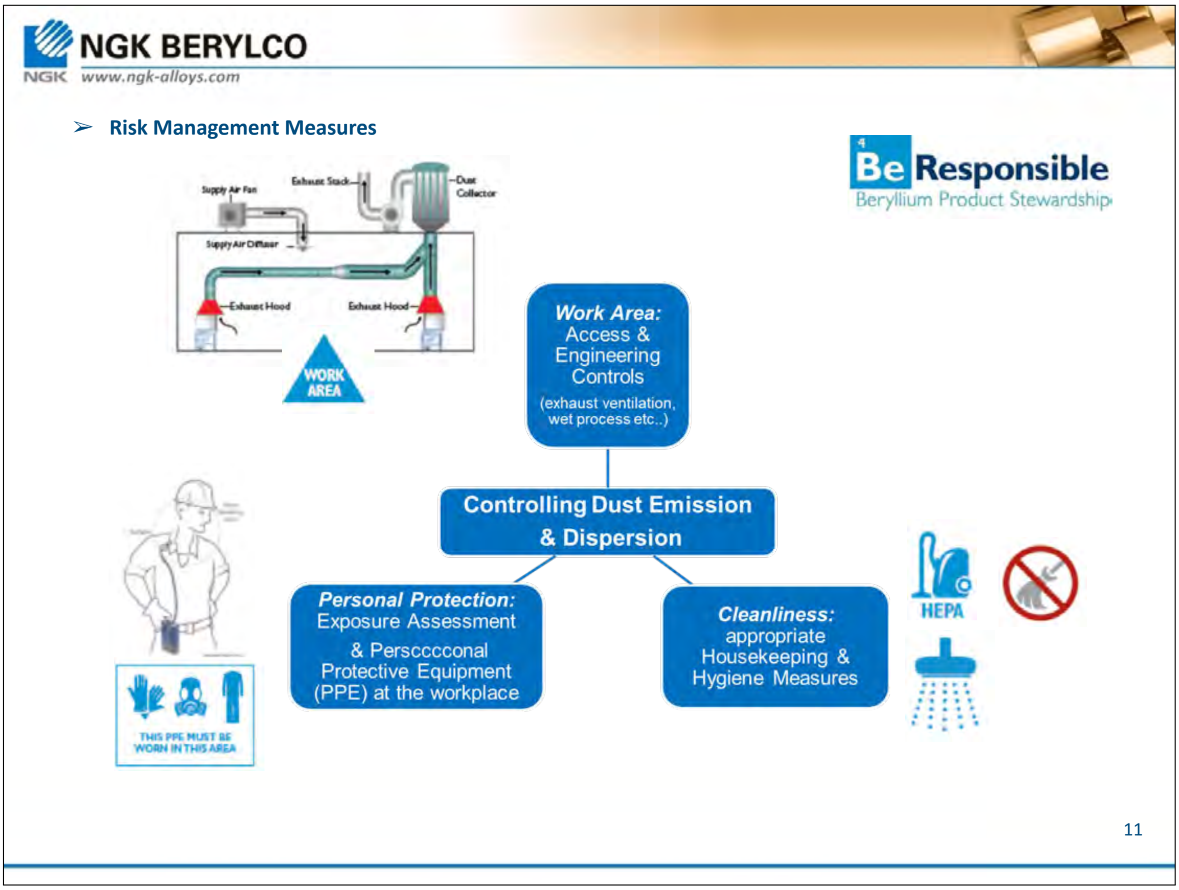
NGK BERYLCO
NGK www.ngk-alloys.com
➢ Risk Management Measures
Be Responsible
Beryllium Product Stewardship
Supply Air Fan
Exhaust Stack
Dust Collector
Supply Air Diffuser
Exhaust Hood
Exhaust Hood
WORK AREA
Work Area: Access & Engineering Controls
(exhaust ventilation, wet process etc..)
Controlling Dust Emission & Dispersion
Personal Protection: Exposure Assessment & Persccccconal Protective Equipment (PPE) at the workplace
Cleanliness: appropriate Housekeeping & Hygiene Measures
HEPA
THIS PPE MUST BE WORN IN THIS AREA
11


NGK BERYLCO
NGK www.ngk-alloys.com
☑ Be Responsible Program – Webinars by BeST « Working safely with Beryllium »
➢ Since 2020, BeST has proposed 3 up to 4 webinars /year: 2 in English, 1 in French and 1 in German - Next in German scheduled on Thursday 20 October 2022
➢ Communication: Newsletters, Easy Guide Blast, Web etc..
BeST
SPRING ISSUE / 2021
BeST Holds First 2021 Beryllium Safety Webinar
Launch of Beryllium Safety websites in 24 languages!
Be Responsible
Beryllium Product Stewardship
Dear Reader
CONTEXT OF THE BE RESPONSIBLE PROGRAMME
OUR PERSONAL PROTECTIVE EQUIPMENT & HYGIENE GUIDE
WWW.BERYLLIUMSAFETY.EU
Be Responsible
WEBINAR: WORKING SAFELY WITH BERYLLIUM
Be Responsible 2021
23 MARCH 2021
15:00 - 16:30 CET
Be Responsible
TRAVAILLER AVEC LE BERYLLIUM EN TOUTE SÉCURITÉ - WEBINAIRE -
16 DÉCEMBRE 2020
16:00 - 17:30
12

NGK BERYLCO
www.ngk-alloys.com

☑ **Beryllium Training courses for ITER workers (INSTN – CEA)**

- ➢ Sessions in French and English (2018, 2019, 2020, 2021)
- ➢ In cooperation with the ITER occupational physician

☑ **Testimony as part of the French Presidency of the EU (conference on occupational cancers – French Labor and Health Ministries on 07 & 08 March 2022 in Paris)**

- ➢ Testimonial from a company that has conducted a prevention initiative : NGK BERYLCO France (Beryllium sector)

13

Beryllium in JET with the ITER-Like Wall: Fuel retention, oxidation, melt erosion, dust

M. Rubel[1], A. Widdowson[2], I. Jepu[2], L. Dittrich[1], T.T. Tran[3], J. Grzonka[4,5], E. Fortuna-Zaleśna[4], S. Moon[1], P. Petersson[1] and JET Contributors*

[1]KTH Royal Institute of Technology, Fusion Plasma Physics, 100 44 Stockholm, Sweden
[2]Culham Science Centre for Fusion Energy, Abingdon OX14 3DB, United Kingdom
[3]Uppsala University, Department of Physics and Astronomy, 751 20 Uppsala, Sweden
[4]Warsaw University of Technology, 02-507 Warsaw, Poland
[5]University of Cadiz, 11003 Cadiz, Spain

Joint European Torus (JET) functions with the ITER-Like Wall (JET-ILW): beryllium in the main chamber and tungsten in the divertor. Be is used in the form of castellated bulk metal limiter blocks and evaporated coatings on the inner wall cladding (IWC) tiles. The operation with Be plasma-facing components (PFC) involves a spectrum of nuclear safety issues arising from plasma-material interactions: erosion, fuel retention, co-deposition with oxygen, melt damage including metal splashing and melt layer propagation, dust generation and mobilization, behaviour under massive water (liquid, vapour) or air leak, impact on invessel diagnostic components.

All above mentioned aspects of Be erosion and migration have been studied in detail with a range of methods including high-resolution in-vessel photographic survey, over twenty exsitu ion-, electron-, photon-based material analysis techniques and dedicated laboratory experiments performed on materials retrieved from JET. Results are summarized as follows.

- Be-based dust occurs in two forms: co-deposited layers peeled off from PFC and droplets released from the limiters following high-heat loads and consequential target melting.
- Be splashes stick firmly to surfaces thus creating a minimal risk for further mobilization.
- The amount of loose Be dust after a full experimental campaign comprising 20 h of plasma operation is assessed at the level of 0.05-0.1 g, i.e. 5-10% of the total mass of dust.
- Deuterium content in co-deposits on so-called wall probes is 1-2x1017 cm-2, i.e. it is low.
- Total D retention in Be coatings on IWC, 5.3×1022, is on the same level as on Be limiters.
- Optical performance of test mirrors in the divertor is fully degraded by Be deposition, while mirrors in the main chamber wall maintained reflectivity.
- Depth profiles of Be and oxygen in co-deposits are of the shape indicating the in-vessel origin of O (gettering) but not post exposure oxidation when PFC was in contact with air.
- No mobilization of Be dust was detected in connection with the operation of remotely handled robotic arm used for in-vessel work at shutdowns.

In summary, all these points answer specific questions formulated at JET and ITER. A comprehensive report will contain research details accompanied by a critical assessment of results with emphasis of their weight and possible impact on the use of Be in future devices.

Corresponding Author:
Prof. Marek Rubel
rubel@kth.se
KTH Royal Institute of Technology, 100 44 Stockholm, Sweden

EUROfusion

Beryllium in JET with the ITER-Like Wall: *Fuel retention, oxidation, melt erosion, dust*

Marek Rubel, Anna Widdowson, Ionut Jepu, Laura Dittrich, Tuan T. Tran, Justyna Grzonka, Elzbieta Fortuna-Zalesna, Sunwoo Moon, Per Petersson and JET Contributors

JET KTH UK Atomic Energy Authority

This work has been carried out within the framework of the EUROfusion Consortium and has received funding from the Euratom research and training programme 2014-2018 under grant agreement No 633053. The views and opinions expressed herein do not necessarily reflect those of the European Commission.

JET tokamak with the ITER-Like Wall: **Plasma-facing components: Beryllium and Tungsten**

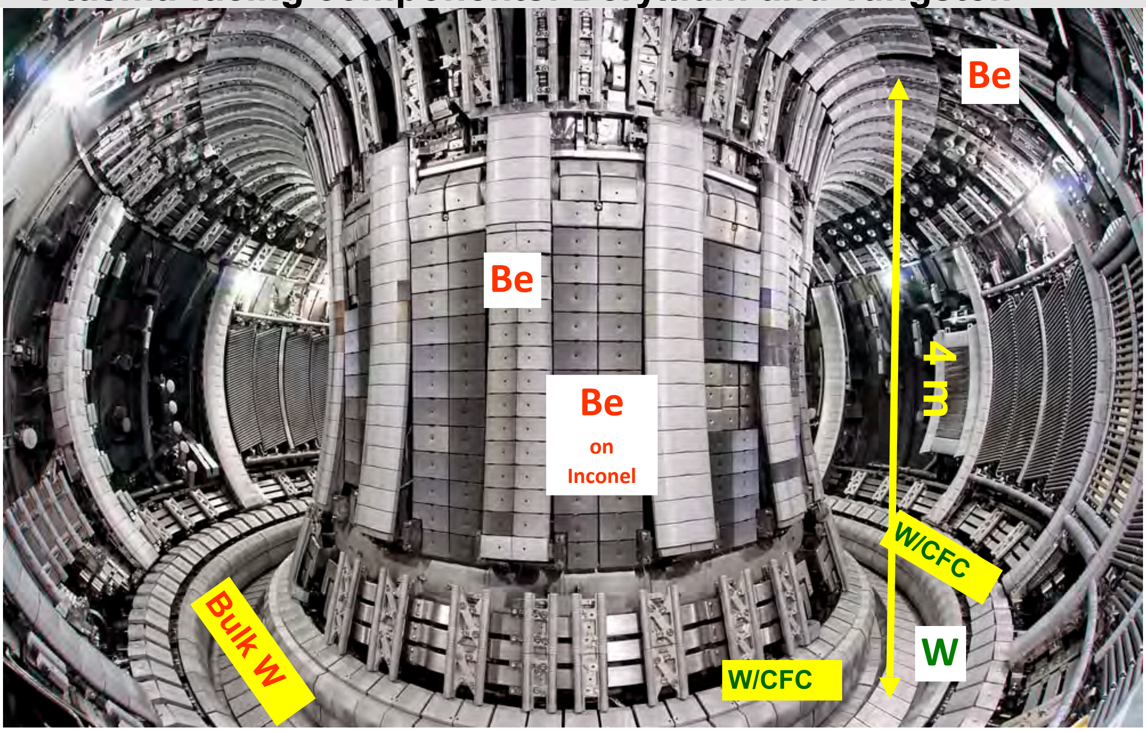

All categories of PFC tiles have special structural features.

Marek Rubel| Workshop on Be Technology & BeYond-IX|Karlsruhe| September 2022| Page 2

JET tokamak with ITER-like wall: JET-ILW

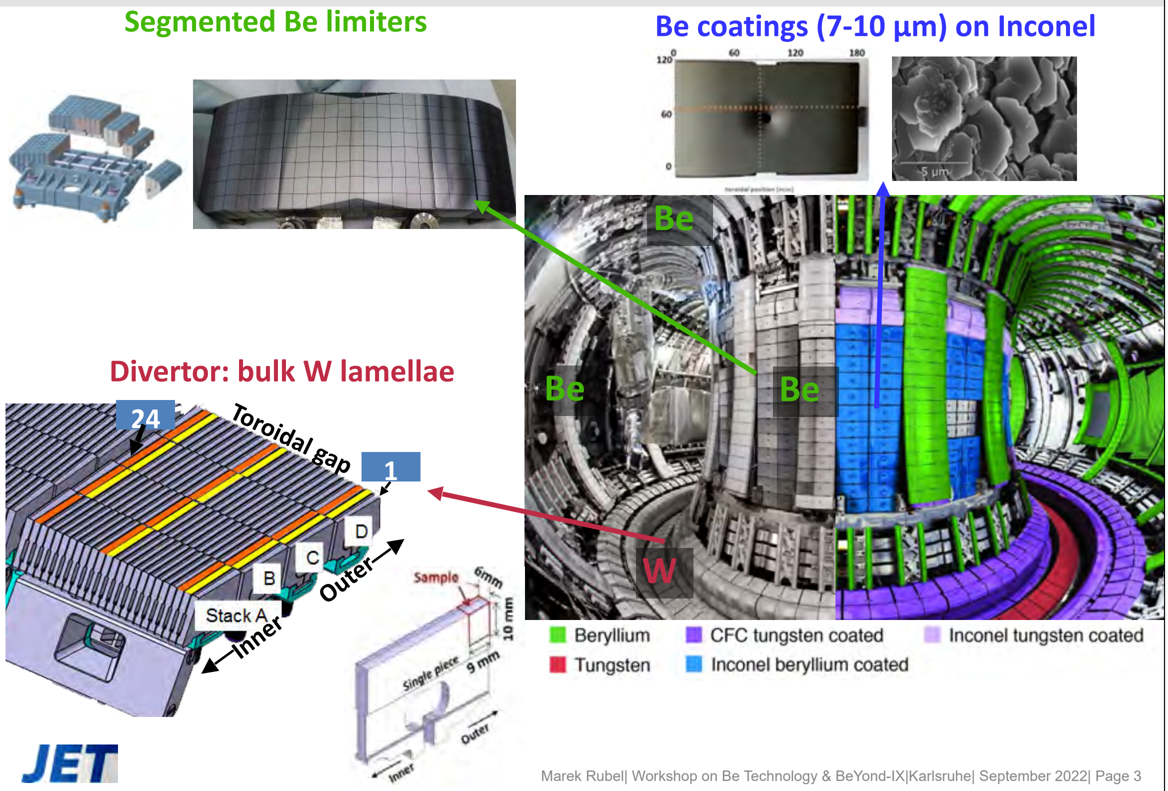

Marek Rubel| Workshop on Be Technology & BeYond-IX|Karlsruhe| September 2022| Page 3

Motivation and Aims

Driving force in studies: Safety & economy of reactor operation.

Operation with Be wall components involves a spectrum of nuclear safety issues arising from plasma-wall interactions:

- *Erosion, migration re-deposition (co-deposition),*
- *Fuel retention,*
- *Melt damage, melt layer propagation & metal splashing,*
- *Dust generation and mobilisation (disruptions),*
- *Impact of erosion products on in-vessel diagnostics,*
- *Risks related to massive coolant (water, vapour) leaks.*

All processes need to be studied and (if possible) **quantified to enable reasonable predictions for a reactor.**

JET

Marek Rubel| Workshop on Be Technology & BeYond-IX|Karlsruhe| September 2022| Page 4

Handling beryllium and tritiated components
Beryllium Handling Facility (BeHF) at JET

All JET materials go through BeHF before shipment for ex-situ studies.

JET

Marek Rubel| Workshop on Be Technology & BeYond-IX|Karlsruhe| September 2022| Page 5

Analysis: A mosaic of methods

A "mosaic" of over 40 different methods has been used in our studies of wall components.

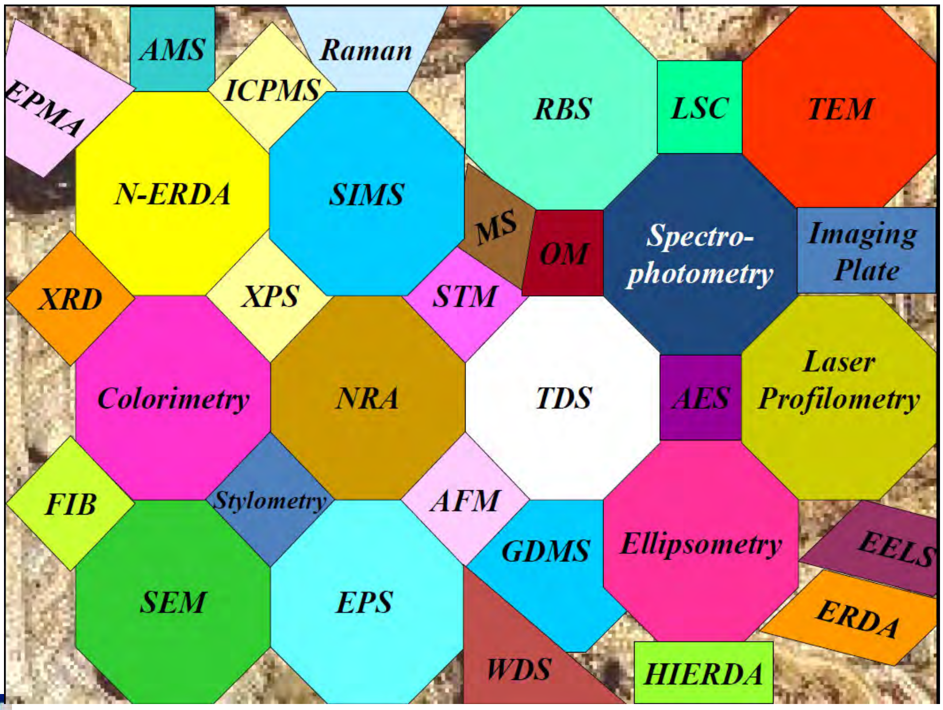

JET

Marek Rubel| Workshop on Be Technology & BeYond-IX|Karlsruhe| September 2022| Page 6

Beryllium Limiters

JET

Fuel retention on Plasma-facing surfaces

Aim: Comparison of retention after campaigns finished with different fueling.

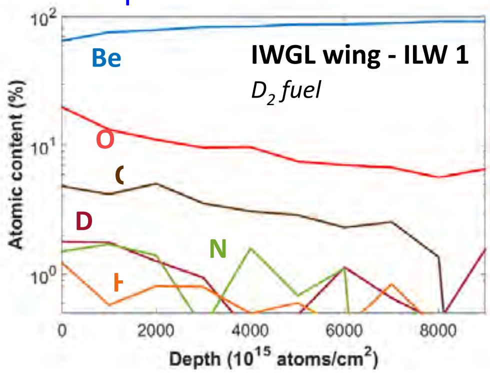

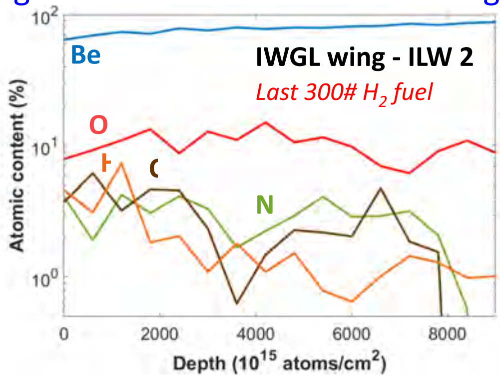

ILW 1: **D: 90×10^{15} cm^{-2},**
H: 61×10^{15} cm^{-2},
→ *D content higher than H*

ILW 2: D: 0 cm^{-2},
H: 185×10^{15} cm^{-2},
→ *No deuterium in the surface layer.*

Messages:

- The content of hydrogen iostopes in Be limiters is small.
- Main impurities: O, C, N and Ni *(Inconel components)*
- Operation with H_2 fuel at the end of ILW-2 eliminated D from the surface layer.

JET **Laura Dittrich, 47th EPS, 2021**

Marek Rubel| Workshop on Be Technology & BeYond-IX|Karlsruhe| September 2022| Page 8

Be upper dump plate ILW1-3: Melt zone composition

Motivation: Analyses of MkI-Be divertor tiles (1995) suggested possible higher fuel retention in molten Be areas.

Aim: To determine the composition of the melt zone.

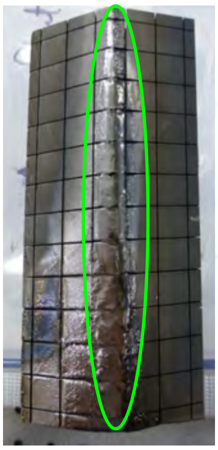

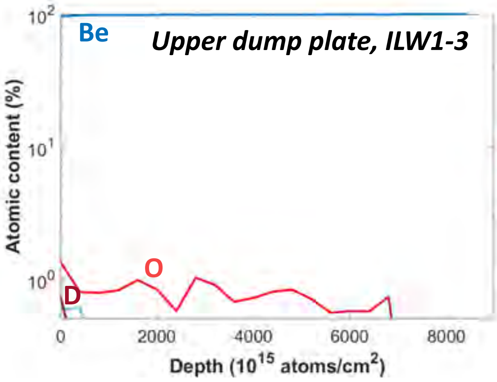

Main results

- On average 99 at.% Be
- ~1 % at. oxygen
- No co-deposited N, C, Ni
- < 0.1 % at. H isotopes

Messages:

➢ Melt zones are cleaner than not melted Be areas.

➢ They are cleaner than unexposed reference samples.

JET Laura Dittrich, 47th EPS, 2021 9

Beryllium-coated Inner Wall Cladding

JET

Be-coated Inconel: Inner Wall Cladding

Aim:
Assess the Be erosion and fuel retention, the share in the total retention in JET

Total Be-coated IWC area $5.36\ m^2$

Analyzed tiles:
- Reference: unexposed
- Tile 403 exposed to JET-ILW 1-3
- Tile 106 exposed to JET-ILW 1-2
- Tile 412 exposed to JET-ILW 1-3

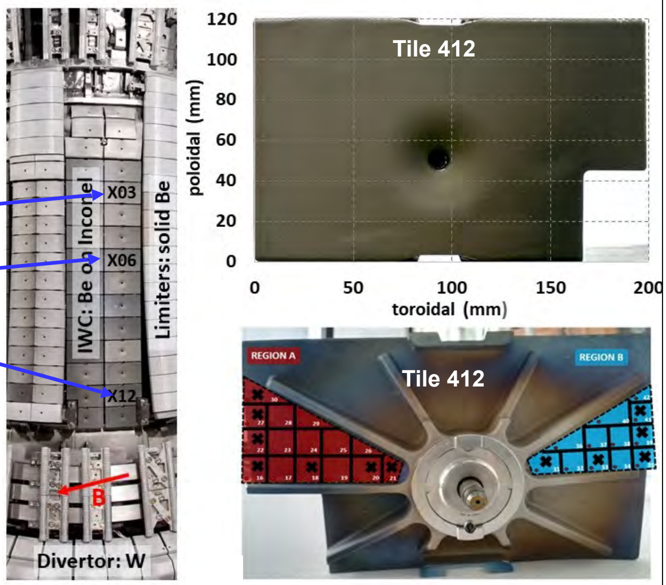

JET

Marek Rubel| Workshop on Be Technology & BeYond-IX|Karlsruhe| September 2022| Page 11

Be-coated Inconel: Inner Wall Cladding

Be erosion and deuterium content.

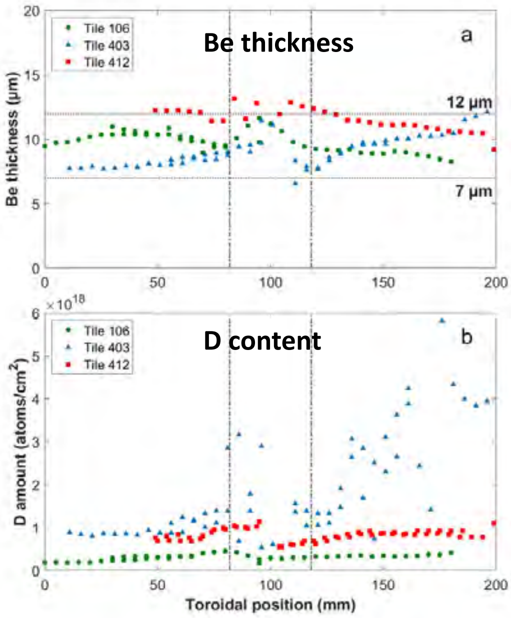

L. Dittrich et al., Phys. Scr. 96 (2021)
A. Widdowson et al., , Phys. Scr. 96 (2021)

Messages:
- ➢ Small variations in the Be layer thickness.
- ➢ No erosion through the whole layer.

- ➢ D content: 0.2 – 4.1 x 10^{18} cm^{-2}.
- ➢ Averaged D content: 1.0 x 10^{18} cm^{-2}.
- ➢ Extrapolated D inventory in IWC: **5.3x10^{22} D** corresponding to **176 mg D.**
- ➢ This is on the same level as in all limiters.

Conclusion:
Retention in the coating cannot be neglected in the accountancy of fuel inventory in the entire tokamak.

JET

12

Be-coated Inconel: Erosion of Inner Wall Cladding

Structure of initial and power-tested Be layers.

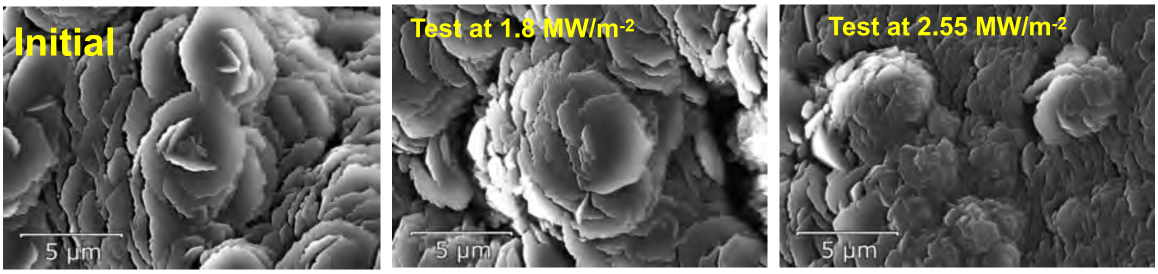

After exposure in JET.

Note: rounded edges with bright rims and a network of small "dots" on Be platelates.

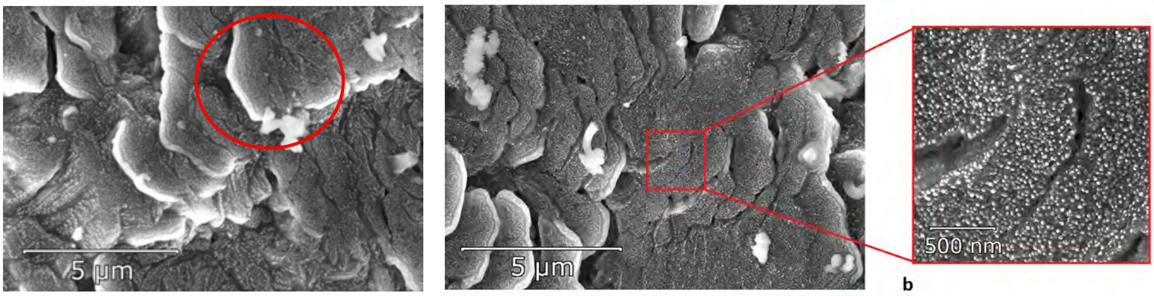

JET L. Dittrich et al., Phys. Scr. 96 (2021)

Marek Rubel| Workshop on Be Technology & BeYond-IX|Karlsruhe| September 2022| Page 13

Inner Wall Cladding: Erosion pathway of Be coatings

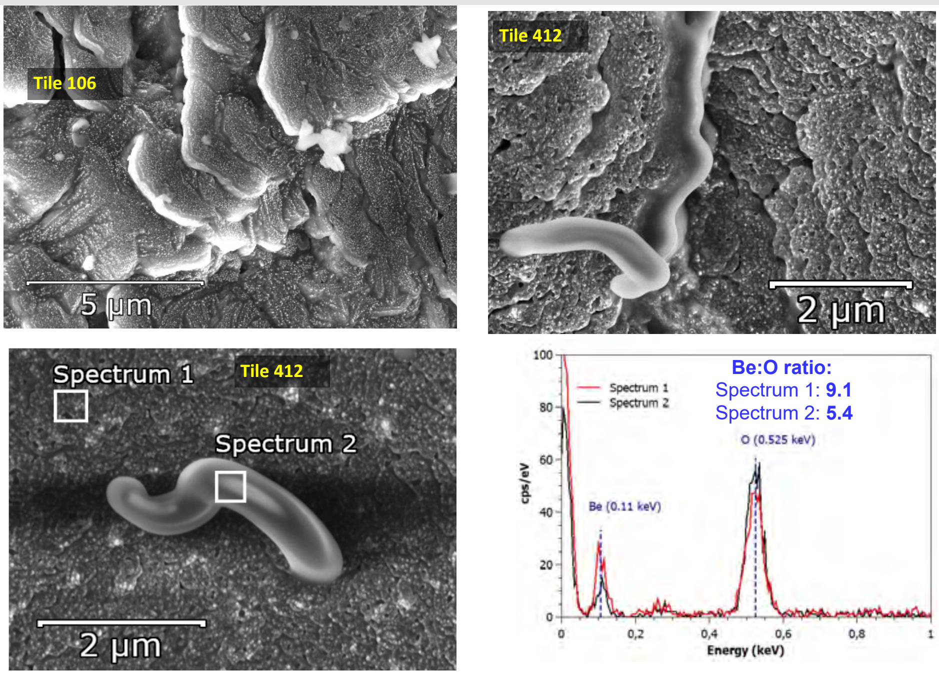

Message:

Layer erosion and disintegration by the formation of tube-like Be-O structures.

JET L. Dittrich et al., Phys. Scr. 96 (2021)

Marek Rubel| Workshop on Be Technology & BeYond-IX|Karlsruhe| September 2022| Page 14

Beryllium melting, splashing and dust

JET

Dust Collection: *Facts, Advantages, Drawbacks*

Vacuum cleaning: 360 °

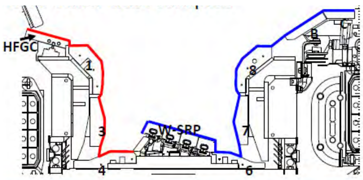

Message:
Around 1 g found after each campaign (20 h of plasma)

Drawbacks:
Composition: a mix of all particles.
Not possible to associate dust morphology with place.

Local sampling: sticky tape

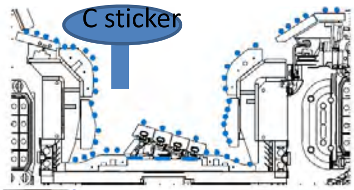

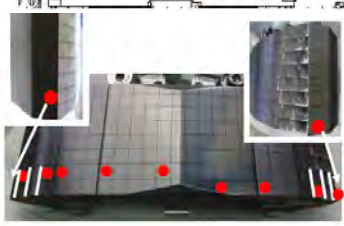

Messages:
- *Fairly small amount sampled.*
- *Good adherence of particles to tiles.*

Advantage: *Detailed local analyses.*

Drawbacks:
The top layer of samples represents the bottom of deposits.
Force applied during collection; more than just dust may be collected.

Dust monitors

Message:
Tiny amount collected.

Advantages:
Collection of undisturbed mobilized particles.
Precise analyses

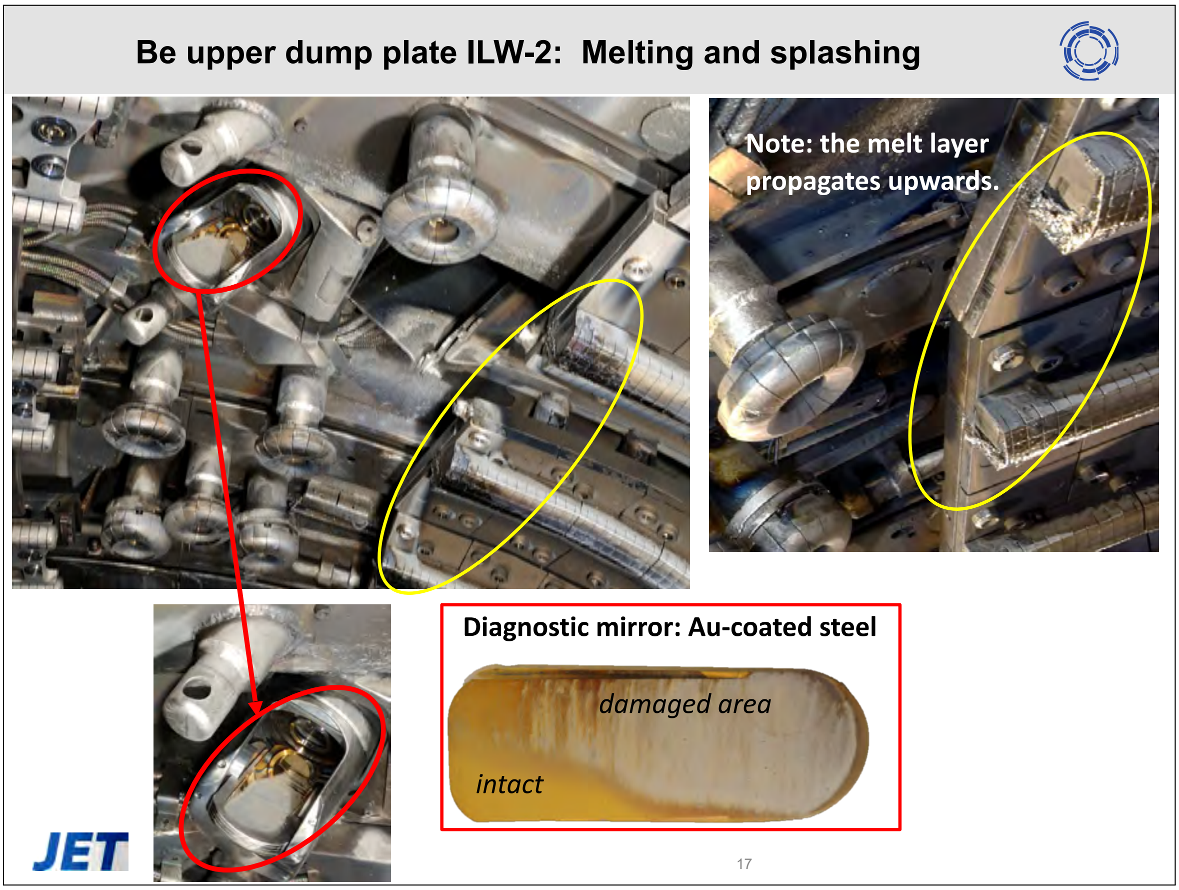
Be upper dump plate ILW-2: Melting and splashing
Note: the melt layer propagates upwards.
Diagnostic mirror: Au-coated steel
damaged area
intact
JET
17

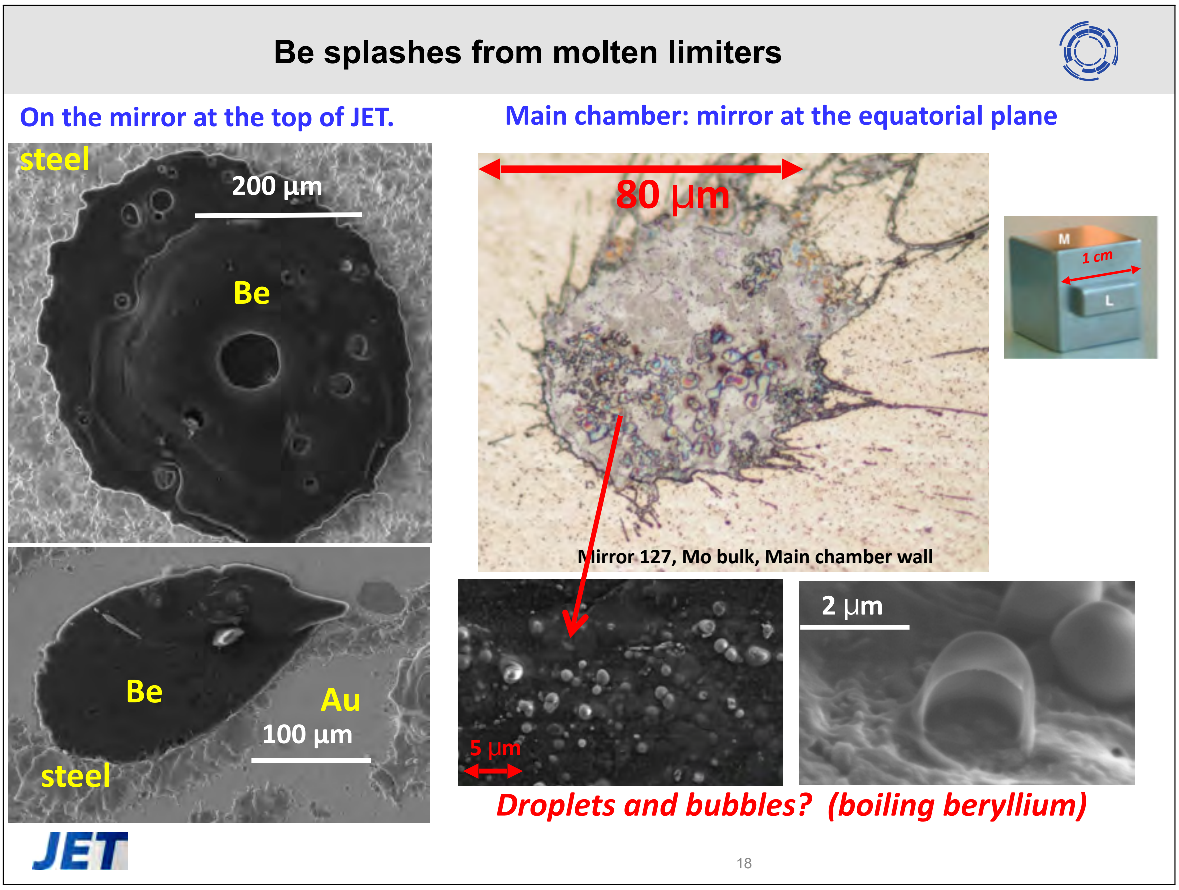
Be splashes from molten limiters
On the mirror at the top of JET.
Main chamber: mirror at the equatorial plane
steel
200 µm
Be
Be
Au
100 µm
steel
80 µm
M
1 cm
L
Mirror 127, Mo bulk, Main chamber wall
5 µm
2 µm
Droplets and bubbles? (boiling beryllium)
JET
18

Be droplets and splashes from molten limiters

On dust monitors above the divertor | On the tungsten divertor plates: bottom of JET

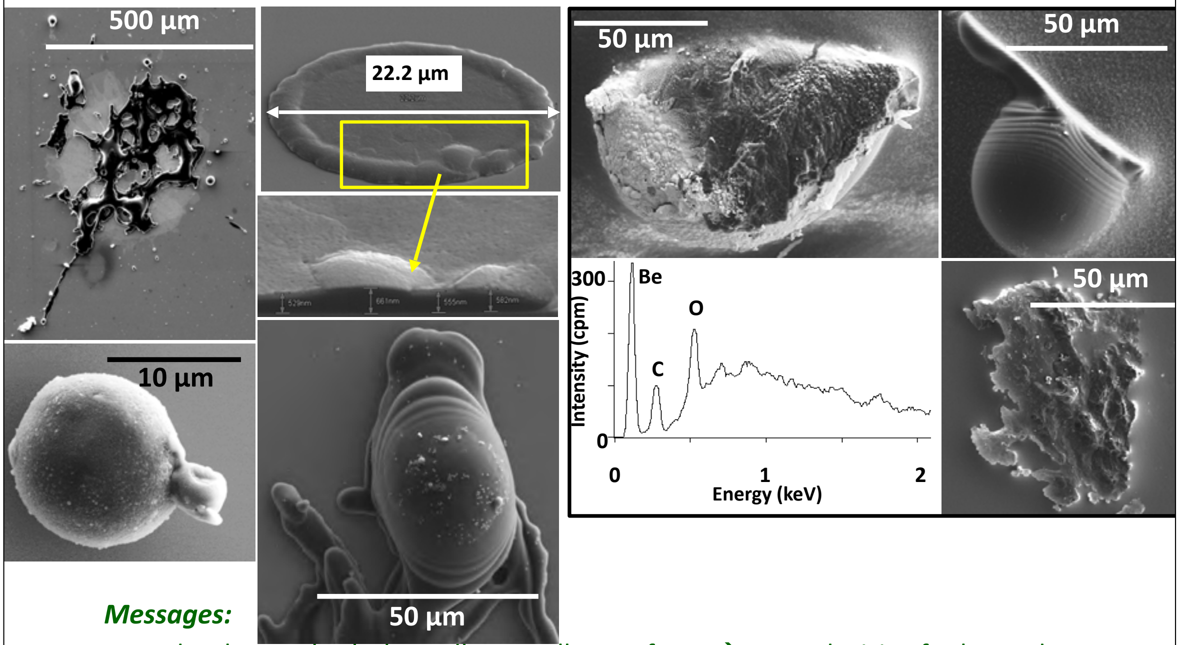

Messages:

- Be droplets and splashes adhere well to surfaces → not decisive for loose dust.
- Splashes are mostly round and only very thinly coated by deposits.

JET

19

Search for mobilized Be dust during in-vessel interventions

JET

Dust on the remotely handled (RH) robotic arm

Exercise performed on the request from the ITER Safety Division.

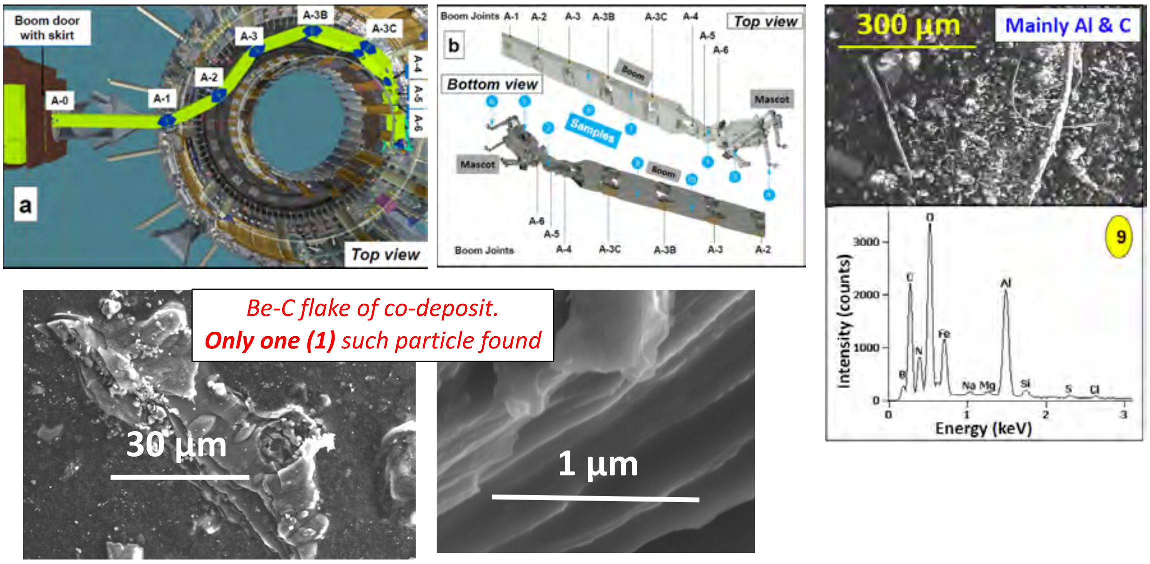

- *Aluminium is the main species: from the RH equipment.*
- *Other species: carbon, copper (NBI), steel/Inconel*
- *Only ONE Be-containing particle was found.*

M. Rubel , W. Widdowson et al. Phys. Scr. T171 (2020)

JET ***Main message:*** No massive Be mobilization.

Concluding Remarks: specific to JET

- **Over 2 tons of beryllium PFC are installed in the main chamber of JET with the ITER-Like Wall.**
- **JET operation with metal walls has led to a significant decrease of fuel inventory and dust production in comparison to the operation with carbon walls.**
- **Beryllium splashes stick firmly to surfaces and do not form loose dust.**
- **Fuel retention in Be coatings is comparible to that in Be limiters. In both cases it is small: < 200 mg after three ILW campaigns (63 h operation).**
- **In-vessel operation with a robotic arm does not cause mobilisation of Be dust. The study was performed to respond to the request of the ITER Safety division.**

JET

Marek Rubel| Workshop on Be Technology & BeYond-IX|Karlsruhe| September 2022| Page 23

Recent papers on Be

Data on erosion and hydrogen fuel retention in beryllium plasma-facing materials
G. De Temmerman, K. Heinola, D. Borodin, S. Brezinsek, R.P. Doerner, M. Rubel, E. Fortuna et al.,
Nucl. Mater. Energy 27 (2021) 100994 https://doi.org/10.1016/j.nme.2021.100994

Dust generation and accumulation in JET-ILW: morphology and stability of co-deposits on main plasma-facing components and wall probes.
E. Fortuna-Zaleśna, T. Płociński, S.W. Moon, P. Petersson, M. Rubel, A. Widdowson
Phys. Scr. 96 (2021) 124038 https://doi.org/10.1088/1402-4896/ac2979

Fuel retention and erosion-deposition on inner wall cladding tiles in JET-ILW
L. Dittrich, P. Petersson, M. Rubel, T.T. Tran, A. Widdowson, I. Jepu, et al.,
Phys. Scr. 96 (2021) 124071 https://doi.org/10.1088/1402-4896/ac379e

Evaluation of tritium retention in plasma facing components during JET tritium operations
A. Widdowson, J.P. Coad, Y. Zayachuk, I. Jepu, E. Alves, N. Catarino, V. Corregidor et al.,
Phys. Scr. 96 (2021) 124075 https://doi.org/10.1088/1402-4896/ac3b30

An overview of tritium retention in dust particles from the JET-ILW divertor
T. Otsuka, S. Masuzaki, N. Ashikawa, Y. Torikai, Y. Hatano, M. Tokitani, Y. Oya et al.,
Phys. Scr. 97 (2022) 024008 https://doi.org/10.1088/1402-4896/ac445b

Marek Rubel| Workshop on Be Technology & BeYond-IX|Karlsruhe| September 2022| Page 24

Tools: Erosion-Deposition Diagnostics in JET-ILW
Marker Tiles and Probes

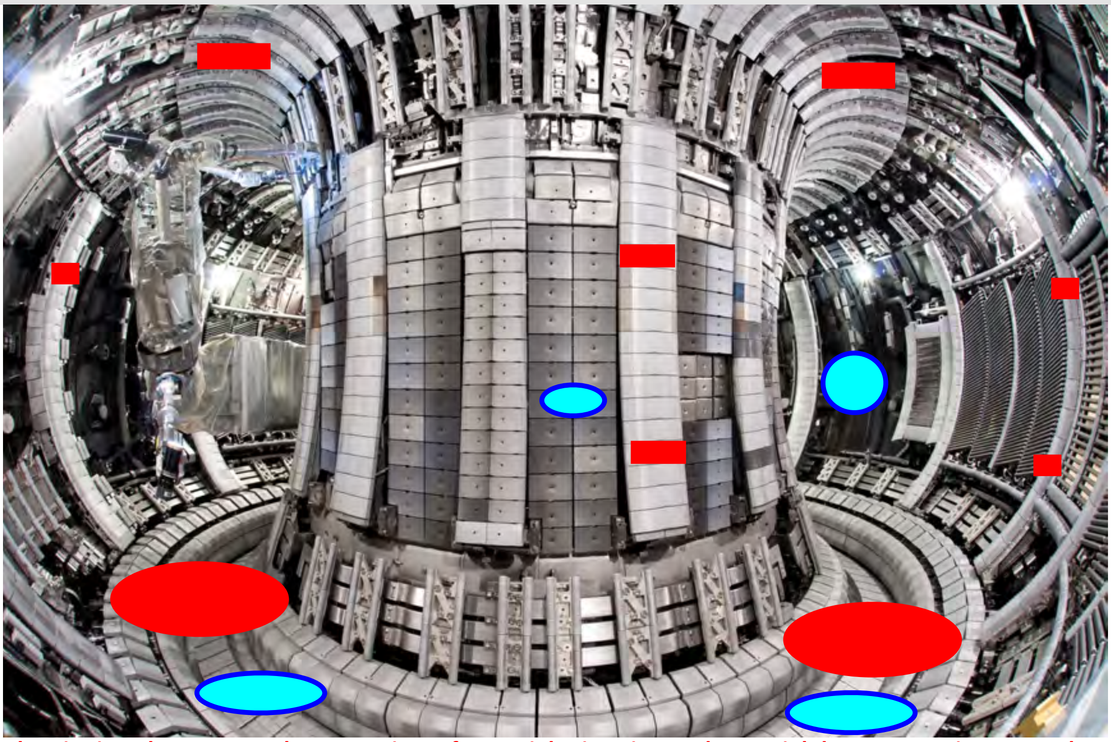

The aim is to have a complete overview of material migration and material damage, not just a number *(even large)* of analysis points and isolated findings.

ILW 2013-2014: Dust monitors

Monitor in the inner divertor

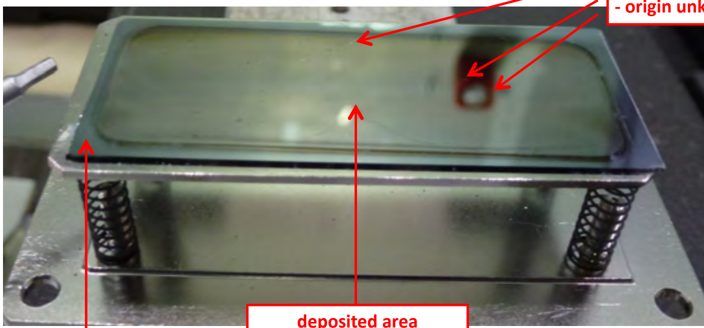

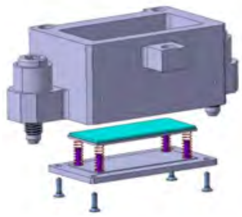

A. Widdowson, NOT published images

JET

Be Limiters: Deposition inside Castellations

Aim: Determine surface composition inside the castellations.

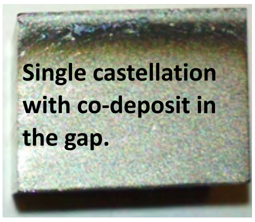

Dump Plate (DP):

O, N, decrease slightly with increasing depth.

C at 0.5×10^{17} cm^{-2}

Outer Poloidal Limiter (OPL):

No D detected close to the surface.

C at 1×10^{17} cm^{-2}

Outer Poloidal Limiter (OPL)
ILW 3

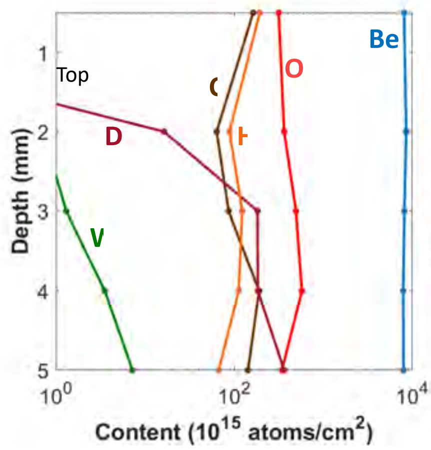

M. Rubel *et al. 2017 Nucl. Fusion* **57** 066027

JET

Thermal desorption of tritium from beryllium plasma-facing components of the JET ITER-like wall

Aigars Vītiņš[1], Elīna Pajuste[1,2], Juris Jansons[1], Gunta Ķizāne[1] and JET Contributors[*]

EUROfusion Consortium JET, Culham Science Centre, Abingdon, OX14 3DB,UK
[1] Institute of Chemical Physics, University of Latvia, One Jelgavas Street, Riga, LV-1004, Latvia
[2]Faculty of Chemistry, University of Latvia, One Jelgavas Street, Riga, LV-1004, Latvia
[*] See the author list of E. Joffrin et al., 2019 Nucl. Fusion, 59, 112021.

The JET ITER-like wall (ILW) has beryllium in the main plasma chamber and tungsten in the divertor as foreseen for the ITER vacuum vessel. Limiters and an upper dump plate of the JET vacuum vessel are bulk beryllium tiles. The goal of the ILW experimental campaigns is to characterize plasma-wall interactions and to compare plasma performance with the previous, carbon wall. One of the scientific objectives of the ILW experimental campaigns is to demonstrate sufficiently low fuel retention and, in particular, to demonstrate ITER-relevant tritium retention mitigation. The aim of the present study is to assess tritium accumulation in the beryllium tiles from the three ILW campaigns (2011-2012, 2013-2014, 2015-2016) and to investigate its thermal desorption patterns with respect to development of possible detritiation techniques. Tritium is a minor component of the fuel in the present study as tritium has not been introduced within the ILW campaigns 2011-2016. Tritium accumulation in plasma-facing tiles can occur as a result of its co-deposition with eroded material and implantation/diffusion in the bulk of the tiles.

Thermal desorption of tritium was performed in a He + 0.1% H_2 flow at 4.8 K/min from 290 to 1300 K. For inner wall samples, the surface concentration of tritium decreased in the three ILW campaigns from 83E11 (2011-2012) to 6E11 (2015-2016) atoms / cm^2. The temperature of 50% detritiation was 697 K and 880 K for these two samples respectively. For outer wall samples, the maximum value of the surface concentration of tritium 13E13 atoms / cm^2 was found for a centre sample of the 2015-2016 campaign, but the minimum value of that 0.52E13 atoms / cm^2 was for a right-hand wing sample of the 2013-2014 campaign. The temperature of 50% detritiation was 966 K and 840 K for these two samples respectively. For the 2011-2012 and 2013-2014 campaigns, both inner and outer wall samples from a tile middle part had higher temperatures of their 50% detritiation than those of the respective wing samples. The different values of the surface concentration of tritium and dissimilarity of tritium desorption patterns of the samples investigated indicate both quantitative and qualitative differences in tritium accumulation in the samples.

Acknowledgment: This work has been carried out within the framework of the EUROfusion Consortium, funded by the European Union via the Euratom Research and Training Programme (Grant Agreement No 101052200 — EUROfusion). Views and opinions expressed are however those of the author(s) only and do not necessarily reflect those of the European Union or the European Commission. Neither the European Union nor the European Commission can be held responsible for them.

Corresponding Author:

Aigars Vītiņš
aigars.vitins@lu.lv
Laboratory of Radiation Chemistry of Solids,
Institute of Chemical Physics, University of Latvia,
Four-storey building, Room 108,
32 Miera Street, Salaspils, LV-2169, Latvia

EUROfusion

UNIVERSITY OF LATVIA
INSTITUTE OF CHEMICAL PHYSICS

Thermal desorption of tritium from beryllium plasma-facing components of the JET ITER-like wall

Aigars Vītiņš[1], Elīna Pajuste[1,2], Juris Jansons[1], Gunta Ķizāne[1]
and JET Contributors*

EUROfusion Consortium JET, Culham Science Centre, Abingdon, OX14 3DB,UK
[1] Institute of Chemical Physics, University of Latvia, One Jelgavas Street, Riga, LV-1004, Latvia
[2] Faculty of Chemistry, University of Latvia, One Jelgavas Street, Riga, LV-1004, Latvia

* See the author list of E. Joffrin et al., 2019 Nucl. Fusion, 59, 112021.

BeWS-15, Karlsruhe, Germany,
14 September 2022 1

Outline

- Introduction
- Experimental procedure
- Results and discussion
- Conclusions

BeWS-15, Karlsruhe, Germany,
14 September 2022 2

Outline

- Introduction
- Experimental procedure
- Results and discussion
- Conclusions

BeWS-15, Karlsruhe, Germany,
14 September 2022 3

The JET ITER-like wall (ILW)

- Limiters and an upper dump plate of the JET vacuum vessel are castellated bulk beryllium tiles.
- One of the scientific objectives of the ILW experimental campaigns is to demonstrate sufficiently low fuel retention and, in particular, to demonstrate ITER-relevant tritium retention mitigation.
- The aim of the present study is to assess tritium accumulation in the beryllium tiles from the three ILW campaigns (2011-2012, 2013-2014, 2015-2016) and to investigate its thermal desorption patterns with respect to development of possible detritiation techniques.

BeWS-15, Karlsruhe, Germany,
14 September 2022 4

Tiles investigated

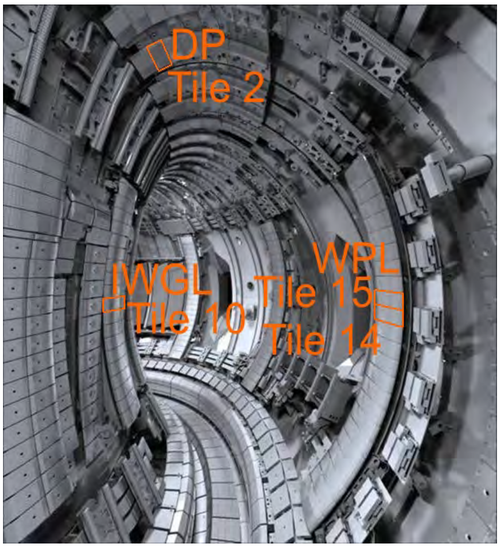

Samples for this study were cut out of the following bulk beryllium tiles of the JET ITER-Like Wall (ILW) main chamber after the JET-ILW campaigns 2011-2012 (ILW1), 2013-2014 (ILW2) and 2015-2016 (ILW3):

- Inner Wall Guard Limiter (IWGL) 2XR10
- Outer Wide Poloidal Limiter (WPL) 4D14, 4D15
- Upper Dump Plate (DP) 2BC2

BeWS-15, Karlsruhe, Germany, 14 September 2022 5

Tritium as a minor component of the fuel

- Tritium is a minor component of the fuel in the present study as tritium has not been introduced within the ILW campaigns 2011-2016 with deuterium plasma. Tritium has remained in the vacuum vessel since D-T experiments (the last of them was in 2003). Tritium can be produced in the D-D reactions and in the beryllium reactions with neutrons.
- Tritium accumulation in plasma-facing tiles can occur as a result of its co-deposition with eroded material and implantation/diffusion in the bulk of the tiles. Subsequently, tritium-containing material can be eroded and re-deposited.

BeWS-15, Karlsruhe, Germany, 14 September 2022 6

Outline

- Introduction
- **Experimental procedure**
- Results and discussion
- Conclusions

Sample preparation

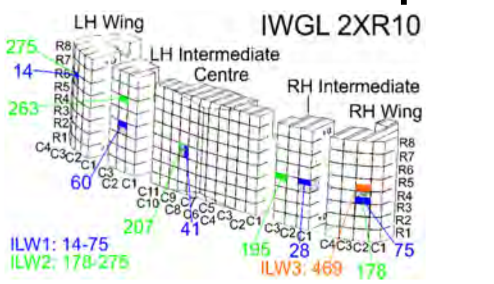

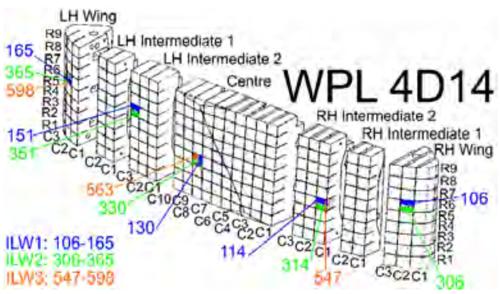

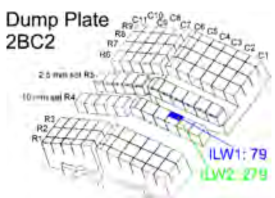

- 10 mm thick beryllium samples have been prepared by cutting individual castellations (about 12 x 12 mm) from the beryllium pieces that make up each of the tiles in the main chamber of JET.
- These samples were further cut into two parts: one for a dissolution experiment and another one for temperature-programmed desorption (TPD) of tritium.
- TPD of tritium was performed for single quarters of samples 547, 563 and 598 and for three quarters of sample 691 separately for each quarter.

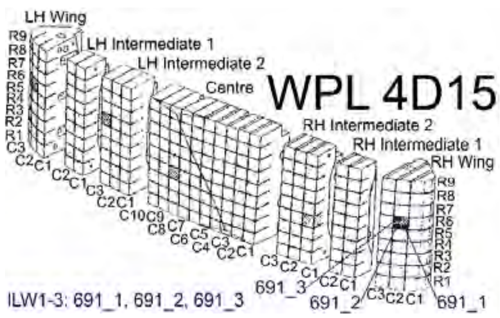

Gas flow schematic drawing of the experimental setup for TPD of tritium

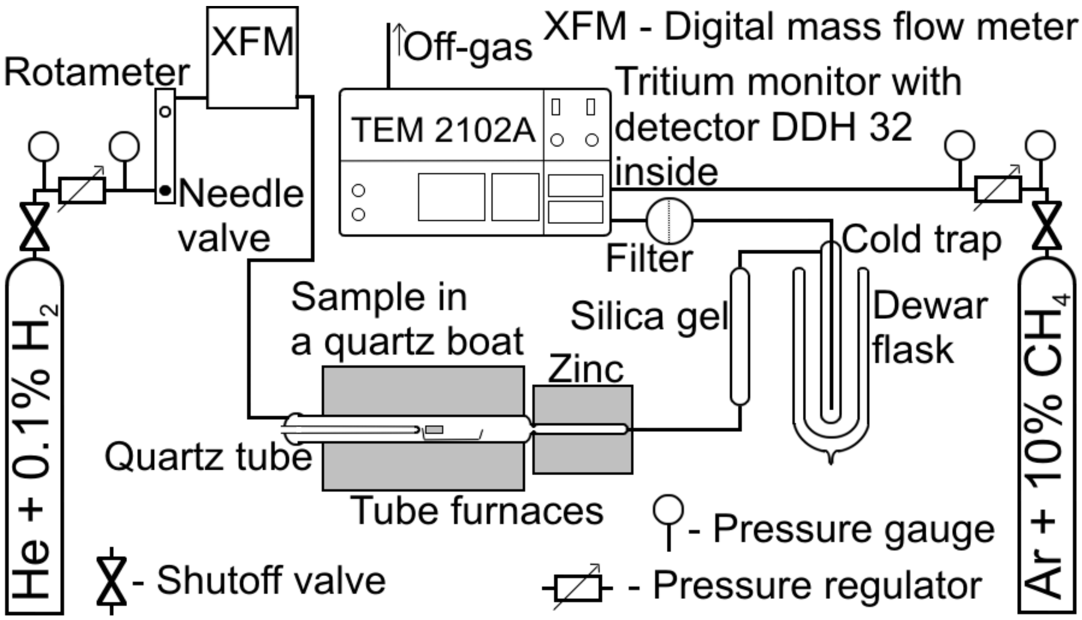

BeWS-15, Karlsruhe, Germany, 14 September 2022 9

Gas exchange time of the tritium TPD setup

- Quartz tube of 156 cm^3: 72 cm^3 - before the sample; 59 cm^3 - after the sample; 25 cm^3 – the zinc compartment.
- Column of 74 cm^3 for silica gel.
- Cold trap of 66 cm^3.
- Gas filter of 20 cm^3.
- Volume of these items of the tritium TPD setup together is about 320 cm^3.
- Purge gas He + 0.1% H_2 14-15 L/h or about 250 cm^3/min.
- The gas exchange time of the tritium TPD setup itself is about 1.3 min.

- Operating volume of tritium detector DDH 32 is 300 cm^3.
- Purge gas He + 0.1% H_2 14-15 L/h or about 250 cm^3/min.
- Counting gas Ar + 10% CH_4 42-45 L/h or about 750 cm^3/min.
- The gas exchange time of the tritium detector itself is about 18 seconds.
- According to the data of the manufacturer of DDH 32 (“MAB”, Germany), there will be 62% of the fresh gas mixture in the detector after 18 s, but 94% will be after 54 s.

- Therefore, the released tritium activity was measured repeatedly with the measuring time of 2 min.

BeWS-15, Karlsruhe, Germany, 14 September 2022 10

Temperature program and temperature measurements

- Samples were heated at a rate of 4.8 K/min to 1300 K and then kept at that temperature for 1 h.
- The temperatures of the sample, the zinc bed and the cold trap were continuously measured with an Agilent 34970A multichannel digital voltmeter with an Agilent 34902A multiplexer and recorded with a PC using the Agilent BenchLink Data Logger 3 software using type S and K thermocouples.

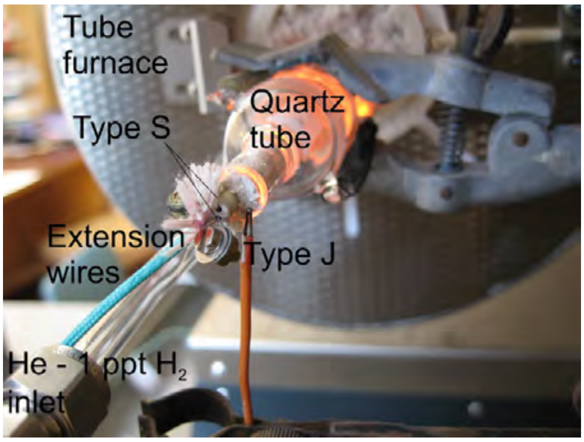

BeWS-15, Karlsruhe, Germany,
14 September 2022 11

Rationale of the tritium TPD experiments

- As tritium was a minor component of the fuel in the JET-ILW operation, the beryllium samples to be investigated may have a low tritium activity and a low tritium release.
- A blank experiment with **an unirradiated beryllium sample** in a quartz boat was performed as the first experiment in the series in order to test the system background.
- The count rate was corrected for the system background for ≥ 1 h time as determined at the start and the end of each experiment.
- The tritium release rate of the sample was calculated from the corrected count rate and the measured flow rate of the purge gas. The calibration factor for tritium was found to be 107.8 (kBq / m^3) / cps.
- The total released tritium activity was calculated by integrating the release rate over the time.
- The radioactivity of tritium released was calculated as kBq/cm^2 to 1 cm^2 of the plasma-facing surface area of the sample. The respective number of tritium atoms was found by dividing their activity [Bq] with λ = 1.782E-9 s^{-1}.
- Subsequent second heating of the same sample in the same setup with the same temperature program to 1300 K caused no significant tritium release.
- As most of tritium released during the temperature ramp of 4.8 K/min to 1300 K, the release rate and the sum release were plotted as functions of temperature.
- **In order to take tritium natural decay into account, the number of tritium atoms has been recalculated to the respective JET shutdown date.**

BeWS-15, Karlsruhe, Germany,
14 September 2022 12

Outline

- Introduction
- Experimental procedure
- **Results and discussion**
- Conclusions

TPD of tritium from the part of ILW3 Be sample 469 (2015-2016: IWGL 2XR10: R5-C2 of RH wing) (1/2)

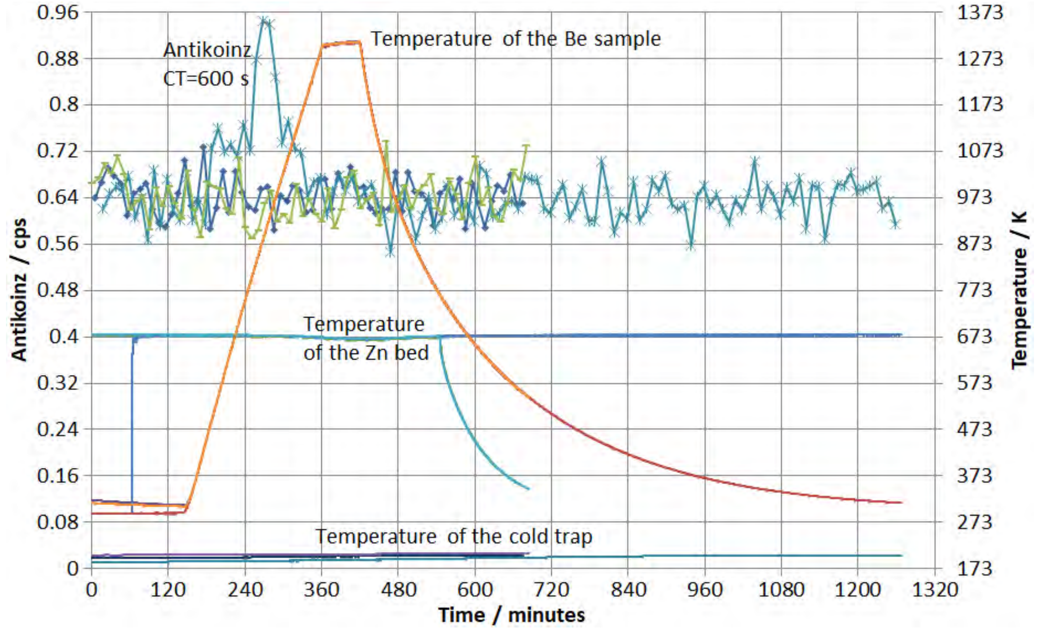

Plasma-facing surface (PFS): 0.81 cm^2

Initial background: 0.6239 cps (78’-178’)

Final background: 0.6133 cps (448’-598’)

TPD of tritium from the part of ILW3 Be sample 469 (2015-2016: IWGL 2XR10: R5-C2 of RH wing) (2/2)

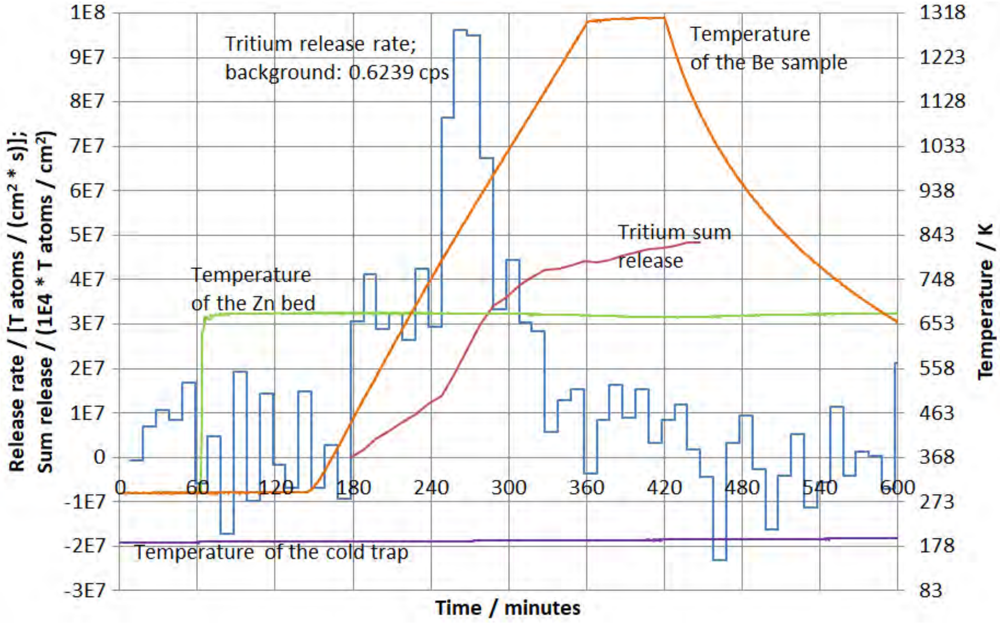

Plasma-facing surface (PFS): 0.81 cm²

Initial background: 0.6239 cps (78'-178')

Final background: 0.6133 cps (448'-598')

BeWS-15, Karlsruhe, Germany,
14 September 2022

15

IWGL: Tritium fractional release rate at 4.8 K/min

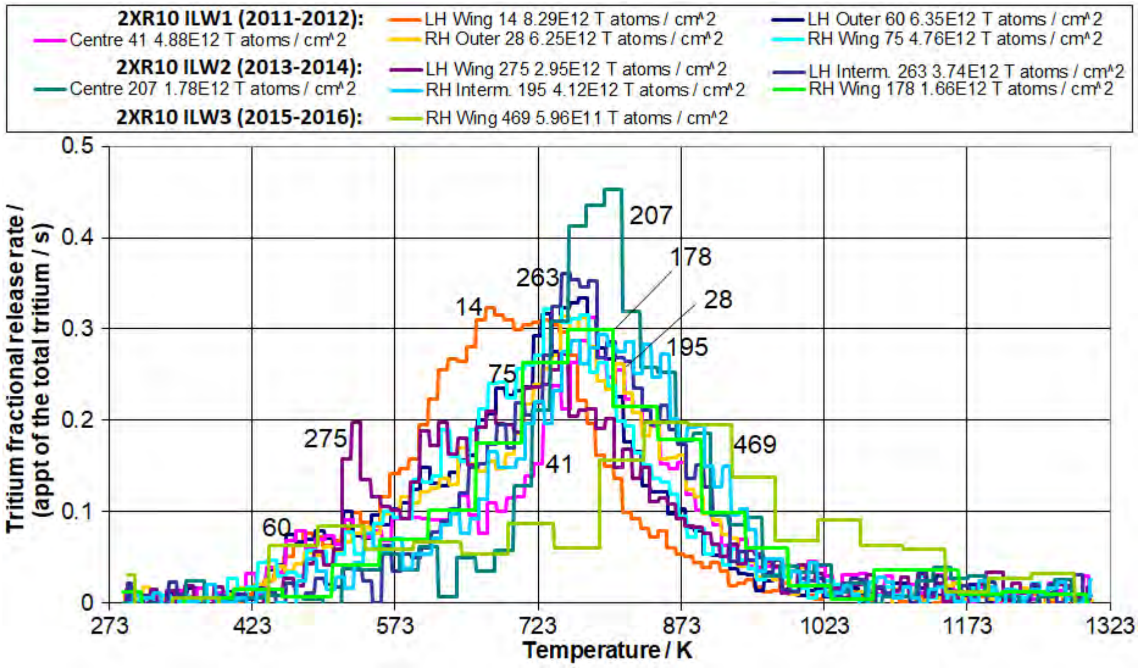

BeWS-15, Karlsruhe, Germany,
14 September 2022

16

IWGL: Released fraction of the total tritium

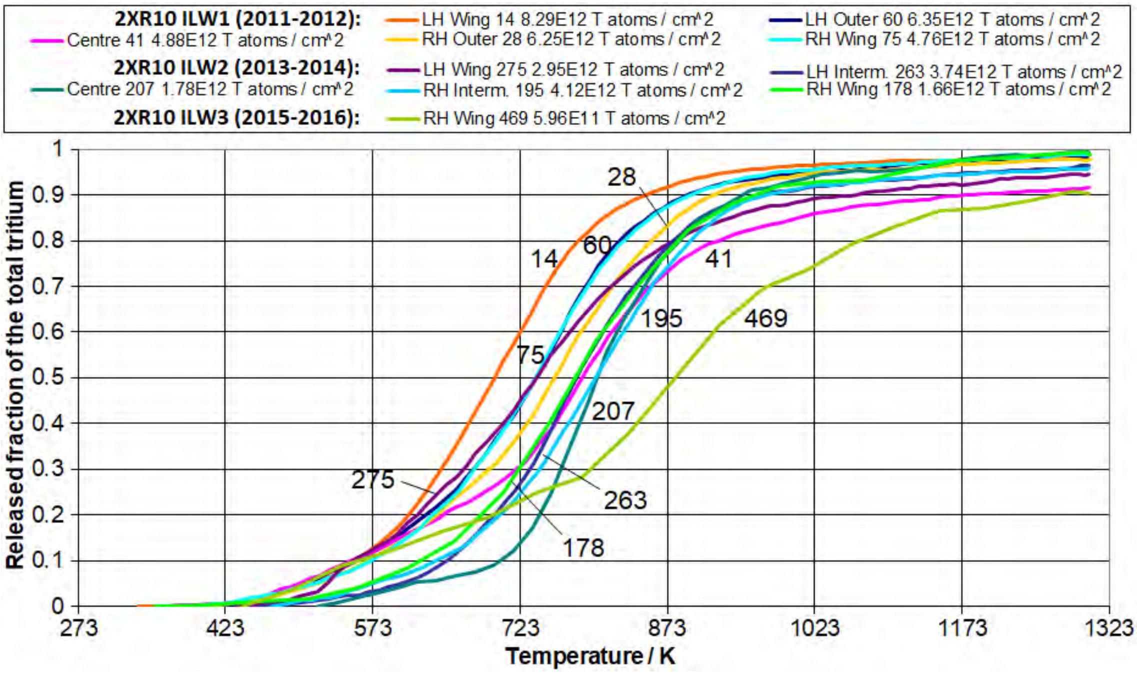

BeWS-15, Karlsruhe, Germany, 14 September 2022 17

IWGL 2XR10: Thermal desorption of tritium

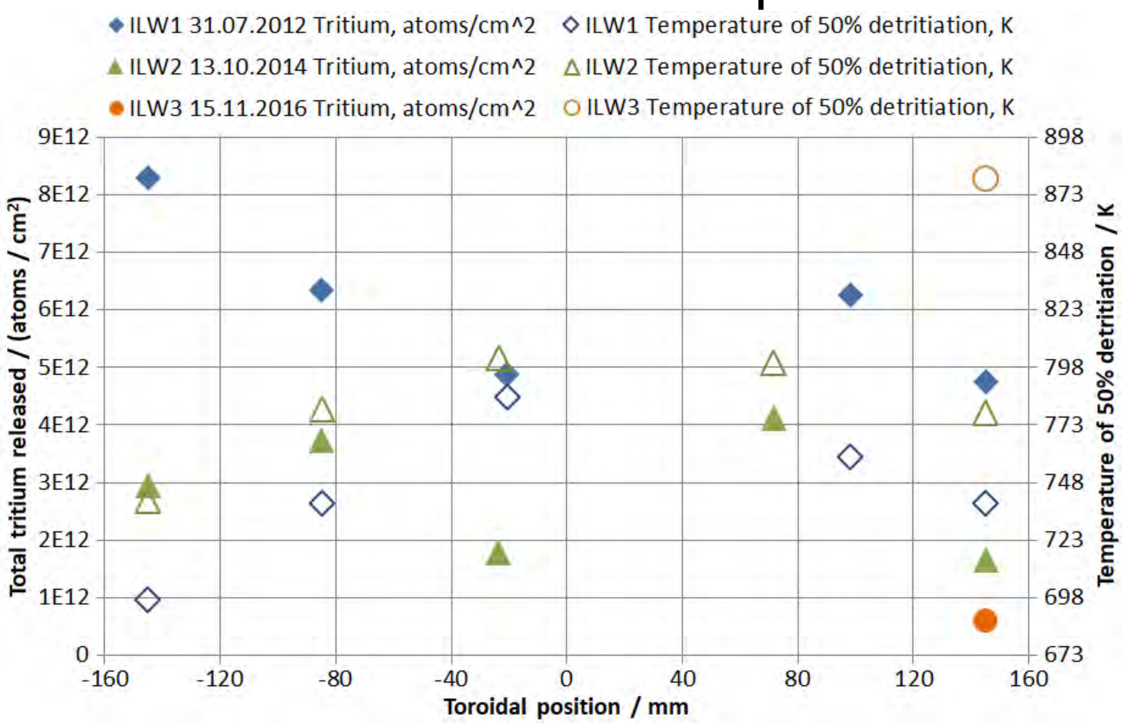

BeWS-15, Karlsruhe, Germany, 14 September 2022 18

Dump plate 2BC2, R4-C3: Thermal desorption of tritium at 4.8 K /min

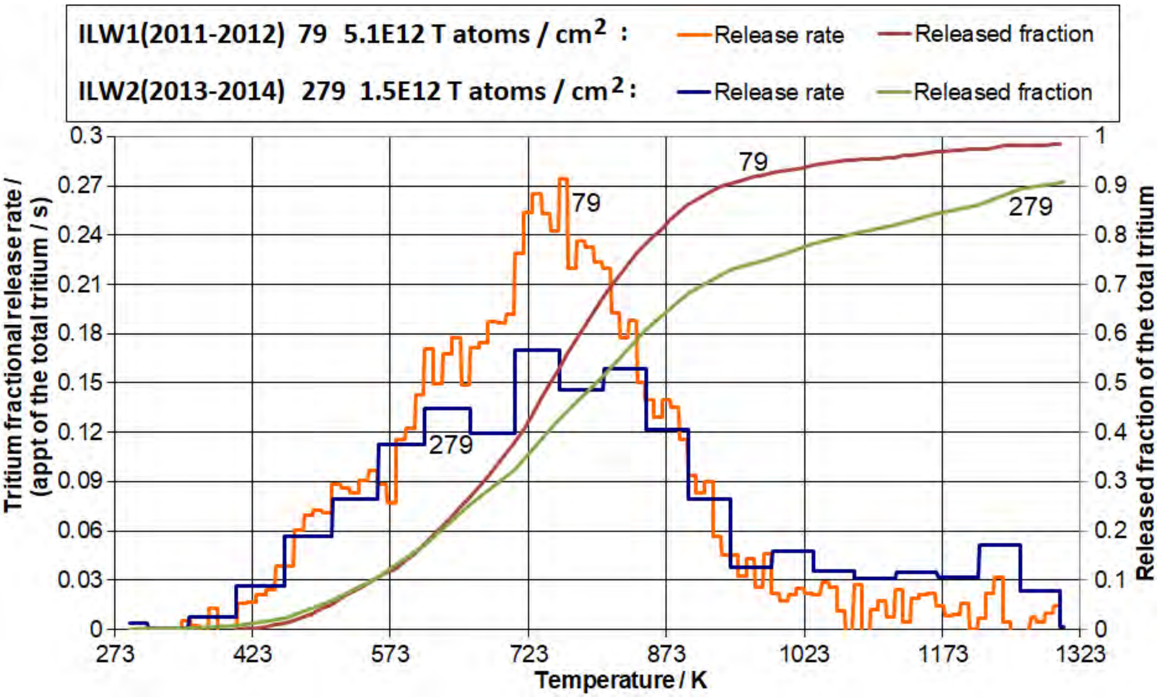

BeWS-15, Karlsruhe, Germany, 14 September 2022 19

TPD of tritium from quarters 1-3 of ILW1-3 Be sample 691 (2011-2016: WPL 4D15: R6-C2 of RH wing) (1/2)

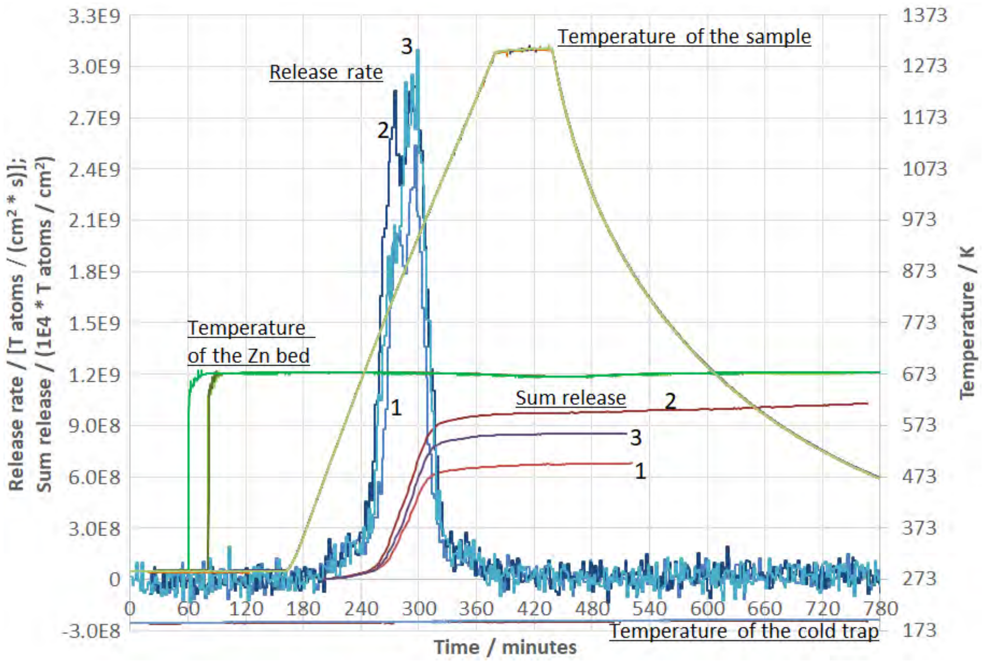

BeWS-15, Karlsruhe, Germany, 14 September 2022 20

TPD of tritium from quarters 1-3 of ILW1-3 Be sample 691 (2011-2016: WPL 4D15: R6-C2 of RH wing) (2/2)

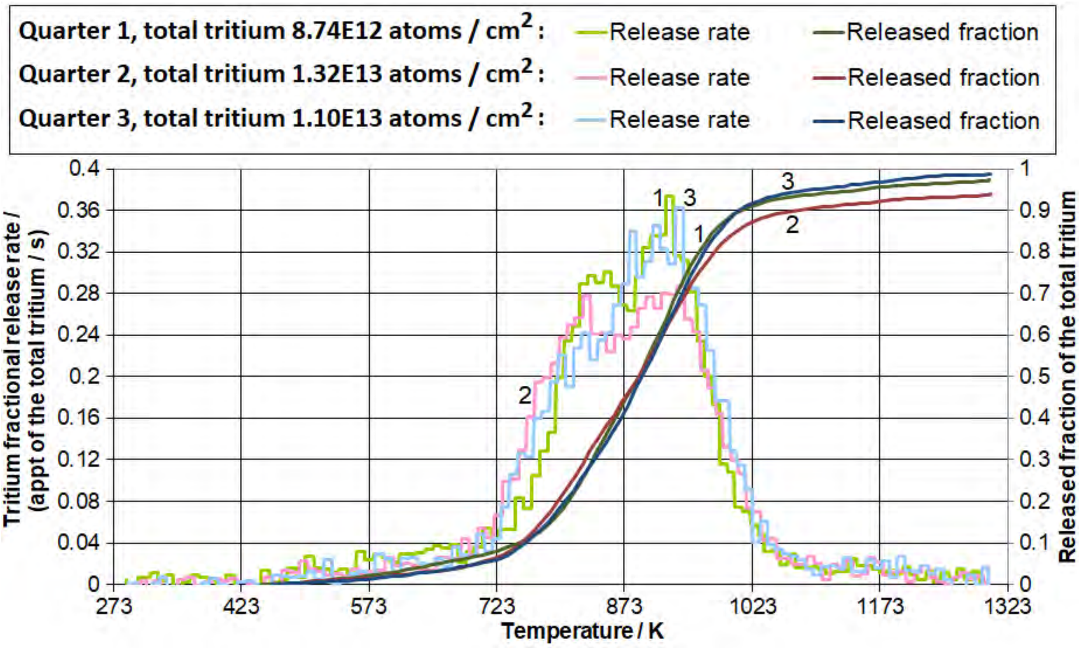

BeWS-15, Karlsruhe, Germany, 14 September 2022 21

WPL: Tritium fractional release rate at 4.8 K/min

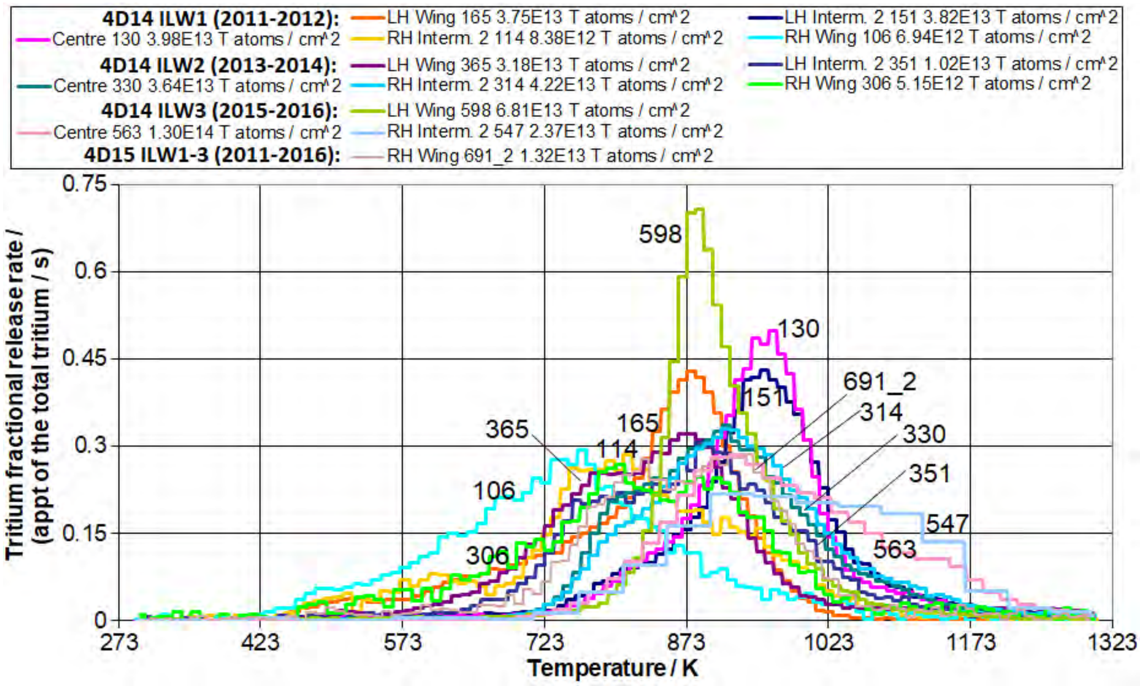

BeWS-15, Karlsruhe, Germany, 14 September 2022 22

WPL: Released fraction of the total tritium

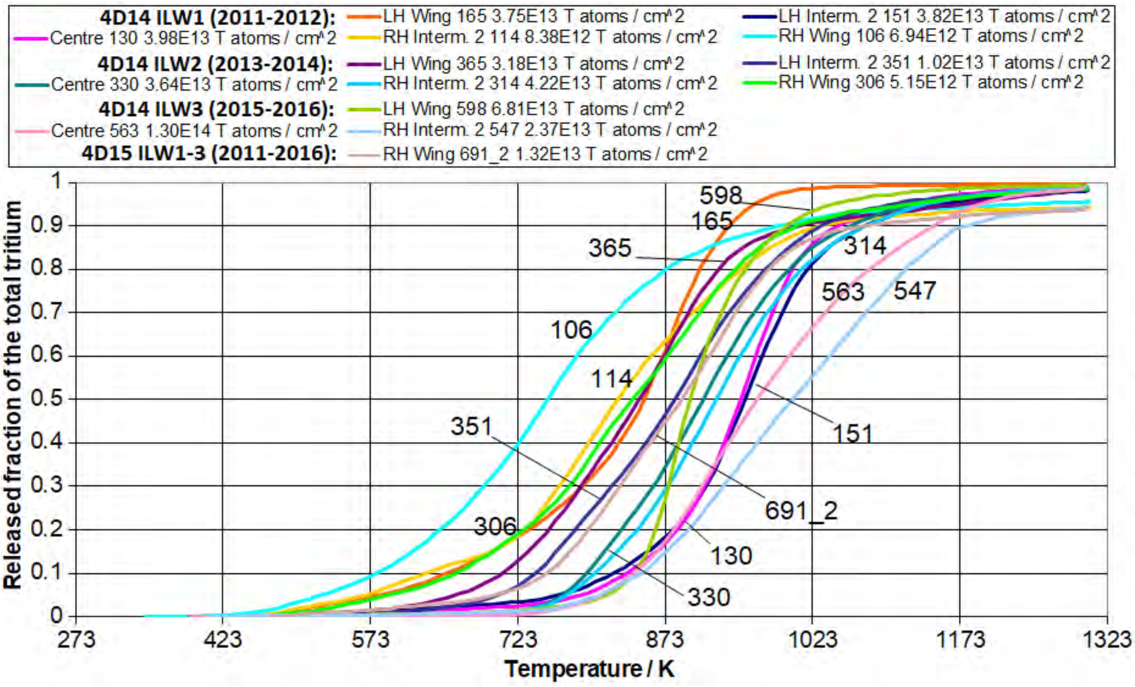

BeWS-15, Karlsruhe, Germany,
14 September 2022 23

WPL: Thermal desorption of tritium

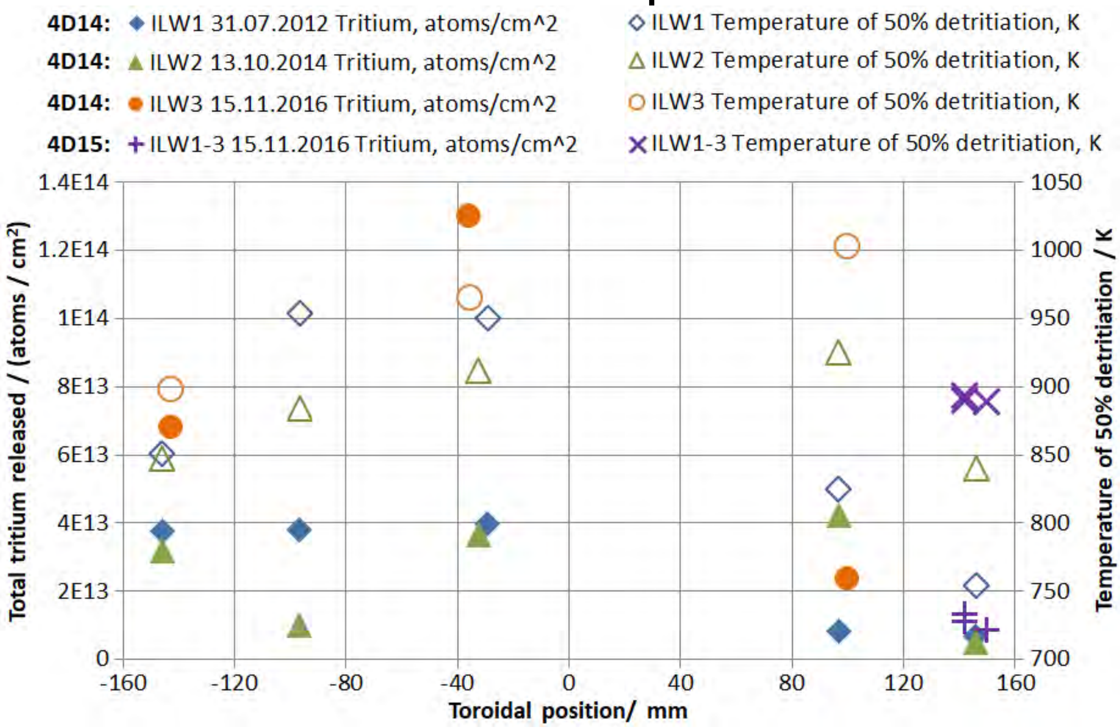

BeWS-15, Karlsruhe, Germany,
14 September 2022 24

Outline

- Introduction
- Experimental
- Results and discussion
- Conclusions

BeWS-15, Karlsruhe, Germany, 14 September 2022 25

Conclusions about IWGL 2XR10 samples

1. For the inner wall samples investigated in the present study, the surface concentration of tritium gradually decreased in the three ILW campaigns. The maximum of 83E11 atoms / cm^2 was found for the LH Wing sample of ILW1 (2011-2012), and the minimum of 6E11 atoms / cm^2 was for the RH Wing sample of ILW3 (2015-2016). The temperature of 50% detritiation was 697 K and 880 K for these two samples respectively.
2. The samples had quite different thermal desorption spectra of tritium indicating different tritium accumulation in the samples. The ILW2 (2013-2014) samples had by 17-43 K higher temperature of 50% detritiation than the respective ILW1 (2011-2012) samples. For ILW1 and ILW2 samples, the temperature of 50% detritiation gradually decreased from the centre towards the wings by 24-88 K. For all the samples, the temperature of 50% detritiation was in the range of 697-880 K.

BeWS-15, Karlsruhe, Germany, 14 September 2022 26

Conclusions about Upper Dump Plate 2BC2 samples

1. The ILW2 (2013-2014) sample had by a factor of >3 lower surface concentration of tritium than that of the respective ILW1 (2011-2012) sample: 1.5E12 and 5.1E12 atoms / cm^2.
2. The tritium release curves had a single main maximum, but the temperature of 50% detritiation of the ILW2 (2013-2014) sample, 796 K, was by 49 K higher than that of the ILW1 (2011-2012) sample, 747 K.

BeWS-15, Karlsruhe, Germany,
14 September 2022 27

Conclusions about WPL samples

1. The surface concentration of tritium of the 4D14 samples depends strongly both on the ILW campaign and on their toroidal position. The highest value of 130E12 atoms / cm^2 was found for the Centre sample of ILW3 (2015-2016), and the lowest value of 5E12 atoms / cm^2 was for the RH Wing sample of ILW2 (2013-2014). The temperature of 50% detritiation was 966 K and 840 K for these two samples respectively.
2. The 4D14 samples had different thermal desorption spectra of tritium indicating different tritium accumulation in the samples. For all the 4D14 samples investigated, the temperature of 50% detritiation was in the range of 754-1003 K. At 1181 K, all the 4D14 samples investigated had ≥90% detritiation.
3. The three quarters of castellation R6-C2 of RH Wing of tile 4D15 from the ILW1-3 (2011-2016) campaigns had following values the total tritium: 8.7E12, 13.2E12 and 11.0 E12 atoms / cm^2. Their temperatures of 50% detritiation were 889-894 K. But their temperatures of 90% detritiation were in a broader range of 1009-1078 K.

BeWS-15, Karlsruhe, Germany,
14 September 2022 28

Acknowledgements

- This work has been carried out within the framework of the EUROfusion Consortium, funded by the European Union via the Euratom Research and Training Programme (Grant Agreement No 101052200 — EUROfusion).
- Views and opinions expressed are however those of the author(s) only and do not necessarily reflect those of the European Union or the European Commission. Neither the European Union nor the European Commission can be held responsible for them.

BeWS-15, Karlsruhe, Germany,
14 September 2022

29

A Study on Technician Variability in Wipe Sampling for Beryllium & Potential Contributions to Robotic Sampling Equipment

Eilish McKEON[1], Amy BLEASDALE[1], Christopher DORN[1], Maddy KEARNEY[1], Jon VERDON[1], and Heather LEWTAS[1]

[1]*UK Atomic Energy Authority, Culham Centre for Fusion Energy, Abingdon, U.K.*

The Joint European Torus (JET) is the largest operational magnetically confined fusion research reactor in the world, beginning operations in 1983. Beryllium (Be) was first installed in JET in 1989, which gives the UKAEA a high level of experience and expertise in the safe handling, storage, and disposal of this high-performance but toxic material.

The UKAEA's Health Physics Group (HPG) is comprised of a team of trained technicians and analysts who support an on-site Be handling facility and operate a Be analysis laboratory, in which accredited processes are certified to UKAS ISO 17025. The laboratory capabilities enable the UKAEA to carry out technical studies involving beryllium in a controlled, safe environment by using established air and surface sampling techniques to monitor conditions over a study's specified experiments and any related activities.

To date, surface sampling for beryllium, known on the Culham site as "smearing", has been performed by HP technicians trained in defined, manual processes. Others' studies in recent years have looked at collection efficiencies between the sampling media being used and the type of beryllium compound being sampled. Given the manual nature of the task, natural variations occur from person to person, and building on the aforementioned research, UKAEA has decided to investigate the impact of force exerted by a technician during the sampling process.

This presentation gives an overview on the history of beryllium use at JET, surface sampling processes used on site, a summary of the pilot study in progress, and how these manual studies are contributing to further research into robotic sampling equipment in challenging environments.

Corresponding Author:

Ms. Eilish McKEON
eilish.mckeon@ukaea.uk
Postal address:
UK Atomic Energy Authority
Culham Centre for Fusion Energy
Abingdon, Oxfordshire OX14 3DB,
United Kingdom

UK Atomic Energy Authority

UKAEA

A Study on Technician Variability in Wipe Sampling for Beryllium & Potential Contributions to Robotic Sampling Equipment

E. McKEON, A. BLEASDALE, C. DORN, M. KEARNEY, J. VERDON & H. LEWTAS

15th International Workshop on Beryllium Technology & BeYOND-IX Industrial Forum

Karlsruhe Institute of Technology, Karlsruhe, Germany • 14-16 September 2022

BeWS-15 2022 15th International Workshop On Beryllium Technology Karlsruhe, Germany 14-15 September 2022

SPECIAL JOINT EVENT

BeYOND-IX 2022 9th Industrial Forum on Beryllium Opportunities & New Developments Karlsruhe, Germany 16 September 2022

UK Atomic Energy Authority

Presentation Plan

- **Part 1: Introduction / Background**
  - ❖ *Presenter: Chris Dorn*
  - Overview of the Joint European Torus (JET)
  - History of Beryllium Use in JET
  - Sampling Programme at UKAEA
- **Part 2: Technician Variability Study**
  - ❖ *Presenter: Eilish McKeon*
  - Assumptions, Impetus & Prior Work
  - Purpose & Scope
  - Project Outline & Milestones
- **Part 3: Robotic Surface Wiping**
  - ❖ *Presenters: Maddy Kearney & Jon Verdon*
  - Background: Robotics & AI in Nuclear (RAIN)
  - Glovebox Wiping
    - Tool Design & Trials
    - Future Work

Culham Centre for Fusion Energy, Abingdon, Oxfordshire, UK

2 Beryllium Wipe Sampling Variability Study – BeWS-15 & BeYOND-IX – Sep-2022

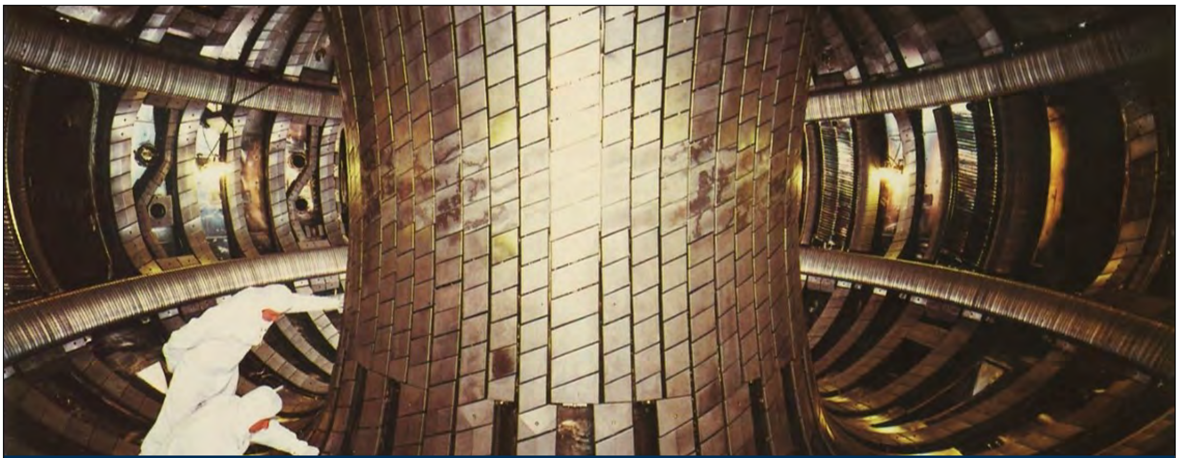

Part 1: Introduction / Background

Presenter: CHRIS DORN

Overview of the Joint European Torus (JET)

UK Atomic Energy Authority

- 1978: JET construction starts
- 1983: First plasma in JET
- 1989: First installation of beryllium in JET
- 1991: First experiments with tritium
- 1997: High-performance, full deuterium-tritium experiments. JET achieves world record fusion power of 16.1MW.
- 2009-10: JET installs ITER-Like Wall: beryllium & tungsten
- 2019-20: Preparations well advanced for new deuterium-tritium experiments, designed to sustain high fusion performance for longer periods.

[1]

Above: Beryllium RF Antenna Tiles Production Sequence [2][3]

Left: JET Reactor c.1982-83

Right: JET Reactor c.1990 with Be Belt Limiters Installed

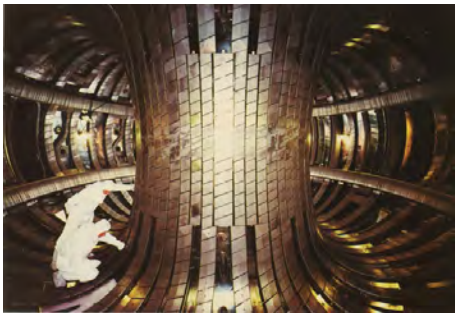

4 Beryllium Wipe Sampling Variability Study – BeWS-15 & BeYOND-IX – Sep-2022

History of Beryllium Use in JET

UK Atomic Energy Authority

- More than just laboratory-scale use of beryllium in fusion research began at JET in 1989
- UKAEA understood the need to monitor for airborne beryllium to comply with applicable UK standards
- Based on experience in radiation protection, UKAEA also foresaw the need to monitor for beryllium surface particulate
- As a result, UKAEA developed a surface sampling method for beryllium, in conjunction with Sandia National Lab (USA)
  - Dry wiping using Whatman Grade 1 filter papers
  - Analysis of collected samples done on site
- Surface sampling is just one part of the overall UKAEA Beryllium Management Programme

Right: JET Reactor c.2010-11 with Beryllium ITER-Like Wall Installed [3][4]

Below: ITER-Like Wall Beryllium Tile (Courtesy of Axsys Technologies PMP) [5]

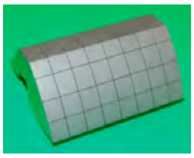

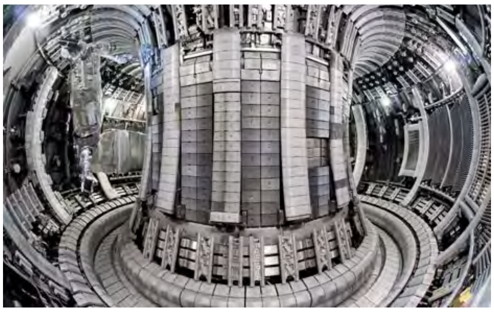

5 Beryllium Wipe Sampling Variability Study – BeWS-15 & BeYOND-IX – Sep-2022

Sampling Programme at UKAEA

UK Atomic Energy Authority

- Unlike for airborne beryllium, there are no national or international standards for beryllium surface contamination
- UKAEA created its own internal standards and action levels for beryllium surface contamination
  - Transfer of items from one designated area to another
  - Clearance of items from designated areas entirely
  - Action levels: trigger the creation of designated areas
- UKAEA has used the same beryllium surface sampling method to support JET operations, but we have also developed other processes for external customers

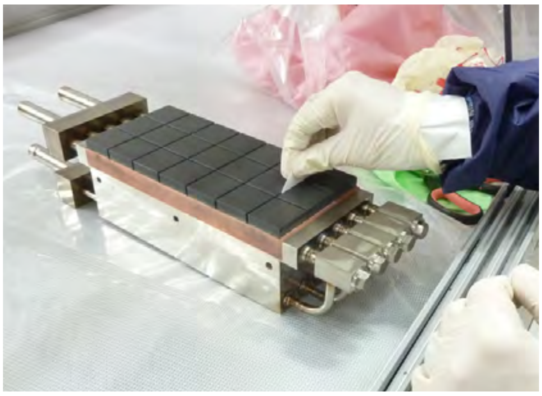

Wipe sampling with dry Whatman filter paper of beryllium tile surfaces

6 Beryllium Wipe Sampling Variability Study – BeWS-15 & BeYOND-IX – Sep-2022

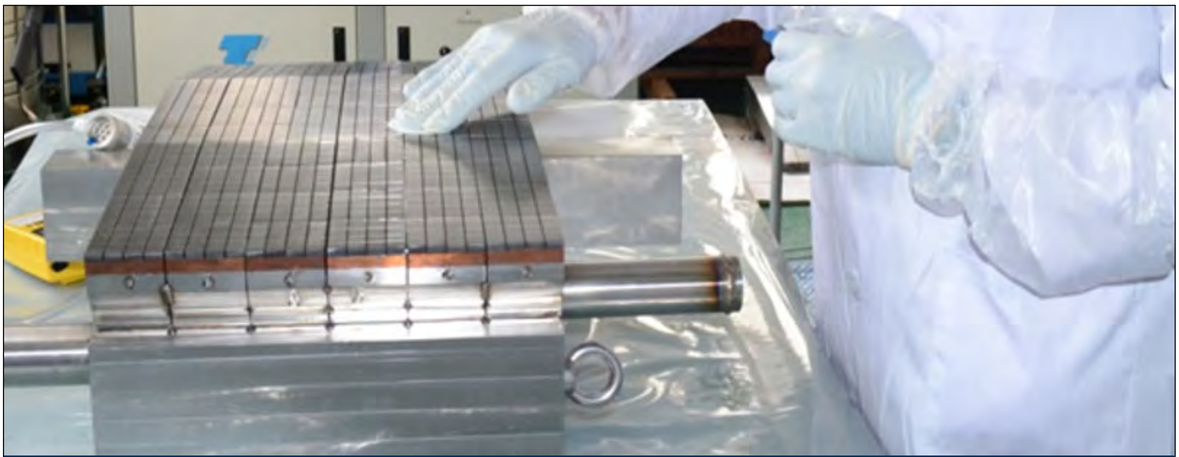

Part 2: Technician Variability Study

Presenter: EILISH McKEON

Background: Assumptions, Impetus & Prior Work

UK Atomic Energy Authority

- **Original Baseline Assumption**
  - Cleaning effect: each successive sample for removable beryllium taken from the same area should give a progressively lower result
  - Does not take into account samples collected from solid Be surfaces
- **Impetus**
  - Long-term study with surface sampling as integral part
  - Due to staff changes over the duration of the study, several technicians were used to collect surface samples
  - Results did not always consistently follow expectations
- **Prior Work**
  - Damjanovic, 2019: *Comparison of Collection Efficiencies of Whatman No. 1 Filter Paper and Ghost Wipes for Loose Beryllium Surface Contamination* (presented at BeWS-14) [6]

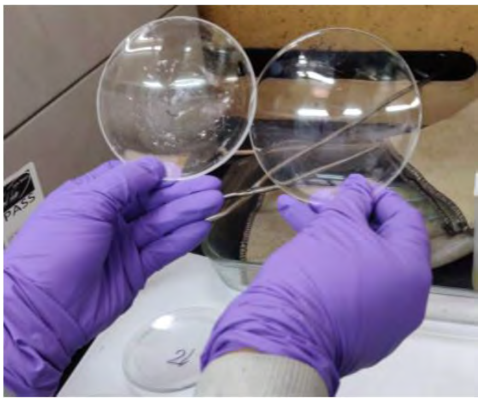

Glass plates spiked with beryllium-containing solution in known amounts were used in the previous study [6]

8 Beryllium Wipe Sampling Variability Study – BeWS-15 & BeYOND-IX – Sep-2022

Purpose & Scope

- **Purpose of the Study**
  - Determine an uncertainty factor that can be applied to surface sampling results for removable beryllium that incorporates the effects of pressure exerted during the sampling process
- **Scope of Work**
  - Procuring pressure-measuring equipment
  - Manufacturing a pressure rig (test fixture)
  - Spiking a defined surface with known concentrations of beryllium
  - Measuring pressure ranges exerted by a number of individual technicians
  - Measuring the amount of beryllium detected
  - Determining the results are correlated and if so, determining an uncertainty factor which can be applied to analytical results incorporating the uncertainty from the sampling and analytical processes. (Analytical uncertainty is already accounted for.)

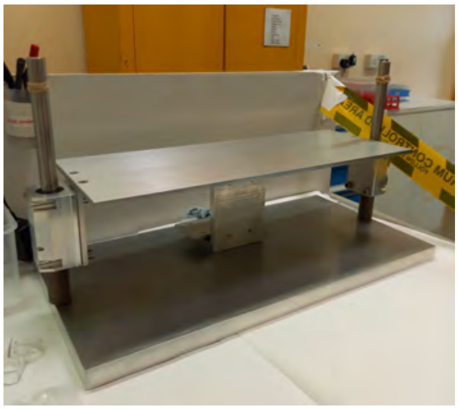

Pressure rig (test fixture) built at UKAEA and used in the study (the force gauge is not installed in this view). Design credit: Materion Corp., Ohio, USA Shown here with kind permission [7]

9 Beryllium Wipe Sampling Variability Study – BeWS-15 & BeYOND-IX – Sep-2022

Project Outline & Milestones

Deliverables have been defined for the project as follows:

- **Preparatory Stage**
  - Experiment Design
  - Intellectual Property Investigation
  - Procurement & Manufacture of Components
  - Data Protection Requirements & Permissions
- **Experimental Stage**
  - Gathering Data
  - Analysing Data
- **Reporting Results**
  - Internal Report Write-Up
  - Authoring a Scientific Paper
  - Peer Review & Publication
- **Future Work**
  - Consider Investigation of Other Variables

Technicians prepare standardised beryllium samples in a temporary controlled area set up in the Analytical Laboratory at UKAEA expressly for the purposes of this study

10 Beryllium Wipe Sampling Variability Study – BeWS-15 & BeYOND-IX – Sep-2022

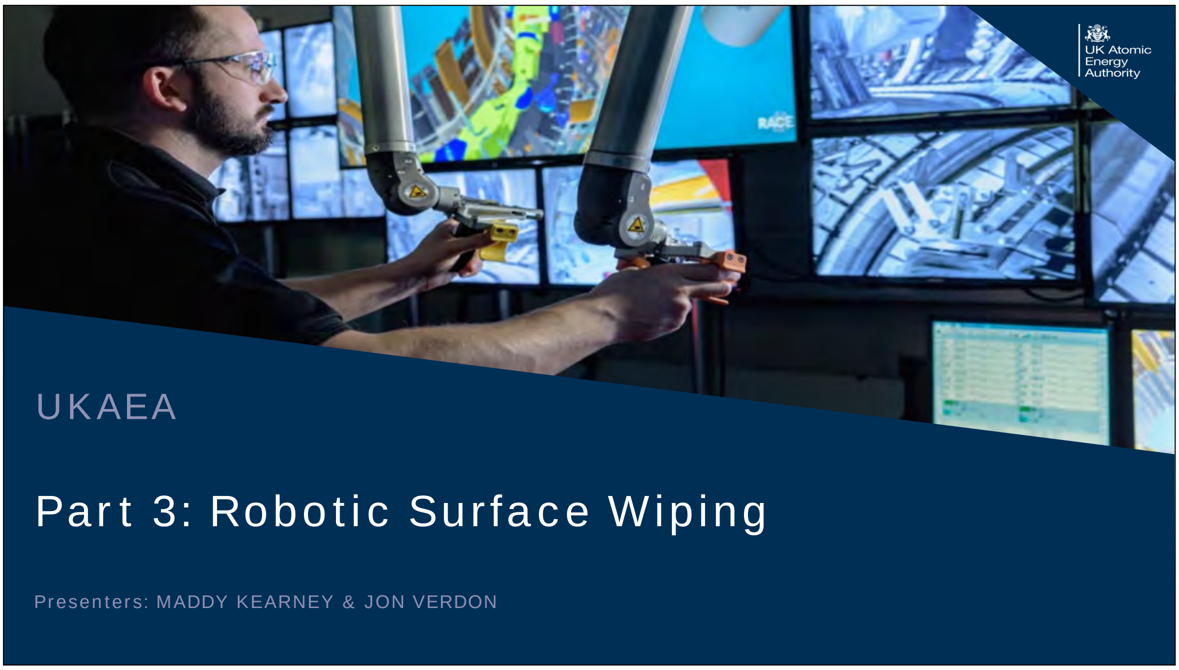
UK Atomic Energy Authority
RACE
UKAEA
Part 3: Robotic Surface Wiping
Presenters: MADDY KEARNEY & JON VERDON

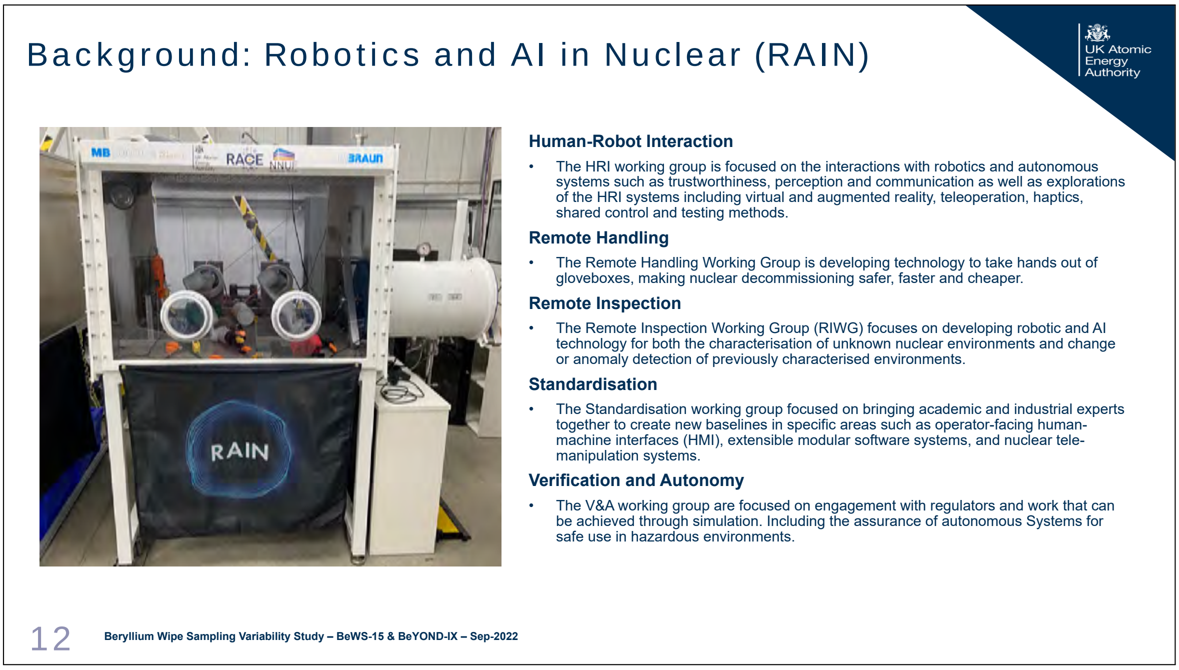
Background: Robotics and AI in Nuclear (RAIN)
UK Atomic Energy Authority
MB
RACE
BRAUN
RAIN
Human-Robot Interaction
• The HRI working group is focused on the interactions with robotics and autonomous systems such as trustworthiness, perception and communication as well as explorations of the HRI systems including virtual and augmented reality, teleoperation, haptics, shared control and testing methods.
Remote Handling
• The Remote Handling Working Group is developing technology to take hands out of gloveboxes, making nuclear decommissioning safer, faster and cheaper.
Remote Inspection
• The Remote Inspection Working Group (RIWG) focuses on developing robotic and AI technology for both the characterisation of unknown nuclear environments and change or anomaly detection of previously characterised environments.
Standardisation
• The Standardisation working group focused on bringing academic and industrial experts together to create new baselines in specific areas such as operator-facing human-machine interfaces (HMI), extensible modular software systems, and nuclear tele-manipulation systems.
Verification and Autonomy
• The V&A working group are focused on engagement with regulators and work that can be achieved through simulation. Including the assurance of autonomous Systems for safe use in hazardous environments.
12
Beryllium Wipe Sampling Variability Study – BeWS-15 & BeYOND-IX – Sep-2022

Glovebox Wiping Tool Design & Trials (1)

UK Atomic Energy Authority

1.

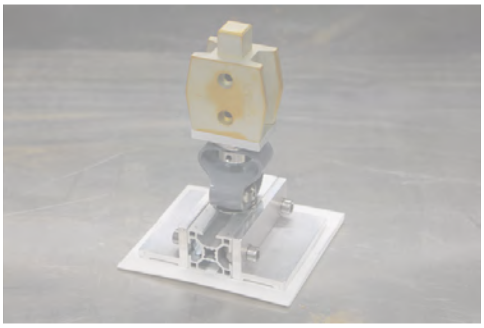

Final prototype wiping tool with robotic interface

2.

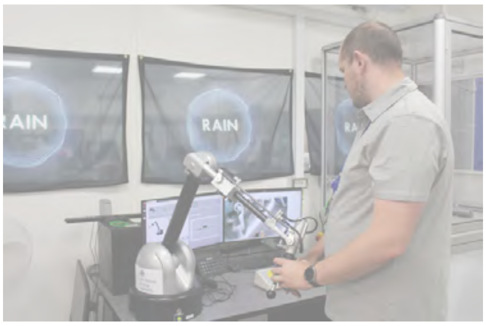

Remote Handling Operator using teleoperation to operate the robot

13 Beryllium Wipe Sampling Variability Study – BeWS-15 & BeYOND-IX – Sep-2022

Glovebox Wiping Tool Design & Trials (2)

UK Atomic Energy Authority

3.

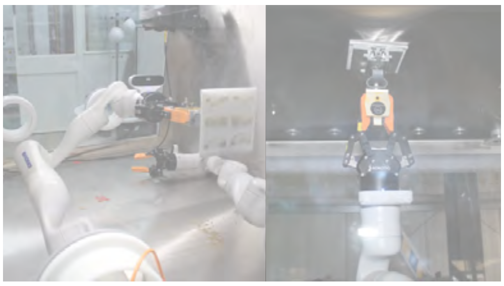

Robot demonstrating that it can wipe all surfaces

4.

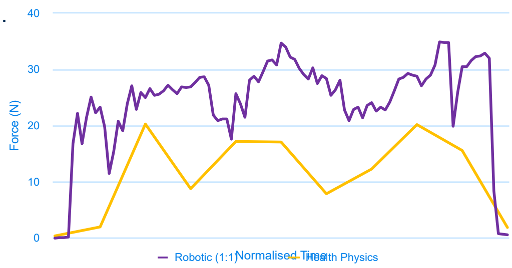

Comparison of forces from a robotic wipe and trained professionals' wipe.

14 Beryllium Wipe Sampling Variability Study – BeWS-15 & BeYOND-IX – Sep-2022

Future Work (1)

- **Redesigning the current hook and loop attachment system**: need to overcome the following issues:
  - Creation of high spots
  - Trapping of contaminants by high surfaces
  - Inability to work with wet media
- Plan to design a quick-release system that will not require the wipe (i.e., the media) to be modified

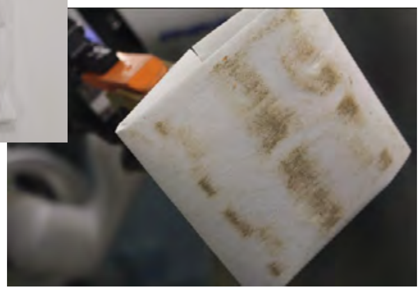

UK Atomic Energy Authority

15 Beryllium Wipe Sampling Variability Study – BeWS-15 & BeYOND-IX – Sep-2022

Future Work (2)

- **Design full life cycle of operation:** involves robotically cleaning an area, swabbing, analysing, and reading results, all within a glovebox using robotics.
  - Picking-up tool
  - Wiping surfaces
  - Removal of wipes
  - Safe disposal of wipes with no human contact

UK Atomic Energy Authority

16 Beryllium Wipe Sampling Variability Study – BeWS-15 & BeYOND-IX – Sep-2022

Future Work (3)

- **Using Health Physics results to automate wiping.**
  - Data taken from observing and recording experienced technicians
  - With automation, all parameters can be controlled.
    - Force
    - Speed
    - Wiping pattern
- **Comparing humans, automation, and teleoperation (future paper).**
  - Speed
  - Pick-up
  - Forces

Pressure rig (test fixture) with force gauge installed taking readings from robotic wiping.

Design credit: Materion Corp., Ohio, USA Shown here with kind permission [7]

17 **Beryllium Wipe Sampling Variability Study – BeWS-15 & BeYOND-IX – Sep-2022**

References & Credits

[1] UK Atomic Energy Authority. URL: https://ccfe.ukaea.uk/research/joint-european-torus/. Accessed on 18-Aug-2022.

[2] Brush Wellman Inc. *Designing With Beryllium*, Section 3 “Properties of Mill Products”. Brush Wellman Inc., Cleveland, Ohio, USA, 1999, pp.9-14.

[3] Dorn, C., Vidal, E., Goods, S. “Beryllium Materials for Fusion Reactor Wall Applications”. *Proceedings of the 13th International Workshop on Beryllium Technology (BeWS-13)*, held in Narita, Japan, 2017.

[4] European Fusion Development Agreement (EFDA) and Joint European Torus (JET). ITER-Like Wall Project, Original URL: http://www.efda.org/jet/, 2009.

[5] Acreman, M., Gossett, D., Dorn, C., Hattan, L. “Manufacturing of Beryllium Tiles for the JET ITER-Like Wall Project”. *Proceedings of the 9th International Workshop on Beryllium Technology (BeWS-9)*, held in Almaty, Kazakhstan, 2009.

[6] Damjanovic, M. “Comparison of Collection Efficiencies of Whatman No. 1 Filter Paper and Ghost Wipes for Loose Beryllium Surface Contamination”. *Proceedings of the 14th International Workshop on Beryllium Technology (BeWS-14)*, held in Long Beach, California, U.S.A., 2019, pp. 324-346. Lemmens Medien GmbH, 2021.

[7] Materion Corp., Mayfield Heights, Ohio, USA, 2021.

18 **Beryllium Wipe Sampling Variability Study – BeWS-15 & BeYOND-IX – Sep-2022**

SESSION 4

Beryllides

Overview of activities in Kazakhstan related to study of beryllium and beryllium compounds

A. Shaimerdenov[1,2], T. Kulsartov[2,3], I. Kenzhina[1,2,4*], Zh. Zaurbekova[2,3], Y. Kenzhin[4], Y.V. Chikhray[2], S. Udartsev[5]

[1]The Institute of Nuclear Physics, Almaty, Kazakhstan - 1
[2]al-Farabi Kazakh National University, Almaty, Kazakhstan - 2
[3]Institute of Atomic Energy of the National Nuclear Center of the Republic of Kazakhstan, Kurchatov, Kazakhstan - 3
[4]Kazakh-British Technical University, Almaty, Kazakhstan - 4
[5]Ulba Metallurgical Plant, Ust-Kamenogorsk, Kazakhstan - 5

Kazakhstan is one of the world leaders in the production of beryllium and beryllium products. Since recently, the Ulba Metallurgical Plant has set up production of beryllium-based intermetallic compounds; in particular, beryllides of titanium, chromium, molybdenum, etc. are produced. Beryllides are candidate materials for fusion plants as a neutron multiplier. In addition, beryllides are considered as a material for hydrogen storage. On the basis of research reactors in Kazakhstan, studies are being conducted on the effects of neutron irradiation on the properties of beryllium and beryllides. This paper provides an overview of research programs in Kazakhstan to study the radiation resistance of metallic beryllium of different grades and beryllides.

Corresponding Author:

Dr. Inesh Kenzhina
kenzhina@physics.kz
99/1 Nauryzbay batyra str., 94 app., 050000, Almaty, Kazakhstan.

15th International Workshop on Beryllium Technology (BeWS-15), Karlsruhe, Germany, September 14-15, 2022

Overview of activities in Kazakhstan related to study of beryllium and beryllium compounds

A.Shaimerdenov[1,2], T.Kulsartov[2,3], I.Kenzhina[1,2,4], Zh.Zaurbekova[2,3], Y. Kenzhin[4], Y.V.Chikhray[2], S. Udartsev[5]

1 - The Institute of Nuclear Physics, Almaty, Kazakhstan
2 - al-Farabi Kazakh National University, Almaty, Kazakhstan
3 - Institute of Atomic Energy of the National Nuclear Center of the Republic of Kazakhstan, Kurchatov, Kazakhstan
4 - Kazakh-British Technical University, Almaty, Kazakhstan
5 - Ulba Metallurgical Plant, Ust-Kamenogorsk, Kazakhstan

Disclaimer:
This presentation summarizes the results of a study of the effect of neutron irradiation on the properties of beryllium and plans for reactor studies of titanium beryllides.

Kazakhstan's research reactors

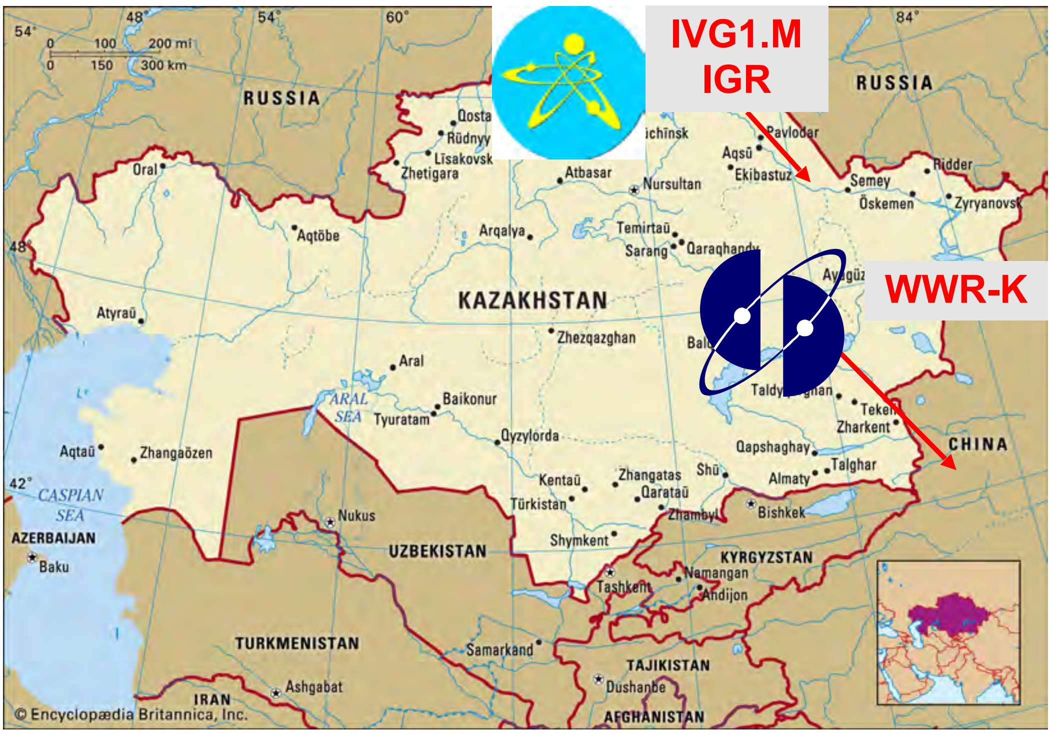

IGR RESEARCH REACTOR

- Type: pulse
- Thermal power: 1 GW
- Moderator: graphite
- Reflector: graphite
- Coolant: graphite/helium
- Pressure: atmospheric
- Type of coolant: natural convection
- Core size: 1400 mm
- Core height: 1463 mm
- Fuel: $UO_2(NO_3)_2$+C (HEU)
- Maximum of thermal neutron flux: $7*10^{16}$ $cm^{-2}s^{-1}$

IVG1.M RESEARCH REACTOR

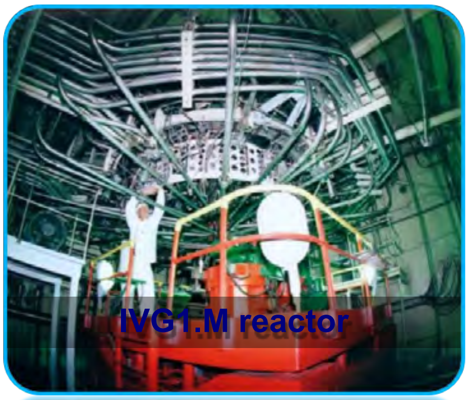

- Type: loop
- Thermal power: 6 MW
- Moderator: light water
- Reflector: beryllium
- Coolant: light water
- Pressure: atmospheric
- Type of coolant: forced
- Core diameter: 548 mm
- Core height: 800 mm
- Fuel: UZr (LEU)
- Maximum of thermal neutron flux: $1.5*10^{14}$ $cm^{-2}s^{-1}$

WWR-K RESEARCH REACTOR

- **Type:** tank
- **Thermal power:** 6 MW
- **Moderator:** demineralized water
- **Reflector:** demineralized water and beryllium
- **Coolant:** demineralized water
- **Pressure:** atmospheric
- **Type of coolant:** forced
- **Coolant circuit:** two
- **Core diameter:** 720 mm
- **Core height:** 600 mm
- **Fuel:** UO_2+Al matrix (LEU)
- **Maximum of thermal/fast neutron flux:** $2*10^{14}/8*10^{13}$ $cm^{-2}s^{-1}$

EXPERIMENTAL POSSIBILITIES OF WWR-K

Two kind of hot cells:
- concrete shielding (5 cells)
- steel shielding (4 cells)

Hydraulic transfer system

Utilized to load and unload of irradiation ampoule to/from the core during reactor operation

Critical assembly

Zero power reactor
Maximum thermal power: 100 W
Reflector: deionized water and/or beryllium
Moderator: deionized water
Fuel composition: UO_2+Al;
Enrichment in U-235: 19.7 % (since 2012)
Max. thermal neutron flux density: 10^9 cm^{-2} s^{-1}
Diameters of experimental channels: 65, 96 and 140 mm.

Pneumatic transfer system

Installed at beam tube #3, allows transfer of ampoule with a sample from laboratory room to the core and return back for gamma spectrometry measurement (neutron activation analysis)

Gas-vacuum loop facility

Gas-vacuum Loop Facility is designed to create a vacuum or gas environment in a sample during in-pile test

VIKA experimental facility

Schematic circuit

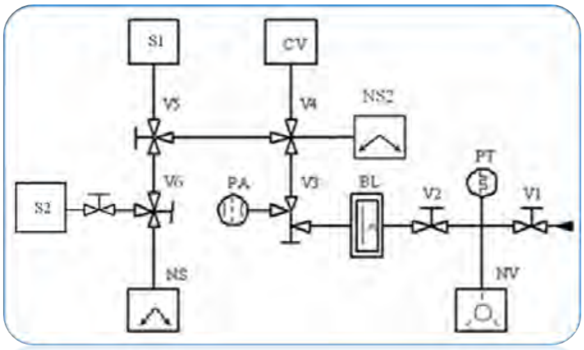

External view

PT – thermocouple vacuum gage;
PA – ionizing vacuum gage;
NS – magnetic-discharge pump NORD – 100;
NS2 – magnetic-discharge pump NORD -250;
S1 – omegatron RMO -13;
S2 – gage of quadropole analizator for remaining gases (RGA-100)
NV – forepump NVR – 5 DM; BL – liquid nitrogen trap ;
CV – vacuum chamber; V – vacuum tap;

Technical parameters

- Range of temperatures 30 ÷ 1500 °**C**;
- Pressure in vacuum chamber at crucible temperature 1500 °**C**, 10^{-4} **Pa**;
- An accuracy of temperature auto control ± 0.5 °**C**;
- A range of heating rate 2 ÷ 50 °**C**/min.

Complex for in-reactor gas release analysis (CIRRA)

Block scheme

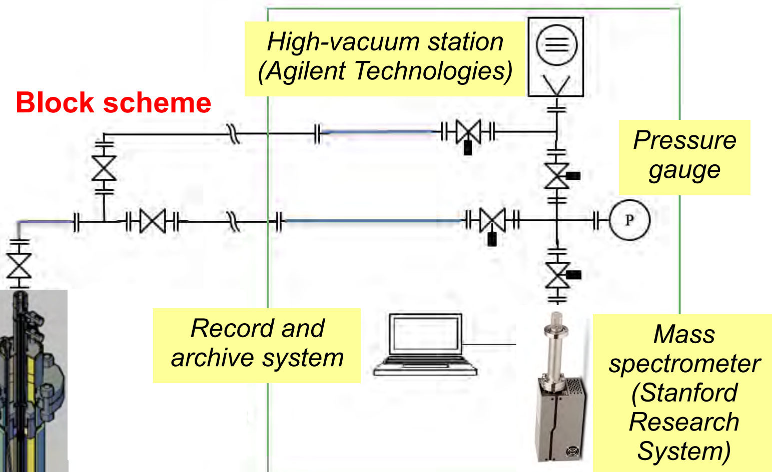

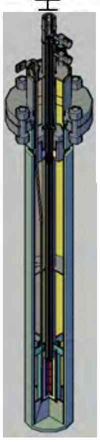

- Irradiation temperature: 50-1500 ºC;
- Measurement of elements mass: up to 100 a.e.m.;
- Measurement method: determination of a separating fluid at the condition of vacuum extraction under uninterrupted exhaustion;
- Temperature control method: by changing gas pressure in capsule gap and using electrical heater;
- Heating method: radiation heating and electrical heater;
- Features: the experimental facility can be connected to the experimental devices installed in any cell of the reactor core; irradiation parameters (temperature, pressure, the neutron flux relative density, etc.) are recorded and archived.

Study of DV-56 and TShG-200 beryllium grade

DV-56 grade irradiated beryllium

Irradiation site – BN-350 reactor (Aktau, RK)

Fluence - 5 · 10^{21} n/sm^2 (E > 1 MeV)

Year of unloading – 1996

Chemical composition	Be	Si	Fe	Al	C	BeO
Mass fraction impurities, %	98,64	0,013	0,055	0,02	0,072	1,2

diameter - 30 mm, lengths- 110 mm
Initial sample

TShG-200 grade irradiated beryllium

Irradiation site – IVG reactor (Kurchatov, RK)

Fluence ~ 10^{19} n/sm^2 (E < 0,1 MeV)

Year of unloading – 2010 г.

Chemical composition	Be	Fe	Al	Si	Cr	F	O	C	Ti
Mass fraction impurities, %	97,8	0,25	0,03	0,04	0,05	0,002	1,3	0,12	0,04

Diameter - 56 mm, lengths - 80 мм
Initial sample

Samples for TDS investigations

Sample shapes	Half-disc		Disk	
Average size, mm	4.5	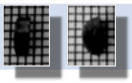	9-10	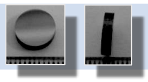
Width, mm	1-1.5		1-3	

Experimental results

Time dependences of sample temperature and partial gas pressure changes

DV-56 grade

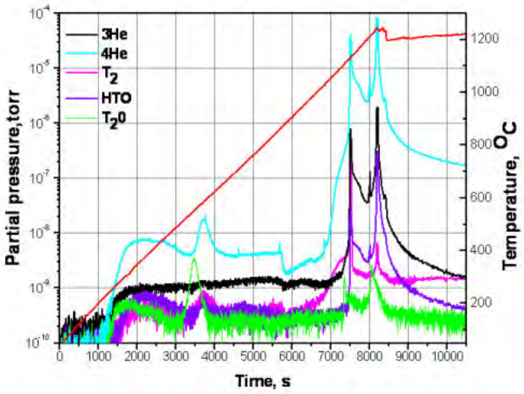

Gas release from irradiated beryllium of DV-56 grade

Heating rate 10 °C/min, sample width – 1 mm

Time dependences of sample temperature and partial gas pressure changes

TShG-200 grade

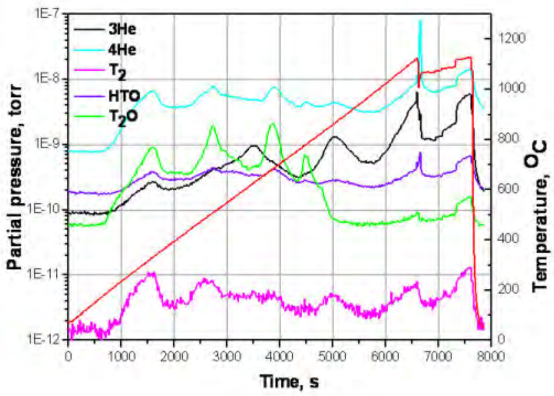

Gas release from irradiated beryllium of TShG-200 grade

Heating rate 10 °C/min, sample width – 1.3 mm

Results of microstructural investigations

Results of microstructural investigation of DV-56 beryllium grade after TDS-experiments

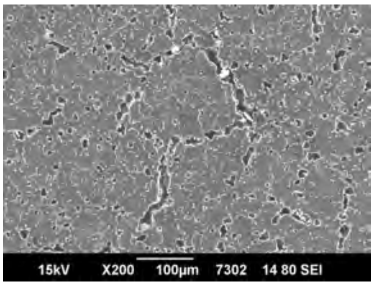

Surface of beryllium sample

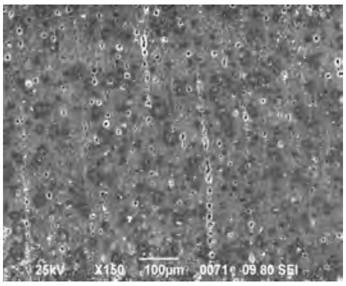

Surface of the sample's cross section

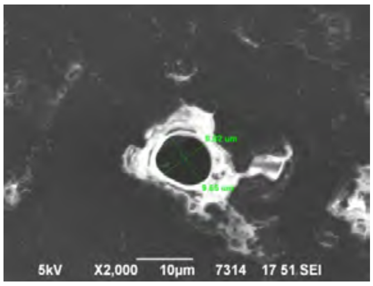

Scaled up view of pore in a sample

Main parameters of tritium interaction with investigated samples

	DV-56 grade	TShG-200 grade
Diffusion coefficient D, m^2/s	$(9,0\pm0,2)*10^{-2}$	150±5
Activation energy of diffusion E_D, кJ/mole	$(3,4\pm0,4)*10^{-4}$	90±5

Analysis of experimental results

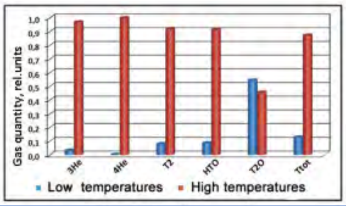

DV-56 beryllium grade

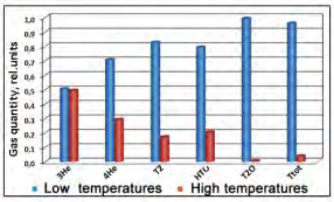

TShG-200 beryllium grade

A histogram of relative gas release from two-types samples during the different temperatures ranges of TDS spectrum

High temperatures

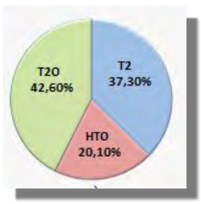

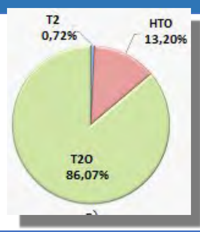

Low temperatures

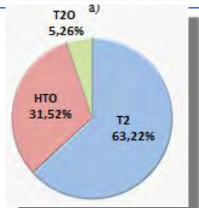

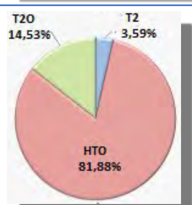

DV-56 beryllium grade

TShG-200 beryllium grade

Relative contribution of integral tritium-containing release to total tritium release from investigated samples

Study of S-200F, S-65H, I-220H beryllium grades

Performed 2010-2013

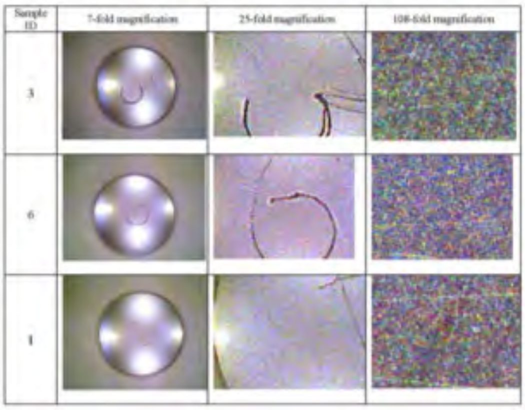

The beryllium grades were the following:

- traditional grade of beryllium, S-200F, which is produced by the vacuum hot pressing (VHP);
- the grade S-65H, which is produced by hot isostatic pressing (HIP); it is characterized by a higher degree of purity;
- the grade I-220H, which is also produced by the HIP technique but is characterized by higher mechanical strength and better extent of isotropy.

Grade	Shape	Dimension (mm) (initial diameter×thickness)	Mass (mg)
S-200F	Disk	⌀10×1.5	217.96
		⌀9.98×1.51	218.3
S-65H	Disk	⌀10×1.51	219.47
		⌀10.0×1.5	219.04
I-220H	Disk	⌀10.01×1.51	219.04

Scope of study:

- measurement of dimensions and weight;
- hardness test;
- SEM observation;
- TDS experiments for measurements of Helium/ Tritium contents.

Irradiation conditions

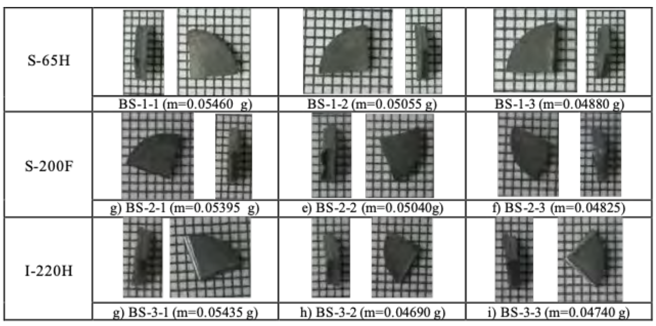

- Samples were irradiated in the WWR-K reactor core;
- Two neutron fluence were reached: ≈$1.5x10^{24}$ and ≈$4x10^{24}$ n/m^2 (E_n > 1 MeV);
- Iron fluence monitor was used for measurement of accumulated neutron fluence;
- Temperature of irradiation: 50ºC;
- Samples environment: helium;

Microstructure study

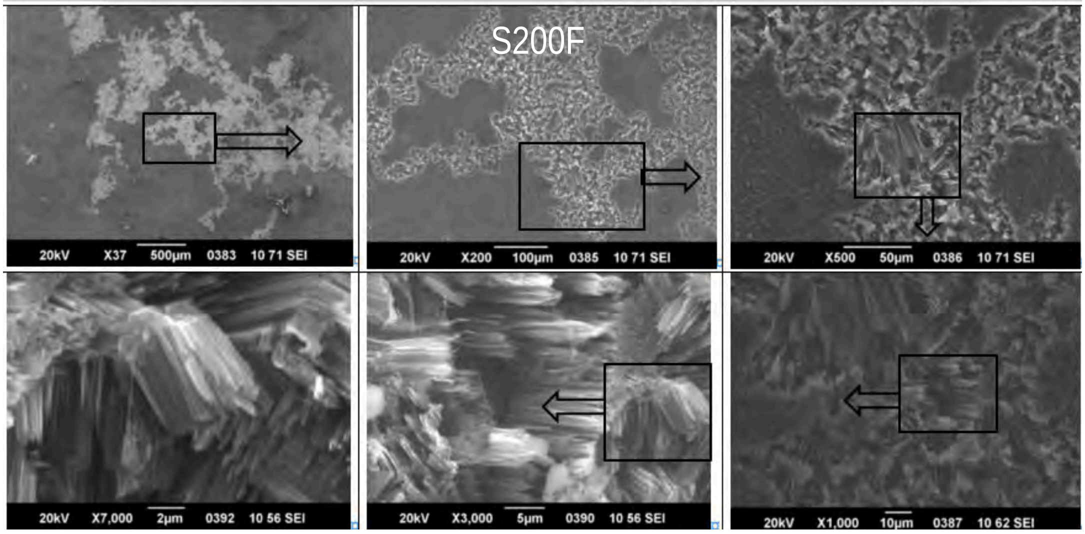

On all samples there is pitting corrosion over the entire surface of the sample

The most pronounced corrosion pitting are observed on a sample of S200F beryllium; less pronounced on the sample of beryllium grade S65H; and the least pronounced on the I220H beryllium grade sample.

Gas release results (1)

Sample heating is carried put in two stages.

- First stage: a sample is heated, by linear law, at a specified rate, to the temperature level close to the sample melting point ($T \approx 0.98T_{melt}$).
- Second stage: the sample heating rate is decreased, and the sample is heated to the beryllium melting point ($T \approx 1283°C$).

Variations in partial pressures of gases was studied (helium ^{3}He ((a.m.u.3), ^{4}He (a.m.u. 4), and tritium (a.m.u. 6)) in the continuously exhausted chamber of the experimental facility are recorded.

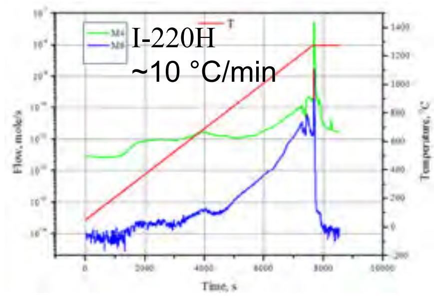

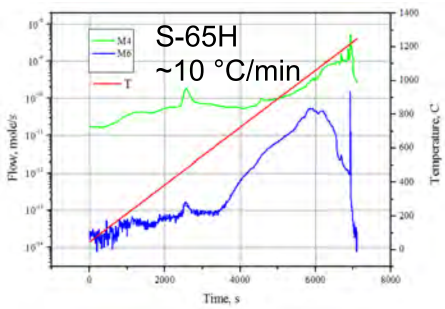

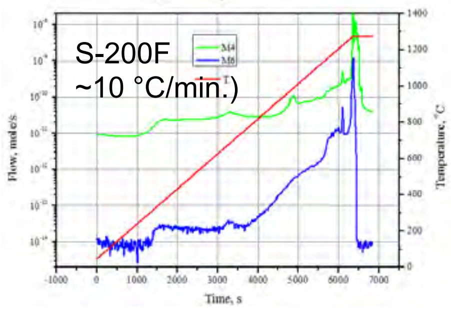

Gas release results (2)

Release of tritium and helium for samples S-200F, I-220H - the main amount of gas (both helium and tritium) is released close to the melting temperature and during melting (while in previous experiments with samples irradiated to a lower fluence, noticeable amounts of released tritium were observed in the temperature range of 900-1150 C).

Beryllium sample of grade S-65H, a noticeable amount of gas is released up to the melting point (with a peak for tritium in the region of about 1100 C). (A similar picture was observed with samples irradiated to a lower fluence).

Beryllium grade	Tritium		Helium	
	mole T_2	ppm	mole ^4He	ppm
S-65H	$4{,}55 \cdot 10^{-9}$	1,5	$1{,}41 \cdot 10^{-7}$	24
S-200F	$4{,}45 \cdot 10^{-9}$	1,5	$1{,}54 \cdot 10^{-7}$	26
I-220H	$4{,}23 \cdot 10^{-9}$	1,4	$1{,}28 \cdot 10^{-7}$	22

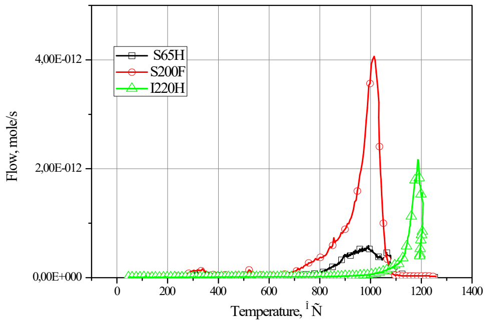

Temperature dependencies of tritium flux from beryllium

Plans for study of radiation resistance of titanium beryllide (1)

In this regard, Kazakhstan has great opportunities, since on its territory Ulba Metallurgical Plant (UMP) is located (a unique enterprise engaged in the production of beryllium, uranium and tantalum products for the needs of nuclear energy). UMP employees have developed a technological method for obtaining titanium beryllide in large quantities by vacuum hot pressing→ **Mr.Udartsev was reported.**

Titanium beryllide is a candidate material for a neutron breeder of a fusion reactor blanket. This is due to its improved mechanical properties compared to metallic beryllium.

Project named as “Influence of reactor irradiation on physical and mechanical properties and gas generation in titanium beryllide” (grant #AP14871445) has been accepted by Kazakhstan government for funding

Plans for study of radiation resistance of titanium beryllide (2)

Samples dimension:
8x8x1.5 mm (LxWxT)

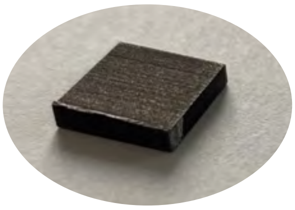

Project will started since October 2022

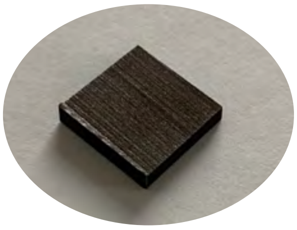

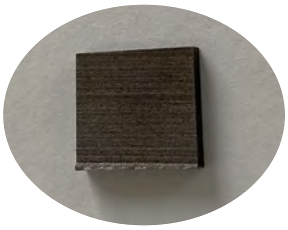

Scope of study:

- ❑ Neutron irradiation by accumulation of two neutron fluence ($5x10^{20}$ cm^{-2} and $\sim 10^{21}$ cm^{-2});
- ❑ Samples density (unirradiated and irradiated);
- ❑ Hardness (unirradiated and irradiated);
- ❑ Microstructure (unirradiated and irradiated);
- ❑ Magnetic permeability (unirradiated and irradiated);
- ❑ Phase structure (unirradiated);
- ❑ TDS experiments for gas release measurements (irradiated);

Summary

- There are three research reactors in Kazakhstan where material science research is being carried out.
- The research centers of Kazakhstan employ highly qualified specialists who have many years of experience in researching materials for fusion
- Two reactors have facilities for TDS experiments (in-situ and PIE). The availability of such an infrastructure makes it possible to study materials in high level, in particular, beryllium and beryllides.
- In Kazakhstan, there is a unique UMP plant that manufactures products from beryllium and can manufactured beryllides. With this in mind, studies of beryllides manufactured at the UMP begin in Kazakhstan.

Taking into account the above, we invite you to cooperation

Beryllides as advanced materials for neutron multiplication

R. Gaisin[1], R. Rolli, V. Chakin, P. Vladimirov

[1] Karlsruhe Institute of Technology, Institute for Applied Materials - Applied Materials Physics, 76344 Eggenstein-Leopoldshafen, Germany

The neutron multiplier is an essential component of the blanket of future thermonuclear reactors, which should provide the tritium breeder with a sufficient amount of neutrons of a certain energy. Among all chemical elements, only beryllium and lead have an advantageous ratio of high neutron multiplication reaction at low neutron absorption rates. However, pure metals – beryllium and lead – for various reasons cannot be used in the harsh operating conditions of a fusion reactor blanket. Intermetallic compounds of beryllium – beryllides have a number of advantages over pure beryllium and are currently considered to be the reference neutron multiplication material for the Helium Cooled Pebble Bed (HCPB) breeding blanket concept of EU DEMO fusion reactor. Recently, a batch of full-size beryllide blocks has been manufactured on an industrial scale in cooperation with the Ulba Metallurgical Plant. The present work is devoted to the characterization and analysis of these beryllide blocks so that the material could be used for the manufacture of a blanket.

Titanium beryllide ($TiBe_{12}$) blocks are hexagonal prisms with an internal hole, while chromium beryllide ($CrBe_{12}$) blocks are solid prisms of complex shape. The resulting blocks have a single-phase structure of the corresponding beryllide with a small impurity in the form of beryllium oxide. One of the titanium beryllide blocks also has about 7% residual beryllium phase. Grains of titanium beryllide have an average size of about 7–8 µm, while grains of chromium beryllide are much larger and reach 40–50 µm. Mechanical compression and bending tests of beryllides showed their very high strength, which is maintained up to 1000°C. In terms of specific compressive strength, the single-phase $TiBe_{12}$ surpasses all materials, except diamond, in the 700–1000°C temperature range. Chromium beryllide and titanium beryllide with 7% of the beryllium phase have lower strength, but higher ductility. Corrosion tests were carried out in air and in He + 2% water vapor at 800–1200°C. Beryllides have high corrosion resistance similar to Ni-base superalloys and high temperature ceramics. Long-term thermal cycling tests with rapid heating and cooling, simulating operation in a fusion reactor, showed high resistance of beryllides to thermal shocks. The results obtained are also discussed from the point of view of the application of beryllides in other areas.

Corresponding Author:

Dr. Ramil Gaisin
ramil.gaisin@kit.edu
Herrmann-von-Helmholtz-Platz 1
76344 Eggenstein-Leopoldshafen

15th International Workshop on
Beryllium Technology, Karlsruhe

Beryllides as advanced materials for neutron multiplication

R. Gaisin, R. Rolli, V. Chakin, M. Dürrschnabel, P. Vladimirov
Institute for Applied Materials – Applied Materials Physics, Karlsruhe Institute of Technology (KIT), Karlsruhe, Germany

S. Udartsev, M. Kolmakov, E. Frantz
Ulba Metallurgical Plant, Ust-Kamenogorsk, Kazakhstan

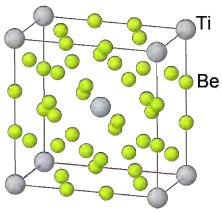

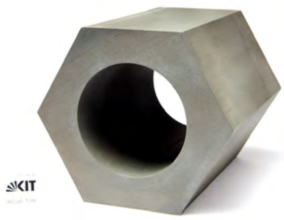

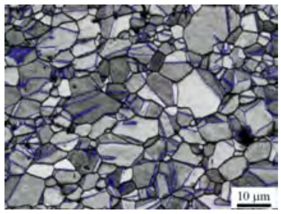

KIT – The Research University in the Helmholtz Association

www.kit.edu

Neutron multiplier materials for breeding blanket

Demonstration power plant: DEMO

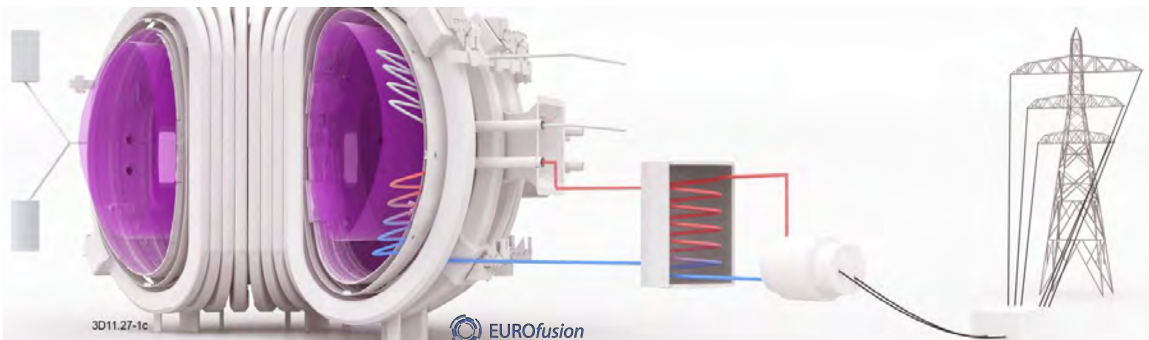

Deuterium-Tritium tokamak
Fusion power 2 GW = 111 kg of tritium/year

2 /44 14.09.2022 Dr. Ramil Gaisin Institute for Applied Materials – Applied Materials Physics

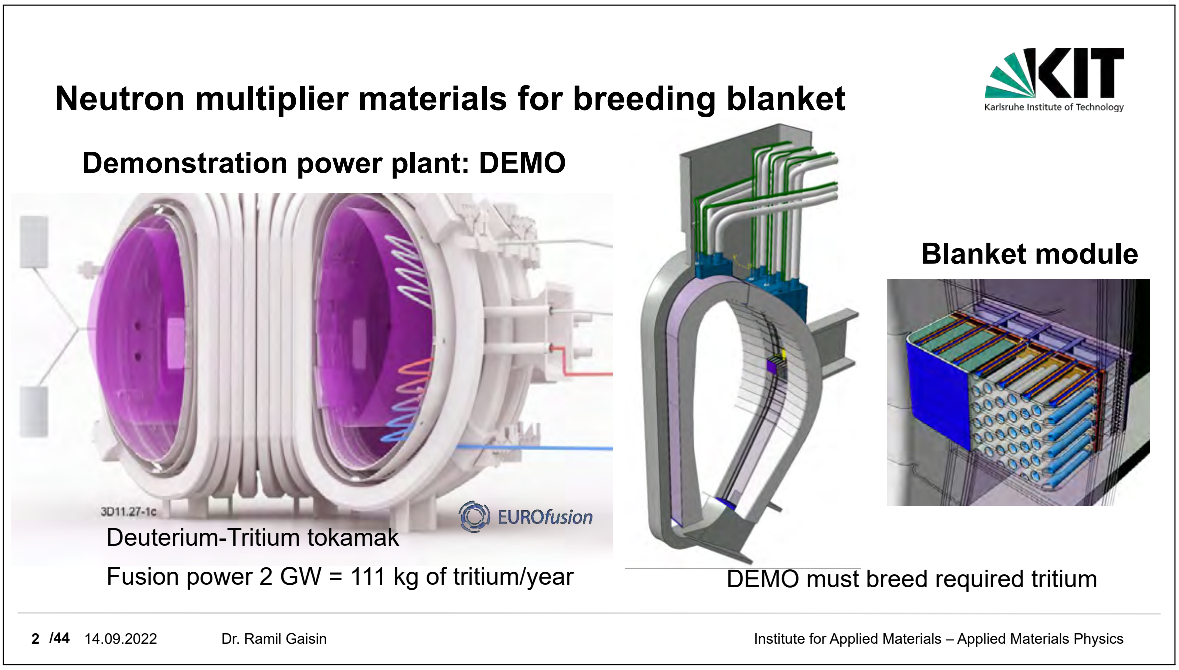
Neutron multiplier materials for breeding blanket
Karlsruhe Institute of Technology
Demonstration power plant: DEMO
Blanket module
3D11.27-1c
EUROfusion
Deuterium-Tritium tokamak
Fusion power 2 GW = 111 kg of tritium/year
DEMO must breed required tritium
2 /44 14.09.2022 Dr. Ramil Gaisin Institute for Applied Materials – Applied Materials Physics

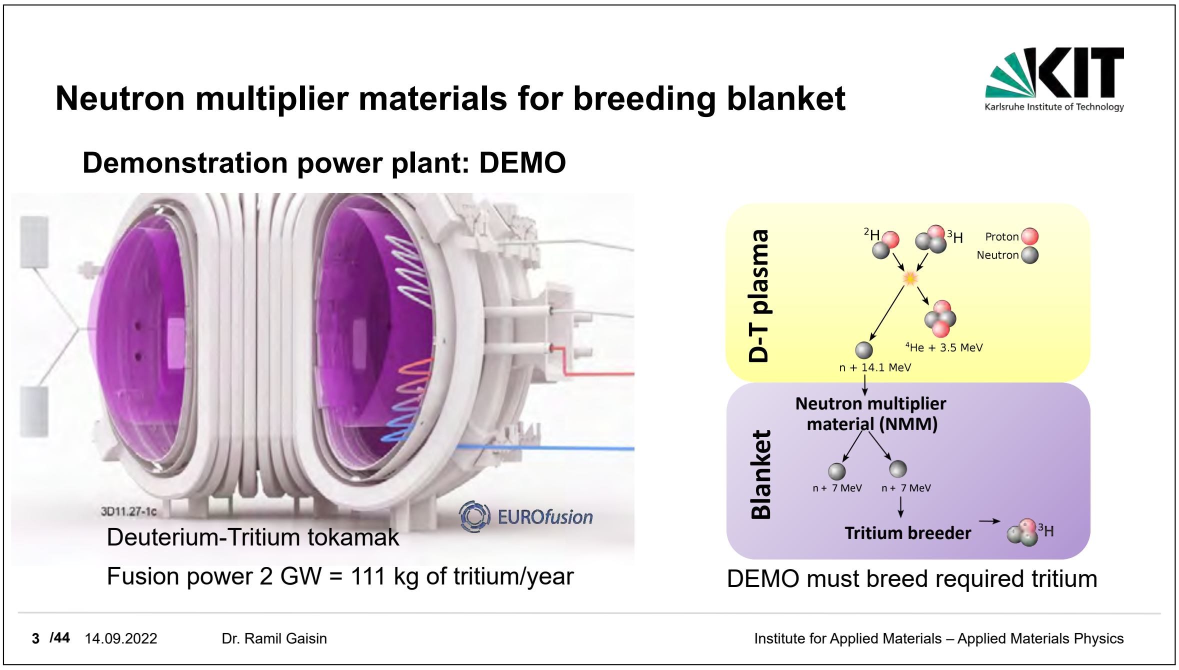
Neutron multiplier materials for breeding blanket
Karlsruhe Institute of Technology
Demonstration power plant: DEMO
3D11.27-1c
EUROfusion
Deuterium-Tritium tokamak
Fusion power 2 GW = 111 kg of tritium/year
D-T plasma
²H
³H
Proton
Neutron
⁴He + 3.5 MeV
n + 14.1 MeV
Blanket
Neutron multiplier material (NMM)
n + 7 MeV
n + 7 MeV
Tritium breeder
³H
DEMO must breed required tritium
3 /44 14.09.2022 Dr. Ramil Gaisin Institute for Applied Materials – Applied Materials Physics

Selection of neutron multiplier material

Karlsruhe Institute of Technology

Relative reaction rates

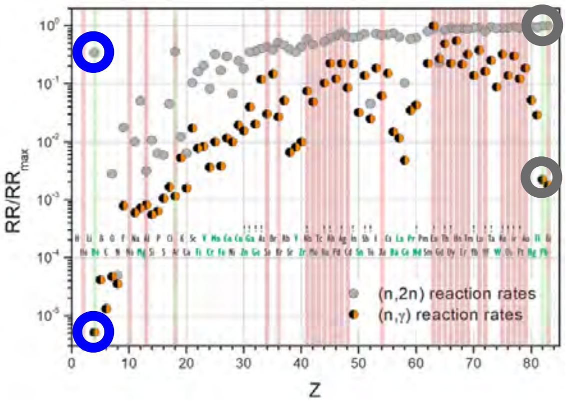

Limits on the use of elements

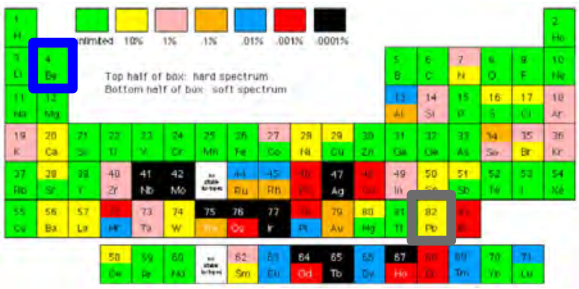

NMM should have: - large (n,2n) cross-section
- low parasitic neutron absorption

F.A. Hernández, P. Pereslavtsev FED 137 (2018) 243-256

4 /44 14.09.2022 Dr. Ramil Gaisin Institute for Applied Materials – Applied Materials Physics

Selection of neutron multiplier material

Karlsruhe Institute of Technology

Relative reaction rates

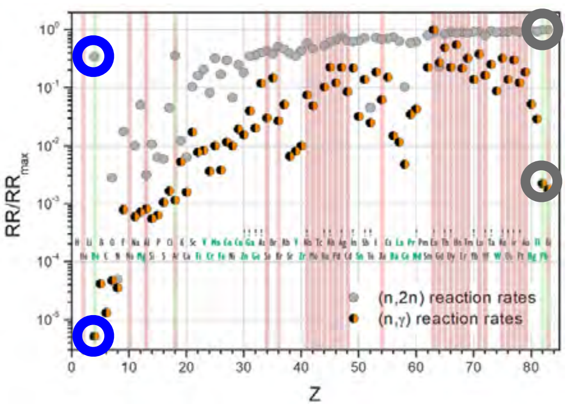

Threshold energy

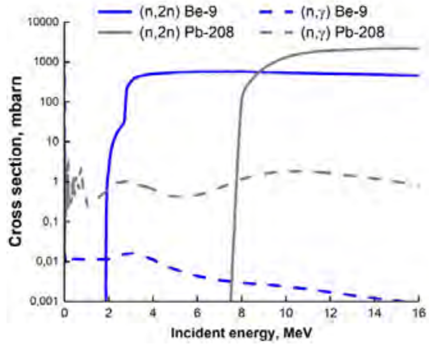

NMM should have: - large (n,2n) cross-section
- low parasitic neutron absorption

(n,2n) threshold energy for Be is much lower than for Pb

5 /44 14.09.2022 Dr. Ramil Gaisin Institute for Applied Materials – Applied Materials Physics

Beryllium as NMM

ADVANTAGES:

+ The best neutron multiplier, dual function as multiplier and fair moderator
+ The most compact T-breeding blanket
+ Allows working with relatively low Li6 enrichment (≈60%)
+ Avoids problems of liquid metal blankets (corrosion, embrittlement, bubbles, magnetohydrodynamics)
+ Can operate above 400°C, thus avoiding irradiation embrittlement of steels

Before irradiation

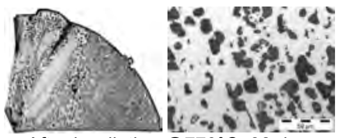

After irradiation @770°C, 38 dpa
*V*porosity = 24%

SHORTCOMINGS:

– High chemical reactivity with steam and air
– High swelling under neutron irradiation above 650°C
– High tritium retention

As received

Corrosion in steam @800°C

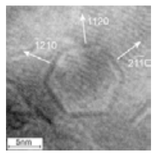

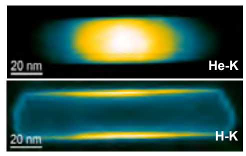

6 /44 14.09.2022 Dr. Ramil Gaisin Institute for Applied Materials – Applied Materials Physics

Solution - Beryllides

- Beryllium forms intermetallic compounds (beryllides) with almost all metals
- Typical compositions: MBe_{12}, MBe_{22}, MBe_{13}, M_2Be_{17}
- High corrosion resistance
- Low swelling and low tritium retention

$TiBe_{12}$

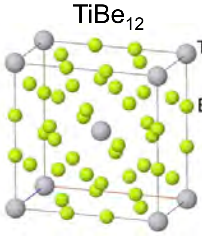

Ti_2Be_{17}

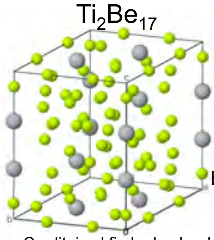

Credit: icsd.fiz-karlsruhe.de

$ZrBe_{13}$

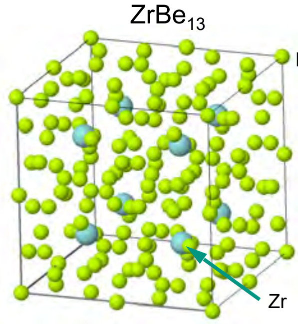

7 /44 14.09.2022 Dr. Ramil Gaisin Institute for Applied Materials – Applied Materials Physics

Selection of beryllides compositions

- Neutron performance – high Be content
- High melting point
- High corrosion resistance
- Reasonable strength
- Low radioactivation

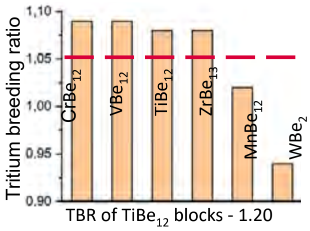

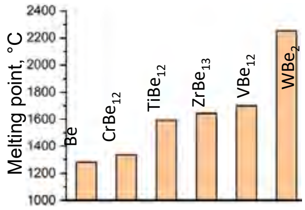

Limits on the use of elements

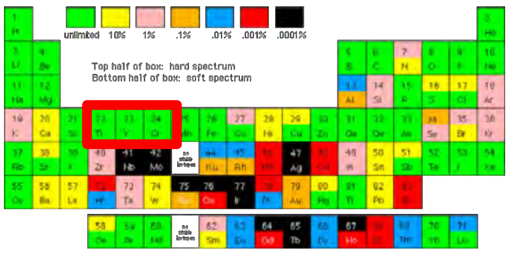

F.A. Hernández et al., FST 75 (2019) 352–364

F.A. Hernández, P. Pereslavtsev FED 137 (2018) 243-256

8 /44 14.09.2022 Dr. Ramil Gaisin Institute for Applied Materials – Applied Materials Physics

Titanium and chromium beryllides

$TiBe_{12}$

- Be-7.7at.%Ti or Be-30.8wt.%Ti
- T_m=1550°C
- ρ=2.28 g/cm³
- High corrosion resistance
- Reasonable thermal conductivity

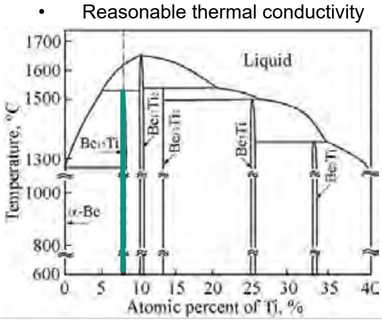

$CrBe_{12}$

- Be-7.7at.%Ti or Be-32.5wt.%Ti
- T_m=1340°C
- ρ=2.44 g/cm³
- Simple phase diagram, no peritectic reaction

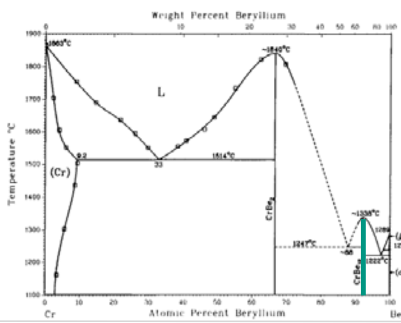

9 /44 14.09.2022 Dr. Ramil Gaisin Institute for Applied Materials – Applied Materials Physics

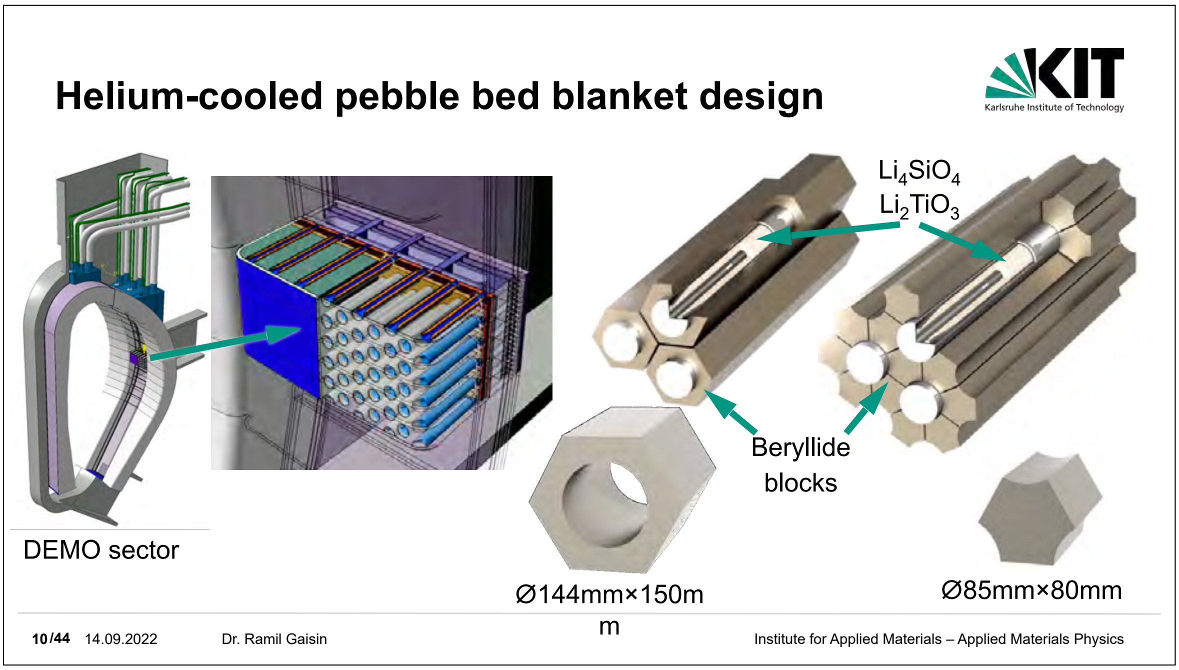
Helium-cooled pebble bed blanket design
Karlsruhe Institute of Technology
Li4SiO4
Li2TiO3
Beryllide
blocks
DEMO sector
Ø144mm×150m
m
Ø85mm×80mm
10/44 14.09.2022
Dr. Ramil Gaisin
Institute for Applied Materials – Applied Materials Physics

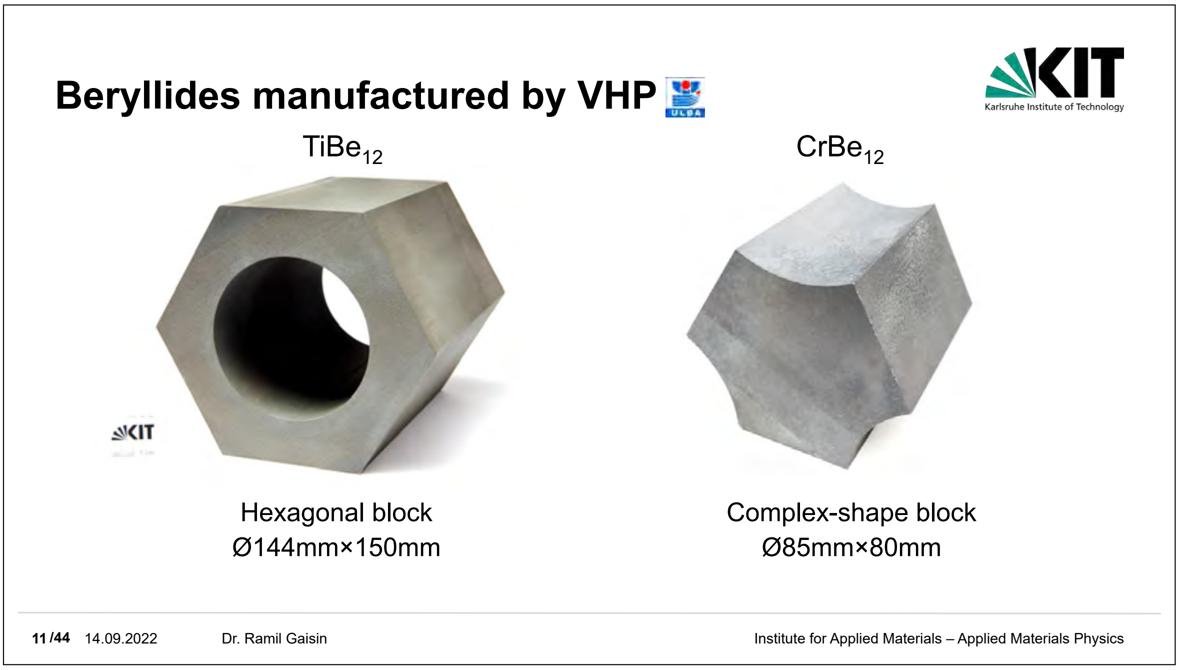
Beryllides manufactured by VHP
Karlsruhe Institute of Technology
TiBe12
CrBe12
Hexagonal block
Ø144mm×150mm
Complex-shape block
Ø85mm×80mm
11/44 14.09.2022
Dr. Ramil Gaisin
Institute for Applied Materials – Applied Materials Physics

Requirements for beryllides as neutron multiplier materials

- High tritium breeding ratio – maximum possible content of Be
- Minimum content of impurities that form long-lived isotopes under irradiation (e.g. Uranium)
- Fine grain structure for easy tritium release and reasonable mechanical properties
- Beryllide blocks must retain their shape and not fracture during operation
- Low corrosion in the air and purge gas atmosphere
- Low interaction with structural materials (e.g. EUROFER steel)
- No fracture or cracks during rapid heating/cooling due to pulsed operation of DEMO

12/44 14.09.2022 Dr. Ramil Gaisin Institute for Applied Materials – Applied Materials Physics

$TiBe_{12}$ manufactured by VHP. XRD

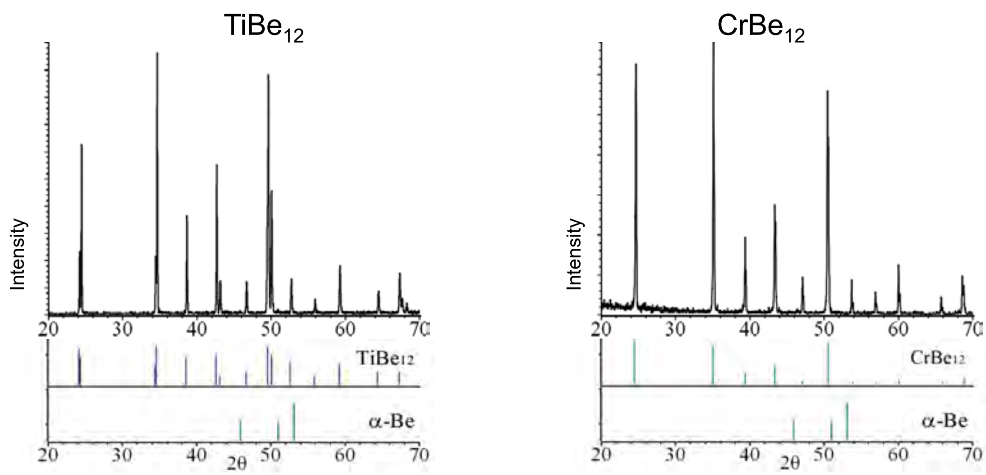

13/44 14.09.2022 Dr. Ramil Gaisin Institute for Applied Materials – Applied Materials Physics

Requirements for beryllides as neutron multiplier materials

- High tritium breeding ratio – maximum possible content of Be
- Minimum content of impurities that form long-lived isotopes under irradiation (e.g. Uranium) – as low as possible activation
- Fine grain structure for easy tritium release and reasonable mechanical properties
- Beryllide blocks must retain their shape and not fracture during operation
- Low corrosion in the air and purge gas atmosphere
- Low interaction with structural materials (e.g. EUROFER steel)
- No fracture or cracks during rapid heating/cooling due to pulsed operation of DEMO

14/44 14.09.2022 Dr. Ramil Gaisin Institute for Applied Materials – Applied Materials Physics

Chemical composition

Material	Ti	Cr	C	N	O	Mg	Al	Si	Ca	Fe	U, ppm	Be
$TiBe_{12}$ UMP	**29.6**	-	0.038	0.0801	0.597	<0.0002	0.0222	0.0213	0.01	0.124	0.51	Bal.
$TiBe_{12}$ + 7vol.% Be UMP	**27.8**	-	0.034	0.106	0.686	<0.00005	0.020	0.0162	0.015	0.118	0.395	Bal.
$CrBe_{12}$ UMP	-	30.8	0.0346	0.0177	0.555	<0.0002	0.0156	0.0237	0.0088	0.114	0.54	Bal.
$TiBe_{12}$ HIP (from Materion Be)	29.11	-	0.0774	0.0028	0.219	0.0355	0.037	0.0215	0.0018	0.102	19.3	Bal.

Almost no uranium in beryllides from UMP

15/44 14.09.2022 Dr. Ramil Gaisin Institute for Applied Materials – Applied Materials Physics

Requirements for beryllides as neutron multiplier materials

- High tritium breeding ratio – maximum possible content of Be
- Minimum content of impurities that form long-lived isotopes under irradiation (e.g. Uranium)
- Fine grain structure for facilitated tritium release and reasonable mechanical properties
- Beryllide blocks must retain their shape and not fracture during operation
- Low corrosion in the air and purge gas atmosphere
- Low interaction with structural materials (e.g. EUROFER steel)
- No fracture or cracks during rapid heating/cooling due to pulsed operation of DEMO

16/44 14.09.2022 Dr. Ramil Gaisin Institute for Applied Materials – Applied Materials Physics

Microstructure of $TiBe_{12}$

$TiBe_{12}$ | $TiBe_{12}$ + 7vol.% Be

SEM

Single phase $TiBe_{12}$ ρ=98.6%

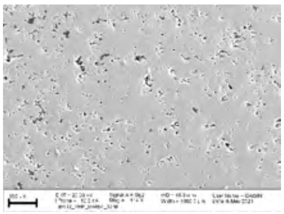

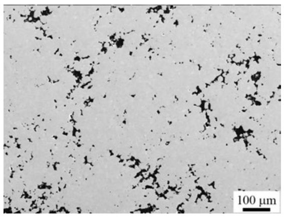

7 vol.% of Be phase (black) ρ=98.3%

EBSD

D = 8±3.5 µm

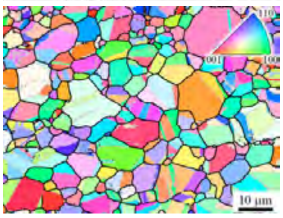

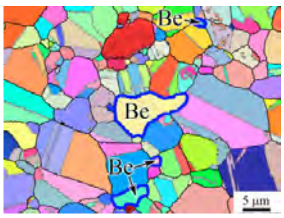

D = 7±3 µm

17/44 14.09.2022 Dr. Ramil Gaisin Institute for Applied Materials – Applied Materials Physics

Microstructure of Ti and Cr beryllides

KIT – Karlsruhe Institute of Technology

$TiBe_{12}$ | $CrBe_{12}$

Single phase $TiBe_{12}$ ρ=98.6%

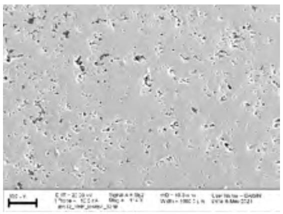

SEM

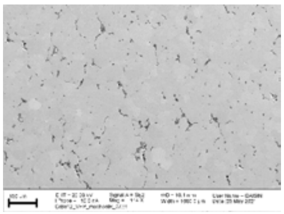

Single phase $CrBe_{12}$ ρ=98.5%

D = 8±3.5 µm

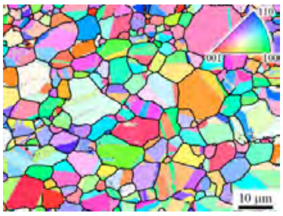

EBSD

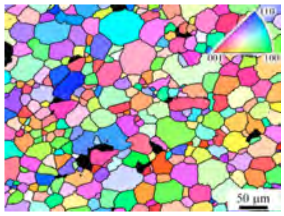

D = 42±18 µm

Requirements for beryllides as neutron multiplier materials

KIT – Karlsruhe Institute of Technology

- High tritium breeding ratio – maximum possible content of Be
- Minimum content of impurities that form long-lived isotopes under irradiation (e.g. Uranium)
- Fine grain structure for easy tritium release and reasonable mechanical properties
- Beryllide blocks must retain their shape and not fracture during operation.
- Low corrosion in the air and purge gas atmosphere
- Low interaction with structural materials (e.g. EUROFER steel)
- No fracture or cracks during rapid heating/cooling due to pulsed operation of DEMO

Compression tests

Karlsruhe Institute of Technology

Cracked Si_3N_4 platens

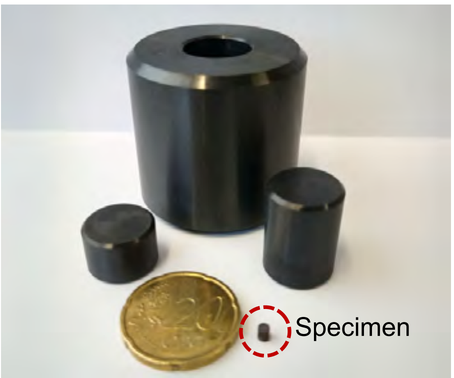

Specimens from Ø2.2mm×2.6mm to Ø4mm×6mm

20/44 14.09.2022 Dr. Ramil Gaisin Institute for Applied Materials – Applied Materials Physics

Compressive properties of $TiBe_{12}$

Karlsruhe Institute of Technology

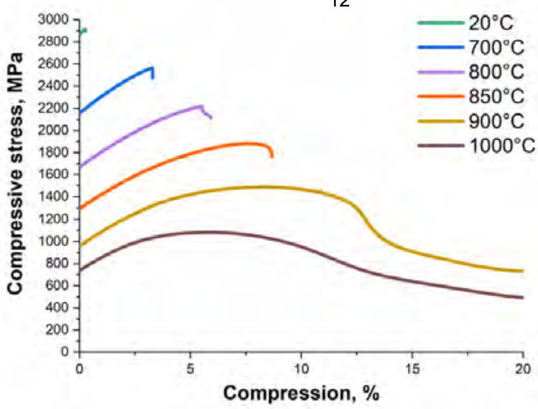

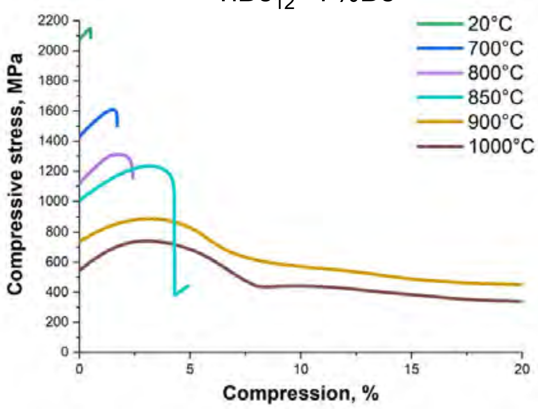

21/44 14.09.2022 Dr. Ramil Gaisin Institute for Applied Materials – Applied Materials Physics

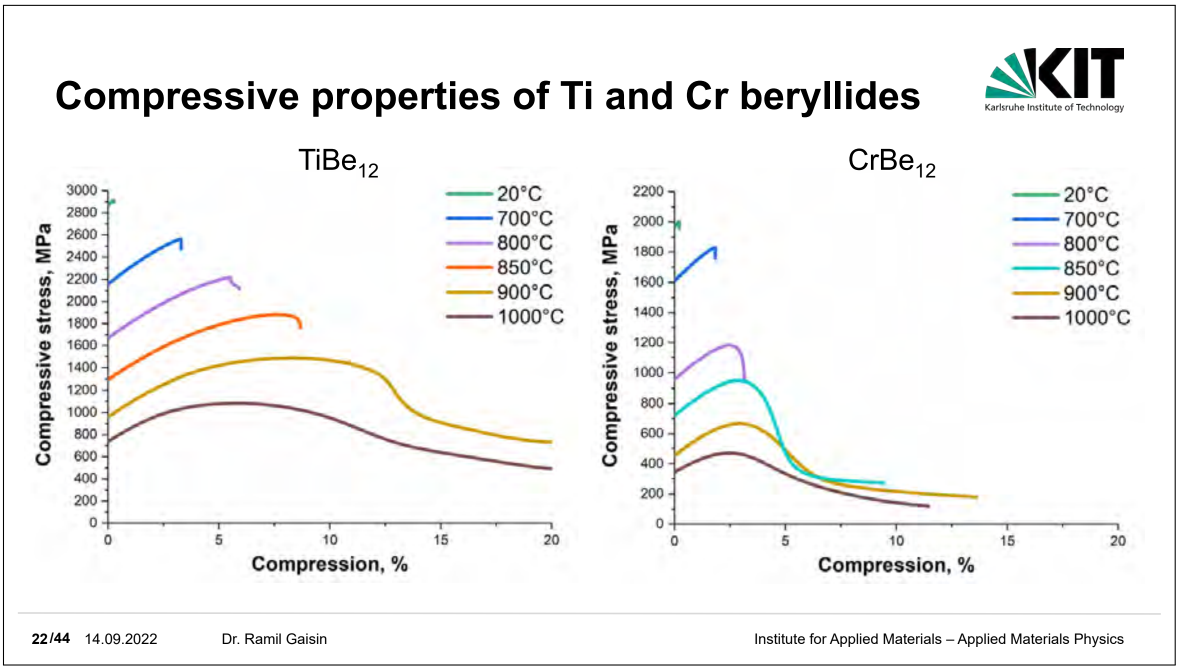
Compressive properties of Ti and Cr beryllides
KIT
Karlsruhe Institute of Technology
TiBe12
CrBe12
Compressive stress, MPa
Compression, %
20°C
700°C
800°C
850°C
900°C
1000°C
22/44 14.09.2022 Dr. Ramil Gaisin Institute for Applied Materials – Applied Materials Physics

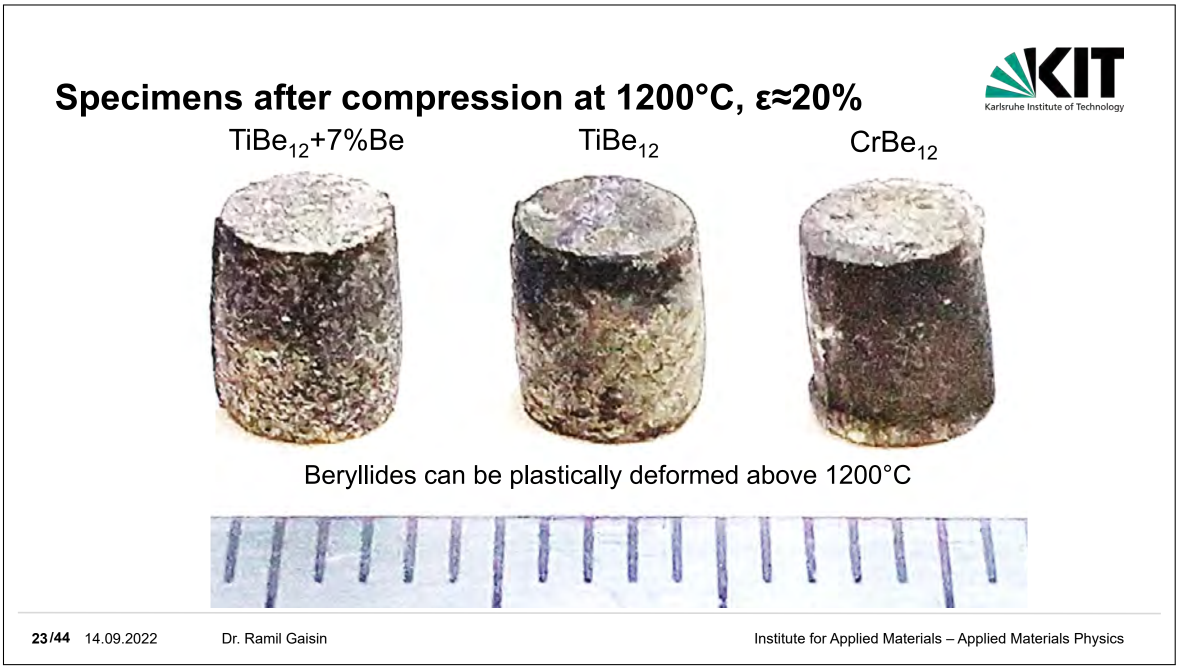
Specimens after compression at 1200°C, ε≈20%
KIT
Karlsruhe Institute of Technology
TiBe12+7%Be
TiBe12
CrBe12
Beryllides can be plastically deformed above 1200°C
23/44 14.09.2022 Dr. Ramil Gaisin Institute for Applied Materials – Applied Materials Physics

Compressive strength of beryllides

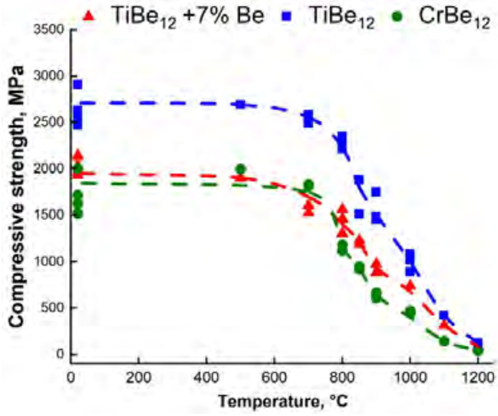

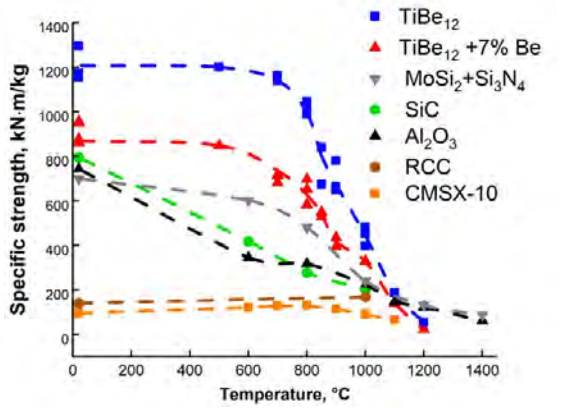

Shackelford, CRC Materials Science and Engineering Handbook, 2000
Hebsur, Handbook of Ceramic Composites, 2005
Reed, The Superalloys, 2006

24/44 14.09.2022 Dr. Ramil Gaisin Institute for Applied Materials – Applied Materials Physics

3 point bending tests

Specimens

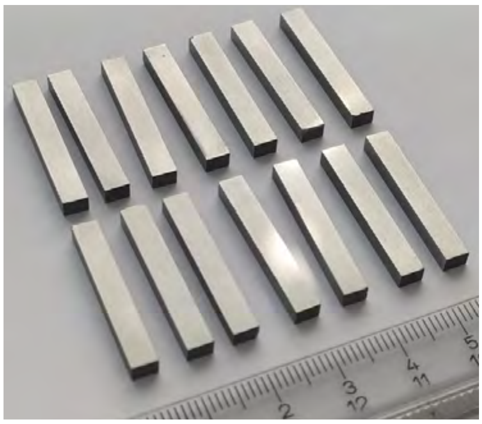

25/44 14.09.2022 Dr. Ramil Gaisin Institute for Applied Materials – Applied Materials Physics

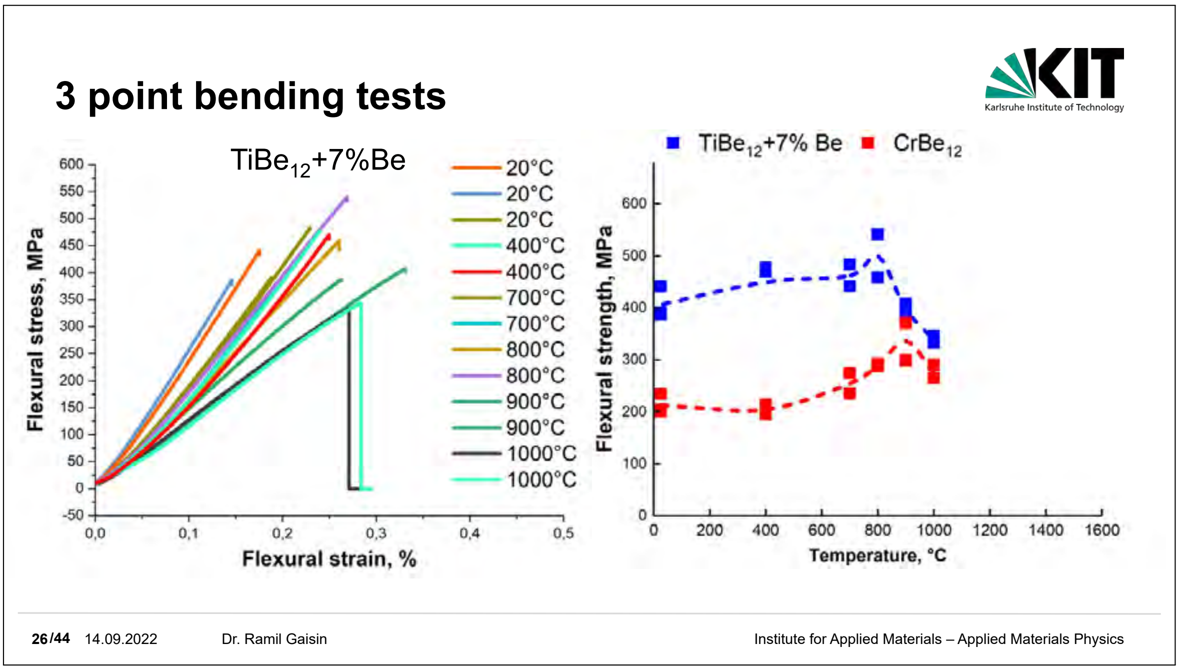
3 point bending tests
KIT
Karlsruhe Institute of Technology
TiBe12+7%Be
Flexural stress, MPa
Flexural strain, %
20°C
20°C
20°C
400°C
400°C
700°C
700°C
800°C
800°C
900°C
900°C
1000°C
1000°C
TiBe12+7% Be
CrBe12
Flexural strength, MPa
Temperature, °C
26/44 14.09.2022 Dr. Ramil Gaisin Institute for Applied Materials – Applied Materials Physics

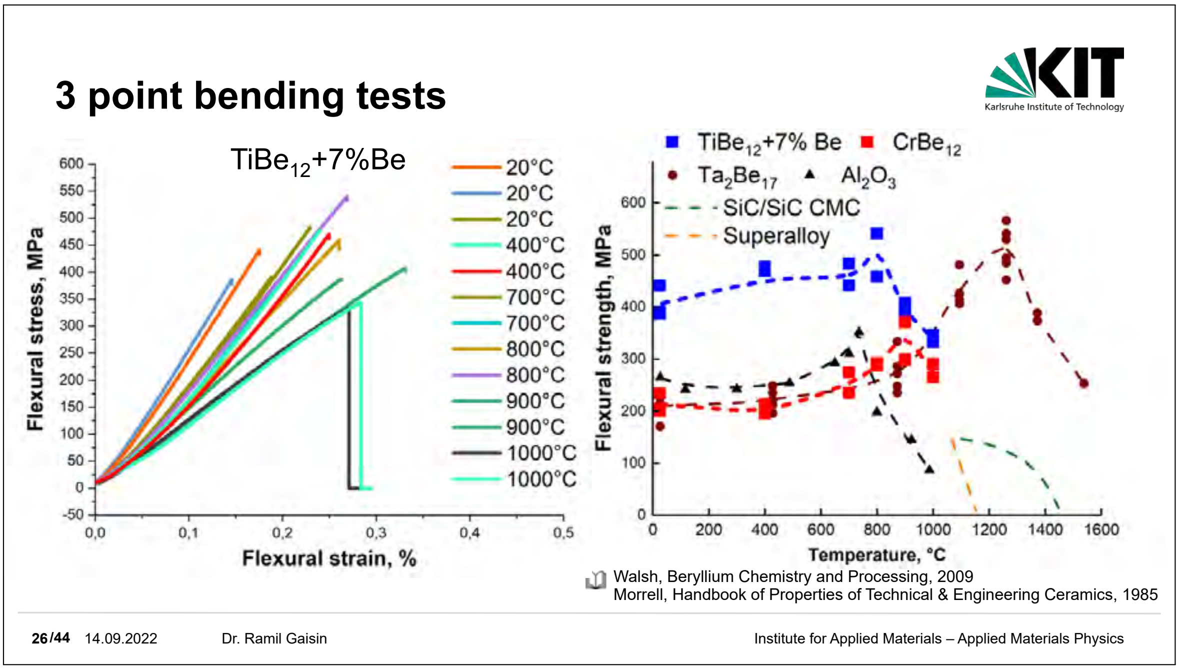
3 point bending tests
KIT
Karlsruhe Institute of Technology
TiBe12+7%Be
Flexural stress, MPa
Flexural strain, %
20°C
20°C
20°C
400°C
400°C
700°C
700°C
800°C
800°C
900°C
900°C
1000°C
1000°C
TiBe12+7% Be
CrBe12
Ta2Be17
Al2O3
SiC/SiC CMC
Superalloy
Flexural strength, MPa
Temperature, °C
Walsh, Beryllium Chemistry and Processing, 2009
Morrell, Handbook of Properties of Technical & Engineering Ceramics, 1985
26/44 14.09.2022 Dr. Ramil Gaisin Institute for Applied Materials – Applied Materials Physics

Requirements for beryllides as neutron multiplier materials

- High tritium breeding ratio – maximum possible content of Be
- Minimum content of impurities that form long-lived isotopes under irradiation (e.g. Uranium)
- Fine grain structure for easy tritium release and reasonable mechanical properties
- Beryllide blocks must retain their shape and not fracture during operation
- Low corrosion in the air and purge gas atmosphere
- Low interaction with structural materials (e.g. EUROFER steel)
- No fracture or cracks during rapid heating/cooling due to pulsed operation of DEMO

27/44 14.09.2022 Dr. Ramil Gaisin Institute for Applied Materials – Applied Materials Physics

Corrosion tests in air and He + 2% H_2O

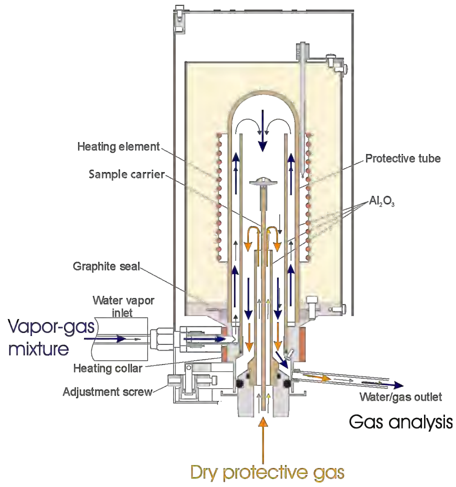

28/44 14.09.2022 Dr. Ramil Gaisin Institute for Applied Materials – Applied Materials Physics

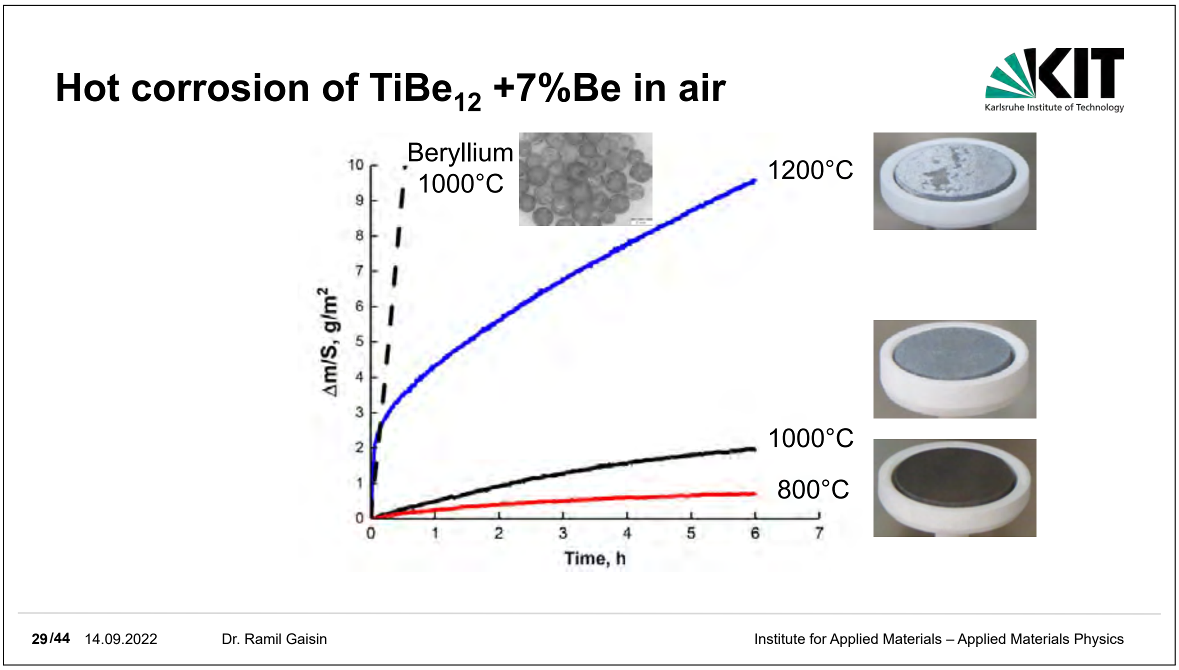
Hot corrosion of $TiBe_{12}$ +7%Be in air
KIT
Karlsruhe Institute of Technology
Beryllium
1000°C
1200°C
1000°C
800°C
$\Delta m/S$, g/m²
Time, h
29/44 14.09.2022
Dr. Ramil Gaisin
Institute for Applied Materials – Applied Materials Physics

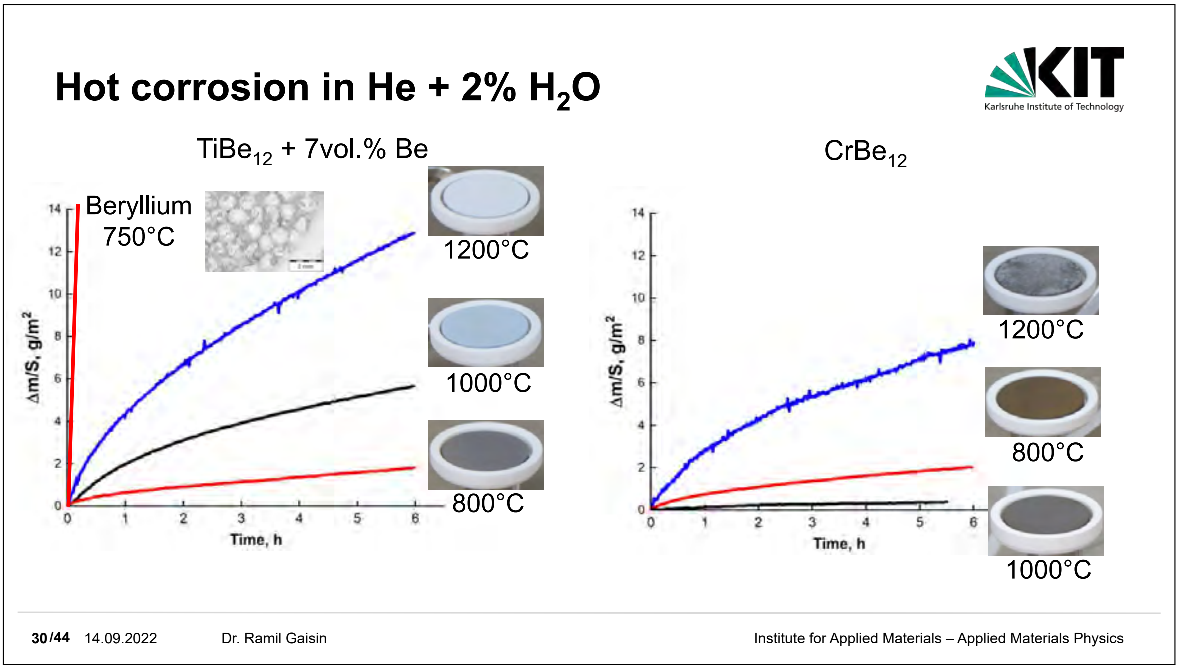
Hot corrosion in He + 2% H_2O
KIT
Karlsruhe Institute of Technology
$TiBe_{12}$ + 7vol.% Be
Beryllium
750°C
1200°C
1000°C
800°C
$\Delta m/S$, g/m²
Time, h
$CrBe_{12}$
1200°C
800°C
1000°C
$\Delta m/S$, g/m²
Time, h
30/44 14.09.2022
Dr. Ramil Gaisin
Institute for Applied Materials – Applied Materials Physics

Hot corrosion in He + 2% H_2O

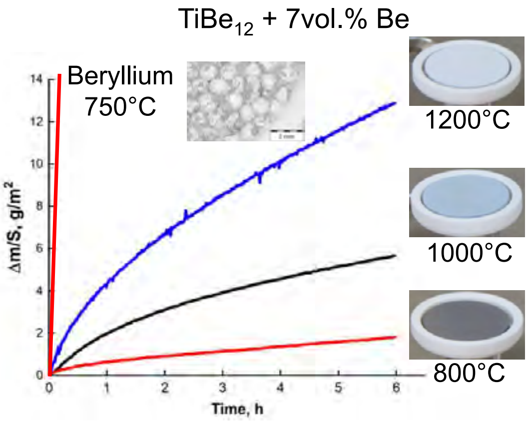

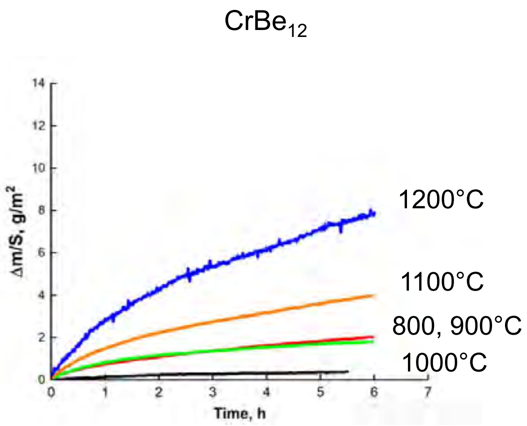

31 /44 14.09.2022 Dr. Ramil Gaisin Institute for Applied Materials – Applied Materials Physics

Requirements for beryllides as neutron multiplier materials

- High tritium breeding ratio – maximum possible content of Be
- Minimum content of impurities that form long-lived isotopes under irradiation (e.g. Uranium)
- Fine grain structure for easy tritium release and reasonable mechanical properties
- Beryllide blocks must retain their shape and not fracture during operation
- Low corrosion in the air and purge gas atmosphere
- Low interaction with structural materials (e.g. EUROFER steel)
- No fracture or cracks during rapid heating/cooling due to pulsed operation of DEMO

32 /44 14.09.2022 Dr. Ramil Gaisin Institute for Applied Materials – Applied Materials Physics

Compatibility of Ti and Cr beryllides with EUROFER

$TiBe_{12}$+7%Be

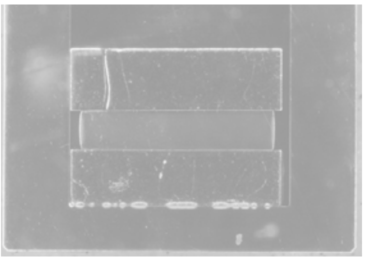

900°C, 1000 N, 100 h

$CrBe_{12}$

33/44 14.09.2022 Dr. Ramil Gaisin Institute for Applied Materials – Applied Materials Physics

Compatibility of Ti and Cr beryllides with EUROFER

$TiBe_{12}$+7%Be

EUROFER

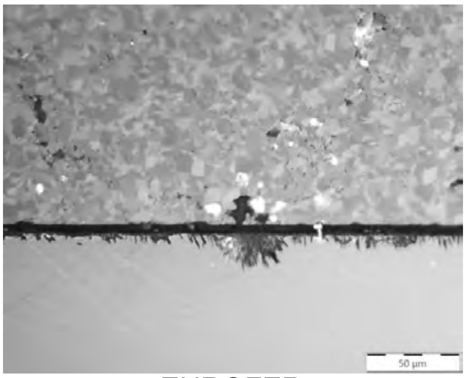

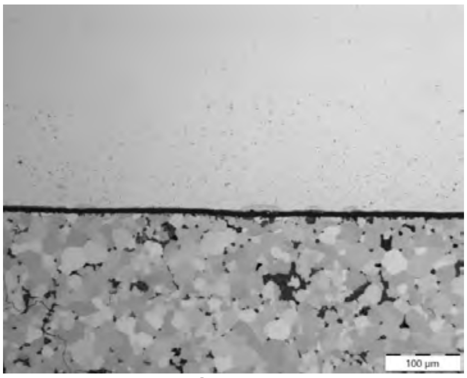

EUROFER

$CrBe_{12}$

34/44 14.09.2022 Dr. Ramil Gaisin Institute for Applied Materials – Applied Materials Physics

Requirements for beryllides as neutron multiplier materials

- High tritium breeding ratio – maximum possible content of Be
- Minimum content of impurities that form long-lived isotopes under irradiation (e.g. Uranium)
- Fine grain structure for easy tritium release and reasonable mechanical properties
- Beryllide blocks must retain their shape and not fracture during operation
- Low corrosion in the air and purge gas atmosphere
- Low interaction with structural materials (e.g. EUROFER steel)
- No fracture or cracks during rapid heating/cooling due to pulsed operation of DEMO

35/44 14.09.2022 Dr. Ramil Gaisin Institute for Applied Materials – Applied Materials Physics

Thermal cycling of test sample

$TiBe_{12}$ Ø40×20

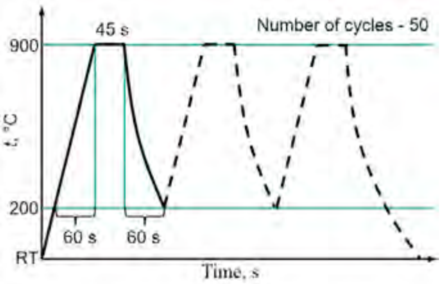

After thermal cycling

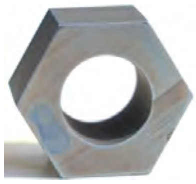

36/44 14.09.2022 Dr. Ramil Gaisin Institute for Applied Materials – Applied Materials Physics

Simulation of DEMO pulse using induction heating

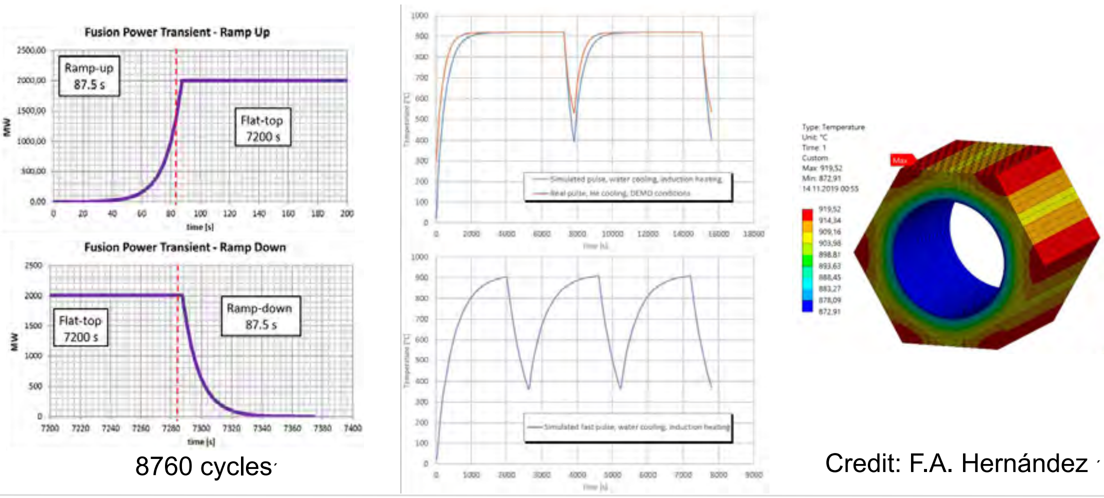

8760 cycles

Credit: F.A. Hernández

37/44 14.09.2022 Dr. Ramil Gaisin Institute for Applied Materials – Applied Materials Physics

Thermal cycling of full-sized blocks

$TiBe_{12}$ Ø144×100

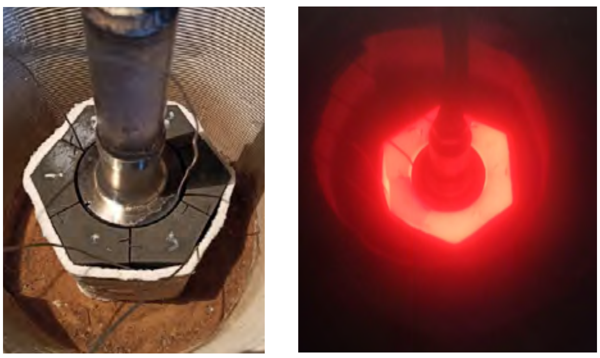

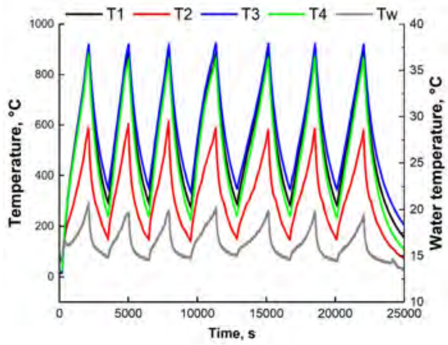

38/44 14.09.2022 Dr. Ramil Gaisin Institute for Applied Materials – Applied Materials Physics

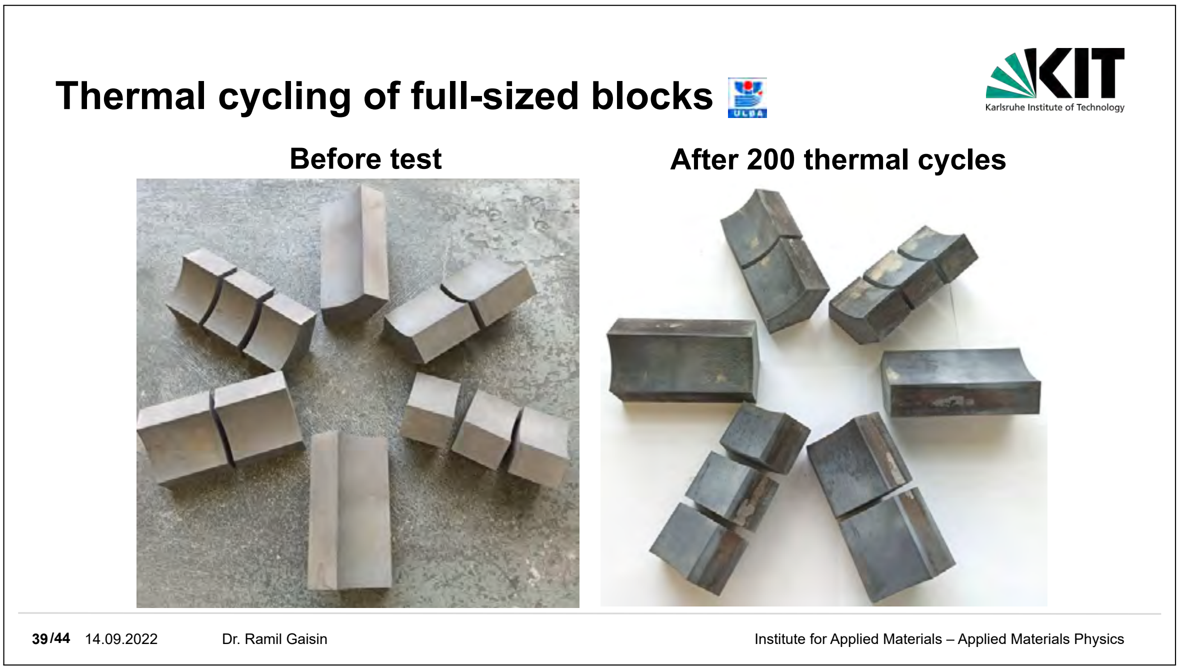
Thermal cycling of full-sized blocks
Karlsruhe Institute of Technology
Before test
After 200 thermal cycles
39/44 14.09.2022
Dr. Ramil Gaisin
Institute for Applied Materials – Applied Materials Physics

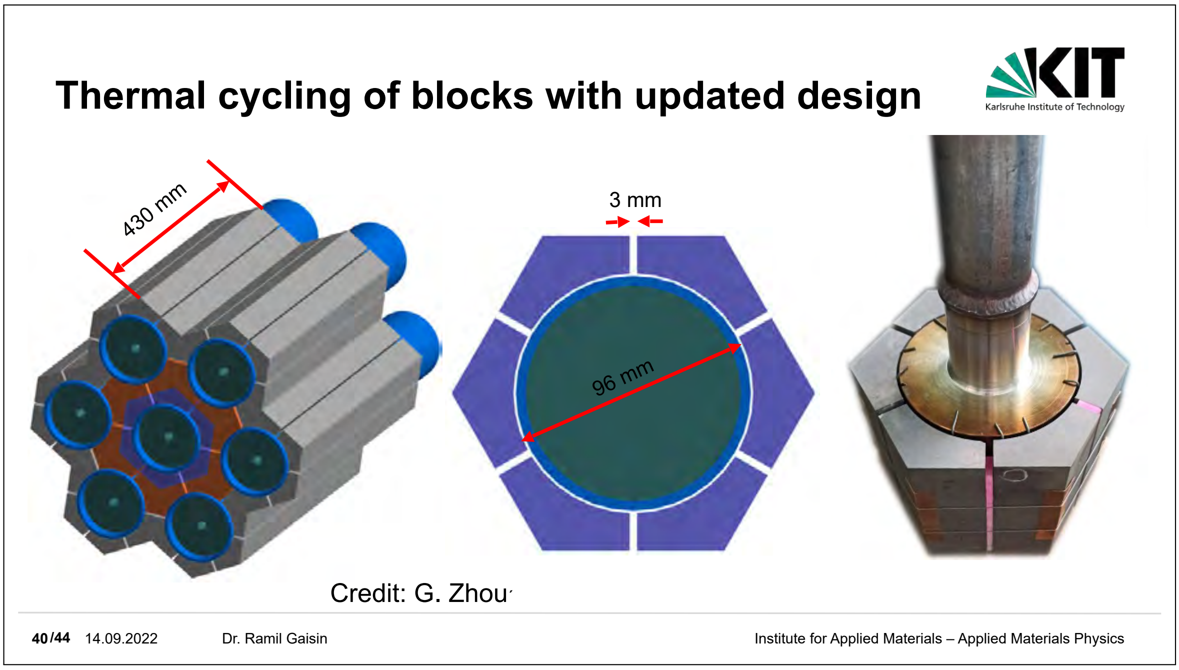
Thermal cycling of blocks with updated design
Karlsruhe Institute of Technology
430 mm
3 mm
96 mm
Credit: G. Zhou
40/44 14.09.2022
Dr. Ramil Gaisin
Institute for Applied Materials – Applied Materials Physics

Thermal cycling of beryllide blocks

KIT Karlsruhe Institute of Technology

Thermal cycling in 2020-2021

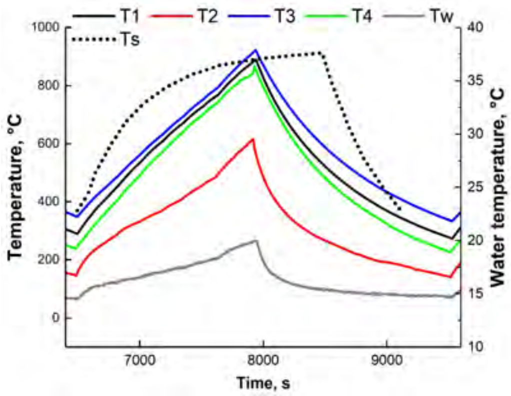

360-930°C
200 cycles

Thermal cycling in 2022-2023

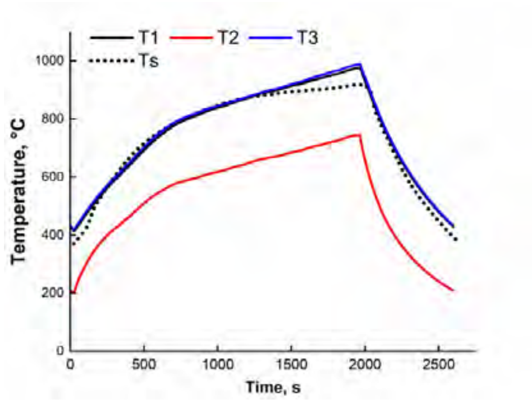

440-990°C
>500 of 1500 cycles

41/44 14.09.2022 Dr. Ramil Gaisin Institute for Applied Materials – Applied Materials Physics

Conclusions

KIT Karlsruhe Institute of Technology

- Single-phase $TiBe_{12}$ meets all the basic requirements for NMM.
- $CrBe_{12}$ is not yet well studied in terms of irradiation and thermal cycling, but may be a good alternative due to better corrosion resistance.
- The presence of a beryllium metal phase in beryllide increases ductility, but can cause accelerated corrosion or interaction with other materials.

Outlook

- New irradiation campaign up to 2-3 dpa and post irradiation examination

42/44 14.09.2022 Dr. Ramil Gaisin Institute for Applied Materials – Applied Materials Physics

Potential applications of beryllides in extreme environments

Karlsruhe Institute of Technology

Neutron multiplier material in fusion power plant blanket

- High-dose irradiation (20-50 dpa) in high-energy neutrons
- High temperature up to 1000°C
- High heating/cooling rates
- Potentially corrosive atmosphere

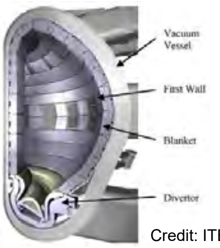

Credit: ITER

Structural material for the skin of spacecraft and hypersonic vehicles

- High temperatures of 1000°C and above
- Thermal shocks
- Corrosive atmosphere
- High loads
- Collision with debris

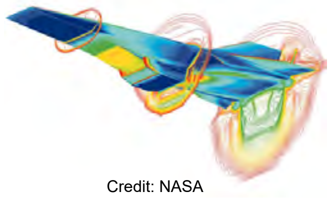

Credit: NASA

Neutron reflector material in fission reactors

- High-dose irradiation in low-energy neutrons
- Low temperature (70-150°C) – cracking / swelling
- Water environment

Credit: Materion Corp.

43/44 14.09.2022 Dr. Ramil Gaisin Institute for Applied Materials – Applied Materials Physics

Karlsruhe Institute of Technology

Thank you for your attention!

44/44 14.09.2022 Dr. Ramil Gaisin Institute for Applied Materials – Applied Materials Physics

Mechanical properties of titanium beryllium intermetallic compounds

Taehyun HWANG[1], Jae-Hwan KIM[1], Yutaka SUGIMOTO[1], Suguru NAKANO[1], Yoshiaski AKATSU[1], Msaru NAKAMICHI[1],

[1] *Fusion Energy Research and Development Directorate, National Institutes for Quantum Science and Technology, Rokkasho, Aomori 2-166, Japan*

Beryllium (Be) has been a promising functional material for the breeding blanket of a fusion reactor. However, Be has disadvantages such as the sharp increase of swelling above 600°C and deterioration for mechanical properties and thermal conductivity due to irradiation damage. Be intermetallic compounds (beryllide) such as $Be_{12}Ti$ and $Be_{12}V$ are considered as promising advanced neutron multipliers for DEMO instead of Be, because of its excellent high-temperature stability and low reactivity with water vapor. Besides, recently, there has been a growing interest in the usage of beryllide block instead of beryllide pebble. However, the evaluation of the mechanical properties of beryllide has not been sufficiently performed. Thus, the aim of this study is to investigate the tensile properties of beryllide.

A mixed powder of Be-7.7at.% Ti, which is the stoichiometric value of $Be_{12}Ti$, was subjected to a single-phase treatment at 1200°C for 24 hours in an argon atmosphere. Also, $Be_{12}Ti$ powder which has been crushed using a planetary ball mill at 300 rpm for 5 hours was prepared for comparison of the effect of refinement. For the fabricating samples, plasma sintering (KE-PAS II, manufactured by Kaken) was conducted using beryllide single-phase powder. Tensile tests were performed on various temperatures with sub-sized tensile specimens, which fabricated by electric discharge machining.

Under the above-mentioned sintering conditions, $Be_{12}Ti$ single-phase berylide was obtained, and the sintering density of $Be_{12}Ti$ was almost 100% above 1000°C. Detail of tensile properties of beryllides will be reported.

Corresponding Author:

Dr. HWANG Taehyun
hwang.taehyun@qst.go.jp
Fusion Energy Research and Development Directorate, National Institutes for Quantum Science and Technology, Rokkasho, Aomori 2-166, Japan

Mechanical properties of titanium beryllium intermetallic compounds

Taehyun HWANG[1], Jae-Hwan KIM[1], Yutaka SUGIMOTO[1], Suguru NAKANO[1], Yoshiaski AKATSU[1], Msaru NAKAMICHI[1],

National Institutes for Quantum Science and Technology

In this presentation ,unfortunately, only published and opened materials will be presented because of export classification's aspect.

1

Introduction

- Developing advanced neutron multipliers

Beryllium(Be) used to be a candidate for **neutron multipliers**

- Swelling by neutron irradiation
- Oxidation resistance at high temperatures
- Hydrogen generation by water vapor
- Deterioration of mechanical properties and thermal conductivity due to irradiation

➡ **Beryllium intermetallic compound（$Be_{12}Ti$, $Be_{12}V$）**

- Design

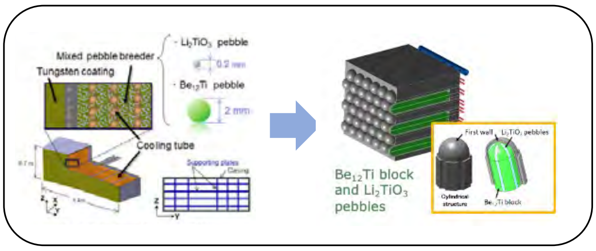

- Objective

To evaluate the mechanical properties of beryllide fabricated by the plasma sintering method for establishment of the material database for DEMO design.

2

Experimental

- Test Material
  - Be-7.7at.%Ti isothermal heat treatment （Ar ATM 1200℃ 24hr）
  - Plasma sintering
  - Ball milling (BM)300rpm、 5hr
- Particle analysis
  - ✓ CAMSIZER X2
- Sintering condition
  - ✓ KE-PASII、 kaken.co.
  - Sintered temp.：900, 1000, 1050℃, 20 min
  - Sintered pressure：15, 17 kN
- Hardness
  - load：300 gf
  - Cal. For toughness：IF method、 load : 5kgf

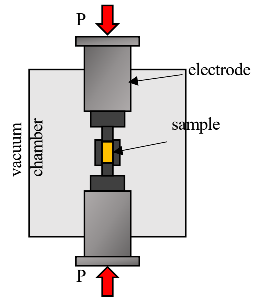

3

Results of XRD and size analysis

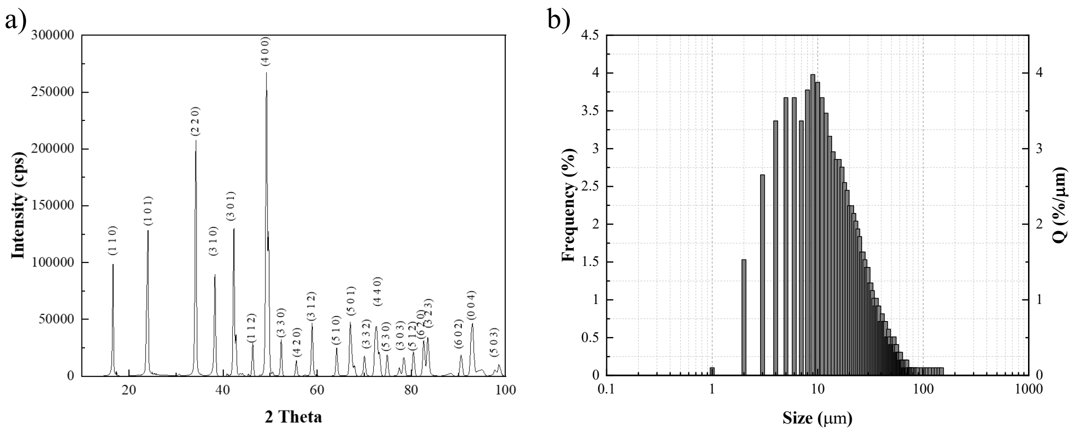

- The diffractogram suggests that no peaks were observed for any impurities, indicating that the $Be_{12}Ti$ intermetallic compound was successfully synthesized.
- The average size of powder was approximately 16.5 μm

4

T. Hwang et al., Nuclear Materials and Energy 30 (2022) 101117

Effect of sintering temperature on density and hardness

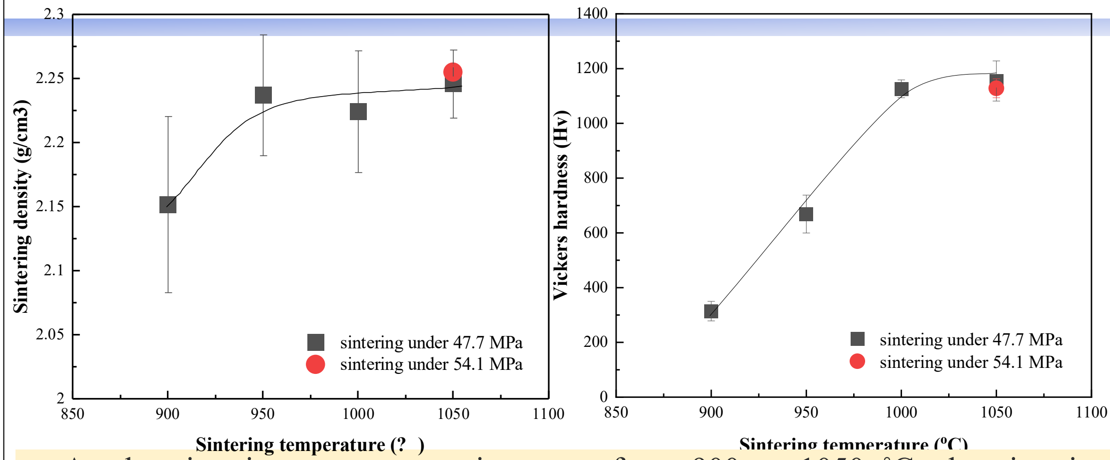

- As the sintering temperature increases from 900 to 1050 ˚C, the sintering density also increases and reaches a theoretical density of 2.26 g/cm^3.
- Beryllide has a low density because the low sintering temperature of 900 ˚C, which corresponds to 60% of the melting point (1500 ˚C), for $Be_{12}Ti$ resulted in insufficient consolidation of powders.
- The plot of Vickers microhardness for $Be_{12}Ti$ seems to be consistent with the sintering density as a function of temperature.

T. Hwang et al., Nuclear Materials and Energy 30 (2022) 101117

Effect of Sintering Temper. on $Be_{12}Ti$ Microstructure

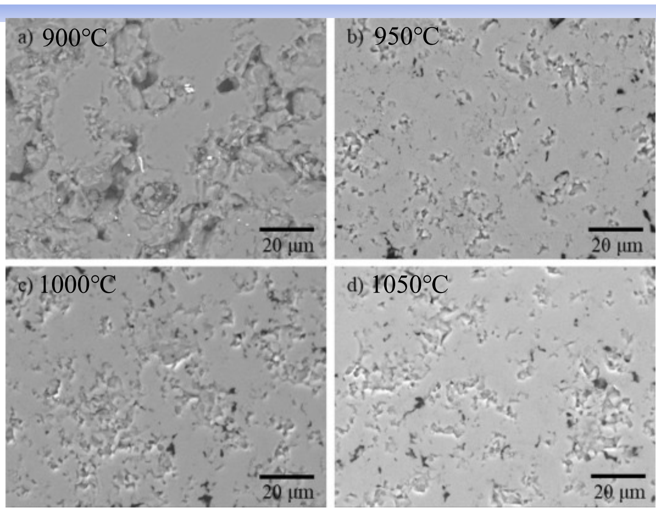

- Due to insufficient sintering temperature (Fig. 4(a)), consolidation between particles was not sufficient during plasma sintering, and many pores were formed on the surface.
- As the sintering temperature increased to 1050 ˚C, the volume fraction of pores decreased.

6

T. Hwang et al., Nuclear Materials and Energy 30 (2022) 101117

Calculation of fracture toughness by IF method

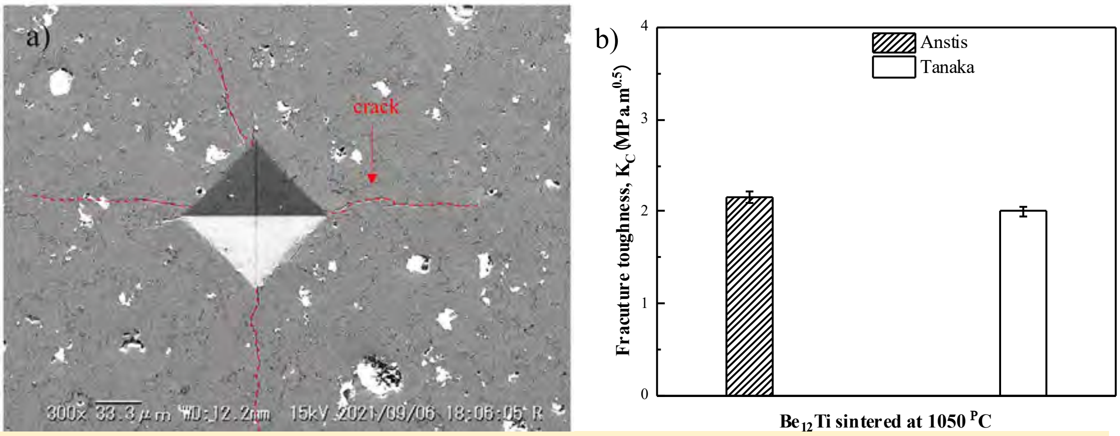

The fracture toughness of plasma-sintered $Be_{12}Ti$ sintered at 1050 ˚C and 54.1 MPa was found to be comparable to that of $Be_{12}Ti$.
The fracture toughness of plasma-sintered $Be_{12}Ti$ was 2.16, and 2.00 MPa·m$^{0.5}$, respectively, based on the calculation formula, indicating that it is brittle compared to Be at 9.0 MPa·m$^{0.5}$.

- *T. Hwang et al., Nuclear Materials and Energy 30 (2022) 101117*
- *G.R. Anstis, P. Chantikul, B.R. Lawn, D.B. Marshall, J. Am. Ceram. Soc. 64 (9) (1981) 533–538,*
- *K. Tanaka, J. Japan Inst. Met. Mater. 48 (12) (1984) 1157–1162*

7

Summary

The mechanical properties of $Be_{12}Ti$ fabricated by plasma sintering were investigated to provide important properties data for the material database for beryllide blocks as advanced neutron multipliers.
From the experimental results, the following conclusions can be drawn:

- Block-type single-phased $Be_{12}Ti$ was successfully fabricated by homogenization treatment and plasma sintering.
- As the sintering temperature increased, the sintering density and microhardness increased up to 1000 ˚C and then saturated.
- The Vickers microhardness was congruent with the sintering density. The microhardness of $Be_{12}Ti$ sintered at 1050 ˚C was 1154 Hv.
- To determine the fracture toughness of beryllide sintered at 1050 ˚C, the IF method was used, and the results showed that the fracture toughness values were 2.16, and 2.00 MPa·m$^{0.5}$ according to Anstis, and Tanaka equations, respectively. There was no significant difference compared with HIP $Be_{12}Ti$ by KIT.

8

SESSION 5

Modeling & experimental validation

Investigation of radiation damage effects in beryllium: updates on recent results obtained on proton, neutron and He-ions irradiated samples

Slava Kuksenko

United Kingdom Atomic Energy Authority, Culham Science Centre, Abingdon, OX14 3DB, UK

Beryllium is an essential material for a wide variety of application such as operating and future nuclear facilities including material testing nuclear fission reactors, fusion energy experimental and future commercial reactors, target component materials in currently running and near-future multi-megawatt particle accelerator sources. Therefore, beryllium and beryllium-based alloys are under extensive investigation by nuclear facility communities.

The paper gives an overview of the recent results obtained in the UK Atomic Energy Authority on beryllium samples, particularly during collaborative studies with the Karlsruhe Institute of Technology (Germany), the University of Horsfield (UK) and the international Radiation Damage In Accelerator Target Environments (RaDIATE) collaboration and include:

- micromechanical test results obtained on high energy proton irradiated and helium implanted samples including novel TiBe12 and CrBe12 alloys;
- atom probe tomography mapping of the fine-scale distribution of impurities and transmutants in beryllium after neutron irradiation at different DEMO relevant conditions during the HIDOBE-2 campaign in the HFR reactor;
- updates on the in-situ and ex-situ TEM studies of He implanted beryllium, TiBe12 and CrBe12 alloys.

The paper will also give an overview of the future plans.

Corresponding Author:

Dr. Viacheslav Kuksenko
slava.kuksenko@ukaea.uk
United Kingdom Atomic Energy Authority
Culham Science Centre, Abingdon, OX14 3DB, UK

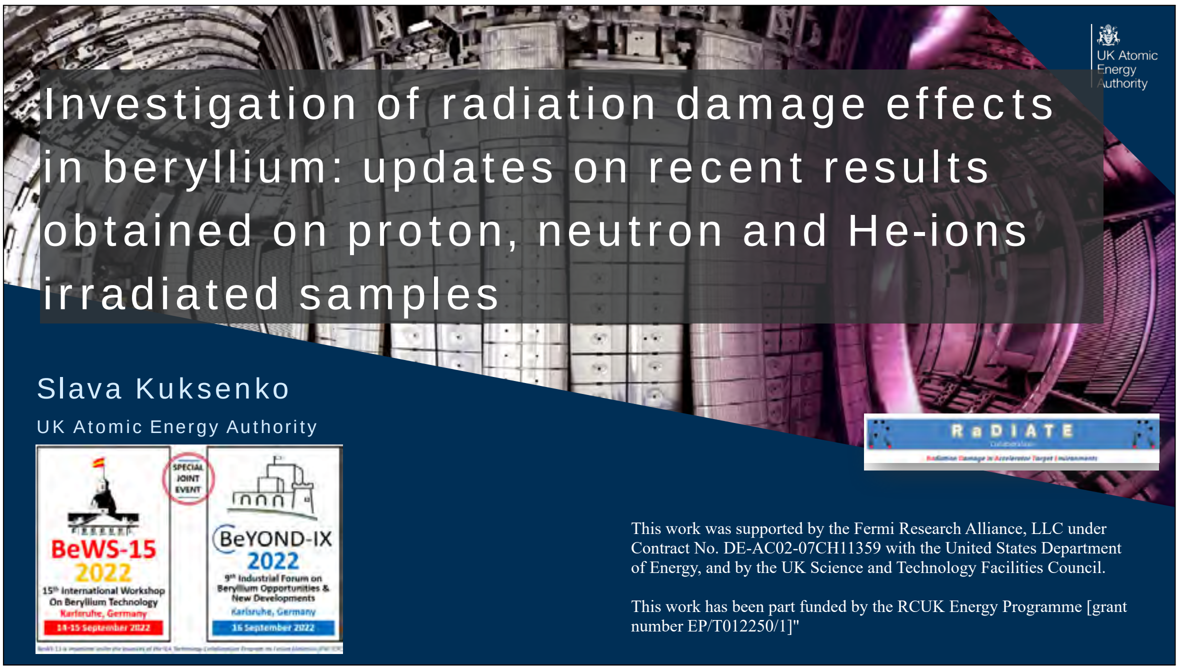
UK Atomic Energy Authority
Investigation of radiation damage effects in beryllium: updates on recent results obtained on proton, neutron and He-ions irradiated samples
Slava Kuksenko
UK Atomic Energy Authority
RaDIATE
BeWS-15 2022
15th International Workshop On Beryllium Technology
Karlsruhe, Germany
14-15 September 2022
SPECIAL JOINT EVENT
BeYOND-IX 2022
9th Industrial Forum on Beryllium Opportunities & New Developments
Karlsruhe, Germany
16 September 2022
This work was supported by the Fermi Research Alliance, LLC under Contract No. DE-AC02-07CH11359 with the United States Department of Energy, and by the UK Science and Technology Facilities Council.
This work has been part funded by the RCUK Energy Programme [grant number EP/T012250/1]"

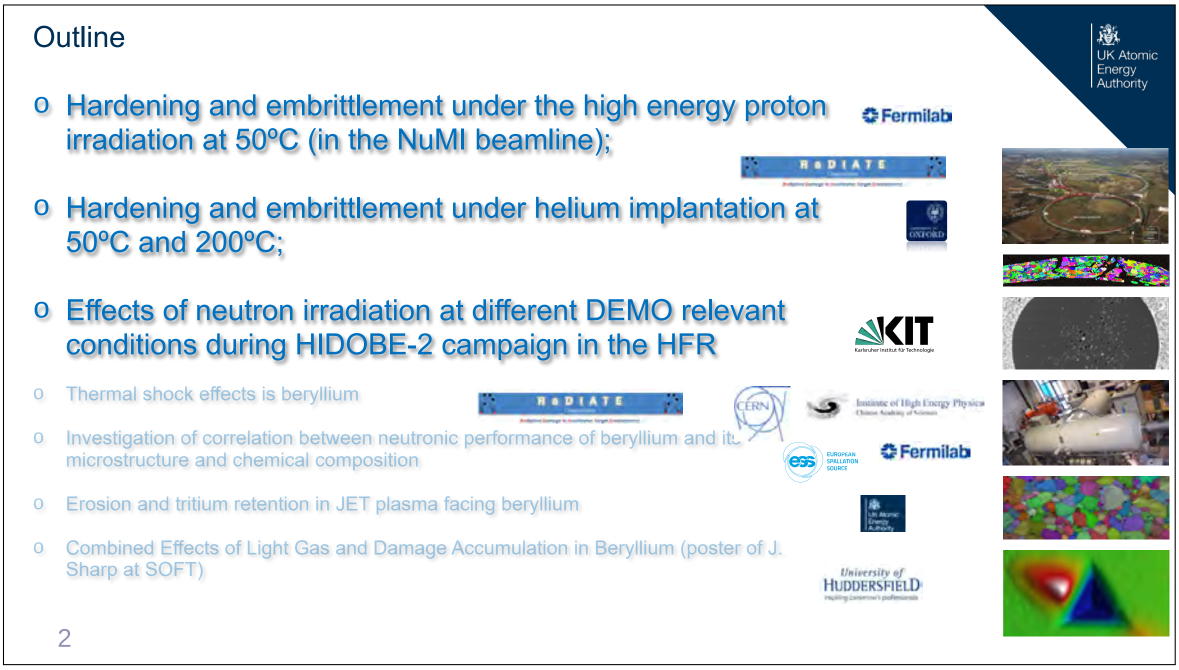
Outline
Hardening and embrittlement under the high energy proton irradiation at 50°C (in the NuMI beamline);
Hardening and embrittlement under helium implantation at 50°C and 200°C;
Effects of neutron irradiation at different DEMO relevant conditions during HIDOBE-2 campaign in the HFR
Thermal shock effects is beryllium
Investigation of correlation between neutronic performance of beryllium and its microstructure and chemical composition
Erosion and tritium retention in JET plasma facing beryllium
Combined Effects of Light Gas and Damage Accumulation in Beryllium (poster of J. Sharp at SOFT)
Fermilab
RaDIATE
KIT
CERN
Institute of High Energy Physics
ess
Fermilab
UK Atomic Energy Authority
University of HUDDERSFIELD
2

4
Be
Beryllium
9.012

Beryllium has a unique combination of mechanical and physical properties:

- High strength
- Low density
- Low nuclear interaction cross-section (so low heat load)
- High heat capacity
- Thermal conductivity
- High melting point

Beryllium is of particular importance for nuclear application:

- First wall material in JET experiment and the currently constructed ITER
- Neutron multiplier candidate material for tritium breeding blanket of the future DEMO and STEP fusion reactors
- Reflector and moderation in research reactors and spallation neutron sources
- Beam windows and target components material in neutrino sources

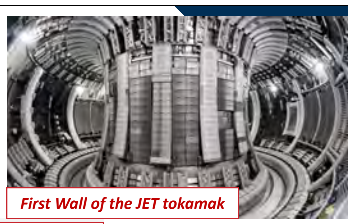
First Wall of the JET tokamak


Primary beam window of the NuMI neutrino source


Be reflector in the ISIS Neutron Source (TS2)

	Very high He production in beryllium, appm/dpa
SM-3 high-flux reactor (Russia)	330
BOR-60 reactor (Russia)	280
HFR, HIDOBE-01 irradiation campaign (Petten, Netherlands)	160
Beryllium reflectors in the ISIS neutron source (RAL, UK)	110 - 220
DEMO fusion reactor	700
Neutrino target component (FNAL, USA)	4000

3

Proton irradiated beam window: (NuMI)

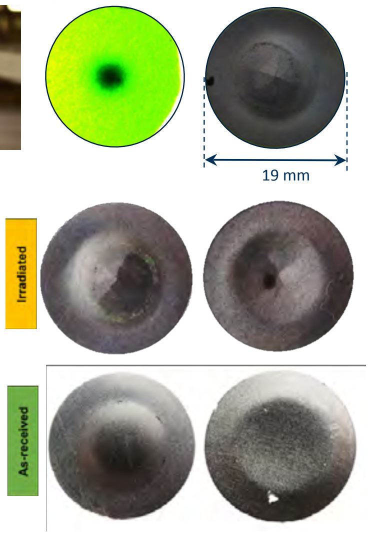

120GeV proton beam
- 1.57×10^{21} protons during its lifetime
- Up to 0.5 dpa and 2000 appm of He
- T ≈ 50ºC

UK Atomic Energy Authority

4

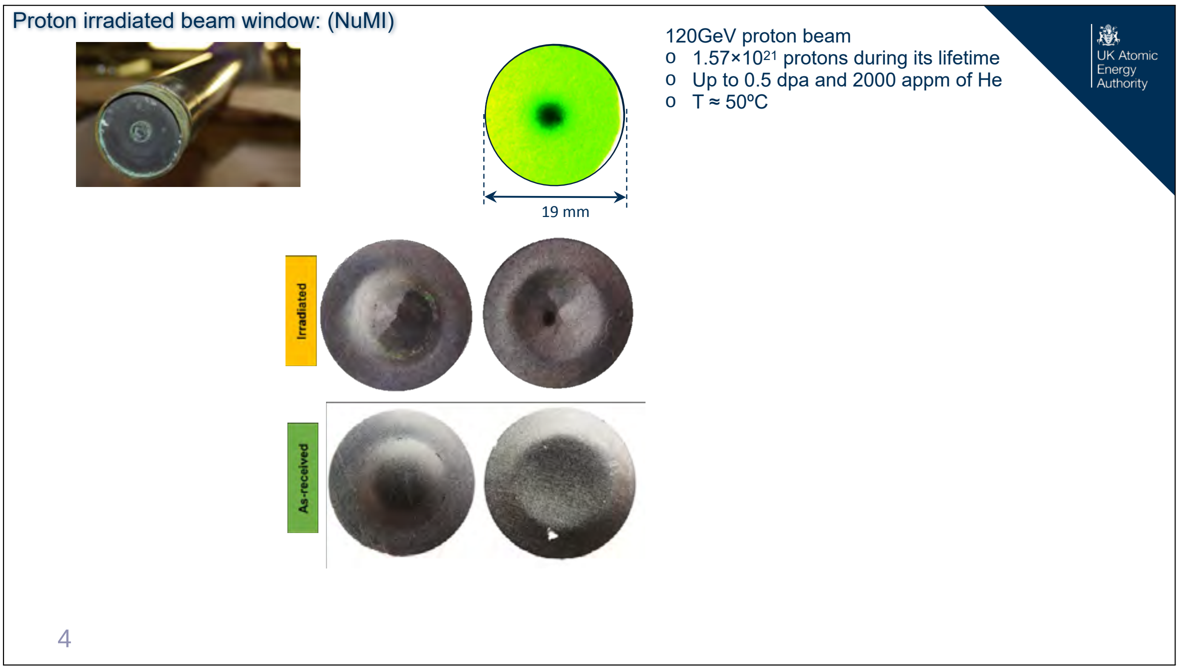
Proton irradiated beam window: (NuMI)
120GeV proton beam
o 1.57×10²¹ protons during its lifetime
o Up to 0.5 dpa and 2000 appm of He
o T ≈ 50ºC
UK Atomic Energy Authority
19 mm
Irradiated
As-received
4

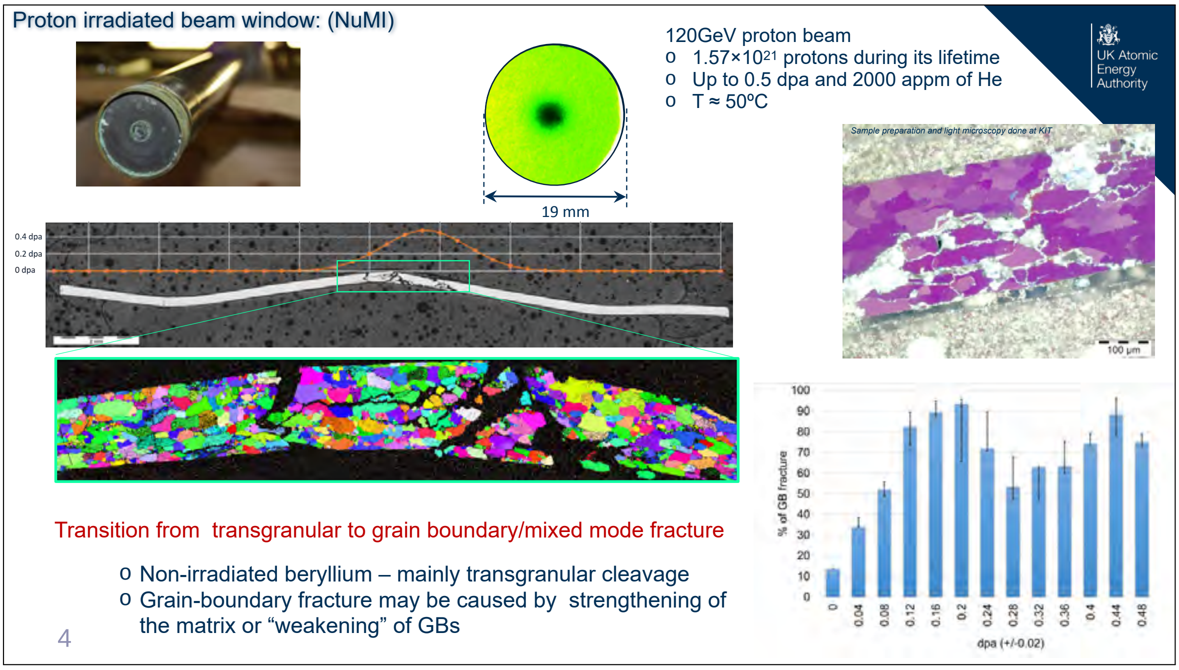
Proton irradiated beam window: (NuMI)
120GeV proton beam
o 1.57×10²¹ protons during its lifetime
o Up to 0.5 dpa and 2000 appm of He
o T ≈ 50ºC
UK Atomic Energy Authority
19 mm
0.4 dpa
0.2 dpa
0 dpa
Sample preparation and light microscopy done at KIT
100 µm
% of GB fracture
dpa (+/-0.02)
Transition from transgranular to grain boundary/mixed mode fracture
o Non-irradiated beryllium – mainly transgranular cleavage
o Grain-boundary fracture may be caused by strengthening of the matrix or “weakening” of GBs
4

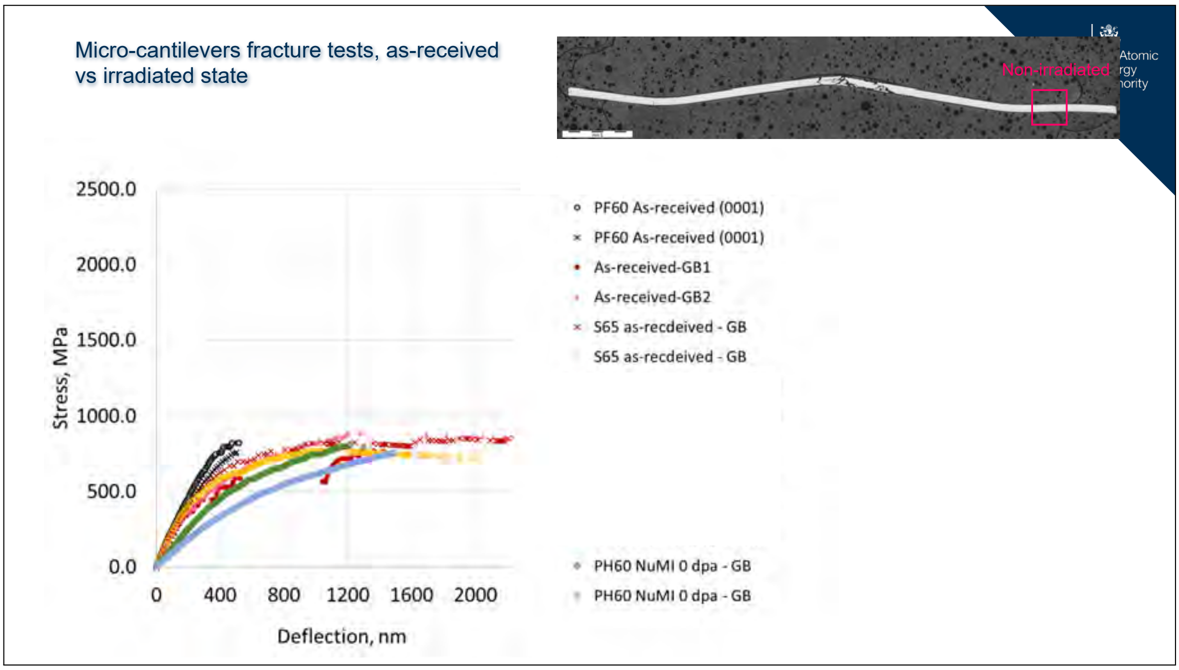
Micro-cantilevers fracture tests, as-received vs irradiated state
Non-irradiated
Stress, MPa
2500.0
2000.0
1500.0
1000.0
500.0
0.0
0
400
800
1200
1600
2000
Deflection, nm
PF60 As-received (0001)
PF60 As-received (0001)
As-received-GB1
As-received-GB2
S65 as-recdeived - GB
S65 as-recdeived - GB
PH60 NuMI 0 dpa - GB
PH60 NuMI 0 dpa - GB

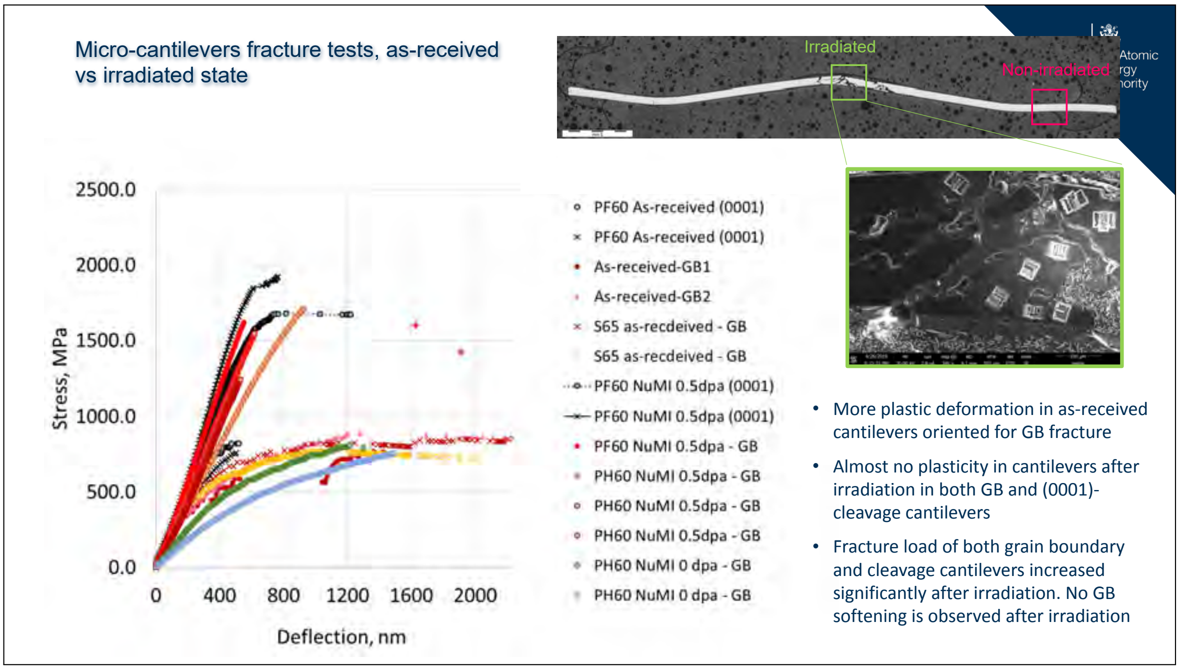
Micro-cantilevers fracture tests, as-received vs irradiated state
Irradiated
Non-irradiated
Stress, MPa
2500.0
2000.0
1500.0
1000.0
500.0
0.0
0
400
800
1200
1600
2000
Deflection, nm
PF60 As-received (0001)
PF60 As-received (0001)
As-received-GB1
As-received-GB2
S65 as-recdeived - GB
S65 as-recdeived - GB
PF60 NuMI 0.5dpa (0001)
PF60 NuMI 0.5dpa (0001)
PF60 NuMI 0.5dpa - GB
PH60 NuMI 0.5dpa - GB
PH60 NuMI 0.5dpa - GB
PH60 NuMI 0.5dpa - GB
PH60 NuMI 0 dpa - GB
PH60 NuMI 0 dpa - GB
• More plastic deformation in as-received cantilevers oriented for GB fracture
• Almost no plasticity in cantilevers after irradiation in both GB and (0001)-cleavage cantilevers
• Fracture load of both grain boundary and cleavage cantilevers increased significantly after irradiation. No GB softening is observed after irradiation

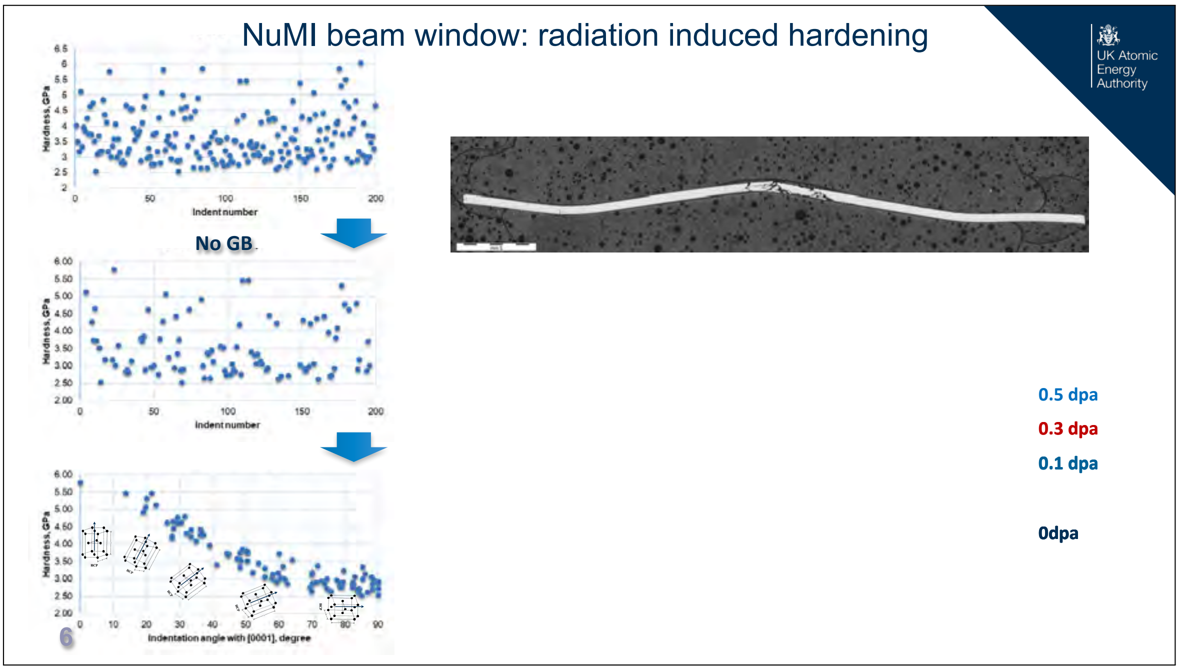
NuMI beam window: radiation induced hardening
UK Atomic Energy Authority
Hardness, GPa
Indent number
No GB
Hardness, GPa
Indent number
Hardness, GPa
Indentation angle with [0001], degree
0.5 dpa
0.3 dpa
0.1 dpa
0dpa

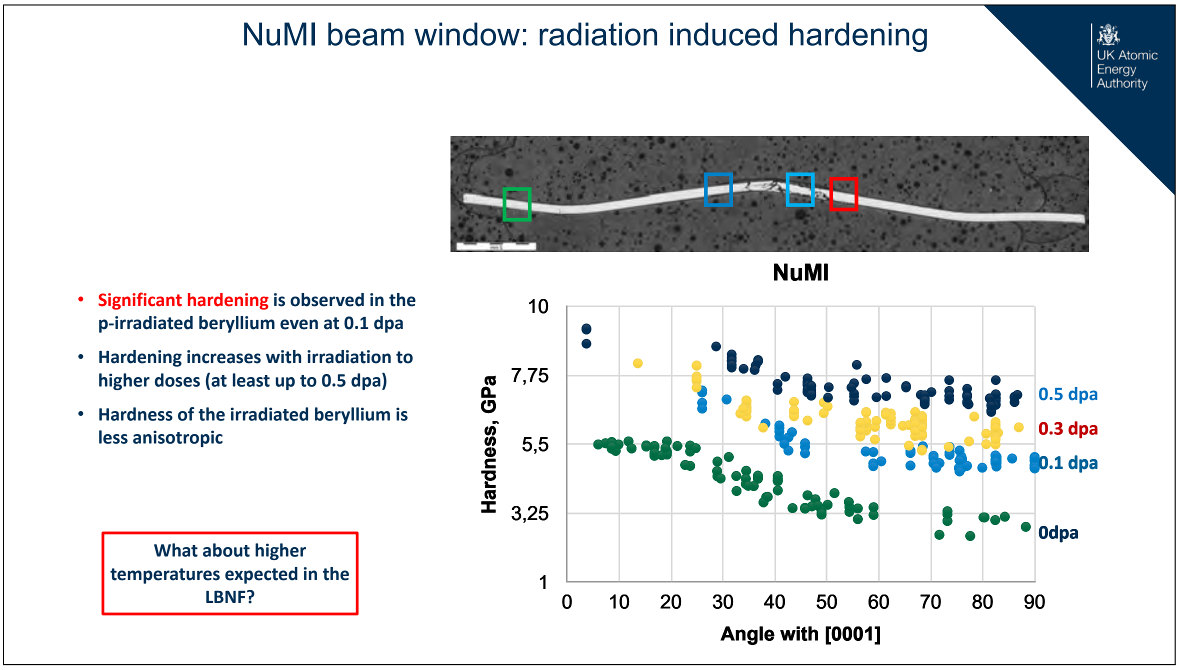
NuMI beam window: radiation induced hardening
UK Atomic Energy Authority
• Significant hardening is observed in the p-irradiated beryllium even at 0.1 dpa
• Hardening increases with irradiation to higher doses (at least up to 0.5 dpa)
• Hardness of the irradiated beryllium is less anisotropic
What about higher temperatures expected in the LBNF?
NuMI
Hardness, GPa
10
7,75
5,5
3,25
1
0
10
20
30
40
50
60
70
80
90
Angle with [0001]
0.5 dpa
0.3 dpa
0.1 dpa
0dpa

He implantation in Be through Al degrader (50°C and 200°C)

UK Atomic Energy Authority

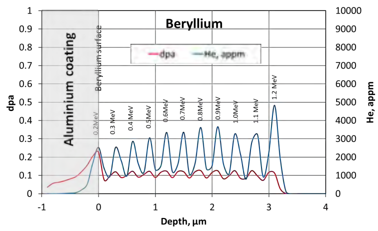

- radiation damage appeared as "black dots" (less than 10 nm) arranged in lines parallel to the surface of samples
- the damaged layers of the samples exposed at 50 and 200°C were very similar and no difference was noticed between two investigated beryllium grades (FIB damage?)
- no cavities or He bubbles at both temperatures, including grain boundary areas.

S-65 irradiated at 50°C

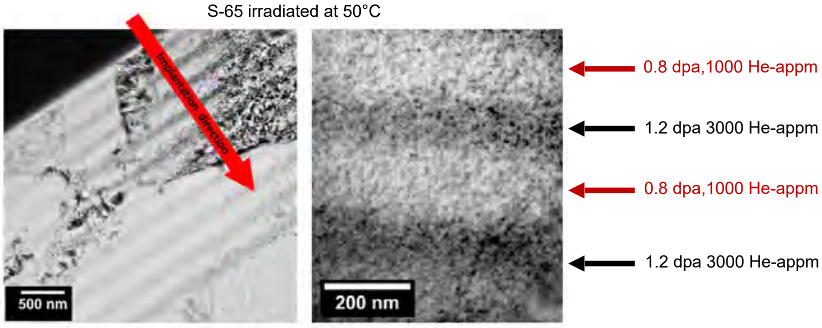

Micro-cantilevers fracture tests, He implantation vs transmutation under proton irradiation

UK Atomic Energy Authority

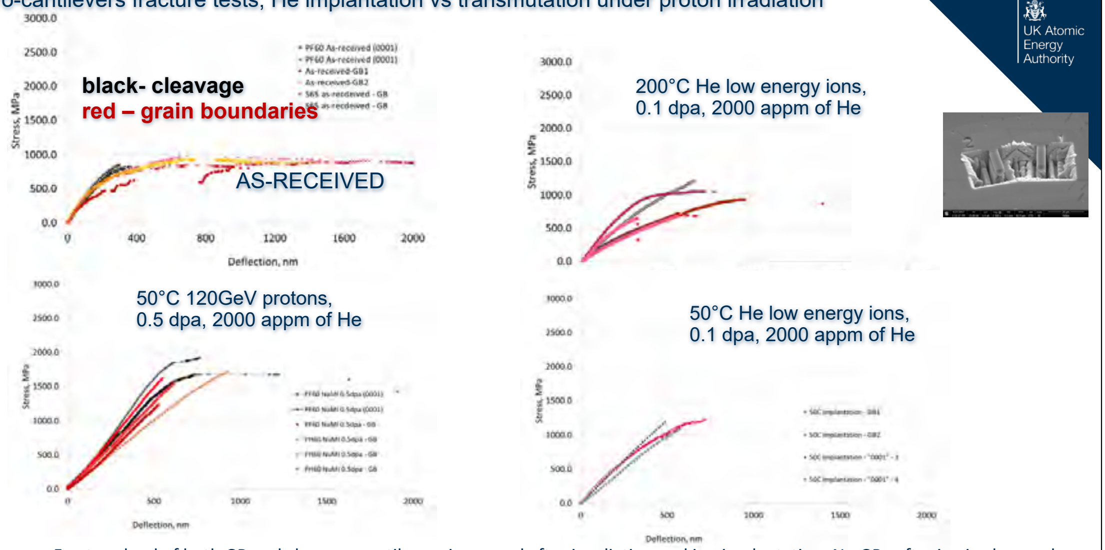

- Fracture load of both GB and cleavage cantilevers increased after irradiation and ion implantation. No GB softening is observed
- Work of fracture is lower for cantilevers pre-notched for the basal cleavage, but the difference between two types of cantilevers is after irradiation

8

Hardening under He implantation: chemistry effect

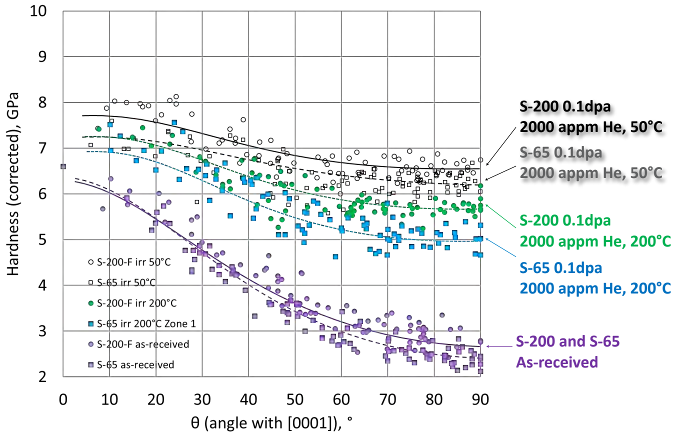

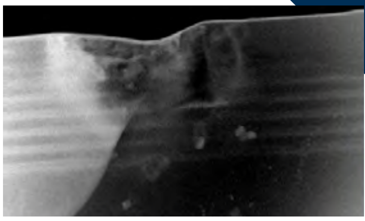

- Low purity grade is harder in as-received state and after implantations
- Irradiation induced hardening after 50°C implantation is about 75% higher than after 200°C.
- Less pure grade (S-200) exhibited higher hardening (especially for “soft” grains)

9

He implantation vs transmutation under proton irradiation at 50°C

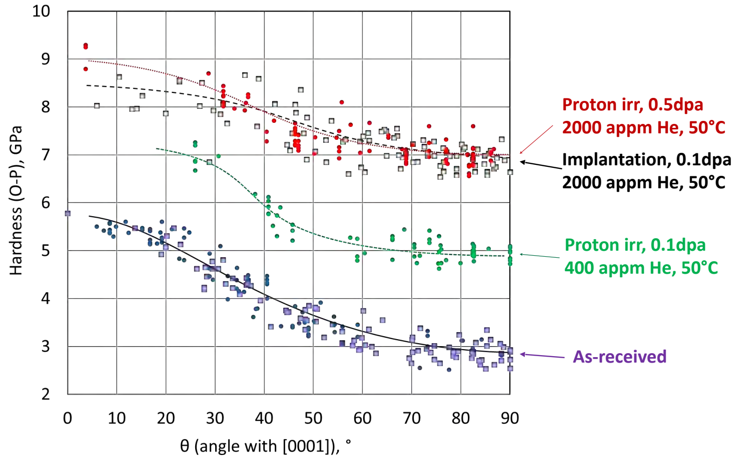

- Same He content introduces similar hardening
- Same displacement damage – less hardening after implantation
- Comparison dpa and He concentrations infuses (>0.1dpa) on hardening suggest that He concentration dominates

10

Hardening of He impanated samples

Dispersed barrier hardening model:

$$\Delta \sigma_y = \alpha M \mu b \sqrt{N \bullet d}$$

(M = 4.3 , μ =133GPa, b = 0.23nm, N $\approx$ 10^{22} m^{-3} d $\approx$ 5nm)

As a first approximation:

$$\Delta H = 3 \Delta \sigma_y$$

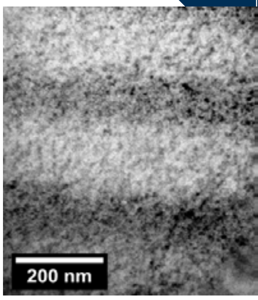

	Implantation at 50°C	Implantation at 200°C
Measured av. hardening	3.3 GPa	2.4 GPa
Black dots hardening, 0.4	From 0.85 to 1.7 GPa depending on	From 0.85 to 1.7 GPa depending on
Non-"black-dots" hardening	From 1.5 to 2.4 GPa	From 0.6 to 1.4 GPa

May it be from solid solution hardening?

$$\Delta \sigma_y = \frac{M}{760} \mu \bullet \delta^{\frac{3}{2}} \bullet c_{He}^{\frac{1}{2}} \approx$$ 33MPa for 2000 appm of He in solid solution

(model of Fleischer, 1963)

So, He should be in invisible by TEM bubbles

More details in Kuksenko et al. JNM 555 (2021)

- calculations suggest that the radius of bubbles should be $\approx$ 0.8...1.5 nm with Nd $>$ 1023m^{-3} and they should be weak obstacles $\alpha \leq 0.2$
- Difference between 50 and 200°C implantation may originate from different sizes or different vacancy/He ratio in bubbles

11

Conclusions (1st part)

1. Radiation induces significant hardening and fracture mechanism change of beryllium even at 0.1 dpa
2. Irradiation at 200°C leads to much lower hardening
3. Less pure grade (S-200) exhibited higher hardening (especially for "soft" grains)
4. Both displacement damage and He atoms cause hardening. We have indications that He content has a dominant effect.
5. He implantation led to increase of fracture strength of pre-notched microcantilevers and decrease of work to fracture, with severe drop for 50°C implantation and high energy proton irradiation
6. Calculations suggest that the radius of bubbles should be $\approx$ 0.8...1.5 nm with Nd $>$ 1023m^{-3} and they should be weak obstacles $\alpha \leq 0.2$

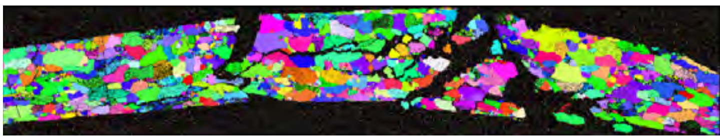

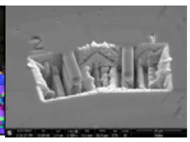

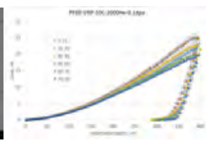

Irradiation at HIDOBE-02 (collaboration with KIT)

UK Atomic Energy Authority

Name	T irr, C	dpa	He, appm	T, appm	Experiments
6bPC2	600	34	5557	600	SEM, EDX, EBSD, APT, Raman
6mPC1	480	28.2	4788	508	SEM, EDX, EBSD, APT
5mPC1	387	19.5	3638	369	SEM, EDX, EBSD
49sPC	370	20.8	3632	367	SEM
8sPC	560	34.4	5524	596	SEM
7sPC	650	37.2	5925	644	SEM
1473-10	20	-	-	-	SEM, EDX, EBSD, Raman

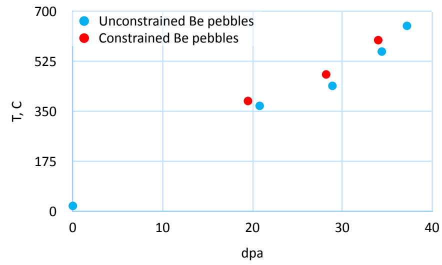

- **6 samples irradiated samples from the HIDOBE-2 campaign were received from KIT.**
- **Every sample has from 8 to 23 pebbles cross-sections polished in KIT to "EBSD quality"**

13

EDX and APT chemical maps: as-received state

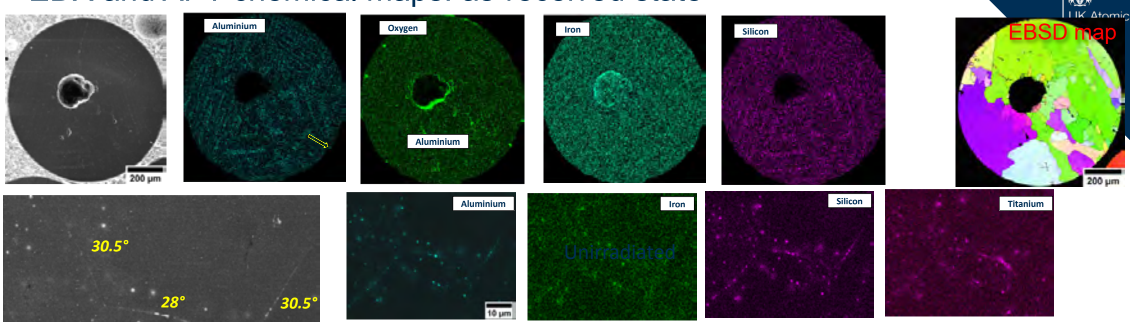

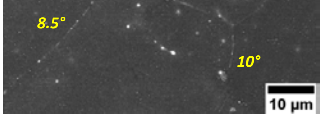

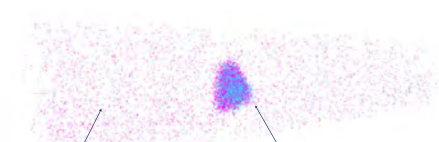

Precipitate
Fe+Al+Si+Mn

Matrix:
Fe (<300 appm); O (< 500 appm); Si (<100 appm); Ni (<50 appm)

- **Precipitates have white contrast on the SEM image and located at high- (>10°) and low-angle (<10°) GB-s as well as inside the grains;**
- **majority of the white contrast particles are enriched with Al, Si, Mg and Ti. Some precipitates enriched by Fe and, rarely, by O and Cr**

14

EDX chemical maps: irradiation at 600°C

UK Atomic Energy

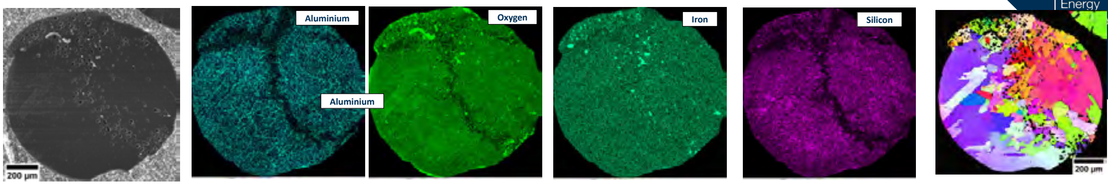

EBSD map

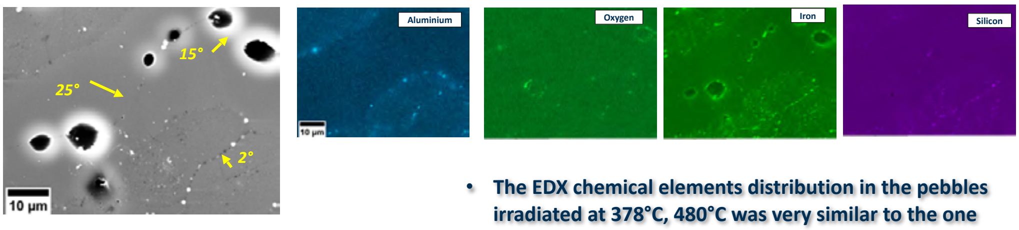

- **The EDX chemical elements distribution in the pebbles irradiated at 378°C, 480°C was very similar to the one observed in the unirradiated pebbles**
- **In the pebbles irradiated at 600°C More than a hundred micrometres wide channels with reduced impurity content and almost free of precipitates were observed**

15

Nanometric-scale investigation of distribution of tritium transmutant

UK Atomic Energy Authority

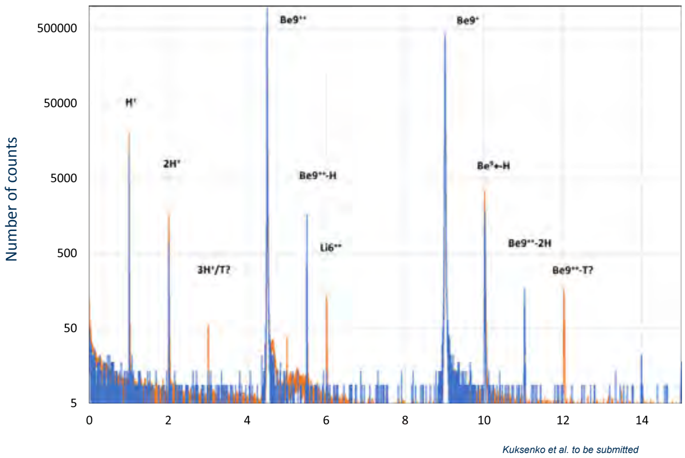

APT mass-to-charge ratio spectrum (before and after n-irradiation), Da

T_{irr}, °C	dpa	He, appm
480	28	4800

$^{9}Be + n \rightarrow {}^{6}He + {}^{3}H$ ($E_n > 0.6$ MeV)

$^{6}He \rightarrow {}^{6}Li + \beta^- + \nu$

$^{6}Li + n \rightarrow {}^{4}He + {}^{3}H$

- **New mass spectrum peaks appear after neutron irradiation at "3", "6" and "12" Da should be related to tritium and/or lithium**

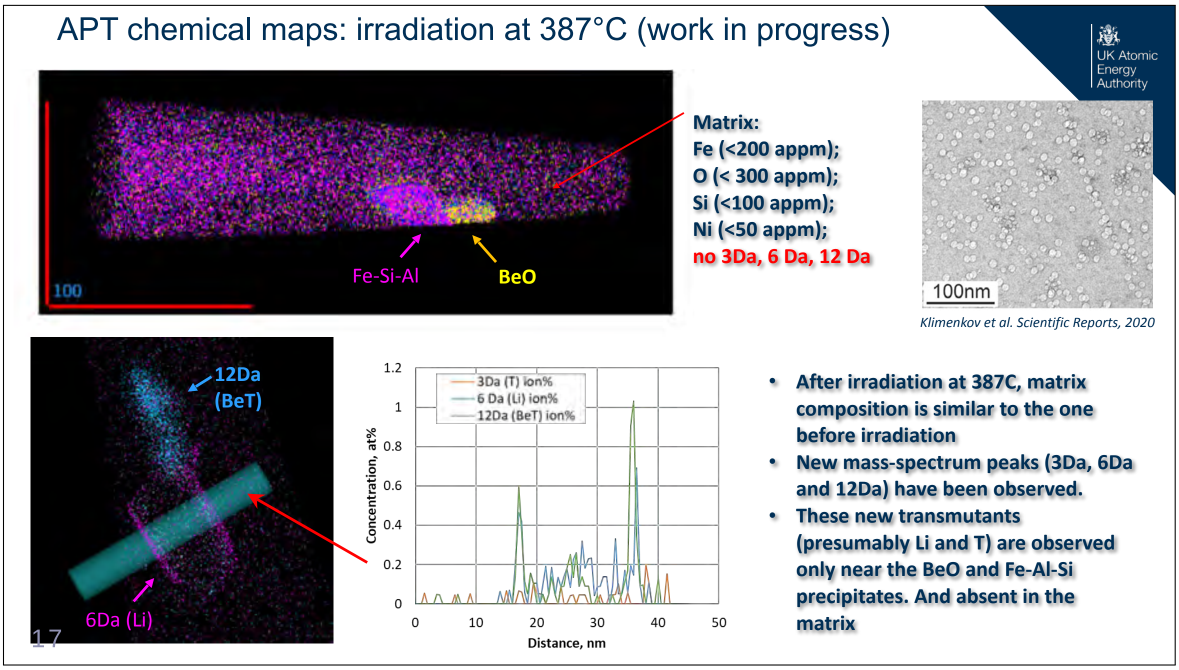
APT chemical maps: irradiation at 387°C (work in progress)
UK Atomic Energy Authority
100
Fe-Si-Al
BeO
Matrix:
Fe (<200 appm);
O (< 300 appm);
Si (<100 appm);
Ni (<50 appm);
no 3Da, 6 Da, 12 Da
100nm
Klimenkov et al. Scientific Reports, 2020
12Da (BeT)
6Da (Li)
3Da (T) ion%
6 Da (Li) ion%
12Da (BeT) ion%
Concentration, at%
Distance, nm
After irradiation at 387C, matrix composition is similar to the one before irradiation
New mass-spectrum peaks (3Da, 6Da and 12Da) have been observed.
These new transmutants (presumably Li and T) are observed only near the BeO and Fe-Al-Si precipitates. And absent in the matrix
17

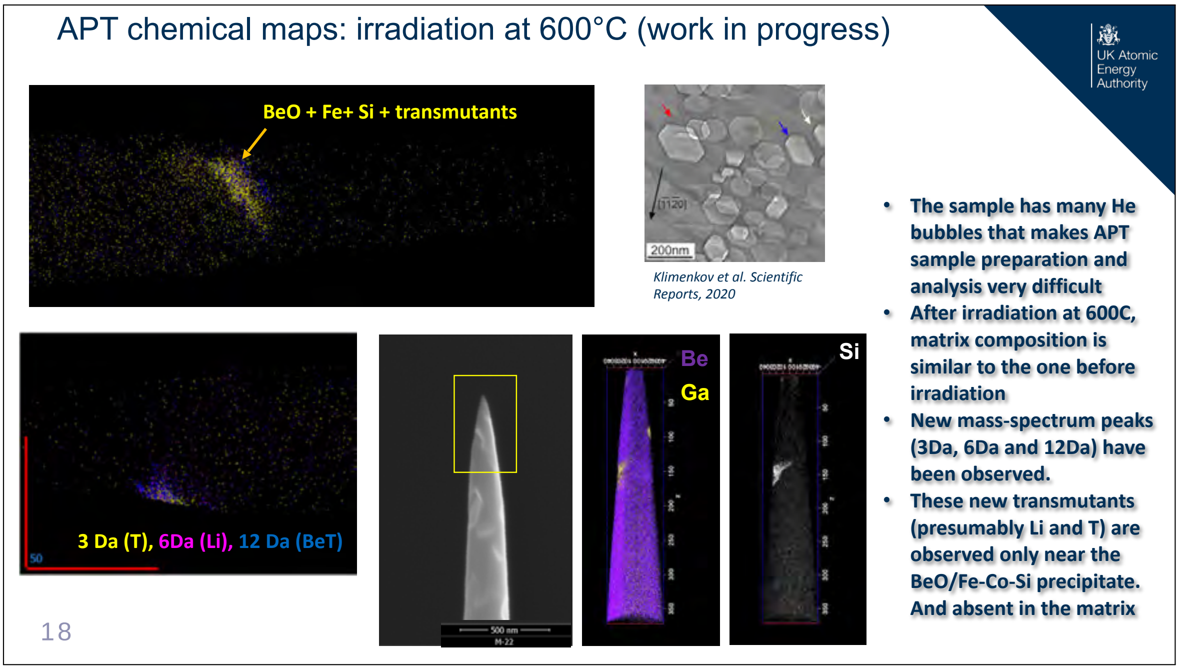
APT chemical maps: irradiation at 600°C (work in progress)
UK Atomic Energy Authority
BeO + Fe+ Si + transmutants
200nm
Klimenkov et al. Scientific Reports, 2020
3 Da (T), 6Da (Li), 12 Da (BeT)
50
Be
Ga
Si
500 nm
The sample has many He bubbles that makes APT sample preparation and analysis very difficult
After irradiation at 600C, matrix composition is similar to the one before irradiation
New mass-spectrum peaks (3Da, 6Da and 12Da) have been observed.
These new transmutants (presumably Li and T) are observed only near the BeO/Fe-Co-Si precipitate. And absent in the matrix
18

APT chemical maps: irradiation at 480°C (work in progress)

UK Atomic Energy Authority

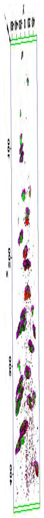

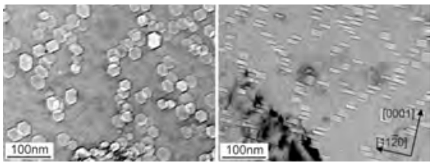

Klimenkov et al. Scientific Reports, 2020

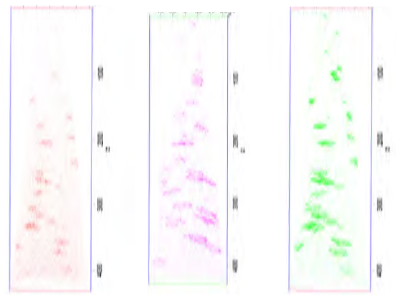

3 Da
T^+?

6 Da
$2T^+/Li_6^+$

12 Da
Be-T complex?

- The "new elements/ isotopes" are non-homogeneously distributed (480°C irradiation).
- Comparison with TEM suggests that the new element(-s) segregate to helium bubbles (hexagon coins shaped).

APT chemical maps: irradiation at 480°C (work in progress)

UK Atomic Energy Authority

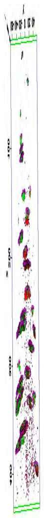

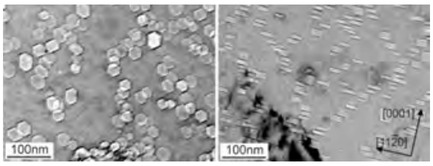

Klimenkov et al. Scientific Reports, 2020

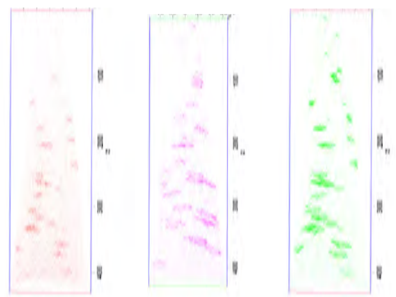

3 Da
T^+?

6 Da
$2T^+/Li_6^+$

12 Da
Be-T complex?

- The "new elements/ isotopes" are non-homogeneously distributed (480°C irradiation).
- Comparison with TEM suggests that the new element(-s) segregate to helium bubbles (hexagon coins shaped).

Conclusions (preliminary)

UK Atomic Energy Authority

- New mass spectrum peaks appear after neutron irradiation at “3”, “6” and “12” Da should be related to tritium
- The “new elements/isotopes” are non-homogeneously distributed
- The transmutants (presumably Li and T) are observed only near the BeO and Fe-Al-Si precipitates in the HIDOBE samples irradiated at 387 and 600C.
- The plate-like shape suggests that in the HIDOBE samples irradiated at 480C the new element(-s) segregate to helium bubbles.
- Matrix composition of n-irradiated HIDOBE samples is similar to the one before irradiation. There is not transmutants detected in the matrix.

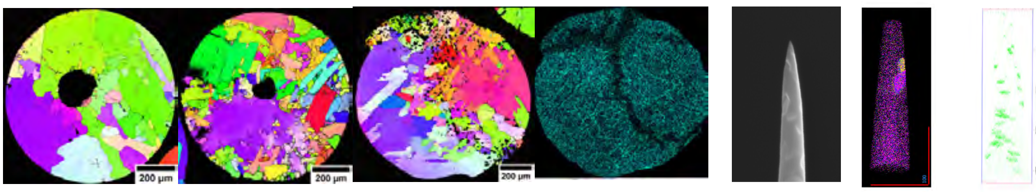

UK Atomic Energy Authority

Acknowledgements:

MRF and health physics teams

This work was supported by the Fermi Research Alliance, LLC under Contract No. DE-AC02-07CH11359 with the United States Department of Energy, and by the UK Science and Technology Facilities Council.

This work has been part funded by the RCUK Energy Programme [grant number EP/T012250/1]"

Thank you!

21

First principles simulation of resistivity recovery in irradiated beryllium

Christopher Stihl[1], Pavel Vladimirov[1]

[1]Karlsruhe Institute of Technology, Institute for Applied Materials – Applied Materials Physics

Future fusion devices like ITER or DEMO require closed fuel cycles. These vitally depend on neutron multiplying materials as part of a breeding blanket module like beryllium pebbles in the European Helium-Cooled Pebble-Bed. During operation the beryllium pebbles will accumulate point defects, tritium, and helium due to inevitable exposure to highly energetic neutron irradiation as emitted by the fusion plasma. A detailed knowledge of the characteristics of point defects is decisive for reliable simulations of microstructure evolution in irradiated beryllium. Such models are a prerequisite for predicting tritium inventory during operation as well as after the blanket´s end of life since tritium retention and release is the paramount safety concern.

A well-established experimental approach to assess the dynamics of relevant atomic defects consists in measuring electrical resistivity recovery (ERR) after irradiation during annealing. Within this approach, temperatures corresponding to electrical recovery steps are correlated with activation energies which are associated with different type of reactions between defects.

In this work, results of our ongoing efforts to model and understand the ERR of beryllium are presented. To that end, we introduce a rate equation-based approach to model ERR spectra (see picture below) utilizing density functional theory results as input. Within this approach, electrical resistivity recovery models comprising the volume of spontaneous recombination of monovacancies and self-interstitial atoms in beryllium as well as various additional defects are considered. As a result, an intricate interplay between different defect dynamics is uncovered, suggesting a clear route for further research to obtain systematically improved electrical resistivity recovery models.

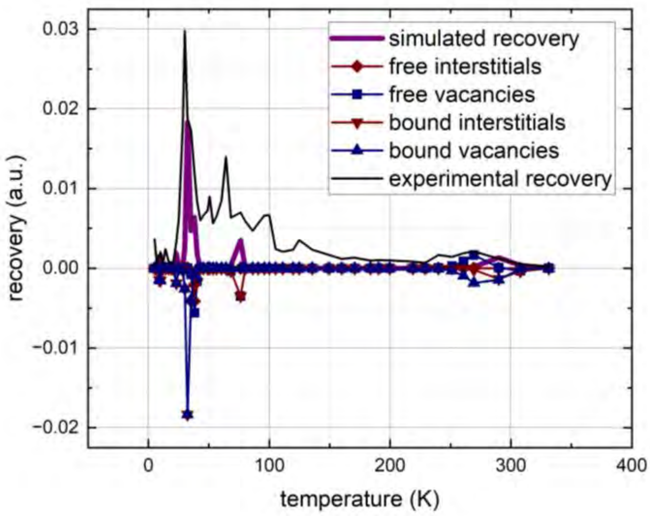

Corresponding Author:

Dr. Christopher Stihl
Christopher.stihl@kit.edu
Hermann-von-Helmholtz-Platz 1,
76344 Eggenstein-Leopoldshafen

Karlsruhe Institute of Technology

First principles simulation of resistivity recovery in irradiated beryllium

Christopher Stihl

KIT – The Research University in the Helmholtz Association

www.kit.edu

Outline

Karlsruhe Institute of Technology

- Resistivity Recovery Experiments
- Resistivity Recovery Modelling
  - Relevant Be properties
  - Model derivation
  - Various models
- Conclusions & outlook

2 15.09.2022 Christopher Stihl Institute for Applied Materials – Applied Materials Physics

Resistivity recovery experiment(s by example)

Karlsruhe Institute of Technology

- sample preparation
  - cool to 4.2 K
  - measure resistivity
  - irradiate
  - measure resistivity
- measurements
  - do annealing cycle
    - heat
    - hold
    - cool
  - measure resistivity
  - repeat at higher T
- process spectrum

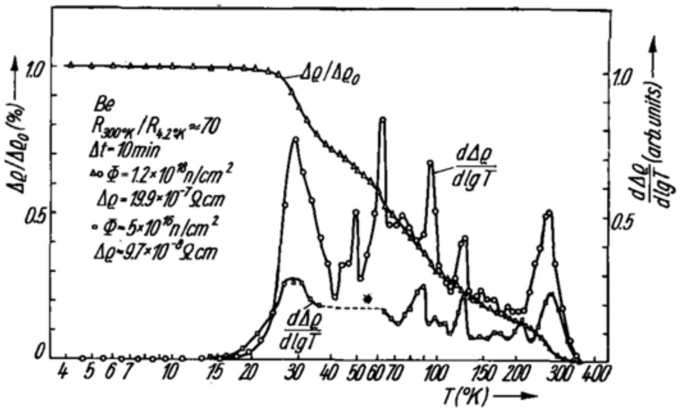

3 15.09.2022 Christopher Stihl Institute for Applied Materials – Applied Materials Physics

Model-relevant Be properties (from DFT)

Karlsruhe Institute of Technology

- HCP structure
- AB-stacked layers
- mono vacancies
  - immobile (0.8 eV)
- basal interstitials
  - mobile (0.12 eV)
- spontaneous recombination hull
  - oblate spheroid
  - with (very) fast recombination

4 15.09.2022 Christopher Stihl Institute for Applied Materials – Applied Materials Physics

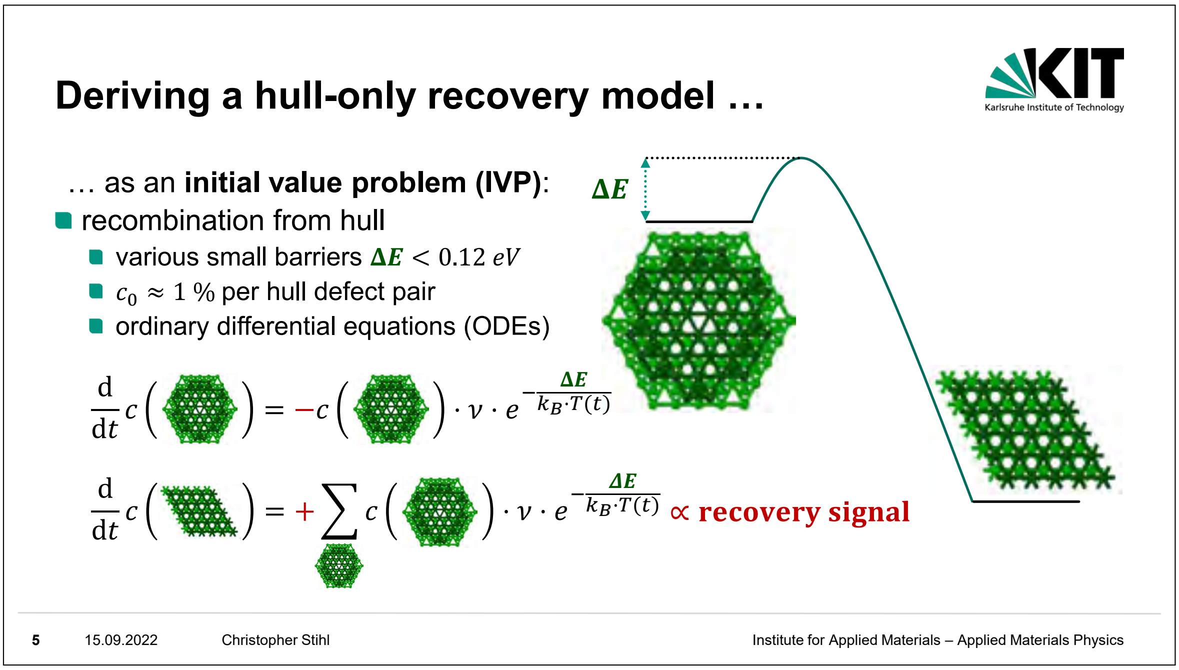
Deriving a hull-only recovery model …
Karlsruhe Institute of Technology
… as an initial value problem (IVP):
recombination from hull
various small barriers $\Delta E < 0.12\ eV$
$c_0 \approx 1\ \%$ per hull defect pair
ordinary differential equations (ODEs)
ΔE
∝ recovery signal
5
15.09.2022
Christopher Stihl
Institute for Applied Materials – Applied Materials Physics

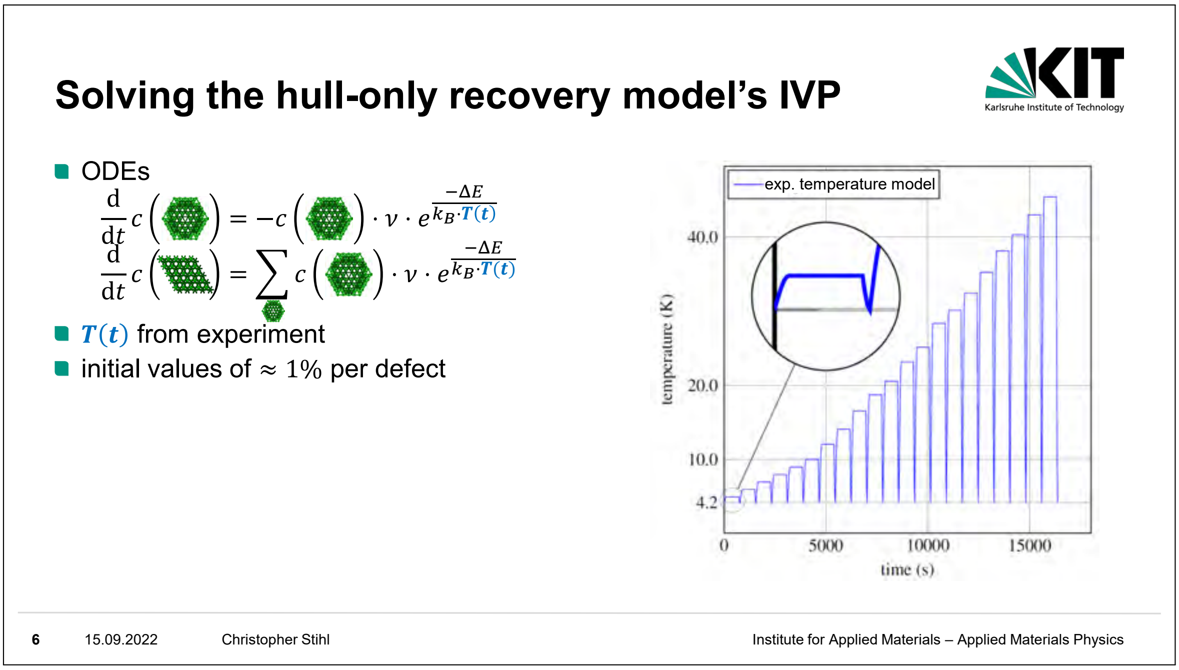
Solving the hull-only recovery model's IVP
Karlsruhe Institute of Technology
ODEs
$T(t)$ from experiment
initial values of ≈ 1% per defect
exp. temperature model
temperature (K)
time (s)
40.0
20.0
10.0
4.2
0
5000
10000
15000
6
15.09.2022
Christopher Stihl
Institute for Applied Materials – Applied Materials Physics

Solving the hull-only recovery model's IVP

Karlsruhe Institute of Technology

- ODEs

$$\frac{\mathrm{d}}{\mathrm{d}t} c(\ ) = -c(\ ) \cdot \nu \cdot e^{\frac{-\Delta E}{k_B \cdot T(t)}}$$

$$\frac{\mathrm{d}}{\mathrm{d}t} c(\ ) = \sum c(\ ) \cdot \nu \cdot e^{\frac{-\Delta E}{k_B \cdot T(t)}}$$

- $T(t)$ from experiment
- initial values of $\approx 1\%$ per defect
- symmetric hull and recovery evolution
- sloped step patterns from annealing cycles

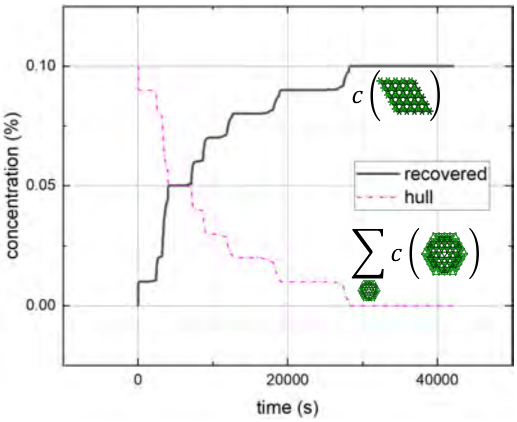

6 15.09.2022 Christopher Stihl Institute for Applied Materials – Applied Materials Physics

Solving the hull-only recovery model's IVP

Karlsruhe Institute of Technology

- ODEs

$$\frac{\mathrm{d}}{\mathrm{d}t} c(\ ) = -c(\ ) \cdot \nu \cdot e^{\frac{-\Delta E}{k_B \cdot T(t)}}$$

$$\frac{\mathrm{d}}{\mathrm{d}t} c(\ ) = \sum c(\ ) \cdot \nu \cdot e^{\frac{-\Delta E}{k_B \cdot T(t)}}$$

- $T(t)$ from experiment
- initial values of $\approx 1\%$ per defect
- symmetric hull and recovery evolution
- sloped step patterns from annealing cycles
- +/- peaks show in/decreasing concentration
- lowest-energy hull pairs decay early
- initial values are important free parameter

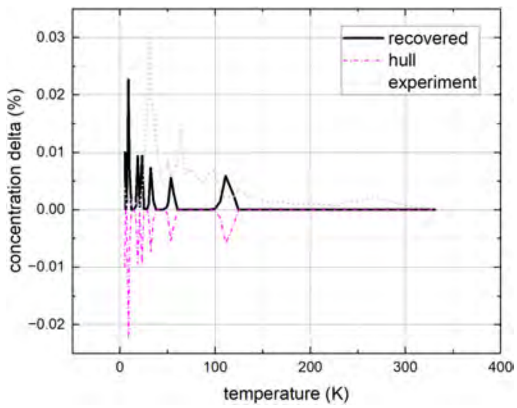

6 15.09.2022 Christopher Stihl Institute for Applied Materials – Applied Materials Physics

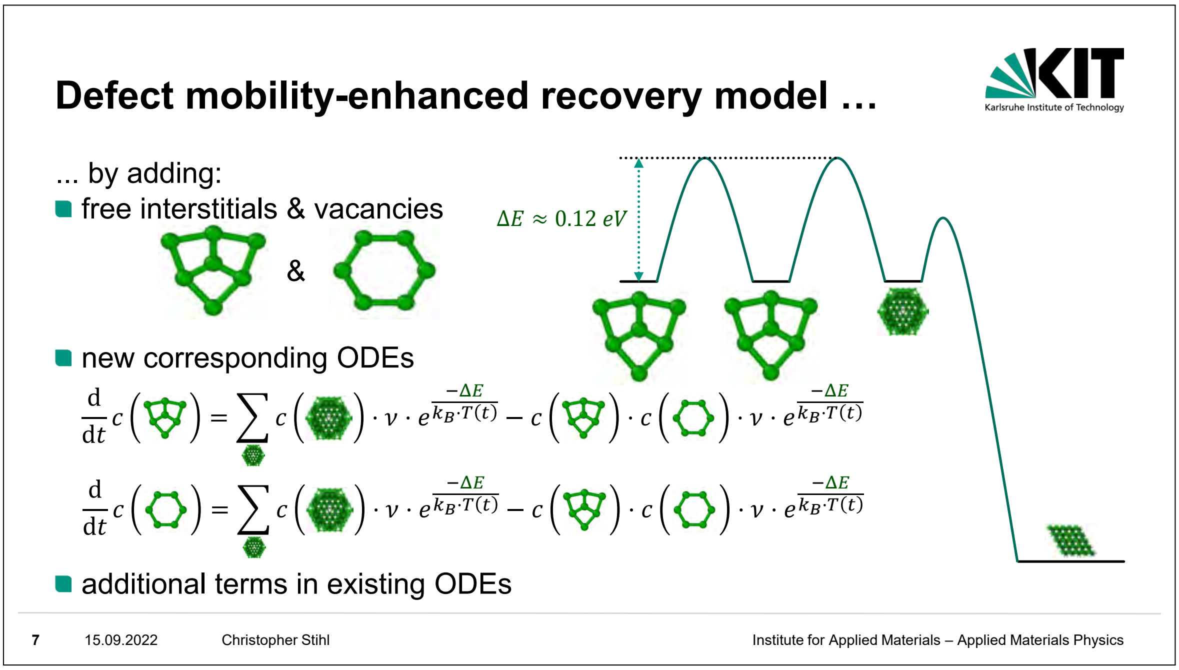
Defect mobility-enhanced recovery model …
KIT
Karlsruhe Institute of Technology
… by adding:
free interstitials & vacancies
&
new corresponding ODEs
additional terms in existing ODEs
$\Delta E \approx 0.12\ eV$
7
15.09.2022
Christopher Stihl
Institute for Applied Materials – Applied Materials Physics

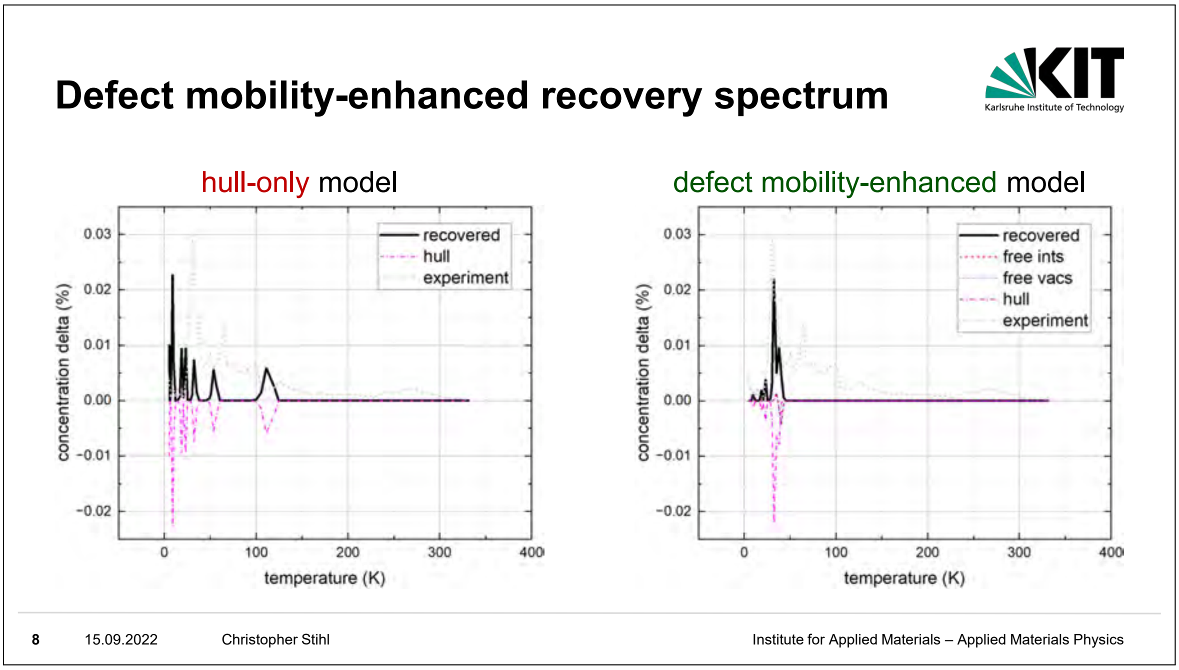
Defect mobility-enhanced recovery spectrum
KIT
Karlsruhe Institute of Technology
hull-only model
defect mobility-enhanced model
recovered
hull
experiment
free ints
free vacs
concentration delta (%)
temperature (K)
8
15.09.2022
Christopher Stihl
Institute for Applied Materials – Applied Materials Physics

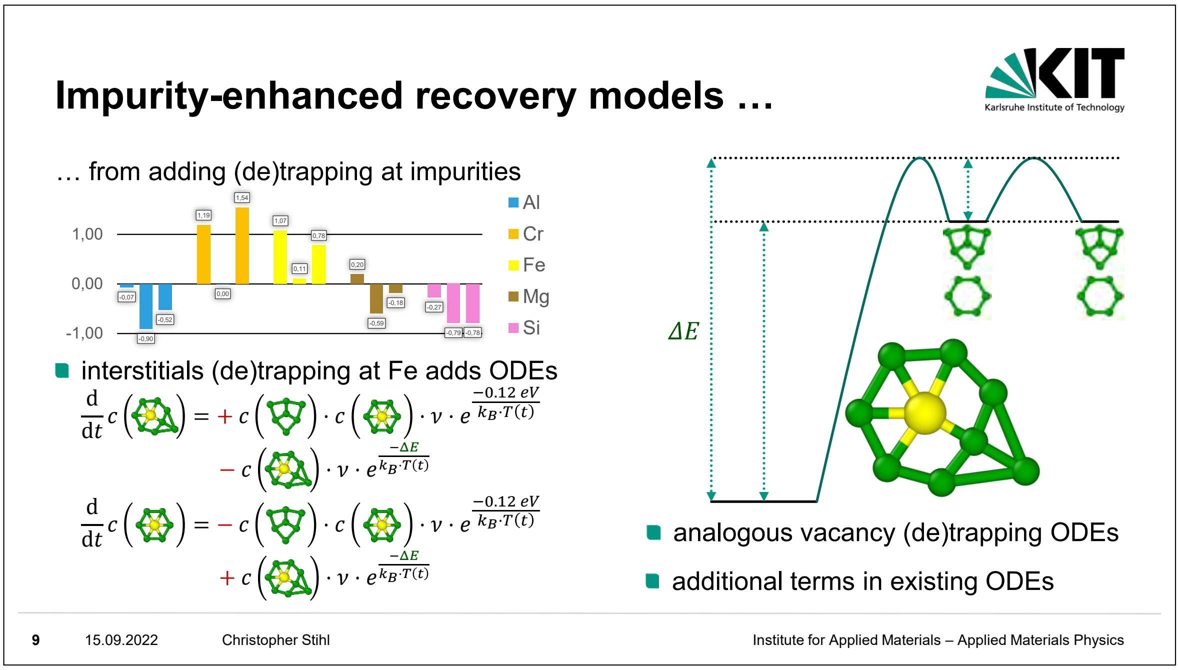
Impurity-enhanced recovery models …
Karlsruhe Institute of Technology
… from adding (de)trapping at impurities
Al
Cr
Fe
Mg
Si
1,00
0,00
-1,00
interstitials (de)trapping at Fe adds ODEs
ΔE
analogous vacancy (de)trapping ODEs
additional terms in existing ODEs
9
15.09.2022
Christopher Stihl
Institute for Applied Materials – Applied Materials Physics

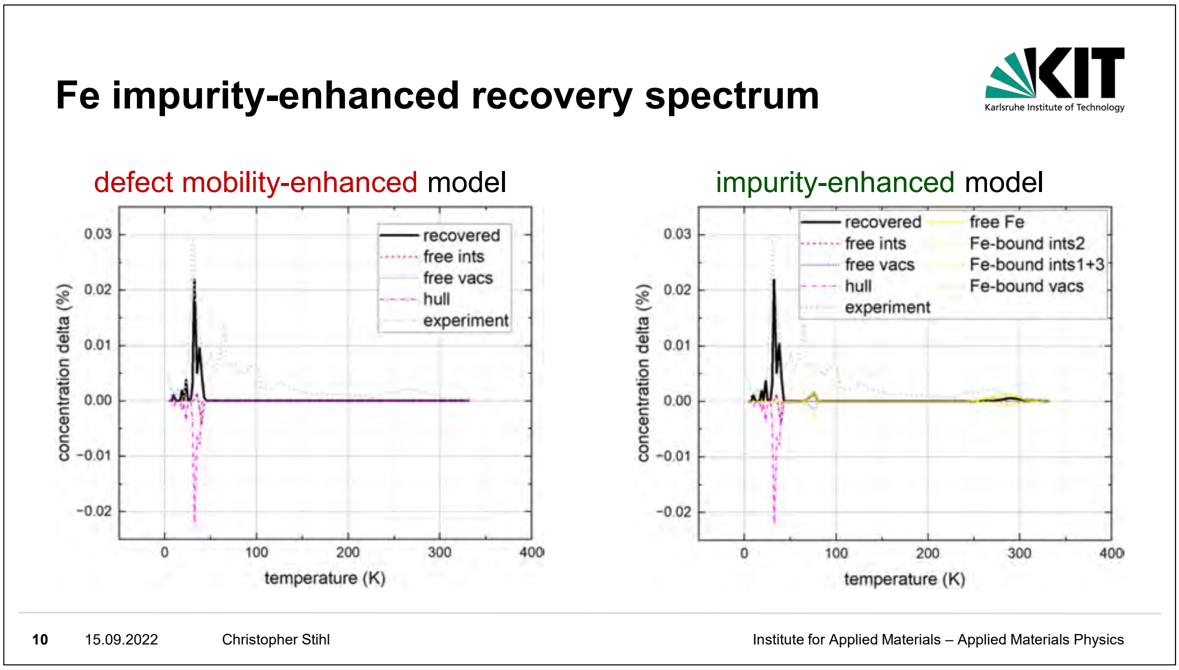
Fe impurity-enhanced recovery spectrum
Karlsruhe Institute of Technology
defect mobility-enhanced model
impurity-enhanced model
recovered
free ints
free vacs
hull
experiment
free Fe
Fe-bound ints2
Fe-bound ints1+3
Fe-bound vacs
concentration delta (%)
temperature (K)
10
15.09.2022
Christopher Stihl
Institute for Applied Materials – Applied Materials Physics

Fe impurity-enhanced recovery spectra

KIT Karlsruhe Institute of Technology

impurity-enhanced model

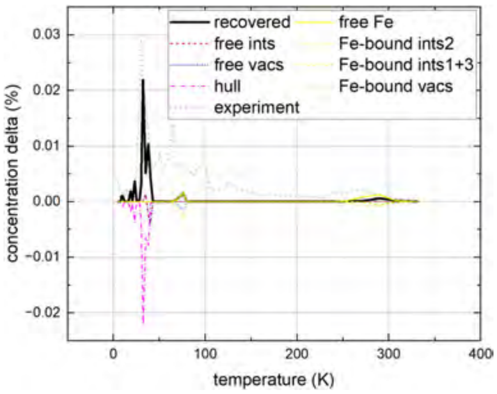

impurity-enhanced, vac-starved model

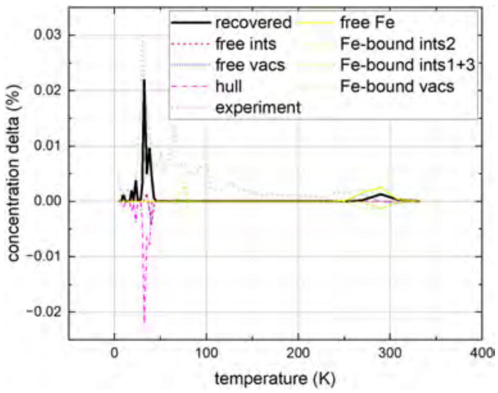

11 15.09.2022 Christopher Stihl Institute for Applied Materials – Applied Materials Physics

Conclusions & outlook

KIT Karlsruhe Institute of Technology

- first peaks due to closely correlated pairs
  - reasonable defect concentrations sufficient
  - gaps likely due to non-exhaustive set of pairs
- diffusion onset decisive for later spectrum
- last peaks due to mobile vacancies
  - here from vacs weakly bound to Fe
- interdependent dynamics of different traps
  - e.g. different traps at Fe (and additional ones …)
- intermediate peaks *likely not* due to impurities
  - concentrations *too low*
  - might still contribute some peaks
- additional Be-only defects to be considered
- model can be extended to calorimetry signals

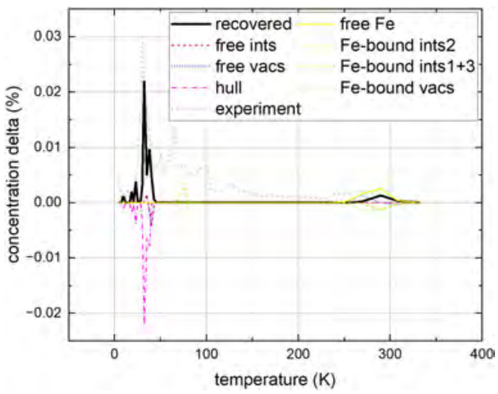

12 15.09.2022 Christopher Stihl Institute for Applied Materials – Applied Materials Physics

Radiation induced formation gas bubbles in beryllium after neutron irradiation up to 6000 appm helium production

Michael Klimenkov, Ute Jäntsch, Vladimir Chakin, Nikolai Zimber and Pavel Vladimirov

Karlsruhe Institut of Technology, Hermann-von-Helmholtz-Platz 1 76344 Eggenstein-Leopoldshafen, Germany

The current interest in mechanical properties and microstructure of neutron irradiated beryllium refers to its planned application in the Helium-Cooled Pebble Bed (HCPB) European concept of a breeding blanket of DEMO. Irradiation experiments in high-neutron flux nuclear research reactors yield information about microstructural evolution of beryllium under conditions relevant to fusion (temperature, damage dose, helium and tritium productions) excluding 14 MeV neutrons impact which is not present in the neutron spectra of fission reactors. The HIDOBE-02 irradiation campaign accomplished at the HFR, Petten corresponds to 1246.5 Full Power Days at a reactor power level of 45 MW in the temperature range from 410°C to 680 °C. Transmission electron microscopy (TEM) has been to study the evolution of voids during neutron irradiation at different temperatures. The target preparation of specimens was performed using focused ion beam (FIB).

TEM study shows the formation of radiation induced hexagonal flat gas bubbles inside the grains, however at the lowest irradiation temperature of 410° the pebbles show the uniform shape. The diameters of the bubbles increase from a few nanometers for 410°C to more than hundred nanometers for 680 °C. The number density of bubbles decreases, correspondingly, by more than two orders of magnitude. The preferable formation of bubbles along the grain boundary and dislocation lines was observed. Analytical investigations using electron energy loss spectroscopy show the presence of He and H23 inside bubbles. Also the Si and Fe segregation on the voids was detected [2].

EDX mapping shows that the precipitates inside the grains and on the GBs have increased iron and aluminum content, indicating the formation of an Fe-Al-Be phase. In the material irradiated at 440°C, most of the precipitates also have Fe-Al-Be composition, while several other single- and multiphase precipitates were found. The Fe-Al-Be phase is observed as 10-15 nm precipitates within the grains and as 200 nm particles bound to a gas bubble at the GB. The present study shows detailed microstructural changes induced by neutron irradiation in beryllium.

[1] M. Klimenkov, et al. Journal of Nuclear Materials 455 (2014) 660–664
[2] M. Dürrschnabel, et al. Scientific Reports, 11, 7572 (2021)

Corresponding Author:
Dr. Michael Klimenkov
michael.klimenkov@kit.edu
Karlsruhe Institut of Technology, Hermann-von-Helmholtz-Platz
1 76344 Eggenstein-Leopoldshafen, Germany

Karlsruhe Institute of Technology

Radiation induced formation gas bubbles in beryllium after neutron irradiation up to 6000 appm helium production

M. Klimenkov, **P. Vladimirov, N. Zimber, U. Jäntsch and A. Möslang**

Institute for Applied Materials - Applied Materials Physics, Karlsruhe Institute of Technology (KIT), Karlsruhe, Germany.

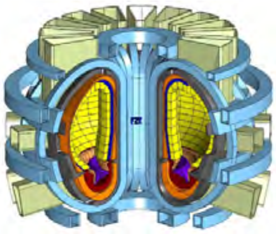

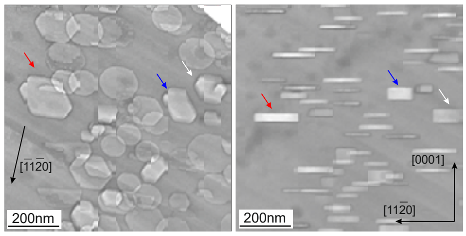

KIT – The Research University in the Helmholtz Association

www.kit.edu

Content

Karlsruhe Institute of Technology

- Introduction
- Microstructural examination of neutron irradiated beryllium at IAM-AWP (HIDOBE I and HIDOBE II)
- Detection of He and ^{3}H inside bubbles
- Distribution of impurity atoms in irradiated Be
- Conclusions

2 Dr. Michael Klimenkov Institute of Applied Materials – Applied Materials Physics (IAM-AWP) IAM

Beryllium application in fusion technology

KIT Karlsruhe Institute of Technology

- Application as a "First Wall" material in ITER.
- As neutron multiplier material in different tritium-breeding blanket concepts for the future demonstration fusion power plant DEMO.

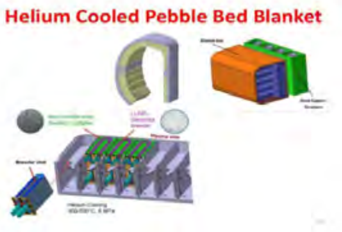

Production of helium and tritium (^3H) by transmutation reactions

$^9Be + n \rightarrow 2\,^4He + 2n$ (E_n>2.7 MeV)

$^9Be + n \rightarrow {}^7Li + {}^3He$ (E_n>10.7 MeV)

$^7Li + n \rightarrow {}^4He + {}^3H + n$

$^9Be + n \rightarrow {}^6He + {}^3H$ (E_n> 0.6 MeV)

$^6He \rightarrow {}^6Li + b^- + \nu$

$^6Li + n \rightarrow {}^4He + {}^3H$

Prediction of irradiation resistance of beryllium pebbles under close-to-fusion conditions.

- operation temperature,
- accumulated damage dose,
- amount of helium and tritium generated by neutron-induced transmutation.

3 Dr. Michael Klimenkov Institute of Applied Materials – Applied Materials Physics (IAM-AWP) IAM Institute for Applied Materials

Neutron irradiation programs 2005 - 2016

KIT Karlsruhe Institute of Technology

High Dose Beryllium irradiation program **(HIDOBE-I) (2005-2007)**
High-Flux Reactor (HFR), Petten, Netherlands
Dose 18 dpa, 3000 appm ^{4}He, **300** appm ^{3}H
Irradiation temperatures: 410°C, 480°C, 590°C, 700°C

High Dose Beryllium irradiation program **(HIDOBE-II) (2005-2011)**
High-Flux Reactor (HFR), Petten, Netherlands
38 dpa displacement per atom **5900** appm ^{4}He, **640** appm ^{3}H
Irradiation temperatures: 370°C, 440°C, 540°C, 650°C

Be pebbles

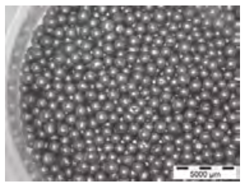

∅ 1mm
∅ 2mm

1mm pebble

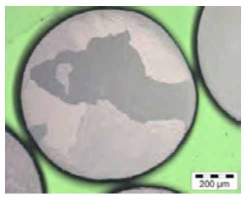

100-300µm grain size

4 Dr. Michael Klimenkov Institute of Applied Materials – Applied Materials Physics (IAM-AWP) IAM Institute for Applied Materials

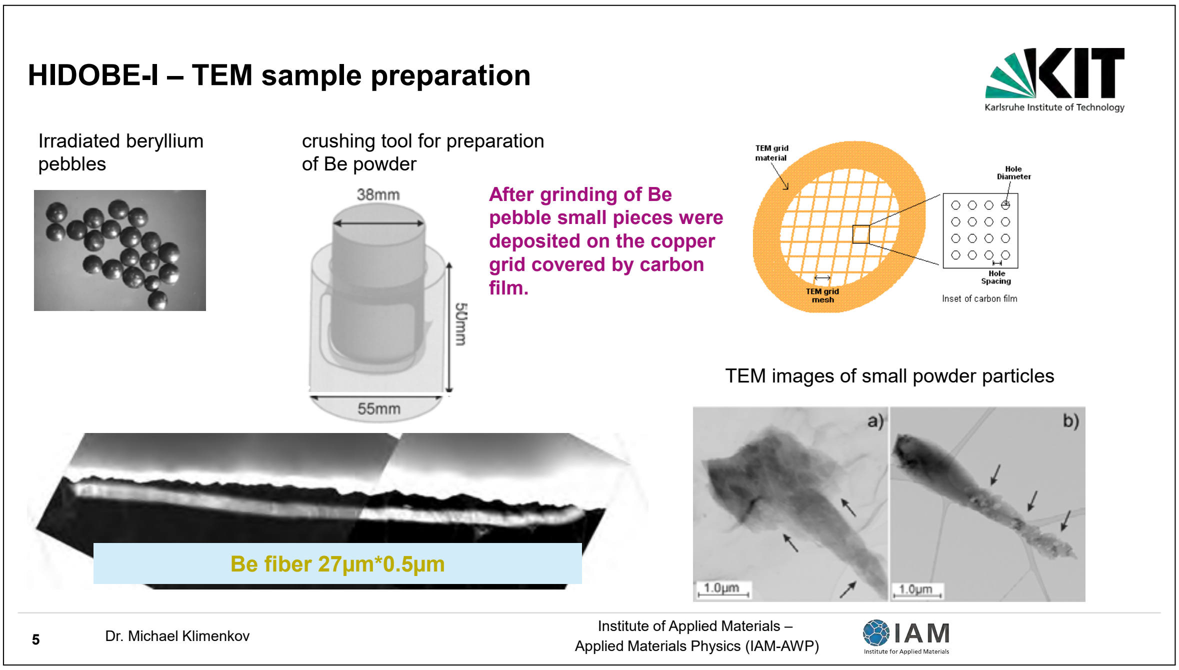
HIDOBE-I – TEM sample preparation
Karlsruhe Institute of Technology
Irradiated beryllium pebbles
crushing tool for preparation of Be powder
38mm
50mm
55mm
After grinding of Be pebble small pieces were deposited on the copper grid covered by carbon film.
TEM grid material
Hole Diameter
Hole Spacing
TEM grid mesh
Inset of carbon film
TEM images of small powder particles
a)
b)
1.0µm
1.0µm
Be fiber 27µm*0.5µm
5
Dr. Michael Klimenkov
Institute of Applied Materials – Applied Materials Physics (IAM-AWP)
IAM

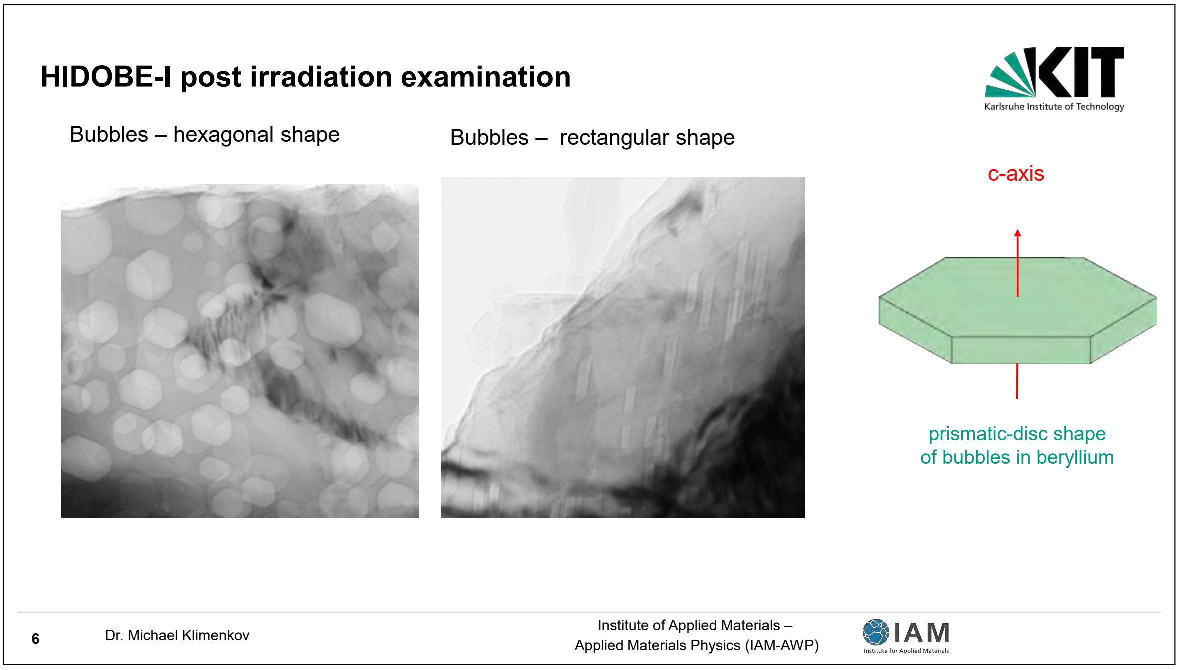
HIDOBE-I post irradiation examination
Karlsruhe Institute of Technology
Bubbles – hexagonal shape
Bubbles – rectangular shape
c-axis
prismatic-disc shape of bubbles in beryllium
6
Dr. Michael Klimenkov
Institute of Applied Materials – Applied Materials Physics (IAM-AWP)
IAM

HIDOBE-I - post irradiation examination

Karlsruhe Institute of Technology

Pecipitates 480°C

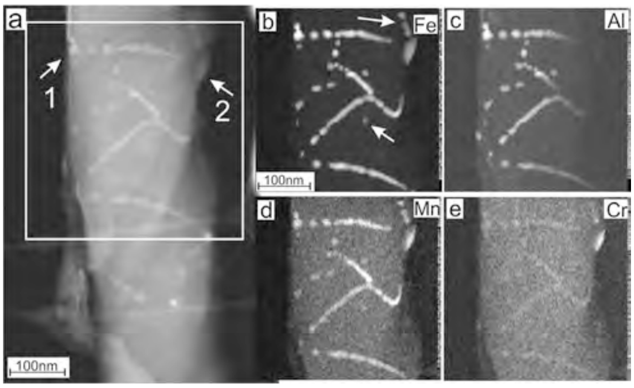

The FeAlMnCr pecipitates located in a fiber of 350 nm thickness.

7 Dr. Michael Klimenkov Institute of Applied Materials – Applied Materials Physics (IAM-AWP) IAM Institute for Applied Materials

HIDOBE-I post irradiation examination

Karlsruhe Institute of Technology

Precipitates contains of FeAlMnCrTi beryllides

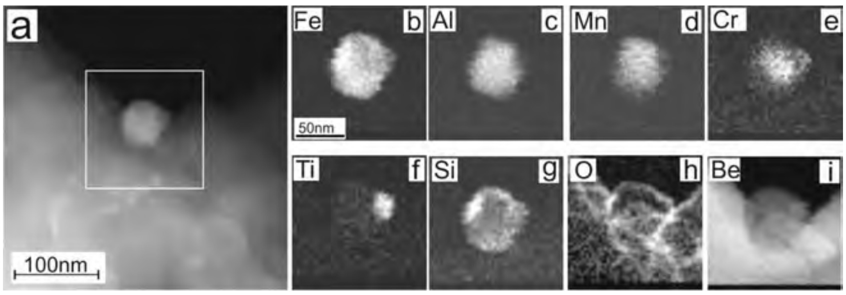

- M.Klimenkov, V.Chakin, A.Moeslang, R.Rolli, Journal of Nuclear Materials 443 (2013) 409-416
- M.Klimenkov, V.Chakin, A.Moeslang, R.Rolli, Journal of Nuclear Materials 455 (2014) 660–664

8 Dr. Michael Klimenkov Institute of Applied Materials – Applied Materials Physics (IAM-AWP) IAM Institute for Applied Materials

HIDOBE-II

High Dose Beryllium irradiation program **(HIDOBE-II)** **(2005-2011)**
High-Flux Reactor (HFR), Petten, Netherlands
38 dpa displacement per atom **5900** appm ^{4}He, **640** appm ^{3}H
Irradiation temperatures: 370°C, 440°C, 540°C, 650°C

Microstructural examination:
2016-2021

TEM lamellae were prepared from irradiated tungsten using focused ion beam (FEI SCIOS) in the FML at KIT.

Transmission Electron Microscope
Talos F200X G2 / 200 kV FEG

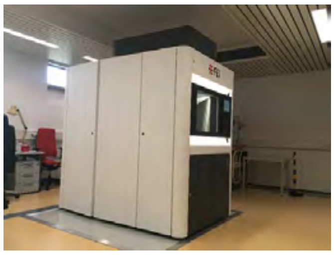

9 Dr. Michael Klimenkov
Institute of Applied Materials – Applied Materials Physics (IAM-AWP)

Specimen preparation using Foccused Ion Beam

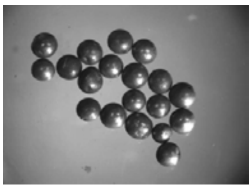

Removal of larger amounts of surrounding material using Ga ion beam.

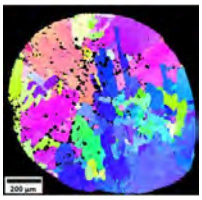

Deposition of prepared lamellae on the Cu greed

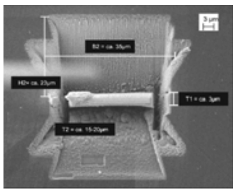

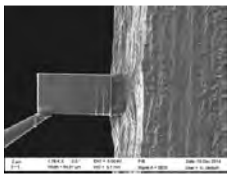

Preparation of thin transparent window for TEM analysis

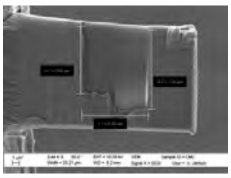

The thickness varried from 120 to 350nm mean path in beryllium ≈0,6-2.1λ

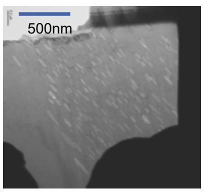

lamella is ready for TEM analysis

10 Dr. Michael Klimenkov
Institute of Applied Materials – Applied Materials Physics (IAM-AWP)

Microstructure of irradiated beryllium

- Bubbles show hexagonal prismatic-disc shape in the transmission electron microscope (TEM)

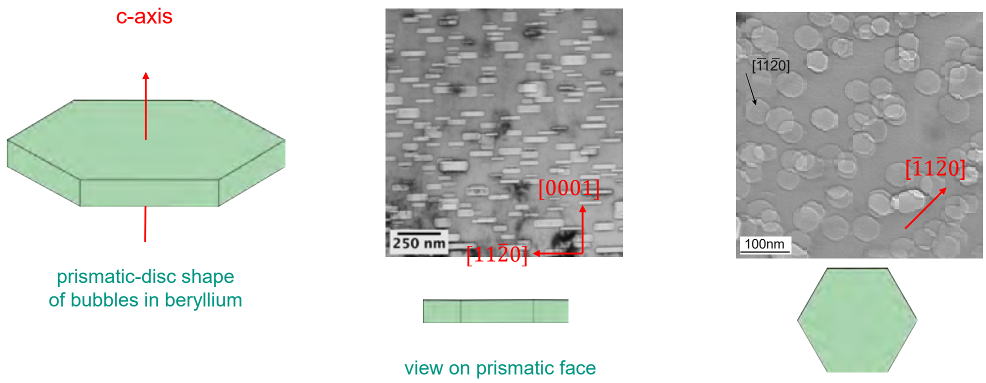

11 Dr. Michael Klimenkov Institute of Applied Materials – Applied Materials Physics (IAM-AWP)

Tomography in TEM

66° total tilt (from -32° to +34°)

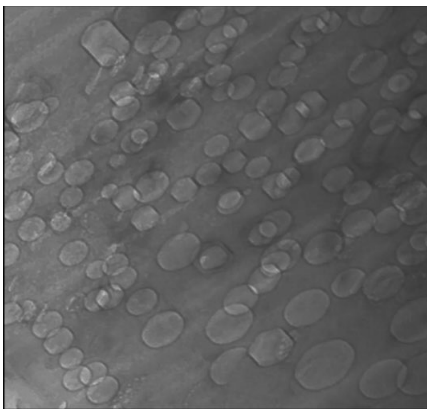

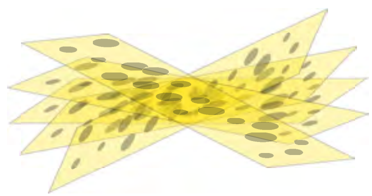

step ~3°
23 images

12 Dr. Michael Klimenkov Institute of Applied Materials – Applied Materials Physics (IAM-AWP)

Bubbles in beryllium irradiated at different temperatures

Images of the bubbles in the basal and prismatic orientations

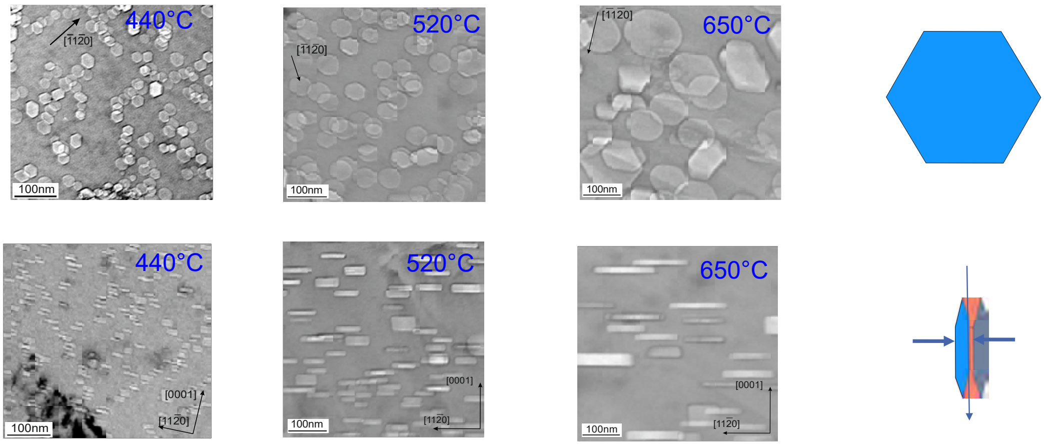

13 Dr. Michael Klimenkov

Institute of Applied Materials – Applied Materials Physics (IAM-AWP)

Bubbles in beryllium irradiated at 370°C

Tilt of 60° between these images

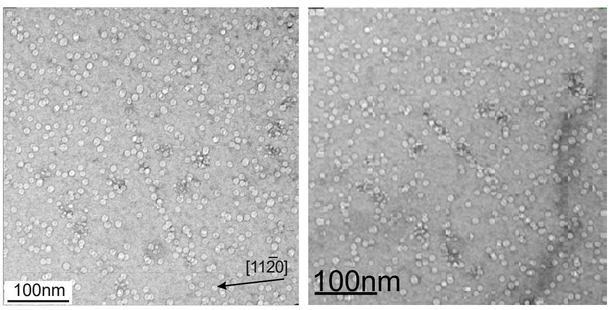

A uniform bubble shape

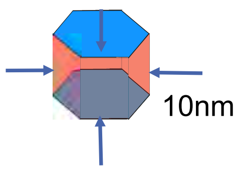

14 Dr. Michael Klimenkov

Institute of Applied Materials – Applied Materials Physics (IAM-AWP)

Quantitative evaluation

Effect of radiation dose on the microstructure of irradiated beryllium

Bubble diameter

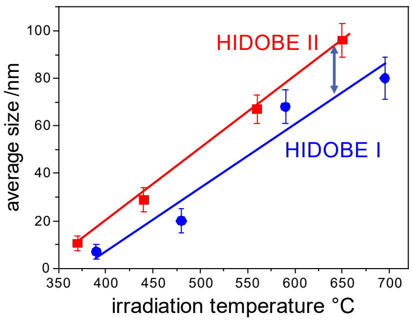

~20% increase

Swelling

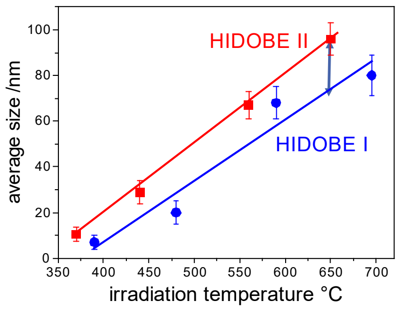

~25% increase

15 Dr. Michael Klimenkov Institute of Applied Materials – Applied Materials Physics (IAM-AWP)

Analytical study of bubbles in irradiated beryllium

Low energy EELS spectra

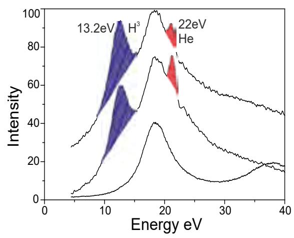

TEM dark field image $^3H_2$ signal He signal

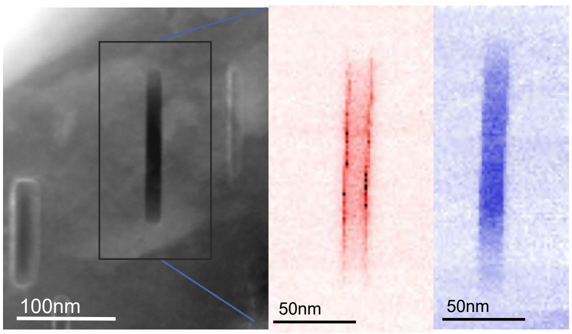

Formation of beryllium hydride BeH_2 layers on internal walls He detection inside bubbles

Calculation of the gas pressure inside the individual bubbles

$$n_x = \frac{I_x}{I_Z * d * \sigma_x}$$

n_x the number density of the gas

I_Z and **I_x** are integrated intensities from the spectra

$\sigma_P(\Delta,\beta)$ is the partial inelastic cross-section for He/H

d is the bubble thickness in the direction of electron beam.

n_{He} =4.2±1.0 at/nm³

n_{H2} =3.5±0.8 at/nm³

16 Dr. Michael Klimenkov Dr. M. Klimenkov Institute of Applied Materials – Applied Materials Physics (IAM-AWP)

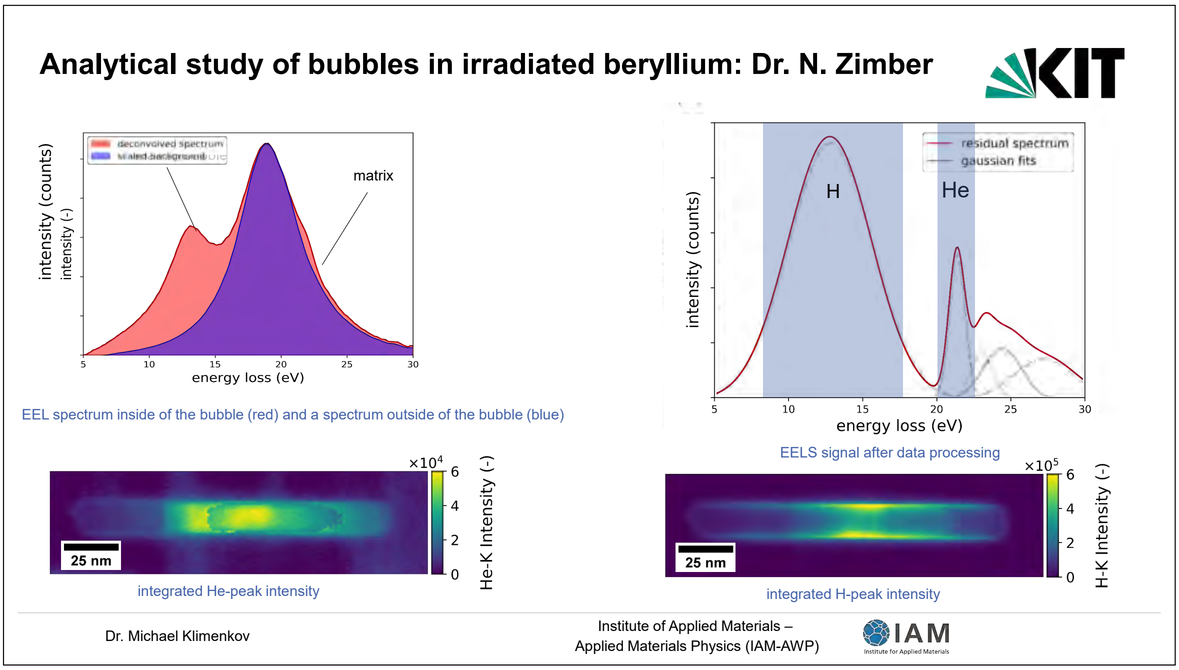

Analytical study of bubbles in irradiated beryllium: Dr. N. Zimber
KIT
deconvolved spectrum
scaled background
matrix
intensity (counts)
intensity (-)
energy loss (eV)
EEL spectrum inside of the bubble (red) and a spectrum outside of the bubble (blue)
residual spectrum
gaussian fits
H
He
intensity (counts)
energy loss (eV)
EELS signal after data processing
×10^4
He-K Intensity (-)
25 nm
integrated He-peak intensity
×10^5
H-K Intensity (-)
25 nm
integrated H-peak intensity
Dr. Michael Klimenkov
Institute of Applied Materials –
Applied Materials Physics (IAM-AWP)
IAM

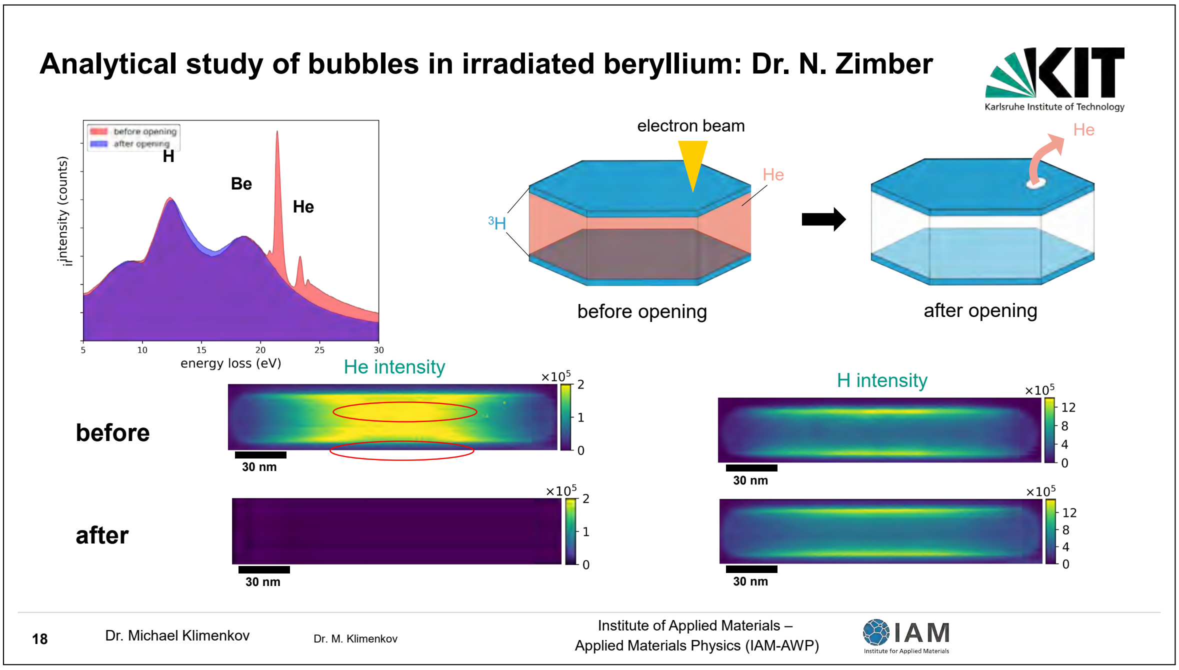

Analytical study of bubbles in irradiated beryllium: Dr. N. Zimber
KIT
Karlsruhe Institute of Technology
before opening
after opening
H
Be
He
intensity (counts)
energy loss (eV)
electron beam
He
³H
before opening
after opening
He
He intensity
H intensity
before
after
30 nm
18
Dr. Michael Klimenkov
Dr. M. Klimenkov
Institute of Applied Materials –
Applied Materials Physics (IAM-AWP)
IAM

HIDOBE II publications

Karlsruhe Institute of Technology

- M. Klimenkov, P. Vladimirov, J. Hoffmann, N. Zimber, A. Möslang, V. Kuksenko “First simultaneous detection of helium and tritium inside bubbles in beryllium” Micron **127** (2019) 102754
- M. Klimenkov, P. Vladimirov, U. Jäntsch, V. Kuksenko, R. Rolli, A. Möslang and N. Zimber “New insights into microstructure of irradiated beryllium based on experiments and computer simulations” Scientific Reports (2020) 10:8042
- N. Zimber, P. Vladimirov, M. Klimenkov, V. Kuksenko “Investigation of a high-dose irradiated beryllium microstructure” Journal of Nuclear Materials **540** (2020) 152374
- N. Zimber, P. Vladimirov, “The role of grain boundaries and denuded zones for tritium retention in high-dose neutron irradiated beryllium” Journal of Nuclear Materials **568** (2022) 153855

19 Dr. Michael Klimenkov Institute of Applied Materials – Applied Materials Physics (IAM-AWP) IAM Institute for Applied Materials

Distribution of impurity elements

Karlsruhe Institute of Technology

presence of pecipitates at 370°C and 440°C

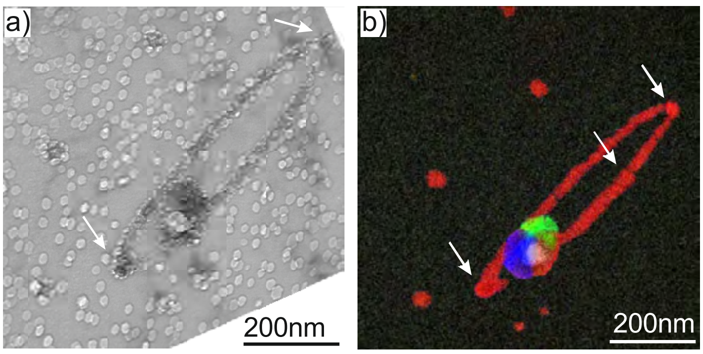

A loop decorated by a segregation of Fe-Al-Be phase pinned by a complex phase precipitate (a) observed at 643 K (370 °C).

Various phases in EDX map are colored as follows

AlFe

MnSi

CrTi

UFe

20 Dr. Michael Klimenkov Institute of Applied Materials – Applied Materials Physics (IAM-AWP) IAM Institute for Applied Materials

Summary

- Successful microstructural examination of neutron irradiated beryllium at IAM-AWP over the past 10 years (6 publications in peer reviewed journal).
- Detection of He and H_2 in bubbles by TEM in neutron irradiated Be was reported for the first time.
- Recent study were focused on the characterization of gas bubbles located inside grains and at the GBs as well as on the study of spatial distribution and composition of secondary phase precipitates.
- **Recent results (HIDOBE II):**
- Helium bubbles were found inside grains at all irradiation temperatures, which is consistent with previous literature. Their shape is spherical at 370°C and changes to a flat hexagonal prism at higher irradiation temperatures. The bubble size increases strongly with irradiation temperature. The apparent swelling estimated from the TEM data reaches ~9% at 650°C
- Precipitation of Fe-Al-Be phase within grains were detected at low irradiation temperatures (370°C and 440°C)
- EELS spectroscopy was used for detection and analysis of He and H_2 gases trapped inside flat hexagonal bubbles formed on the basal planes of beryllium under neutron irradiation.
- The number densities of both gases inside the bubbles were calculated using atomic scattering cross-section and the intensity of the zero-loss peak. The values He=(4.2±1) at/nm^3 and nH_2=(3.5±1.2) molecules/nm^3 were determined for a bubble with a diameter of 160nm.

21 Dr. Michael Klimenkov Institute of Applied Materials – Applied Materials Physics (IAM-AWP)

Effect of impurities on microstructural evolution under irradiation in beryllium

P.V. Vladimirov[1], D.V. Bachurin[1], C. Stihl[1] and N. Zimber[1]

[1]*Karlsruhe Institute of Technology, Institute for Applied Materials - Applied Materials Physics,*
76344 Eggenstein-Leopoldshafen, Germany

Impurities are known to affect mechanical properties of beryllium, but their effect on development of irradiation induced microstructure is still unknown. In this contribution we are making further attempt to reveal behavior of impurities in neutron irradiated beryllium pebbles by using both analytical transmission electron microscope (TEM) and first principles computer simulations.

TEM studies have revealed Al-Fe-Be precipitates, complex multiple phase precipitates, homogeneous segregations of elements to grain boundaries as well as abundant precipitation along dislocations. All precipitates are richly decorated with helium bubbles which are smaller in size than typical bubbles inside grains. Precipitate-free and helium-bubble-free zones were observed along grain boundaries.

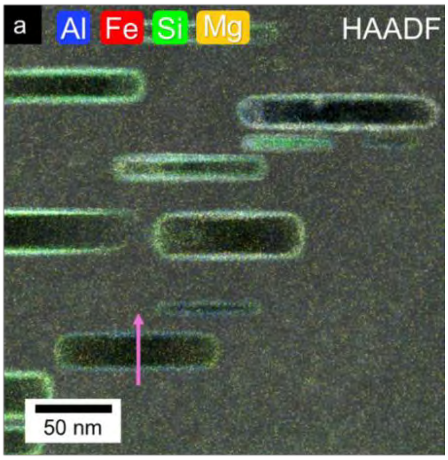

Using density functional theory approach, we have calculated interaction of typical solutes found in beryllium, namely, Al, Fe, Cr, Mg and Si with vacancies, interstitials and free surfaces which can simulate a surface of helium bubbles. Interesting correlation has been revealed: an impurity which has attractive binding with a vacancy has also positive affinity to free surface. In particular, Al, Mg and Si are strongly bound with vacancies and also attracted by the free surfaces. This result is supported by the EDX measurements, (see Fig. above) which reveal decoration of He bubbles with Al, Si and Mg, while Fe is homogeneously distributed. Those impurities which repulse vacancies are attracted by self-interstitials, however, no correlation with the formation volume of respective substitutional atoms was found in this case.

Corresponding Author:
Dr. Pavel Vladimirov,
pavel.vladimirov@kit.edu
Karlsruhe Institut of Technology,
Hermann-von-Helmholtz-Platz 1
76344 Eggenstein-Leopoldshafen, Germany

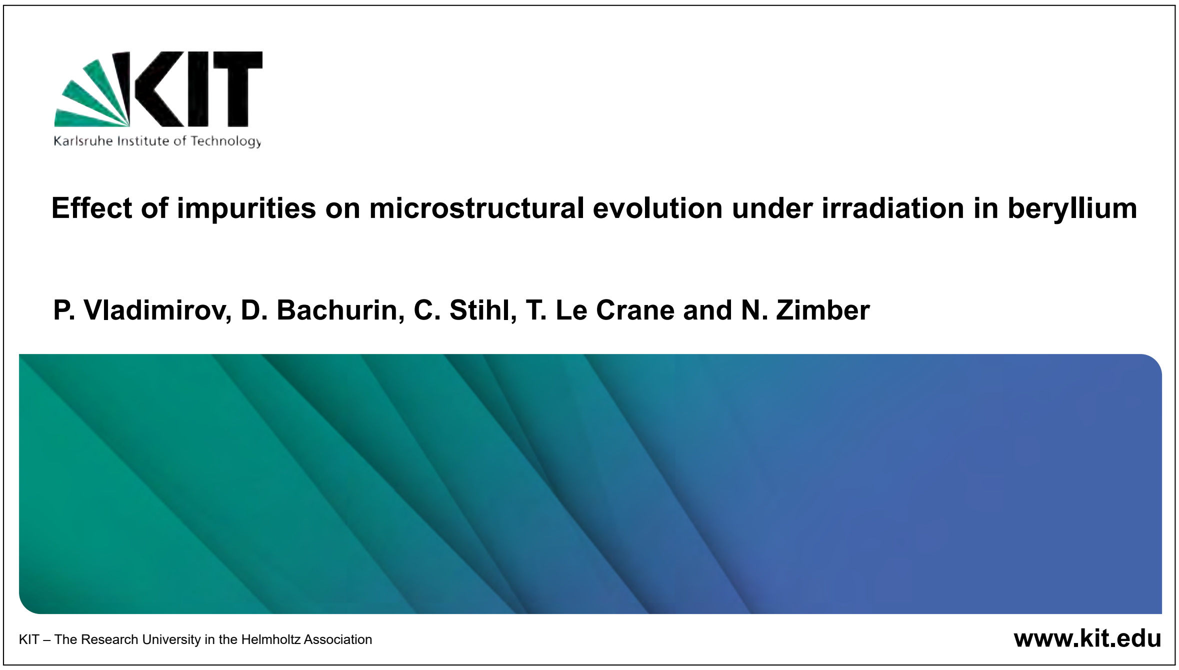
Karlsruhe Institute of Technology
Effect of impurities on microstructural evolution under irradiation in beryllium
P. Vladimirov, D. Bachurin, C. Stihl, T. Le Crane and N. Zimber
KIT – The Research University in the Helmholtz Association
www.kit.edu

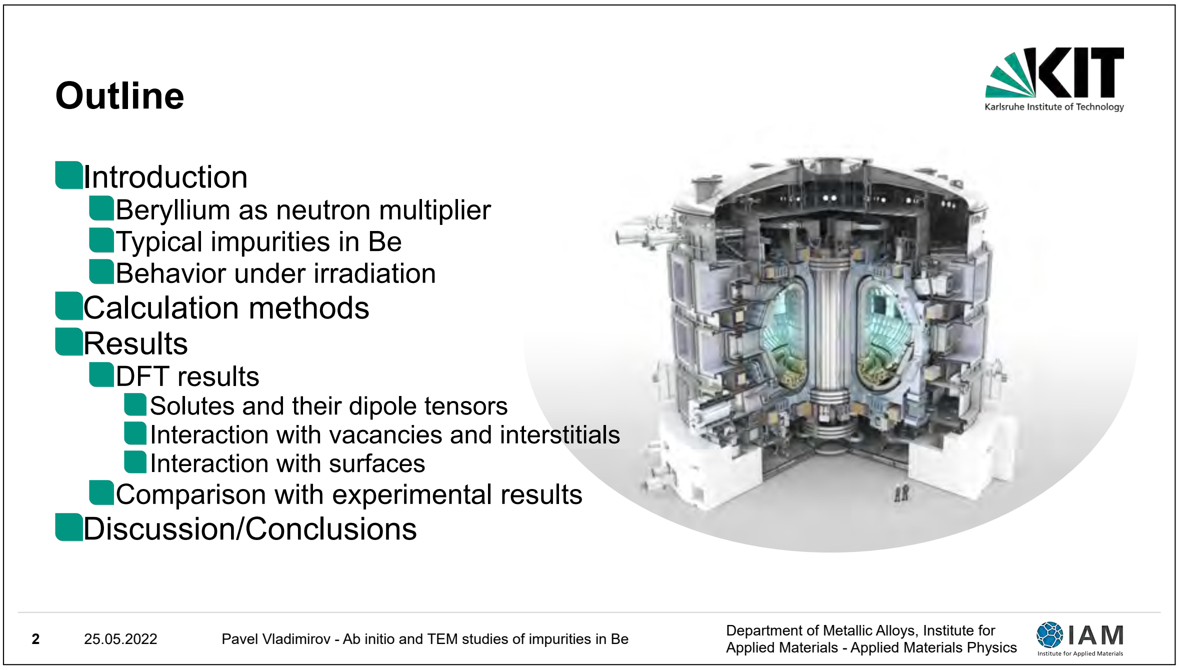
Outline
Karlsruhe Institute of Technology
Introduction
Beryllium as neutron multiplier
Typical impurities in Be
Behavior under irradiation
Calculation methods
Results
DFT results
Solutes and their dipole tensors
Interaction with vacancies and interstitials
Interaction with surfaces
Comparison with experimental results
Discussion/Conclusions
2
25.05.2022
Pavel Vladimirov - Ab initio and TEM studies of impurities in Be
Department of Metallic Alloys, Institute for Applied Materials - Applied Materials Physics
IAM

Beryllium as neutron multiplier in ITER TBM

- Lithium and beryllium are needed to increase TBR and close fuel cycle
- Beryllium will be used as 1-mm pebbles filling space within BU around Li-ceramic layers

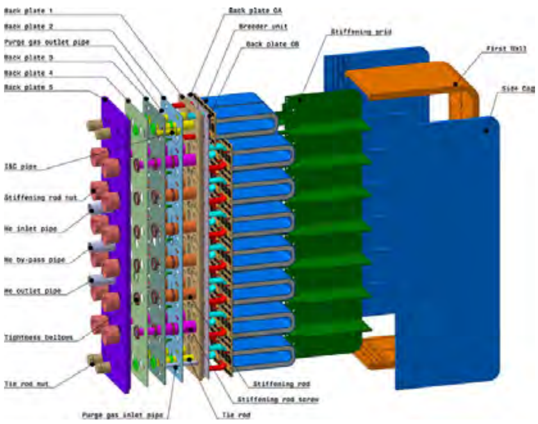

M. Zmitko, et al. *Development and qualification of functional materials for the European HCPB TBM*, https://doi.org/10.1016/j.fusengdes.2018.05.014

3 25.05.2022 Pavel Vladimirov - Ab initio and TEM studies of impurities in Be Department of Metallic Alloys, Institute for Applied Materials - Applied Materials Physics

Beryllium as neutron multiplier in ITER TBM

- Lithium and beryllium are needed to increase TBR and close fuel cycle
- Beryllium will be used as 1-mm pebbles filling space within BU around Li-ceramic layers
- Formation of gas filled bubbles (swelling) is critical for tritium accumulation

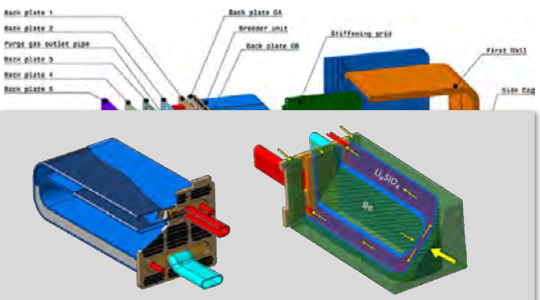

BU = Breeder Unit
Consists of Li-cermics and Be interchanging pebble beds

M. Zmitko, et al. *Development and qualification of functional materials for the European HCPB TBM*, https://doi.org/10.1016/j.fusengdes.2018.05.014

3 25.05.2022 Pavel Vladimirov - Ab initio and TEM studies of impurities in Be Department of Metallic Alloys, Institute for Applied Materials - Applied Materials Physics

Impurities in Be

KIT
Karlsruhe Institute of Technology

- Why impurities are important:
  - Mechancial properties (hot shortness)
  - Activation under irradiation (e.g., U)
  - Affect microstructure development under irradiation
- Major metallic impurities are
  - Mg, Al, Si,
  - Cr, Fe
- Major non-metals:
  - C, O
- Impurities produced by neutron-induced nuclear transmutations:
  - He, Li

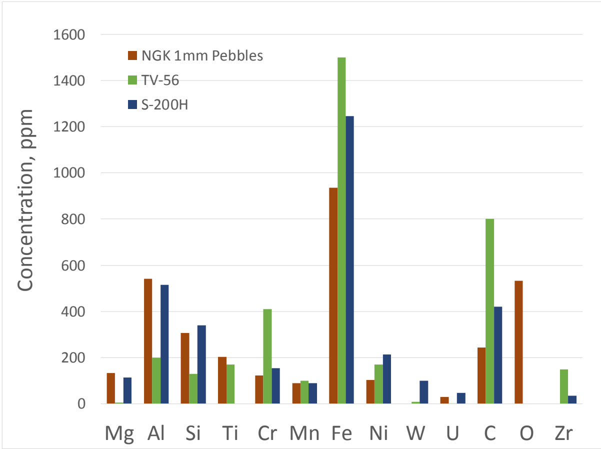

4 25.05.2022 Pavel Vladimirov - Ab initio and TEM studies of impurities in Be

Department of Metallic Alloys, Institute for Applied Materials - Applied Materials Physics

IAM
Institute for Applied Materials

Impurities in as received Be

KIT
Karlsruhe Institute of Technology

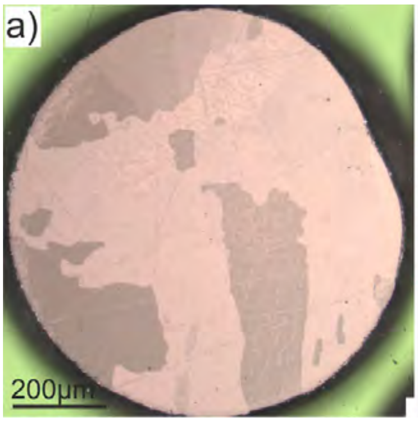

N. Zimber PhD Thesis,
10.5445/IR/1000139959

5 25.05.2022 Pavel Vladimirov - Ab initio and TEM studies of impurities in Be

Department of Metallic Alloys, Institute for Applied Materials - Applied Materials Physics

IAM
Institute for Applied Materials

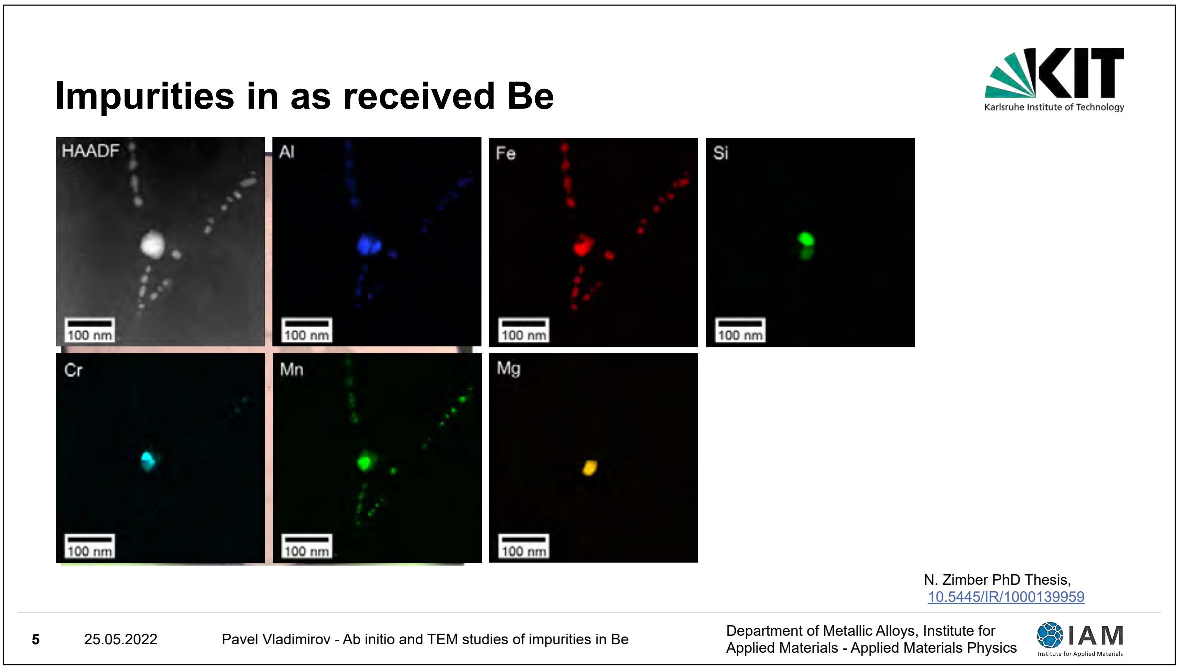
Impurities in as received Be
Karlsruhe Institute of Technology
HAADF
Al
Fe
Si
Cr
Mn
Mg
100 nm
N. Zimber PhD Thesis,
10.5445/IR/1000139959
5
25.05.2022
Pavel Vladimirov - Ab initio and TEM studies of impurities in Be
Department of Metallic Alloys, Institute for Applied Materials - Applied Materials Physics
IAM

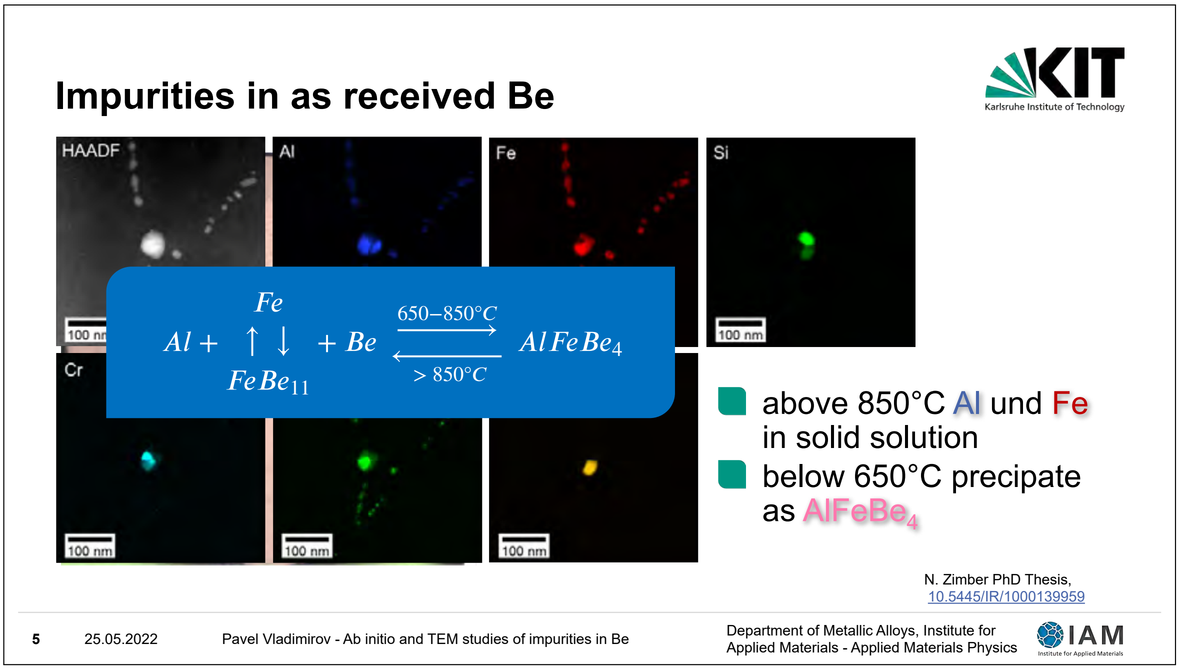
Impurities in as received Be
Karlsruhe Institute of Technology
HAADF
Al
Fe
Si
Cr
100 nm
$Al + \overset{Fe}{\underset{FeBe_{11}}{\uparrow\downarrow}} + Be \underset{>850°C}{\overset{650-850°C}{\rightleftarrows}} AlFeBe_4$
above 850°C Al und Fe in solid solution
below 650°C precipate as $AlFeBe_4$
N. Zimber PhD Thesis,
10.5445/IR/1000139959
5
25.05.2022
Pavel Vladimirov - Ab initio and TEM studies of impurities in Be
Department of Metallic Alloys, Institute for Applied Materials - Applied Materials Physics
IAM

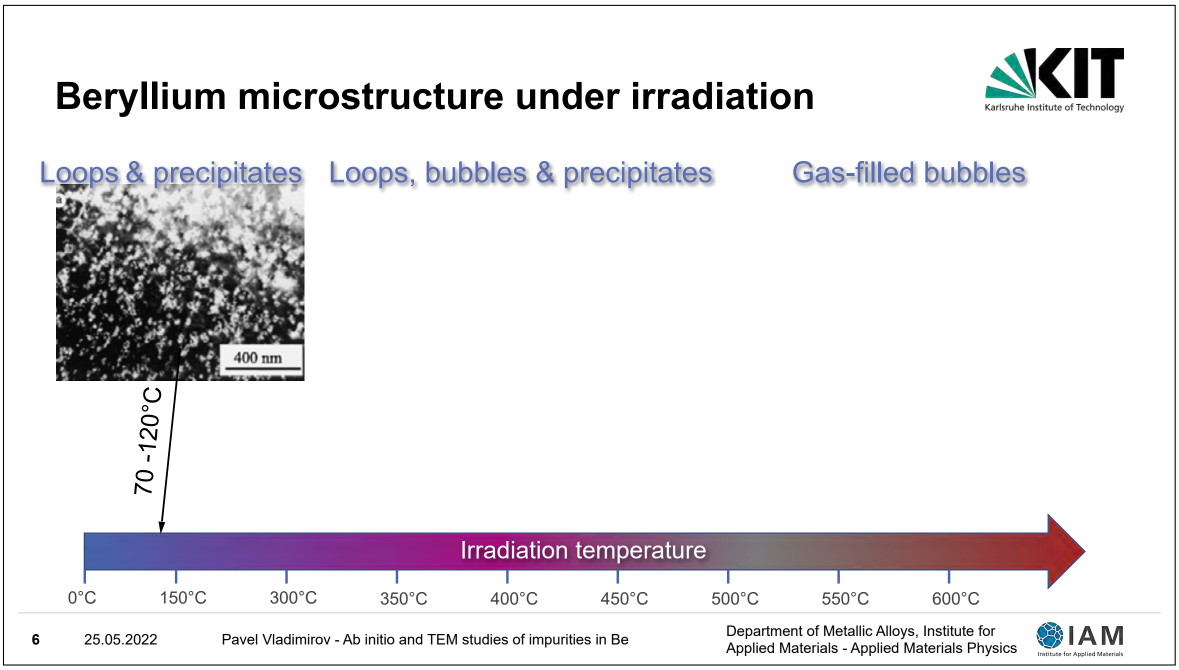
Beryllium microstructure under irradiation
Karlsruhe Institute of Technology
Loops & precipitates
Loops, bubbles & precipitates
Gas-filled bubbles
400 nm
70 -120°C
Irradiation temperature
0°C
150°C
300°C
350°C
400°C
450°C
500°C
550°C
600°C
6
25.05.2022
Pavel Vladimirov - Ab initio and TEM studies of impurities in Be
Department of Metallic Alloys, Institute for Applied Materials - Applied Materials Physics
IAM

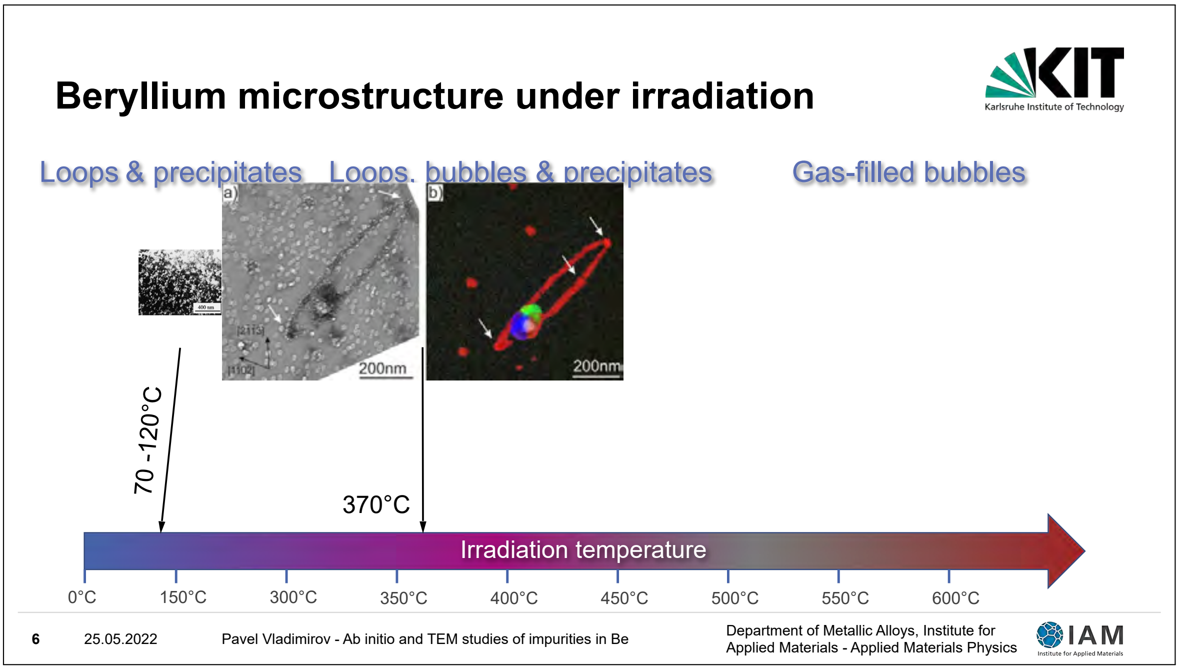
Beryllium microstructure under irradiation
Karlsruhe Institute of Technology
Loops & precipitates
Loops, bubbles & precipitates
Gas-filled bubbles
a)
b)
200nm
200nm
70 -120°C
370°C
Irradiation temperature
0°C
150°C
300°C
350°C
400°C
450°C
500°C
550°C
600°C
6
25.05.2022
Pavel Vladimirov - Ab initio and TEM studies of impurities in Be
Department of Metallic Alloys, Institute for Applied Materials - Applied Materials Physics
IAM

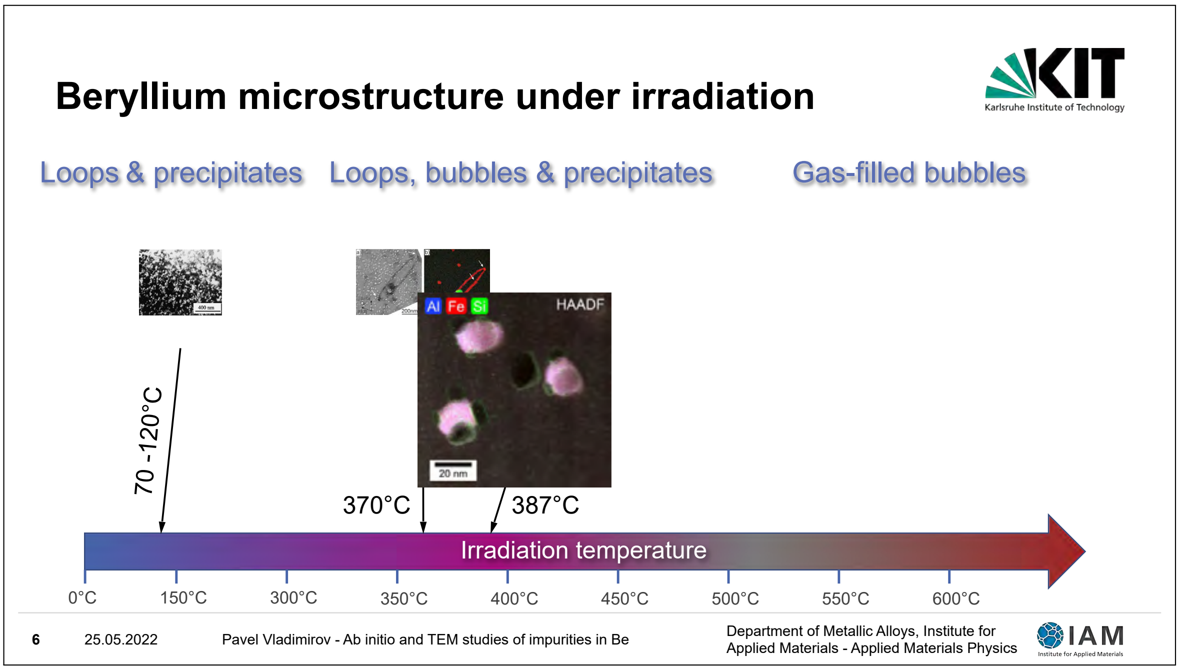

Beryllium microstructure under irradiation
Karlsruhe Institute of Technology
Loops & precipitates
Loops, bubbles & precipitates
Gas-filled bubbles
Al Fe Si
HAADF
20 nm
70 -120°C
370°C
387°C
Irradiation temperature
0°C
150°C
300°C
350°C
400°C
450°C
500°C
550°C
600°C
6
25.05.2022
Pavel Vladimirov - Ab initio and TEM studies of impurities in Be
Department of Metallic Alloys, Institute for Applied Materials - Applied Materials Physics
IAM

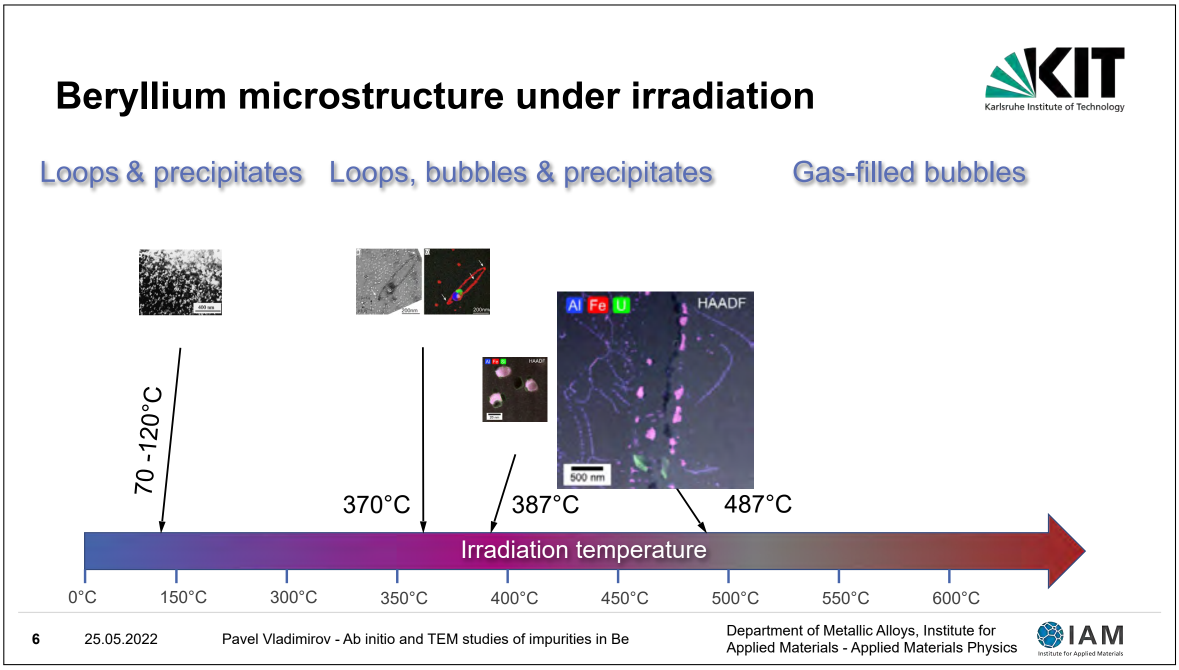

Beryllium microstructure under irradiation
Karlsruhe Institute of Technology
Loops & precipitates
Loops, bubbles & precipitates
Gas-filled bubbles
Al Fe U
HAADF
500 nm
70 -120°C
370°C
387°C
487°C
Irradiation temperature
0°C
150°C
300°C
350°C
400°C
450°C
500°C
550°C
600°C
6
25.05.2022
Pavel Vladimirov - Ab initio and TEM studies of impurities in Be
Department of Metallic Alloys, Institute for Applied Materials - Applied Materials Physics
IAM

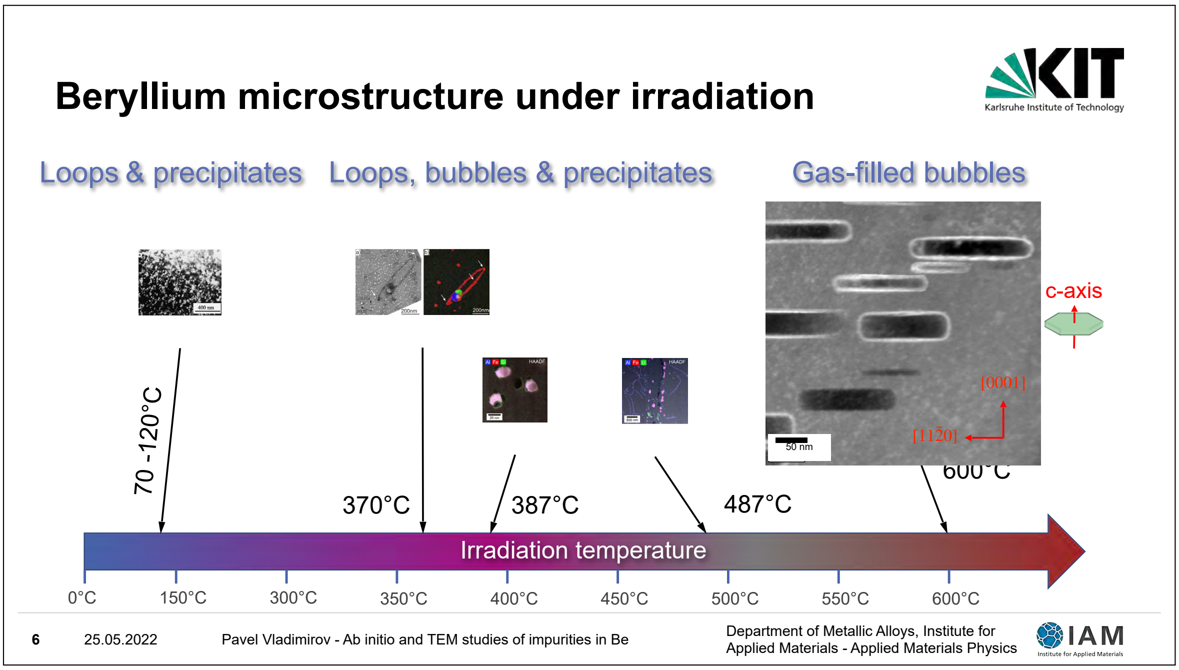
Beryllium microstructure under irradiation
KIT
Karlsruhe Institute of Technology
Loops & precipitates
Loops, bubbles & precipitates
Gas-filled bubbles
c-axis
[0001]
50 nm
70 -120°C
370°C
387°C
487°C
600°C
Irradiation temperature
0°C
150°C
300°C
350°C
400°C
450°C
500°C
550°C
600°C
6
25.05.2022
Pavel Vladimirov - Ab initio and TEM studies of impurities in Be
Department of Metallic Alloys, Institute for Applied Materials - Applied Materials Physics
IAM
Institute for Applied Materials

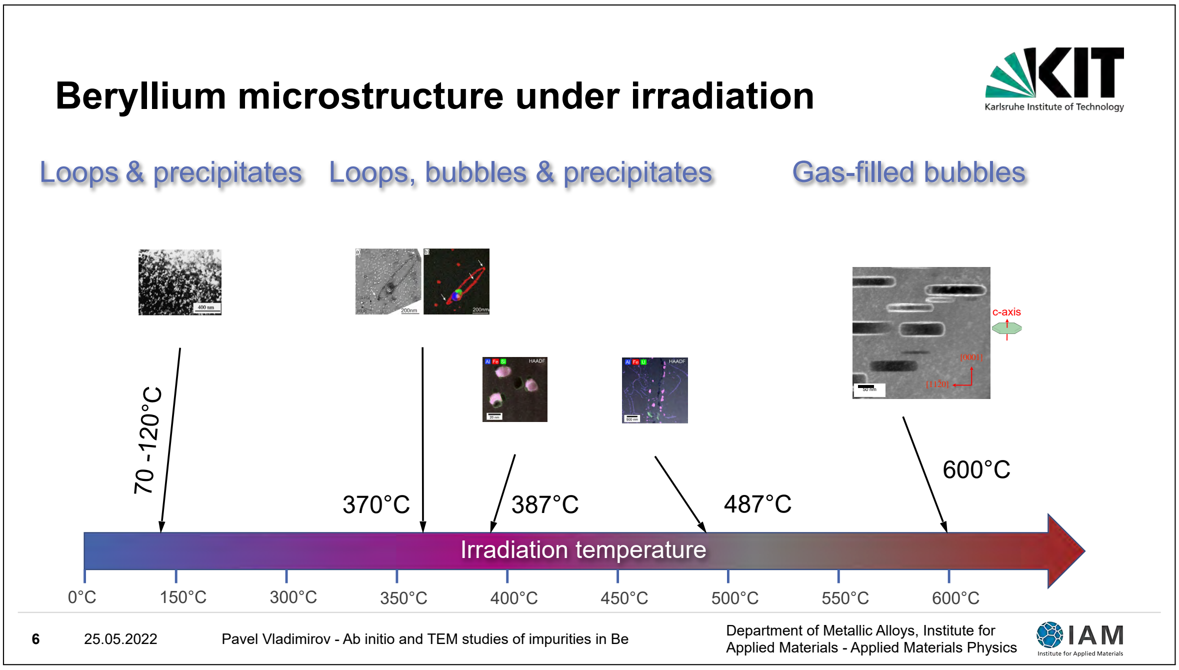
Beryllium microstructure under irradiation
KIT
Karlsruhe Institute of Technology
Loops & precipitates
Loops, bubbles & precipitates
Gas-filled bubbles
c-axis
70 -120°C
370°C
387°C
487°C
600°C
Irradiation temperature
0°C
150°C
300°C
350°C
400°C
450°C
500°C
550°C
600°C
6
25.05.2022
Pavel Vladimirov - Ab initio and TEM studies of impurities in Be
Department of Metallic Alloys, Institute for Applied Materials - Applied Materials Physics
IAM
Institute for Applied Materials

Beryllium microstructure under irradiation

Loops & precipitates | Loops, bubbles & precipitates | Gas-filled bubbles

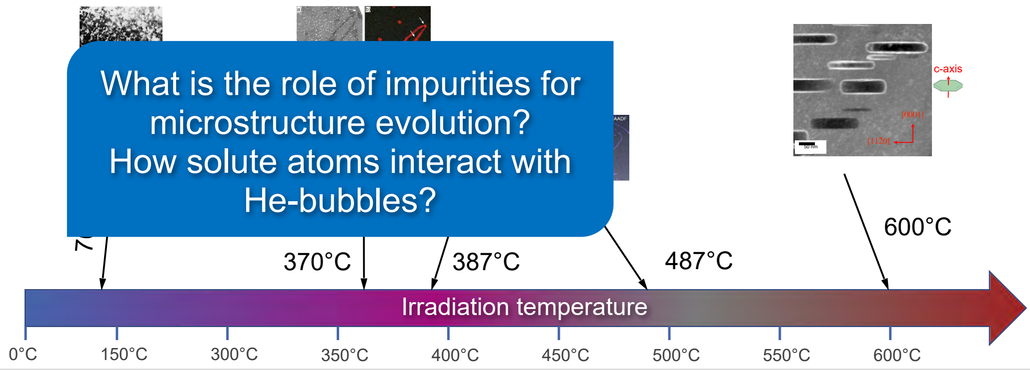

6 25.05.2022 Pavel Vladimirov - Ab initio and TEM studies of impurities in Be

Department of Metallic Alloys, Institute for Applied Materials - Applied Materials Physics

Simulation methods

Density Functional Theory

- VASP 5.3 or 6.2.0
- Generalized Gradient Approximation (GGA)
- Pseudopotentials:
  - Plain Augmented Waves (PAW), xc=PBE_54
  - Li: 2s1 Al: 3s2 3p1
  - Be: 2s2 Si: 3s2 3p2
  - Mg: 3s2 Cr: 4s1 3d5
  - Fe: 3d6 4s2
- Gamma centered Monkhorst-Pack k-point grid
  13 × 13 × 13 or KSPACING = 0.12016
- Energy cutoff ENCUT $\geq$ 450 eV

- Simulation cell sizes for solute-vacancy interaction:
  - 4 × 4 × 3 – 96 atoms
  - 5 × 5 × 3 – 150 atoms
  - 6 × 6 × 3 – 216 atoms
- Simulation cell sizes for slabs:
  - (0001) 4×4×12 – 384 atoms
  - $(1\bar{1}00)$ 3×4×17 – 168 atoms
- Migration barrier calculations:
  - NEB
  - Dimer

7 25.05.2022 Pavel Vladimirov - Ab initio and TEM studies of impurities in Be

Department of Metallic Alloys, Institute for Applied Materials - Applied Materials Physics

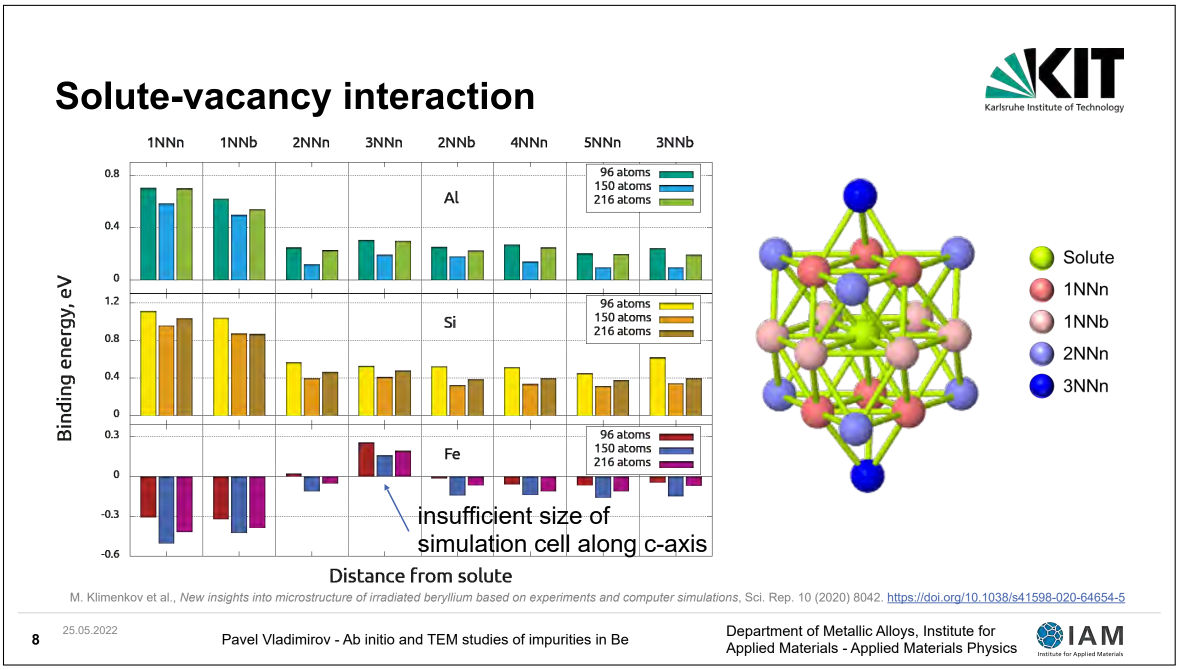
Solute-vacancy interaction
KIT
Karlsruhe Institute of Technology
1NNn
1NNb
2NNn
3NNn
2NNb
4NNn
5NNn
3NNb
Al
Si
Fe
96 atoms
150 atoms
216 atoms
Binding energy, eV
0.8
0.4
0
1.2
0.3
-0.3
-0.6
insufficient size of
simulation cell along c-axis
Distance from solute
Solute
1NNn
1NNb
2NNn
3NNn
M. Klimenkov et al., New insights into microstructure of irradiated beryllium based on experiments and computer simulations, Sci. Rep. 10 (2020) 8042. https://doi.org/10.1038/s41598-020-64654-5
8
25.05.2022
Pavel Vladimirov - Ab initio and TEM studies of impurities in Be
Department of Metallic Alloys, Institute for
Applied Materials - Applied Materials Physics
IAM

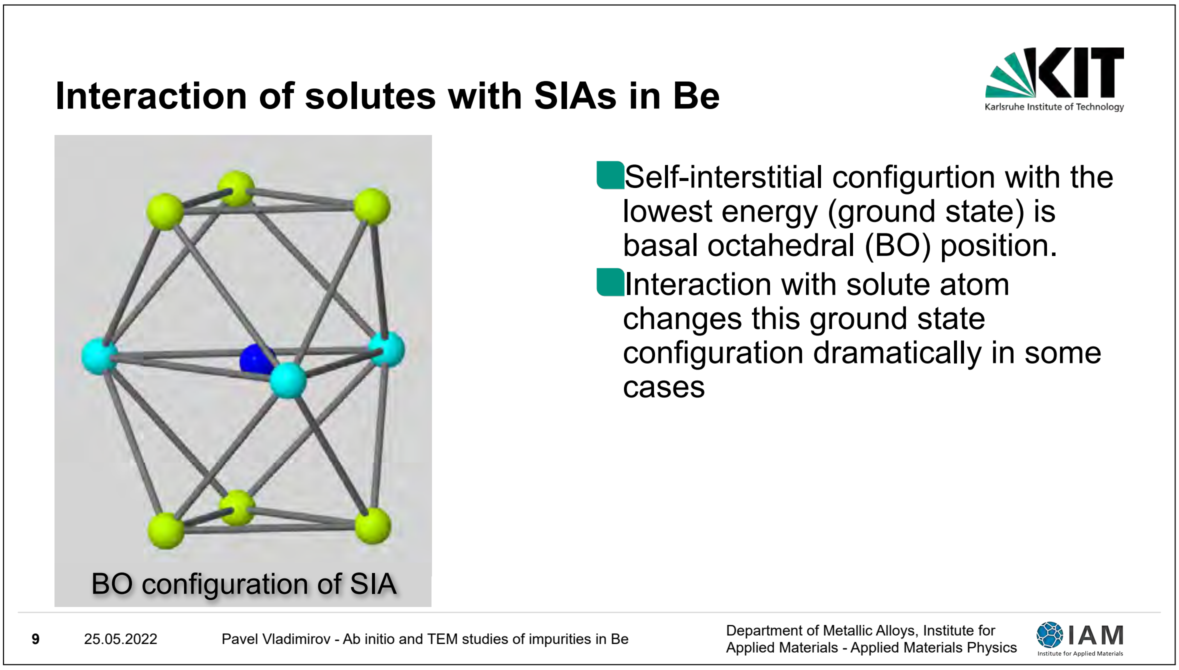
Interaction of solutes with SIAs in Be
KIT
Karlsruhe Institute of Technology
BO configuration of SIA
Self-interstitial configurtion with the lowest energy (ground state) is basal octahedral (BO) position.
Interaction with solute atom changes this ground state configuration dramatically in some cases
9
25.05.2022
Pavel Vladimirov - Ab initio and TEM studies of impurities in Be
Department of Metallic Alloys, Institute for
Applied Materials - Applied Materials Physics
IAM

Interaction of solutes with SIAs

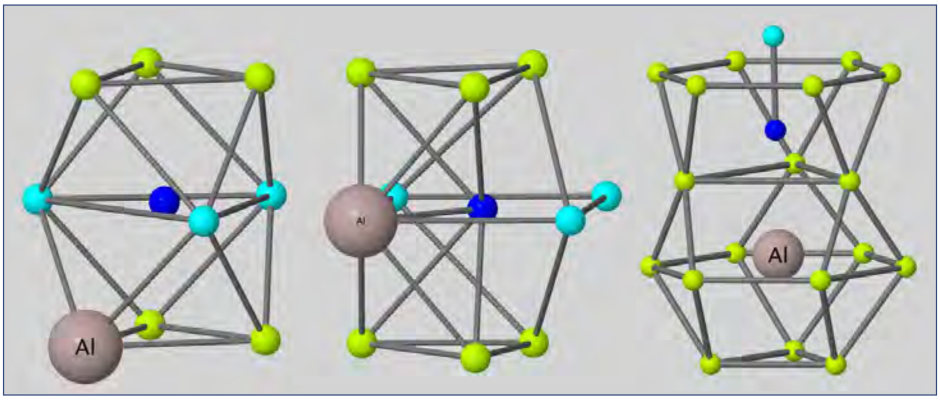

adjacent plane | same basal plane | along c-axis

10 25.05.2022 Pavel Vladimirov - Ab initio and TEM studies of impurities in Be

Department of Metallic Alloys, Institute for Applied Materials - Applied Materials Physics

Interaction of solutes with SIAs

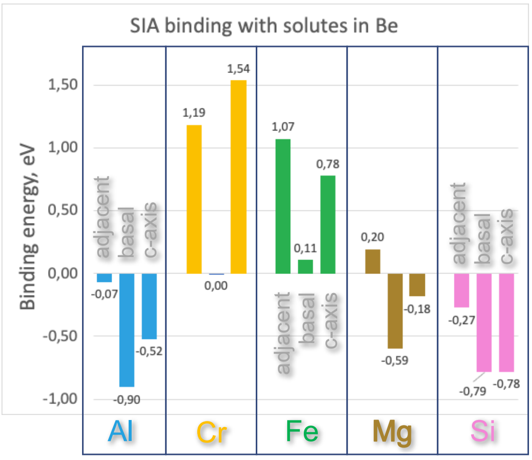

- SIAs are bound to Cr and Fe in non-basal configurations, but are repelled from Al, Mg and Si.
- Largest repulsion and lowest binding are observed for basal configurations.
- For both Cr and Fe, basal configuration is loosely bound => conversion from non-basal to basal configuration might be an important step for SIA detrapping.

11 25.05.2022 Pavel Vladimirov - Ab initio and TEM studies of impurities in Be

Department of Metallic Alloys, Institute for Applied Materials - Applied Materials Physics

Interlayer distance after slab relaxation

KIT Karlsruhe Institute of Technology

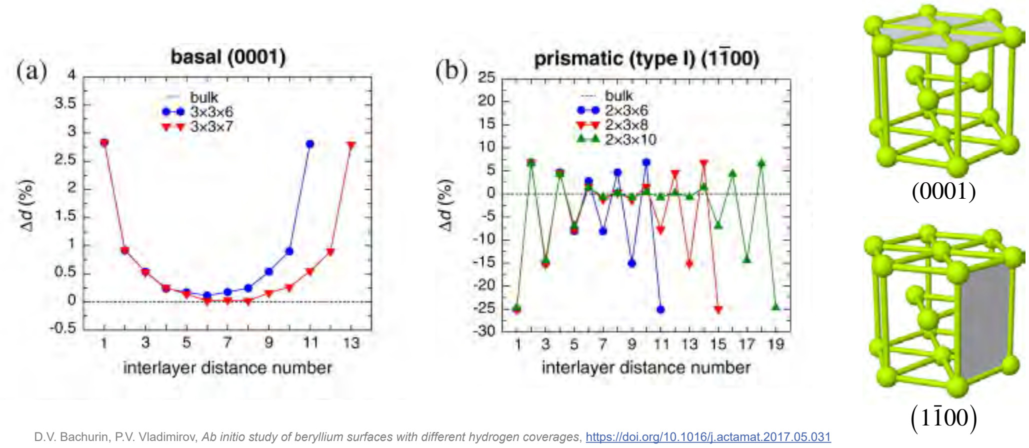

D.V. Bachurin, P.V. Vladimirov, *Ab initio study of beryllium surfaces with different hydrogen coverages*, https://doi.org/10.1016/j.actamat.2017.05.031

12 25.05.2022 Pavel Vladimirov - Ab initio and TEM studies of impurities in Be

Department of Metallic Alloys, Institute for Applied Materials - Applied Materials Physics

IAM Institute for Applied Materials

Impurities near Be (0001) surface

KIT Karlsruhe Institute of Technology

- He is slightly repeled by surface, but favorable inside vacuum

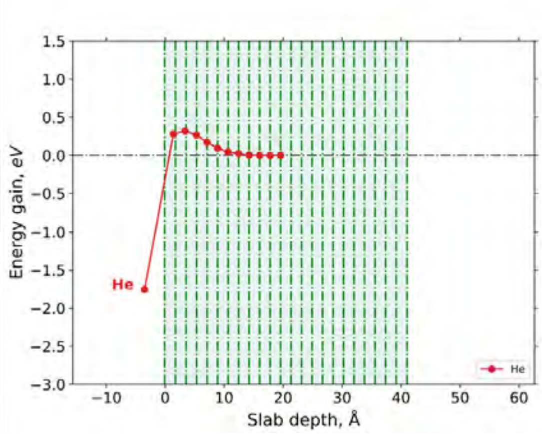

13 25.05.2022 Pavel Vladimirov - Ab initio and TEM studies of impurities in Be

Department of Metallic Alloys, Institute for Applied Materials - Applied Materials Physics

IAM Institute for Applied Materials

Impurities near Be (0001) surface

- He is slightly repeled by surface, but favorable inside vacuum
- Li is also slighly repeled, but favorable at the surface

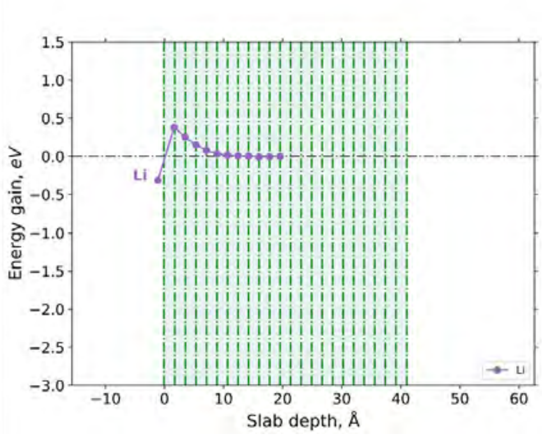

13 25.05.2022 Pavel Vladimirov - Ab initio and TEM studies of impurities in Be

Department of Metallic Alloys, Institute for Applied Materials - Applied Materials Physics

Impurities near Be (0001) surface

- He is slightly repeled by surface, but favorable inside vacuum
- Li is also slighly repeled, but favorable at the surface
- Mg is attracted by surface

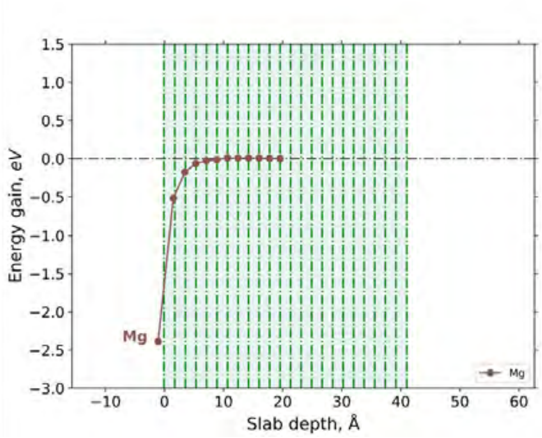

13 25.05.2022 Pavel Vladimirov - Ab initio and TEM studies of impurities in Be

Department of Metallic Alloys, Institute for Applied Materials - Applied Materials Physics

Impurities near Be (0001) surface

KIT Karlsruhe Institute of Technology

- He is slightly repeled by surface, but favorable inside vacuum
- Li is also slighly repeled, but favorable at the surface
- Mg is attracted by surface
- Al is similar to Mg

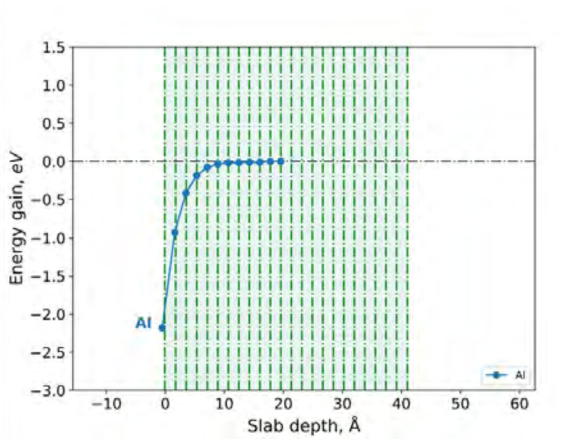

13 25.05.2022 Pavel Vladimirov - Ab initio and TEM studies of impurities in Be Department of Metallic Alloys, Institute for Applied Materials - Applied Materials Physics IAM Institute for Applied Materials

Impurities near Be (0001) surface

KIT Karlsruhe Institute of Technology

- He is slightly repeled by surface, but favorable inside vacuum
- Li is also slighly repeled, but favorable at the surface
- Mg is attracted by surface
- Al is similar to Mg
- Si is the most favorable impurity at the surface

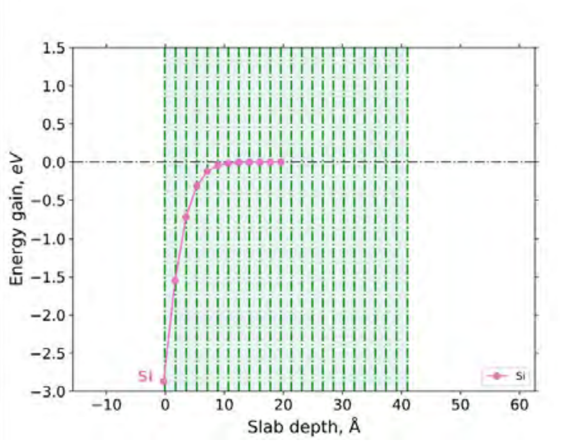

13 25.05.2022 Pavel Vladimirov - Ab initio and TEM studies of impurities in Be Department of Metallic Alloys, Institute for Applied Materials - Applied Materials Physics IAM Institute for Applied Materials

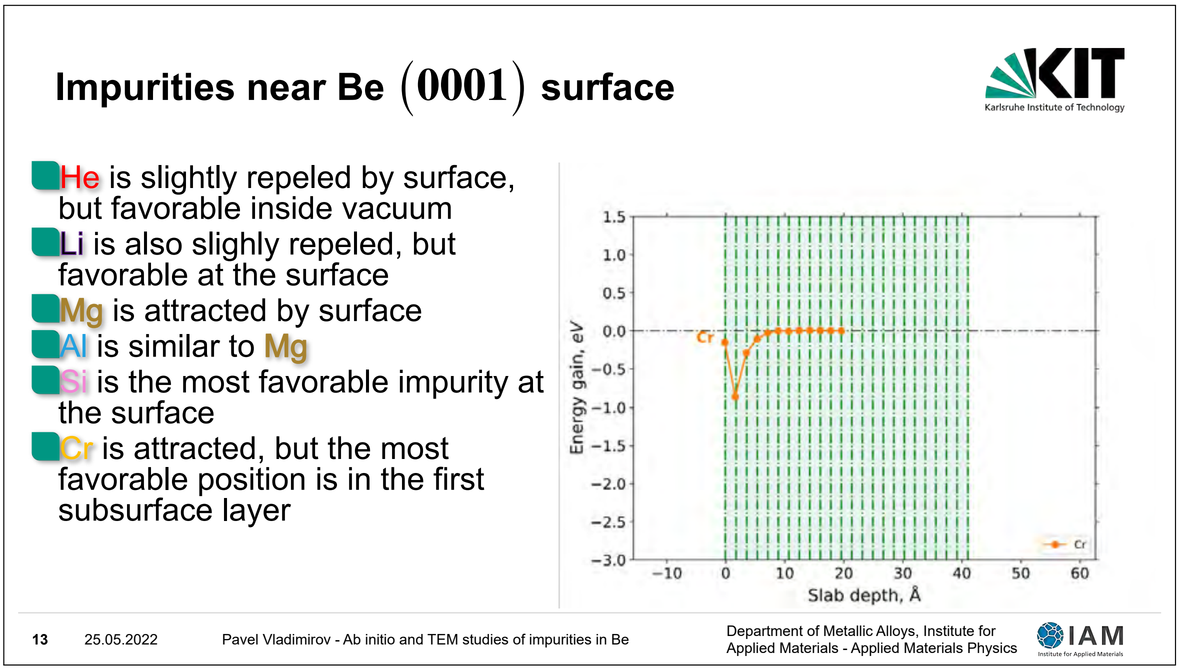
Impurities near Be (0001) surface
KIT
Karlsruhe Institute of Technology
He is slightly repeled by surface, but favorable inside vacuum
Li is also slighly repeled, but favorable at the surface
Mg is attracted by surface
Al is similar to Mg
Si is the most favorable impurity at the surface
Cr is attracted, but the most favorable position is in the first subsurface layer
Energy gain, eV
Slab depth, Å
Cr
13
25.05.2022
Pavel Vladimirov - Ab initio and TEM studies of impurities in Be
Department of Metallic Alloys, Institute for Applied Materials - Applied Materials Physics
IAM
Institute for Applied Materials

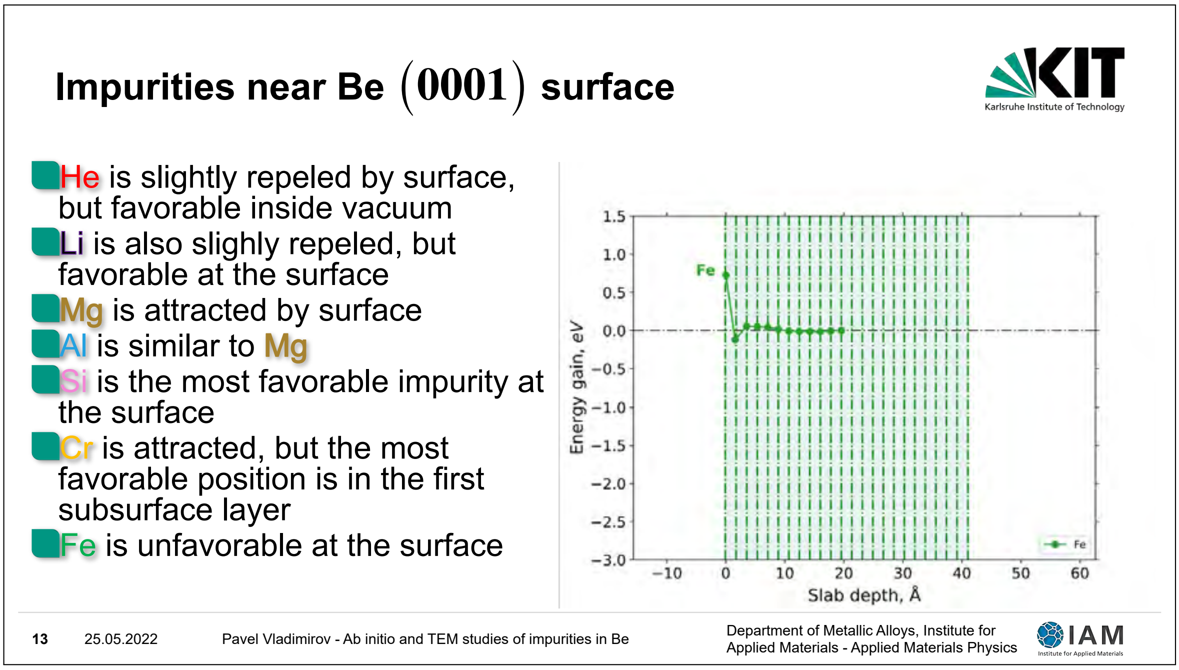
Impurities near Be (0001) surface
KIT
Karlsruhe Institute of Technology
He is slightly repeled by surface, but favorable inside vacuum
Li is also slighly repeled, but favorable at the surface
Mg is attracted by surface
Al is similar to Mg
Si is the most favorable impurity at the surface
Cr is attracted, but the most favorable position is in the first subsurface layer
Fe is unfavorable at the surface
Energy gain, eV
Slab depth, Å
Fe
13
25.05.2022
Pavel Vladimirov - Ab initio and TEM studies of impurities in Be
Department of Metallic Alloys, Institute for Applied Materials - Applied Materials Physics
IAM
Institute for Applied Materials

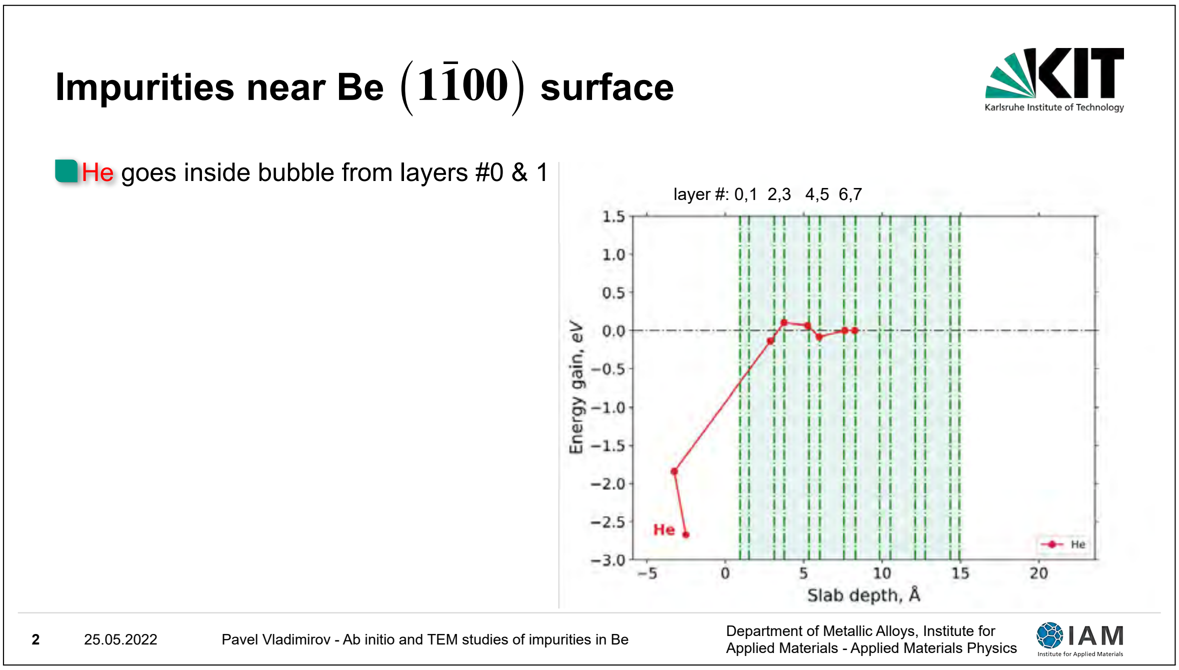
Impurities near Be $(1\bar{1}00)$ surface
Karlsruhe Institute of Technology
He goes inside bubble from layers #0 & 1
layer #: 0,1 2,3 4,5 6,7
Energy gain, eV
Slab depth, Å
He
2
25.05.2022
Pavel Vladimirov - Ab initio and TEM studies of impurities in Be
Department of Metallic Alloys, Institute for Applied Materials - Applied Materials Physics
IAM

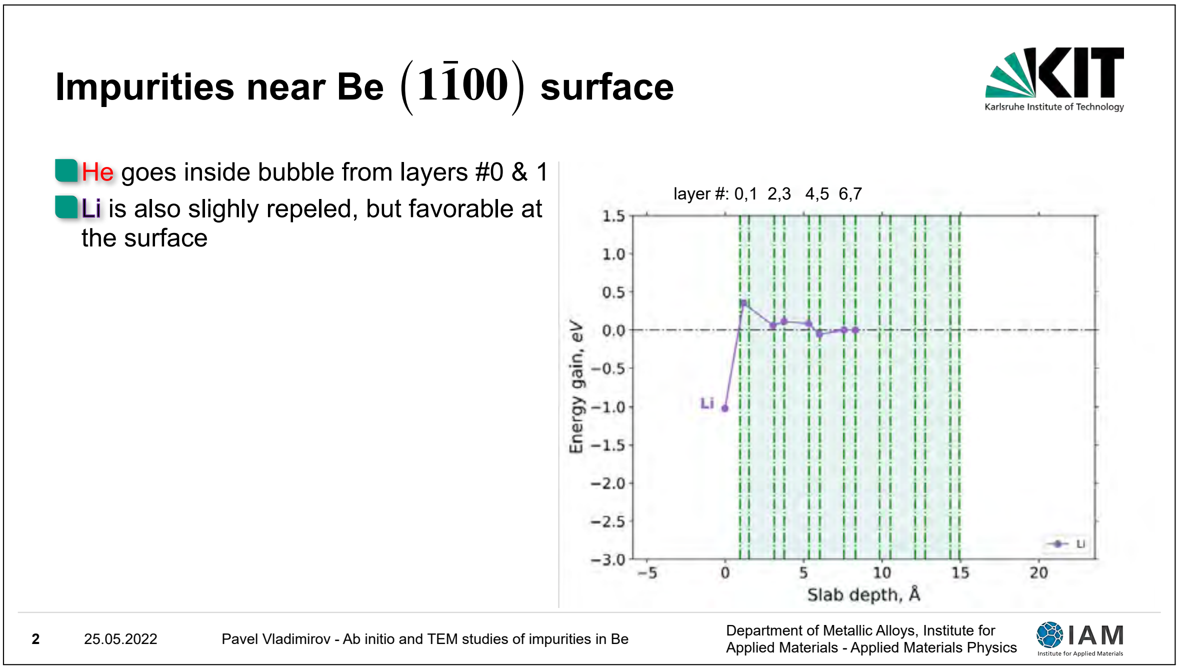
Impurities near Be $(1\bar{1}00)$ surface
Karlsruhe Institute of Technology
He goes inside bubble from layers #0 & 1
Li is also slighly repeled, but favorable at the surface
layer #: 0,1 2,3 4,5 6,7
Energy gain, eV
Slab depth, Å
Li
2
25.05.2022
Pavel Vladimirov - Ab initio and TEM studies of impurities in Be
Department of Metallic Alloys, Institute for Applied Materials - Applied Materials Physics
IAM

Impurities near Be $\left(1\bar{1}00\right)$ surface

- He goes inside bubble from layers #0 & 1
- Li is also slighly repeled, but favorable at the surface
- Mg goes to the surface from layers #0 & 1

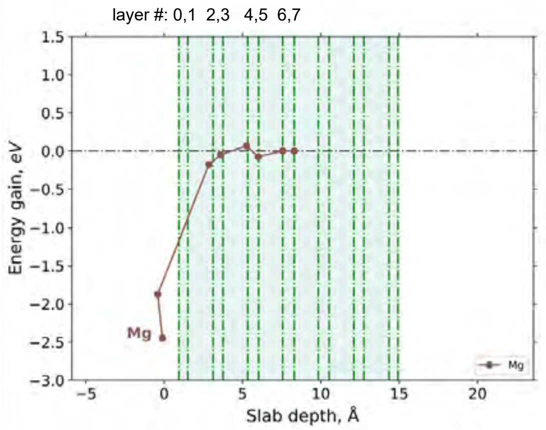

2 25.05.2022 Pavel Vladimirov - Ab initio and TEM studies of impurities in Be

Department of Metallic Alloys, Institute for Applied Materials - Applied Materials Physics

Impurities near Be $\left(1\bar{1}00\right)$ surface

- He goes inside bubble from layers #0 & 1
- Li is also slighly repeled, but favorable at the surface
- Mg goes to the surface from layers #0 & 1
- Al is similar to Mg

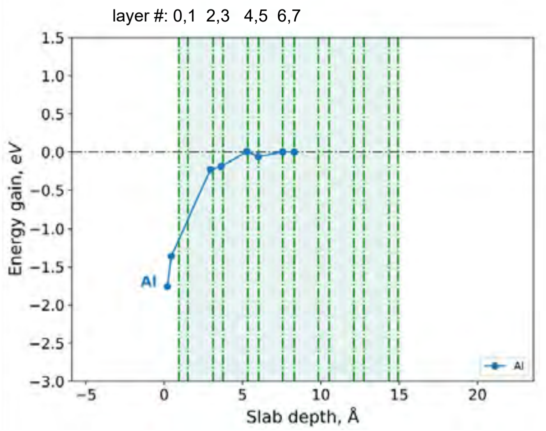

2 25.05.2022 Pavel Vladimirov - Ab initio and TEM studies of impurities in Be

Department of Metallic Alloys, Institute for Applied Materials - Applied Materials Physics

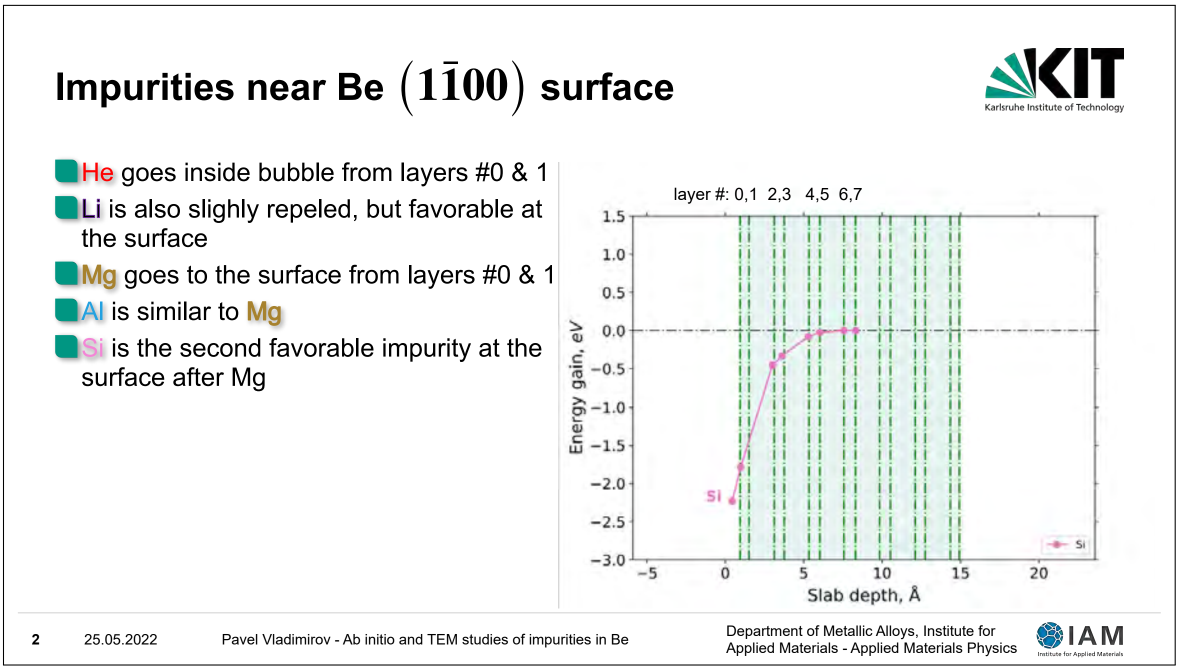
Impurities near Be $(1\bar{1}00)$ surface
Karlsruhe Institute of Technology
He goes inside bubble from layers #0 & 1
Li is also slighly repeled, but favorable at the surface
Mg goes to the surface from layers #0 & 1
Al is similar to Mg
Si is the second favorable impurity at the surface after Mg
layer #: 0,1 2,3 4,5 6,7
Energy gain, eV
Slab depth, Å
Si
2
25.05.2022
Pavel Vladimirov - Ab initio and TEM studies of impurities in Be
Department of Metallic Alloys, Institute for Applied Materials - Applied Materials Physics
IAM
Institute for Applied Materials

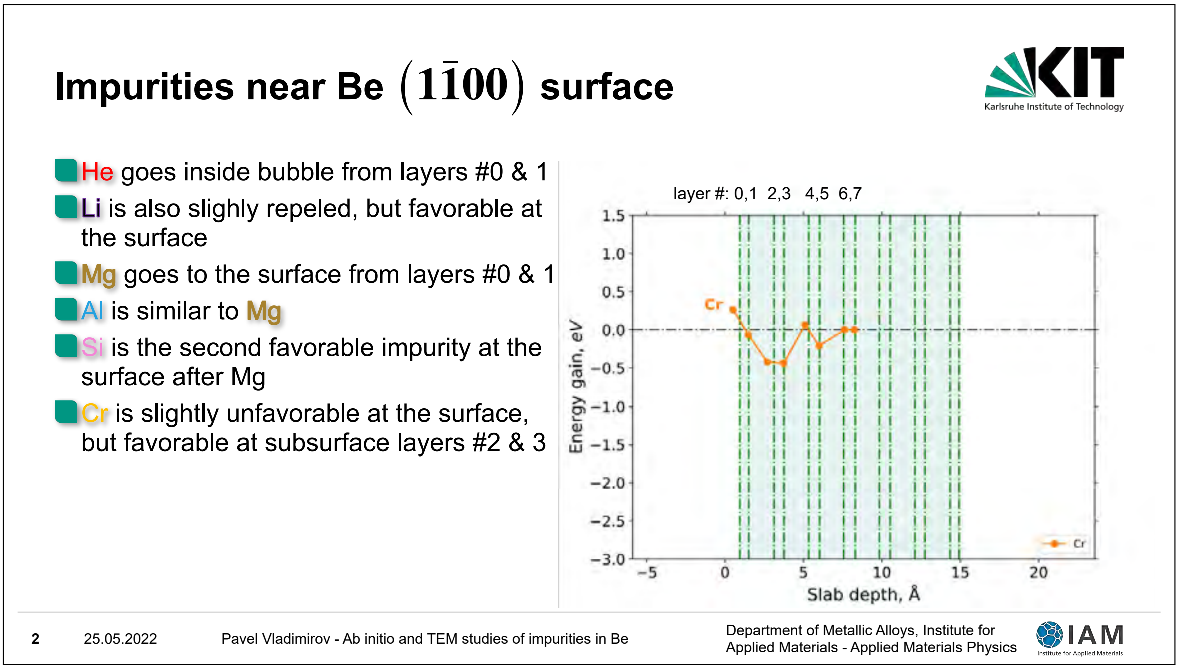
Impurities near Be $(1\bar{1}00)$ surface
Karlsruhe Institute of Technology
He goes inside bubble from layers #0 & 1
Li is also slighly repeled, but favorable at the surface
Mg goes to the surface from layers #0 & 1
Al is similar to Mg
Si is the second favorable impurity at the surface after Mg
Cr is slightly unfavorable at the surface, but favorable at subsurface layers #2 & 3
layer #: 0,1 2,3 4,5 6,7
Energy gain, eV
Slab depth, Å
Cr
2
25.05.2022
Pavel Vladimirov - Ab initio and TEM studies of impurities in Be
Department of Metallic Alloys, Institute for Applied Materials - Applied Materials Physics
IAM
Institute for Applied Materials

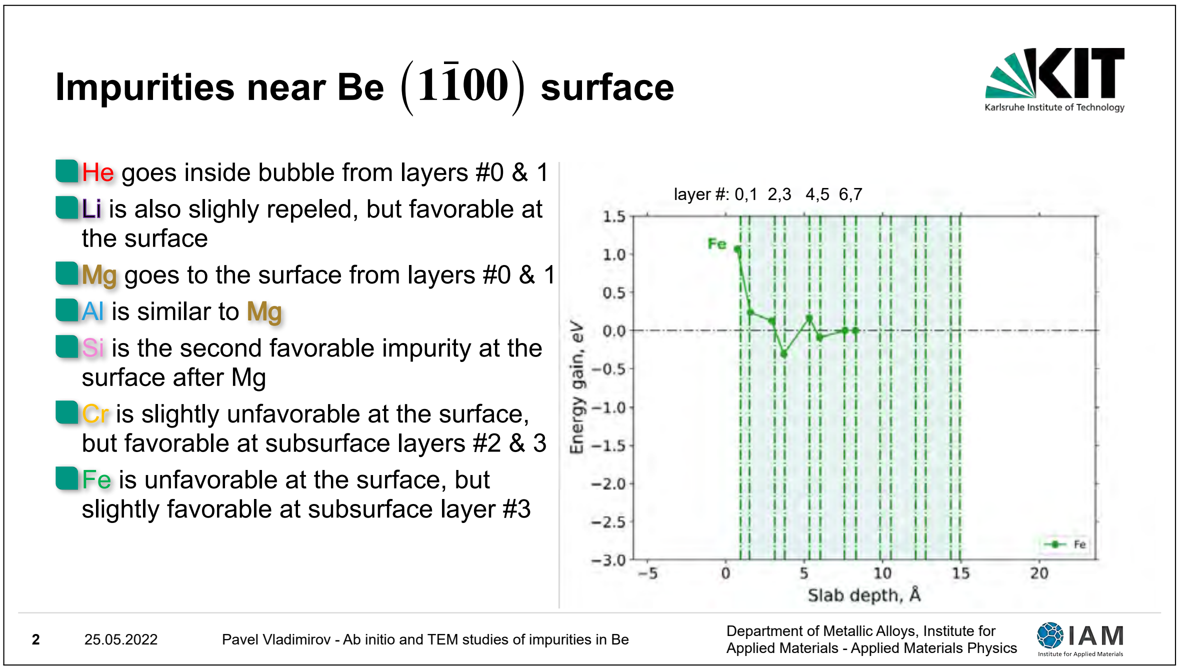
Impurities near Be $(1\bar{1}00)$ surface
Karlsruhe Institute of Technology
He goes inside bubble from layers #0 & 1
Li is also slighly repeled, but favorable at the surface
Mg goes to the surface from layers #0 & 1
Al is similar to Mg
Si is the second favorable impurity at the surface after Mg
Cr is slightly unfavorable at the surface, but favorable at subsurface layers #2 & 3
Fe is unfavorable at the surface, but slightly favorable at subsurface layer #3
layer #: 0,1 2,3 4,5 6,7
Energy gain, eV
Slab depth, Å
Fe
2
25.05.2022
Pavel Vladimirov - Ab initio and TEM studies of impurities in Be
Department of Metallic Alloys, Institute for Applied Materials - Applied Materials Physics
IAM
Institute for Applied Materials

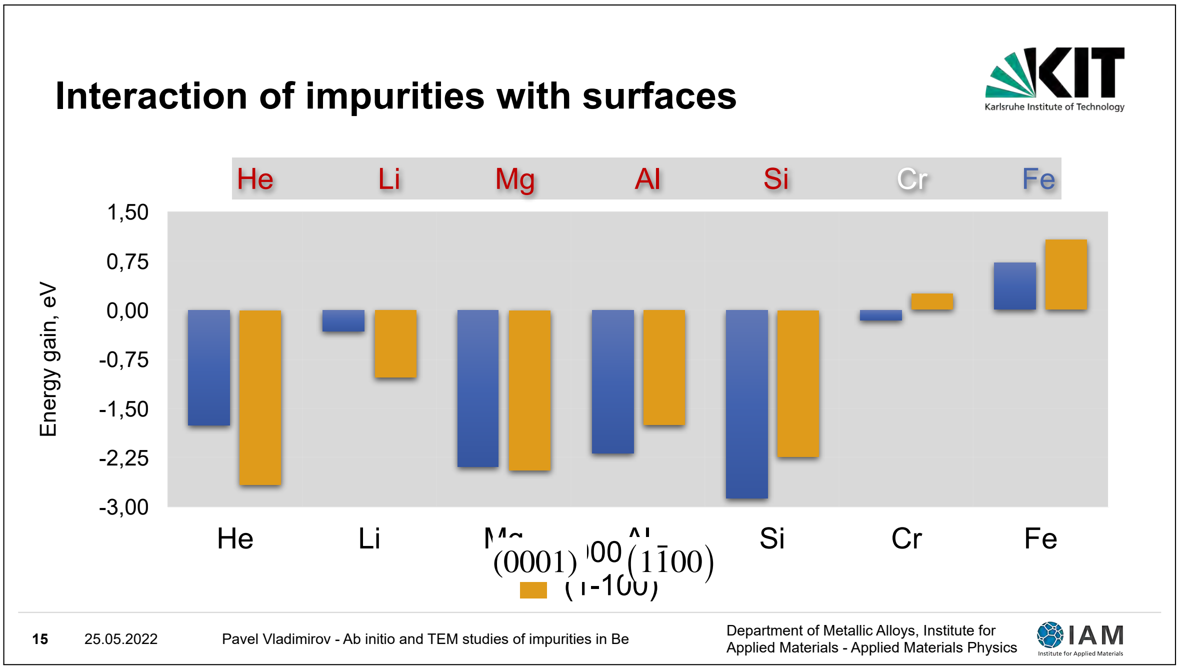
Interaction of impurities with surfaces
Karlsruhe Institute of Technology
He Li Mg Al Si Cr Fe
Energy gain, eV
1,50
0,75
0,00
-0,75
-1,50
-2,25
-3,00
He Li Mg Al Si Cr Fe
(0001)
$(1\bar{1}00)$
15
25.05.2022
Pavel Vladimirov - Ab initio and TEM studies of impurities in Be
Department of Metallic Alloys, Institute for Applied Materials - Applied Materials Physics
IAM
Institute for Applied Materials

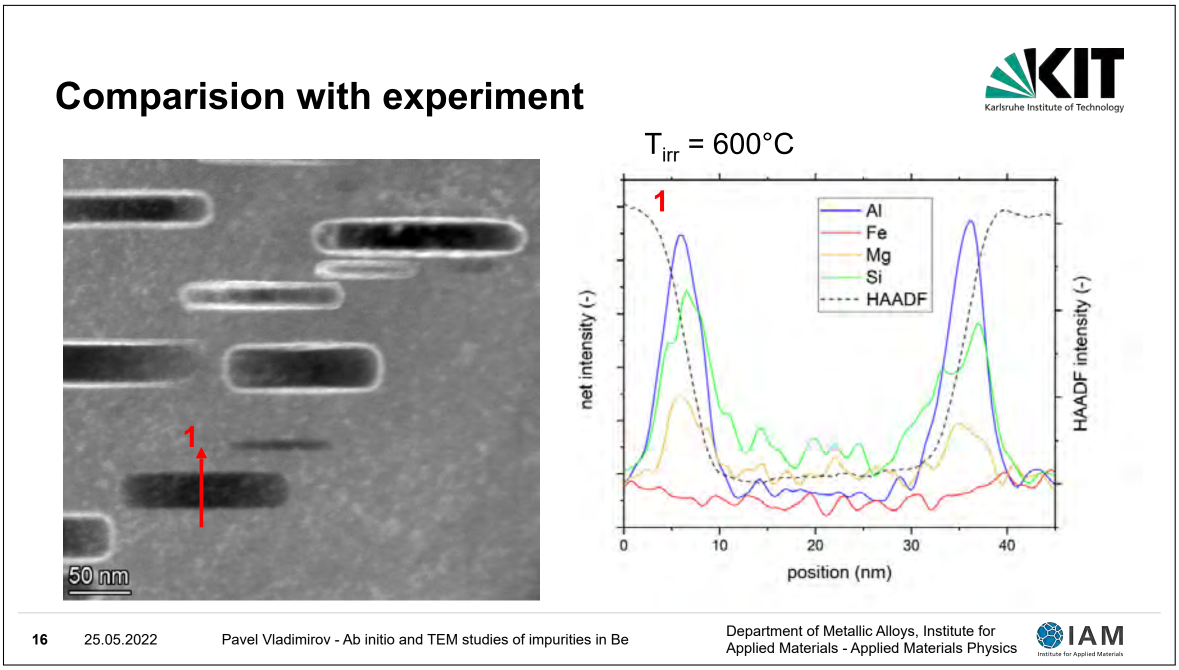
Comparision with experiment
KIT
Karlsruhe Institute of Technology
T_{irr} = 600°C
1
50 nm
1
Al
Fe
Mg
Si
HAADF
net intensity (-)
HAADF intensity (-)
0
10
20
30
40
position (nm)
16
25.05.2022
Pavel Vladimirov - Ab initio and TEM studies of impurities in Be
Department of Metallic Alloys, Institute for Applied Materials - Applied Materials Physics
IAM

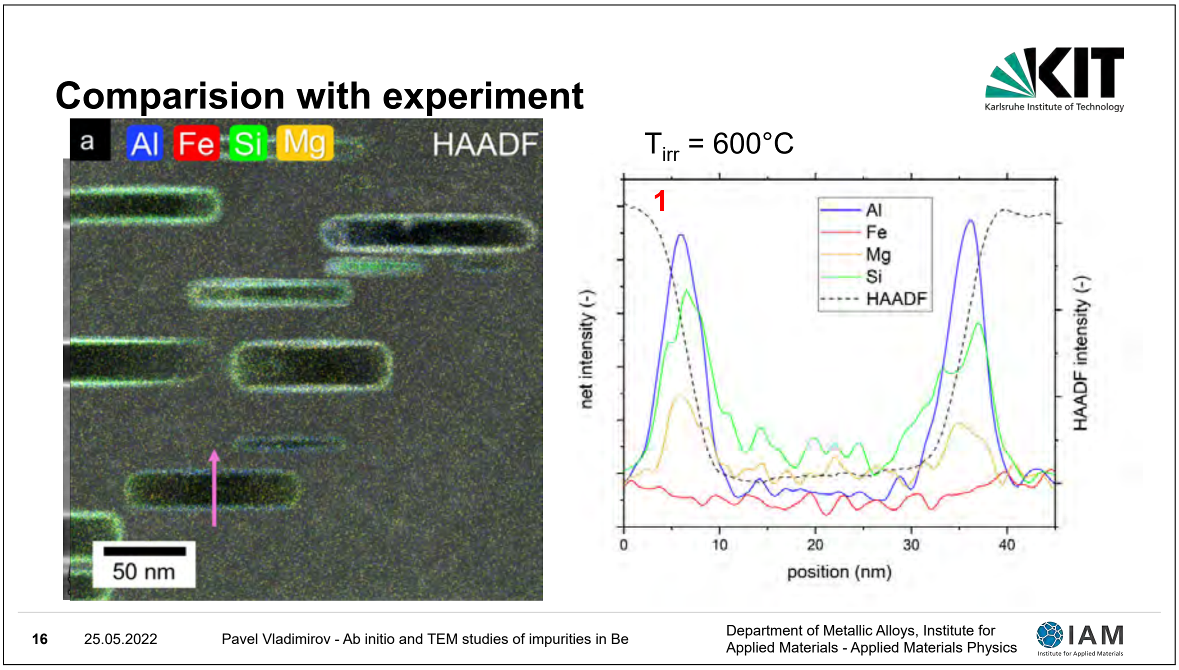
Comparision with experiment
KIT
Karlsruhe Institute of Technology
a
Al
Fe
Si
Mg
HAADF
50 nm
T_{irr} = 600°C
1
Al
Fe
Mg
Si
HAADF
net intensity (-)
HAADF intensity (-)
0
10
20
30
40
position (nm)
16
25.05.2022
Pavel Vladimirov - Ab initio and TEM studies of impurities in Be
Department of Metallic Alloys, Institute for Applied Materials - Applied Materials Physics
IAM

Comparision with experiment

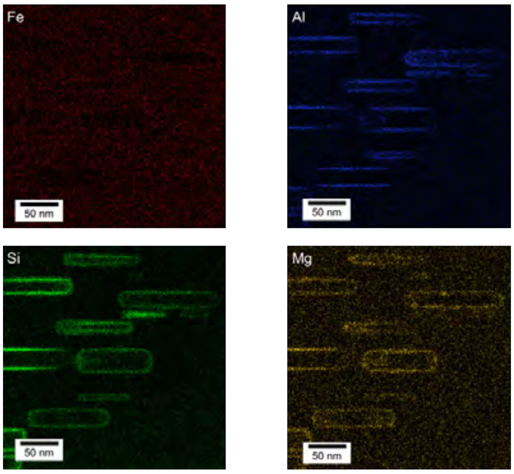

- Fe is homogeneously distributed over beryllium matrix
- Al, Si and Mg cover surfaces of helium bubbles

T_{irr} = 600°C

17 25.05.2022 Pavel Vladimirov - Ab initio and TEM studies of impurities in Be Department of Metallic Alloys, Institute for Applied Materials - Applied Materials Physics

Conclusions

- DFT caclulations suggest that
  - there is a correlation between interaction of solutes with vacancies, surfaces and self-interstitials: those which have binding with vacancies are also attracted by free surfaces and repelled by self-interstitials.
  - Mg, Al, Si have positive binding with vacancies and free surfaces
  - Cr and Fe have no binding with vacancies, also have no binding or even slightly repeled by surfaces, but have attraction to SIAs
- Consequences for diffusion mechanisms
  - Fe and Cr migrate against vacancy gradient
  - Si and Al migrate along vacancy gradient as Solute-Vac complex (e.g. to bubbles or dislocations)
- These findings were confirmed experimentally using TEM equipped with EDX:
  - formation of Mg, Al, Si enriched zones anround gas bubbles in beryllium under irradiation.
  - formation of gas bubbles on $FeAlBe_4$ precipitates as a consequence of Vac-Al complex diffusion
- Obtained results will be used to evaluate the effect of impurities on gas bubble growth, swelling and tritium retention inside helium bubbles.

18 25.05.2022 Pavel Vladimirov - Ab initio and TEM studies of impurities in Be Department of Metallic Alloys, Institute for Applied Materials - Applied Materials Physics

Ab initio study of hydrogen behavior in titanium beryllides

D.V. Bachurin[1], C. Stihl[1], P.V. Vladimirov[1]
[1]*Karlsruhe Institute of Technology, Institute for Applied Materials, Hermann-von-Helmholtz-Platz 1, 76344 Eggenstein-Leopoldshafen, Germany*

An interest in titanium beryllides as candidate materials for advanced neutron multiplier for the Helium Cooled Pebble Bed breeding blanket of European DEMO fusion reactor is related to their lower tritium retention, lower swelling and higher oxidation resistance in comparison with pure beryllium. The latter was initially suggested as neutron multiplier in the International Thermonuclear Experimental Reactor (ITER) and for the above reasons has a number of limitations compared to beryllides.

One of the most important questions is how much weaker tritium, which is formed as a result of the interaction of high-energy neutrons with the pebbles is bound in titanium beryllides in contrast to pure beryllium. Such an interaction awakes formation of helium bubbles and degradation of the material properties. One of the main promising methods for studying the behavior of hydrogen in titanium beryllides is first-principles modeling technique based on density functional theory.

The present work is devoted to *ab initio* study of hydrogen (isotope effects were neglected and hydrogen was considered instead of tritium) behavior in three titanium beryllides (Be_2Ti, $Be_{17}Ti_2$, $Be_{12}Ti$). All of them have different crystal structure and contain a different number of crystallographically non-equivalent interstitial hydrogen sites.

Both the hydrogen solution energy in defect-free lattice and binding energy with a vacancy are important characteristics in terms of tritium dissolution, retention and release. Static *ab initio* calculations demonstrate that hydrogen solution energy in all interstitial non-equivalent sites is noticeably lower as compared with pure beryllium suggesting an easier dissolution of hydrogen atoms in titanium beryllides. Computation of binding energy of single hydrogen atom with all non-equivalent monovacancies reveals that hydrogen might be trapped by a vacancy without being inside it. The obtained results sheds light on the understanding of earlier tritium release in different titanium beryllides during thermo-desorption experiments and expand our knowledge of their properties.

Corresponding Author:
Dr. Dmitry Bachurin
dmitry.bachurin@kit.edu
Hermann-von-Helmholtz-Platz 1,
76344 Eggenstein-Leopoldshafen, Germany

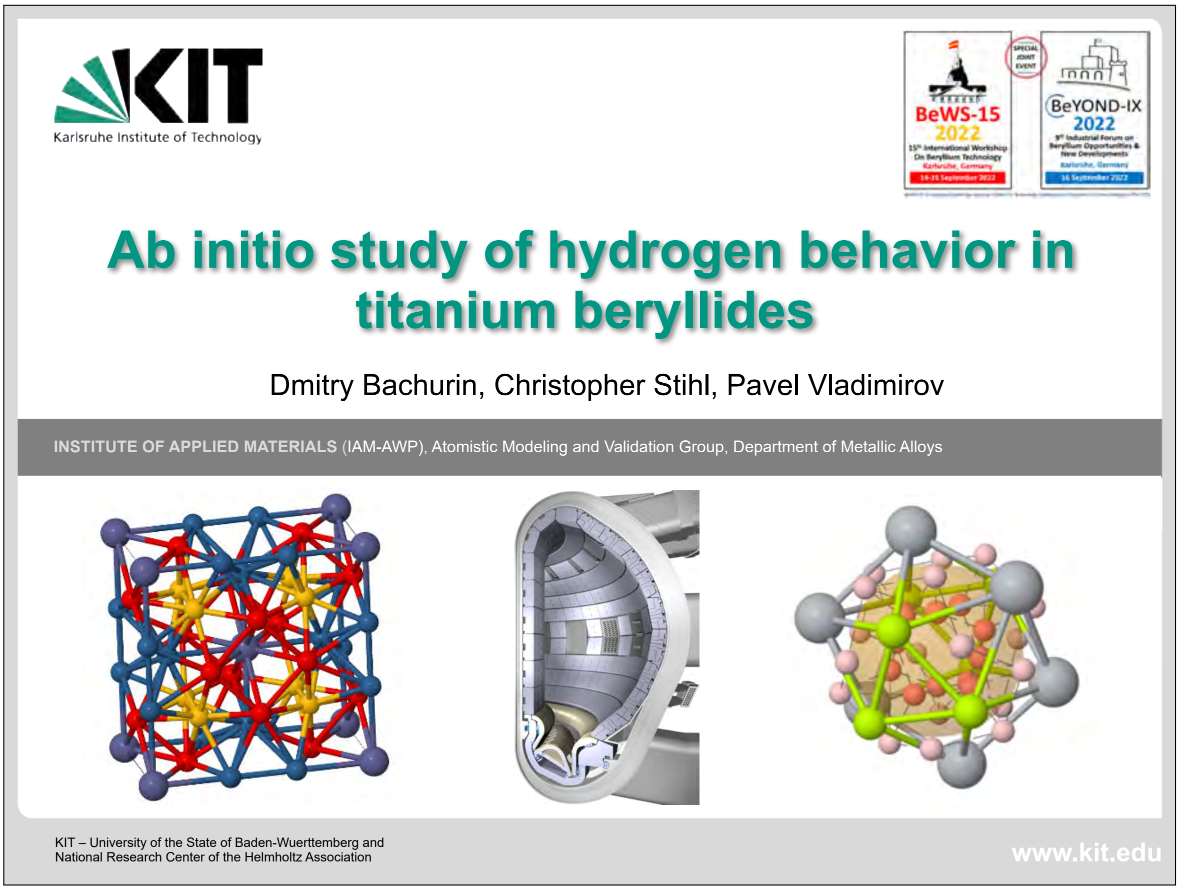
Karlsruhe Institute of Technology
BeWS-15 2022
BeYOND-IX 2022
Ab initio study of hydrogen behavior in titanium beryllides
Dmitry Bachurin, Christopher Stihl, Pavel Vladimirov
INSTITUTE OF APPLIED MATERIALS (IAM-AWP), Atomistic Modeling and Validation Group, Department of Metallic Alloys
KIT – University of the State of Baden-Wuerttemberg and National Research Center of the Helmholtz Association
www.kit.edu

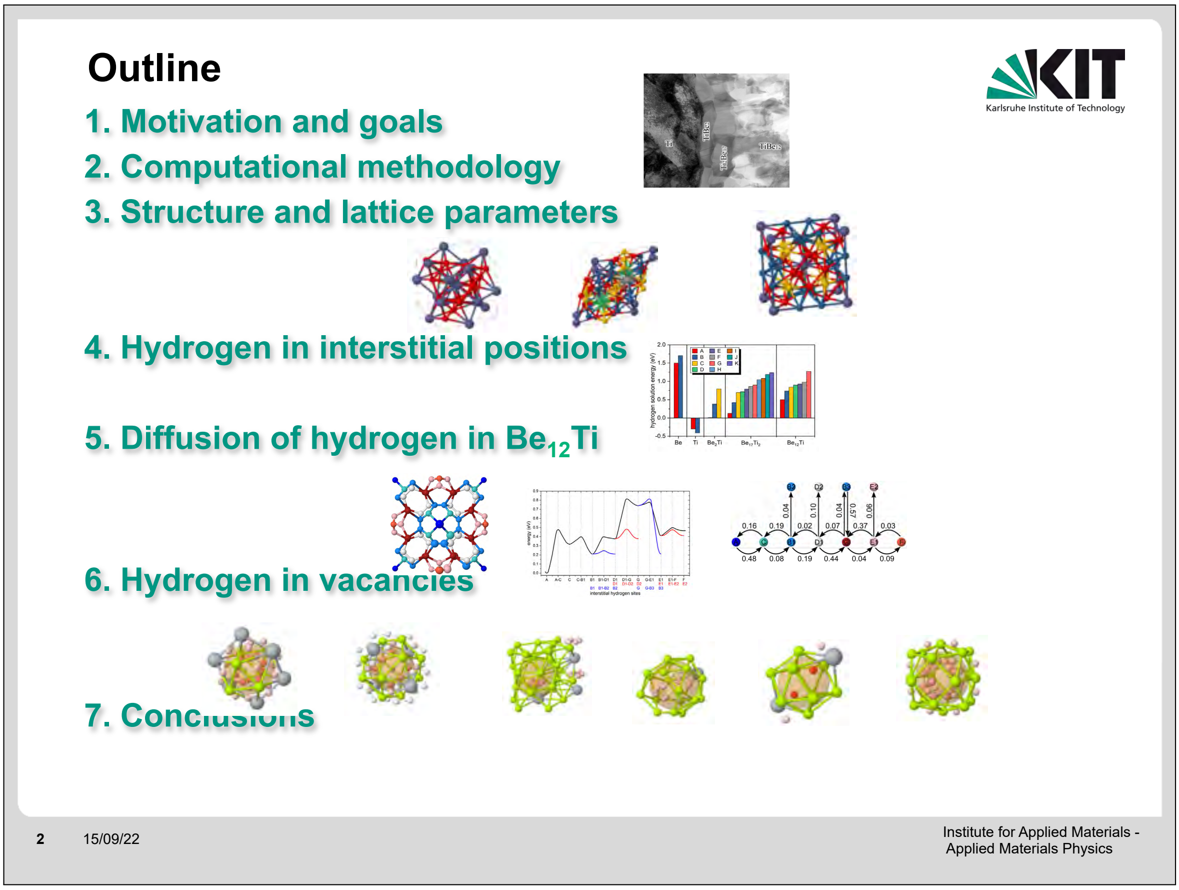
Outline
1. Motivation and goals
2. Computational methodology
3. Structure and lattice parameters
4. Hydrogen in interstitial positions
5. Diffusion of hydrogen in Be12Ti
6. Hydrogen in vacancies
7. Conclusions
Karlsruhe Institute of Technology
2
15/09/22
Institute for Applied Materials - Applied Materials Physics

Beryllium in fusion reactor

- Be is considered as plasma facing material and as effective neutron multiplier for tritium breeding blanket (HCPB)
- Hydrogen isotopes and impurities are implanted into Be first wall tiles
- He and T are produced in Be under neutron irradiation

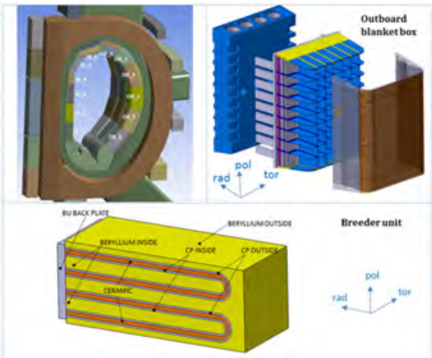

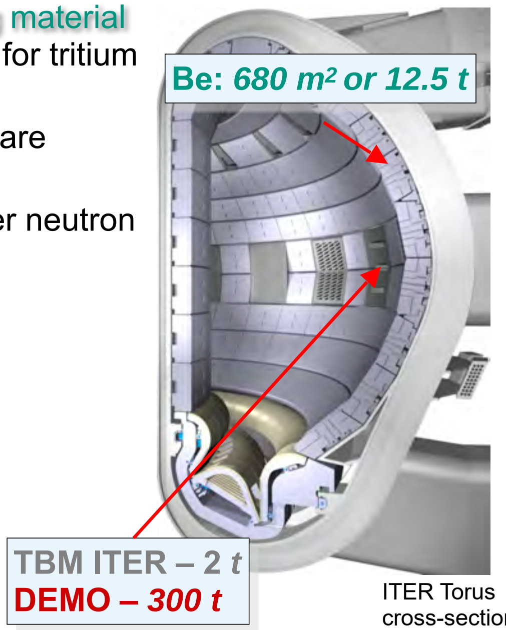

ITER Torus cross-section

K. Ioki et al. Nucl.Fusion **41**(3) 2001 265-275

3 15/09/22 Institute for Applied Materials - Applied Materials Physics

Motivation and goals

- **Motivation:** Intermetallic beryllium compounds as $Be_{12}Ti$, $Be_{12}V$ and $Be_{12}Zr$ are considered as possible candidates for fusion applications, namely as neutron multiplier for the DEMO breeder blanket to be used instead of pure beryllium.
- **Global Goal:** Elucidation of the origin of the superior properties of beryllides affecting the hydrogen release at lower temperatures by performing comparison of its properties with pure Be.
- **Goal:** elucidation of the origin of the superior properties of titanium beryllides (Be_2Ti, $Be_{17}Ti_2$, $Be_{12}Ti$) and its effect on the hydrogen isotope retention rate
- **Approach:** Ab initio methods

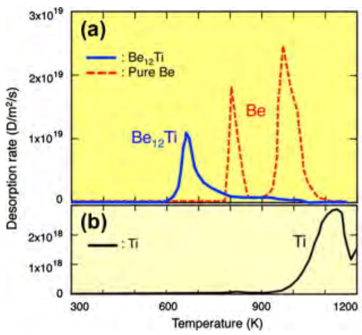

M. Nakamichi et al. JNM 442, 1-3, S465-S471 (2013)

4 15/09/22 Institute for Applied Materials - Applied Materials Physics

Why do we choose titanium beryllides?

Beryllium vs. **Titanium beryllides**

Beryllium	Titanium beryllides
❑ high neutron multiplication efficiency	❑ lower neutron multiplication efficiency
❑ lower melting point	❑ higher melting point
❑ lack of oxidation resistance	❑ higher oxidation resistance
❑ higher tritium retention	❑ lower tritium retention
❑ higher swelling	❑ lower swelling
❑ bad compatibility with the structural material	❑ good compatibility with the structural materials

5 15/09/22 Institute for Applied Materials - Applied Materials Physics

Why do we choose titanium beryllides?

Microstructure of Be-Ti composite after extrusion and hot isostatic pressing at 900°C

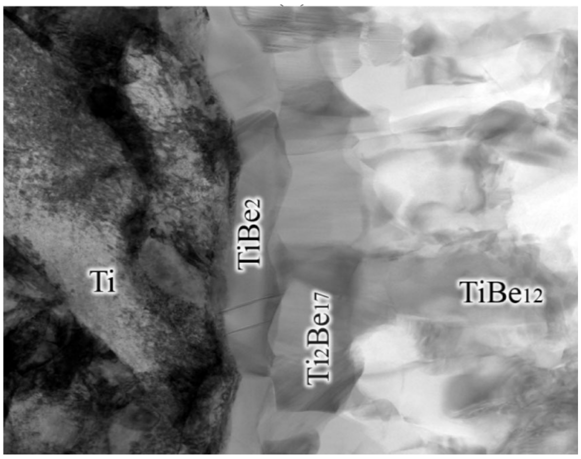

The structure along with the main phase of $Be_{12}Ti$ contains inclusions of other phases: Be_2Ti, $Be_{17}Ti_2$, pure Ti and Be

- ❑ **Be_2Ti in the form of a thin layer surrounding the pure Ti phase;**
- ❑ **$Be_{17}Ti_2$ in the form of small particles located at the prior Ti phase locations;**
- ❑ **pure Ti and Be phases, which do not dissolve completely**

R.G. Gaisin, V. Chakin, M. Duerrschnabel et al. Nucl Mater Energy 24 (2020) 100771.

6 15/09/22 Institute for Applied Materials - Applied Materials Physics

Computational methodology

KIT Karlsruhe Institute of Technology

- Static ab-initio calculations (using VASP)
- Projector augmented wave potential (PAW)
- Generalized gradient approximation (GGA)

- Fermi broadening: 0.2 eV
- Cut-off energy: 487 eV

- No volume and shape relaxation
- No restrictions on relaxation of atoms

Hydrogen solution energy

$$E_s = E_{total}^{\mathrm{Be+H}} - E_{total}^{\mathrm{Be}} - E_{ref}^{\mathrm{H}}$$

$E_{total}^{\mathrm{Be+H}}$ and E_{total}^{Be} are the total energies of the simulation cells with and without hydrogen

$E_{ref}^{\mathrm{H}} = -3.3590\ \mathrm{eV}$ is the energy of hydrogen atom in H_2 molecule

Hydrogen binding energy

$$E_b = E(H+V) - E(V) + E(H_I) - E_{bulk}$$

$E(H+V)$ and $E(V)$ are the total energies of the simulation cells with vacancy and one hydrogen atom and only with a vacancy

$E(H_I)$ is the energy of hydrogen atom in interstitial position

E_{bulk} is the energy of the bulk

7 15/09/22 Institute for Applied Materials - Applied Materials Physics

Structure and lattice parameters

KIT Karlsruhe Institute of Technology

	Be_2Ti cubic	$Be_{17}Ti_2$ hexagonal	$Be_{12}Ti$ tetragonal
	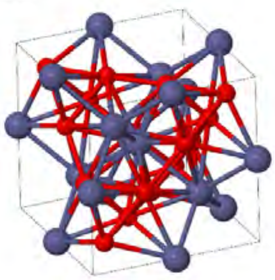	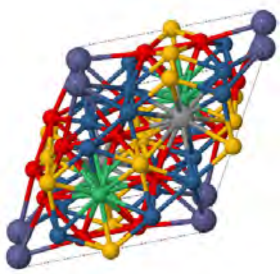	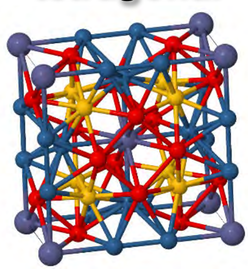
Lattice parameters	a = 4.539 Å	a = 7.333 Å c = 7.164 Å	a = 7.234 Å c = 4.151 Å
Computational cell	32 Be atoms 16 Ti atoms	34 Be atoms 4 Ti atoms	48 Be atoms 4 Ti atoms
Cryst. non-eq. atomic sites	2 (1Be+1Ti)	6 (4Be+2Ti)	4 (3Be+1Ti)

8 15/09/22 Institute for Applied Materials - Applied Materials Physics

Hydrogen in interstitial positions

KIT Karlsruhe Institute of Technology

Be
hexagonal

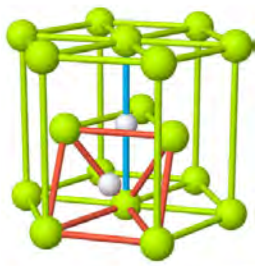

● Octahedral (O)
● Basal Tetrahedral (BT)

Hydrogen was placed in the center of all possible non-equivalent tetrahedra

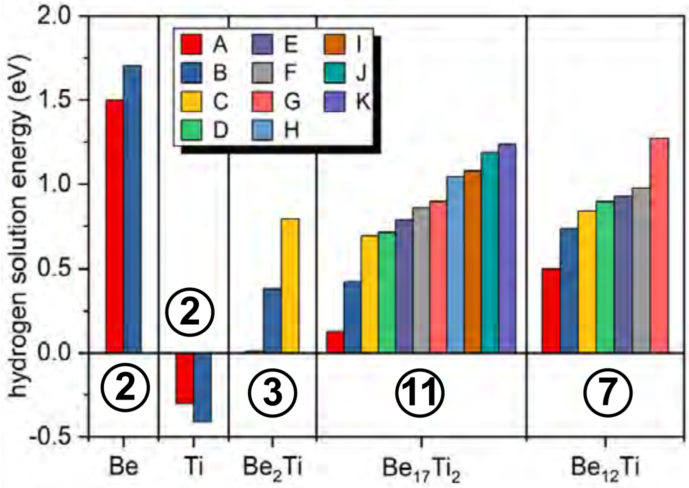

Positive solution energy (endothermic)
Negative solution energy (exothermic)

Easier dissolution of hydrogen atoms in the beryllides

9 15/09/22 Institute for Applied Materials - Applied Materials Physics

Diffusion in $Be_{12}Ti$

KIT Karlsruhe Institute of Technology

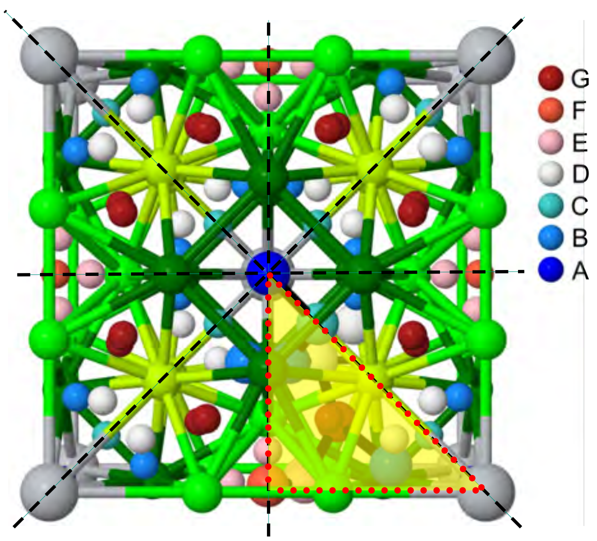

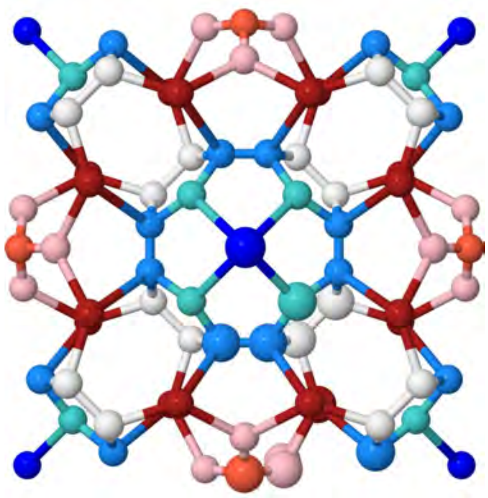

7 energetically nonequivalent hydrogen interstitial sites (A-G) within $Be_{12}Ti$ lattice

Hydrogen path through non-equivalent interstitial sites and 10 jumps between them

D.V. Bachurin, C. Stihl, P.V. Vladimirov, Comp. Mat. Sci. 187 (2021) 109921.

10 15/09/22 Institute for Applied Materials - Applied Materials Physics

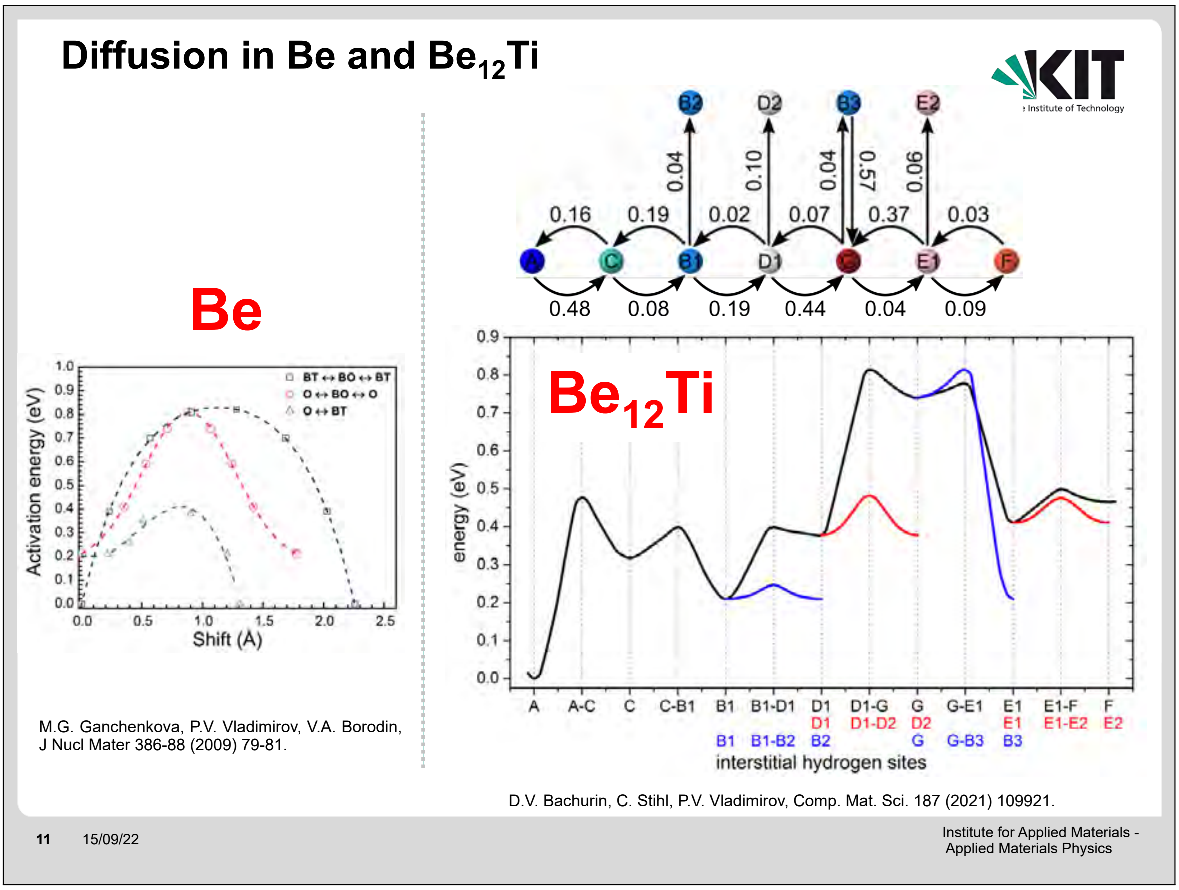
Diffusion in Be and Be12Ti
Be
Activation energy (eV)
Shift (Å)
BT ↔ BO ↔ BT
O ↔ BO ↔ O
O ↔ BT
M.G. Ganchenkova, P.V. Vladimirov, V.A. Borodin, J Nucl Mater 386-88 (2009) 79-81.
Be12Ti
energy (eV)
interstitial hydrogen sites
A A-C C C-B1 B1 B1-D1 D1 D1-G G G-E1 E1 E1-F F
D1 D1-D2 D2 E1 E1-E2 E2
B1 B1-B2 B2 G G-B3 B3
0.16 0.19 0.02 0.07 0.37 0.03
0.48 0.08 0.19 0.44 0.04 0.09
0.04 0.10 0.04 0.57 0.06
D.V. Bachurin, C. Stihl, P.V. Vladimirov, Comp. Mat. Sci. 187 (2021) 109921.
11 15/09/22
Institute for Applied Materials - Applied Materials Physics

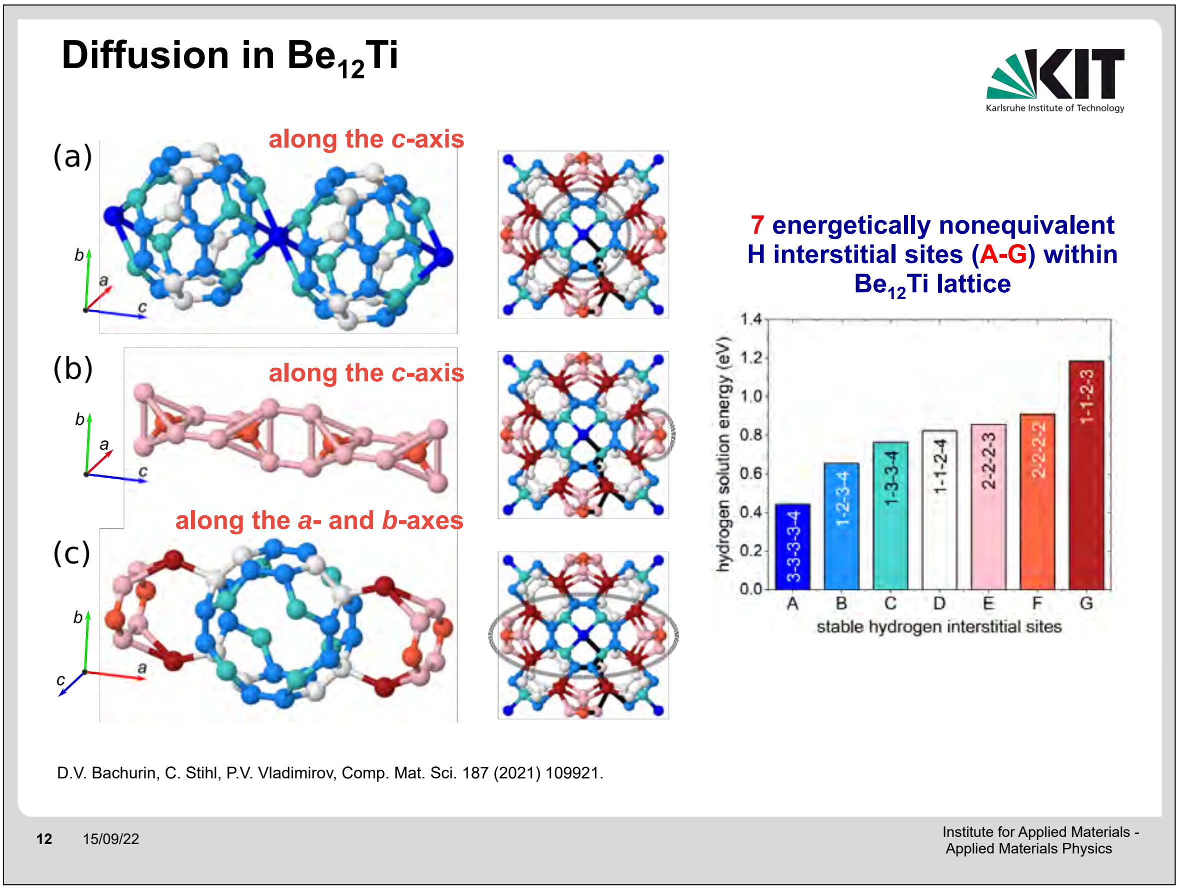
Diffusion in Be12Ti
Karlsruhe Institute of Technology
(a) along the c-axis
(b) along the c-axis
(c) along the a- and b-axes
7 energetically nonequivalent H interstitial sites (A-G) within Be12Ti lattice
hydrogen solution energy (eV)
stable hydrogen interstitial sites
3-3-3-4 1-2-3-4 1-3-3-4 1-1-2-4 2-2-2-3 2-2-2-2 1-1-2-3
D.V. Bachurin, C. Stihl, P.V. Vladimirov, Comp. Mat. Sci. 187 (2021) 109921.
12 15/09/22
Institute for Applied Materials - Applied Materials Physics

Vacancy formation energy

Karlsruhe Institute of Technology

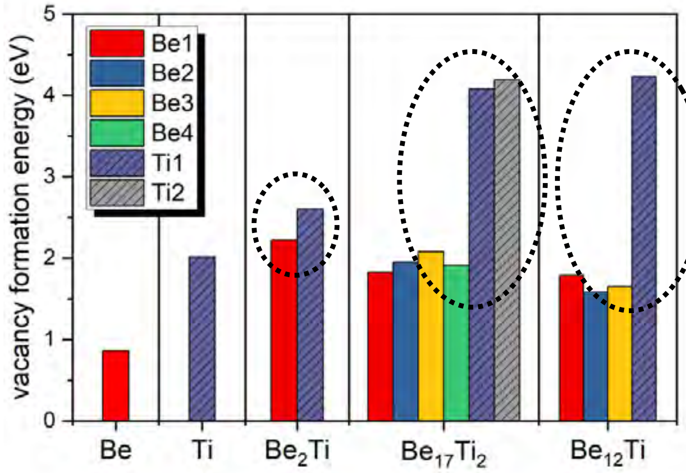

$$E_f^V = E_{n-1}^V - E_n + E_{coh}^{Be,Ti}$$

E_{n-1}^V and E_n are the total energies of the simulation cells with and without vacancy

E_{coh}^{Be} = -3.7660 eV

E_{coh}^{Ti} = -7.7627 eV

- The formation energies of Be vacancies in $Be_{12}Ti$ and $Be_{17}Ti_2$ are circa two times less then those of Ti vacancies (except for Be_2Ti)

13 15/09/22 Institute for Applied Materials - Applied Materials Physics

Vacancy formation energy

Karlsruhe Institute of Technology

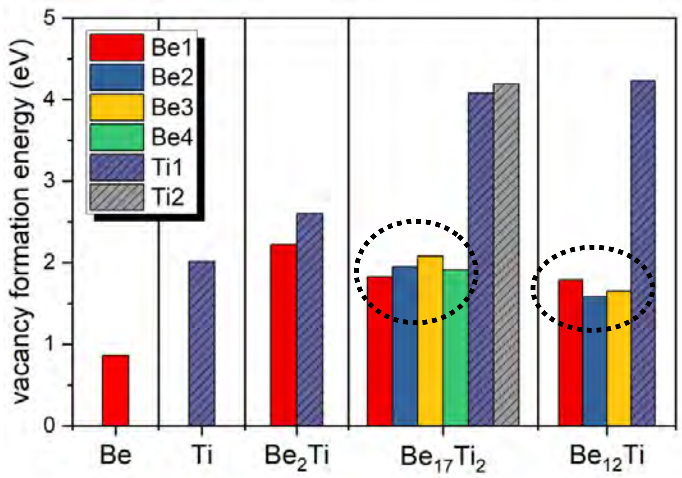

$$E_f^V = E_{n-1}^V - E_n + E_{coh}^{Be,Ti}$$

E_{n-1}^V and E_n are the total energies of the simulation cells with and without vacancy

E_{coh}^{Be} = -3.7660 eV

E_{coh}^{Ti} = -7.7627 eV

- The formation energies of Be vacancies in $Be_{12}Ti$ and $Be_{17}Ti_2$ are circa two times less than those of Ti vacancies (except for Be_2Ti)
- The formation energies of Be vacancies in $Be_{12}Ti$ and $Be_{17}Ti_2$ are very close to each other

14 15/09/22 Institute for Applied Materials - Applied Materials Physics

Binding energy of hydrogen atom in vacancy

KIT Karlsruhe Institute of Technology

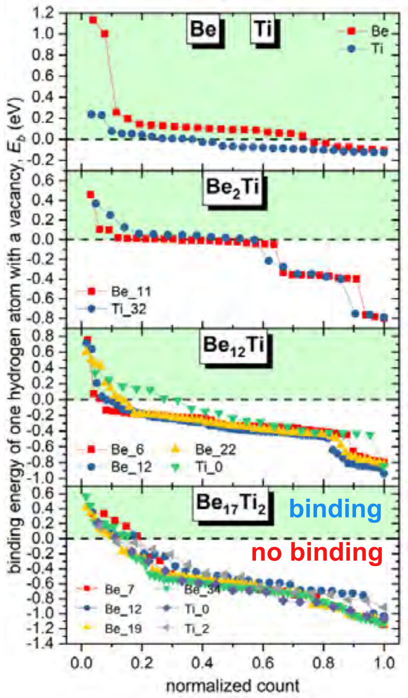

- Binding energy of H atom in Ti vacancy is circa 0.9 eV lower than that in Be
- (Be_2Ti) Binding energies of H atom with Be and Ti vacancies are 0.36 and 0.46eV, respectively
- ($Be_{12}Ti$) Binding energies of H atom with Be vacancies are 0.76, 0.71 and 0.60eV, with Ti vacancy is 0.34eV
- ($Be_{17}Ti_2$) Binding energies of H atom with Be vacancies are 0.34, 0.36, 0.41 and 0.56eV, with Ti vacancies are 0.21 and 0.16eV
- Binding energy of H atom with Be vacancy is always higher than with Ti vacancy

15 15/09/22 Institute for Applied Materials - Applied Materials Physics

Binding energy of hydrogen atom in vacancy

KIT Karlsruhe Institute of Technology

Be

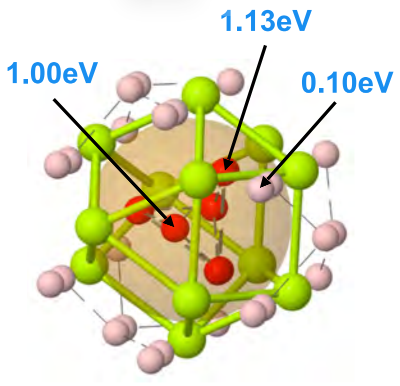

Be vacancy

Ti

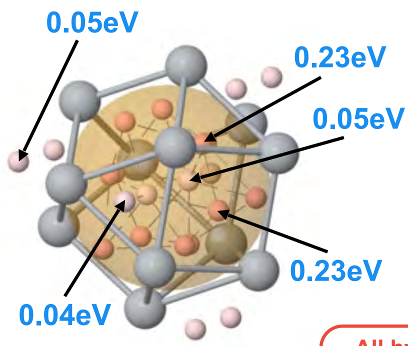

Ti vacancy

All hydrogen atoms with negative binding energy were made invisible

Binding energy of H atom with Be vacancy is significantly higher than that in Ti

Some hydrogen atoms located outside a vacancy are trapped by it

16 15/09/22 Institute for Applied Materials - Applied Materials Physics

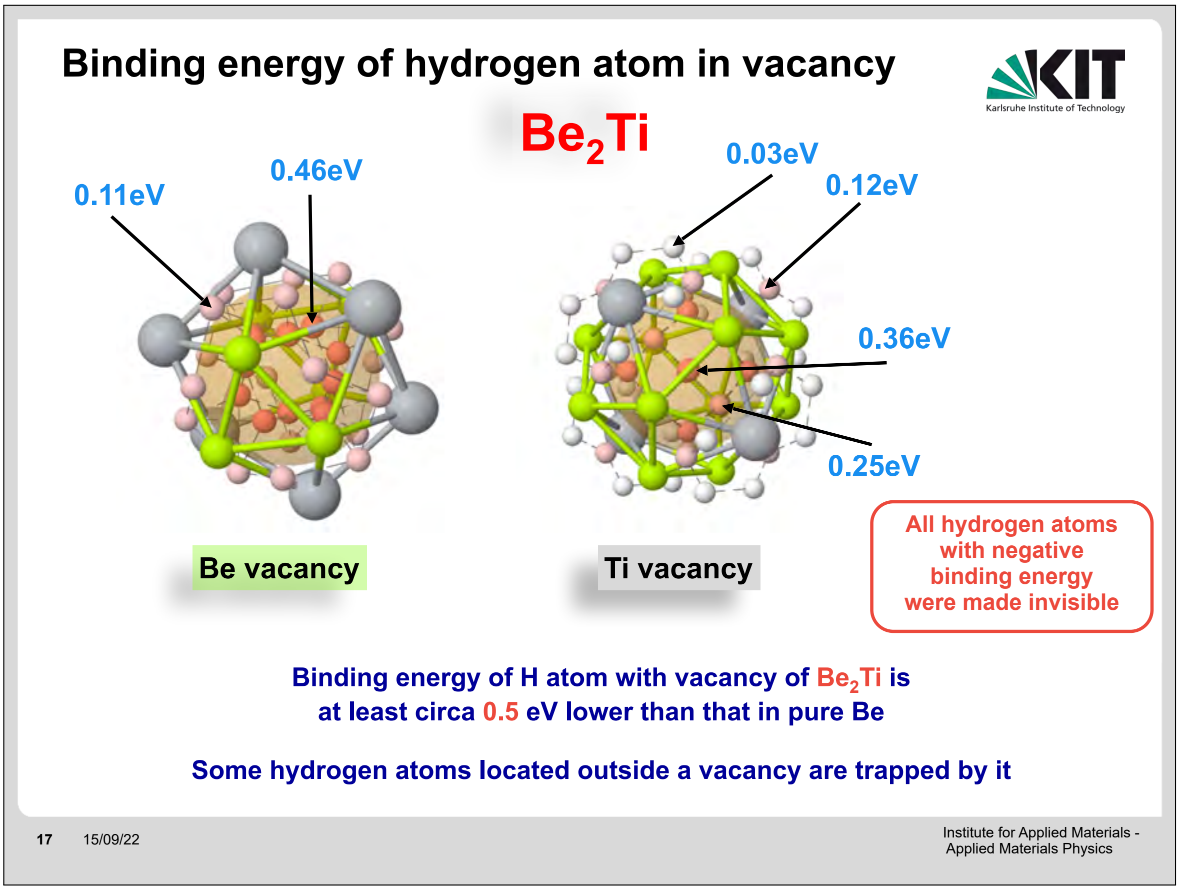
Binding energy of hydrogen atom in vacancy
KIT
Karlsruhe Institute of Technology
Be_2Ti
0.11eV
0.46eV
0.03eV
0.12eV
0.36eV
0.25eV
Be vacancy
Ti vacancy
All hydrogen atoms with negative binding energy were made invisible
Binding energy of H atom with vacancy of Be_2Ti is at least circa 0.5 eV lower than that in pure Be
Some hydrogen atoms located outside a vacancy are trapped by it
17 15/09/22
Institute for Applied Materials - Applied Materials Physics

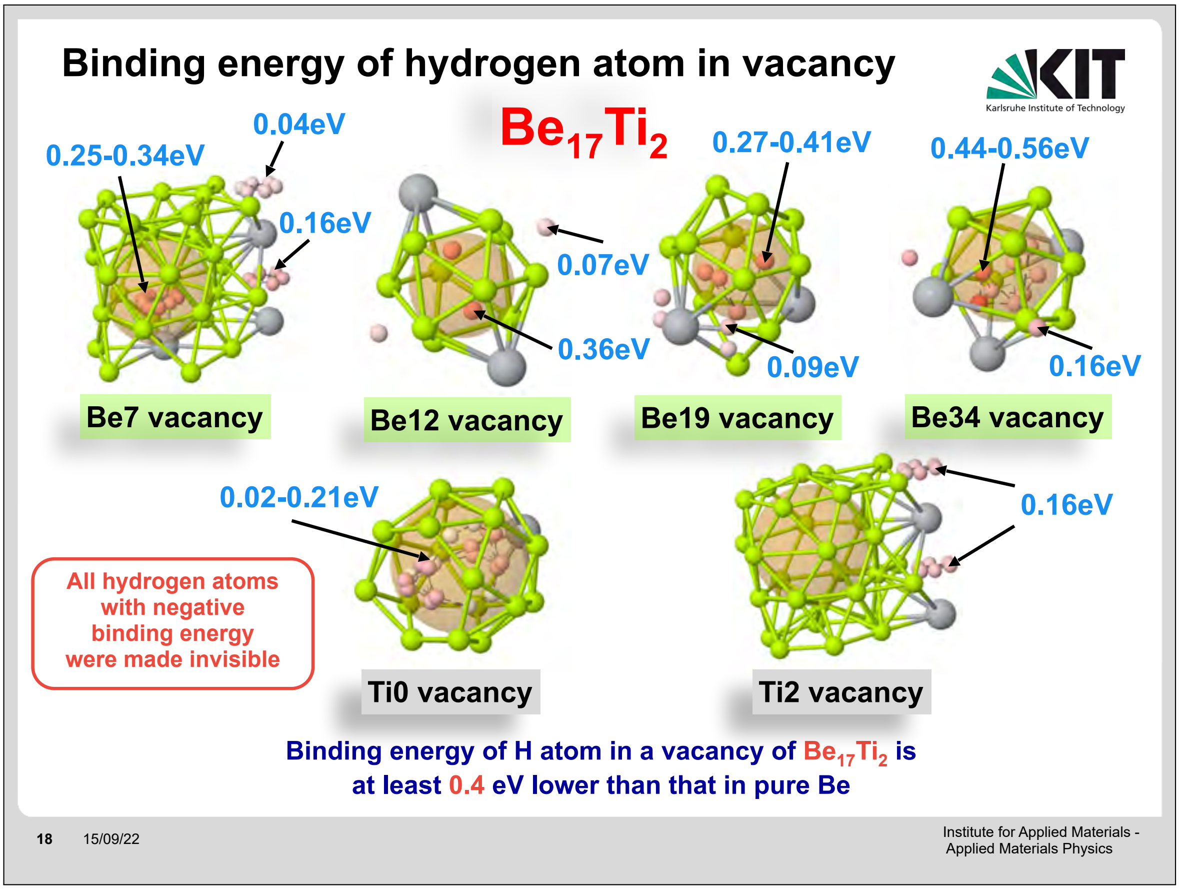
Binding energy of hydrogen atom in vacancy
KIT
Karlsruhe Institute of Technology
$Be_{17}Ti_2$
0.25-0.34eV
0.04eV
0.16eV
0.07eV
0.36eV
0.27-0.41eV
0.09eV
0.44-0.56eV
0.16eV
Be7 vacancy
Be12 vacancy
Be19 vacancy
Be34 vacancy
0.02-0.21eV
0.16eV
All hydrogen atoms with negative binding energy were made invisible
Ti0 vacancy
Ti2 vacancy
Binding energy of H atom in a vacancy of $Be_{17}Ti_2$ is at least 0.4 eV lower than that in pure Be
18 15/09/22
Institute for Applied Materials - Applied Materials Physics

Binding energy of hydrogen atom in vacancy

KIT Karlsruhe Institute of Technology

$Be_{12}Ti$

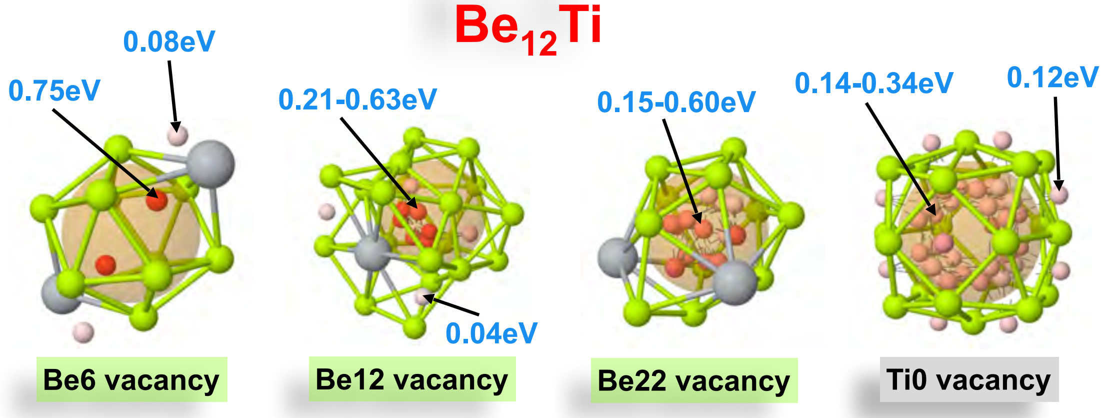

Binding energy of H atom in a vacancy of $Be_{12}Ti$ is at least 0.4 eV lower than that in pure Be

Binding energy of H atom inside the vacancies of titanium beryllides is always lower then outside them and is in the range of 0.04-0.16 eV

19 15/09/22 Institute for Applied Materials - Applied Materials Physics

Conclusions

KIT Karlsruhe Institute of Technology

- Hydrogen solution energy in interstitial positions of titanium beryllides are at least 0.2-0.7 eV lower then that for Be suggesting easier dissolution of hydrogen atoms in the studied beryllides.
- In titanium beryllides hydrogen atoms prefer to occupy the interstitial sites near Ti.
- Formation energy of Be vacancies is circa two times less than the corresponding energy for Ti vacancies in $Be_{12}Ti$ and $Be_{17}Ti_2$. In Be_2Ti the formation energies of Be and Ti vacancies does not differ much from each other.
- Some hydrogen atoms might be trapped by a vacancy without being inside it.
- Hydrogen binding with a monovacancy is 0.4-0.5 eV lower in the studied titanium beryllides, suggesting easier release of hydrogen from beryllides as compared to pure Be.
- The latter conclusion is consistent with the experimental data on deuterium release from Be and $Be_{12}Ti$ after deuterium implantation.

20 15/09/22 Institute for Applied Materials - Applied Materials Physics

Nanoscale characterization of beryllide materials

M. Duerrschnabel[1], R. Gaisin[1], P. Valdimirov[1], M. Rieth[1]

[1] *Institute of Applied Materials- Applied Material Physics, Herrmann-von-Helmholtz-Platz 1, 76344 Eggenstein-Leopoldshafen*

The most recent version of the Helium Cooled Pebble Bed (HCPB) foreseen for the European DEMO blanket considers solid blocks of titanium beryllide as neutron multiplicator material. The advantage of beryllide materials over pure beryllium is their higher operating temperature, higher corrosion resistance, lower swelling, and retention of tritium under neutron irradiation. Understanding the micro- and nanostructure especially after neutron irradiation is of crucial importance for the qualification process of the material.

The focus of this work will lie on the transmission electron microscopy (TEM) characterization of a titanium beryllide/beryllium composite material irradiated at two different temperatures during the HIDOBE neutron irradiation campaign. In particular, the structure and chemistry of the nanosized cavities in the pure beryllium region and the beryllide region was analyzed and is compared to each other. Apart from the cavities, structural defects were observed in the beryllide region that are not known from irradiated pure beryllium.

The presented results can be used for understanding and quantifying for example tritium retention in beryllide materials and to further optimize the material synthesis and the breeding blanked design in general.

Corresponding Author:

Dr. Michael Duerrschnabel
michael.duerrschnabel@kit.edu

Institute of Applied Materials
Applied Material Physics
Herrmann-von-Helmholtz-Platz 1
76344 Eggenstein-Leopoldshafen


Karlsruhe Institute of Technology
EUROfusion
Nanoscale characterization of beryllide materials
M. Duerrschnabel, R. Gaisin, P. Vladimirov, M. Rieth
Institute of Applied Materials- Applied Material Physics, Herrmann-von-Helmholtz-Platz 1, 76344 Eggenstein-Leopoldshafen
KIT – The Research University in the Helmholtz Association
www.kit.edu

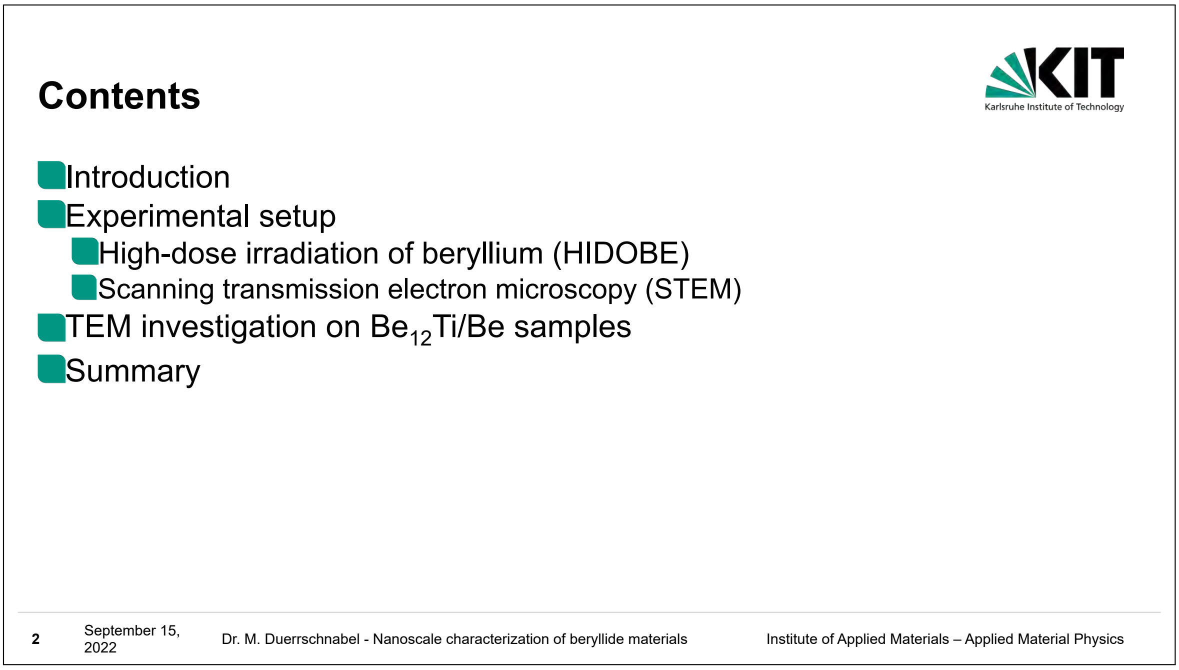
Contents
Karlsruhe Institute of Technology
Introduction
Experimental setup
High-dose irradiation of beryllium (HIDOBE)
Scanning transmission electron microscopy (STEM)
TEM investigation on $Be_{12}Ti$/Be samples
Summary
2
September 15, 2022
Dr. M. Duerrschnabel - Nanoscale characterization of beryllide materials
Institute of Applied Materials – Applied Material Physics

Introduction

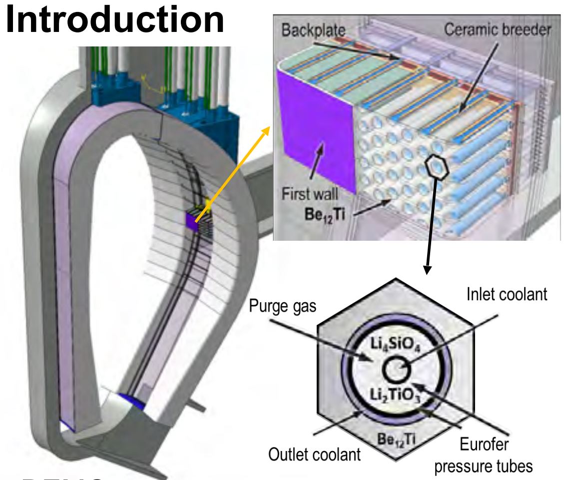

DEMO sector

- Beryllide materials foreseen as an effective *neutron multiplier materials* in future fusion reactors.
- Questions needed to be answered:
  - Understanding the evolving beryllide *microstructure under neutron irradiation*.
  - Understanding of atomic scale mechanisms of *tritium trapping* and release is necessary for assessment of radioactive inventory.

tritium breeding

Neutron losses require a neutron multiplicator

[1] F.A. Hernández et al., Fusion Science and Technology 75 (2019) 352–364

3 September 15, 2022 Dr. M. Duerrschnabel - Nanoscale characterization of beryllide materials Institute of Applied Materials – Applied Material Physics

High-dose irradiation of beryllium (HIDOBE)

HIDOBE-01 and HIDOBE-02 irradiation campaigns.

	HIDOBE-01	HIDOBE-02
Fluence ($E_n > 0.1$ MeV, $\times 10^{26}$ n/m^2)	1.5	3
Fluence ($E_n > 1$ MeV, $\times 10^{26}$ n/m^2)	0.7	1.4
Helium production in Be (appm)	3000	6000
Tritium production in Be (appm)	250	700
Neutron damage in Be (dpa)	17.9	35.8
Helium production in $Be_{12}Ti$ (appm)	2740	5480
Tritium production in $Be_{12}Ti$ (appm)	235	562
Neutron damage in $Be_{12}Ti$ (dpa)	19.5	38.9
Irradiation target temperature (°C)	425, 525, 650, 750	425, 525, 650, 750

Fedorov et al. - Post irradiation characterization of beryllium and beryllides after high temperature irradiation up to 3000 appm helium production in HIDOBE-01, Fusion Engineering and Design **102** (2016), pp. 74–80.

- STEM analyses on two Be/ $Be_{12}Ti$ samples will be presented:
  - T_{irr} = 664°C
  - T_{irr} = 768°C

4 September 15, 2022 Dr. M. Duerrschnabel - Nanoscale characterization of beryllide materials Institute of Applied Materials – Applied Material Physics

Electron microscopy: Methods & Machines

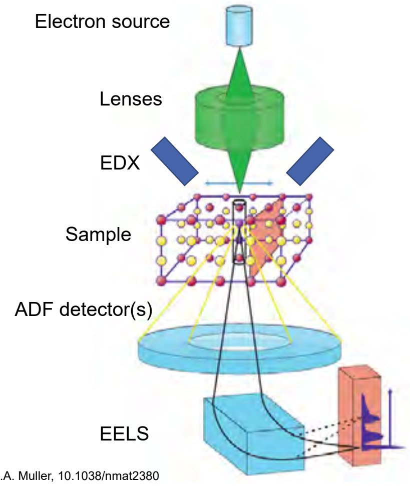

D.A. Muller, 10.1038/nmat2380

- A high-brightness electron source produces a **100-300 keV** electron beam with an energy spread of **0.3-1 eV**.
- Round magnetic lenses focus the beam to a spot size of between **0.05 and 1 nm**, which is scanned across an electron-transparent sample.
- **Signals** from scattered electrons and ionized atoms (**simultaneously**) recorded as the beam is scanned across the sample.
- **Chemical and bonding information** can be obtained by measuring the energy lost by transmitted electrons (e.g., by EELS).

5 15.09.2022 Dr. M. Duerrschnabel - Nanoscale characterization of beryllide materials Institute of Applied Materials – Applied Material Physics

Electron microscopy: Methods & Machines

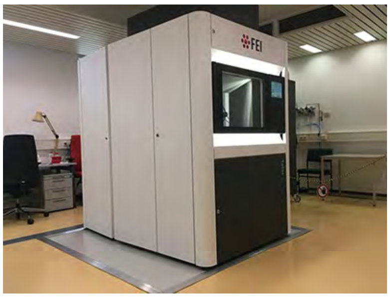

https://www.thermofisher.com/de/de/home/electron-microscopy/products/transmission-electron-microscopes/talos-f200x-tem.html#specifications

- Thermofisher Talos F200X
- Acceleration voltage up to **200 kV**
- High brightness XFEG: 1.8×10^9 A /cm^2 srad (@200kV)
- Super-X EDS system: **4 windowless SDD detectors** in a symmetric design; energy resolution ≤136 eV for Mn-K$_\alpha$ and 10 kcps (output)
- Gatan Enfinium EEL spectrometer capable of acquiring up to **1000 spectra/s**; energy resolution up to **0.7 eV**
- TEM information limit: 1.2 Å (@ 200 kV)
- STEM point resolution: **1.6 Å** (@ 200 kV)

6 15.09.2022 Dr. M. Duerrschnabel - Nanoscale characterization of beryllide materials Institute of Applied Materials – Applied Material Physics

Results of $Be_{12}Ti$ sample irradiated at 664°C

TEM $Be_{12}Ti$ T_{irr} = 664°C

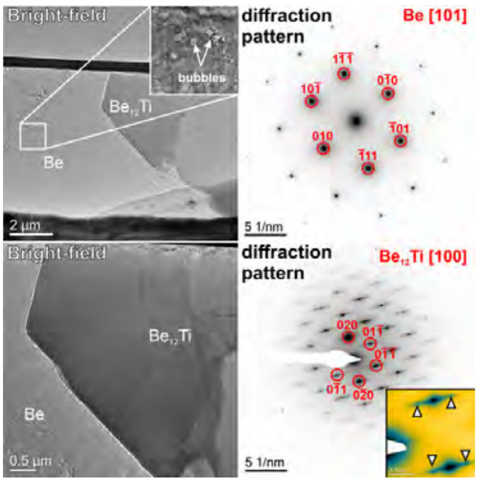

- Bright-field imaging of the Be region shows bubbles.
- Selected area diffraction shows that Be is single crystalline.
- Contrast in the bright-field image of $Be_{12}Ti$ looks homogeneous. Are there bubbles?
- SAED of $Be_{12}Ti$ shows streaking in c-axis direction → stacking faults?

$Be_{12}Ti$ T_{irr} = 664°C bubble sizes

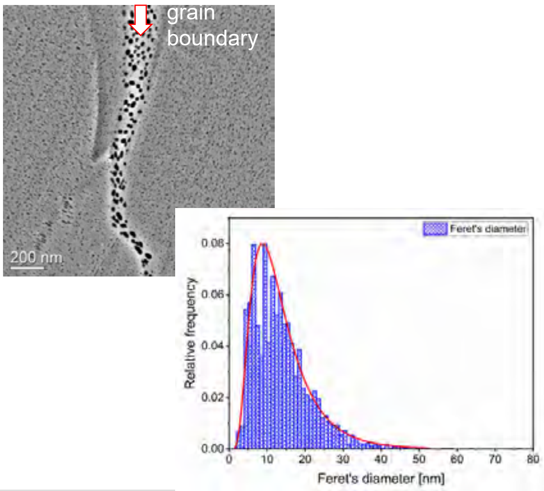

- Bubbles in $Be_{12}Ti$ are log normally distributed and have an average size of about 14 nm.
- The bubble number density can be estimated using STEM-EELS (t ≈ 250 nm) → 6.86 10^{21} m^{-3}

$Be_{12}Ti$ T_{irr} = 664°C STEM imaging

$Be_{12}Ti$ [100] zone-axis orientation

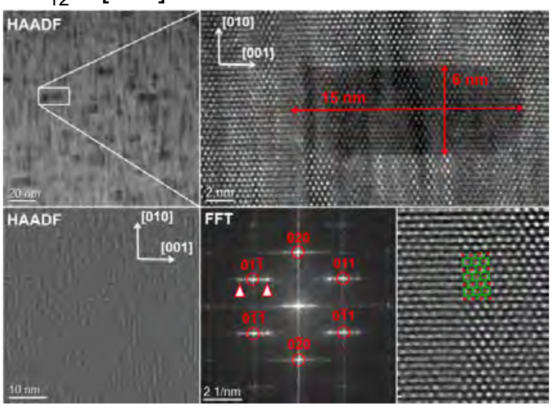

- Bubbles have a rounded cuboid shape with the round surface along [001] (not clear yet, APT?).
- Bubble surfaces are atomically sharp.
- Wavy contrast is due to distorted lattice along $Be_{12}Ti$ c-axis → result of neutron irradiation?
- Streaking in FFT result of (partial) shift of Ti atoms along $Be_{12}Ti$ c-axis.

$Be_{12}Ti$ T_{irr} = 664°C STEM imaging

Karlsruhe Institute of Technology

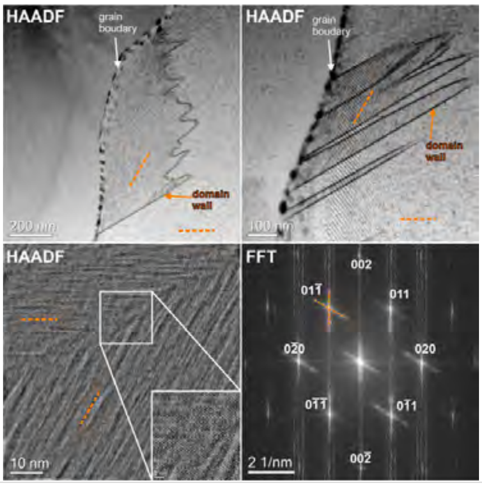

- Presence of domain-like regions at $Be_{12}Ti$ GB having different disorder inclination.
- „Domains“ are separated by a ~5 nm thick domain wall.
- Stacked 30-40 nm sized bubbles at GB.
- “Domain walls” are regions of undisturbed $Be_{12}Ti$ lattice.

11 September 15, 2022 Dr. M. Duerrschnabel - Nanoscale characterization of beryllide materials Institute of Applied Materials – Applied Material Physics

$Be_{12}Ti$ T_{irr} = 664°C STEM-EELS

Karlsruhe Institute of Technology

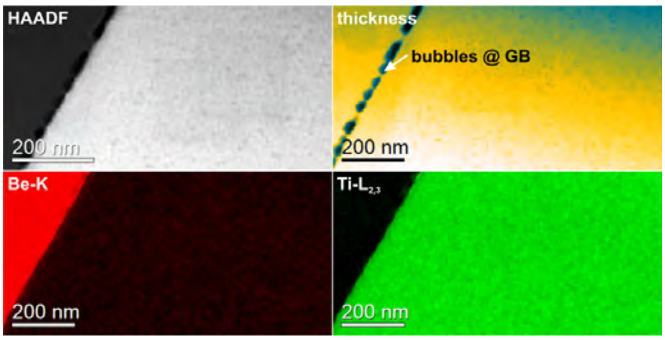

- Homogeneous element distribution.
- STEM-EELS quantification reveals phase composition of $Be_{12}Ti$:
  - Be: 93.8 ± 0.33 at% (nominal: 92.3 at%)
  - Ti: 6.2 ± 0.33 at% (nominal: 7.7 at%)

12 September 15, 2022 Dr. M. Duerrschnabel - Nanoscale characterization of beryllide materials Institute of Applied Materials – Applied Material Physics

Results of $Be_{12}Ti$ sample irradiated at 768°C

TEM $Be_{12}Ti$ T_{irr} = 768°C

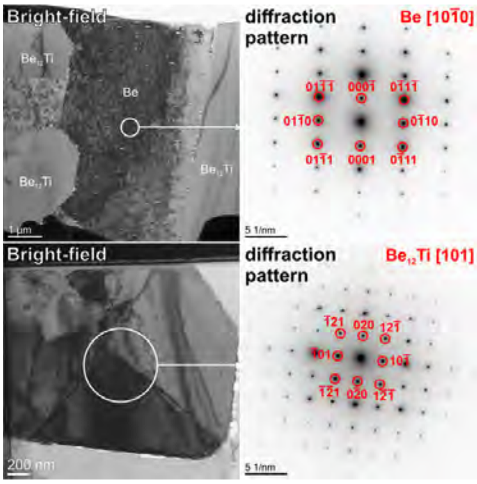

- Be and $Be_{12}Ti$ are both crystalline at T_{irr} = 768°C.
- Be/$Be_{12}Ti$ interfaces are faceted.
- No visible bubbles in $Be_{12}Ti$ at this magnification.
- Large bubbles in Be region and at the Be side of the Be/$Be_{12}Ti$ interface.

STEM-EELS $Be_{12}Ti$ T_{irr} = 768°C

Karlsruhe Institute of Technology

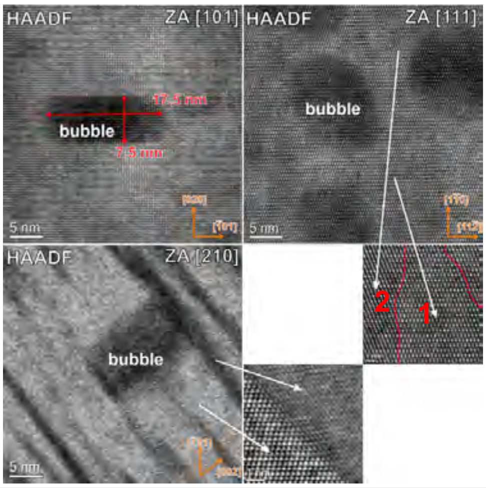

- Bubbles in [101] zone-axis (ZA) orientation have atomically sharp interfaces at (020).
- Bubble sizes comparable to T_{irr} = 668°C sample.
- No visible atomic disturbance in [101] ZA orientation.
- Disturbed areas of 2-5 nm in height perpendicular to c-axis in [210] ZA visible.
- In [111] ZA two regions observed.
  - Region 1: Normal [111]-type HAADF contrast
  - In region 2 Ti atoms are shifted into the center of the (1-10) planes

15 September 15, 2022 Dr. M. Duerrschnabel - Nanoscale characterization of beryllide materials Institute of Applied Materials – Applied Material Physics

STEM-EDX $Be_{12}Ti$ T_{irr} = 768°C

Karlsruhe Institute of Technology

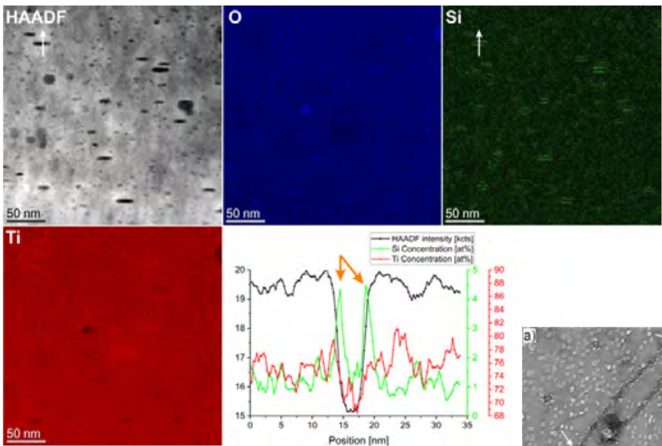

- Bubble edges in $Be_{12}Ti$ covered with a 1.5 nm thin Si layer.
- $Be_{12}Ti$ less prone to oxidation compared to pure Be (→ open bubbles).
- No other foreign elements (Fe, U…) found as in pure Be.

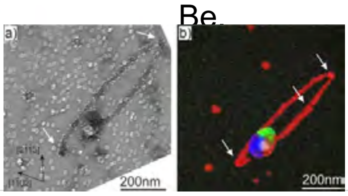

Pure Be: Various phases in EDX map (**b**) are colored as follows: Al-Fe-Be (red), Mg-Si (blue), Cr-Ti (green) and U-Fe (white).

Klimenkov et al. - New insights into microstructure of irradiated beryllium based on experiments and computer simulations, Sci. Rep. **10** (2020), 8042.

16 September 15, 2022 Dr. M. Duerrschnabel - Nanoscale characterization of beryllide materials Institute of Applied Materials – Applied Material Physics

STEM-EELS $Be_{12}Ti$ T_{irr} = 768°C

Reminder: bubble contents in pure Be:

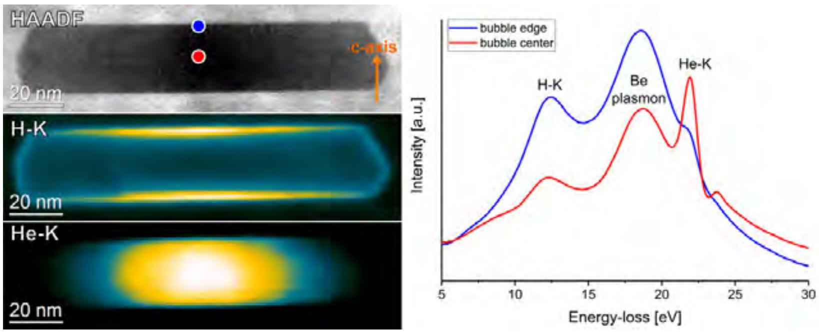

- ^3H is preferentially located on bubble c-axis surfaces
- He is in the bubble center.

Further reading:
1) Klimenkov et al. - First simultaneous detection of helium and tritium inside bubbles in beryllium, Micron **127** (2019), 102754.
2) Klimenkov et al. - New insights into microstructure of irradiated beryllium based on experiments and computer simulations, Sci. Rep. **10** (2020), 8042.
3) Zimber et al. - Investigation of a high-dose irradiated beryllium microstructure, JNUCMAT **540** (2020), 152374.
4) Zimber & Vladimirov - The role of grain boundaries and denuded zones for tritium retention in high-dose neutron irradiated beryllium, JNUCMAT **568** (2022), 153855.

17 September 15, 2022 Dr. M. Duerrschnabel - Nanoscale characterization of beryllide materials Institute of Applied Materials – Applied Material Physics

STEM-EELS $Be_{12}Ti$ T_{irr} = 768°C

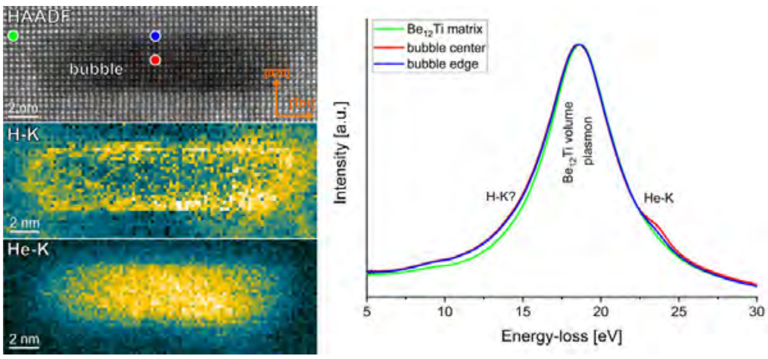

- ^3H is preferentially located on bubble surfaces.
- He is in the bubble center.
- Situation in $Be_{12}Ti$ less clear than in pure Be due to experimental limitations.

18 September 15, 2022 Dr. M. Duerrschnabel - Nanoscale characterization of beryllide materials Institute of Applied Materials – Applied Material Physics

Summary

KIT Karlsruhe Institute of Technology

- A thorough TEM investigation of $Be_{12}Ti$ neutron irradiated at 2 different temperatures was carried out.
- Bubbles generated by neutron irradiation are roughly 10x smaller in $Be_{12}Ti$ than in pure Be.
- Extended structural defects (domain-like regions) observed in $Be_{12}Ti$ besides bubbles for both irradiation temperatures
- In both materials – Be and $Be_{12}Ti$ – ^3H is located at bubble surfaces and He is in the bubble center. In case of $Be_{12}Ti$ monochromated, C_S-corrected (S)TEM experiments can yield better datasets.
- STEM-EDX shows the presence of 1.5 nm thin Si layers on bubble surfaces.
- STEM-EELS quantification reveals phase composition of $Be_{12}Ti$ close to the nominal values.

19 September 15, 2022 Dr. M. Duerrschnabel - Nanoscale characterization of beryllide materials Institute of Applied Materials – Applied Material Physics

KIT Karlsruhe Institute of Technology

Thank you for your attention!

20 15.09.2022 Dr. M. Duerrschnabel - Nanoscale characterization of beryllide materials Institute of Applied Materials – Applied Material Physics

SESSION 6

Mechanical properties & irradiation damage

Mechanical compression behaviors and microstructure change under He ion irradiation of single phase Be and binary $Be_{12}Ti$ pebbles

Pingping Liu[1,*], Qian Zhan[1], Wen Hu[1], Yumei Jia[1], Farong Wan[1]

[1] *School of Materials Science and Engineering, University of Science and Technology Beijing, Beijing 100083, China*

The world urgently needs a carbon-free, safe, clean and limitless energy source. Fusion energy has the potential to meet this need. International thermonuclear fusion experimental reactor (ITER) and future commercial power demonstration reactor (DEMO) were designed and developed by scientists around the world. However, one key problem of “tritium fuel self-sustaining” needs to be solved firstly. Thus, tritium breeding blanket module (TBM) was developed. Beryllium (Be) pebbles with a diameter of 1 mm are planned to be used as a neutron multiplier in the helium-cooled ceramic breeder (HCCB) test TBM of ITER, which is also the primary option of the Chinese TBM program. Meanwhile, beryllium intermetallic compounds (beryllides) such as $Be_{12}Ti$ are the most promising advanced neutron multipliers in advanced DEMO fusion reactors because of high melting point and high stability at high temperatures.

In this study, in the prospect of establishing a database of advanced neutron multipliers for fusion reactor, the preparation, mechanical properties test and irradiation damage of Be and beryllides pebbles were carried out. The process of producing pure Be and Be-Ti alloy pebbles can be roughly divided into two stages: fabrication of Be and beryllide electrode rods and granulation of Be and beryllide pebbles. The Be-Ti beryllides synthesized by hot isostatic pressing (HIP) with a pressure of 230 MPa at 1073 K for 2 h. The Be and $Be_{12}Ti$ granulation process by rotating electrode process (REP). Then, surface analysis, mechanical compression and irradiation were performed to evaluate surface microstructure, mechanical properties and irradiation resistance.

Be pebbles with diameter of 1 mm and $Be_{12}Ti$ pebbles with diameter of 0.7 mm were successfully fabricated by combining HIP and REP methods. According to the XRD results, the phase composition of the Be pebbles was identified as Be with little BeO. The phase composition of the as-granulated Be-7.7 at.%Ti pebbles was identified as $Be_{12}Ti$ with little Be and BeO. The AFM and SEM results revealed that Be and $Be_{12}Ti$ pebble were well shaped with small surface fluctuates. During mechanical compression tests, Be pebbles exhibited very good ductility (no fracture at 50% deformation), which is better than that of $Be_{12}Ti$ pebbles. Rupture of $Be_{12}Ti$ pebbles occurred at the deformation beyond 10%. After high dose helium ion irradiation, the surface blistering and internal damage structure were examined and analysed by SEM and TEM, which may provide experimental basis for good understanding of irradiation damage mechanism and design optimization of advanced neutron multipliers for the fusion reactor.

Corresponding Author:
Dr. Pingping Liu
ppliu@ustb.edu.cn
University of Science and Technology Beijing,
No. 30 Xueyuan Road,
Haidian District, Beijing

Fabrication and surface irradiation damage of advanced neutron multiplier for fusion blankets

Pingping Liu, Qian Zhan, Farong Wan

School of Materials Science and Engineering, University of Science and Technology Beijing, China

2022.09.15

Outline

- **Background: Fusion T-self & Neutron multiplier**
- **Fabrication of Be, $Be_{12}Ti$ and $Be_{12}W$ pebble**
- **Mechanical compression of neutron multiplier beryllium and beryllide pebble**
- **Surface irr. damage of Be, $Be_{12}Ti$ and $Be_{12}W$ pebble**
- **Summary**

Background

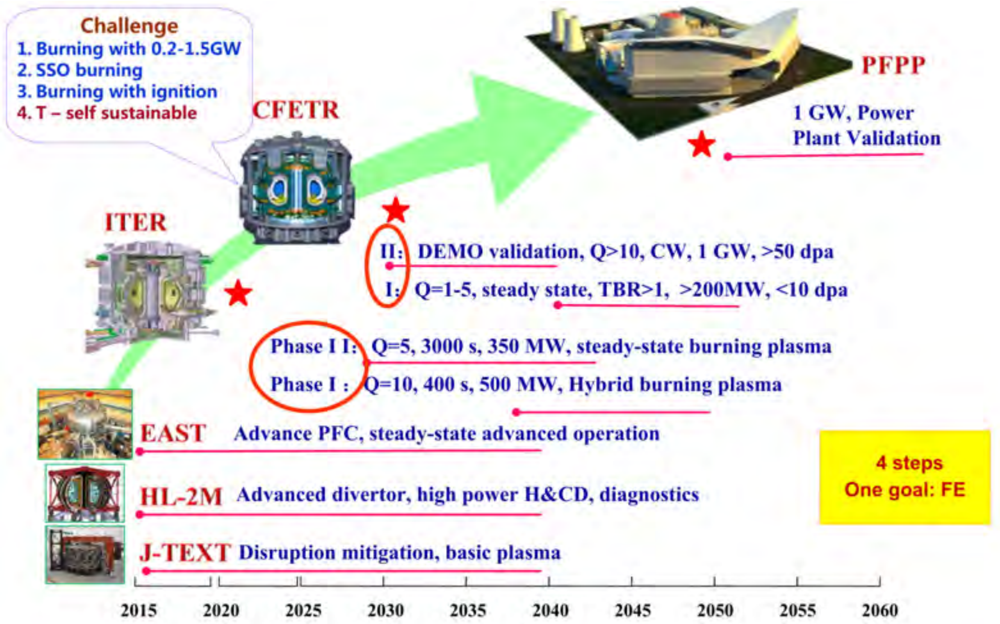

*Part of the schematic diagram from Y.X. Wan., 2020.

Background

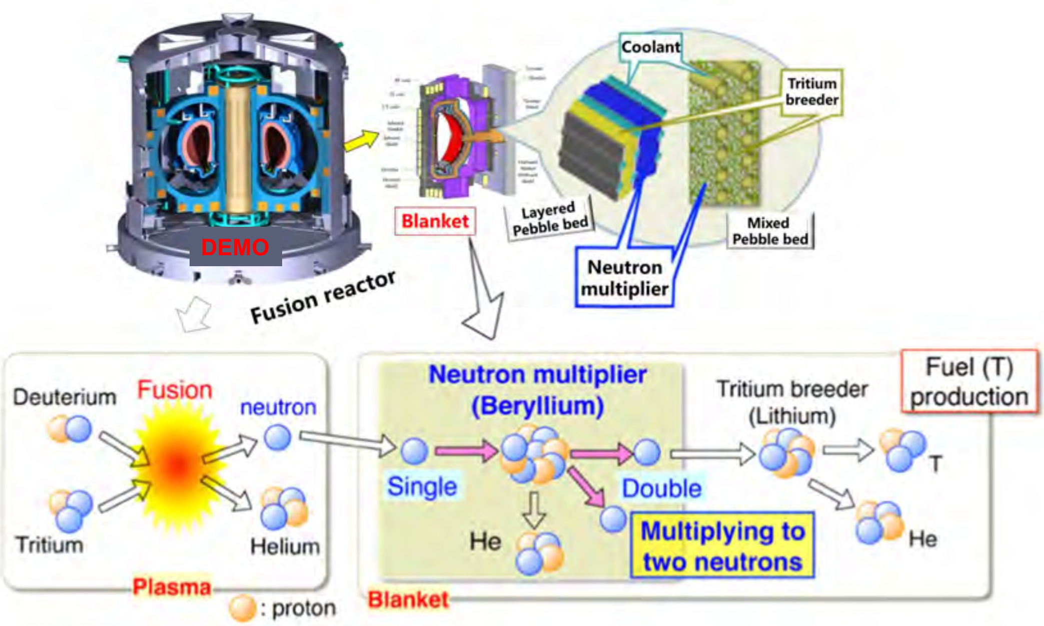

*Part of the schematic diagram from M. Nakamichi, J. Kim, M.M. Nakamura et al., Beryllium and its Alloys as Neutron Multiplying Materials, 2020.

Background

Some parameters of Blanket of different fusion reactor

Items	ITER	CFETR	DEMO Reactor
Temperature (.)	150~350	<650	600~900
He (appm)	~3000	~10 000	~20 000
Irr. damage (dpa)	10	~30	50
Be pebbles	√	?	×

Neutron Multiplier of DEMO

--High beryllium content

--Low activation

--High melting point

Materials	Be	$Be_{12}Ti$	$Be_{12}W$
Melting point	1280 ℃	~1550 ℃	~1750 ℃
Be content(at.)	100%	92.3%	92.3%

Background

Initial Motivation:

1、Fabrication of high-melting-point neutron multiplier pebbles.

2、Evaluation of irradiation resistance of the pebbles.

D-T fusion produces an extremely energetic (14.1-MeV) neutron, which is potentially useful for breeding more tritium but also creates challenges for the materials (**Irradiation damage**).

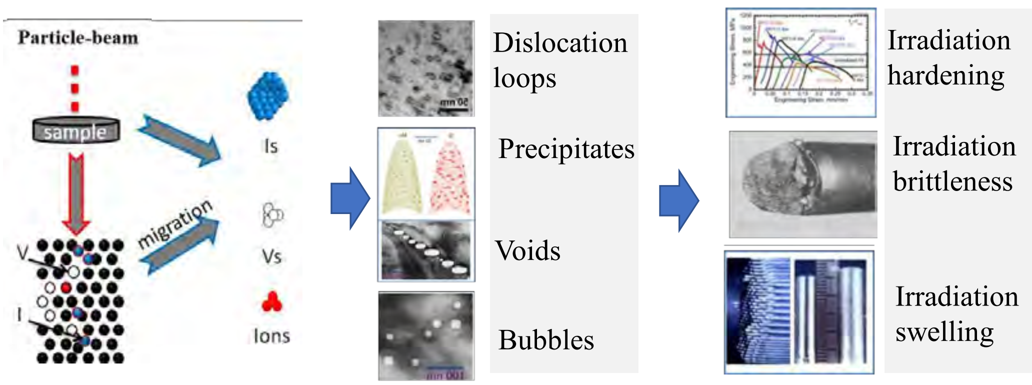

Outline

- Background: Fusion T-self & Neutron multiplier
- **Fabrication of Be, $Be_{12}Ti$ and $Be_{12}W$ pebble**
- Mechanical compression of neutron multiplier beryllium and beryllide pebble
- Surface irradiation damage of Be and $Be_{12}Ti/W$ pebble
- Summary

Fabrication of neutron multiplier pebbles

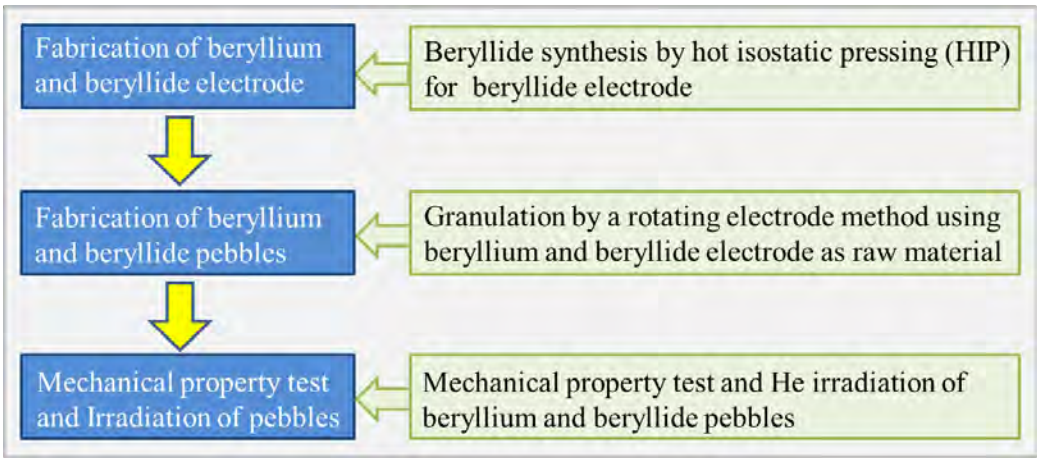

Flowchart for the fabrication of neutron multiplier.

Fabrication of neutron multiplier pebbles

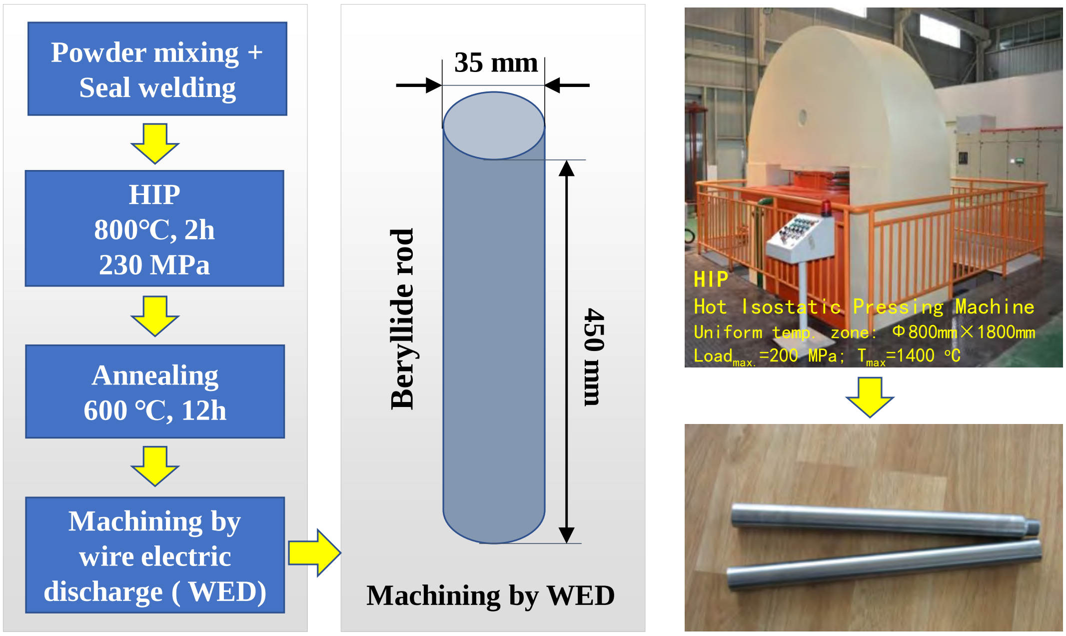

Fabrication scheme of the beryllium rode by hot isostatic pressing.

Fabrication of neutron multiplier pebbles

Rotating electrode process:

(1) Rotating of beryllium electrode
(2) Discharge between beryllium and W electrode
(3) Solidification to spherical particles

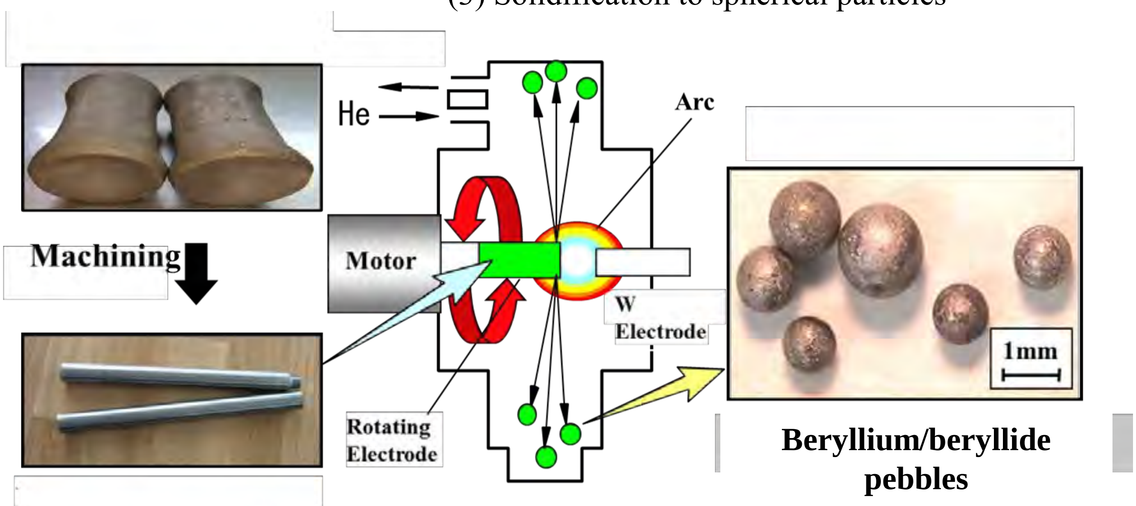

Rotation electrode process (REP)

*Part of the schematic diagram from K. Tsuchiya (JAEA), 2005.

Fabrication of neutron multiplier pebbles

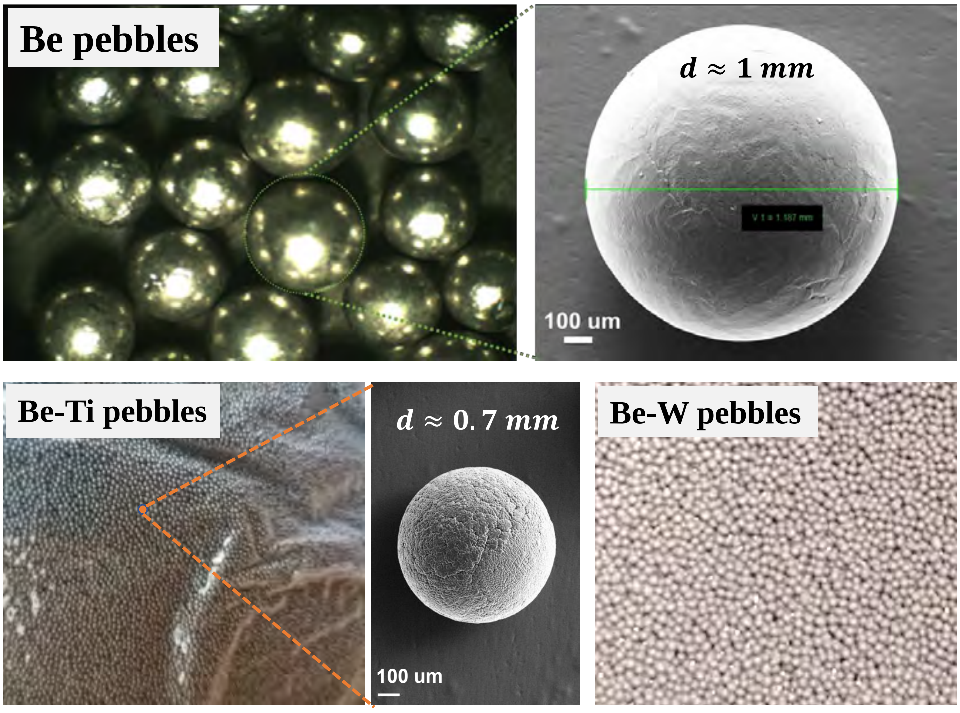

Fabrication of neutron multiplier pebbles

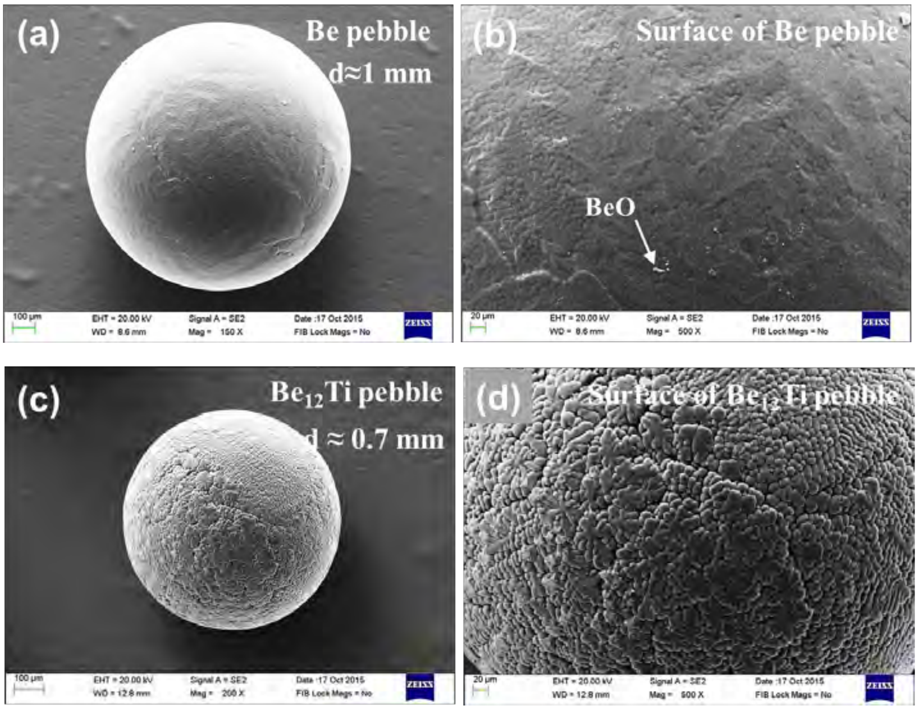

Surface microstructure of Be and BeTi pebble produced by REP.

Fabrication of neutron multiplier pebbles

Table 1. Chemical compositions of the Be, BeTi and BeW pebbles (wt.%).

Samples	Al	Fe	Mg	O	W	Ti	Be
Be pebble	0.02	0.088	<0.001	0.986	——	——	98.1
BeTi pebble	0.06	0.19	<0.010	0.081	——	28.27	71.27
BeW pebble	0.18	0.25	<0.039	0.721	62.3	——	36.51

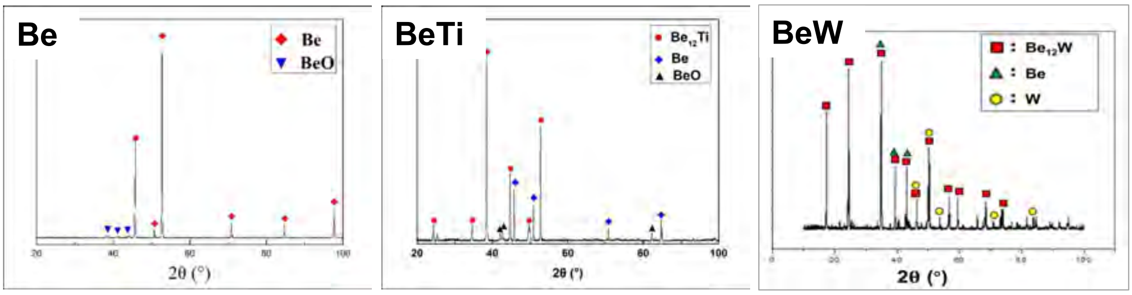

X-ray diffraction spectrum of the Be, BeTi and BeW pebbles.

Be, $Be_{12}Ti$ and $Be_{12}W$ pebbles were fabricated.

P.P. Liu, et al., Fusion Engineering and Design 144 (2019) 202-208

Outline

- Background: Fusion T-self & Neutron multiplier
- Fabrication of Be, $Be_{12}Ti$ and $Be_{12}W$ pebble
- **Mechanical compression of neutron multiplier beryllium and beryllide pebble**
- Surface irradiation damage of Be and $Be_{12}Ti/W$ pebble
- Summary

Compression of Be and $Be_{12}Ti$ pebbles

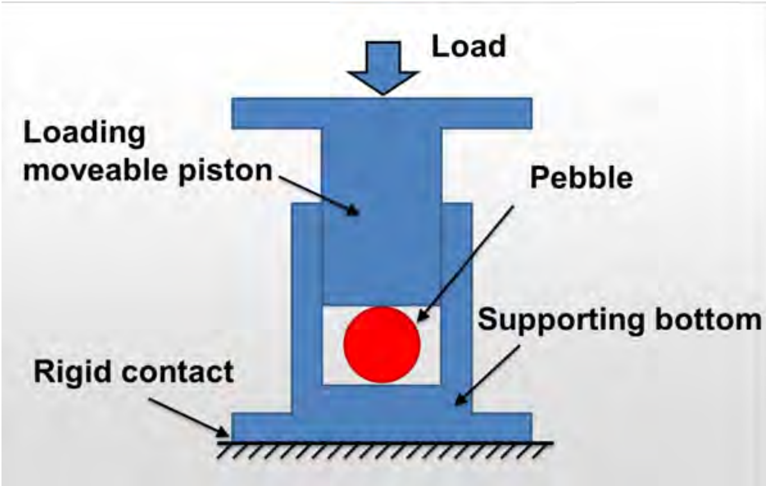

The scheme of loading of a pebble (Be or BeTi) during the compression test.

Compression of Be and $Be_{12}Ti$ pebbles

(0.05 mm, 45 N), (0.1 mm, 88 N), (0.5 mm, 316 N)

(0.035 mm, 76 N) , (0.07 mm, 174 N)

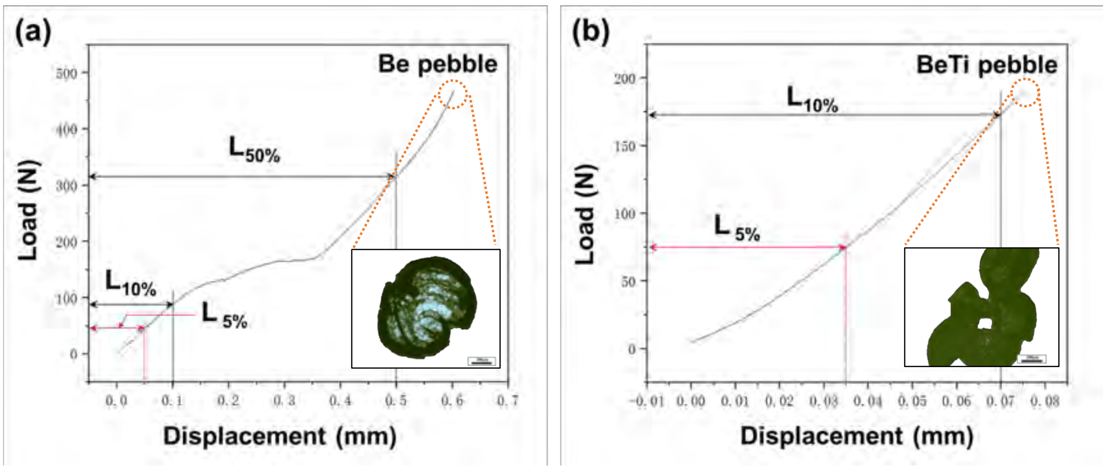

Load curves in compression tests of Be (a) and BeTi (b) pebbles with load speed of 0.2 mm/min.

Compression of Be and $Be_{12}Ti$ pebbles

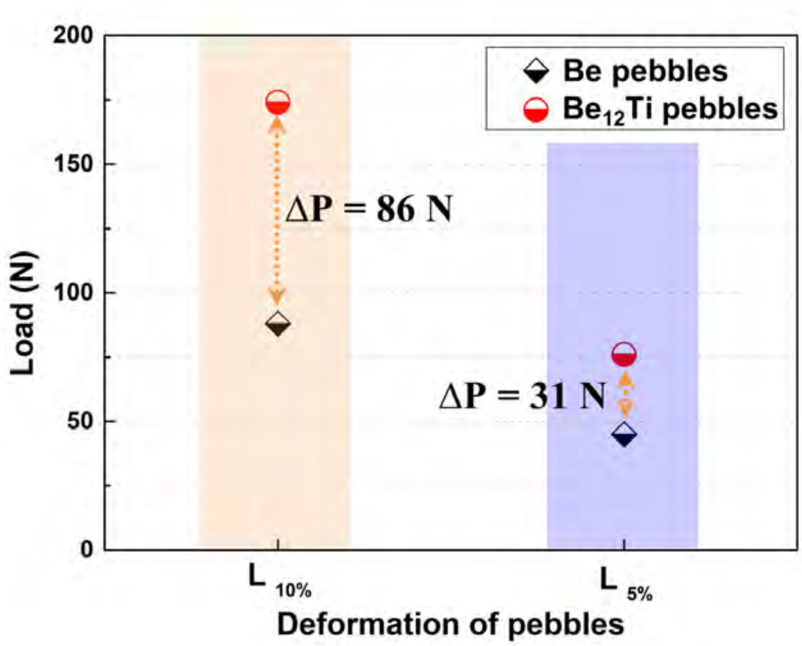

Compression of Be and $Be_{12}Ti$ pebbles

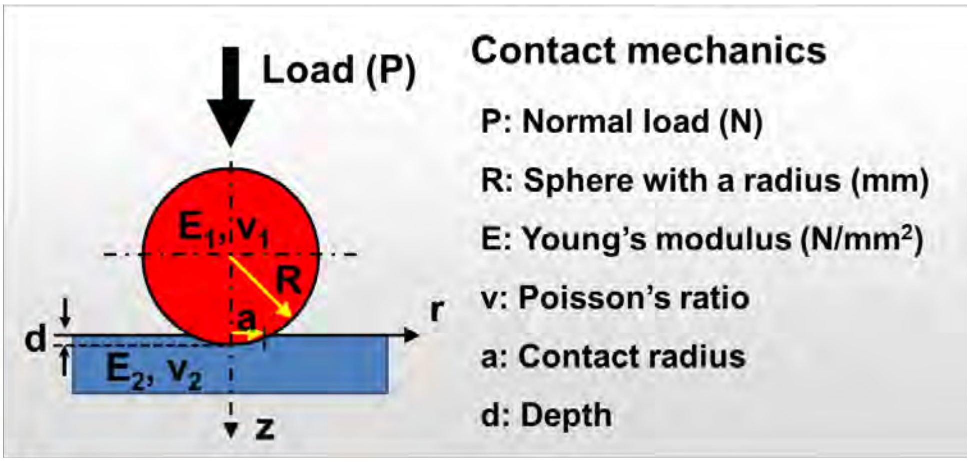

[*]https://en.wikipedia.org/wiki/Contact_mechanics

K. Tsuchiya, E. Ishitsuka, H. Kawamura, et al. Contact Strength Evaluation Of Irradiation Beryllium Pebbles, 7th IEA International Workshop on Beryllium Technology, 2008.

Compression of Be and $Be_{12}Ti$ pebbles

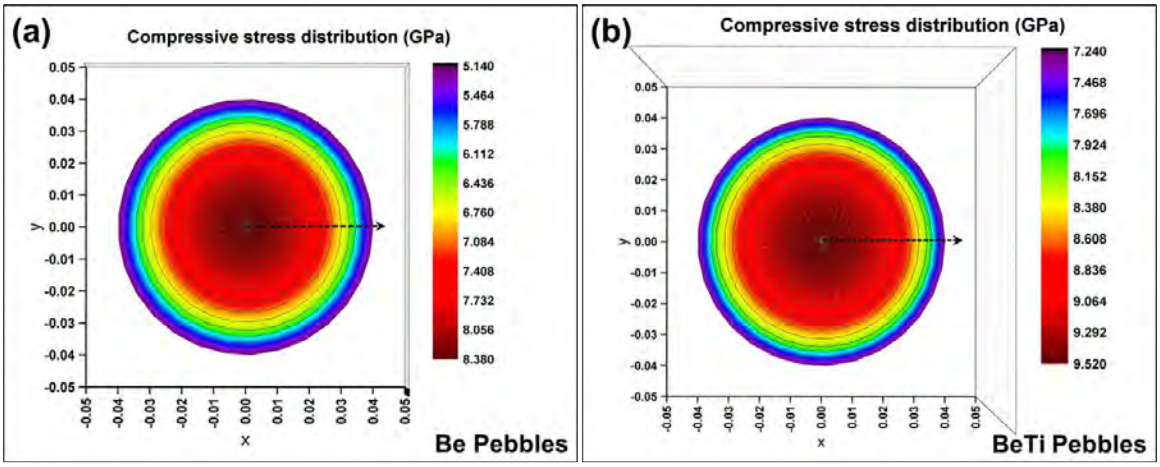

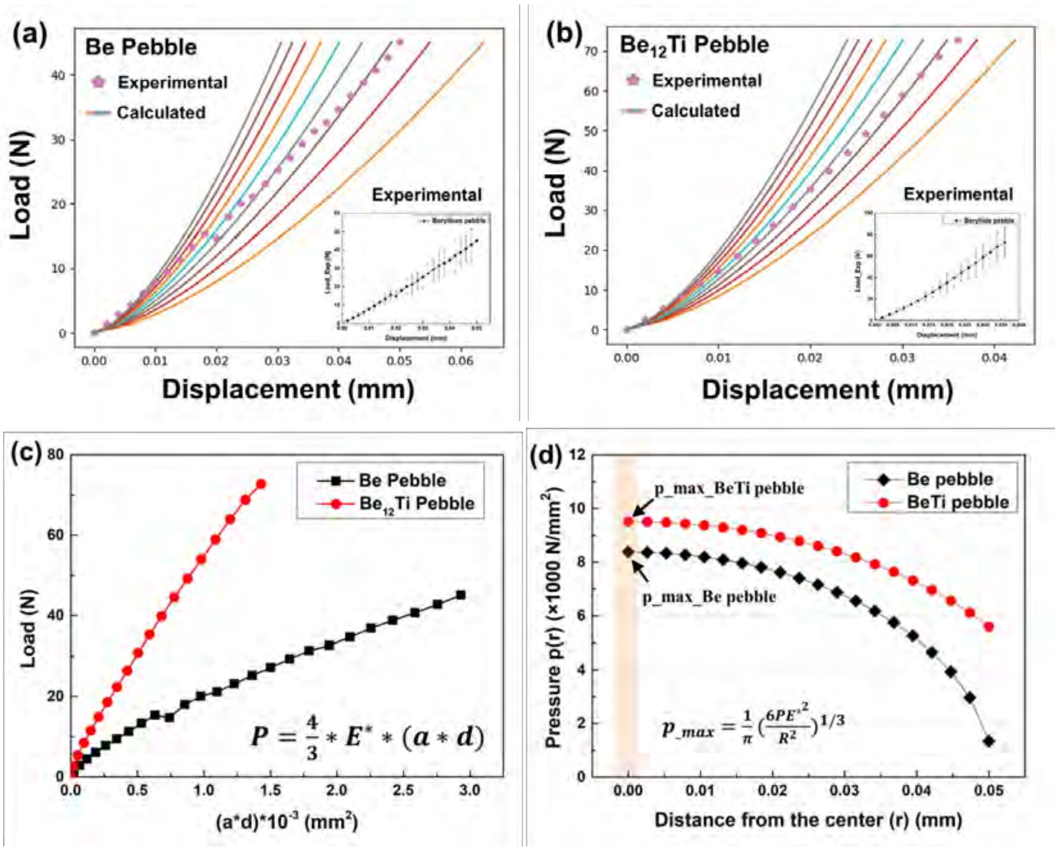

Outline

- Background: Fusion T-self & Neutron multiplier
- Fabrication of Be, $Be_{12}Ti$ and $Be_{12}W$ pebble
- Mechanical compression of neutron multiplier beryllium and beryllide pebble
- **Surface irradiation damage of Be and $Be_{12}Ti/W$ pebble**
- Summary

He ion irradiation (30 keV, 10^{18} ion/cm^2)

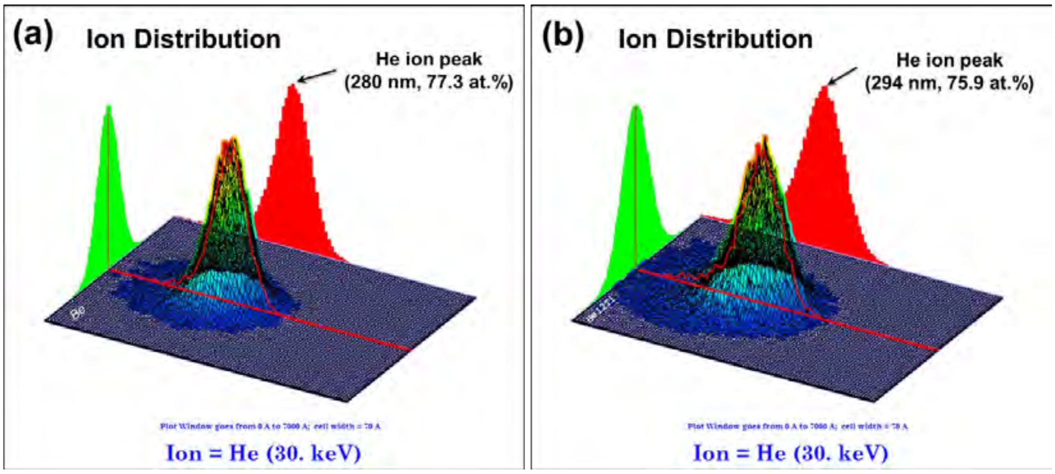

Helium content profile in Be (a) and Be12Ti (b) pebbles calculated by SRIM.

Materials	Be	$Be_{12}Ti$	$Be_{12}W$
He ion peak	280 nm	290 nm	300 nm
He content	77.3 at.%	75.9 at.%	57.5 at.%

Surface of Be pebble after He ion irradiation

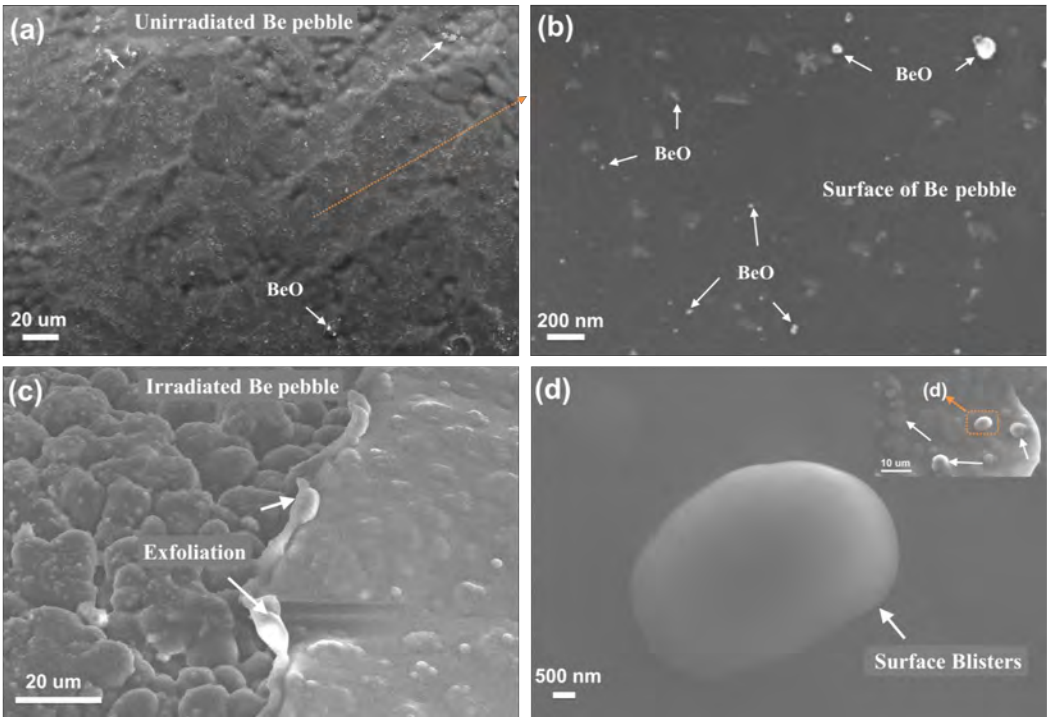

Surface of $Be_{12}Ti$ pebble after He ion irradiation

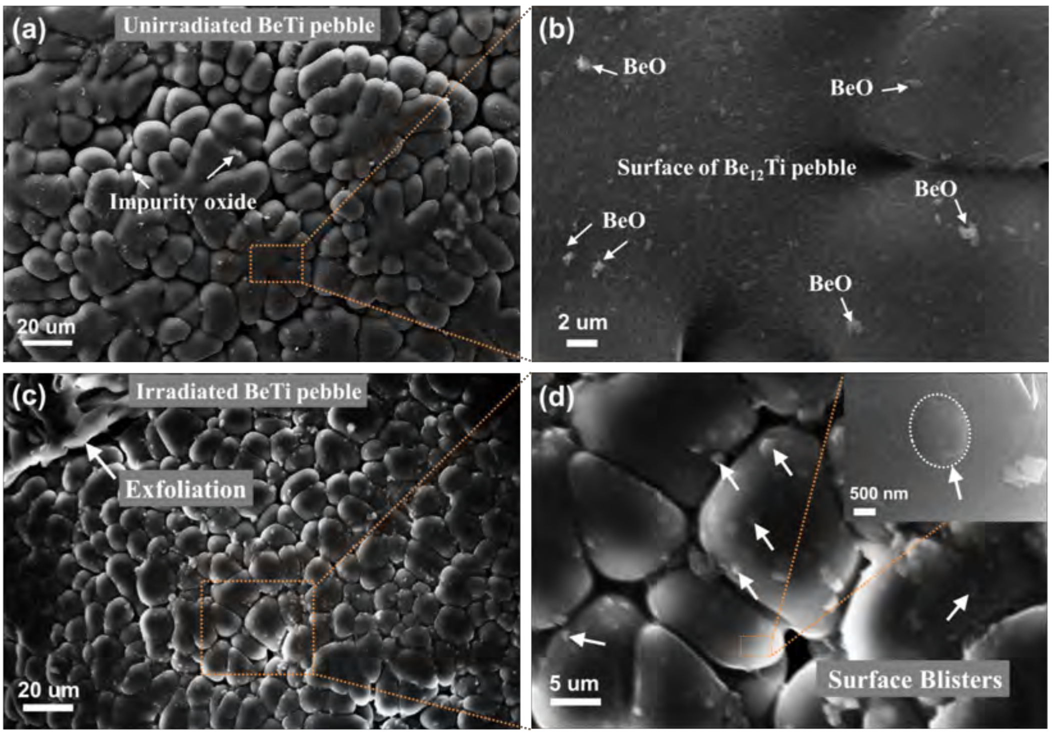

Surface of $Be_{12}W$ pebble after He ion irradiation

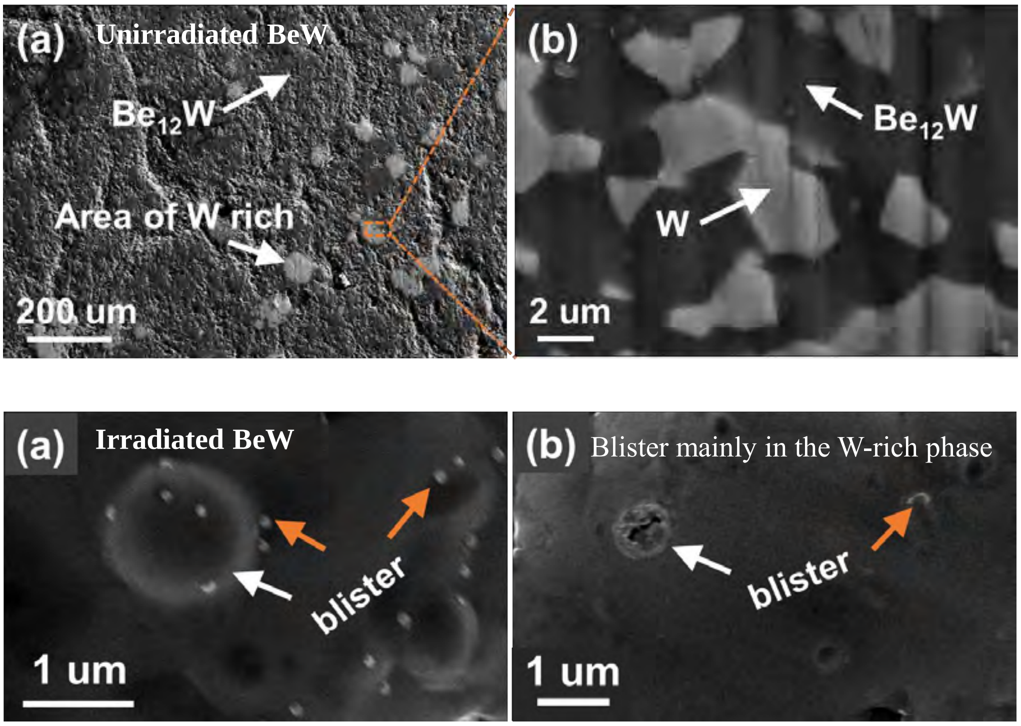

Surface swelling of Be, $Be_{12}Ti$ and $Be_{12}W$ pebble

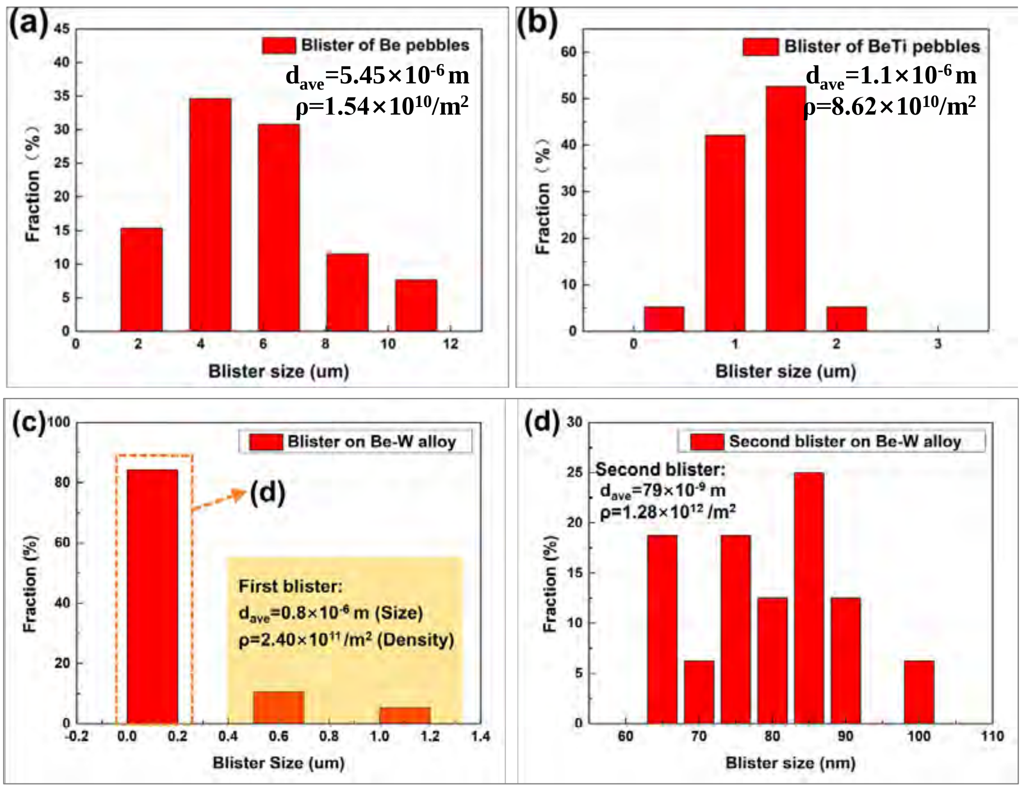

Surface swelling of Be and $Be_{12}Ti$ pebble

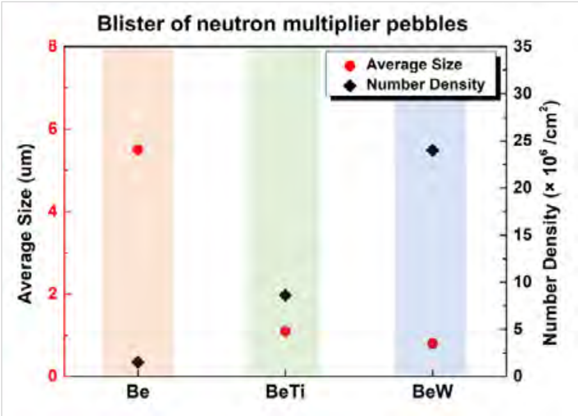

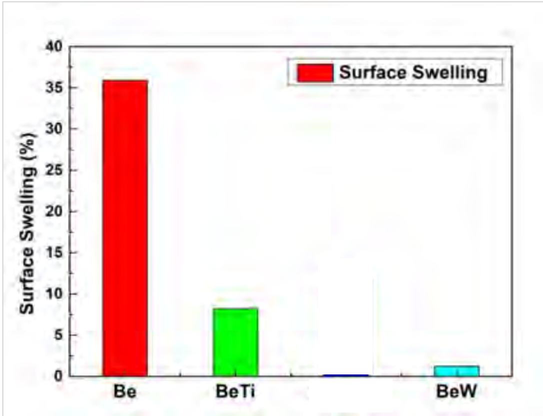

Surface swelling rate:

Be:	**35.91%**
Be-Ti:	**8.19%**
Be-W:	**~1.21%**

Microstructure of Be before irradiation

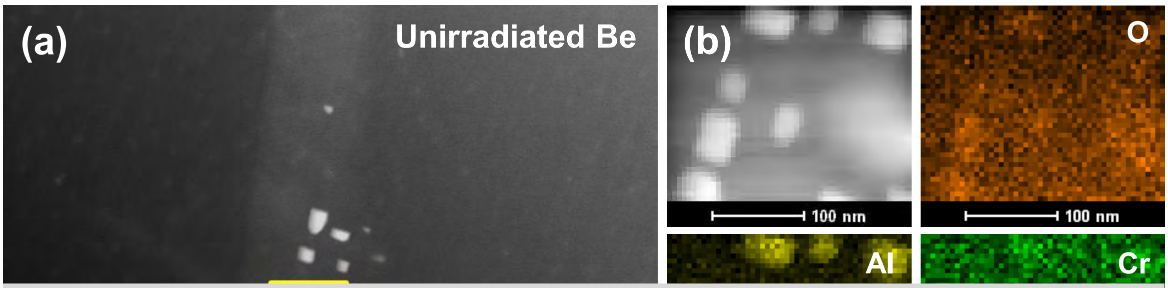

The grain size of the metal fall in the range from several microns to several hundred microns.

"Clean"--No damage

Few impurity particles in the marked beryllium matrix were observed as shown in the morphology. However, some precipitates were observed near the grain boundary.

Microstructure (TEM) of Be after He ion irradiation

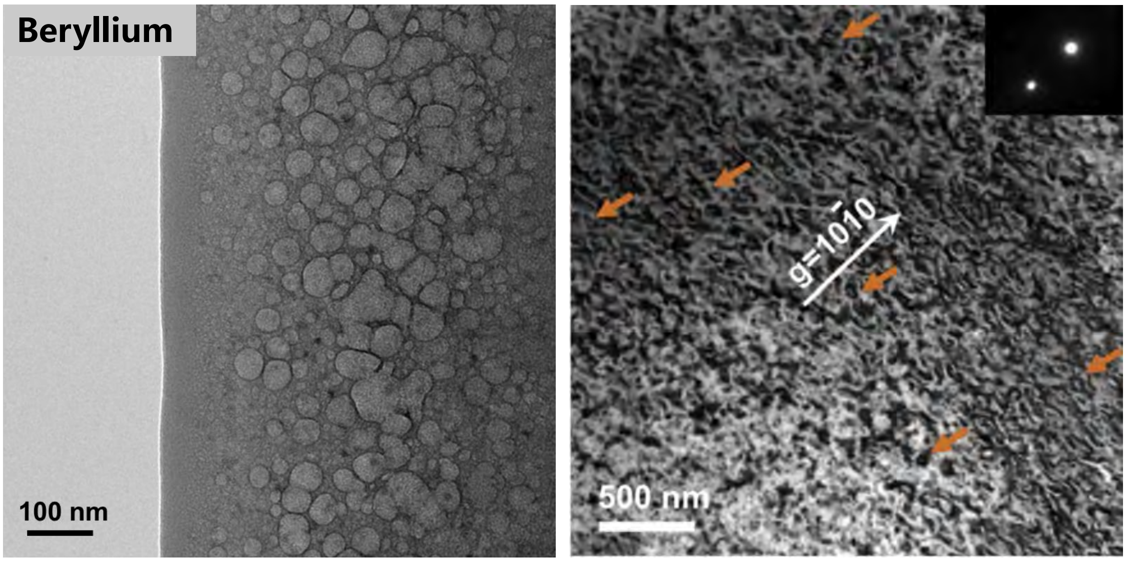

Large bubbles and dislocation loops of high density were induced by 1×10^{18} /cm^2 He ion irradiation.

Summary

1) Be, BeTi and BeW pebbles could be fabricated by REP.

2) Compression properties of Be and Be12Ti pebbles were evaluated by mechanical compression.

----Beryllium pebbles displayed high ductility (50% deformation without fracture), which is better than that of beryllide pebbles.

3) Be, BeTi and BeW were irradiated by high dose He-ion beam.

----The surface swelling-resistance of BeTi and BeW is better than beryllium.

Creep of beryllium pebbles after neutron irradiation to 6000 appm helium production

Vladimir Chakin[1], Rolf Rolli[1], Milan Zmitko[2]

[1]Institute for Applied Materials - Applied Materials Physics, Karlsruhe Institute of Technology, Hermann-von-Helmholtz-Platz 1, 76344 Eggenstein-Leopoldshafen, Germany
[2]Fusion for Energy, c/ Josep Pla, nº 2, Torres Diagonal Litoral Edificio B3, 08019 Barcelona,
Spain

Beryllium pebbles with 1 mm diameter are the reference neutron multiplier material in the Helium Cooled Pebble Bed (HCPB) blanket of ITER. High energy fusion neutrons cause swelling of the beryllium pebbles at the HCPB operation temperatures to 923 K. The radiation-induced swelling of beryllium as well as different thermal expansions of the beryllium pebbles and the structural material can cause the high thermal stresses in the pebble bed. Thermal creep of the pebbles should reduce the stresses because the relaxation. Neutron irradiation leads to degradation of mechanical properties, what expresses in the hardening and the embrittlement. This radiation effect hinders the effect of the relaxation.

In this study, creep properties of beryllium pebbles with 1 mm diameter produced by Rotating Electrode Method (REM) at NGK, Japan were studied. These beryllium pebbles were irradiated in the HFR, Petten, the Netherlands, at temperatures of 643, 723, 833, 923 K to 6000 appm helium production. The creep tests of individual pebbles were performed at temperatures which were equal to the irradiation temperatures by using of three different loadings per each temperature. For two lowest irradiation temperatures of 643 and 723 K, no creep effect was observed. The radiation hardening only occurs that manifests itself in significant reduction of the pebble deformation under loading. At higher irradiation temperatures of 833 and 923 K, the creep rates have significant values. The creep rates strongly depend on the testing temperatures and the loadings. At high irradiation temperatures the ability of beryllium pebbles to the significant deformation under applied loadings should provide the complete relaxation of the internal stresses in the beryllium pebbles.

Corresponding Author:

Dr. Vladimir Chakin
vladimir.chakin@kit.edu

Institute for Applied Materials - Applied Materials Physics,
Karlsruhe Institute of Technology, Hermann-von-Helmholtz-Platz 1, 76344 Eggenstein-Leopoldshafen, Germany

The 15th IEA International Workshop on Beryllium Technology (BeWS-15), September 14-15, 2022 Karlsruhe, Germany

Creep of beryllium pebbles after neutron irradiation to 6000 appm helium production

Vladimir Chakin[1], Rolf Rolli[1], Milan Zmitko[2]

[1]Karlsruhe Institute of Technology, Institute for Applied Materials, Hermann-von-Helmholtz-Platz 1, 76344 Eggenstein-Leopoldshafen, Germany

[2]Fusion for Energy (F4E), Josep Pla 2, Barcelona, Spain

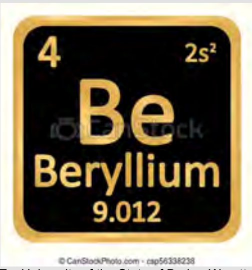

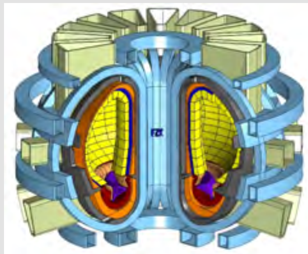

KIT – University of the State of Baden-Wuerttemberg and National Research Center of the Helmholtz Association

www.kit.edu

Outline

Materials, pebbles, creep testing at FML

HIDOBE-02: irradiation of unconstrained (free filled) Be pebbles and constrained Be pebble beds

Optical microstructure of irradiated Be pebbles

Creep behaviour of irradiated unconstrained and constrained Be pebbles

Conclusions

1 Institute for Applied Materials – Applied Materials Physics

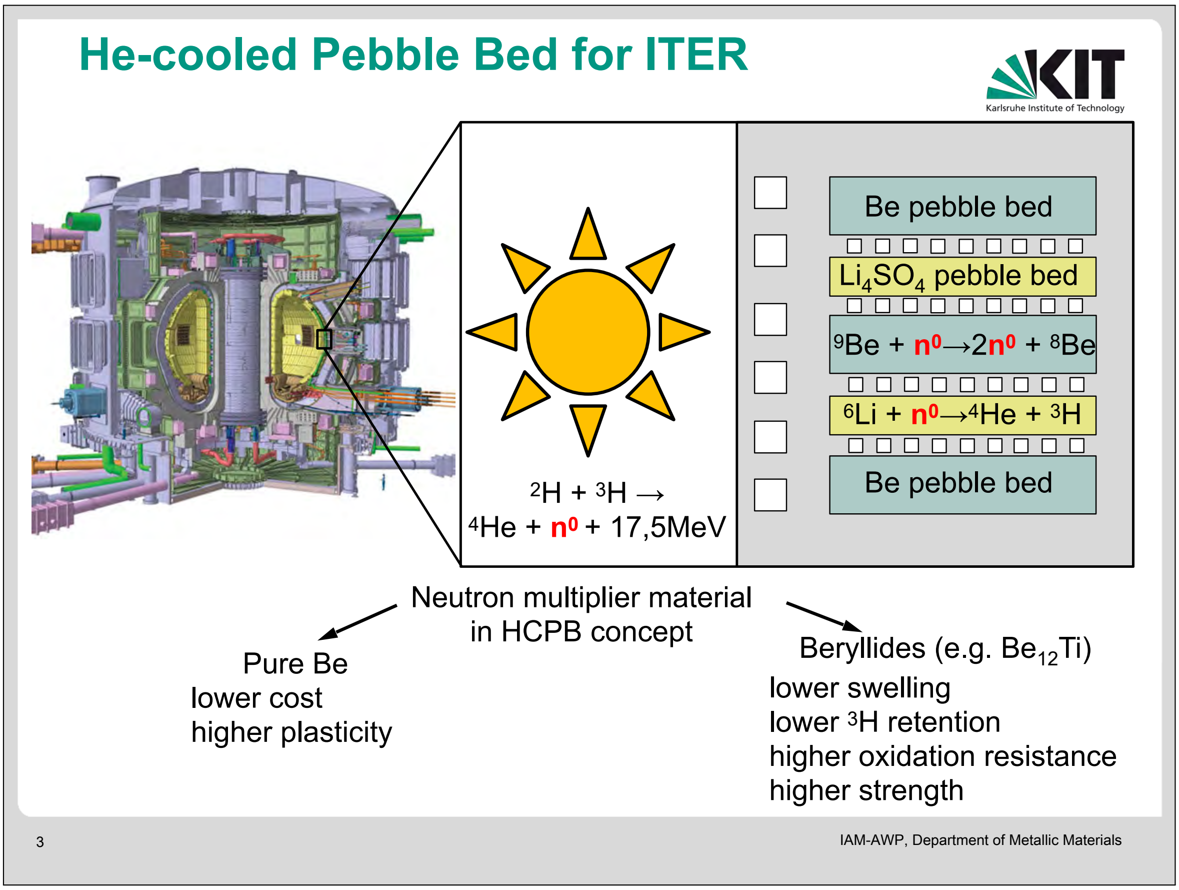
He-cooled Pebble Bed for ITER
KIT
Karlsruhe Institute of Technology
Be pebble bed
Li4SO4 pebble bed
9Be + n0→2n0 + 8Be
6Li + n0→4He + 3H
Be pebble bed
2H + 3H →
4He + n0 + 17,5MeV
Neutron multiplier material
in HCPB concept
Pure Be
lower cost
higher plasticity
Beryllides (e.g. Be12Ti)
lower swelling
lower 3H retention
higher oxidation resistance
higher strength
3
IAM-AWP, Department of Metallic Materials

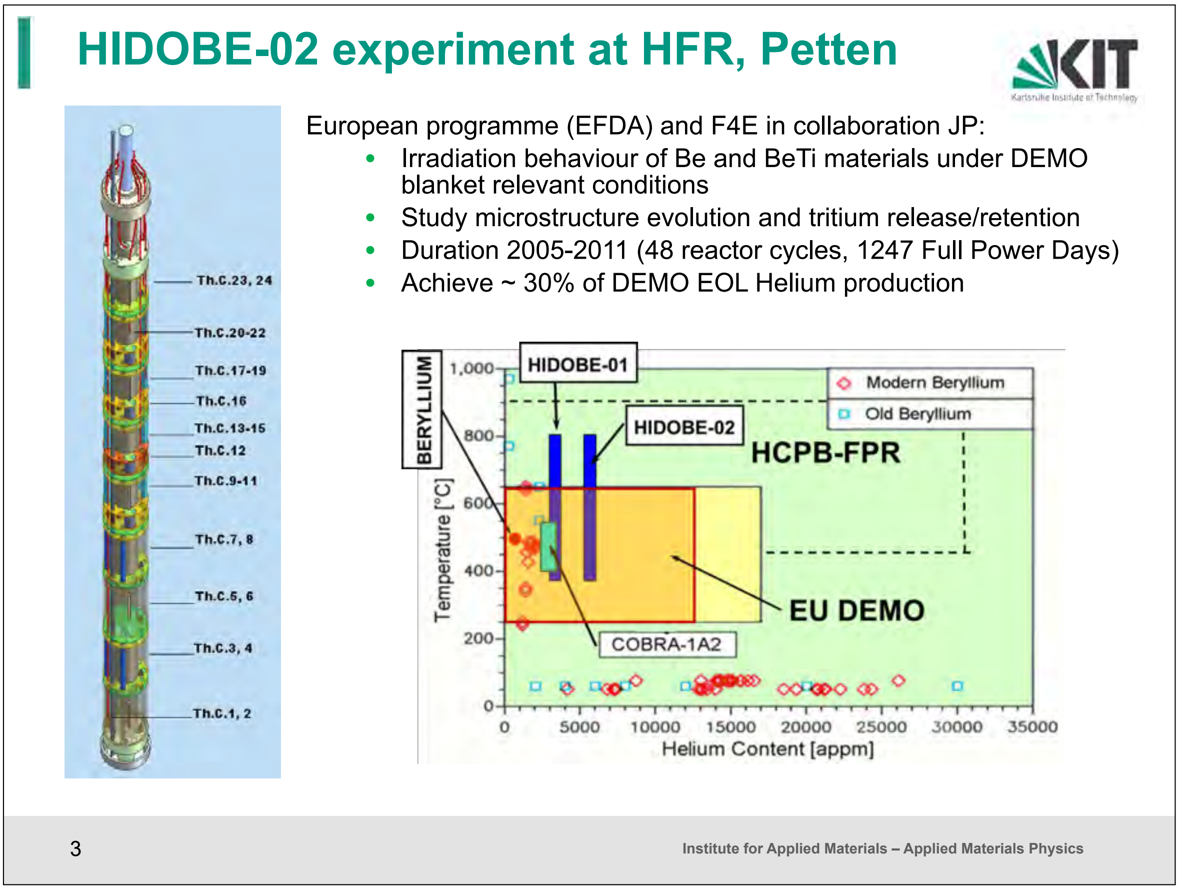
HIDOBE-02 experiment at HFR, Petten
KIT
European programme (EFDA) and F4E in collaboration JP:
Irradiation behaviour of Be and BeTi materials under DEMO blanket relevant conditions
Study microstructure evolution and tritium release/retention
Duration 2005-2011 (48 reactor cycles, 1247 Full Power Days)
Achieve ~ 30% of DEMO EOL Helium production
Th.C.23, 24
Th.C.20-22
Th.C.17-19
Th.C.16
Th.C.13-15
Th.C.12
Th.C.9-11
Th.C.7, 8
Th.C.5, 6
Th.C.3, 4
Th.C.1, 2
BERYLLIUM
HIDOBE-01
HIDOBE-02
HCPB-FPR
EU DEMO
COBRA-1A2
Modern Beryllium
Old Beryllium
Temperature [°C]
Helium Content [appm]
0
200
400
600
800
1,000
5000
10000
15000
20000
25000
30000
35000
3
Institute for Applied Materials – Applied Materials Physics

HIDOBE-02 experiment at HFR, Petten

Euro ... ration JP:
... erials under DEMO

... n release/retention
... 247 Full Power Days)
... oduction

M. Dalle Donne
G.R. Longhurst
H. Kawamura
A. Moeslang
J.G. Van der Laan
J.B.J. Hegeman
I.B. Kupriyanov
F. Scaffidi-Argentina
A. Goraieb

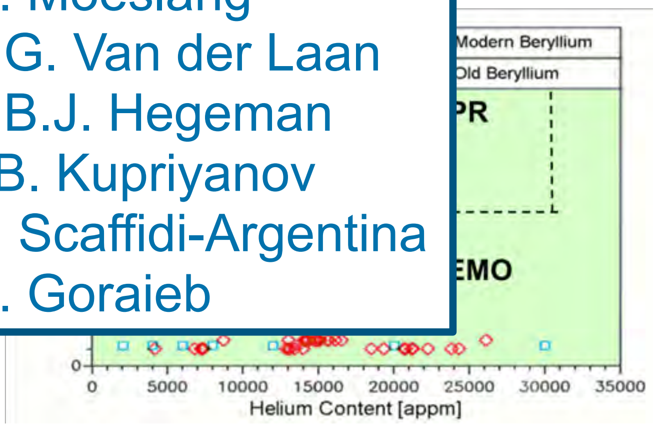

Irradiation parameters of Be pebbles in HIDOBE-02 compaign

Be pebble with Ø1 mm	T_{irr} , K	F, $\times10^{26}$, m^{-2}, E>1MeV	D, dpa	^4He, appm	^3H, appm
Unconstrained (free filled)	644	1.06	21	3632	367
	716	1.43	29	4751	502
	832	1.68	34	5524	596
	919	1.81	37	5925	644
Constrained	660	1.06	21	3632	367
	754	1.43	29	4751	502
	874	1.68	34	5524	596
	958	1.81	37	5925	644

Chemical composition of Be pebbles with Ø 1 mm

Element	Content, wt.%
Be	99.5
BeO	0.36
Fe	0.094
Al	0.048
Mg	0.024
Si	0.029
U	<0.01

5 Institute for Applied Materials – Applied Materials Physics

Placement of Ø 1 mm Be pebbles in HIDOBE-02

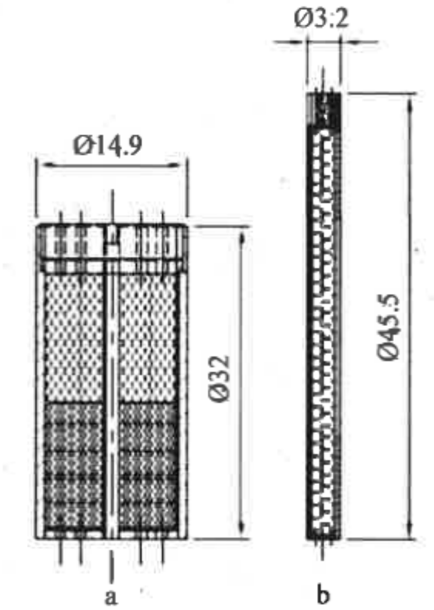

Unconstrained Be pebbles are placed in capsule with Ø 3.2 mm. The pebbles were filled free in the capsule.

Constrained Be pebble beds are placed in capsule with Ø 14.9 mm. It was filled by pebbles and then, screwed on with screw cap with torque wrench. In particular, after contact of the cap with the pebbles, another forced turn of the cap along the thread was done. In this position, the cap was spot welded to the capsule. In this way, additional internal stresses were created in the pebbles.

This allows to simulate internal state of the pebbles swelled after irradiation to higher neutron dose than that in HIDOBE-02 experiment.

6 Institute for Applied Materials – Applied Materials Physics

Pebble loading scheme in creep machine

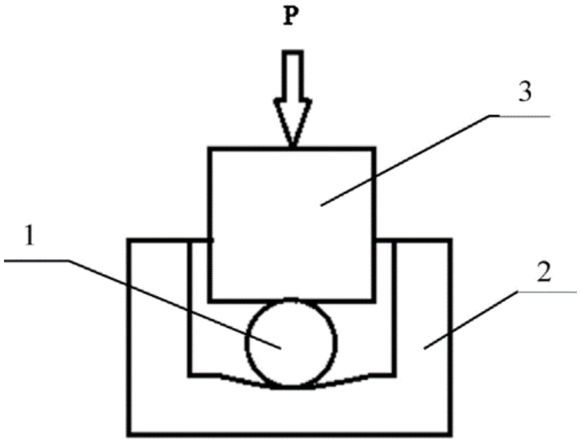

1 – pebble
2 – bottom
3 – loading piston

P – constant during creep test

$T_{test} = T_{irr}$ for each testing pebble

t = 80 h

7 Institute for Applied Materials – Applied Materials Physics

Creep testing parameters and shortly about results

State	T_{irr}, K	T_{test}, K	P, N	Result
Unconstrained	644	643	100	no deformation
			110	cracks
			120	cracks
			150	cracks
	716	723	100	no deformation
			110	cracks
			120	cracks
	832	833	55	no deformation
			60	deformation
			70	deformation
	919	923	15	no deformation
			20	no deformation
			25	no deformation
Constrained	660	643	35	deformation
			50	deformation
			70	deformation
			100	cracks
	754	723	70	deformation
			100	deformation
			120	deformation
	874	833	35	deformation
			50	deformation
			70	cracks
	958	923	-	not dismantled

"No deformation" means that the load is not enough to produce deformation or destruction of the pebble.

"Cracks" means that cracks appeared as a result of loading.

"Deformation" means that as a result of loading, the pebble deformed through creep.

Therefore, only 10 diagrams (by red) from 23 diagrams of performed tests include really creep behavior therefore, they can be processed.

8 diagrams from 10 "red" diagrams ("deformation") are constrained pebbles. This means that constrained pebbles have comparatively better creep behavior.

8 Institute for Applied Materials – Applied Materials Physics

Examples of "no deformation" case after creep tests

Unconstr., T_{test} = 643 K, P = 100 N

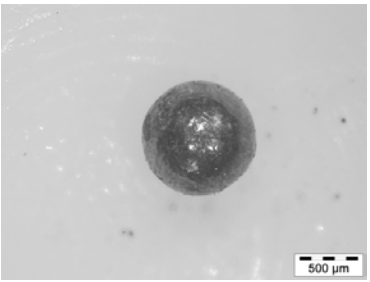

Unconstr., T_{test} = 833 K, P = 80 N

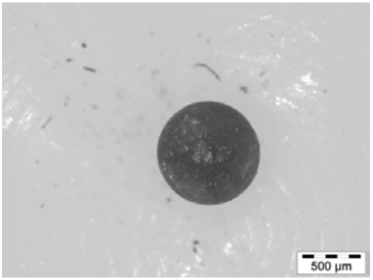

Unconstr., T_{test} = 923 K, P = 25 N

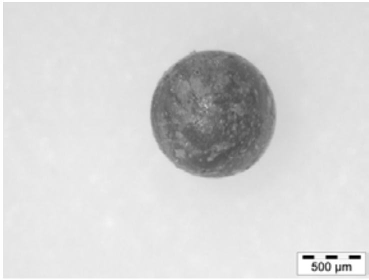

"No deformation" case was only for unconstrained Be pebbles (6 creep tests).

Reason for "no deformation" case is that was not enough load to deform or to break the tested pebble.

9 Institute for Applied Materials – Applied Materials Physics

Examples of "cracks" case after creep tests

Unconstr., T_{test} = 643 K, P = 120 N

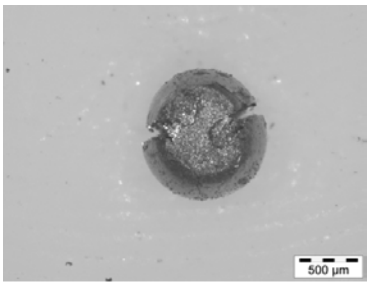

Unconstr., T_{test} = 723 K, P = 120 N

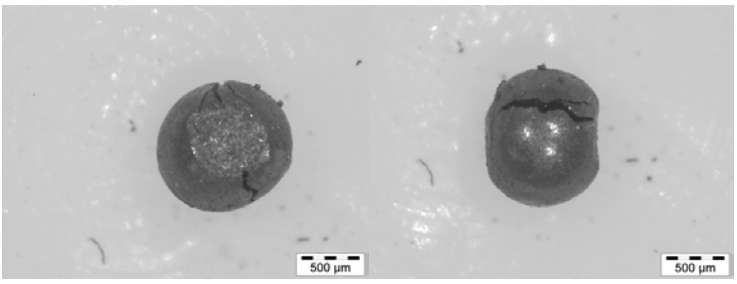

Constr., T_{test} = 643 K, P = 100 N

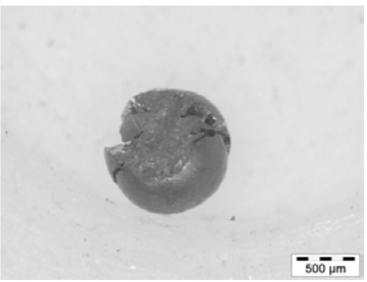

Constr., T_{test} = 833 K, P = 70 N

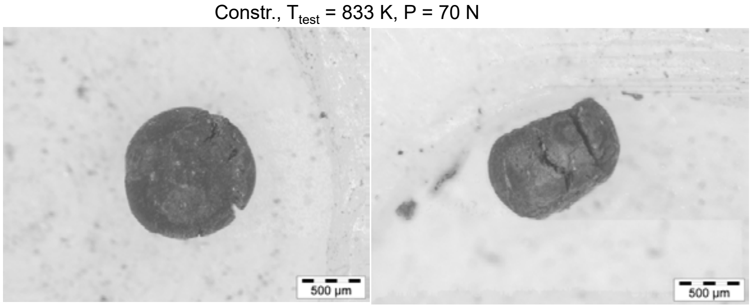

5 "cracks" cases are for unconstrained pebbles, 2 cases are for constrained pebbles.

10 Institute for Applied Materials – Applied Materials Physics

Examples of "deformation" case

KIT Karlsruhe Institute of Technology

Unconstr., T_{test} = 833 K, P = 60 N

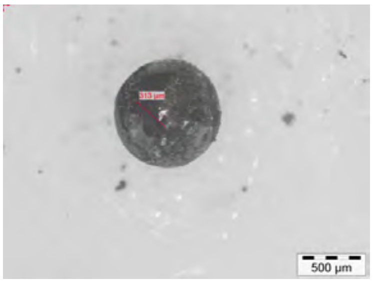

Unconstr., T_{test} = 833 K, P = 70 N

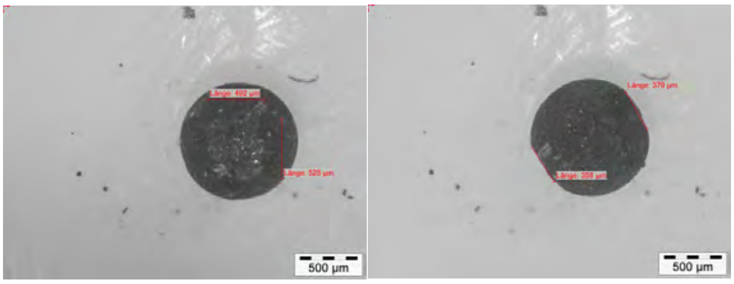

Constr., T_{test} = 643 K, P = 70 N

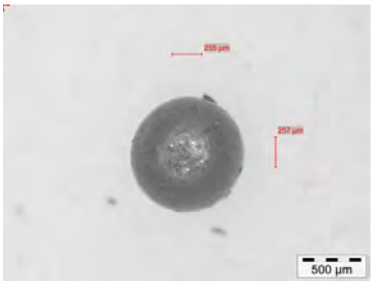

Constr., T_{test} = 833 K, P = 50 N

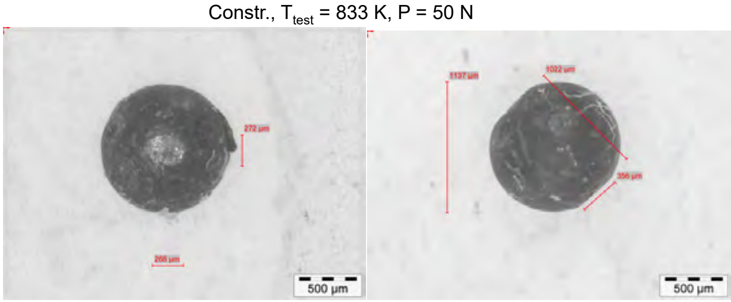

2 "deformation" cases are for unconstrained pebbles, 8 cases are for constrained pebbles.

11 Institute for Applied Materials – Applied Materials Physics

Parameters of indentations on irradiated Be pebbles after creep testing

KIT Karlsruhe Institute of Technology

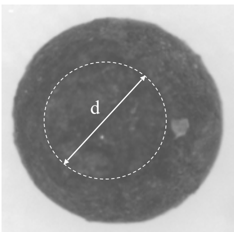

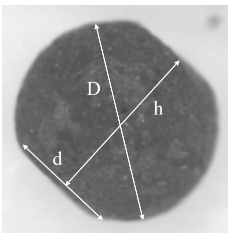

D is diameter of pebble

d is indentation diameter as a result of the creep process

h is distance between opposite indentations

$\sigma = P/S = 4P/\pi d^2$, where σ is internal stress in the pebble under loading P, S is area of indentation with diameter of d

12 Institute for Applied Materials – Applied Materials Physics

Microstructure of unconstrained Be pebbles after irradiation

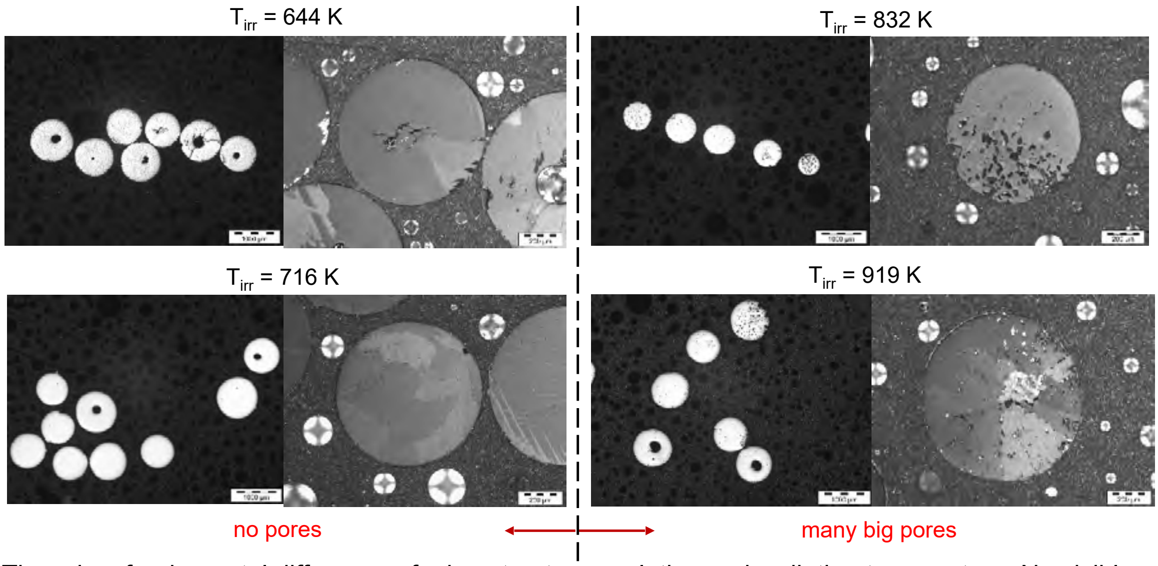

There is a fundamental difference of microstructure evolution on irradiation temperature. No visible pores are after irradiation at two lowest T_{irr} (644 and 716 K). Many big pores are after irradiation at two highest T_{irr} (832 and 919 K).

Microstructure of constrained Be pebble beds after irradiation

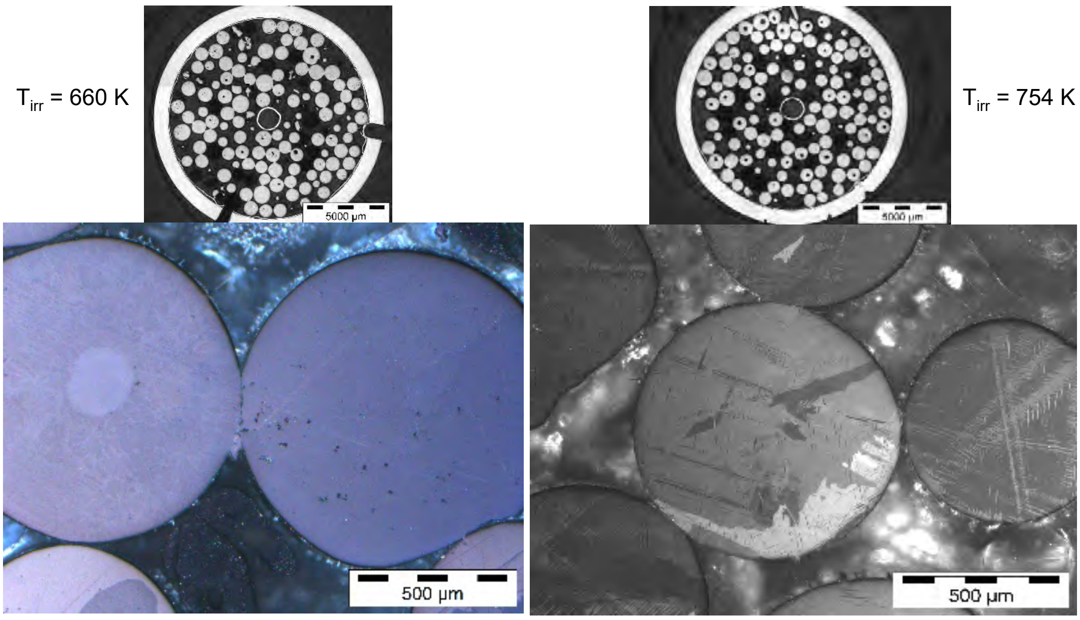

Also, no pores but constrained pebbles have much more sub-grains and twins compared to unconstrained pebbles.

Microstructure of constrained Be pebbles after irradiation at 874 K

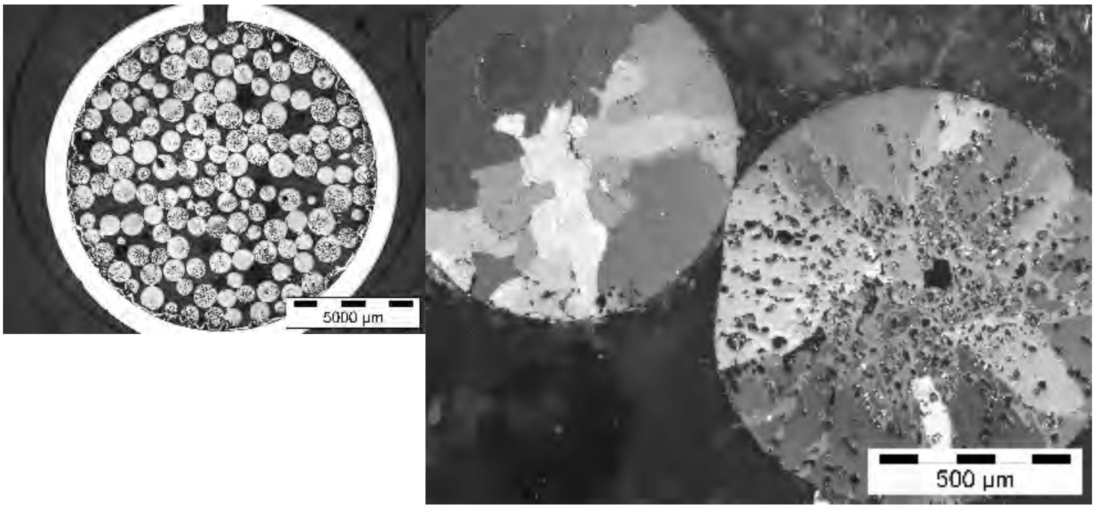

There are many big pores and developed sub-grain microstructure.

15 Institute for Applied Materials – Applied Materials Physics

Failure load on loading of irradiated Be pebbles at T_{test} = 723 and 833 K

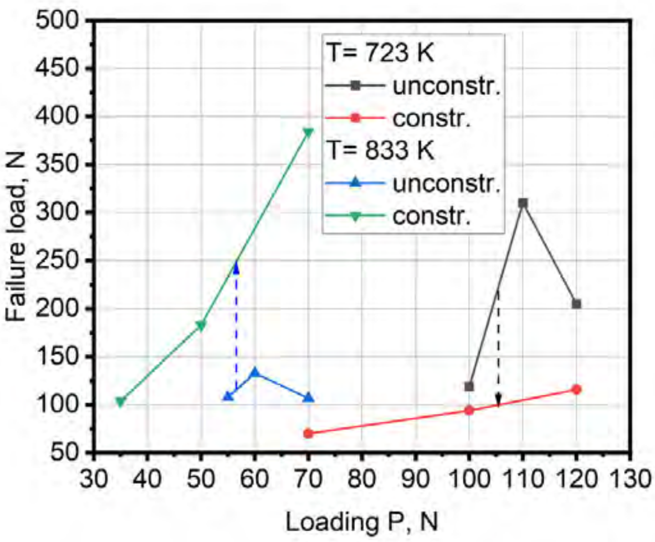

T_{test} = 643 K (0.412 T_m)
723 K (0.463 T_m)
Creep starts at T_{test}>0.5T_m
833 K (0.534 T_m)
923 K (0.592 T_m)

At 723 K is no creep: failure load of unconstrained pebbles is higher than that of constrained pebbles, and failure occurs at higher loading.

At 833 K is creep: failure load of unconstrained pebbles is lower than that for constrained pebbles, and failure occurs at lower loading.

16 Institute for Applied Materials – Applied Materials Physics

Examples of creep curves for unconstrained and constrained irradiated Be pebbles

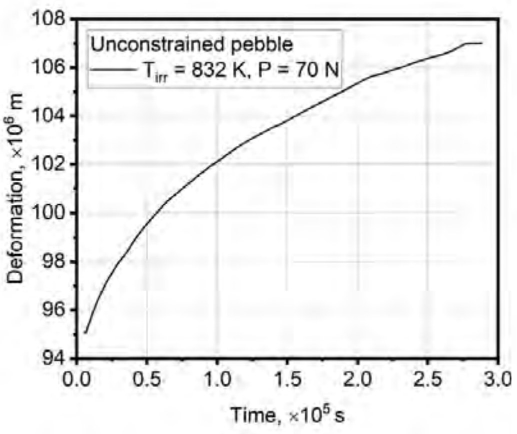

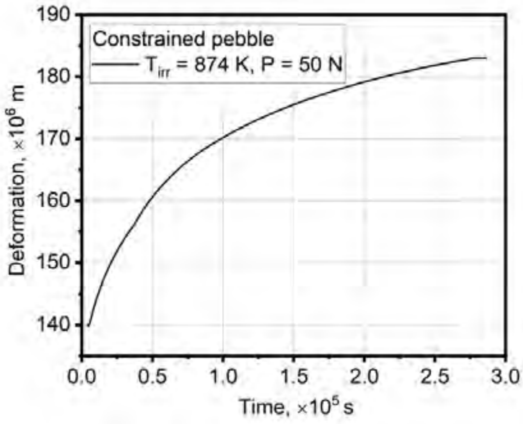

Both samples were tested at the same temperature of 833 K.

Shape of both curves is typical for creep tests.

Deformation for constrained pebble is significantly higher to unconstrained pebbles even though the loading was relatively less for constrained pebble (50 to 70 N).

Creep rate determination in second stage

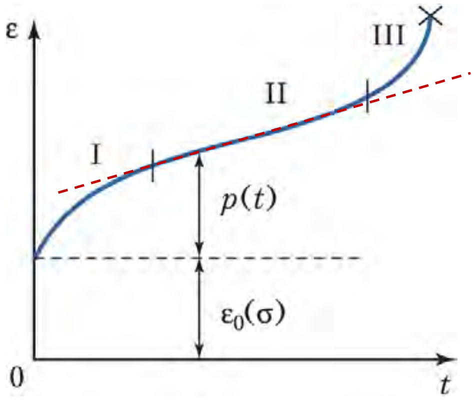

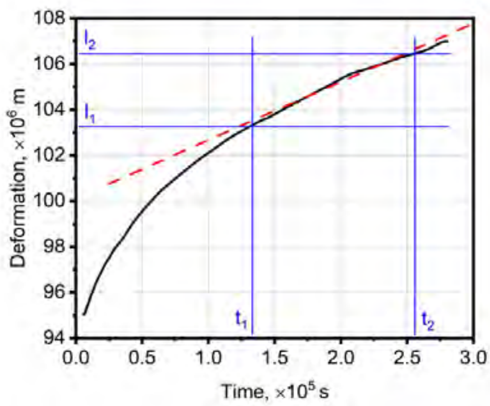

Creep rate determination in second stage

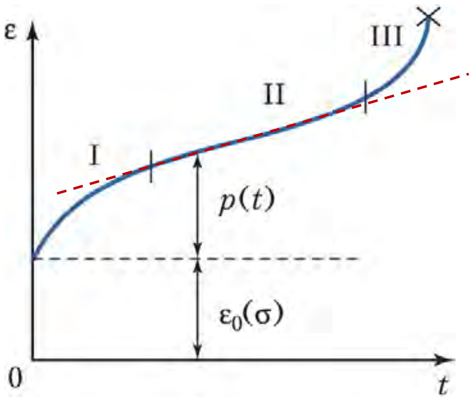

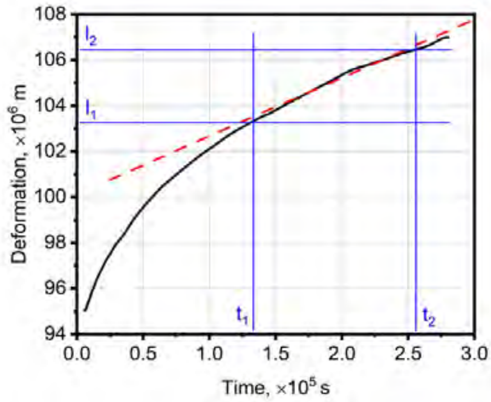

We carry out a linear approximation at second stage using experimental creep curve.

Steady-state strain-rate $\dot{\varepsilon} = (l_2 - l_1)/[(t_2 - t_1)\times h]$,
where l_1 and l_2 are deformation at beginning and end of selected segment of creep curve, t_1 and t_2 are time to reach beginning and end of selected deformation segment, h is distance between opposite indentations on tested pebble.

18 Institute for Applied Materials – Applied Materials Physics

Creep rate determination in second stage

Classical creep curve has three stages

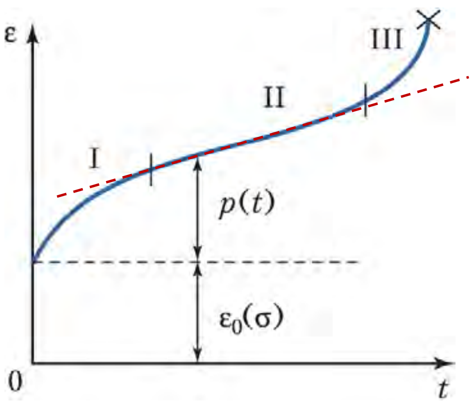

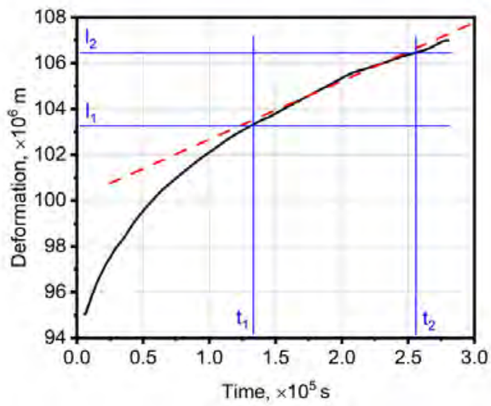

We carry out a linear approximation at second stage using experimental creep curve.

Steady-state strain-rate $\dot{\varepsilon} = (l_2 - l_1)/[(t_2 - t_1)\times h]$,
where l_1 and l_2 are deformation at beginning and end of selected segment of creep curve, t_1 and t_2 are time to reach beginning and end of selected deformation segment, h is distance between opposite indentations on tested pebble.

18 Institute for Applied Materials – Applied Materials Physics

Creep rate determination in second stage

Classical creep curve has three stages

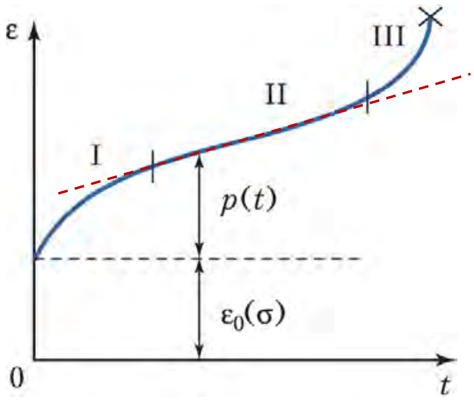

Experimental creep curve has only two incomplete stages

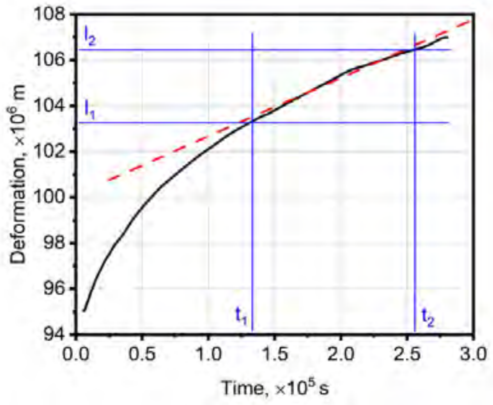

We carry out a linear approximation at second stage using experimental creep curve.

Steady-state strain-rate $\dot{\varepsilon} = (l_2 - l_1)/[(t_2 - t_1)\times h]$,
where l_1 and l_2 are deformation at beginning and end of selected segment of creep curve, t_1 and t_2 are time to reach beginning and end of selected deformation segment, h is distance between opposite indentations on tested pebble.

18 Institute for Applied Materials – Applied Materials Physics

Dependence of steady-state strain-rate $\dot{\varepsilon}$ to stress σ

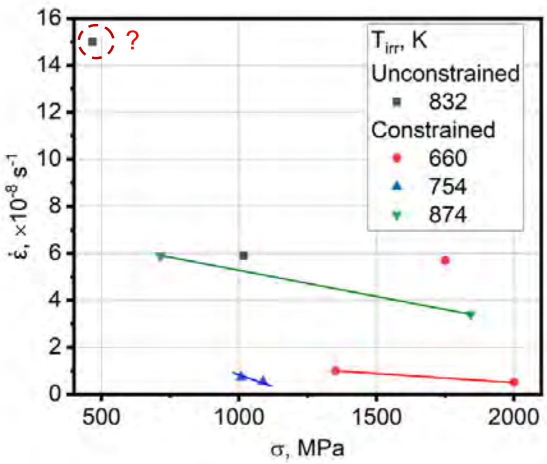

19 Institute for Applied Materials – Applied Materials Physics

Dependence of steady-state strain-rate $\dot{\varepsilon}$ to stress σ

KIT Karlsruhe Institute of Technology

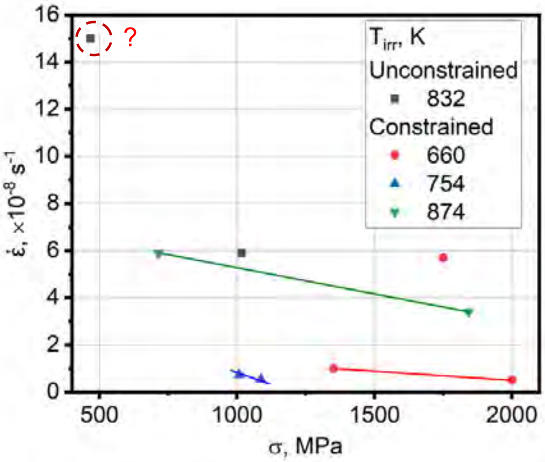

Creep behavior of constrained pebbles is logical. Creep rate at lowest temperature 660 K is similar to that at 754 K but it has higher applied stress. Creep rate at highest temperature 874 K is higher than that at lower temperatures.
Creep behavior of unconstrained pebbles is unclear because it was obtained a limited number of successful creep tests.

19 Institute for Applied Materials – Applied Materials Physics

Comparison of behavior of constrained pebble beds after irradiation at low- and high-temperatures

KIT Karlsruhe Institute of Technology

T_{irr} = 660 K (0.423 $_{m}$) – no creep T_{irr} = 874 K (0.56T_m) – by creep

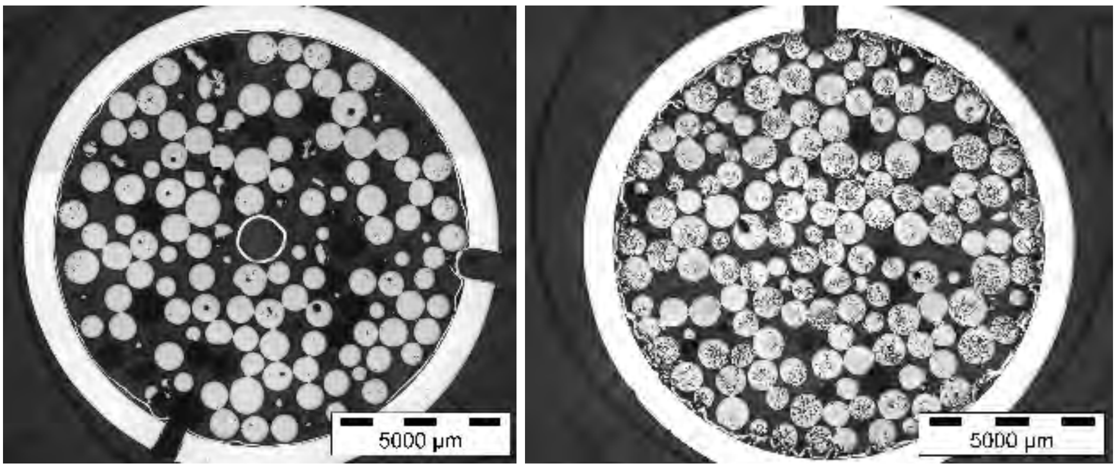

20 Institute for Applied Materials – Applied Materials Physics

Comparison of behavior of constrained pebble beds after irradiation at low- and high-temperatures

T_{irr} = 660 K (0.423 $_{m}$) – no creep

T_{irr} = 874 K (0.56T_m) – by creep

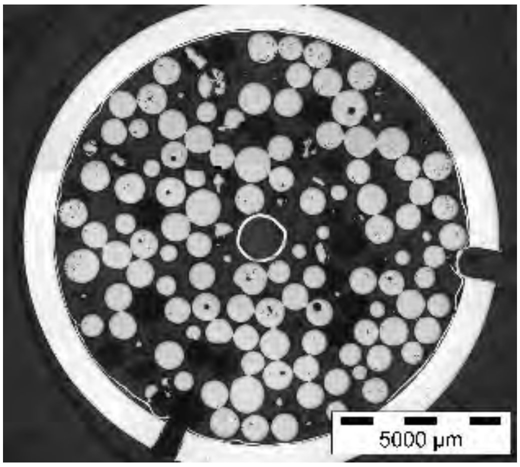

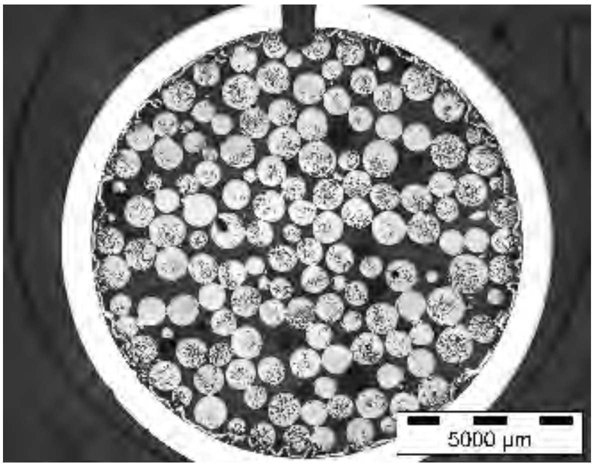

Constrained pebble bed, if it concerns level of internal stresses in the pebbles, means state of the pebble bed after high-dose irradiation because high internal stresses were created in the pebbles already before irradiation.

Low-temperature irradiation (<0.5T_m) – no pores, not high swelling, formation of dislocation sub-grain microstructure but no creep deformation therefore, defragmentation of pebbles occurs.
High-temperature irradiation (>0.5T_m) – many big pores and high swelling, but sub-grains and creep deformation are available therefore, stress relaxation exists resulting comparatively less pebble defragmentation comparing to low-temperature irradiation.

20 Institute for Applied Materials – Applied Materials Physics

Conclusions

Creep tests of Ø 1 mm Be pebbles irradiated to 6000 appm He production show difference of creep behavior of unconstrained (free filled) and constrained pebbles.

There are points:
- 10 from 23 performed tests include really creep behavior as "deformation" case. And 8 from 10 diagrams were obtained on constrained pebbles.
- There is transition to creep behavior between 723 K (0.463 T_m) and 833 K (0.534 T_m). Constrained pebbles at 833 K have comparatively higher failure load than that for unconstrained pebbles.
- Optical metallography shows very developed sub-gran microstructure in constrained pebbles. Unconstrained pebbles have practically no sub-grains.
- Concerning calculation of dependence of steady-state strain-rate to stress for constrained pebbles, it is logical behavior. For unconstrained pebbles, it was performed not enough successful creep tests (there were mainly "no deformation" or "cracks" cases).

This means that constrained pebbles have comparatively better creep behavior than unconstrained pebbles especially for irradiation at higher temperatures than 0.5T_m.

21 Institute for Applied Materials – Applied Materials Physics

4th IEA International Workshop on Beryllium Technology for Fusion, September 15-17, 1999, Karlsruhe, Germany

22 Institute for Applied Materials – Applied Materials Physics

4th IEA International Workshop on Beryllium Technology for Fusion, September 15-17, 1999, Karlsruhe, Germany

1999-2022
BeWS-4 ➡ BeWS-15

22 Institute for Applied Materials – Applied Materials Physics

Thank you for your attention!

See you again on BeWS-16?

23 Institute for Applied Materials – Applied Materials Physics

Thermo-mechanical behavior of titanium beryllide pebble beds at elevated temperatures

J. Reimann[1], E. Cilingir[2], R. Gaisin[1], A. Goraieb[2],
M. Nakamichi[3], P. Vladimirov[1]

[1] Karlsruhe Institute of Technology, Institute for Applied Materials, Hermann-von-Helmholtz-Platz 1, 76344 Eggenstein-Leopoldshafen, Germany
[2] Karlsruhe Beryllium Handling Facility (KBHF GmbH), Hermann-von-Helmholtz-Platz 1, 76344 Eggenstein-Leopoldshafen, Germany
[3] National Institutes for Quantum and Radiological Science and Technology, 2-166 Omotedate, Obuchi, Rokkasho, Aomori 039-3212, Japan

The thermomechanical behavior of titanium beryllide pebble beds was investigated experimentally at temperatures between 200 and 500°C in helium atmosphere at atmospheric pressure. The pebbles consist of a mixture of $TiBe_{12}$ and Ti_2Be_{17} titanate beryllide phases and a small residual amount of Be phase, denominated as Be-7.7Ti.

Like previous experiments at ambient temperature [1], the pebble beds were compressed uniaxially up to 4.5MPa and the effective thermal conductivity k was measured using the hot wire technique.

Compared to ambient temperature, the stress-strain curves do not differ significantly in investigated temperature range. Because the thermal conductivity of solid $TiBe_{12}$ is fairly constant in a wide temperature range [2], k increases moderately with increasing temperature because of the increasing thermal conductivity of helium.

Compared to beryllium pebble beds, the k of the Be-7.7Ti pebble beds increases again much lesser because of the significantly smaller thermal conductivity of the solid material and the mechanically harder behavior resulting in smaller contact surfaces.

[1] J. Reimann et al, Fusion Eng. Des. 165 (2021) 112249
[2] M. Uchida, E. Ishitsuka, H. Kawamura, Fusion Eng. Des. 69 (2003) 499-503.

Corresponding Author:
Dr. Joerg Reimann
reimann-langhans@web.de

Karlsruhe Institute of Technology

Thermo-mechanical behavior of titanium beryllide pebble beds at elevated temperatures

J. Reimann[1], E. Cilingir[2], R. Gaisin[1], A. Goraieb[2], M. Nakamichi[3], P. Vladimirov[1]

[1] Karlsruhe Institute of Technology, Institute for Applied Materials, Hermann-von-Helmholtz-Platz 1, 76344 Eggenstein-Leopoldshafen, Germany
[2] Karlsruhe Beryllium Handling Facility (KBHF GmbH), Hermann-von-Helmholtz-Platz 1, 76344 Eggenstein-Leopoldshafen, Germany
[3] National Institutes for Quantum and Radiological Science and Technology, 2-166 Omotedate, Obuchi, Rokkasho, Aomori 039-3212, Japan)

KIT – The Research University in the Helmholtz Association

www.kit.edu

Outline

- Introduction
  - Modelling parameters of the thermo-mechanical behaviour of pebble beds
  - Previous investigations at ambient temperature
- Experimental set-up
- Results
  - A) Uniaxial Stress-Strain dependence
  - B) Effective thermal conductivity of pebble beds
  - C) Thermal creep
- Discussion/Conclusions

2 15.09.2022 J. Reimann – Thermal-mechanical behavior of TiBe12 pebble beds Department of Metallic Alloys, Institute for Applied Materials - Applied Materials Physics IAM Institute for Applied Materials

General Remarks

- *This paper is an extension of recent investigations at ambient temperature T_a [1]. In all experiments, a simple experimental facility was used, therefore, the experimental results should be considered as screening exps.*
- *The beryllium-titanate pebbles (d=0.8-1.2mm) were produced with the stoichiometric composition of Be and 7.7at% Ti, ideally resulting in single phase Be12Ti pebbles. However, it was found that the used pebbles have also a Be13Ti2 and a Be phase, for details, see [1]. Therefore, the denomination Be-7.7Ti was chosen.*

[1] Reimann et al, FED 165 (2021) 112249

3 15.09.2022 J. Reimann – Thermal-mechanical behavior of TiBe12 pebble beds Department of Metallic Alloys, Institute for Applied Materials - Applied Materials Physics

Main Parameters for the modelling of the thermo-mechanical behaviour of blanket pebble beds, pbs

BOL:

- stress-strain relationship $\sigma = f(\varepsilon, T, \ldots)$,
- pebble bed effective thermal conductivity $k_{eff} = f(\varepsilon, T, \ldots)$,
- thermal creep ε_{cr}.

EOL: Irradiation effects,

- Same parameters as above, see e.g. [2] analyses of Be-based materials from the ADOBE exps.

Previous investigations

Exps at ambient temperature, Ta, [1]

[2] Chakin et al, JNM 559 (2022) 153430

4 15.09.2022 J. Reimann – Thermal-mechanical behavior of TiBe12 pebble beds Department of Metallic Alloys, Institute for Applied Materials - Applied Materials Physics

Experimental set-up

Uniaxial Compression Test facility combined with a Hot Wire, HW, set-up.

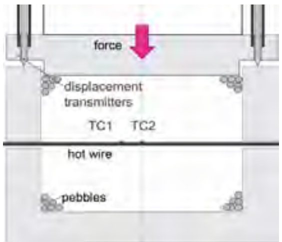

Set-up used for exps at Ta [1] . For details of the HW-system, see also [1].

Now: Use of the container with additional heating on cylindrical part and the heating system of HECOP facility [3]

Parameter range:

- max. pressure (uniaxial stress): 6MPa
- max. T: 500°C

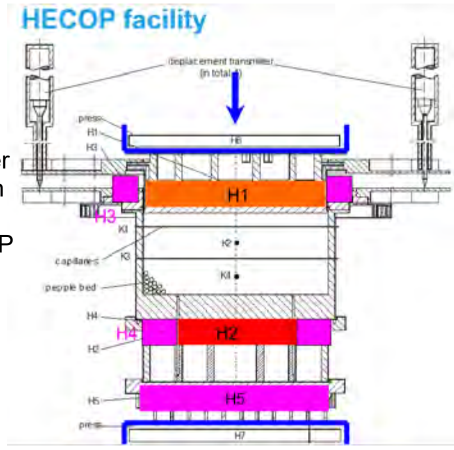

[3] Reimann et al, FED 81 (2006) 449-454

Results: A) σ–ε relationship

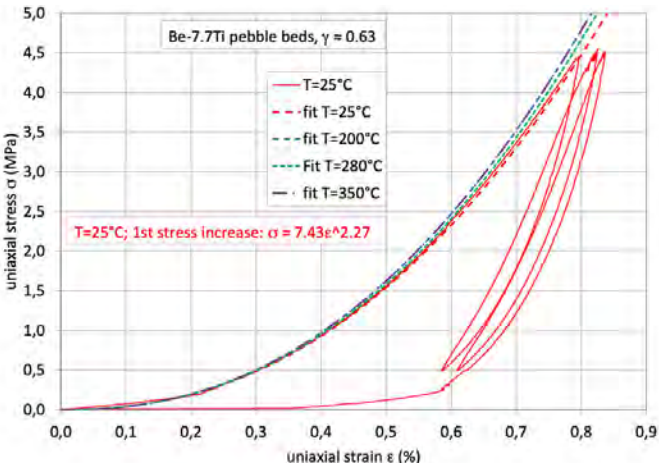

- Besides the first stress increase curve, the subsequent stress release and following cycles are also blanket relevant.
- As already observed for Be pbs [3], the σ–ε dependence of 1st σ-increase curve is negligibly dependent on T as long as thermal creep is of no concern.
- The cycling curves curves indicate an elastic pebble material.

KIT Karlsruhe Institute of Technology

Results: B) Thermal conductivity of solid materials, k_s, and helium, k_{-he}

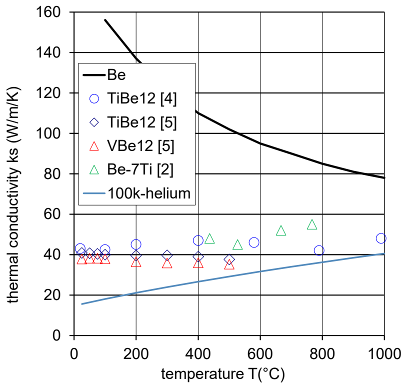

Beryllide pbs, are superior to Be pbs in many aspects (irradiation, compatibility, oxidation…)

However, there is a significant drawback: the thermal conductivity of the solid materials, k_s, is significantly smaller than that of Be [2,4,5].

Because the present Be-7.7Ti pebbles consist of several phases, the exact k_s value is not known. In the following, a constant value of k_s = 40 W/(mK) is assumed.

The thermal conductivity of helium increases with T.

[4] Uchida et al, FED 69 (2003) 499-503

[5] Reimann et al, SOFE 2009, IEEE CFP09SOF-PRT, 305-309

7 15.09.2022 J. Reimann – Thermal-mechanical behavior of TiBe12 pebble beds Department of Metallic Alloys, Institute for Applied Materials - Applied Materials Physics IAM

KIT Karlsruhe Institute of Technology

B) Non-compressed pbs, k_{eff-0} = f(T)

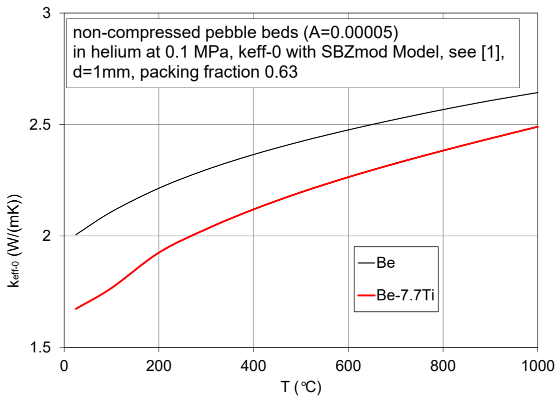

- Pebble bed thermal conductivities much smaller than solid material conductivities.
- k_{eff-0} for Be-7.7Ti at 600C about 10% lower than that of Be (although $k_{s\text{-}Be7.7} \approx 0.5 k_{s\text{-}Be}$).
- However: for Be pbs, k_{eff} increases drastically with compression (uniaxial stress); how about Be-7.7Ti?

8 15.09.2022 J. Reimann – Thermal-mechanical behavior of TiBe12 pebble beds Department of Metallic Alloys, Institute for Applied Materials - Applied Materials Physics IAM

B) 1st stress increase, compressed pbs, Ta [1], k_{eff} = f(stress σ)

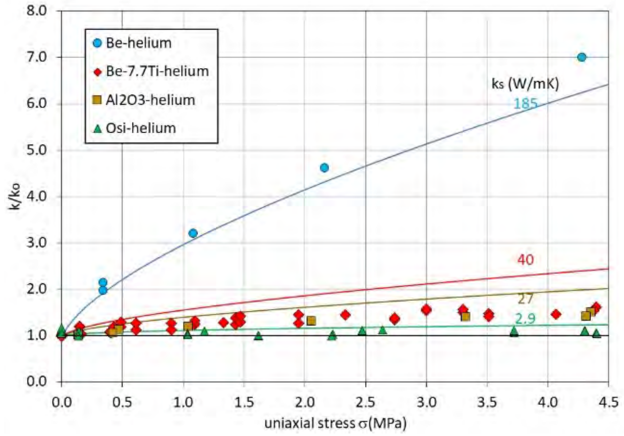

- For Be pbs, k_{eff} increases drastically with σ in contrast to other pb materials.
- What is the reason for this?
  - ductility?
  - solid material thermal conductivity k_s?
- Answer: both; assuming the same increase of contact surfaces as for Be pbs, the measured data for non-ductile materials are below the calculated curves.

B) 1st stress increase, compressed pbs, Ta [1], k_{eff} = f(strain ε)

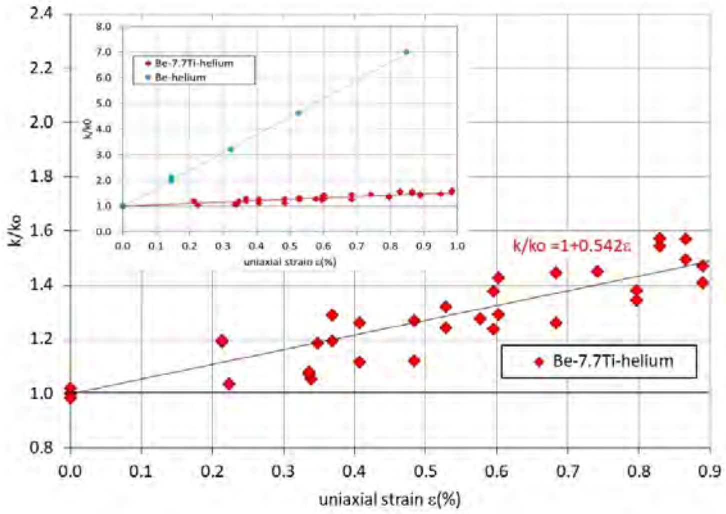

- In blankets, strain is the prime parameter.
- As observed for Be pbs [3], a fairly linear dependence is obtained.

B) Temperature dependence of keff for first stress increase

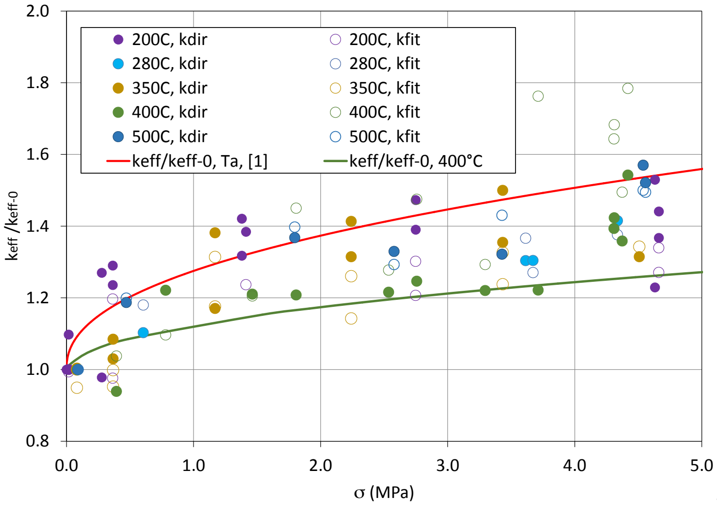

- With increasing temperature, the data are generally below the curve for Ta. The reason is that keff-0 increases with T because of the increasing helium thermal conductivity.
- Additionally, the contribution of contact surfaces decreases also with increasing gas thermal conductivity.

11 15.09.2022 J. Reimann – Thermal-mechanical behavior of TiBe12 pebble beds

Department of Metallic Alloys, Institute for Applied Materials - Applied Materials Physics

B) Temperature dependence of keff during mech. cycling

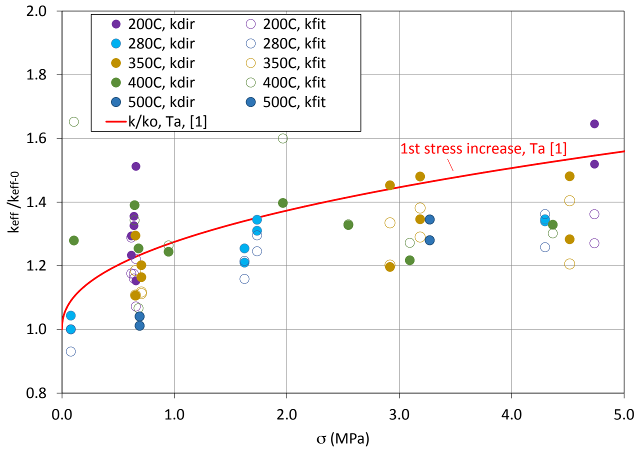

- For ductile pb materials, e.g. Be, keff does not decrease significantly with stress decrease in a wide σ-range.
- For Be-7.7Ti, this effect is not expressed, indicating again the elastic pebble behavior.

12 15.09.2022 J. Reimann – Thermal-mechanical behavior of TiBe12 pebble beds

Department of Metallic Alloys, Institute for Applied Materials - Applied Materials Physics

C) Thermal creep strain ε_{cr}

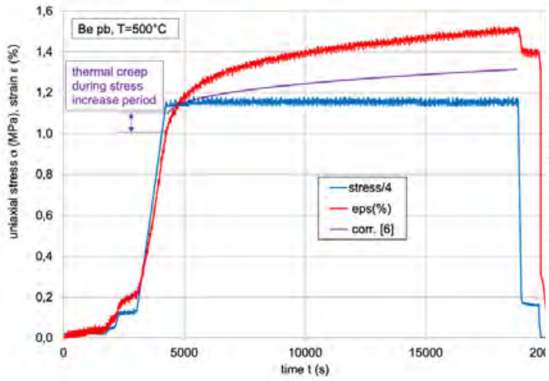

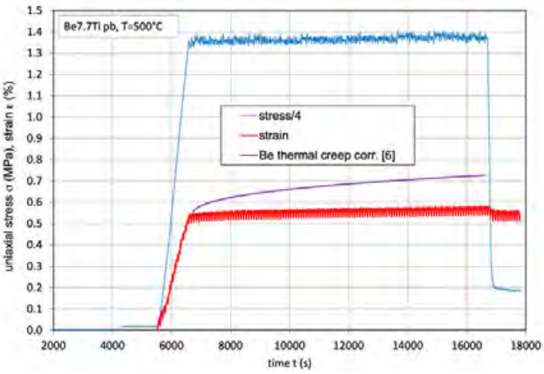

[6] Reimann et al, FED 75-79 (2005) 1043-1046

- Thermal creep increases contact surfaces and with this increases effectively keff.
- At 500°C, thermal creep is significant for Be pbs [6] and negligible for Be7.7Ti pbs. (Corresponding keff results can not be shown because of HW failure).

13 15.09.2022 J. Reimann – Thermal-mechanical behavior of TiBe12 pebble beds Department of Metallic Alloys, Institute for Applied Materials - Applied Materials Physics

Discussions/Conclusions

- The thermo-mechanical behavior of beryllium titanate Be-7.7Ti pbs was investigated at temperatures up to 500°C.
- Compared to Be pbs, Be-7.7Ti pbs have a considerably smaller keff during compression because of the smaller ductility and the smaller solid material conductivity.
- Thermal creep effects, causing also an increase of contact surfaces, are marginal for Be-7.7Ti in the investigated temperature range.
- keff can be impoved by using binary pbs instead of monosized pbs [7].
- Beryllide pbs can be superior to Be pbs, if mixed breeder and neutron multiplyer pbs are a viable option, requiring irradiation exps.
- Recent analyses of the HIDOBE irradiation programme showed much smaller swelling of Be5Ti and Be7Ti disks compared to Be disks, and smaller swelling rates for Be pebbles compared to Be disks. Again, irradiation exps with non-constrained/ constrained beryllide pebbles are required.
- First thermal creep results on irradiated Be pebbles were presented by [8].

[7] Reimann et al, BeWS 13
[8] Chakin et al, BeWS 15

14 15.09.2022 J. Reimann – Thermal-mechanical behavior of TiBe12 pebble beds Department of Metallic Alloys, Institute for Applied Materials - Applied Materials Physics

APPENDIX A

Workshop photos

Figure 1: Group picture of the BeWS-15 participants (courtesy of J. Reimann). From left to right:
1st row: S. Udartsev, A. Goraieb, M. Klimenkov, E. McKeon, M. Kearney, J.-H. Kim, R. Pearson, P. Vladimirov, J. Reimann, I. Kenzhina, D. Radloff, M. Ionescu-Bujor, K. Hesch, A. Renier, H. Huang;
2nd row: S. Kuksenko, S. Kovalskiy, J. Verdon, C. Baus, G. Kizane, K. Ashley, P. Späh, P. Dvoráková-Ruskayová, M. Rubel, T. Knudson, K. Smith, R. Gaisin;
3rd row: M. Dürrschnabel, A. Möslang, M. Rieth, R. Stieglitz, D. Bachurin, A. Frehn, A. Shaimerdenov, Y. Frants, P. Mählmann, M. Voß, K. Zenkov, D. Sioui, A. Vitins, T. Scherer, C. Dorn, L. Whalen, L. Vandermark, R. Jilek, L. Toupal.

Figure 2: Group picture of the BeWS-15 participants without J. Reimann, who was taking this photo (courtesy of J. Reimann)

Figure 3: Workshop dinner in Hoepfner Schalander Hall

Figure 4: Awarding the Prof. Mario Dalle Donne Award to Aniceto Goraieb during the Workshop dinner in Hoepfner Schalander Hall

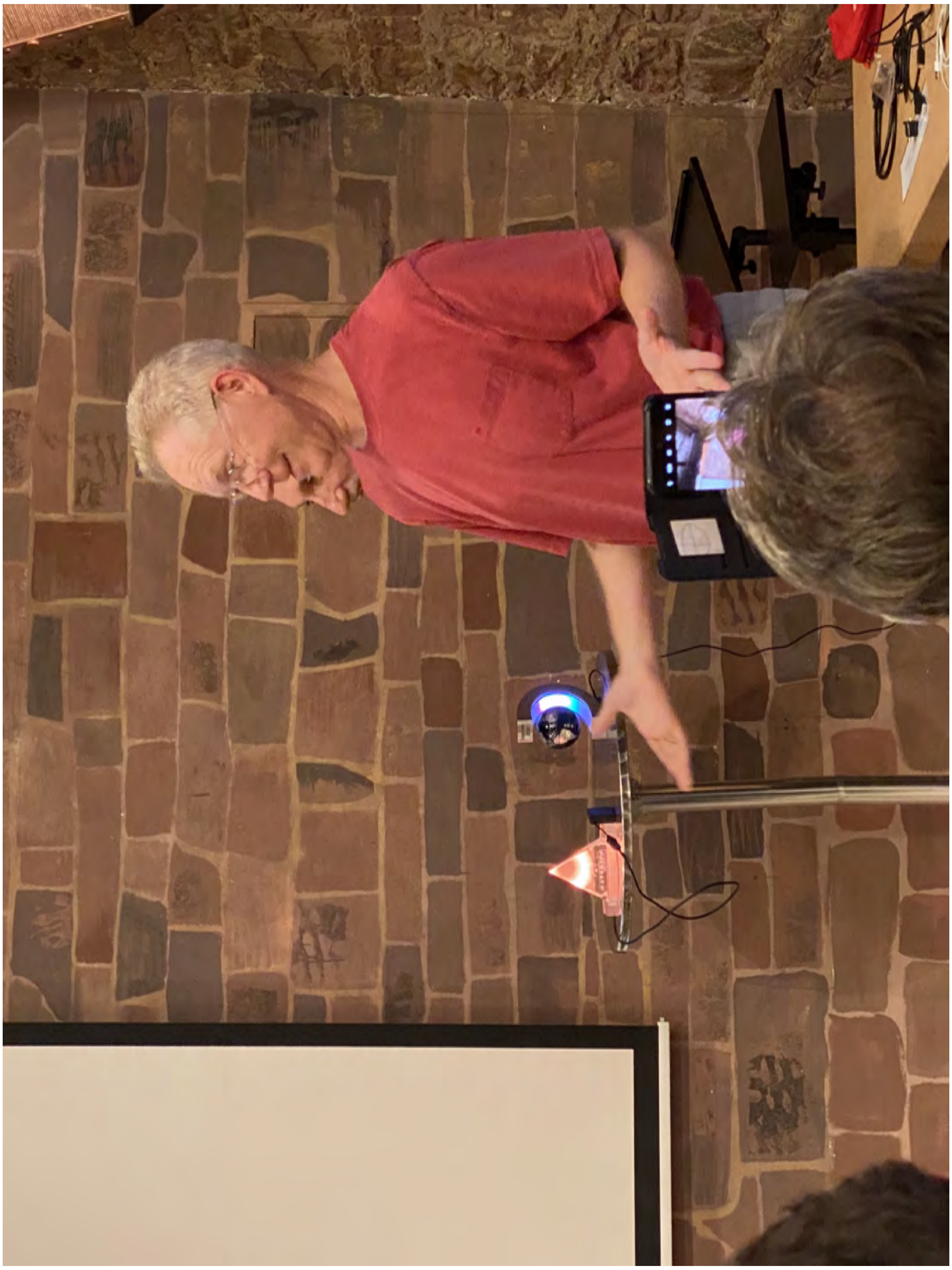

Figure 5: Awarding the Prof. Glen Longhurst Award to Christopher Dorn during the Workshop dinner in Hoepfner Schalander Hall

Figure 6: Guided tour of the Hoepfner Burghof Brewery

Figure 7: Group photo (from left to right): R. Gaisin, K. Zenkov, S. Udartsev, Ye. Frants, P. Vladimirov

Figure 8: Group photo (from left to right): P. Vladimirov, S. Kuksenko, R. Gaisin

APPENDIX B

BeWS-15 Technical Program

Title:	The 15th International Workshop on Beryllium Technology (BeWS-15)
Location:	Karlsruhe Institute of Technology, Karlsruhe, Germany
Date:	14-16.09.2022

BeWS-15: 14.09.22

Start	End	Time	Item	Presenter	Session	Chair
9:00 AM	9:15 AM	0:15	Welcome	Pavel Vladimirov	**In memory of Glen Longhurst**	Ch. Dorn
9:15 AM	9:45 AM	0:30	The HCPB Test Blanket Module: Current Status in Development and Qualification of Beryllium Materials and an Overview of Open Issues	Milan Zmitko (online)		
9:45 AM	10:15 AM	0:30	Overview of R&D activities on Neutron Multipliers in QST	Jae-Hwan Kim		
10:15 AM	10:35 AM	0:20	Break & Exhibition			
10:35 AM	11:00 AM	0:25	Overview of the United States Beryllium Industry - 2022 Update	Keith J. Smith	**News from Industry**	M. Zmitko
11:00 AM	11:25 AM	0:25	Beryllides - experience of UMP JSC in development and testing	Sergey Udartsev		
11:25 AM	11:50 AM	0:25	Beryllium Additive Manufacturing	FritzCarl Grensing		
11:50 AM	12:15 PM	0:25	Current design of the EU DEMO Helium Cooled Pebble Bed breeding blanket	Guangming Zhou	**DEMO, ITER & JET**	V. Chakin / S.Kuksenko
12:15 PM	1:45 PM	1:30	Lunch			
1:45 PM	2:10 PM	0:25	Regulatory situation of Beryllium in EU and France – Update Beryllium Good Practices at the Workplace - Be Responsible Program - Update	Angélique Renier		
2:10 PM	2:35 PM	0:25	Beryllium in JET with the ITER-Like Wall: Fuel retention, oxidation, melt erosion, dust	Marek Rubel		
2:35 PM	3:00 PM	0:25	Thermal desorption of tritium from beryllium plasma-facing components of the JET ITER-like wall	Aigars Vītiņš		
3:00 PM	3:20 PM	0:20	Break & Exhibition			
3:20 PM	3:45 PM	0:25	A Study on Technician Variability in Wipe Sampling for Beryllium & Potential Contributions to Robotic Sampling Equipment	Eilish McKeon	**Beryllides**	P. Vladimirov
3:45 PM	4:10 PM	0:25	Overview of activities in Kazakhstan related to study of beryllium and beryllium compounds	Inesh Kenzhina		
4:10 PM	4:35 PM	0:25	Beryllides as advanced materials for neutron multiplication	Ramil Gaisin		
4:35 PM	5:00 PM	0:25	Mechanical properties of titanium beryllium intermetallic compounds	Jae-Hwan Kim		
5:00 PM			ADJOURN			
Total		**8:00**				

BeWS-15: 15.09.22

Start	End	Time	Item	Presenter	Session	Chair
9:00 AM	9:25 AM	0:25	Investigation of radiation damage effects in beryllium: updates on recent results obtained on proton, neutron and He-ions irradiated samples	Viacheslav Kuksenko	**Modeling & experimental Validation**	A. Möslang / R. Gaisin
9:25 AM	9:50 AM	0:25	First principles simulation of resistivity recovery in irradiated beryllium	Christofer Stihl		
9:50 AM	10:15 AM	0:25	Radiation induced formation gas bubbles in beryllium after neutron irradiation up to 6000 appm helium production	Michael Klimenkov		
10:15 AM	10:35 AM	0:20	Break & Exhibition			
10:35 AM	11:00 AM	0:25	Effect of impurities on microstructural evolution under irradiation in beryllium	Pavel Vladimirov	**cont'd**	
11:00 AM	11:25 AM	0:25	Ab initio study of hydrogen behavior in titanium beryllides	Dmitry Bachurin		
11:25 AM	11:50 AM	0:25	Nanoscale characterization of beryllide materials	Michael Dürrschnabel		
11:50 AM	12:15 PM	0:25	Mechanical compression behaviors and microstructure change under He ion irradiation of single phase Be and binary $Be_{12}Ti$ pebbles	Pingping Liu (online)	**Mechanical properties & irradiation damage**	M. Rubel
12:15 PM	1:45 PM	1:30	Lunch			
1:45 PM	2:10 PM	0:25	Creep of beryllium pebbles after neutron irradiation to 6000 appm helium production	Vladimir Chakin		
2:10 PM	2:35 PM	0:25	Thermo-mechanical behavior of titanium beryllide pebble beds at elevated temperatures	Jörg Reimann		
2:35 PM	2:45 PM	0:10	Closing remarks	Pavel Vladimirov		
2:45 PM	3:15 PM	0:30	Break & Exhibition			
3:15 PM	4:00 PM	0:45	Networking			
Total		**7:00**				

5:00 PM	Guided Tour over brewery Hoepfner (time to be confirmed)
7:00 PM	Conference Dinner at Hoepfner Burghof Restaurant

APPENDIX C

The list of participants

	Last Name	First Name	Institution	Country
1	Ashley	Kevin	Ashley Analytical Associates LLC	USA
2	Bachurin	Dmitry	Karlsruhe Institute of Technology	Germany
3	Baus	Colin	Kyoto Fusioneering	Japan
4	Chakin	Vladimir	Karlsruhe Institute of Technology	Germany
5	Dorn	Chris	UKAEA	UK
6	Dürrschnabel	Michael Thomas	Karlsruhe Institute of Technology	Germany
7	Dvoráková Ruskayová	Petra	ELI Beamlines	Czech Republic
8	Frants	Yevgeniy	Ulba Metallurgical Plant JSC	Kazakhstan
9	Frehn	Andreas	MATERION Brush GmbH	USA
10	Gaisin	Ramil	Karlsruhe Institute of Technology	Germany
11	Goraieb	Aniceto	KBHF GmbH	Germany
12	Gorr	Bronislava	Karlsruhe Institute of Technology	Germany
13	Grensing	Fritz Carl	Materion	USA
14	Hesch	Klaus	Karlsruhe Institute of Technology	Germany
15	Huang	Haibo	General Atomics	USA
16	Ionescu-Bujor	Mihaela	Karlsruhe Institute of Technology	Germany
17	Jamieson	Valerie	UKAEA	UK
18	Jilek	Richard	Centrum vyzkumu Rez s.r.o.	Czech Republic
19	Kearney	Maddy	UKAEA	UK
20	Kenzhina	Inesh	Kazakh-British Technical University	Kazakhstan
21	Kim	Jae-Hwan	National Institutes for Quantum Science and Technology	Japan
22	Kizane	Gunta	University of Latvia	Latvia
23	Klimenkov	Michael	Karlsruhe Institute of Technology	Germany
24	Knudson	Ted	Materion Corporation	USA
25	Kovalskiy	Sergey	Karlsruhe Institute of Technology	Germany
26	Kuksenko	Viacheslav	United Kingdom Atomic Energy Authority	UK
27	Liu	Pingping	University of Science and Technology Beijing	China
28	Mählmann	Peter	TROPAG Oscar H. Ritter Nachf. GmbH	Germany
29	McKeon	Eilish	UKAEA	UK
30	Möslang	Anton	Karlsruhe Institute of Technology	Germany
31	Pearson	Richard	Kyoto Fusioneering UK Ltd	UK
32	Liu	Pingping	School of Materials Science and Engineering, University of Science and Technology Beijing	China
33	Radloff	Dirk	Karlsruhe Institute of Technology (KIT)	Germany
34	Reimann	Joerg	Karlsruhe Institute of Technology	Germany
35	Renier	Angélique	NGK BERYLCO FRANCE	France
36	Rieth	Michael	Karlsruhe Institute of Technology	Germany
37	Rubel	Marek	KTH Royal Institute of Technology	Sweden
38	Scherer	Theo Andreas	Karlsruhe Institute of Technology	Germany
39	Seko	Kiyoshi	Kyoto Fusioneering	Japan

	Last Name	First Name	Institution	Country
40	Shaimerdenov	Asset	Institute of Nuclear Physics, Almaty	Kazakhstan
41	Sioui	Daniel	General Atomics	USA
42	Smith	Keith	Materion	USA
43	Späh	Peter	Karlsruhe Institute of Technology	Germany
44	Stieglitz	Robert	Karlsruhe Institute of Technology	Germany
45	Stihl	Christopher	Karlsruhe Institute of Technology	Germany
46	Toupal	Lukas	Centrum vyzkumu Rez s.r.o.	Czech Republic
47	Udartsev	Sergey	Ulba Metallurgical Plant JSC	Kazakhstan
48	Vandermark	Lee	General Dynamics Mission Systems PSO	USA
49	Verdon	Jon	UKAEA	UK
50	Vitins	Aigars	University of Latvia	Latvia
51	Vladimirov	Pavel	Karlsruhe Institute of Technology	Germany
52	Voß	Michael	TROPAG Oscar H. Ritter Nachf. GmbH	Germany
53	Whalen	Lance	General Dynamics	USA
54	Zenkov	Konstantin	Ulba Metallurgical Plant JSC	Kazakhstan
55	Zhou	Guangming	Karlsruhe Institute of Technology	Germany
56	Zmitko	Milan	F4E	Spain

APPENDIX D

Author Index

ISBN 978-3-7315-1284-4
9 783731 512844

ISSN 1869-9669
ISBN 978-3-7315-1284-4

Gedruckt auf FSC-zertifiziertem Papier